Hierarchical Control and Input Redundancy

Jean-François Trégouët

Université Claude Bernard Lyon 1

INSA INSTITUT NATIONAL DES SCIENCES APPLIQUÉES LYON

N° Identificateur : 2025HDR014 Année 2025

HABILITATION A DIRIGER DES RECHERCHES

présentée devant

l'Institut National des Sciences Appliquées de Lyon et l'Université Claude Bernard Lyon I

Commande hiérarchique et redondance d'entrée

par

Jean-François TRÉGOUËT
Docteur en Automatique

Soutenue le 9 juillet 2025 devant la commission d'examen

Composition du jury

Président :	Pr. Sorin OLARU	CentraleSupélec
Rapporteurs :	DR Jean Jacques LOISEAU	LS2N
	Pr. Andrea SERRANI	Università di Bologna
	DR Luca ZACCARIAN	LAAS
Examinateurs :	PU Éric BIDEAUX	INSA de Lyon
	MCF – HDR Antoneta Iuliana BRATCU	Grenoble INP – UGA
	PU Jamal DAAFOUZ	ENSEM – Université de Lorraine
	PU Bernhard MASCHKE	Université Lyon I
	Pr. Sorin OLARU	CentraleSupélec

Laboratoire Ampère — UMR 5005

Thanks / Remerciements

Merci à Léa, Isabelle et Paul d'une part, et Émile, d'autre part, sans qui ce travail aurait été terminé beaucoup plus tard et beaucoup plus tôt, respectivement.

Let me warmly thank the jury members and apologize for being long. I was afraid of being unclear.

Contents

List of Figures

Part I

Éléments de carrière

Part II

Scientific content

Notations and acronyms

General formatting rules[2]

a, b, c	Scalar or vector
A, B, C	Linear mapping or matrix
$\mathsf{A}, \mathsf{B}, \mathsf{C}$	Operator or subsystem
$\mathcal{A}, \mathcal{B}, \mathcal{C}$	Subset (not necessarily linear) of Euclidean spaces
$\mathfrak{A}, \mathfrak{B}, \mathfrak{C}$	Class, i.e. set of sets
$\mathbf{A}, \mathbf{B}, \mathbf{C}$	Function space

Notations of general purpose

$\mathbf{0}$	Anything that is not a real number and is zero (a vector, matrix, map, or subspace), according to the context
E [V]	Physical variable E is expressed in volt
$\wedge, \vee, \neg$	Logical operators "and", "or" and "not", respectively
$a \mod b$	a modulo b
$[\![a, b]\!]$	$\{a, \dots, b\} = [a, b] \cap \mathbb{Z}$ if $a \leq b$ and $\{\varnothing\}$ otherwise
$\mathbb{S}^n$	$\{x \in \mathbb{R}^{n+1} : \|x\|_2 = 1\}$
$A \succ \mathbf{0}, A \prec \mathbf{0}$	Matrix A is positive and negative definite matrix, respectively
J'	Derivative of real-valued function J, i.e. $\begin{bmatrix}\partial J/\partial u_1 & \partial J/\partial u_2 & \dots\end{bmatrix}$
∇J	$(J')^\intercal$
x^{-1}	Component-wise inversion of the vector x, i.e. $\begin{bmatrix}x_1^{-1} & x_2^{-1} & \dots\end{bmatrix}$
$\sigma(A)$	Spectrum of A *counting multiplicity*, e.g. $\sigma(\mathbf{I}_2) = \{1, 1\}$
$\mathbf{I}_n, \mathrm{id}_{\mathcal{X}}$	Identity matrix of size $n \times n$ and identity mapping of the set $\mathcal{X}$, respectively
$\mathbf{1}_n, \mathbf{1}_{p\times m}$	Vector of size $n \times 1$ and matrix of size $p \times m$ whose entries are all one, respectively
$\mathrm{sat}_{\mathcal{X}}$	Any application mapping the vector x to some vector in $\arg\min_{\eta\in\mathcal{X}} \|\eta - x\|_2$
$\mathbb{C}^0, \mathbb{C}^-, \mathbb{C}^+$	Imaginary axis, open left-half plan, open right-half plan, respectively
$u \leq v$	Vectors u, v satisfying $u_k \leq v_k$ for all k
$\min x, \max x$	Minimum and maximum of entries of x, i.e. $\min\{x_1, x_2, \dots\}$ and $\max\{x_1, x_2, \dots\}$, respectively
$A_1 \sim A_2$	Maps A_1 and A_2 are similar, i.e. there exists P such that $P^{-1}A_1P = A_2$

[2]Generally speaking, those rules apply. Exceptions exist, though. They include $E \in \mathbb{R}$ corresponding to voltage source magnitude in Chap. 5 and Chap. 10, and $\mathbf{I}$ standing for the identity matrix.

Indexing

$x_{a:b}$	Subvector made of entries of x whose indices[3] belong to $[\![a, b]\!]$, i.e. $x_{a:b} = \begin{bmatrix} \mathbf{0} & \mathbf{I}_{b-a+1} & \mathbf{0} \end{bmatrix} x$
$P_{a:b} \in \mathbb{R}^{p \times m}$	Submatrix made of columns of P whose indices belong to $[\![a, b]\!]$, i.e. $P_{a:b} = P \begin{bmatrix} \mathbf{0} & \mathbf{I}_{b-a+1} & \mathbf{0} \end{bmatrix}^\intercal$

Sets

$\uplus$	Union with any common elements repeated
$\mathcal{X}_{1:m}$	For $\mathcal{X} \subset \mathbb{R}^n$, coordinates in $\mathcal{P} = \text{span}\left\{ \begin{bmatrix} \mathbf{I}_m \\ \mathbf{0} \end{bmatrix} \right\} \subset \mathbb{R}^n$ of the orthogonal projection of $\mathcal{X}$ on $\mathcal{P}$, i.e. $\{x_{1:m} \mid \exists x_{m+1:n} : x \in \mathcal{X}\}$
$x + S$	$\{x + s : s \in S\}$
$\text{co}\,\{S\}$	Convex hull of S
$\mathcal{A} \subset \mathcal{B}$	$\mathcal{A}$ is included in $\mathcal{B}$ (and possibly equal to $\mathcal{B}$)
$\mathcal{A} \subsetneq \mathcal{B}$	$\mathcal{A}$ is a proper subset of $\mathcal{B}$, i.e. $\mathcal{A}$ is included in $\mathcal{B}$ but not equal to $\mathcal{B}$
$\text{int}(S)$	Interior of S
$\lvert S \rvert$	Cardinality[4] of S
$[u, v]$	$\{x : u \leq x \leq v\}$ if vectors u and v satisfy $u \leq v$
$\min S$	Minimum of S
$x(\cdot) \in \mathcal{V}$	Identical set membership of $t \mapsto x(t)$ to $\mathcal{V}$, i.e. $x(t) \in \mathcal{V}$ holds for all t
$\mathcal{V} \simeq \mathcal{W}$	Sets $\mathcal{V}$ and $\mathcal{W}$ are isomorphic
$M(\mathcal{A})$	Image of the set $\mathcal{A}$ under the map M, i.e. $\{M(x) : x \in \mathcal{A}\}$

Function spaces

B	Set of causal[5] and bounded vector-valued signals
P	Set of causal and persistent vector-valued signals, i.e. $\mathbf{P} = \{x(\cdot) \in \mathbf{B} : \text{if } x^\star = \lim_{t \to +\infty} x(t) \text{ exists, then } x^\star \neq \mathbf{0}\}$
C	Set of causal and continuous vector-valued signals
PC	Set of causal and piecewise continuous vector-valued signals
D	Set of causal vector-valued signals that are differentiable on $]0, +\infty[$
PD	Set of causal and piecewise differentiable vector-valued signals
$\mathbf{X}(\mathcal{M})$	$\{x(\cdot) \in \mathbf{X} : \forall t \geq 0, x(t) \in \mathcal{M}\}$

[3] Indices start at 1.

[4] $\lvert S \rvert$ is said to be greater than or equal to $\alpha \in \mathbb{N}$ if S admits at least α distinct members. In particular, if $\mathbf{S} \subset \{u : \mathbb{R} \to \mathbb{R}^n\}$ is a function space, then $\lvert \mathbf{S} \rvert > \alpha$ means that there exist $u_1, \ldots, u_\alpha \in \mathbf{S}$ such that every u_i, u_j differ on a strictly positive measure set, i.e. $\int \left\| u_i(\tau) - u_j(\tau) \right\| \mathrm{d}\tau > 0$ for all $i \neq j \in \{1, \ldots, \alpha\}$.

[5] By causal signal, we mean a signal which is zero for all strictly negative time instant.

Control theory

$u(t) \in \mathbb{R}^m$	Input vector at time t
$x(t) \in \mathbb{R}^n$	State vector at time t
$y(t) \in \mathbb{R}^p$	Output vector at time t
$\mathrm{H}_x[x_0;\cdot]$	Input-to-state operator with x_0 as the initial state
$\mathrm{H}[x_0;\cdot]$	Input-to-output operator with x_0 as the initial state
$\mathfrak{L}[u]$	Laplace transform of u
$x^\star$	Steady-state value of the signal or argument of some extremum, according to the context
$\left[\begin{array}{c\|c} A & B \\ \hline C & D \end{array}\right]$	Quadruple[6] of the linear system Σ governed by $\dot{x} = Ax + Bu,\ y = Cx + Du$
$\mathbf{Q}(x_0)$	$\{(u,x,y) \in \mathbf{U} \times \mathbf{X} \times \mathbf{Y} \mid \mathrm{H}_x[x_0;u] = x,\ \mathrm{H}[x_0;u] = y\}$
$\mathbf{W}(x_0)$	$\{(u,y) \in \mathbf{U} \times \mathbf{Y} \mid \exists x : (u,x,y) \in \mathbf{Q}(x_0)\}$
$\mathfrak{S}$	System deriving from Σ by ruling the trajectories violating input or state constraints out
$P_\Sigma(s)$	System matrix $\left[\begin{smallmatrix} s\mathbf{I}-A & -B \\ C & D \end{smallmatrix}\right]$
$G(s)$	Transfert function matrix, i.e. $G(s) = C(s\mathbf{I} - A)^{-1}B + D$

Geometric control theory[7]

$B\|\mathcal{N}$	Domain restriction of $B : \mathcal{U} \to \mathcal{X}$ to $\mathcal{N} \subset \mathcal{U}$
$\mathcal{V}\|B$	Codomain restriction of $B : \mathcal{U} \to \mathcal{X}$ from $\mathcal{V} \supset \mathcal{X}$ if $\mathrm{Im}\{B\} \subset \mathcal{V}$
$B^{-1}\mathcal{V}$	Pre-image of $\mathcal{V}$ under B, i.e. $\{u : Bu \in \mathcal{V}\}$
$\mathcal{K}$	$\mathrm{Ker}\{C\}$
$\langle \mathcal{K}\|A \rangle$	Largest A-invariant subspace contained in $\mathcal{K}$
$\langle A\|\mathcal{B} \rangle$	Smallest A-invariant subspace containing the subspace $\mathcal{B} \subset \mathcal{X}$
$\sup \mathfrak{V}$,$\inf \mathfrak{V}$	Supremum and infimum of the class $\mathfrak{V}$ containing linear sets, respectively
$\mathbb{F}(\mathcal{V})$	Set of friends of the subspace $\mathcal{V}$, i.e. $\{F : (A+BF)\mathcal{V} \subset \mathcal{V} \subset \mathrm{Ker}\{C+DF\}\}$
$\mathcal{Z}$	Set of invariant zeros, i.e. $\sigma((A+BF)\|\mathcal{V}^*/\mathcal{R}^*)$ where F is arbitrary in $\mathbb{F}(\mathcal{V}^*)$
$\mathcal{Z}_{\mathrm{od}}$	Set of output decoupling zeros, i.e. $\sigma(A\|\langle \mathcal{K}\|A \rangle)$

Acronyms

a-IOA	asymptotic Input-to-Output Annihilator
as-LI	asymptotic strong Left Invertible
bp	bounded and persistant
bp-WIR	bounded and persistant Weak Input Redundant/Redundancy
CAM	Classical Allocation Methodology
CCM/DCM	Continuous/Discontinuous Conduction Mode
IOA	Input-to-Output Annihilator
IR	Input Redundant/Redundancy
ISA	Input-to-State Annihilator
LI	Left-Invertible/Invertibility
PC	Power Converter(s)
MPC	Model Predictive Control
SLI	Strong Left-Invertible/Invertibility
WIR	Weak Input Redundant/Redundancy

[6] Sometimes, the quadruple is simply denoted by (A,B,C,D).
[7] See Appendix A for more details.

Preliminary: Overview of my research interests

Nothing is as practical as a good theory.

Taking up the above quotation, attributed to Kurt Lewin, the research activities I carry out are mainly at the intersection of automatic control on the one hand, ElectroTechnics and Power Electronics (ETPE), and, more recently, Fluid Power (FP) on the other. Fig. 4.1 illustrates the relationship between these topics. My contributions are mainly methodological. Drawing on the department's multidisciplinary environment, I endeavor:

1. to make appropriate use of control methodologies, i.e. a suitable choice of modeling assumptions and a relevant knowledge of technological obstacles, as well as of the various control goals and the trade-off that can be considered between them;
2. to formulate and address in a general framework the obstacles corresponding to methodological shortcomings *issued from practice, and then tested by it*.

The joint design of the system and its control law is the culmination of this approach; see the last chapter devoted to the perspectives.

My research interests are outlined below. The second item, namely "Modular converters as input redundant systems", is the topic of the rest of the manuscript.

Power electronics converters seen as hybrid dynamical systems

The electrical systems are controlled via power converters. These can be seen as the interconnection of passive components (diodes, coils, and capacitors) and controlled switches (transistors). This interconnection naturally gives rise to affine piecewise (owing to diodes) and relay (owing to transistors) models, because the input vector belongs to a set of finite cardinality.

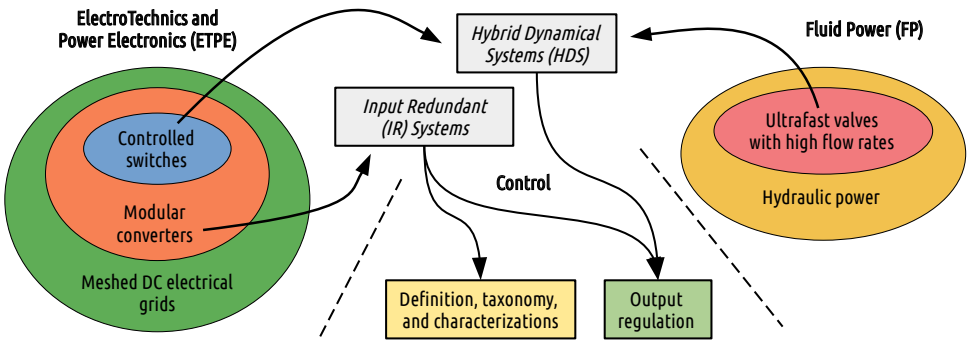

Figure 4.1: Personal current research topics.

Practical contribution to ETPE In this field, my contribution consisted in discarding, theoretically and practically, an assumption that underlies many publications in the field of automatic control, but which is unrealistic in application terms, that is, all model parameters, including the value of the load of power converters, are constant and perfectly known.

Methodological contribution in control For this particular class of Hybrid Dynamical Systems (HDS), I have contributed to the extension of robust output control by internal model (Davison, Francis, Wonham), originally thought for continuous systems with unconstrained inputs.

Publications [**Ndo+19**; **Ndo+22**; **NT24**]

Supervised Phd student Aboubacar NDOYE

Modular converters as input redundant systems

In the context of major disruptions in energy systems, the reconfigurability of power converters is a decisive criterion. The aim is to design systems that are resilient in the event of failure and upgradeable to incorporate the latest technological advances. Modular design is a response to these requirements, based on components whose overall functionality is not ensured by a monolithic component but distributed between different modules that coordinate with each other.

Practical contribution to ETPE The parallel interconnection of converters supplying a single load is the result of such an approach. For this type of modular converter, my contributions have resulted in a control law that guarantees output voltage regulation while ensuring optimum current distribution without assuming that the value of the load is known. Particular effort has been made to handle the hierarchical nature of the set of specifications.

Methodological contribution in control Since each converter/module is controllable, there are more control inputs than are required by load voltage regulation alone, so this system falls into the category of Input Redundant (IR) systems. In addition to applying these techniques (historically confined to aeronautics) to ETPE, my contributions focus on :

1. the definition, characterization and classification of constrained and unconstrained IR systems;
2. the exploitation of input redundancy for the output regulation problem;
3. bridging the gap between the historical approach to control allocation (Durham, Bodson, Johansen, etc.) with the new approaches proposed over the last two decades (Zaccarian, Serrani, Galeani, etc.), particularly for the management of dynamic actuators.

Publications [**TDG16**; **TD17**; **Kre+18a**; **TD19**; **Del+19**; **Kre+19**; **Kre+21b**; **KT21**; **Kre+21a**; **Sad+22**; **TK24**]

Supervised Phd student Jérémie KREISS

Modular converters for power grids

Power grids face unprecedented technical challenges. On the one hand, not only consumption but also production are now concerned by intermittence. Second, the latest generation of terminals connected to the grid has the dual effect of dangerously lowering grid inertia, and making the use of direct current (DC) more appropriate. Meshing the network structure and orienting it towards DC are relevant technical responses to these challenges, as they enable finer, and reconfigurable management of the transport of electrical power.

Practical contribution to ETPE Smart Nodes (SN) are multi-branch converters capable of directing power flows in a network, among other features. I have worked on the design and control of a modular SN for mixed DC/AC grids.

Methodological contribution in control Designed via forwarding or singular perturbation methods, the control laws in this SN can be seen as ad-hoc solutions for the output regulation of uncertain bilinear models subject to input constraints, which remains an open problem.

Publications [**Lin+21**; **Sim+21a**; **Sim+21b**; **Sim+23a**; **Sim+23b**]

Supervised Phd students Tanguy SIMON, Lukas CAFRAN (on-going Phd)

On-off control for hydraulic power

The recent advent of ultrafast valves with high flow rates and low pressure drops represents a major technological advance in the field of hydraulic power. By enabling sub-millisecond switching, this technology promises a significant improvement in the efficiency of the overall energy chain. Compared with the proportional valves conventionally used for flow control, however, the on-off control of such devices remains a challenge because the models to be manipulated are relay-based and nonlinear.

Practical contribution to FP Recently involved in this theme, in which Ampere Laboratory has a long-standing and recognized expertise, I have been working on the development of a conceptual framework for the design of control laws for these systems. More generally, the aim is to explore the analogy between FP and ETPE, both technologically and methodologically, and in terms of design and control.

Methodological contribution in control By neglecting some fast dynamics, the input-to-output relationship of 3-pistons motors can be captured by a parameter-dependent affine static IR system. The expression of the inverse of this system has been obtained in closed-form.

Publications [**DBT23**; **Dar+24**]

Supervised Phd student Justin DARNET

The social-technical analysis of digital objects

On a technical level, the energy transition aims to make electricity a universal energy carrier in the context of intermittent demand and supply. To this end, digital technology, and automatic control in particular, are called upon as the right tools to approach optimality in an uncertain

context. However, this enabling digital technology is deployed on material support, whose ecological impact can no longer be ignored. At the same time, society's relationship with this "decision-making technology" needs to be questioned.

Interrest Exploring the intrinsic ambivalence of technology, and particularly digital technology, is a theme of great interest to me, particularly in the current context of multicrisis (ecological, economic and political). Bringing these issues into the public debate is a task to which I strive to contribute, within my abilities.

Publications [**RST20b**; **RST20a**]

Supervised master student Baptiste BEGUINET

Miscellaneous

This chapter ends with a list of past/dormant research topics.

- Robust control of periodic systems: [**Tré+11a**; **Tré+12b**; **Tré+12a**; **Tré+13b**]
- Globally monotonic tracking control of multivariable systems: [**Nto+16b**; **Nto+16a**]
- Robust control of network controlled systems: [**TSD16**]
- Control of electrical motors: [**Kre+18b**; **Zha+21**]
- Attitude control of satellites using both magnetorquers and reaction wheels: [**Tré+11b**; **Tré+13a**; **Tré+15**]
- Eco-driving assistance system: [**Jav+17**] (Setareh JAVANMARDI was a Phd student, I have supervised on this topic)

General introduction

Considerations from control practitioners

Our starting point comprises the following two observations, described by adopting a control practitioner's perspective.

A technological trend

An increasingly popular technological trend involves substituting a single high-capacity actuator with multiple actuators that work in concert. This strategy aims to increase the overall capacity and systemic robustness of the actuation subsystem. Examples include state-of-health and/or thermal management, resilience to actuator failure, and enhanced control capabilities, see [BBF17; **Tré+15**; JF13; HT07] to cite a few. Systems of this type are known as over-actuated systems.

Control designs dedicated to overactuated systems have been proposed in various fields, including aerospace and aeronautics [ODB11], marine vessels [FJ06], and power electronics [BBF17; **TD19**]. Typically, two distinct control specifications are addressed simultaneously.

S1 that is related to the main control objective of the plant;

S2 that translates some preferences of the *overall* actuation subsystem, e.g. minimizing its energy consumption or preserving its state-of-health.

This manuscript aims to contribute to the methodological side of control problems related to overactuated systems. This class of systems falls into the category of input-redundant (IR) systems, for which the input can be either manipulable or not. Therefore, this manuscript also contributes to the analysis of this general class of IR systems.

Dealing with a set of conflicting specifications

A standard control problem is the combination of a model and specification. In most textbooks, the latter reduces to make the origin of the state space a stable equilibrium. If the refinement of this statement is used in the output regulation context, the stabilization of a single (possibly moving) set point remains at the heart of most control problems.

However, in many practical cases, one must consider *a set of specifications*. **S1** and **S2** constitutes a typical example of this fact. In this case, as in many others, **S1** and **S2** are conflicting: Serving **S2** exclusively will jeopardize **S1**. Indeed, the preferred state of each actuator is usually switched off, which would obviously sacrifice **S1** in general.

In many cases, this misalignment between **S1** and **S2** is resolved naturally by considering the implicit hierarchy between **S1** and **S2**. This allows for the recovery of a well-posed problem. This hierarchy is typically implemented using one of the two strategies that are now exposed. To illustrate them, it is assumed that **S1** $>$ **S2** holds in the sense that priority should

be given to **S1** over **S2**. We also adopt the optimal control point of view, where the problem is to design the manipulable input u that is optimal.

(i) Soft hierarchy relies on a trade-off between **S1** and **S2**. This idea can be captured via the following optimization problem:

$$\max_u \alpha \mathbf{S1} + (1-\alpha)\mathbf{S2} \tag{SH}$$

where $\alpha \in [0,1]$ reflects the trade-off level and is typically closer to 1 than to 0. The LQ optimal control problem is the mainstream solution along this line.

(ii) Hard hierarchy imposes that **S1** must be fulfilled "as much as possible" before addressing **S2** via the remaining degrees-of-freedom (if any). This strategy boils down to the following two-stage optimization problem:

$$\max_u \mathbf{S2} \quad \text{s.t.} \quad u \in \mathbf{F} := \arg\max_{\hat{u}} \mathbf{S1} \tag{HH}$$

This manuscript is concerned with methodological tools that are helpful to construct a solution to (HH).[8] To make the discussion concrete, we define the output y as the (possibly vector-valued) signal related to **S1**, in the sense that addressing **S1** amonts to shape y. Let $\mathrm{H} : u \mapsto y$ be the resulting input-output map. Furthermore, assume that there exists a unique output $y = y^\star$ in the range of H that maximizes **S1**. In this case, **F** reads:[9]

$$\mathbf{F} := \{u : \mathrm{H}(u) = y^\star\}. \tag{4.1}$$

Clearly, (HH) is relevant only if **F** is not reduced to a singleton. Otherwise, there will be no degrees of freedom to deal with **S2**. The next section aims to use this condition to define IR. This makes IR a pivotal concept between the aforementioned technological trend and the handling of conflicting specifications.

Three views of the IR mount

Hereafter, and throughout this manuscript, the standing assumption is that H is linear. In this framework, the following questions are now addressed:

> **Q1)** How to characterize the set of systems for which (HH) is relevant? How can this class of systems be related to IR systems? How can these types of systems be characterized?
>
> **Q2)** How to derive an expression of **F** in closed-form?
>
> **Q3)** How to build a control architecture allowing to solve (HH)?

In what follows, answers to the question **Qi)** are labelled **Ai)**.

[8] Let us emphasize that (SH) with $\alpha = 1$ is distinct from (HH). In particular, if **F** does not reduce to a singleton, then the former cannot be well posed (the minimum is not unique), unlike the latter.

[9] $y^\star \in \mathrm{Im}\,\{\mathrm{H}\}$ implies $\mathbf{F} \neq \varnothing$.

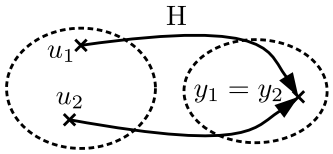

Figure 4.2: IR is non injectivity.

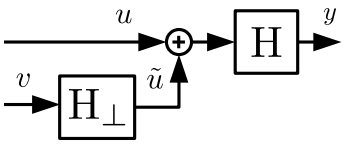

Figure 4.3: If $\mathrm{H}_\perp$ is an annihilator, then $\tilde{u}$ is invisible from the output y. Thus, v can address **S2**, letting **S1** unchanged.

Inversion perspective

As illustrated by Fig. 4.2, assume that there exist distinct inputs $u_1 \neq u_2$ producing identical output y:

$$\exists u_1 \neq u_2 : \mathrm{H}(u_1) = \mathrm{H}(u_2) \tag{4.2}$$

The following development shows that this property does not depend on u_2.

$$(4.2) \overset{\mathrm{H\,linear}}{\iff} \exists u_1 - u_2 =: \tilde{u} \neq \mathbf{0} : \mathrm{H}(\tilde{u}) = \mathbf{0} \tag{4.3}$$

$$\iff \forall u_2, \exists u_1 = u_2 + \tilde{u} \neq u_2 : \mathrm{H}(u_1) = \mathrm{H}(u_2) \tag{4.4}$$

This proves that addressing **S1** by shaping y does not uniquely define the corresponding u. In particular, for any u_2 satisfying $\mathrm{H}(u_2) = y^\star$, $u_1 := u_2 + \tilde{u}$ also induces an optimal output $y^\star$. This proves $\{u_1, u_2\} \subset \mathbf{F}$, so that $\mathbf{F}$ does not reduce to a singleton and, in turn, (HH) is relevant. Conversely, if (4.2) does not hold, the nonempty set $\mathbf{F}$ is obviously a singleton.

Clearly, this situation corresponds to the non-injectivity of H. The idea promoted in this manuscript is that this property shall be used as the definition of IR.[10]

> **A1)** The mapping H is said IR if it is non injective, i.e. non left-invertible. This property is necessary and sufficient for (HH) to be relevant, i.e. for $\mathbf{F}$ not to reduce to a singleton.

By linearity, the noninjectivity of H can be characterized by the nontriviality of the kernel of this map, see (4.3).

> **A1)** The mapping H is IR iff Ker $\{\mathrm{H}\} := \{\tilde{u} : \mathrm{H}(\tilde{u}) = \mathbf{0}\}$ is non trivial.

Signal injection perspective

By renaming u_2 as u, one can rewrite (4.4) as follows:

$$\exists u, \exists \tilde{u} \neq \mathbf{0} : \mathrm{H}(u + \tilde{u}) = \mathrm{H}(u) \tag{4.5}$$

From a control perspective, the situation is insightful: The incremental input $\tilde{u}$ can be injected into the input channel without affecting the output, i.e. $\tilde{u}$ is invisible from the output. Thus, $\tilde{u}$ can be added to address the secondary goal **S2**, and let **S1** remain unchanged.

From (4.3), $\tilde{u}$ is to be selected in Ker $\{\mathrm{H}\}$, which is nontrivial. Because Ker $\{\mathrm{H}\}$ inherits the linearity of H, an infinite number of distinct $\tilde{u}$ satisfy $\mathrm{H}(u + \tilde{u}) = \mathrm{H}(u)$. This is a motivation to

[10] Here, and in the remainder of the manuscript, IR stands for "input redundancy" or "input redundant" depending on the context.

introduce the map $\mathrm{H}_\perp$ that is in charge of selecting the appropriate $\tilde{u}$ by way of v, see Fig. 4.3. By definition, $\mathrm{H}_\perp$ is a non-zero map whose range is included in $\mathrm{Ker}\,\{\mathrm{H}\}$, so that

$$\mathrm{H} \circ \mathrm{H}_\perp = \mathbf{0} \tag{4.6}$$

holds. For this reason, $\mathrm{H}_\perp$ is called an annihilator of H. Clearly, IR is a necessary and sufficient condition for the existence of $\mathrm{H}_\perp$.

> **A1)** H is IR iff it admits an annihilator, i.e. a non trivial map $\mathrm{H}_\perp$ satisfying $\mathrm{H} \circ \mathrm{H}_\perp = \mathbf{0}$.
>
> **A3)** The computation of u can be performed via the control structure of Fig. 4.3.

Input space decomposition perspective

Another control structure can be obtained by decomposing the input space $\mathbf{U}$ as follows:

$$\mathbf{U} = \mathrm{Ker}\,\{\mathrm{H}\} \oplus \mathbf{L} \tag{4.7}$$

for an arbitrary $\mathbf{L} \subset \mathbf{U}$. Let us decompose $u = \tilde{u} + u_L$ accordingly so that $\tilde{u} \in \mathrm{Ker}\,\{\mathrm{H}\}$ and $u_L \in \mathbf{L}$ hold. As shown on Fig. 4.4, those two signals can be driven via $i_\perp : \mathrm{Ker}\,\{\mathrm{H}\} \to \mathbf{U}$ and $i_L : \mathbf{L} \to \mathbf{U}$ the natural embeddings.[11] Note that by construction, $i_\perp$ is an annihilator of H (with maximal range), so that $\mathrm{H} \circ i_\perp = \mathbf{0}$ holds.

This leads to the following relationship:

$$\mathrm{H}(u) = \mathrm{H}(i_\perp v + i_L \varphi) \overset{\text{H is linear}}{=} (\mathrm{H} \circ i_\perp)(v) + (\mathrm{H} \circ i_L)(\varphi) = (\mathrm{H} \circ i_L)(\varphi) \tag{4.8}$$

which is illustrated in Fig. 4.5. The comments are as follows:

- $\mathrm{H} \circ i_\perp = \mathbf{0}$ induces that v is invisible on y, and can therefore be used to address **S2**;
- $\mathrm{H} \circ i_L$ is injective so that the problem of shaping y via φ is well-posed in the sense that, if the equation $(\mathrm{H} \circ i_L)(\varphi) = y$ of unknown φ is solvable, then the solution is unique.

This highlights that the rationale behind the decomposition (4.7) is (i) to isolate φ, the minimal part of u that is uniquely determined by the equality $\mathrm{H}(u) = y$, and (ii) to optimize v, the remaining part of u.

> **A3)** The computation of u can be performed via the control structure of Fig. 4.4.

In conclusion, the injectivity of $\mathrm{H} \circ i_L$ proves the existence of a left-inverse $(\mathrm{H} \circ i_L)^+$. This suggests that imposing a desired achievable value y_d on the output amounts to assigning $(\mathrm{H} \circ i_L)^+(y^d)$ to φ. Indeed, $(\mathrm{H} \circ i_L) \circ (\mathrm{H} \circ i_L)^+(y_d) = y_d$ holds for all y_d in the range of H. Letting

$$\varphi^\star := (\mathrm{H} \circ i_L)^+(y^\star),$$

this allows to express $\mathbf{F}$ in closed form:[12]

$$\mathbf{F} \overset{(4.8)}{=} \{i_\perp v + i_L \varphi : (\mathrm{H} \circ i_L)(\varphi) = y^\star \Leftrightarrow \varphi = \varphi^\star\} = i_L \varphi^\star + \mathrm{Im}\,\{i_L\} = i_L \varphi^\star + \mathrm{Ker}\,\{\mathrm{H}\}$$

[11] By definition, $i_\perp$ and i_L are injective maps whose ranges are $\mathrm{Ker}\,\{\mathrm{H}\}$ and $\mathbf{L}$, respectively.

[12] Let us emphasize that, to arrive at this result, neither H is assumed to be right invertible nor is the dimension of the input space $\mathbf{U}$ assumed to be finite.

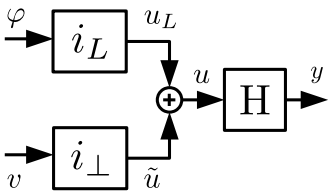

Figure 4.4: Control structure resulting from the decomposition (4.7).

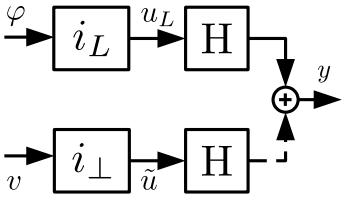

Figure 4.5: From linearity of H, this figure can be deduced from Fig. 4.4. The upper stream $\mathrm{H} \circ i_L$ is left-invertible, whereas the lower one $\mathrm{H} \circ i_\perp$ is zero as shown by the dashed arrow that conveys zero signal.

A2) **F** reads $i_L\varphi^\star + \mathrm{Ker}\,\{\mathrm{H}\}$.

One recovers the fact that **F** does not reduce to a singleton iff H is IR. In this framework, the high-level subproblem of (HH) reduces to set $\varphi = \varphi^\star$, whereas the low-level subproblem reads:

$$\max_v \mathbf{S2} \quad \text{s.t.} \quad u = i_L\varphi^\star + i_\perp v$$

Structure of the manuscript

This manuscript addresses questions **Q1)** to **Q3)** for linear mapping H, by joggling with the three points of view on IR. This goes beyond the discussion above in three ways. First, the input is not always assumed to freely take arbitrary values. Second, H sometimes models the input-output relationship of a dynamical system. In this case, state constraints can apply and the initial condition x_0 plays a crucial role.[13] Third, some power electronics control problems pertaining to this framework are discussed and solved, not only as an illustration of the general case but also as a source of inspiration.

A graphical illustration of the table of contents of the manuscript is now offered using the acronym CAM, which stands for Classical Allocation Methodology.

[13] Discussing the impact of x_0 can be seen as the core of the added value of Chap. 9 wrt to Chap. 8.

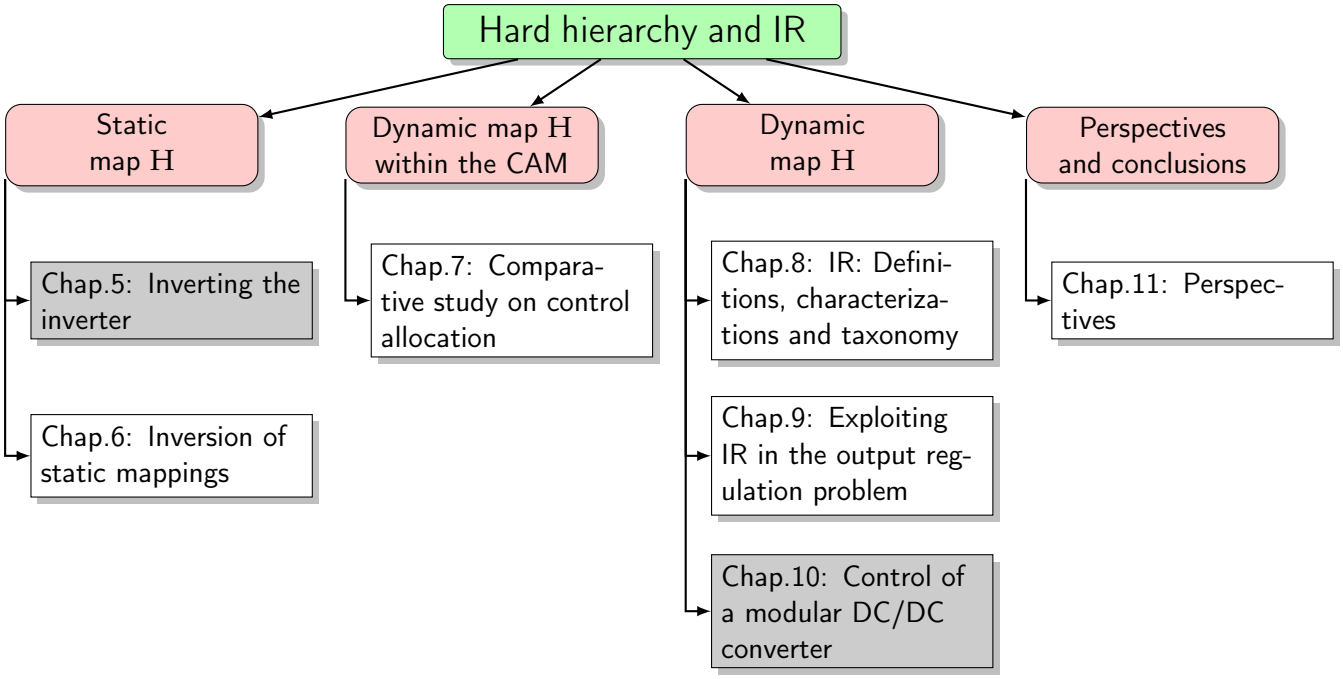

Let us now discuss this figure.

- The two chapters colored in gray are concerned with power electronics problems. The purpose of Chap. 5 is didactical, because it shows how (HH) is treated for a well-known real system. It is intended to be readable by members of the control community as well as those belonging to the power electronics community. Chap. 10 is more control-oriented. It provides a (hopefully nice) particularization of the results of Chap. 8 and Chap. 9. It also goes beyond these chapters on robustness issues.

- When H is a static map, the challenge is to deal with nonlinear input domain $\mathbf{U}$. Both Chap. 5 and Chap. 6 address this problem.

- The CAM is the standard tool to address control problems for over-actuated systems. It can be viewed as a control architecture that embeds real-time inversion of a static map with input constraints to achieve a certain level of closed-loop performance. Chap. 7 offers an extensive discussion on how a stability certificate can be obtained in this framework. Supported by numerous simulation results obtained from a running academic example, the blind spot of dynamic actuators is treated in this chapter as a crucial scientific question related to the CAM. In doing so, the latest stream of the literature devoted to IR systems is introduced [Zac09; Ser12] and compared with the CAM. In contrast, Chap. 8 tackles the dynamic nature of input-output mappings head-on. This chapter somehow implements the above discussion on IR for dynamic systems that are possibly affected by input and/or state constraints. Chap. 9 investigates the applicability of IR to the classical output regulation problem. This shows that trajectory generation should rely on a new definition of IR, coined "bounded persistent weak input redundancy". In doing so, suitable tools to compare the most relevant existing definitions of IR (including the proposed ones) are constructed and utilized. As a by-product, new characterizations of various notions of left invertibility are derived.

Note to the reader

Let us end this introduction with some information for the reader.

- After others, I feel that offering the reader a broad perspective on the considered problem is more informative than artificially inflate my own personal contribution. This manuscript follows these guidelines.
  Notwithstanding, the bibliographical notes ending each chapter is divided with the intention to ease the reviewer and other jury members[14] task in their assessment.[15] Also, citations to the personal bibliography are in bold, like as in the beginning of this introduction.

- Many results are not already published. Any formal statements like theorems, propositions, etc. without any references belong to this category. This comment applies particularly to Chap. 9. For this reason, the technical statements supporting these results are collected in the appendices.

- In this manuscript, essential is standard theory on multi-input multi-output linear time-invariant system. It relies on two types of mathematical tools. The first category uses the so-called system/Rosenbrock matrix, a particular matrix pencil. The second is about decomposing the input and state spaces into suitable linear subspaces using a coordinate-free framework. In this manuscript, we focus on the latter, called geometric control theory, mainly for personal taste, and secondly, owing to its natural extension out of the class of linear dynamics and linear spaces. For reader convenience, the core of the background required for this theory is provided in Appendix A.

[14] Let me thank them once again.

[15] One of the subsections of these bibliographical notes is "Rephrased existing works". This introduction falls entirely into this category.

Chapter 5

Inverting the inverter

Contents

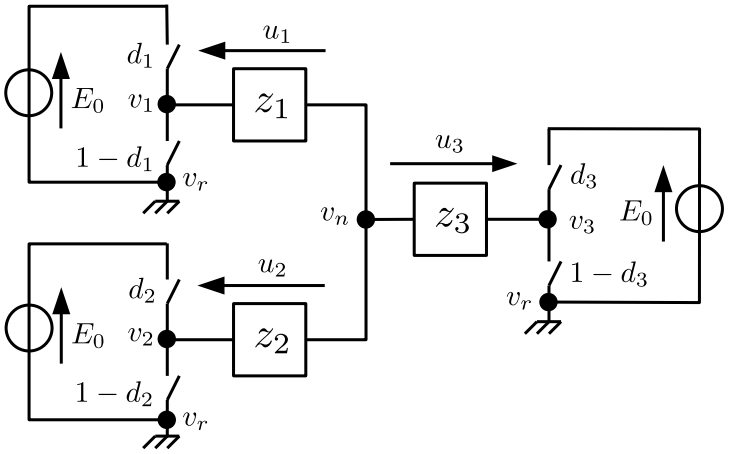

Figure 5.1: Electrical circuit of the three-leg two-level inverter. Potential at the nodes are denoted by $v_{1,2,3}$, v_n and v_r [V].

This first chapter deals with a system originating from power electronics, that is a 3-phases inverter. This system is treated with a mathematical flavor and with the aim of illustrating the philosophy exposed in the introduction and serving as a source of inspiration.

5.1 Problem statement

This first section exposes the control problem associated with the 3-phases inverter.

5.1.1 System description

Consider the three-load inverter depicted in Fig. 5.1. Voltage $v_k - v_r$ on one side of the load z_k is imposed by way of $s_k(t) \in \{0, 1\}$, the binary input of the k-th leg. Thus, voltage $v_k - v_r$ equals $s_k E_0$ where E_0 [V] is the magnitude of the voltage generator. The goal is to control the output voltages $u_{1,2,3}$ [V] at each load via binary-controlled inputs $s_{1,2,3}$. Note that the inverter depicted in Fig. 5.1 implements the so-called "star-connected" topology, which is characterized by the existence of a common interconnection pin for each load.

A synchronous Pulse Width Modulation (PWM) strategy at frequency $1/T$ [Hz] is implemented, so that the actual control signal of each leg is the duty cycle

$$[0, 1] \ni d_k(t) = \frac{1}{T} \int_{t-T}^{t} s_k(s) \mathrm{d}s.$$

The three duty cycles being controlled independently, the input space in which the vector $d(t)$ belongs to is

$$\mathcal{D} := [0, 1]^3. \tag{5.1}$$

The signal to be controlled is the mean value $\bar{u}_k$ of the output voltage u_k at each load.

$$t \mapsto \bar{u}_k(t) := \frac{1}{T} \int_{t-T}^{t} u_k(s) \mathrm{d}s.$$

Under the assumption of balanced loads, it is well-known that d is mapped to $\bar{u}$ via the linear algebraic relationship $\bar{u} = E_0 H d$ with

$$H := \frac{1}{3} \begin{bmatrix} 2 & -1 & -1 \\ -1 & 2 & -1 \\ -1 & -1 & 2 \end{bmatrix}.$$

For the sake of simplicity, let us lighten the notation by redefining u_k as $\bar{u}_k/E_0$, that is, normalized adimensional output voltage is considered and mean value is implicit. Henceforth, the following relationship:

$$u = Hd \tag{5.2}$$

will be used in place of $\bar{u} = E_0 Hd$.

5.1.2 Problem setting

The engineering problem to be solved is as follows.

Problem 5.1. Given a desired *feasible output voltage* u^d, i.e.

$$u^d \in \mathcal{U} := \{u : \exists d \in \mathcal{D}, u = Hd\} \subset \mathbb{R}^3, \tag{5.3}$$

compute a corresponding duty cycle vector $d \in \mathcal{D}$ satisfying $u^d = Hd$. If such a vector d is non-unique, select the optimal one according to some criterion to be defined.

As a starting point, observe that (5.2) might suggest that the considered problem apparently boils down to "invert" the matrix H, that is: To define a mapping $u^d \mapsto d$ leading to $u^d = u$, as shown by Fig. 5.2. This task is not as trivial as inverting the matrix H, though, for two reasons that are now exposed.

1) Matrix H is singular

Therefore, even if the existence of solutions is assumed via the feasibility of u^d, the problem remains ill-posed owing to the lack of unicity in general, that is, there exist distinct vectors d inducing identical u. This issue can be handled via the following optimization problem:

$$\min_{d \in \mathbb{R}^3} J(d) \quad \text{s.t.} \quad u^d = Hd,$$

so that the optimal vector d^* is selected among the ones leading to u^d, that is, the feasibility set is the image of u^d by the inverse map H^{-1} of H:

$$H^{-1}(u^d) = \{d \in \mathbb{R}^3 : u^d = Hd\}. \tag{5.4}$$

This allows us to rewrite the optimization problem as follows:

$$\min_{d \in H^{-1}(u^d)} J(d). \tag{5.5}$$

In the sequel, we will sometimes refer to the *unconstrained problem* defined as Prob. 5.1 with $\mathcal{D} = \mathbb{R}^3$, i.e. duty cycles d_k can be arbitrarily selected, even outside $[0, 1]$. Reference to this artificial problem aims to highlight features specifically related to this first difficulty of non-unicity.

2) The input space $\mathcal{D}$ is a proper subset of $\mathbb{R}^3$

As a result, the mapping $u^d \mapsto d$ to be defined must be tailored in such a way that d always belongs to $\mathcal{D}$, whatever is u^d, i.e. the actual optimisation problem is the following:

$$\min_{d \in \mathcal{D}} J(d) \quad \text{s.t.} \quad u^d = Hd.$$

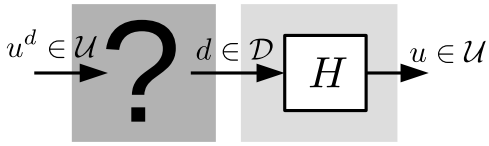

Figure 5.2: Graphical illustration of the control problem associated with the inverter.

Imposing this constraint can be implemented by ruling the duty cycle vector d which is outside $\mathcal{D}$, out of $H^{-1}(u^d)$. Saying it differently, actual feasibility set shall be constructed by intersecting $H^{-1}(u^d)$ with $\mathcal{D}$, so that previous optimisation problem reads

$$\min_{d \in \mathcal{S}} J(d), \tag{5.6}$$

with

$$\mathcal{S} := H^{-1}(u^d) \cap \mathcal{D}. \tag{5.7}$$

In view of these two reasons, the aim of this section is to provide an expression of $\mathcal{S}$ in closed form, adopting an inversion perspective and making intensive use of block diagrams as a graphical tool.

5.2 Problem solution of the unconstrained problem

5.2.1 Change of input coordinates

To better grasp the geometry of the problem, let us change the input basis by performing the following change of variables:

$$d_{\alpha\beta 0} := \begin{bmatrix} d_\alpha \\ d_\beta \\ d_0 \end{bmatrix} := P^{-1} d \tag{5.8}$$

where orthogonal matrix $P^{-1} = P^\intercal$ reads

$$\mathbb{R}^{3\times 3} \ni P^{-1} := \sqrt{\frac{2}{3}} \left[\begin{array}{ccc} 1 & -1/2 & -1/2 \\ 0 & \sqrt{3}/2 & -\sqrt{3}/2 \\ \hline 1/\sqrt{2} & 1/\sqrt{2} & 1/\sqrt{2} \end{array}\right] =: \left[\begin{array}{c} P_{\alpha\beta}^\intercal \\ \hline P_0^\intercal \end{array}\right] \tag{5.9}$$

so that d can be computed from $d_{\alpha\beta 0}$ via the following equality, which is just another way to write (5.8) down:

$$d = P d_{\alpha\beta 0} = P_{\alpha\beta} d_{\alpha\beta} + P_0 d_0. \tag{5.10}$$

Defining

$$H_{\alpha\beta 0} := HP = \begin{bmatrix} H_{\alpha\beta} & H_0 \end{bmatrix}, \quad H_{\alpha\beta} := HP_{\alpha\beta} = \begin{bmatrix} \sqrt{2/3} & 0 \\ -1/\sqrt{6} & 1/\sqrt{2} \\ -1/\sqrt{6} & -1/\sqrt{2} \end{bmatrix}, \quad H_0 := HP_0 = \begin{bmatrix} 0 \\ 0 \\ 0 \end{bmatrix} \tag{5.11}$$

this change of basis (called "Concordia transformation") allows to rewrite (5.2) as follows:

$$u = HP\, P^{-1} d = H_{\alpha\beta 0} d_{\alpha\beta 0} = H_{\alpha\beta} d_{\alpha\beta} + H_0 d_0 = H_{\alpha\beta} d_{\alpha\beta} \tag{5.12}$$

The decomposition can be graphically summed up in Fig. 5.3.

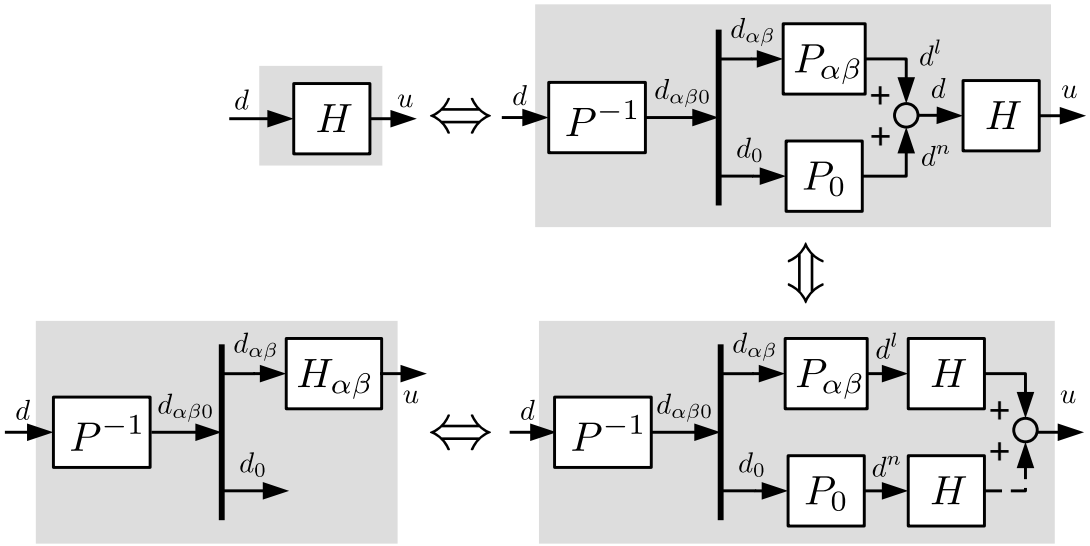

Figure 5.3: Decomposition of the inverter model (dashed arrow conveys null signal due to equality $HP_0 = \mathbf{0}$).

5.2.2 Input space decomposition

The quantity $d_0 = P_0^\intercal d$ is called the "homopolar duty cycle", since it is proportional to $\sum_k d_k$, see the expression of P_0. It is well-known that this quantity has no impact on output voltage u.[1]

Observe that the columns of the submatrix $H_{\alpha\beta} \in \mathbb{R}^{3\times 2}$ are linearly independent, so that $H_{\alpha\beta}$ is left-invertible, i.e. there exists a matrix $H_{\alpha\beta}^+$ which is the left-inverse of $H_{\alpha\beta}$ in the sense that $H_{\alpha\beta}^+ H_{\alpha\beta} = \mathbf{I}_2$. This means that (5.12) implies

$$d_{\alpha\beta} = H_{\alpha\beta}^+ u \tag{5.13}$$

A possible expression for $H_{\alpha\beta}^+$ reads:

$$\mathbb{R}^{2\times 3} \ni H_{\alpha\beta}^+ := (H_{\alpha\beta}^\intercal H_{\alpha\beta})^{-1} H_{\alpha\beta}^\intercal = \sqrt{\frac{2}{3}} \begin{bmatrix} 1 & -1/2 & -1/2 \\ 0 & \sqrt{3}/2 & -\sqrt{3}/2 \end{bmatrix} = P_{\alpha\beta}^\intercal.$$

From (5.13), the crucial comment regarding (5.12) is that u uniquely defines $d_{\alpha\beta}$.

Remark 5.2 (The input decomposition perspective). The two previous paragraphs already give a concret application of the discussion proposed in the introduction: By decomposing the unconstrained input space $\mathbb{R}^3$ into $\mathcal{N} \oplus \mathcal{L}$ with $\mathcal{L} := \operatorname{Im}\{P_{\alpha\beta}\}$ and $\mathcal{N} = \operatorname{Im}\{P_0\}$, one solves the unconstrained problem. Indeed, d can always be uniquely decomposed as $d^n + d^l$ with $d^n = P_0 d_0 \in \mathcal{N}$ and $d^l = P_{\alpha\beta} d_{\alpha\beta} \in \mathcal{L}$, see Fig. 5.3. This construction ensures that input d^n leads to zero output, and that input d^l, and in turn $d_{\alpha\beta}$, satisfying $Hd^l = u^d$ is unique. •

[1] Indeed, d_0 impacts both $v - \mathbf{1}_3 v_r = d = P_{\alpha\beta} d_{\alpha\beta} + P_0 d_0$ and $(v_n - v_r)\mathbf{1}_3 = P_0 d_0$ in such a way that

$$u = v - v_n \mathbf{1}_3 = (v - \mathbf{1}_3 v_r) - (v_n - v_r)\mathbf{1}_3 = P_{\alpha\beta} d_{\alpha\beta}$$

remains unaffected by d_0: Voltages $v_k - v_r$ and $v_n - v_r$ are "translated" by $d_0/\sqrt{3}$ but $u = (v_k - v_r) - (v_n - v_r)$ does not change. This physical observation is mathematically recovered by the fact that $H_0 = \mathbf{0}$, so that d_0 does not contribute at all to u, see (5.12). Saying it differently, d_0 is the coordinate of d in $\mathcal{N} := \operatorname{Ker}\{H\}$.

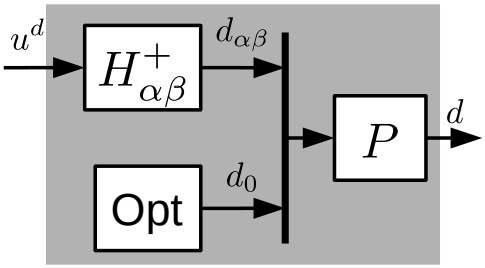

Figure 5.4: Schematic of the solution of the *unconstrained* inverter control problem.

5.2.3 Solution of the unconstrained problem

This discussion already leads to the solution of the unconstrained version of Prob. 5.1, i.e. the simplified problem for which d can be arbitrarily selected in $\mathbb{R}^3$. Bearing in mind that recovering the appropriate d from u^d reduces to "invert" the mapping H, any solution d can be constructed by "walking backward" along the path from d to u on Fig. 5.3. Consider the last subplot of Fig. 5.3 located at the bottom left-hand corner. From (5.13), taking the path at the top of this subplot gives the first two entries of $d_{\alpha\beta 0}$ by way of $H^+_{\alpha\beta}$. The last component d_0 can be arbitrarily selected because the path at the bottom does not contribute to the output voltage. The construction of the following set formalizes these observations:

$$H^{-1}_{\alpha\beta 0}(u^d) \coloneqq \{d_{\alpha\beta 0} \in \mathbb{R}^3 : H_{\alpha\beta 0} d_{\alpha\beta 0} = u^d\} = \left\{ \begin{bmatrix} d_{\alpha\beta} \\ d_0 \end{bmatrix} : d_{\alpha\beta} = H^+_{\alpha\beta} u^d, d_0 \in \mathbb{R} \right\} = \{H^+_{\alpha\beta} u^d\} \times \mathbb{R} \tag{5.14}$$

Note that d can eventually be computed from $d_{\alpha\beta 0}$ using (5.10).

Fig. 5.4 presents a graphical illustration of this inverse mapping. Bearing in mind that $H^+_{\alpha\beta} H_{\alpha\beta} = \mathbf{I}_2$ holds, the key observation is that when connecting the controller in Fig. 5.4 to H as decomposed in Fig. 5.3, one gets $u = u^d$ *regardless* of the value of d_0 which can thus be computed via an optimizer, depicted by the block called "Opt". Comparing Fig. 5.4 and Fig. 5.3, one can say that the controller $u^d \mapsto d$ was built via *mirror construction of the decomposition of the system*.

5.3 Dealing with constraints

5.3.1 Propagation of the input set $\mathcal{D}$ through the inverter

So far, the discussion implicitly relies on the assumption that input d is allowed to take any value in $\mathbb{R}^3$. In fact, the components of d are duty cycles, which are enforced to belong to $[0, 1]$, so that $d \in \mathcal{D} = [0, 1]^3$ must be ensured. Imposing this constraint on the previous development can be implemented by ruling out the duty cycle vector $d_{\alpha\beta 0}$ which does not belong to $\mathcal{D}_{\alpha\beta 0}$. Here, $\mathcal{D}_{\alpha\beta 0}$ refers to $\mathcal{D}$ in the new coordinates, i.e.

$$\mathcal{D}_{\alpha\beta 0} \coloneqq \{d_{\alpha\beta 0} : P d_{\alpha\beta 0} = d \in \mathcal{D}\}.$$

so that $d_{\alpha\beta 0} \in \mathcal{D}_{\alpha\beta 0}$ is equivalent to $d \in \mathcal{D}$. Therefore, the admissible set for $d_{\alpha\beta 0}$ is the following:

$$\mathcal{S}_{\alpha\beta 0} \coloneqq H^{-1}_{\alpha\beta 0}(u^d) \cap \mathcal{D}_{\alpha\beta 0} \tag{5.15}$$

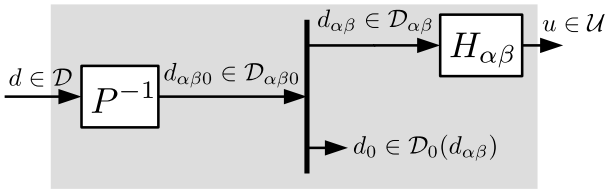

Figure 5.5: Propagation of the input set through the decomposition of the inverter model.

To give this set a formulation in closed-form, one can first compute $\mathcal{D}_{\alpha\beta 0}$ and then intersect it with $H_{\alpha\beta 0}^{-1}(u^d)$ already computed. Here, we follow a different path by pursuing the idea that inversion can be performed by reversing the decomposition of the system.

Specifically, we investigate how $\mathcal{D}$ impacts the problem solution by propagating this set through the inverter model depicted in Fig. 5.3, from the left-hand side to the right-hand side. The resulting image is shown in Fig. 5.5. The first step is the forward transportation of $\mathcal{D}$ through P^{-1}, that is, the computation of $P^{-1}\mathcal{D}$. The next development shows that this set is nothing but $\mathcal{D}_{\alpha\beta 0}$:

$$P^{-1}\mathcal{D} = \{P^{-1}d : d \in \mathcal{D}\} = \{P^{-1}Pd_{\alpha\beta 0} : Pd_{\alpha\beta 0} \in \mathcal{D}\} = \{d_{\alpha\beta 0} : Pd_{\alpha\beta 0} \in \mathcal{D}\} = \mathcal{D}_{\alpha\beta 0}$$

The next step is to transport the set $\mathcal{D}_{\alpha\beta 0}$ through the mapping extracting both $d_{\alpha\beta}$ and d_0 from $d_{\alpha\beta 0}$. Two solutions exist depending on which component has priority:

(i) If priority is given to $d_{\alpha\beta}$, then one defines

$$\mathcal{D}_{\alpha\beta} \coloneqq \{d_{\alpha\beta} : \exists d_0, d_{\alpha\beta 0} \in \mathcal{D}_{\alpha\beta 0}\} \tag{5.16}$$

so that the "slave" variable d_0 belongs to

$$\mathcal{D}_0(d_{\alpha\beta}) \coloneqq \{d_0 : d_{\alpha\beta 0} \in \mathcal{D}_{\alpha\beta 0}\}; \tag{5.17}$$

(ii) If priority is given to d_0, then one defines $\mathcal{D}_0 \coloneqq \{d_0 : \exists d_{\alpha\beta}, d_{\alpha\beta 0} \in \mathcal{D}_{\alpha\beta 0}\}$ and the "slave" variable becomes $d_{\alpha\beta}$ that belongs to $\mathcal{D}_{\alpha\beta}(d_0) = \{d_{\alpha\beta} : d_{\alpha\beta 0} \in \mathcal{D}_{\alpha\beta 0}\}$.[2]

As illustrated on Fig. 5.5, solution (i) is retained because d_0 has no impact on the output voltage u, so this component is naturally chosen as the "slave" variable.

5.3.2 Handeling the input set $\mathcal{D}$ in the inversion procedure

Once again, the problem solution can be constructed by "walking backward" on the path from d to u in Fig. 5.5. Recall that u^d uniquely defines $d_{\alpha\beta}$ using (5.13), as in the unconstrained case. This implies that taking the path at the top of Fig. 5.5 from u^d to $d_{\alpha\beta}$, the constraint $d_{\alpha\beta} \in \mathcal{D}_{\alpha\beta}$ is satisfied under the assumption of the feasibility of u^d. From $d_{\alpha\beta}$, the last component d_0 is then computed to ensure that $d_0 \in \mathcal{D}_0(d_{\alpha\beta})$ holds.

These observations are formalized in two directions. First, by providing an expression for $\mathcal{S}_{\alpha\beta 0}$ corresponding to $\mathcal{S}$ in the new coordinates:

$$\mathcal{S}_{\alpha\beta 0}(u^d) = \left\{ \begin{bmatrix} d_{\alpha\beta} \\ d_0 \end{bmatrix} : d_{\alpha\beta} = H_{\alpha\beta}^{+} u^d, d_0 \in \mathcal{D}_0(d_{\alpha\beta}) \right\} = \{H_{\alpha\beta}^{+} u^d\} \times \mathcal{D}_0(H_{\alpha\beta}^{+} u^d) \tag{5.18}$$

[2]Let us emphasize that $\mathcal{D}_0(d_{\alpha\beta})$ and $\mathcal{D}_0$ are distincts, just like $\mathcal{D}_{\alpha\beta}(d_0)$ differs from $\mathcal{D}_{\alpha\beta}$.

When compared with (5.14), this expression clearly shows that the set membership constraint $d \in \mathcal{D}$ modifies the set of solutions by reducing the set in which d_0 can be selected. Second, via Fig. 5.6 which builds on Fig. 5.4 and proposes a graphical representation of the problem solution. Once again, connecting the controller in Fig. 5.6 to H as decomposed in Fig. 5.5, one obtains $u = u^d$ *regardless* of the value of d_0, provided that

(i) $d_{\alpha\beta} \in \mathcal{D}_{\alpha\beta}$ holds, which is equivalent to saying that u is feasible;

(ii) d_0 is selected in $\mathcal{D}_0(d_{\alpha\beta})$, so that $d_{\alpha\beta 0} \in \mathcal{D}_{\alpha\beta 0}$ and, in turn, $d \in \mathcal{D}$ are ultimately ensured. The saturation block in Fig. 5.6 delivering d_0 aims to formalize that $d_0 \in \mathcal{D}_0(d_{\alpha\beta})$ holds.

For this reason, d_0 is computed via an optimizer. Again, comparing Fig. 5.6 and Fig. 5.5, the controller $u^d \mapsto d$ arises from the mirror construction of the decomposition of the inverter.

5.3.3 Computing $\mathcal{D}_0(d_{\alpha\beta})$

The last task is to formulate $\mathcal{D}_0(d_{\alpha\beta})$ in closed-form. To do so, let us adopt a component-wise notation for inequalities, which is illustrated via the following reformulation of $\mathcal{D}$:

$$\mathcal{D} = \left\{ \begin{bmatrix} d_a \\ d_b \\ d_c \end{bmatrix} : 0 \leq d_k \leq 1, (k \in \{a, b, c\}) \right\} = \{d : \mathbf{0}_3 \leq d \leq \mathbf{1}_3\} \tag{5.19}$$

so that $\mathcal{D}_{\alpha\beta 0}$ can be first manipulated in the following way:

$$\begin{aligned} d_{\alpha\beta 0} \in \mathcal{D}_{\alpha\beta 0} &\overset{(5.10)}{\iff} \mathbf{0}_3 \leq P_{\alpha\beta} d_{\alpha\beta} + P_0 d_0 \leq \mathbf{1}_3 \overset{(5.9)}{\iff} -\sqrt{3} P_{\alpha\beta} d_{\alpha\beta} \leq \mathbf{1}_3 d_0 \leq \sqrt{3}(\mathbf{1}_3 - P_{\alpha\beta} d_{\alpha\beta}) \\ &\iff \underline{d}_0(d_{\alpha\beta}) := -\sqrt{3} \min\{P_{\alpha\beta} d_{\alpha\beta}\} \leq d_0 \leq \sqrt{3}(1 - \max\{P_{\alpha\beta} d_{\alpha\beta}\}) =: \bar{d}_0(d_{\alpha\beta}) \end{aligned} \tag{5.20}$$

where $\min\{\cdot\}$ and $\max\{\cdot\}$ extract the minimum and maximum of the components of their argument vectors, respectively. Clearly, the last equivalence allows us to conclude on the expression of $\mathcal{D}_0(d_{\alpha\beta})$:

$$\mathcal{D}_0(d_{\alpha\beta}) = [\underline{d}_0(d_{\alpha\beta}), \bar{d}_0(d_{\alpha\beta})] \tag{5.21}$$

Remark 5.3 (Two expressions of $\mathcal{D}_{\alpha\beta 0}$). The following alternative expression for $\mathcal{D}_{\alpha\beta 0}$ can be derived from (5.20):

$$\mathcal{D}_{\alpha\beta 0} = \left\{ \begin{bmatrix} d_{\alpha\beta} \\ d_0 \end{bmatrix} : d_0 \in \mathcal{D}_0(d_{\alpha\beta}) \right\} \tag{5.22}$$

When combined with (5.14) and $\mathcal{S}_{\alpha\beta 0} = H_{\alpha\beta 0}^{-1}(u^d) \cap \mathcal{D}_{\alpha\beta 0}$, this allows to recover (5.18). •

5.4 The feasible set of output voltages

Let us now investigate the problem of existence of solution, i.e. let us construct the feasibility set $\mathcal{U}$ to which u^d has to belong to for a solution d to exist.

To this end, consider the following change of variables on the output u:[3]

$$u_{\alpha\beta 0} = Q^{-1} u \quad \text{with} \quad Q = P \tag{5.23}$$

[3] P and Q are matrices of the change of variables in the input and output spaces, respectively. If they fortuitously coincide for the inverter, they are distinct in general. In the same vein, if R is invertible in general, see (5.26), it is distinct from the identity. This motivates the use of R instead of $\mathbf{I}_2$ and of different notations for (i) P and Q and (ii) $\mathcal{D}_{\alpha\beta}$ and $\mathcal{U}_{\alpha\beta}$.

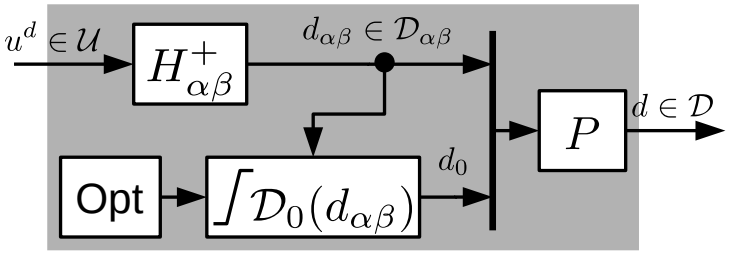

Figure 5.6: Schematic of the solution of the inverter control problem.

This equation leads to:

$$u_{\alpha\beta 0} = \hat{H}_{\alpha\beta 0} d_{\alpha\beta 0}, \tag{5.24}$$

with

$$\hat{H}_{\alpha\beta 0} := Q^{-1} H P = \left[\begin{array}{cc|c} & R & 0 \\ & & 0 \\ \hline 0 & 0 & 0 \end{array}\right] \quad \text{with} \quad R = \mathbf{I}_2. \tag{5.25}$$

Hence, (5.24) reads

$$\left\{\begin{array}{rcl} u_{\alpha\beta} & = & R d_{\alpha\beta} = d_{\alpha\beta}, \\ u_0 & = & 0. \end{array}\right. \tag{5.26}$$

As a result, $u_{\alpha\beta 0}$ is feasible iff (i) $u_0 = 0$ and (ii) $u_{\alpha\beta} \in \mathcal{U}_{\alpha\beta}$ with

$$\mathcal{U}_{\alpha\beta} := R\mathcal{D}_{\alpha\beta} = \mathcal{D}_{\alpha\beta} \tag{5.27}$$

In view of (5.16), item (ii) is equivalent to saying that there exists d_0 such that $d_{\alpha\beta 0} \in \mathcal{D}_{\alpha\beta 0}$ with $d_{\alpha\beta} = u_{\alpha\beta}$. Observe that d_0 does not appear in those equations because of the equality $HP_0 = \mathbf{0}$ already mentioned. This discussion can be summarized by the following derivation of the feasibility set $\mathcal{U}_{\alpha\beta 0}$ in $\alpha\beta 0$ coordinates:

$$\mathcal{U}_{\alpha\beta 0} := \{u_{\alpha\beta 0} : \exists d_{\alpha\beta 0} \in \mathcal{D}_{\alpha\beta 0}, u_{\alpha\beta 0} = \hat{H}_{\alpha\beta 0} d_{\alpha\beta 0}\} = \left\{ \begin{bmatrix} u_{\alpha\beta} \\ u_0 \end{bmatrix} : u_{\alpha\beta} \in \mathcal{U}_{\alpha\beta}, u_0 = 0 \right\} = \mathcal{U}_{\alpha\beta} \times \{0\} \tag{5.28}$$

From (5.20), the set $\mathcal{U}_{\alpha\beta} = \mathcal{D}_{\alpha\beta}$ can be rewritten in closed-form as follows:

$$\mathcal{D}_{\alpha\beta} = \{d_{\alpha\beta} : \mathcal{D}_0(d_{\alpha\beta}) \neq \{\varnothing\}\} = \{d_{\alpha\beta} : \underline{d}_0(d_{\alpha\beta}) \leq \bar{d}_0(d_{\alpha\beta})\} \tag{5.29}$$

A graphical summary of this discussion is shown in Fig. 5.7, which enriches both Fig. 5.5 and Fig. 5.6.

Remark 5.4 (Key role plays by (5.20)). Let us emphasize that (5.20) gives an expression in closed-form not only of $\mathcal{D}_0(d_{\alpha\beta})$ but also of $\mathcal{D}_{\alpha\beta}$, that is, the two sets arising when splitting $\mathcal{D}_{\alpha\beta 0}$ and giving priority to $d_{\alpha\beta}$ over d_0. •

Remark 5.5 (From $\mathcal{U}_{\alpha\beta 0}$ to $\mathcal{U}$). The feasible set in the original coordinates can be simply derived using the following expression:

$$\mathcal{U} := \{Q u_{\alpha\beta 0} : u_{\alpha\beta 0} \in \mathcal{U}_{\alpha\beta 0}\} = Q\mathcal{U}_{\alpha\beta 0} \tag{5.30}$$

•

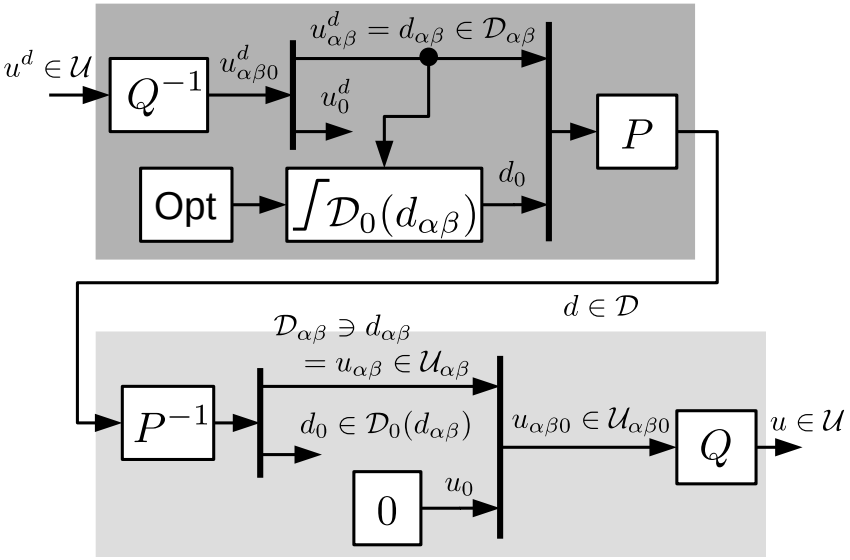

Figure 5.7: Schematic of the ultimate solution of the inverter control problem where the feasible set explicitly appears. If u^d belongs to $\mathcal{U}$ or, equivalently, if $u^d_0 = 0$ and $u^d_{\alpha\beta} \in \mathcal{U}_{\alpha\beta}$ hold, then u equals the desired output voltage u^d.

Remark 5.6 (Homopolar output voltage). The voltage u_0 is called the "homopolar output voltage", since it is proportional to $\sum_{k\in\{a,b,c\}} u_k$, see the expression of P_0. For a star-connected topology, the assumption of balanced loads implies that $u_0 = 0$ holds. This explains why u_0 can only be null regardless of the input vector. This physical observation is mathematically recovered because $u_0 = 0$ characterizes $\mathrm{Im}\,\{H\}$. •

5.5 Simulation results

As an illustration of the proposed algorithm, let us consider the following desired output voltage trajectory parameterized by $\theta \in [0, 4\pi]$:

$$u^d(\theta) = k(\theta) \begin{bmatrix} \cos(\theta) \\ \cos(\theta - 2\pi/3) \\ \cos(\theta + 2\pi/3) \end{bmatrix} \quad \text{with} \quad k(\theta) = \bar{k} \times \begin{cases} \theta/(2\pi), & (\theta \in [0, 2\pi[), \\ 1, & (\theta \in [2\pi, 4\pi]), \end{cases} \tag{5.31}$$

and where $\bar{k} \in \mathbb{R}$. Expressed in the new coordinates, $u^d(\theta)$ reads:

$$u^d_{\alpha\beta 0}(\theta) = Q^{-1} u(\theta) = k(\theta) \sqrt{\frac{3}{2}} \begin{bmatrix} \cos(\theta) \\ \sin(\theta) \\ 0 \end{bmatrix}.$$

Let $\bar{k} = 1/\sqrt{3}$. A graphical representation of $u(\cdot)$ is shown in Fig. 5.8 as a function of θ in both coordinates. Fig. 5.9 and Fig. 5.10 depict $u(\cdot)$ in the output spaces in both coordinates. It can be seen that $u^d(\theta)$ is feasible for all θ since $u^d_0(\theta) = 0$ and $u^d_{\alpha\beta}(\theta) = \mathcal{U}_{\alpha\beta}$ hold for all θ (see (5.28)).

In the new coordinates, the inversion reduces to the simple relationship $d_{\alpha\beta} = u^d_{\alpha\beta}$ (see (5.26)). Since $u^d(\theta)$ is feasible, $d_{\alpha\beta}(\theta)$ always belongs to $\mathcal{D}_{\alpha\beta}$ so that $\mathcal{D}_0(d_{\alpha\beta}(\theta))$ is never empty. This last set is depicted in Fig. 5.11 together with $d_{\alpha\beta}(\theta)$. Observe that the closer $u^d(\theta)$ is to the boundaries of the feasible set $\mathcal{U}_{\alpha\beta 0}$, the smaller is $\mathcal{D}_0(d_{\alpha\beta}(\theta))$, that is, the degree of freedom

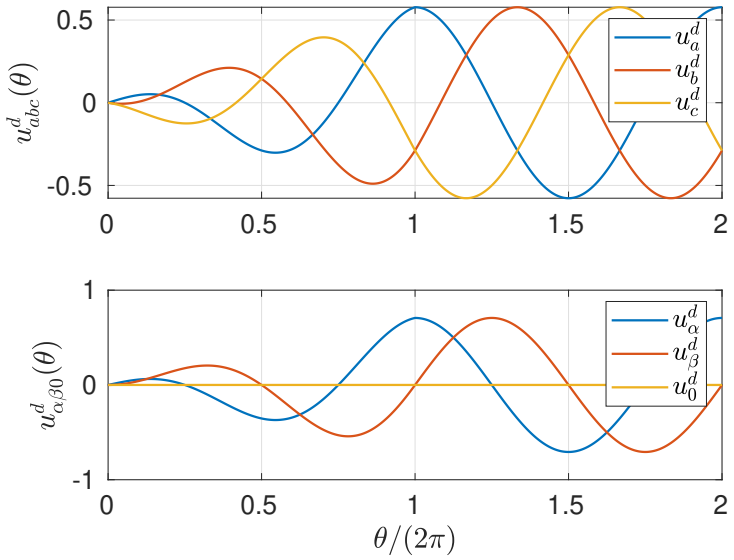

Figure 5.8: u^d defined by (5.31) as a function of θ in both coordinates.

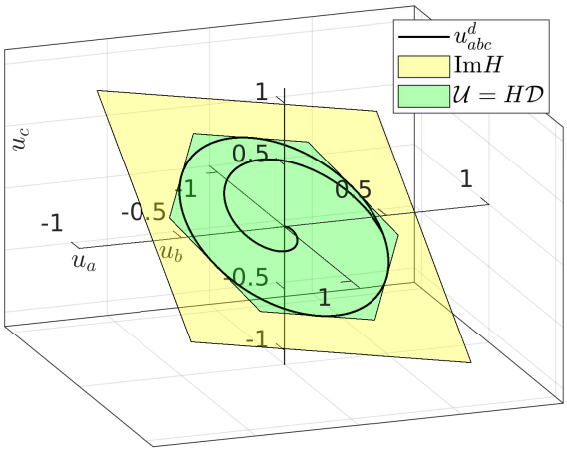

Figure 5.9: Output space in the original coordinates. The feasible unconstrained set $\mathrm{Im}\{H\}$ includes the actual feasible constrained set $\mathcal{U}$.

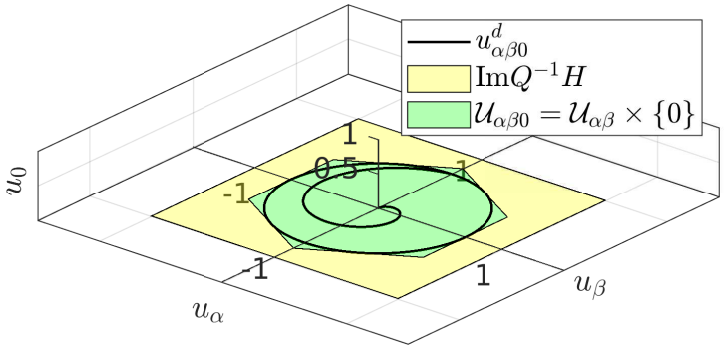

Figure 5.10: Output space in the new coordinates, so that u_0 can now simply be read on the third axis. The feasible unconstrained set is the plan containing the first two axes. It includes the actual feasible constrained set $\mathcal{U}_{\alpha\beta 0}$.

in the selection of $d_0 \in \mathcal{D}_0(d_{\alpha\beta}(\theta))$ vanishes each time this set collapses to a single set-point, as for $\theta \in 2\pi(1 + \{1/9, 3/9, 5/9, \ldots\})$. This observation can be recovered by examining the input set depicted in Fig. 5.12 in the new coordinates. The cube is the input set $\mathcal{D}_{\alpha\beta 0}$. The construction of the input trajectory can be interpreted as the selection of the appropriate value of d_0 (on the third axis) for $d_{\alpha\beta 0}$ to belong to the cube and bearing in mind that the first two coordinates of this vector, that is, $d_{\alpha\beta} = u^d_{\alpha\beta}$, are imposed by the desired output voltage. The set in which d_0 can be selected is depicted by the vertical green surface. Once again, observe that this surface shrinks as the output voltage pushes it close to the external corners of the cube, that is, the corners that are not above the origin. Fig. 5.12 is analogous to Fig. 5.13 in the original coordinates, where d_0 is read on the first diagonal span $\{\mathbf{1}_3\}$. To better relate the figures, note that the particular value

$$\theta_p := \pi/2$$

is identified via the dashed black segments of Fig. 5.11, Fig. 5.12 and Fig. 5.13.

Input $d(\theta)$ can be further represented by Fig. 5.14: To arrive at this picture, different values of d_0 has been selected via $\iota \in [0, 1]$ and according to the following relationship

$$d_0(d_{\alpha\beta}, \iota) = \underline{d}_0(d_{\alpha\beta}) + \iota(\bar{d}_0(d_{\alpha\beta}) - \underline{d}_0(d_{\alpha\beta})).$$

Then, the corresponding d is computed and depicted. Observe that all the curves meet for the value of θ where $\mathcal{D}_0(d_{\alpha\beta}(\theta))$ contains a single point.

Remark 5.7 (Intersective and vector PWM). A typical problem is to compute the largest value of $\bar{k}$ for which the reference $u^d(\theta)$ defined in (5.31) is feasible for all $\theta \in [2\pi, 4\pi]$ and, in turn, for all $\theta \in [0, 4\pi]$. Since $u^d_0(\theta)$ is identically zero, feasibility is achieved iff $u^d_{\alpha\beta}(\theta) \in \mathcal{D}_{\alpha\beta}$ holds for all $\theta \in [2\pi, 4\pi]$, see (5.28). From (5.29), this is equivalent to

$$-\min\{P_{\alpha\beta} d_{\alpha\beta}(\theta)\} \leq (1 - \max\{P_{\alpha\beta} d_{\alpha\beta}(\theta)\}) \quad \text{with} \quad d_{\alpha\beta}(\theta) = u^d_{\alpha\beta}(\theta) = \bar{k}\sqrt{\frac{3}{2}} \begin{bmatrix} \cos\theta \\ \sin\theta \end{bmatrix}$$

for all $\theta \in [2\pi, 4\pi]$. It can be verified that $\bar{k} = 1/\sqrt{3}$ is the answer to the problem because $\underline{d}_0 = \bar{d}_0$ for e.g. $\theta = 2\pi/9 + 2\pi$. The fact that this situation is a limit case is confirmed by the fact that $d(\theta)$ touches the faces of the cube $\mathcal{D}$ for some θ in Fig. 5.13. First subfigure of Fig. 5.15 (corresponding to the second part of the time simulation of Fig. 5.11) illustrates this fact.

Recall that $u^d_{\alpha\beta} \in \mathcal{D}_{\alpha\beta} \Leftrightarrow \mathcal{D}_0(d_{\alpha\beta}) \neq \{\varnothing\}$, see (5.29). Hence, the previous problem is concerned with the case where $\mathcal{D}_0(d_{\alpha\beta}(\theta))$ is never empty. Another problem is to find the

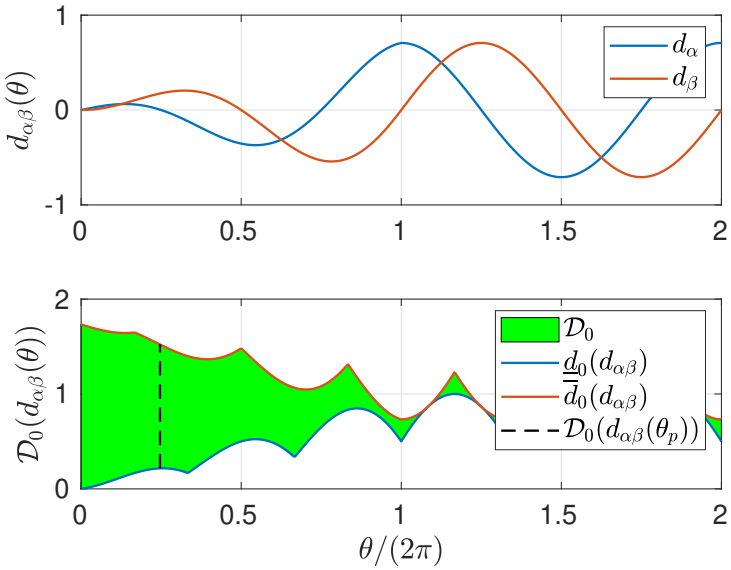

Figure 5.11: Input trajectory leading to the desired output voltages. The selection of d_0 in $\mathcal{D}_0(d_{\alpha\beta})$ is the degree of freedom of this inversion.

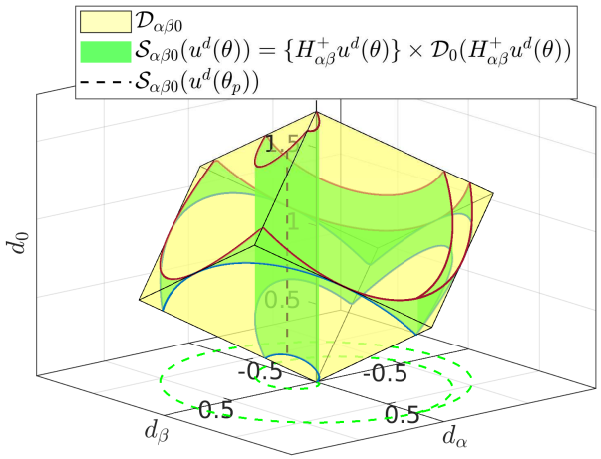

Figure 5.12: Input space in the new coordinates.

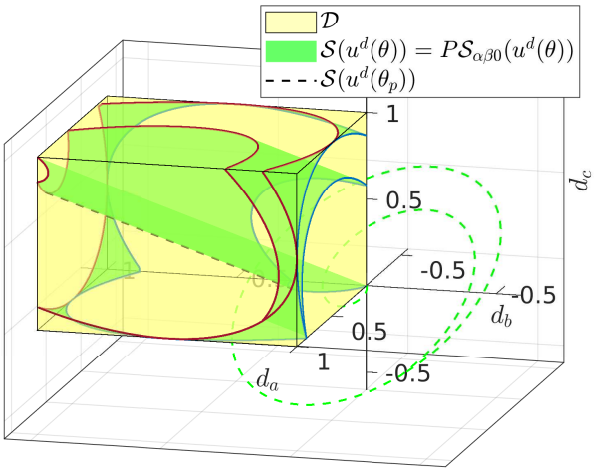

Figure 5.13: Input space in the original coordinates.

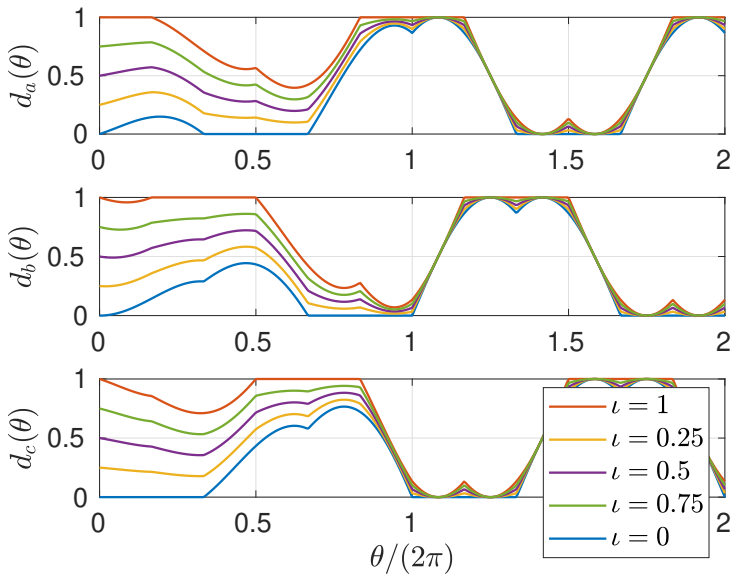

Figure 5.14: Different input trajectories arising from different selection of d_0 in $\mathcal{D}_0(d_{\alpha\beta})$.

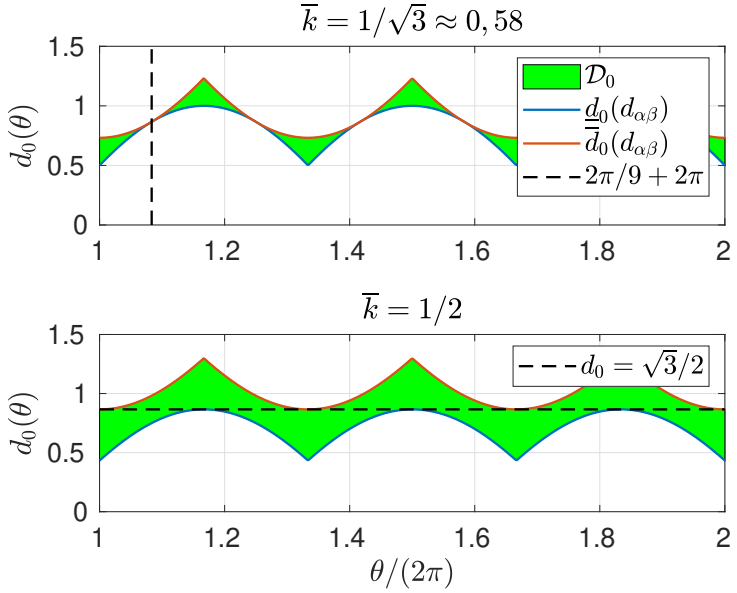

Figure 5.15: Maximize the size of $\overline{k}$ (upper subplot) under the constraint of constant d_0 (lower subplot).

largest value of $\overline{k}$ such that there exists a *constant* $\breve{d}_0 \in \mathbb{R}$, that is, independent of θ, satisfying $\breve{d}_0 \in \mathcal{D}_0(d_{\alpha\beta}(\theta))$ for all $\theta \in [2\pi, 4\pi]$ and, in turn, for all $\theta \in [0, 4\pi]$. As illustrated in the second subfigure of Fig. 5.15, the answer to this problem is $\overline{k} = 1/2$ and $\breve{d}_0 = \sqrt{3}/2$. This corresponds to the following input

$$d(\theta) = \frac{1}{2}\begin{bmatrix} \cos(\theta) \\ \cos(\theta - 2\pi/3) \\ \cos(\theta + 2\pi/3) \end{bmatrix} + \frac{1}{2}\mathbf{1}_3 = u^d(\theta) + \frac{1}{2}\mathbf{1}_3 \tag{5.32}$$

for all $\theta \in [2\pi, 4\pi]$. •

5.6 Conclusions

As a summary of this chapter, let us recall its essential message.

- Control of 3-phases inverter is about:
  - Electrical engineering statement: Adjusting the homopolar duty cycle d_0 in order to cope with the input constraint $\mathcal{D}$ and to meet secondary control purpose;
  - Mathematical statement: Right-inverting a non invertible static linear map subject to input constraints;
- Inverting this map amounts to build a controller via mirror construction of a suitable decomposition of the system, obtained via the "Concordia transformation" and implementing appropriate projections of the input space, see Fig. 5.7. An explicit expression of the range of the system is readily obtained as a byproduct of this study.
- The obtained control law is static and time-invariant, so that it can equally operate in transient or in steady-state.

5.7 Bibliographical notes

Existing works

An up-to-date state-of-the-art for the control of inverters can be found in [Bou22, Chap.1], see also [Pat15, Fig.2.21, p.79]. Material of Rem. 5.7 can be recovered from [Pat15, Chap.2], see, in particular, Tab.2.2 p.74 of this reference, where the intersective PWM is renamed "Sinus PWM".

Two control strategies Most of the time, the literature treats the following two modulation strategies. They are usually exposed as follows:

- Intersective PWM (see e.g. [Pat15, Sec.2.4.2.]): The analysis focuses on the steady state, where the desired output voltage vector is a balanced 3-phases sinusoidal signal, as in the second part of the simulation performed in Sec. 5.5. From the analysis of the waveforms of the carrier and duty cycle (see e.g. [MUR07, see Fig.8.22]) and the observation that $u_{\alpha\beta} = d_{\alpha\beta}$ (see (5.26)), it is immediately concluded that d_0 can be selected as $\sqrt{3}/2$, thus leading to d as in (5.32).
- Vector PWM modulation (see e.g. [Pat15, Sec.2.4.4.] and [NL96, p.115-116]): Adopting a completely different perspective, the focus is set on the hexagon of Fig. 5.9 that is represented in a plan, i.e. $H(\mathcal{D})$ in $\mathrm{Im}\,\{H\}$. Then, solving Prob. 5.1 amounts to identifying every barycentric coordinate of a given output voltage $u^d \in \mathcal{U}$, respectively to the vertices and the center of the hexagon. This process can be graphically performed.

Geometric point of view Pioneering studies on the geometric perspective in this chapter can be found in [RLD99]. The H-bridge and star-connected three- and four-leg inverters are treated. The changes of basis, and their geometric interpretations, are introduced.[4] However, their algebraic origins (in terms of the image and kernel of H) are not discussed, unlike in the remarks of the next chapter. The same comment applies to the input constraints: No guidelines on how to select V_0^* in (4), (12), and (19) of [RLD99] are provided.

Optimization criteria The selection of the optimal value of $d_0 \in \mathcal{D}_0(d_{\alpha\beta})$ is beyond the scope of this chapter. Following e.g. [Pat15; GGL17; Vid+19], it can be made on the basis of the following commonly used criteria: DC bus utilization, spectral content of the output voltage signal, reduction of power losses particularly by clamping, etc.

Paul-Étienne Vidal and its co-authors Recently, a point of view very close to the one used in this chapter has been *independently* adopted by Paul-Étienne Vidal and its co-authors from ENIT, Tarbes France. For the content of this chapter, the most relevant reference is perhaps [Vid+19]. Unlike in [RLD99], the input constraints are explicitly taken into account, see [Vid+19, (24)] and compare it with (5.20). Interestingly, the existing literature on PWM strategies is reviewed in terms of the selection policy of d_0, see [Vid+19, Tab.1] where λ corresponds to d_0. As in this chapter, it is explicitly shown that the proposed point of view is universal in the sense that any existing PWM strategy can be coded as a particular function selecting d_0.

[4] The discussion in [RLD99] is sometimes confusing from a mathematical point of view. For instance, the input space, called "leg voltage space", is depicted on the same graph as the output voltage space, see e.g. [RLD99, Fig.2], even though these sets do not belong to the same euclidien spaces. As another example, [RLD99, Fig.2] suggests that the projection related to H is orthogonal to the first axis, whereas the mapping H is actually related to an oblique projection parallel to the kernel of H.

Rephrased existing work

Let us comment on this state of the literature.

- In both strategies, it is seldom recognized that the problem amounts to invert a static map. [Vid+19] is a notable exception with that respect. If the expression of H can be found in any standard textbook on power electronics, see e.g. [Pat15, (2.31)] or [MUR07, p.232], it is surprisingly seldom used. Perhaps this explains why the inverse map is rarely provided, and why the transient regime remains apparently out of the scope of most studies.

- Comparison between the intersective and vector PWM strategies are often convoluted, see e.g. [KD02; BY97]. In the framework of this chapter, the distinction between the two approaches can be simply viewed as the result of a different parametrization of $\mathcal{D}$. Indeed, instead of defining this hypercube as follows

$$\mathcal{D} = [0,1] \times [0,1] \times [0,1], \tag{5.33}$$

  one can characterize $\mathcal{D}$ as the convex hull of the vertices $\hat{s}_k$ of this hypercube, i.e.

$$\mathcal{D} = \text{conv}\{\hat{s}_1 = \begin{bmatrix}0\\0\\0\end{bmatrix}, \hat{s}_2 = \begin{bmatrix}1\\0\\0\end{bmatrix}, \hat{s}_3 = \begin{bmatrix}1\\1\\0\end{bmatrix}, \dots, \hat{s}_8 = \begin{bmatrix}1\\1\\1\end{bmatrix}\} = \{\sum_{k=1}^{8} \lambda_k \hat{s}_k : \mathbf{0}_8 \leq \lambda \leq \mathbf{1}_8, \sum_{k=1}^{8} \lambda_k = 1\} \tag{5.34}$$

  Eq. (5.33) highlights that each entry of $d \in \mathcal{D}$ takes value in $[0,1]$, *independently*. Eq. (5.34) emphasizes that any $d \in \mathcal{D}$ can selected as the barycenter of the vertices $\hat{s}_k$, weighted by scalars λ_k, so that $d \in \mathcal{D}$ is equivalent to the existence of λ in the unit simplex $\{\lambda : \mathbf{0}_8 \leq \lambda \leq \mathbf{1}_8, \sum_{k=1}^{8} \lambda_k = 1\} \subset \mathbb{R}^8$ such that $d = \sum_{k=1}^{8} \lambda_k \hat{s}_k$.

  The key idea underlying the vector PWM modulation is to write $u = Hd$ for the second parametrization, i.e. $u = \begin{bmatrix} H\hat{s}_1 & \dots & H\hat{s}_8 \end{bmatrix} \lambda$. Solving the problem then boils down to determine the most appropriate weighting vector λ among those that make u a barycenter of the points $\{H\hat{s}_1, \dots, H\hat{s}_8\}$. This can be done graphically, since these points correspond to the center and vertices of the hexagon $\mathcal{U}$, see e.g. [Pat15, Sec.2.4.4.].

- Both parametrization of $\mathcal{D}$ leads to the same reachable output voltage. From the perspective of this chapter (see Rem. 5.7), "constant homopolar duty cycle" and "time-varying homopolar duty cycle" seem more appropriate names for what is called "intersective PWM" and "vector PWM", respectively, in the literature. In addition, the essences of the two strategies do not differ by the reachable output voltage set, but rather by the way the input set $\mathcal{D}$ is parameterized. Hence, the point of view associated to "intersective PWM" and "vector PWM" could be renamed as "cartesian product PWM" and "barycentric PWM", respectively. The following quote confirms this comment: "Vector-based and intersective approaches may therefore be considered complementary for understanding the operation of an inverter for a given control, from both load and source perspectives, and for synthesizing control laws.", [Pat15, p.81].

Hopefully, this chapter will be viewed as a valuable attempt to enrich and strengthen the study of [Vid+19] by mathematically formalizing the discussion and offering a graphical representation of both the input and output spaces. Unlike in [Vid+19], the hexagon $H(\mathcal{D})$ is also clearly computed and represented. In this chapter, it is also firmly said that the scope of the discussion is not confined to sinusoidal output references.

Chapter 6

Inversion of static mappings

Contents

The previous chapter is intended to motivate this one, in which the inversion of input-constrained, static, and affine systems is considered with full generality. It is shown how the case of the 3-phases inverter can be generalized in this context using the same philosophy. Note that the case of parametric dependency of the system is also investigated (see Sec. 6.2) after the exposition of two other engineering motivating examples.

Let us already emphasize that the results of this chapter are useful tools, even in the dynamic system context. Chap. 7 shows that by playing with different time scales, the controller design can exploit algebraic models as approximations of differential relationships, which are locally valid around a particular time scale. Sec. 8.4.3 of Chap. 8 also shows that in some particular cases (namely, $F = \mathbf{0}$ is a friend of a particular subspace of the state-space), dealing with constraints for dynamical systems amounts to handling those limitations on a specific static model. Chap. 10 illustrates this feature for a relevant example of power electronics.

6.1 The affine case

The discussion in the previous chapter is now immersed in the more general context of arbitrary affine input-output mapping. The pictures in both chapters are intended for comparison.

6.1.1 Problem setting

Let the *affine* map $H : \mathbb{R}^m \to \mathbb{R}^p$ capture the following input/output relationship:

$$y = H(u) =: Au + b, \tag{6.1}$$

for some vector $b \in \mathbb{R}^p$ and matrix $A \in \mathbb{R}^{p\times m}$. Our goal is to invert this equation, i.e. given the output $y \in \mathbb{R}^p$, find all inputs $u \in \mathbb{R}^m$ satisfying (6.1), with the additional constraint that u belongs to a given non-empty set $\mathcal{U} \subset \mathbb{R}^m$. This amounts to providing an expression for the following mapping.

$$\begin{aligned}(H|\mathcal{U})^+ : \mathbb{R}^p &\rightrightarrows \mathcal{U},\\ y &\mapsto \{u \in \mathcal{U} : H(u) = y\}.\end{aligned}$$

Of particular importance is the image $\mathcal{Y}$ of $H|\mathcal{U}$, because the output y must belong to $\mathcal{Y}$ for (6.1) to admit solutions:

$$\mathcal{Y} := H(\mathcal{U}) = \{y \in \mathbb{R}^p : \exists u \in \mathcal{U}, H(u) = y\}. \tag{6.2}$$

Problem 6.1. Express both $(H|\mathcal{U})^+(y)$ and $\mathcal{Y}$ in closed-form.

In this section, we aim equipping both $(H|\mathcal{U})^+$ and $\mathcal{Y}$ with an expression in closed-form.[1]

To better grasp the specific difficulties related to the input constraints, we often refer to the

[1]Consider $\mathcal{Y}|H|\mathcal{U}$, that is the codomain restriction to $\mathcal{Y}$ of the domain restriction of H to $\mathcal{U}$. By definition, any right inverse $(\mathcal{Y}|H|\mathcal{U})^+$ of this mapping satisfies $(\mathcal{Y}|H|\mathcal{U}) \circ (\mathcal{Y}|H|\mathcal{U})^+ = \mathrm{id}_{\mathcal{Y}}$. The mapping $(H|\mathcal{U})^+$ gathers the domain extension of every $(\mathcal{Y}|H|\mathcal{U})^+$ to $\mathbb{R}^p$.

sets analogous to $\mathcal{Y}$ and $(H|\mathcal{U})^+(y)$ in the unconstrained context, that is, $H(\mathbb{R}^m)$ and

$$\begin{aligned} H^+ : \mathbb{R}^p &\rightrightarrows \mathbb{R}^m, \\ y &\mapsto \{u \in \mathbb{R}^m : H(u) = y\}, \end{aligned}$$

respectively.[2]

Remark 6.2 (Coordinate-free expressions). Clearly, $\mathcal{Y} = b + A\mathcal{U}$ and $(H|\mathcal{U})^+(y) = H^+(y) \cap \mathcal{U}$ hold. All the materials offered in the sequel can be regarded as an effort to provide an implementable and more informative version of these coordinate-free expressions. Specifically, we want to further support the idea that constructing an inverse reduces to build a block diagram via mirror construction of an appropriate decomposition of the system, as performed in Chap. 5. Such a block diagram of the inverse is more amenable to an algorithm, which is obviously desirable for real-time implementation. •

6.1.2 Problem solution

Input/output change of coordinates Define

$$r := \operatorname{rank}\{A\}.$$

Let us select an orthonormal basis of $\mathbb{R}^m$ that is adapted to $\operatorname{Ker}\{A\}^\perp$, i.e. define a non-singular matrix $P \in \mathbb{R}^{m\times m}$ satisfying $P^{-1} = P^\intercal$ and such that the first $\dim \operatorname{Ker}\{A\}^\perp = r$ columns of P form a basis of $\operatorname{Ker}\{A\}^\perp$. Similarly, let Q be a matrix whose columns form an orthonormal basis of $\mathbb{R}^p$ which is adapted to $\operatorname{Im}\{A\}$. In this case, it is well known that the following relationship holds

$$Q^{-1}AP = \begin{bmatrix} \mathbf{I}_r \\ \mathbf{0}_{(p-r)\times r} \end{bmatrix} R \begin{bmatrix} \mathbf{I}_r & \mathbf{0}_{r\times(m-r)} \end{bmatrix}, \tag{6.3}$$

where $R \in \mathbb{R}^{r\times r}$ is invertible.

Define the following new variables.

$$\hat{y} := Q^{-1}y, \qquad \hat{u} := P^{-1}u, \qquad \hat{b} := Q^{-1}b, \tag{6.4}$$

together with the sets

$$\hat{\mathcal{Y}} := Q^{-1}\mathcal{Y}, \qquad \hat{\mathcal{U}} := P^{-1}\mathcal{U}.$$

By using the following development, (6.1) can be expressed as follows:

$$y = QQ^{-1}(APP^{-1}u + b) \overset{(6.3)}{=} Q(\underbrace{\begin{bmatrix} \mathbf{I}_r \\ \mathbf{0} \end{bmatrix} R \begin{bmatrix} \mathbf{I}_r & \mathbf{0} \end{bmatrix} \overbrace{P^{-1}u}^{=\hat{u}} + \overbrace{Q^{-1}b}^{=\hat{b}}}_{=\hat{y}}), \tag{6.5}$$

so that

$$\hat{y} = \hat{H}(\hat{u}) \quad \text{with} \quad \hat{H}(\hat{u}) := \begin{bmatrix} \mathbf{I}_r \\ \mathbf{0} \end{bmatrix} R \begin{bmatrix} \mathbf{I}_r & \mathbf{0} \end{bmatrix} \hat{u} + \hat{b}, \tag{6.6}$$

or, equivalently,

$$\begin{bmatrix} \hat{y}_{1:r} \\ \hat{y}_{r+1:p} \end{bmatrix} = \begin{bmatrix} R\hat{u}_{1:r} + \hat{b}_{1:r} \\ \hat{b}_{r+1:p} \end{bmatrix}. \tag{6.7}$$

This leads to the decomposition of H proposed by Fig. 6.1.

[2] Clearly, $H(\mathbb{R}^m) \supset \mathcal{Y}$ and $H^+(y) \supset (H|\mathcal{U})^+(y)$ hold for all $y \in \mathcal{Y}$.

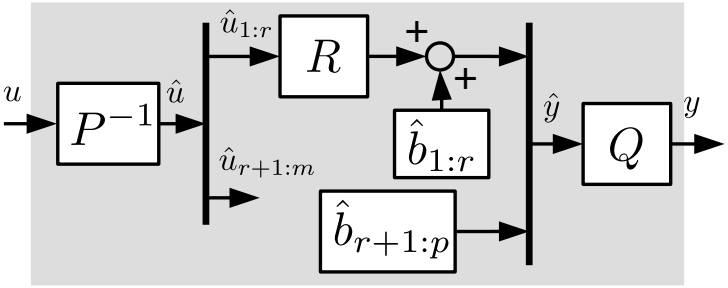

Figure 6.1: Decomposition of H using the new coordinates.

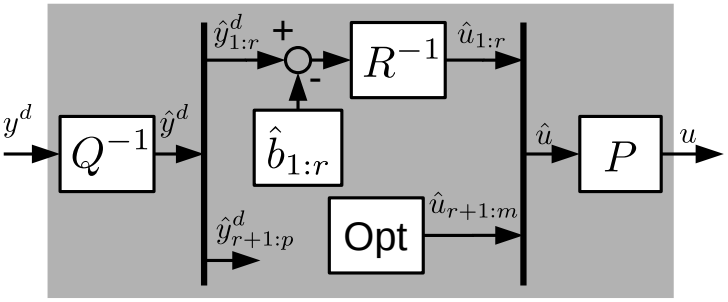

Figure 6.2: Controller built by inversion of Fig. 6.1. Note that the last $m - r$ components of $\hat{u}$ are arbitrary and can thereby be optimised.

Example 6.3 (3-phases inverter of Chap. 5)**.** Observe that the kernel and the image of $H = A$ are as follows:

$$\begin{aligned}\mathrm{Ker}\,\{A\} &= \mathrm{Im}\,\{\mathbf{1}_3\}\,,\\ \mathrm{Im}\,\{A\} &= \{y : \mathbf{1}_3^{\mathsf{T}} y = 0\} = \mathrm{Im}\,\{\mathbf{1}_3\}^{\perp}\,,\end{aligned}$$

so that the same matrix $P = Q$ allows to decompose both input and output spaces, by selecting last column of $P = Q$ in $\mathrm{Im}\,\{\mathbf{1}_3\} \setminus \{\mathbf{0}\}$. The Concordia transformation given by (5.9) satisfies this requirement. From the fact that $\dim \mathrm{Im}\,\{A\} = 2$ and $\dim \mathrm{Ker}\,\{A\} = 1$, it holds

$$Q^{-1}A = \begin{bmatrix} \star & \star & \star \\ \star & \star & \star \\ 0 & 0 & 0 \end{bmatrix}, \quad AP = \begin{bmatrix} \star & \star & 0 \\ \star & \star & 0 \\ \star & \star & 0 \end{bmatrix},$$

as in (5.25).

Solution of the unconstrained problem The essential benefits of the change of basis are the following two key features: (i) $\hat{u}_{r+1:m}$ does not appear in (6.7), which is also visible in Fig. 6.1 where $\hat{y}$ is independent of $\hat{u}_{r+1:m}$ and (ii) R is invertible. As shown below, this allows to derive explicit expressions not only for the achievable output set $\hat{\mathcal{Y}}$ but also for $(H|\mathcal{U})^+$ in the new coordinates, i.e.

$$(\hat{H}|\hat{\mathcal{U}})^+(\hat{y}) := \{\hat{u} \in \hat{\mathcal{U}} : \hat{H}(\hat{u}) = \hat{y}\} = P^{-1}(H|\mathcal{U})^+(Q\hat{y}),$$

To this end, and as a preliminary step, let us consider the unconstrained problem, i.e. $\mathcal{U} = \mathbb{R}^m$. As shown on Fig. 6.2, controller $y^d \mapsto u$ can be readily built via mirror construction of the decomposition of the system depicted in Fig. 6.1. From Fig. 6.1 and Fig. 6.2, observe that

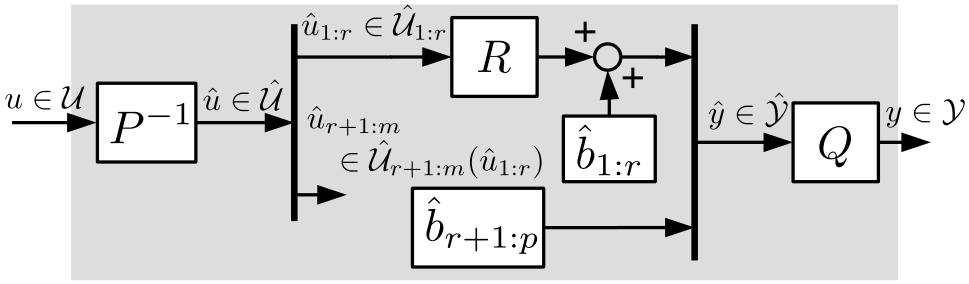

Figure 6.3: Forward propagation of $\mathcal{U}$ toward y in the schematic of Fig. 6.1.

the interconnection of the controller and the system leads to $y^d = y$ iff $\hat{y}^d_{r+1:p} = \hat{b}_{r+1:p}$ holds or, equivalently, if $\hat{y} \in \hat{H}(\mathbb{R}^m)$ with

$$\hat{H}(\mathbb{R}^m) = \mathbb{R}^r \times \{\hat{b}_{r+1:p}\} \tag{6.8}$$

In this case, and as shown in Fig. 6.2, the last $m - r$ components of $\hat{u}$ are arbitrary, whereas the first r ones are entirely determined by y^d via the following mapping $\hat{u}_{1:r}(\cdot) : \mathbb{R}^p \to \mathbb{R}^r$:

$$\hat{u}_{1:r}(\cdot) : \hat{y} \mapsto R^{-1}(\hat{y}_{1:r} - \hat{b}_{1:r}) \tag{6.9}$$

As a result, the unconstrained inverse reads:[3]

$$\hat{H}^+ : \hat{y} \mapsto \{\hat{u}_{1:r}(\hat{y})\} \times \mathbb{R}^{m-r}. \tag{6.10}$$

Handeling the input set $\mathcal{U}$ Fig. 6.3 is constructed from Fig. 6.1 by forward propagation of $\mathcal{U}$ toward y. In doing so, the definitions of the following sets arise naturally by prioritizing $\hat{u}_{1:r}$ over $\hat{u}_{r+1:m}$ because only the former impacts y:

$$\hat{\mathcal{U}}_{1:r} := \left\{\hat{u}_{1:r} \in \mathbb{R}^r : \exists \hat{u}_{r+1:m} \in \mathbb{R}^{m-r}, \hat{u} \in \hat{\mathcal{U}}\right\}, \tag{6.11}$$

$$\hat{\mathcal{U}}_{r+1:m}(\hat{u}_{1:r}) := \{\hat{u}_{r+1:m} : \hat{u} \in \hat{\mathcal{U}}\}, \tag{6.12}$$

together with the relationships $\hat{u}_{1:r} \in \hat{\mathcal{U}}_{1:r}$ and $\hat{u}_{r+1:m} \in \hat{\mathcal{U}}_{r+1:m}(\hat{u}_{1:r})$. This immediately leads to

$$\hat{\mathcal{Y}} = \left(\hat{b}_{1:r} + R\hat{\mathcal{U}}_{1:r}\right) \times \{\hat{b}_{r+1:p}\}, \tag{6.13}$$

$$(\hat{H}|\hat{\mathcal{U}})^+(\hat{y}) = \{\hat{u}_{1:r}(\hat{y})\} \times \hat{\mathcal{U}}_{r+1:m}(\hat{u}_{1:r}(\hat{y})), \tag{6.14}$$

Compare the two expressions with (6.8) and (6.10) to appreciate the impact of the input constraints.

Building on Fig. 6.2, the controller scheme is enriched by Fig. 6.4 via mirror construction of Fig. 6.3. Note that this graphical reasoning can easily be confirmed using (6.7).

Remark 6.4 (Back to the original basis). In the original basis, the two sets above are as follows:

$$\mathcal{Y} = b + Q_{1:r}R\hat{\mathcal{U}}_{1:r},$$
$$(H|\mathcal{U})^+(y) = P_{1:r}\hat{u}_{1:r}(Q^{-1}y) + P_{r+1:m}\hat{\mathcal{U}}_{r+1:m}(\hat{u}_{1:r}(Q^{-1}y)),$$

[3]The same conclusions can be recovered by adopting a purely algebraic view point using (6.7): Provided that $\hat{y}_{r+1:p} = \hat{b}_{r+1:p}$ holds, $\hat{u}$ solving the unconstrained problem exists. Its first r entries are uniquely defined via $\hat{u}_{1:r}(\hat{y})$, whereas its last $m - r$ ones are free.

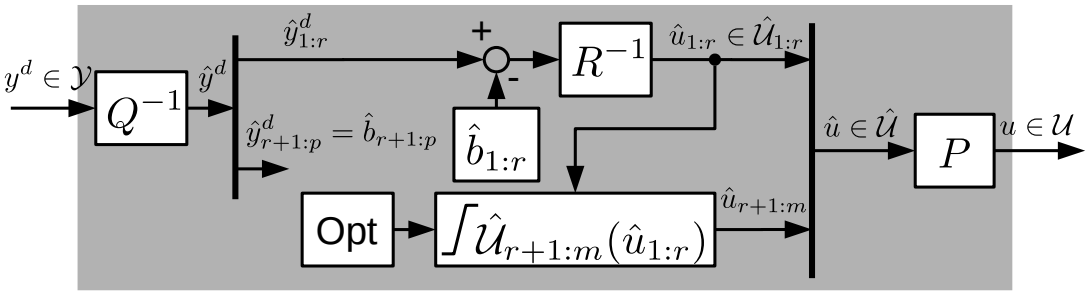

Figure 6.4: Controller build by inversion of Fig. 6.3. Note that the last $m - r$ components of $\hat{u}$ are arbitrary in $\mathcal{U}_{r+1:m}(\hat{u}_{1:r})$ and can thereby be optimised *in this set*.

where P and Q have been split as follows

$$P =: \begin{bmatrix} P_{1:r} & P_{r+1:m} \end{bmatrix}, \quad Q =: \begin{bmatrix} Q_{1:r} & Q_{r+1:m} \end{bmatrix}$$

with $P_{1:r} \in \mathbb{R}^{m \times r}$ and $Q_{1:r} \in \mathbb{R}^{p \times r}$. To arrive at $(H|\mathcal{U})^+(y)$, the following relationship:

$$(\hat{H}|\hat{\mathcal{U}})^+(\hat{y}) = P^{-1}(H|\mathcal{U})^+(Q\hat{y}),$$

has been exploited. •

6.1.3 Outer description of $\hat{\mathcal{Y}}$ and $(\hat{H}|\hat{\mathcal{U}})^+(\hat{y})$

The next step is now to derive a tractable expression for both $\hat{\mathcal{Y}}$ and $(\hat{H}|\hat{\mathcal{U}})^+(\hat{y})$. To this end, assume that $\mathcal{U}$ and $\hat{\mathcal{U}}_{1:r}$ admit the following outer descriptions:

$$\mathcal{U} = \{u \in \mathbb{R}^m : g(u) \leq 0\}, \tag{6.15}$$
$$\hat{\mathcal{U}}_{1:r} = \{\hat{u}_{1:r} \in \mathbb{R}^r : \chi(\hat{u}_{1:r}) \leq 0\}, \tag{6.16}$$

for some mappings $g : \mathbb{R}^m \to \mathbb{R}^\kappa$ and $\chi : \mathbb{R}^r \to \mathbb{R}^\beta$, the latter depending on the former.

Construction of χ from g is the key Expressing $\mathcal{U}$ in the new coordinates

$$\hat{\mathcal{U}} = \{\hat{u} \in \mathbb{R}^m : \hat{g}(\hat{u}) := g(P\hat{u}) \leq 0\}.$$

and using both (6.13) and (6.14) yields

$$\hat{\mathcal{Y}} = \{\hat{b}_{1:r} + \hat{c} : \chi(R^{-1}\hat{c}) \leq 0\} \times \{\hat{b}_{r+1:p}\} \tag{6.17a}$$
$$(\hat{H}|\hat{\mathcal{U}})^+(\hat{y}) = \{\hat{u}_{1:r}(\hat{y})\} \times \{\hat{u}_{r+1:m} \in \mathbb{R}^{m-r} : g(P \begin{bmatrix} \hat{u}_{1:r}(\hat{y}) \\ \hat{u}_{r+1:m} \end{bmatrix}) \leq 0\} \tag{6.17b}$$

If this expression of $(\hat{H}|\hat{\mathcal{U}})^+(\hat{y})$ is tractable, the one of $\hat{\mathcal{Y}}$ requires an explicit expression of χ. Thus, the remaining challenge is to relate g to χ or equivalently, $\mathcal{U}$ to $\hat{\mathcal{U}}_{1:r}$. Observe that $\hat{\mathcal{U}}_{1:r}$ can also be equivalently written as follows:

$$\hat{\mathcal{U}}_{1:r} = \begin{bmatrix} \mathbf{I}_r & \mathbf{0} \end{bmatrix} \hat{\mathcal{U}}$$

This allows to interpret $\hat{\mathcal{U}}_{1:r}$ geometrically as the first r coordinates of the orthogonal projection of $\hat{\mathcal{U}}$ on $\text{Im} \left\{ \begin{bmatrix} \mathbf{I}_r \\ \mathbf{0} \end{bmatrix} \right\} \subset \mathbb{R}^m$, as illustrated in Fig. 6.5. Indeed, $\hat{\mathcal{U}}_{1:r}$ equals $\begin{bmatrix} \mathbf{I}_r & \mathbf{0} \end{bmatrix} \hat{\mathcal{U}}$.

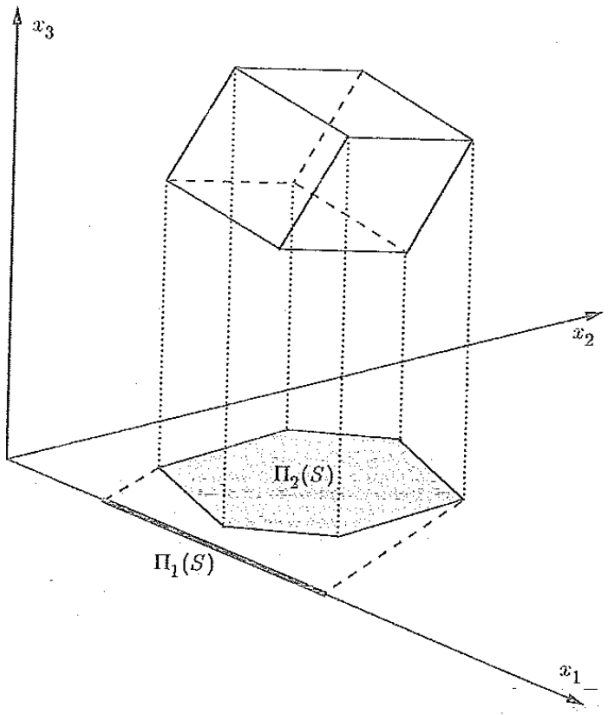

Figure 6.5: Illustration for $m = 3$ and $r = 1$ of the construction of $\hat{\mathcal{U}}_{1:r}$ (denoted by $\Pi_1(S)$ on the picture) from $\hat{\mathcal{U}}$ (the tilted cube). (read $\hat{u}_k$ in place of x_k)[BT97, p.71]

The polyhedron case Motivated by the quest to derive constructive results, let us assume that g is affine so that $\mathcal{U}$ reads

$$\text{H-rep:} \quad \mathcal{U} = \{u \in \mathbb{R}^m : Cu \leq d\} \tag{6.18}$$

for some $C \in \mathbb{R}^{\kappa \times m}$ and $d \in \mathbb{R}^\kappa$. This is equivalent to saying that $\mathcal{U}$ is the intersection of κ half-spaces, i.e. $\mathcal{U}$ is a polyhedron, which is described in (6.18) via its outer description, called H-representation.

Perhaps, the most interesting feature of the set of polyhedrons is that it is closed under affine mapping and intersection with affine space. Therefore, both $\mathcal{Y} = H(\mathcal{U})$ and $(H|\mathcal{U})^+(y) = H^+(y) \cap \mathcal{U}$ are polyhedra because $H^+(y)$ is an affine space, as shown in (6.10). As a result, $\hat{\mathcal{Y}} = Q^{-1}\mathcal{Y}$ and $(\hat{H}|\hat{\mathcal{U}})^+(\hat{y}) = P^{-1}(H|\mathcal{U})^+(Q\hat{y})$ are also polyhedra. As a matter of fact, one can verify that

$$(\hat{H}|\hat{\mathcal{U}})^+(\hat{y}) = \{\hat{u}_{1:r}(\hat{y})\} \times \left\{\hat{u}_{r+1:m} \in \mathbb{R}^{m-r} : CP_{r+1:m}\hat{u}_{r+1:m} \leq d - CP_{1:r}\hat{u}_{1:r}(\hat{y})\right\}.$$

For the same reason, $\hat{\mathcal{U}}$ and, in turn, $\hat{\mathcal{U}}_{1:r} = \begin{bmatrix}\mathbf{I}_r & \mathbf{0}\end{bmatrix}\hat{\mathcal{U}}$ are polyhedron as well. Thus, χ is affine.

Computation of parameters of χ from those of $\hat{g}$ is performed algorithmically.[4] The Fourier-Motzkin algorithm achieves this purpose. It is similar in spirit to Gaussian elimination for systems of linear equations, but applies to systems of linear inequalities. The idea is to isolate the variable $\hat{u}_m$ in $\hat{g}(\hat{u}) \leq \mathbf{0} \Leftrightarrow CP\hat{u} \leq d$ and then eliminate it by comparing its bounds (depending on $\hat{u}_{1:m-1}$). Starting from the resulting inequalities and proceeding in the same way, one can eliminate then $\hat{u}_{m-2}$, and so on and so forth, up to the step where the remaining variables are $\hat{u}_{1:r}$. Ex. 6.5, proof of the forthcoming Lem. 6.7 and (unrelated) Fig. 6.5 all illustrate this iterative procedure.

[4] From (6.18), $\hat{g}(\hat{u}) \leq \mathbf{0}$ simply reads $CP\hat{u} \leq d$.

Note that this elimination method generates a quadratic number of new vectors or inequalities *at each step*, leading to a combinatorial explosion. Fortunately, many new vectors or inequalities are redundant and can therefore be eliminated. Various methods exist for detecting redundancies. Interested readers can refer to [Zie95, p.48].

Example 6.5 (3-phases inverter of Chap. 5 (continued))**.** For this example, the set $\mathcal{U} = \{u : \mathbf{0}_3 \leq u \leq \mathbf{1}_3\}$ can be coded as $g(u) = Cu - d \leq \mathbf{0}$ by defining $C = \begin{bmatrix} -\mathbf{I}_3 \\ \mathbf{I}_3 \end{bmatrix}$ and $d = \begin{bmatrix} \mathbf{0}_3 \\ \mathbf{1}_3 \end{bmatrix}$. Then, observe that (5.20) is an implementation of the Fourier-Motzkin algorithm. Starting from the inequalities $CP\hat{u} \leq d \Leftrightarrow \mathbf{0}_3 \leq P_{\alpha\beta}d_{\alpha\beta} + P_0 d_0 \leq \mathbf{1}_3$ coding $\hat{\mathcal{U}}$, the variable d_0 (corresponding to $\hat{u}_{r+1:m} = \hat{u}_m$) has been isolated to obtain $-\sqrt{3}P_{\alpha\beta}d_{\alpha\beta} \leq \mathbf{1}_3 d_0 \leq \sqrt{3}(\mathbf{1}_3 - P_{\alpha\beta}d_{\alpha\beta})$. Clearly, such a d_0 exists iff $\underline{d}_0(d_{\alpha\beta}) := -\sqrt{3}\min\{P_{\alpha\beta}d_{\alpha\beta}\}$ is equal to or less than $\bar{d}_0(d_{\alpha\beta}) := \sqrt{3}(1 - \max\{P_{\alpha\beta}d_{\alpha\beta}\})$. Thus, $\mathcal{D}_{\alpha\beta} = \{d_{\alpha\beta} : \exists d_0, d_{\alpha\beta 0} \in \mathcal{D}_{\alpha\beta 0}\}$ is nothing but $\{d_{\alpha\beta} : \underline{d}_0(d_{\alpha\beta}) \leq \bar{d}_0(d_{\alpha\beta})\}$. This set corresponds to $\hat{\mathcal{U}}_{1:r}$ so no further elimination is required.

The polytope case A second algorithm applies when $\mathcal{U}$ is bounded, i.e. $\mathcal{U}$ is a polytope. In such a case, $\mathcal{U}$ admits an inner description, called V-representation, as the convex hull of a finite number of vector of $\mathbb{R}^m$ which corresponds to its extreme points, i.e. there exists $u^{[1]}, \ldots, u^{[v]} \in \mathbb{R}^m$ such that

$$\text{V-rep:} \quad \mathcal{U} = \text{co}\left\{u^{[1]}, \ldots, u^{[v]}\right\}. \tag{6.19}$$

From this formulation, a V-representation of $\hat{\mathcal{U}}_{1:r}$ can be immediately obtained:

$$\hat{\mathcal{U}}_{1:r} = \begin{bmatrix} \mathbf{I}_r & \mathbf{0} \end{bmatrix} P^{-1}\mathcal{U} = P_{1:r}^{\mathsf{T}}\mathcal{U} = \text{co}\left\{\hat{u}_{1:r}^{[1]}, \ldots, \hat{u}_{1:r}^{[v]}\right\} \tag{6.20}$$

where $\hat{u}_{1:r}^{[k]} := P_{1:r}^{\mathsf{T}} u^{[k]}$.[5] Subsequently, the computation of χ reduces to the construction of an H-representation from (6.20). Multiple algorithms exist for this nontrivial task, as outlined in [JT13, Chap.5].

The zonotope case Images of the d-hypercube $[-1, 1]^d$ obtained by affine mappings are particular polytopes called zonotopes. Hence, $\mathcal{U}$ is a zonotope if it can be described as follows:

$$\text{G-rep:} \quad \mathcal{U} = \{c + \sum_{j \in [\![1,d]\!]} \lambda_j G_j : \|\lambda\|_\infty \leq 1\} \tag{6.21}$$

for some $c \in \mathbb{R}^m$ and $G = \begin{bmatrix} G_1 & \ldots & G_d \end{bmatrix} \in \mathbb{R}^{m \times d}$ characterizing the affine mapping $\lambda \mapsto c + G\lambda$ relating $[-1, 1]^d$ to $\mathcal{U}$, i.e. $\mathcal{U} = c + G[-1, 1]^d$.

From (6.21), one gets that $\hat{\mathcal{U}}_{1:r}$ is a zonotope whose G-representation can be trivially obtained:

$$\hat{\mathcal{U}}_{1:r} = P_{1:r}^{\mathsf{T}}\mathcal{U} = \{\hat{c} + \sum_{i \in [\![1,d]\!]} \lambda_i \hat{G}_i : \|\lambda\|_\infty \leq 1\}$$

where $\hat{c} := P_{1:r}^{\mathsf{T}} c$ and $\hat{G} = P_{1:r}^{\mathsf{T}} G$. Providing an expression to χ reduces to compute the H-representation corresponding to this G-representation, see [ASB10] for algorithms achieving this goal.

[5] Note that, the inner description of $\hat{\mathcal{U}}_{1:r}$ proposed by (6.20) may not be fully relevant. Indeed, there is no guaranty that it is minimal (even if (6.19) is), in the sense that might exists $j \in [\![1, v]\!]$ such that removing $\hat{u}^{[j]}$ from the list of $\hat{u}^{[k]}$s forming co $\left\{\hat{u}_{1:r}^{[1]}, \ldots, \hat{u}_{1:r}^{[v]}\right\}$ let this convex hull unchanged, i.e. $\hat{u}^{[j]}$ can be obtained by a convex combinaison of $\{\hat{u}^{[k]}\}_{k \in [\![1,v]\!] \setminus \{j\}}$.

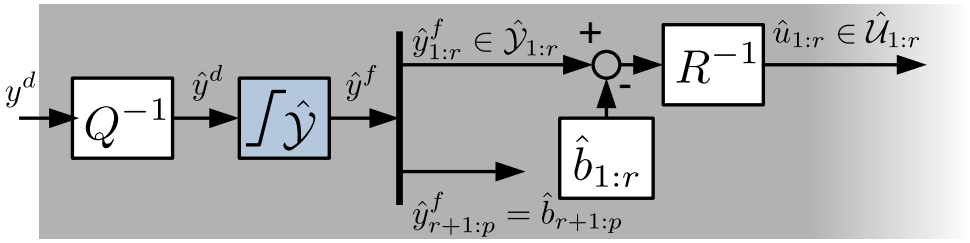

Figure 6.6: Controller of Fig. 6.4 equipped with an upstream saturation bloc to handle unfeasible output reference $y^d \notin \mathcal{Y}$.

Remark 6.6 (Zonotopes set captures decentralized saturations). The decentralized saturation leads to $\mathcal{U} = [\underline{u}_1, \overline{u}_1] \times \ldots \times [\underline{u}_m, \overline{u}_m]$. From the fact that

$$[a, b] = \frac{b-a}{2}[-1, 1] + \frac{a+b}{2}$$

for any $a, b \in \mathbb{R}$, this set $\mathcal{U}$ is a zonotope whose G-representation is characterized by $G = \text{diag}\{(\overline{u} - \underline{u})/2\}$ and $c = (\overline{u} + \underline{u})/2$. •

6.1.4 Discussion

Fault tolerance and reconfiguration Construction of the controller depicted by Fig. 6.4 can easily be reduced to an algorithm. Therefore, if H is affected by some faults, so that either its parameters or its dimension change, then the new post-fault control law can be automatically obtained.

The unfeasible case Let us now consider the case where the desired output y^d does not belong to $\mathcal{Y}$, so that there is no $u \in \mathcal{U}$ such that $H(u) = y^d$. From the discussion above, this situation occurs iff one (at least) of the following conditions holds:

$$\hat{y}^d_{r+1:p} \neq \hat{b}_{r+1:p} \tag{6.22a}$$

$$\hat{u}_{1:r}(\hat{y}^d) \notin \hat{\mathcal{U}}_{1:r} \tag{6.22b}$$

To mitigate the impact of the unavoidable mismatch between y^d and the output y, one can somehow saturate the output vector y^d, that is, implement a pretreatment upstream from the controller or, at least, immediately after the change of coordinates corresponding to the multiplication by Q^{-1} in Fig. 6.4. This boils down to the design of the following mapping:

$$\begin{aligned} \text{sat}_{\hat{\mathcal{Y}}} : \mathbb{R}^p &\to \hat{\mathcal{Y}} \\ \hat{y}^d &\mapsto \hat{y}^f := \text{sat}_{\hat{\mathcal{Y}}}(\hat{y}^d) \end{aligned}$$

The left-hand side of the enriched control scheme is depicted on Fig. 6.6. Observe that none of the conditions (6.22) with $\hat{y}^d$ in place of $\hat{y}^f$ are satisfied, by construction.

Perhaps, the most natural definition of $\text{sat}_{\hat{\mathcal{Y}}}$ is the projection of $\hat{y}^d$ on the closed set $\hat{\mathcal{Y}}$, i.e.

$$\hat{y}^f \in \underset{\check{y} \in \hat{\mathcal{Y}}}{\arg\min} \|\check{y} - \hat{y}^d\|$$

Note that if $\hat{\mathcal{Y}}$ is convex and the considered norm is strictly convex (e.g. the Euclidean norm), then the projection $\hat{y}^f$ of $\hat{y}^d$ is unique; thus, $\text{sat}_{\hat{\mathcal{Y}}}$ is a well-defined mapping. In general, this

strategy does not preserve the direction of $\hat{y}^d$ though, i.e. there is no guarantee that $\hat{y}^d$ and $\hat{y}^f$ are colinear. In the case where this property is desirable, then the following "directionality preserving" definition could to be preferred:[6]

$$\hat{y}^f \in \underset{\check{y}\in\hat{\mathcal{Y}}\cap(\mathbb{R}\hat{y}^d)}{\arg\min} \|\check{y}-\hat{y}^d\|$$

The bottom line of this discussion is that the definition of $\text{sat}_{\hat{\mathcal{Y}}}$ is not unequivocal. The most cautious strategy is probably to define this mapping in accordance with some in-depth study of how the mismatch between $\hat{y}^d$ and $\hat{y}^f$ impacts the rest of the control scheme.

6.2 The linear parameter varying (LPV) case

In this section, we extend the framework of the study by allowing $H(\cdot)$ to depend on a parameter vector $\theta \in \Theta$. The input/output relationship becomes

$$y = H(\theta; u) =: A(\theta)u + b(\theta) \quad \text{with} \quad u \in \mathcal{U} \tag{6.23}$$

for some mapping $\theta \mapsto b(\theta) \in \mathbb{R}^p$ and $\theta \mapsto A(\theta) \in \mathbb{R}^{p\times m}$. Vector θ can gather time t, physical parameters, endogenous/exogenous signals, etc.

Two engineering examples are first introduced to motivate the study. Then, it is shown that they can be captured via a single model that is treated analytically by implementing the inversion strategy described in the previous section using θ as a parameter. A discussion on the continuity of the solution wrt θ ends this chapter.

6.2.1 Two motivating examples

The hydraulic radial piston motor Consider a radial piston motor equipped with three pistons as depicted on Fig. 6.7.[7] The driving torque γ [N.m] is the sum of the individual torques γ_k resulting from the forces exerted by each of the three came rollers on the cameshaft, i.e.

$$\gamma = \sum_{k=1}^{3} \gamma_k.$$

Each elementary torque γ_k depends on both the pressure p_k [bar] in the k-th piston and the angular position between this piston axis and the cameshaft. This can be modeled as follows:

$$\gamma_k = g_k(\theta)p_k,$$

where θ [rad] is the angular position of the crankshaft, and $g_k(\cdot) : [0, 2\pi] \to \mathbb{R}$ [N.m.bar^{-1}] results from geometrical consideration taking the motor architecture and the cam profile into account. In the sequel, we assume that $g(\cdot)$ reads:

$$g_{pm}^{\intercal}(\theta) = \sqrt{\frac{2}{3}}\left[\sin(\theta) \quad \sin(\theta+\tfrac{2\pi}{3}) \quad \sin(\theta-\tfrac{2\pi}{3})\right].$$

[6] Note that the set $\hat{\mathcal{Y}}\cap(\mathbb{R}\hat{y}^d)$ might be empty, depending on $\hat{y}^d$ and $\hat{\mathcal{Y}}$. In this case, the "less bad" direction could be computed before hand.

[7] Note that a larger number of pistons can be treated using the methodology exposed in this subsection.

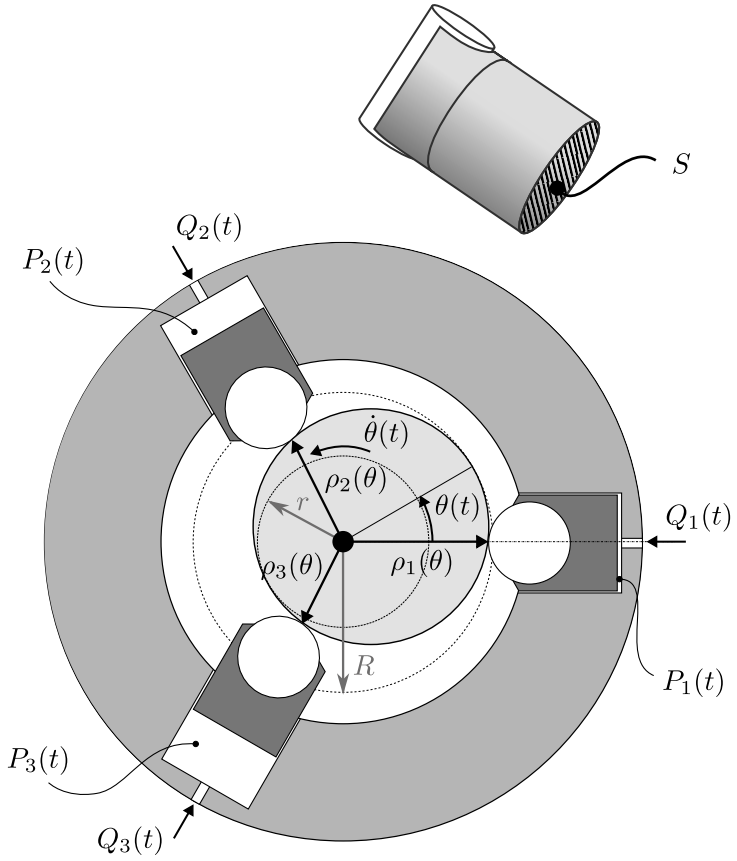

Figure 6.7: Radial hydraulic motor composed of three pistons. *Read $p_{1,2,3}$ (lower-case) instead of $P_{1,2,3}$ (upper-case).*

By neglecting the pressure dynamics, let us assume that p_k can be instantaneously set to either a high value $\overline{p}$ or a low value $\underline{p}$ of the pressure distribution system by way of the binary control signal opening or closing the valves controlling the fluid volume in the k-th cylinder. In this case, the pressure vector $p \in \{\underline{p}, \overline{p}\}^3$ can be considered as the (virtual) control input vector. This discussion can be summarized by the following equation, which captures the input/output relationships of the motor:

$$\gamma = g_{pm}^{\mathsf{T}}(\theta) p.$$

Just like for the electronic inverter, a PWM strategy can be implemented so that the averaged output torque (over a given period of time T [s]) can be controlled by means of the average input pressures. Assuming that T is sufficiently small for $t \mapsto \theta(t)$ to be considered constant over a period of time, the average I/O relationship is as follows:

$$\int_{t-T}^{t} \gamma(\tau) \mathrm{d}\tau = g_{pm}^{\mathsf{T}}(\theta(t)) \int_{t-T}^{t} p(\tau) \mathrm{d}\tau.$$

The integral on the left-hand side is controlled by the integral on the right-hand side, that is the new input. Comparing this equation with the previous one, we conclude that averaging via a PWM strategy keeps the I/O relationships unchanged, but enlarges the input space from $\{\underline{p}, \overline{p}\}^3$ to $[\underline{p}, \overline{p}]^3$.

Table 6.1: How (6.25) captures the considered models of the piston motor and the inverter.

	$u(t)$	$y(t)$	$\underline{u}$	$\overline{u}$
Piston motor	$\int_{t-T}^{t} p(\tau)\mathrm{d}\tau$: averaged input pressures	$\int_{t-T}^{t} \gamma(\tau)\mathrm{d}\tau$: averaged torque	$\underline{p}$	$\overline{p}$
Inverter	$d(t)$: duty cycles	$u_q(t)$: coordinate q of the averaged voltage $u(t)$	$\mathbf{0}_3$	$\mathbf{1}_3$

The inverter in the $dq0$ coordinates The desired output voltage of 3-phases inverter (see Chap. 5) is often expressed in the so-called $dq0$ coordinates,[8] which are obtained via $u_{dq0} = P^{-1}(\theta)u$ where $P(\theta)$ reads:

$$P(\theta) = \sqrt{\frac{2}{3}} \begin{bmatrix} \cos(\theta) & -\sin(\theta) & 1/\sqrt{2} \\ \cos(\theta - 2\pi/3) & -\sin(\theta - 2\pi/3) & 1/\sqrt{2} \\ \cos(\theta + 2\pi/3) & -\sin(\theta + 2\pi/3) & 1/\sqrt{2} \end{bmatrix}. \tag{6.24}$$

In the case of the star-connected inverter, the relationship between the averaged signals u_{dq0} [V] and d reads[9]

$$u_{dq0} = P^{-1}(\theta)Hd = \sqrt{\frac{2}{3}} \begin{bmatrix} \cos(\theta) & \cos(\theta - 2\pi/3) & \cos(\theta + 2\pi/3) \\ -\sin(\theta) & -\sin(\theta - 2\pi/3) & -\sin(\theta + 2\pi/3) \\ 0 & 0 & 0 \end{bmatrix} d = \begin{bmatrix} g^\intercal(\theta) \\ g^\intercal(\theta + \pi/2) \\ \mathbf{0}_3^\intercal \end{bmatrix} d$$

For a synchronous electrical motor, the component of foremost importance is u_q, as it drives the current i_q which is proportional to the electrical torque exerted by the motor.[10] This suggests that u_q should be considered as the output, thus leading to the following input-output model:

$$u_q = g_{em}^\intercal(\theta)d \quad \text{with} \quad g_{em}^\intercal(\theta) = -\sqrt{\frac{2}{3}} \begin{bmatrix} \sin(\theta) & \sin(\theta - \frac{2\pi}{3}) & \sin(\theta + \frac{2\pi}{3}) \end{bmatrix}.$$

Inverting this relationship means computing the duty-cycle vector d such that $d \in \mathcal{D}$ holds, and u_q has the desired value.

6.2.2 Solution for $A(\theta) = g^\intercal(\theta)$ and $\mathcal{U} = [\underline{u}, \overline{u}]^3$

As made explicit by Tab. 6.1, the next specialization of (6.23) is general enough to capture the two examples exposed in the previous subsection:[11]

$$y = A(\theta)u \quad \text{with} \quad A(\theta) = g^\intercal(\theta) \quad \text{and} \quad u \in \mathcal{U} = [\underline{u}, \overline{u}]^3, \tag{6.25}$$

with

$$g^\intercal(\theta) = \sqrt{\frac{2}{3}} \begin{bmatrix} \cos(\theta) & \cos(\theta - \frac{2\pi}{3}) & \cos(\theta + \frac{2\pi}{3}) \end{bmatrix}. \tag{6.26}$$

Using θ as a parameter, the implementation of the methodology of this chapter leads to an analytical expression of the two fundamental sets associated with the inversion of (6.25).

[8] Also called "Concordia + Park" transformation.

[9] As in Chap. 5, notation are lighten by making mean values implicit.

[10] Provided that the coupling term $L\omega i_d$ can be canceled out.

[11] Up to a change of origin of θ and the exchange of the last two components of g.

Lemma 6.7. *Given the input–output relationship in* (6.25) *with* (6.26). *Pick any* $\theta \in [0, 2\pi[- \pi/6$ *and define* $k_\theta \in [\![0, 5]\!]$ *and* $r_\theta \in [-\pi/6, \pi/6[$ *such that* $\theta = r_\theta + k_\theta \pi/3$ *holds. Let*

$$C := \begin{bmatrix} 0 & 0 & -1 \\ -1 & 0 & 0 \\ 0 & -1 & 0 \end{bmatrix}. \tag{6.27}$$

Then, it holds:

$$\mathcal{Y}(\theta) = \overline{y}(r_\theta)[-1, 1] \quad \textit{with} \quad \overline{y}(r_\theta) := \sqrt{\frac{2}{3}}(\overline{u} - \underline{u}) \cos(r_\theta) \tag{6.28}$$

$$\begin{aligned}(H(\theta)|\mathcal{U})^+(y) =& C^{-k_\theta} \left(P_1(r_\theta)\, y \right. \\ &\left. + P_{2:3}(r_\theta) \left\{ \hat{u}_{2:3} : \mathbf{1}_3 \underline{u} - P_1(r_\theta) y \leq P_{2:3}(r_\theta) \hat{u}_{2:3} \leq \mathbf{1}_3 \overline{u} - P_1(r_\theta) y \right\} \right). \end{aligned} \tag{6.29}$$

Proof. See Appendix B.1. □

6.2.3 On continuity wrt θ and the existence of general expression of $P(\theta)$

Lem. 6.7 shows that the methodology outlined in this chapter can be parameterized by θ. A natural question is then how the obtained sets $\mathcal{Y}(\theta)$ and $(H(\theta)|\mathcal{U})^+(y)$ are affected by this parameter. In particular, what type of continuity of $\theta \mapsto \mathcal{Y}(\theta)$ can be expected ?[12] If those questions go beyond the scope of this manuscript, a glimpse of the underlying difficulties is now offered around the subquestion of the continuity of $\theta \mapsto P(\theta)$. Recall that $P(\theta)$ decomposes the input space and is a key ingredient to arrive at the expression of $\mathcal{Y}(\theta)$ in closed-form.

Obstruction to the construction of continuous $P(\cdot)$ Consider the linear, constant rank and single output case

$$H(\theta) = A(\theta) = g^\intercal(\theta)$$

for some *nonvanishing* continuous mapping $g : \Theta \to \mathbb{R}^m \setminus \{\mathbf{0}\}$, that not necessarily coincides with the map defined in (6.26). For $m = 2$, one can define P as follows:

$$P(\theta) = \frac{1}{\|g(\theta)\|} \begin{bmatrix} g_1(\theta) & -g_2(\theta) \\ g_2(\theta) & g_1(\theta) \end{bmatrix}, \tag{6.30}$$

so that $P^\intercal(\theta)P(\theta) = \mathbf{I}_2$ and $g^\intercal(\theta)P(\theta) = \begin{bmatrix} \|g(\theta)\| & 0 \end{bmatrix}$, so that $P(\theta)$ is an orthogonal matrix adapted to $\mathrm{Ker}\,\{g^\intercal(\theta)\}^\perp$. In this case, observe that P inherits continuity from that of g. Implicitly, this has been achieved by decomposing P as $\Phi \circ g$ where *continuous* mapping $\Phi : \mathbb{R}^2 \setminus \{\mathbf{0}\} \to \mathbb{R}^{2\times 2}$ reads

$$g \mapsto \Phi(g) = \frac{1}{\|g\|} \begin{bmatrix} g & \varphi_2(g) \end{bmatrix} \quad \text{with} \quad g \mapsto \varphi_2(g) = \begin{bmatrix} -g_2 \\ g_1 \end{bmatrix}.$$

This is in contrast to the case in which $m = 3$ for which an analogous continuous expression of Φ cannot be derived. Let us prove this assertion. Without loss of generality, first assume that $\|g(\theta)\| = 1$ for all θ.[13] This allows to restrict the domain of Φ to $\mathbb{S}^2$. Then, observe that if a suitable Φ exists, then it can be defined as follows:[14]

$$\Phi(g) = \begin{bmatrix} \Phi_1(g) & \Phi_2(g) & \Phi_3(g) \end{bmatrix} \quad \text{with} \quad \Phi_1(g) = g$$

[12] See [AF09, Chap.1] for the notion of continuity for set-valued mappings.

[13] Any u solving $y = g^\intercal u$ can be recovered from the solution $\hat{u} = \|g\| u$ of $y = \hat{g}^\intercal \hat{u}$ where $\hat{g} = g/\|g\| \in \mathbb{S}^2$, provided that g is non vanishing.

[14] By "suitable", it is meant that $P(\theta) = (\Phi \circ g)(\theta)$ is orthogonal and adapted to $\mathrm{Ker}\,\{g^\intercal(\theta)\}^\perp$, for all θ.

and such that

$$\Phi_i^\intercal(g)\Phi_j(g) = \begin{cases} 1, & (\text{if } i = j) \\ 0, & (\text{otherwise}) \end{cases} \tag{6.31}$$

holds for all $i, j \in [\![1,3]\!]$ and for all $g \in \mathbb{S}^2$. Geometrically, this means that columns of $\Phi_{2,3}(g) = \begin{bmatrix}\Phi_2(g) & \Phi_3(g)\end{bmatrix}$ form an orthonormal basis of the tangent space of $\mathbb{S}^2$ at g. Unfortunately, such a mapping $\Phi_{2,3}$ cannot be continuous. Indeed, the so-called "hairy ball theorem" states that there is no nonvanishing continuous tangent vector field on $\mathbb{S}^n$ if n is even [BG05, p.77], i.e. for any continuous mapping $\Phi_{2,3}$ such that $\Phi_1^\intercal(g)\Phi_{2,3}(g) = g^\intercal\Phi_{2,3}(g)$ is identically null, there exists $g_0 \in \mathbb{S}^2$ such that $\Phi_{2,3}(g_0) = \mathbf{0}$. This implies $\Phi_k^\intercal(g_0)\Phi_k(g_0) = 0, (k \in [\![2,3]\!])$, so that (6.31) cannot hold for all $g \in \mathbb{S}^2$. This proves that, for $m = 3$, there is no continuous Φ leading to a suitable $P = \Phi \circ g$. This example shows that for some cases (e.g. linear, constant rank, single output and odd number of inputs), P cannot be constructed from the entries of A in a continuous way, as it is done in (6.30).

A workaround in the non surjective case If $g(\cdot)$ is continuous and $P(\cdot)$ must also enjoy this property, then the previous obstruction can be avoided if $g : \Theta \to \mathbb{S}^2$ is not surjective, though. For instance, consider the case where $m = 3$ and assume that there exists $g_0 \in \mathbb{S}^2$ such that $g(\theta)$ is distinct from $\pm g_0$ for all $\theta \in \Theta$. Subsequently, define $\Phi_{2,3}$ as follows:

$$\Phi_1(g) = g, \quad \Phi_2(g) = \frac{g_0 \wedge g}{\|g_0 \wedge g\|}, \quad \Phi_3(g) = \frac{g \wedge \Phi_2(g)}{\|g \wedge \Phi_2(g)\|}, \tag{6.32}$$

where $\wedge$ is the usual cross product. In this case, we can verify that (i) $\Phi : \mathbb{S}^2 \setminus \{\pm g_0\} \to \mathbb{R}^{3\times 3}$ is continuous and (ii) (6.31) is satisfied for all $i, j \in [\![1,3]\!]$ and for all $g \in \mathbb{S}^2 \setminus \{\pm g_0\}$. When g is continuous, this in turn proves that $\theta \mapsto P(\theta) = (\Phi \circ g)(\theta)$ is continuous on Θ and is an orthogonal matrix adapted to $\text{Ker}\,\{g^\intercal(\theta)\}^\perp$. Note that $P(\theta)$ given by (6.24) can be constructed in this manner by selecting $g_0 = \mathbf{1}_3/\sqrt{3} \in \mathbb{S}^2$, i.e.

$$\Phi_2(g) = \frac{g_0 \wedge g(\theta)}{\|g_0 \wedge g(\theta)\|} = -\sqrt{\frac{2}{3}}\begin{bmatrix}\sin(\theta) \\ \sin(\theta - 2\pi/3) \\ \sin(\theta + 2\pi/3)\end{bmatrix}, \quad \Phi_3(g) = \frac{g(\theta) \wedge \Phi_2(g(\theta))}{\|g(\theta) \wedge \Phi_2(g(\theta))\|} = \frac{1}{\sqrt{3}}\begin{bmatrix}1 \\ 1 \\ 1\end{bmatrix}$$

where $g(\theta)$ reads as in (6.26). In fact, $g(\theta) \in \mathbb{S}^2 \setminus \{\pm g_0\}$ holds for all $\theta \in [0, 2\pi[$.

Universal expression of P The construction of P as $\Phi \circ g$ is motivated by the requirement for the continuity of P. As a byproduct, this decomposition gives a universal expression of P, in the sense that such a matrix is not only suitable for all θ but also for any definition of $g(\cdot)$, up the discussion on the requirement of nonsurjectivity. This has obvious advantages when a new expression of g must be considered during operating conditions, i.e. for adaptive control.

6.3 Conclusions

As a summary of this chapter, we recall the following essential messages:

- For input constrained and affine systems, a relevant control problem is to derive expressions of the output feasible set $\mathcal{Y}$ as well as the pre-image $(H|\mathcal{U})^+(y)$ of any given feasible output $y \in \mathcal{Y}$, see Prob. 6.1.
- Decomposition of the input and output sets according to the fundamental subspaces

of linear part of H, as well as implementation of the Fourrier-Motzkin algorithm in the case of polyhedral input sets, allow to express both $\mathcal{Y}$ and $(H|\mathcal{U})^+(y)$ in closed-form, see (6.17) and the subsequent developments.

- From those results, a controller can be readily derived via mirror construction of the underlying decomposition of the system, see Fig. 6.4.
- If the methodology can be implemented verbatim in the case of parametric dependency of H, continuity of the solution wrt to the parameters can be challenged, see Sec. 6.2. Workarounds exist for some physically relevant problems.

6.4 Bibliographical notes

Existing works

Relevant references to the topic of this chapter can be found in different fields in the literature. This section follows this partitioning.

Model Predictive Control (MPC), computational geometry and optimization The equivalence between the inner and outer descriptions of a polytope, that is, the V-representation and the H-representation, respectively, is a nontrivial theorem usually attributed to Weyl and Minkowski, see e.g. [Gal08, Th.4.7]. Algorithms that construct the outer description from the inner description have been outlined in [JT13, Chap.5]. This problem is occasionally called facet enumeration [JT03]. See also [De +08, Sec.1.1] for a nice didactical introduction to this last topic. The fact that $H(\mathcal{U})$ equals $\text{co}\left\{H(u^{[1]}),\dots,H(u^{[v]})\right\}$ if $\mathcal{U} = \text{co}\left\{u^{[1]},\dots,u^{[v]}\right\}$ is proved in e.g. [Gal08, Prop.4.2], see (6.20).

For a concise and didactical presentation of the Fourier-Motzkin algorithm, the reader is referred to [BT97, Sec.2.8]. A more in-depth treatment is proposed in [Zie95, Chap.1]. Methods for detecting the redundancy of inequalities arising at each step are reviewed in [Zie95, p.48] and [Kar+83], see also [Tøn03, Appendix B]. For a guide to historical sources, one can consult [Sch11, Notes on Sec.12.2], with references to the original papers by Fourier, Dines, and Motzkin.

Nice introduction and general results on polyhedra can be found in [Gal08, Chap.4]. See also [BM08, Prop.3.28] for a short recap of basic operations w.r.t which the class of polyhedral sets is closed. Note also that a freeware dedicated to computation related to polyhedra has been developed by Michael Joswig, Ewgenij Gawrilow and other contributors [GJ00; GJ]. For a more in-depth treatment of polyhedra, including the particular case of zonotopes, see [Zie95].

The projection of points on sets, discussed in the paragraph dedicated to the unfeasible case, is addressed in [BV04, Sec.8.1]. Interestingly, the analytical expression of this projection can be found in this reference in the case where $\hat{\mathcal{Y}}$ is a half plan or a hyperrectangle. For general polyhedral sets, computing the projection boils down to solve linear program.

Image of a polyhedron via a linear map associated with *a full column rank matrix* is given in [MB76] and proved in [Ker01, p.47]. Note that the result is given as the intersection of a linear set and an outer described polyhedron and not as a usual outer representation. As shown in this chapter, the general case where the mapping is not assumed to be injective leads to projection of polyhedron. The dimension of this projection is discussed in [BO98]. In addition to the Fourier elimination and vertex enumeration (in the case of polytope) outlined in this section, two other classes of projection methods exist: block elimination and gift-wrapping

approaches, see [JKM08] and [Jon05, Sec. 2.1] for details and references. Note that the correspondence between parametric linear program and projection of polyhedron is exhibited in [JKM08].

Robotic In the field of robotics, the topic of this chapter is related to the so-called "inverse kinematics" problem. A typical illustration of this problem arises when controlling a mechanical arm composed of several joints actuated by motors [Whi69; Nen89]. Typically, the goal is to let the arm's hand track a given trajectory in coordinate axes that are convenient for the operator, i.e. Cartesian coordinates are the most frequently used. The vector x of these coordinates is related to the motor positions by the "direct kinematics equation" $x = f(\theta)$, where θ gathers the angular joint positions. In this relationship, x is the output and θ is the input so that the control inverts f. This task is typically involved because (i) f is usually complex and (ii) a smooth inverse of f is highly desirable to facilitate the tracking of θ via the motors. For all those reasons, the most wide-spread technique uses the variational version of the above equation, that is

$$\delta_x = Df(\theta)\delta_\theta \tag{6.33}$$

called "differential kinematics equation" relating the infinitesimal displacements δ_x and δ_θ via the jacobian Df evaluated at θ [Lie77]. From a given angular vector θ, the angular increment δ_θ required to perform an incremental displacement δ_x of the hand arm is obtained via any right inverse of the matrix $Df(\theta)$. See also [Lie77, Fig. 2] for an example of the overall control scheme. For a redundant manipulator, the dimension of x is smaller than the dimension of θ so that $Df(\theta)$ is a noninjective map. This problem is similar to the LPV case outlined in this chapter: Variable correspondances read $\delta_x = y$, $\delta_\theta = u$ and $H(\theta; u) = Df(\theta)u$, but $\mathcal{U} = \mathbb{S}^m$ is not polytopic. An important issue is driving θ via δ_θ away from the singularities of $Df(\theta)$. See [CSE94] for an example of how this problem can be addressed by means of SVD.

Note that the inversion of $x = f(\theta)$ has also been investigated head-on, adopting a global perspective. Appropriate mathematical tools for this task comes from mathematical field of topology. See [Bur88; Bur89; Got86] for pioneer works and e.g. [Mic09; EMW14; DSB96] for more recent references. See also [KH83] for a comparison between local and global inversions.

The solution set $\mathcal{S} = H^+(y) \cap \mathcal{U}$ is seldom explicitly computed, though. Instead, one identifies a particular u in $\mathcal{S}$ based on a given criterion. The most common strategies are (i) solving the optimisation problem

$$\min_{u \in \mathcal{S}(y)} J(u), \tag{6.34}$$

(ii) considering an additional linear equality constraint $A_a u = y_a$, such that the vertical concatenation of A and A_a gives an invertible matrix [Bai85; Ser89] and (iii) adding a vector in $u_\perp \in \mathrm{Ker}\,\{A\}$ to any particular solution $u_p \in \mathcal{S}$ [Lie77]. Clearly, all those methods are equivalent, in the sense that any point in $\mathcal{S}(y)$ can be obtained by appropriately select the parameters (i) J, (ii) A_a, y_a or (iii) $u_\perp$. Note that early contributions use pseudoinverse to compute analytical solutions of (i) when $\mathcal{U} = \mathbb{R}^m$ [KH83; Whi69].

Control allocation Control allocation, which is discussed in the next chapter, is yet another research field for which the computation of the feasibility set $\mathcal{Y}$ and the solution set $\mathcal{S}$ is also of particular interest. In this context, y is often denoted by τ^d and corresponds to the overall actuation effort (moment, forces, etc.) computed using a higher control unit. Control allocation involves distributing τ^d among the actuators, that is, finding $u \in \mathcal{U}$ such that $\tau^d = H(u)$. Observe that both control allocation and kinematics problems amount to partially invert the causal chain from the input to the output of the system. However, what is inverted in robotics

is kinematics (at the end of the causal chain), whereas control allocation focuses on the actuation subsystem (at its beginning of the causal chain).

In the control allocation literature, several heuristic methods well surveyed in [Bor96; JF13; ODB11; Enn98; Sad+19] have been proposed to deal with (6.34) in the particular case where $\mathcal{U}$ is a hyperrectangle.

(a) The starting point is the analytical solution obtained in the particular case where $\mathcal{U} = \mathbb{R}^m$ and $J(u) = (u - u_p)^\intercal W(u - u_p)$ hold for some $u_p \in \mathbb{R}^m$, that is the solution $u^\star$ obtained via the *weighted pseudoinverse* of A translated via u_p. To comply with the actuation limits of $\mathcal{U}$, a rule of thumb is to define W to penalize the entries u_i that are more likely to saturate.

(b) *Daisy chain* and *cascaded generalized inverse* are both iterative techniques. At each step, the unsaturated entry u_i is modified to compensate for the saturated ones, until the overall vector u (hopefully) belongs to $\mathcal{S}$, see [VB94] and [Ada+94, p.108]. As shown in [BD95a], neither (a) nor (b) guarantees that, for all feasible $y \in \mathcal{Y}$, an admissible solution $u \in \mathcal{S}(y)$ can be obtained. This is in contrast with the forthcoming group (c) of methods.[15]

(c) If $u^\star$ does not belong to $\mathcal{U}$, *direct allocation* aims preserving the direction of y by scaling down this vector via $\alpha > 0$ until $Bu = \alpha y$ holds [Dur93].[16] Several ad-hoc (sometimes heuristic) algorithms have been proposed to achieve this non-trivial task, see the contributions of [Dur93; Dur94; Dur01] outlined in [Bod02, §2 II-C]. It was subsequently recognized that this problem can be cast into a linear program [Bod02, Sec. IV-B]. Referring to (6.34), if the obtained solution u is feasible, let us stress that it is not optimal. Hence, none of these three methods leads to a complete solution of (6.34).

This motivates the derivation of the analytical solutions of (6.34), which depends on y in a piecewise affine manner when J is linear or quadratic. Along this line of research, an important contribution to the application of control allocation are the thesis [Tøn03; Spj08] and other related works surveyed in [JF13, Sec. 2.2.5], among which is the MATLAB toolbox [Her+13]. This is an important point of connection with the optimization literature. In this respect, see the already cited reference [JKM08].

In the control allocation context, the feasible set $\mathcal{Y}$ is sometimes called the "atteignable set", or the "atteignable moments" for aircraft control. When $y \in \mathbb{R}^3$ and $\mathcal{U}$ is an hyperrectangle, ad-hoc algorithms to compute $\mathcal{Y}$ have been proposed, together with the solution of methods (c), again see the contributions of [Dur93; Dur94; Dur01] outlined in [Bod02, §2 II-C].

Previous studies have focused on aeronautics and aerospace control. The literature on ships and underwater vehicles is yet another source of methods for control allocation, often referred to as "thrust allocation" in this context. Using the notations of [FJ06], where this research field is well-surveyed, the allocation problem is associated with the equation $\tau = B(\alpha)u$. If α has a constant value, the problem is treated in Subsec. 6.1. Otherwise, it corresponds to the LPV problem outlined in Subsec. 6.2 only apparently. In this case, corresponding to vessels equipped with azimuth thrusters, not only the actuator command vector u but also the azimuth angle vector α are to be determined. Therefore, in addition to the quest for optimality, a important challenge is to control α to avoid rank loss of $B(\alpha)$. SVD can be used for that purpose, see [Sør97].

[15] Note that the (very misleading) term "optimal" is sometimes used to distinguished method enjoying this property (for all feasible $y \in \mathcal{Y}$, an admissible solution $u \in \mathcal{S}(y)$ can be obtained) from other "non-optimal" techniques [Bec02].

[16] As noted in [Bod02], "the implicit assumption is that directionality is an important characteristic of multivariable control systems and flight control in particular". See [Hor09; WS93] on this topic.

Rephrased existing works

Formulating the inversion problem as mirror construction of an appropriate decomposition of the system can be regarded as the added value of Subsec. 6.1 wrt the existing literature. This generalizes the analysis of Chap. 5 beyond the particular case of 3-phases inverter. Hopefully, the impact of a known obstruction on the continuity of the input change of variables (see Subsec. 6.2.3) could be useful for an audience unfamiliar with differential geometry.

We also believe that the above analysis of the literature is useful as it brings closer research fields that are often disconnected, even if they all tackle the same problem. For instance, it is remarkable that the computational geometry literature has largely been ignored in attempts to compute $\mathcal{Y}$. In addition, and after, for example, [AF09], it seems to us that the vocabulary of set-valued mapping could clarify many (sometimes unnecessarily convoluted) statements of parametric optimization problems.

Works never seen elsewhere in those terms ($\approx$ new)

The example of piston motor is exposed in [**DBT23**]. See also [**Dar+24**] for direct control of the pressure vector p, instead of its mean value, as in this chapter. See e.g. [KBL94, p.71] for the use of the inverter in the $dq0$ coordinates to controlling a 3-phases synchronous motor. Lem. 6.7 is unpublished material.

Chapter 7

Comparative study on control allocation

Contents

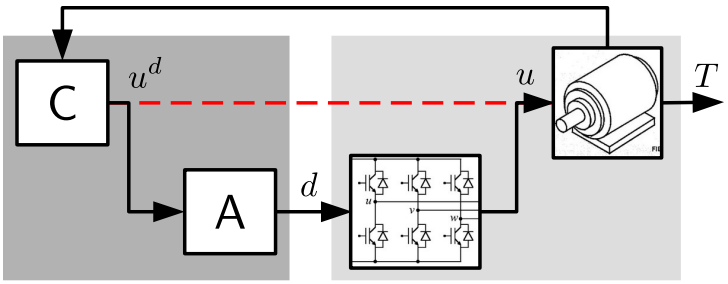

Figure 7.1: Typical architecture implemented to control a 3-phases inverter driving a three phase AC motors.

To drive 3-phases AC motors, the inverter introduced in Chap. 5 is an instrumental device. Fig. 7.1 illustrates the typical interconnection of this inverter with such a motor: The former feeds the latter with the three voltages denoted by u in Sec. 6. Hence, the inputs of the overall system are the three duty cycles whereas the output is the torque T produced by the motor.

To control this system, the classical methodology relies on the modular control scheme displayed by Fig. 7.1, where a high level control unit C achieves torque control by delivering voltage references u^d to a low level control block A. The role of the latter is to compute the duty cycles in such a way that the actual voltage u matches the reference one u^d, as represented by the dashed red line on Fig. 7.1. This is just Prob. 5.1 of Chap. 5.

Such a control architecture is a particular implementation of the one of the Control Allocation Methodology (CAM) depicted by Fig. 7.2. Compare this picture with Fig. 7.1 and observe, that the inverter plays the role of the actuation subsystem Σ_a. In this framework, the mapping A is implicitly defined via an optimisation problem selecting the optimal duty cycles among the ones achieving the voltage references. Since the reference $u^d(\cdot)$ is a time-varying signal, this problem is solved online in a quasi-continuous way.

In this chapter, the CAM is introduced. The emphasis is put on its architecture, its key features, its limitations and its mathematical foundations in terms of stability and optimality, rather than on the details of its algorithm and the gains computation. An in-depth analysis is performed on its applicability to the case of dynamical actuators, where Σ_a is governed by differential equations. Finally, the strikingly innovative approaches to this problem proposed in the last two decades are outlined, illustrated and compared with the CAM.

7.1 The classical control scheme

7.1.1 A modular control scheme

The CAM is concerned with systems which can be decomposed into a set of actuators, gathered in Σ_a, driving a plant Σ_p via the signal τ corresponding to the global actuation effort, see the right-hand side of Fig. 7.2. Specifically, the CAM tackles the case where there exist more actuators than strictly necessary to meet the control objectives. This statement is often translated in mathematical terms by the fact that there exist distinct input vector u leading to the same global actuation effort τ, i.e. τ does not uniquely define u. Thus, a secondary control objective is to distribute the global actuation effort τ among the actuators.

To tackle this problem, the CAM introduces the two-layers control scheme depicted on the left-hand side of Fig. 7.2. The so-called allocator A is a low-level control unit dedicated to the computation of the optimal distribution of the desired global effort τ^d on the actuators, i.e. A

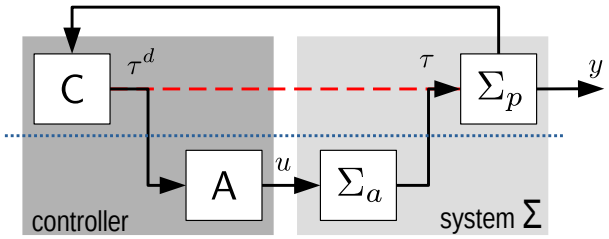

Figure 7.2: Control architecture of the classical control allocation strategy.

implements the following map

$$\Xi : \tau^d(t) \mapsto u(t) \in \arg\min_{\breve{u} \in \mathcal{U}} J(\breve{u}) \quad \text{s.t.} \quad \tau^d(t) = \Sigma_a(\breve{u}) \tag{7.1}$$

where J is a real-valued cost function. Three comments are to be made on the above expression. First, the mapping Σ_a is algebraic, i.e. the attention is implicitly restricted to static actuators. Second, $\breve{u}$ is to be selected in the set $\mathcal{U} \subset \mathbb{R}^m$. This allows to take actuation limits into account, by coding them in the definition of $\mathcal{U}$. Third, $\tau^d(\cdot)$ is a time-varying signal, as made explicit in (7.1). For this reason, and because there is no closed-form expression of $\tau^d \mapsto u(\tau^d)$ in general, the optimisation problem is solved online, frequently enough for (7.1) to be considered as valid for all t. In particular, the constraint $\tau^d(t) = \Sigma_a(u(t))$ of the optimization problem (7.1) is assumed to be always valid. Together with the $\Sigma_a(u(t)) = \tau(t)$, this leads to:

$$\tau^d(t) = \tau(t). \tag{7.2}$$

This equality is the corner stone of the CAM. It is graphically represented by the dashed red line on Fig. 7.2.

The main benefits of the CAM are now outlined:

- Modular control scheme: Instead of dealing with the full problem of controlling Σ head-on, the CAM breaks down complexity of the control design by associating a control unit to each of the component of the system. The control distribution, performed by A, is separated from the regulation task achieved via C. The modular control scheme thus obtained has numerous advantages. This first one is the simplicity of the controller synthesis. Indeed, A is designed disregarding not only the dynamics of the plant but also how reference τ^d has been generated. If A operates properly, then equality $\tau = \tau^d$ is valid. Thus, the high-level controller C can consider τ as the (virtual) control variable, disregarding how this signal is actually produced. The second advantage is related to fault-tolerance and reconfiguration. Indeed, it is often emphasize that, in the event of failure of a particular actuators, the allocator A is the only control unit that has to be updated, i.e. C can remain unchanged.

- Actuation limits accommodation: Virtually, any actuation limits can be considered by defining $\mathcal{U}$ appropriately, even the most complex coupling between entries of the input vector u. Historically, this feature was regarded as one of the main benefits of the CAM, see e.g. [Dur93].

- Optimality: The retained formulation of the allocator (7.1) guaranties optimality of the distribution of the global actuation effort τ, not only at the steady-state but also during transient.[1]

[1] Achieving optimality in a very simple way from the designer point of view (just defined J, Σ_a and $\mathcal{U}$ properly)

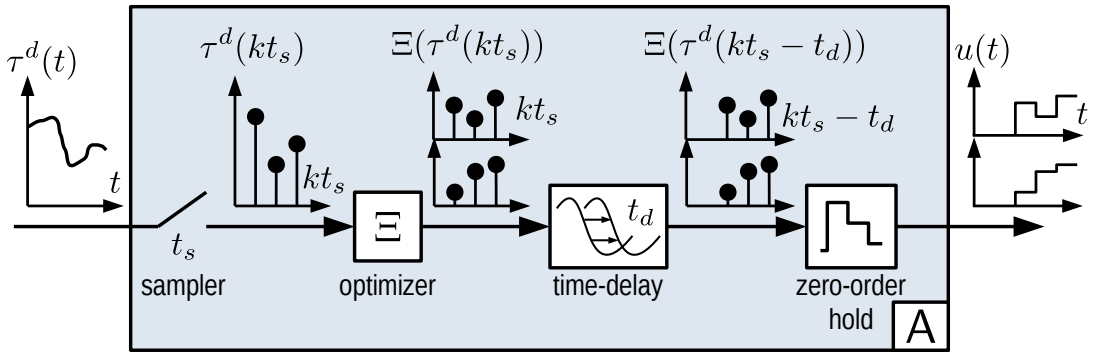

Figure 7.3: Model of the allocator A with typical shape of the involved signals. Throughout this chapter, equality $t_s = t_d$ is imposed to simplify the analysis.

Optimality and constraint satisfaction of the optimisation problem (7.1) are not always simultaneously satisfied in the literature. One often merely focuses on one of those desirable properties, disregarding the other, see the bibliographical notes at the end of Chap. 6.

7.1.2 How to make it works ?

The CAM entirely hinges on the fact that equality $\tau = \tau^d$ is valid, that is, the dashed red line of Fig. 7.2 links signals that are assumed to be equal. This assumption is the key to ensuring independence of the design of both C and A.

However, in practice, this assumption is inevitably violated because the implicit expression of A given by (7.1) is repeatedly resolved online via a sample-and-hold mechanism. To see this, let us model the allocation block A as in Fig. 7.3 where the shapes of the involved signals are also represented. From τ^d to u, signal τ^d is first sampled at a period t_s. This allows the optimization problem (7.1) to be solved with $\tau^d(t) = \tau^d(kt_s)$. A time delay of magnitude $t_d \leq t_s$ models the computation time required by the solver, whose output is connected to a zero-order hold mechanism. In general, the computational effort needed to solve (7.1) is not constant, so that t_d is time-dependent. However, to keep things simple, we consider that t_d is constant and equal to t_s. The following relationship captures the input-output behavior of A, and is valid for all $k \in \mathbb{N}$:

$$u(t) = \Xi\left(\tau^d\left((k-1)t_s\right)\right), \forall t \in [kt_s, (k+1)t_s[\tag{7.3}$$

Let us now compare $\tau(t) = \Sigma_a(u(t))$ with $\tau^d(t)$. As a preliminary step, observe that any $\tau^d(t)$ is mapped by Ξ to some vector $u(t)$ satisfying $\tau^d(t) = \Sigma_a(u(t))$, provided that the optimization problem admits solution, see (7.1). Therefore, the following identity holds:

$$\Sigma_a(\Xi(\tau^d(t))) = \tau^d(t) \tag{7.4}$$

for all $\tau^d(t)$ for which (7.1) is solvable, i.e. for all $\tau^d(t)$ in $\Sigma_a(\mathcal{U})$. In this case, one gets:

$$\tau(t) = \Sigma_a(u(t)) \overset{(7.3),(7.4)}{=} \tau^d\left((k-1)t_s\right), \forall t \in [kt_s, (k+1)t_s[\tag{7.5}$$

Using this equality and some arbitrary signal τ^d, Fig. 7.4 illustrates the relationship between τ^d and τ. Clearly, these two signals are not equal, so $\tau = \tau^d$ is violated. Let us emphasize that this conclusion depends neither on the parameter of the optimization problem associated with Ξ, that is, J and Σ_a, nor on the shape of τ^d, as soon as this signal is not constant.

is often regarded as one of the main benefits of the CAM. Perhaps this feature can be considered as the main reason

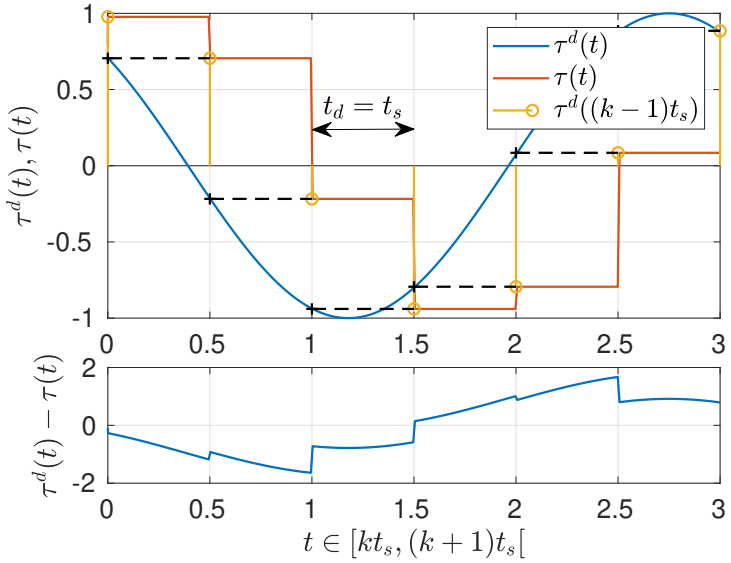

Figure 7.4: Illustration of how τ derives from τ^d for $t_s = t_d = 1$, and comparison of those two signals.

Let us now try to provide guidelines under which $\tau = \tau^d$ can be considered a reasonable assumption anyway, i.e. $\tau^d(t) - \tau(t)$ is small in magnitude.

(a) Use efficient solver to implement A: This amounts to reduce the magnitude of $t_d = t_s$. From the above discussion, this is expected to decrease the peak value of $\tau^d(t) - \tau(t)$;

(b) Slow down τ^d: The rational behind this second suggestion is that the time required to process τ^d should be small with respect to the speed of variation of this signal;

(c) Saturate τ^d to prevent unfeasible constraint: Another reason for which equality $\tau = \tau^d$ might be challenged is that τ^d can make (7.1) unfeasible. In this case, the desired global control effort cannot be achieved within the range of Σ_a and the actuation limits. To prevent this event to occur, the controller C should be designed in such a way that

$$\tau^d(t) \in \Sigma_a(\mathcal{U}) \tag{7.6}$$

is ensured at all time.[2] If Σ_a is static, recall that Chap. 6 contains the material to construct $\Sigma_a(\mathcal{U})$.

(d) Use fast actuators: When defining the optimisation problem Ξ, it has been implicitly assumed that the algebraic mapping Σ_a models the actuation system at a satisfactory level. To ensure the validity of this assumption, fast actuators shall be used so that variation of u immediately impacts τ, as coded by the constraint of Ξ.

Appart from the third point, any of the above guidelines can be interpreted as an effort to impose two distinct time scales on the resulting closed-loop system: On Fig. 7.2, signals associated with the top blocks C and Σ_p (above the blue dotted line) must behave slower than those related to the bottom blocks A and Σ_a (below the blue dotted line). If imposing this two

for the spread of this technique, even out of the control community. This is not without reminding the history of MPC, as outlined in e.g. [May14].

[2]This point of view is far from being shared in the literature, see the discussion in Subsec. 7.6.1 at the end of this chapter.

Table 7.1: Contexts of the different simulations. The first line corresponding to Fig. 7.6 is the nominal case. On each other line, only variations with respect to this nominal case are reported, e.g. for Fig. 7.7, C and Σ_a are as in the nominal case, that is smooth and static, respectively.

Fig. num.	$t_d = t_s$	C	Σ_a
7.6	0.2	smooth	static ($\alpha \to +\infty$)
7.7	1	–	–
7.8	–	aggressive	–
7.9	–	–	dynamic ($\alpha = 1$)
7.10	0.4	–	dynamic ($\alpha = 1$)
7.11	0.4	–	–

time-scales scheme does not prevent $\tau^d(t) - \tau(t)$ from being non-zero, it brings this difference close to zero and, in turn, makes equality $\tau = \tau^d$ a reasonable assumption.

The next example aims to illustrate the strategies discussed in this chapter. Simulations are performed for each of them. To better relate the different simulation contexts, the reader is referred to Tab. 7.1.

Example 7.1 (Toy example)**.** Let us introduce an academic example that is linear to keep things simple, even if the CAM applies to nonlinear systems. The quadruple defining the linear plant reads:

$$\Sigma_p : \left[\begin{array}{c|c} -1 & 1 \\ \hline 1 & 0 \end{array}\right],$$

and $m = 2$ static actuators contribute to the overall control effort according to the following model of Σ_a:

$$\Sigma_a : u \mapsto \tau = \begin{bmatrix} 1 & 2 \end{bmatrix} u.$$

Also assume that

$$\mathcal{U} = [-0.5, 0.5] \times [-1, 1]$$

In this context, the set of achievable τ is

$$\Sigma_a(\mathcal{U}) = [-0.5, 0.5] + 2[-1, 1] = [-2.5, 2.5].$$

We use the closed-loop scheme depicted by Fig. 7.2, where the dynamical behavior of the allocator A is modeled as shown in Fig. 7.3 and via (7.3). The cost function $J : \mathbb{R}^2 \to \mathbb{R}$ associated with Ξ reads

$$J(u) = \frac{1}{2} u_1^2$$

so that $u_1(t)$ is kept at zero as much as possible, i.e. the second actuator produces the entire control effort as much as it can. Fig. 7.5 illustrates the input-output relationship of Ξ, see (7.1). Besides, let $t_s = t_d = 0.2$.

The high-level controller is simply selected as a PI control law whose output is saturated to keep $\tau(t)$ within $\Sigma_a(\mathcal{U})$, i.e. controller C produces the following signal:

$$\tau^d(t) = \mathrm{sat}_{[-2.5,2.5]} \left(k_p(y_r - y(t)) + k_i \int_0^t y_r - y(s) \mathrm{d}s \right) \tag{7.7}$$

with $k_p = 2$ and $k_i = 1$. The constant reference y_r is equal to 2.

Starting from zero initial conditions, the simulation results are depicted in Fig. 7.6. A perturbation of magnitude 1 is produced at $t = 20$s. This signal is added to $\tau(t)$ at the output of Σ_a. The following comments can be made: Signals y and y_c (see the caption in Fig. 7.6) are close to each other, which indicates that if $\tau = \tau^d$ is not perfectly valid, it remains a reasonable assumption. This is confirmed by the second subplot, where one also observes that $\tau^d(t)$ remains within

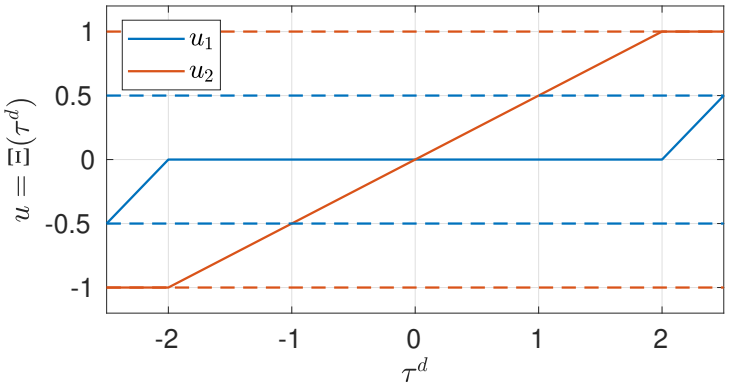

Figure 7.5: Input-output relationship of Ξ for Ex. 7.1. The horizontal dashed lines represent the actuator limits. Note that Ξ is unfeasible for $\tau^d \notin \Sigma_a(\mathcal{U}) = [-2.5, 2.5]$.

$\Sigma_a(\mathcal{U}) = [-2.5, 2.5]$. On the third subplot, it is shown that the piecewise constant input signal u is saturated appropriately by the optimization algorithm. Remarkably, $u_1(t)$ is almost always equal to zero, which is consistent with the definition of J. The beginning of the simulation is an exception in this respect. The high magnitude of $\tau^d(t)$ saturates not only u_2 but also u_1. After this first part of the simulation, $u_2(t)$ alone can cop with the requested $\tau^d(t)$ so that $u_1(t)$ returns to zero.

Remark 7.2 (On (c)). Among the guidelines listed above, the third issue is often addressed in the literature by redefining Ξ as follows:

$$\tau^d(t) \mapsto \underset{\breve{u} \in \mathcal{U}}{\arg\min}\, J(\breve{u}) + \lambda^\intercal(\tau^d(t) - \Sigma_a(\breve{u})),$$

for some *fixed* values of λ, see [Bod02]. The larger is the entries of λ, the more penalized the difference $\tau^d(t) - \Sigma_a(\breve{u})$, and thus the closer the optimal value from the satisfaction of the constraint $\tau^d(t) = \Sigma_a(\breve{u})$. Note that if λ is a decision variable of the optimization problem, then the cost function is the Lagrangian. Under certain conditions, the solution of this new problem coincides with that of the original problem (7.1). Here, by imposing (7.6), we advocate for a control scheme where any signal delivered by a high-level control unit C to a lower-level one A is *feasible*, thus preserving the strict hierarchy of the architecture. •

7.1.3 Intrinsic limitations of the approach

Apart from (c), which can be handled by dealing with the control architecture properly, any of the above guidelines lead to intrinsic limitations of the CAM:

- Inefficient solver is likely to destabilize the closed-loop system, so that the CAM is demanding in terms of computational ressources. Fig. 7.7 confirms this intuition.
- Aggressive controller C has to be avoided, so that closed-loop bandwidth induced by C is inevitably narrowed. When attempting to bypass this guideline, Fig. 7.8 shows that one can challenge the stability of the closed loop.
- Slow actuators lag the transient of τ and, in turn, challenge the equality $\tau = \tau^d$, so that fast actuation system should be preferred.

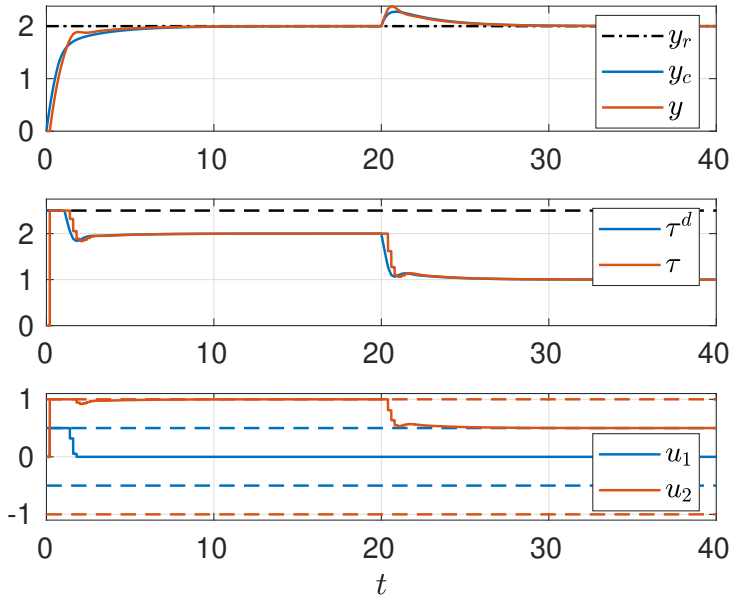

Figure 7.6: Simulation results obtained for Ex. 7.1 and using Fig. 7.2. The dashed lines indicate the saturation limits of $\tau(t)$ and entries of $u(t)$. Signal y_c on the first subplot corresponds to the chronograph obtained under the assumption that $\tau = \tau^d$ holds, that is, C directly feeds Σ_p. This signal is intended to show what is expected when implementing the CAM.

Any of the above limitations are likely to induce over-lapping of the two timescales and, in turn, to challenge equality $\tau = \tau^d$.

Note that the first two points (inefficient solver and aggressive controller) can be dealt with at the cost of increasing the computational capacity of the hardware supporting the control or decreasing the dynamical performance of the closed loop by smoothing the controller C. An other direction is exposed in the next Subsec. 7.1.4.

The last point (slow actuators) is different in nature because it is related to the system itself. This suggests that the CAM can simply be inapplicable to systems with slow actuators. Forthcoming Subsec. 7.2 is devoted entirely to this issue.

7.1.4 Continuous-time optimum-seeking

The problem underlying the CAM is considered in [Joh04] from a completely different perspective. Instead of using a numerical solver surrounded by a sample-and-hold mechanism, as shown in Fig. 7.3, the core idea is to implement the allocator A as a *continuous-time* subsystem. Equations governing the new version of A aim inducing the asymptotic convergence of the overall system toward a setpoint where the input u solves the optimization problem, i.e. $u(t) = \Xi(\tau^d(t))$ holds asymptotically. To achieve this result, two ingredients are required: First, the Lagrangian l of Ξ which is defined as follows:

$$l : (u, \lambda) \mapsto J(u) + \lambda^\intercal(\tau^d - \Sigma_a(u))$$

where λ is the vector of Lagrange multipliers and τ^d acts as a parameter. Second, a Lyapunov function V_0 ensures that the direct interconnection of C and Σ_p makes the origin an asymptotically stable equilibrium. Then, the following composite controlled Lyapunov function is introduced:

$$V(x, u, \lambda) = \sigma V_0(x) + \frac{1}{2}\|\nabla l(u, \lambda)\|_2^2$$

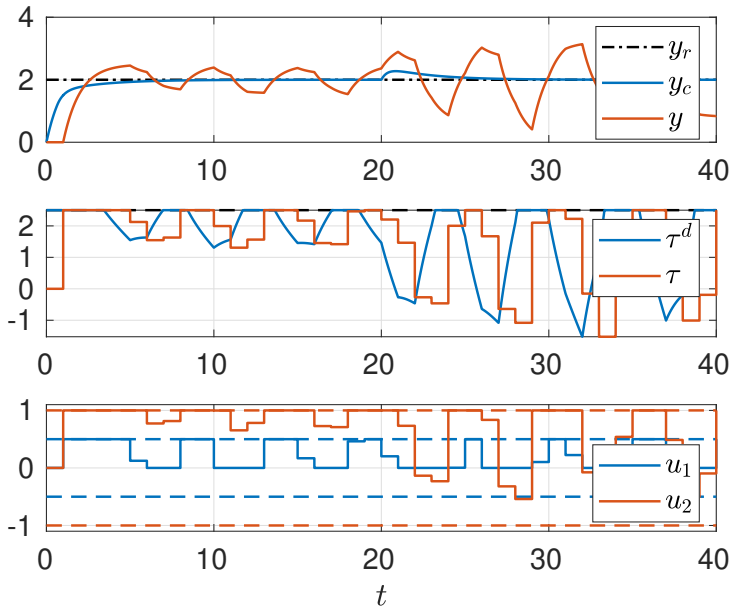

Figure 7.7: Simulation results obtained in the same context as the one of Ex. 7.1 but with $t_s = t_d = 1$ (instead of 0.2). Compare width of the steps of piecewise constant signals of the third subplot, with the analogous subplot of Fig. 7.6.

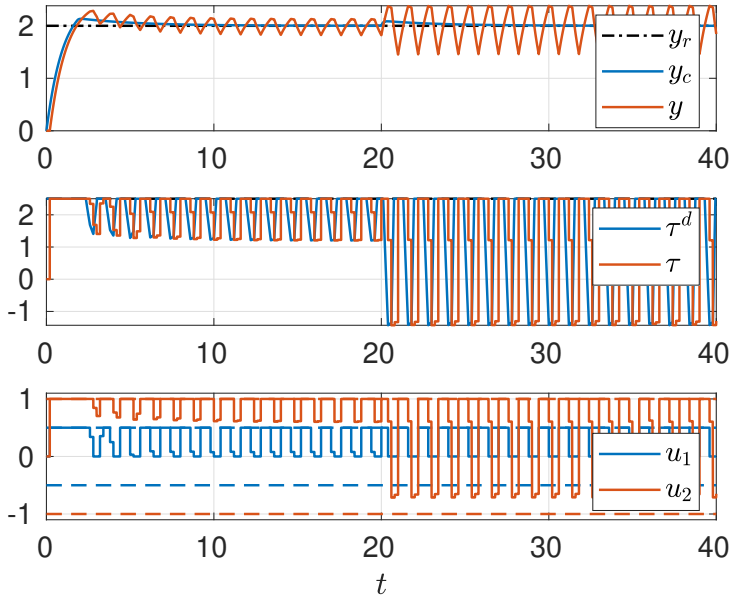

Figure 7.8: Simulation results obtained in the same context as the one of Ex. 7.1 but with a more aggressive high-level controller C: $k_p = 10$ and $k_i = 3$ (instead of $k_p = 2$ and $k_i = 1$). Compare the speed of signal y_c on the first subplot, with the analogous signal of Fig. 7.6.

for some $\sigma > 0$ together with guidelines to shape $\dot{u}$ and $\dot{\lambda}$ in such a way that $V(x(t), u(t), \lambda(t))$ tends to 0. This indeed achieves the first-order optimality condition $\nabla l(u, \lambda) = \mathbf{0}$ in an asymptotic way.

Let us now give an interpretation of the rationale behind the above methodology. Suppose that the computational resources dedicated to the numerical solver Ξ are insufficient. When implementing the CAM, the first option is (i) to enlarge t_s. However, this may challenge the stability, as shown in Fig. 7.7. Another option one may think about is (ii) to feed Σ_a with the current value of the solver when time t_s elapsed, even if the optimization algorithm has not yet converged. In this case, a mismatch exists between the optimal solution and input vector $u(kts)$. This difference could be acceptable, though. This is because the equality $\tau^d(t) = \Sigma_a(u(kt_s))$ may have reached a level of accuracy that is already satisfactory. Alternatively, this mismatch can be handled by C by treating it as a perturbation. In a sense, the methodology introduced in [Joh04] can be seen as an implementation of (ii), since C continuously updates its output without waiting for the convergence of A solving the optimization problem. Optimality $u(t) = \Xi(\tau^d(t))$ is recovered asymptotically, though, so that this method deserves the name "dynamic optimum-seeking" as coined in [JF13]. The key benefit of the approach is therefore that the separation timescale is no longer required, thus allowing for less demanding computational resources for implementing A.

Note that in doing so, the equality $\tau(t) = \tau^d(t)$ is relaxed. This only apparently opens the door to bad interaction between the upper and lower parts of Fig. 7.2. Indeed, the allocator controls these interactions via the controlled Lyapunov function V.

Remark 7.3 (Sequential design). In the CAM, the overall closed-loop behavior is shaped by intermediate designs of C and A. Independence of the individual designs is guaranteed by ensuring the validity of the equality $\tau(t) = \tau^d(t)$ (or at least (7.5)). With the methodology of [Joh04], those design step are not independent anymore but rather sequential: C is first defined and serves as the basis for the definition of A. •

7.2 Handling dynamical actuators within the CAM

Comparing Fig. 7.1 and Fig. 7.2 allows the identification of the inverter and motor with the actuator and plant, respectively. By its very nature, the inverter is an "actuator" with no dynamics. More precisely, the dynamics of the inverter is extremely fast with respect to that of the motor. Therefore, the algebraic model considered in Chap. 5 captures the behavior of the inverter accurately.

In this section, we investigate the case where the hierarchy of the timescales relevant for Σ_p and Σ_a is not so clear. The following quotation emphasizes that this problem has been recognized as a relevant direction of research by the control community working on CAM more than a decade ago:

> "A review of the constrained control allocation literature shows that the coupling effects that result from combining constrained control allocators and actuator dynamics has largely been ignored. [...] The underlying assumption of most previous work is that actuators respond instantaneously to commands." [ODB11]

The intention is to widen the applicability of the CAM. In doing so, the CAM itself is deeply revisited.[3]

[3]Up to a point where one could legitimately contest that the name CAM remains appropriated for the derived methodology.

Example 7.4 (Ex. 7.1 with dynamical actuator)**.** Let us consider that the second actuator is actually dynamic. Assume further that it is governed by a first-order linear internal dynamics characterized by the time constant $1/\alpha > 0$, that is, its transfer function reads:

$$\frac{2}{s/\alpha + 1} = \frac{2\alpha}{s + \alpha}.$$

In this case, the quadruple of Σ_a can be expressed as follows:

$$\Sigma_a : \left[\begin{array}{c|cc} -\alpha & 0 & \alpha \\ \hline 2 & 1 & 0 \end{array}\right]. \tag{7.8}$$

One can check that the DC gain $\Sigma_a^\star$ of Σ_a corresponds to the algebraic mapping $u \mapsto \tau = \begin{bmatrix} 1 & 2 \end{bmatrix} u$ considered in Ex. 7.1, so that this algebraic mapping is indeed a relevant approximation of Σ_a for large α:

$$\lim_{s \to 0^+} B_a(s\mathbf{I} - A_a)^{-1}C_a + D_a = \lim_{s \to 0^+} \begin{bmatrix} 1 & \frac{2\alpha}{s+\alpha} \end{bmatrix} = \begin{bmatrix} 1 & 2 \end{bmatrix}$$

Let us reproduce the simulation context of Ex. 7.1. The constraint of the optimization part of the allocator now reads $\tau^d(t) = \Sigma_a^\star \breve{u}$, instead of $\tau^d(t) = \Sigma_a(\breve{u})$ as in (7.1), that is,

$$\Xi_a : \tau^d(t) \mapsto u(t) \in \underset{\breve{u} \in \mathcal{U}}{\arg\min}\, J(\breve{u}) \quad \text{s.t.} \quad \tau^d(t) = \Sigma_a^\star \breve{u} \tag{7.9}$$

One gets the results depicted in Fig. 7.9. If the results may be regarded as acceptable in terms of regulation performance, equality $\tau = \tau^d$ is much more challenged than in the context where α tends to infinity, see Fig. 7.6, so that y is barely predictable from y_c. Hence, the CAM should only be considered as a coarse strategy in this context.
This conclusion is emphasized when performing new simulations with an inefficient solver. Comparing Fig. 7.10 and Fig. 7.11, one can appreciate that the sensitivity of the control to the efficiency of the solver is increased in the context of dynamical actuators, see also Fig. 7.7.

7.2.1 Inversion of the individual actuators dynamics

One of the first solutions proposed to deal with slow dynamical actuators is to overdrive them, that is, to introduce an additional control layer commanding more from the actuators so that their actual outputs are the desired values. The enriched control scheme is depicted in Fig. 7.12. This picture is derived from Fig. 7.2 as follows:

- Σ_a is decomposed as follows:

  $$\Sigma_a = \Sigma_a^\star \circ \Sigma_a^n$$

  where $\Sigma_a^\star$ is the DC gain matrix of Σ_a, so that Σ_a^n is the dynamical part of Σ_a with DC gain equal to $\mathbf{I}_m$. Such decomposition is possible whenever individual actuators have uncoupled dynamics and a well-defined DC gain[4], i.e. transfert function matrix of Σ_a^n is diagonal and related to stable dynamics.

- The new control unit C_a has been introduced in between the allocator A and the actuators Σ_a. Note that the output of the allocator has been renamed y_a^d and this signal now feeds C_a. This last mapping is responsible for canceling the lag induced by the slow actuators as much as possible.

[4] A power electronics system for which this assumption does not hold is introduced in Chap. 10.

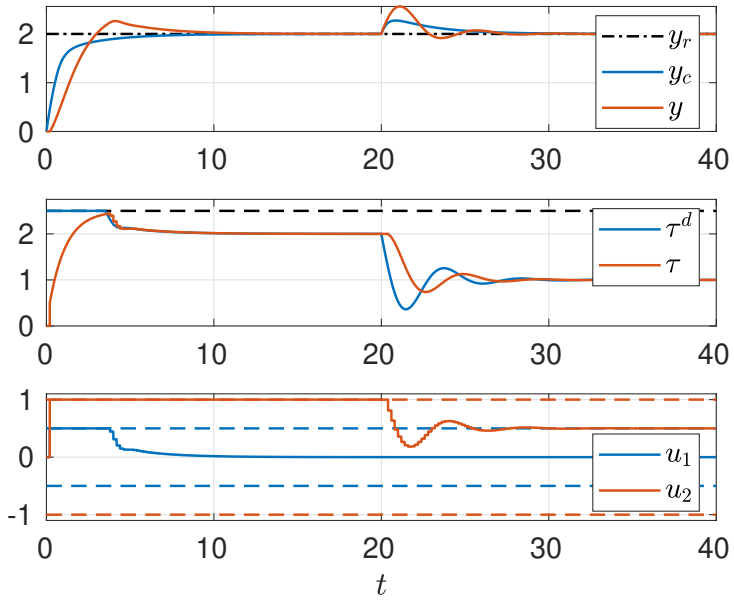

Figure 7.9: Simulation results obtained in the same context as the one of Ex. 7.1 but with dynamical actuators, as described in Ex. 7.4 and for $\alpha = 1$ so that the bandwidths of Σ_a and Σ_p are identical. Compare the settling time of τ on the second subplot with the analogous signal of Fig. 7.6. The difference between τ and τ^d induces the one between y_c and y.

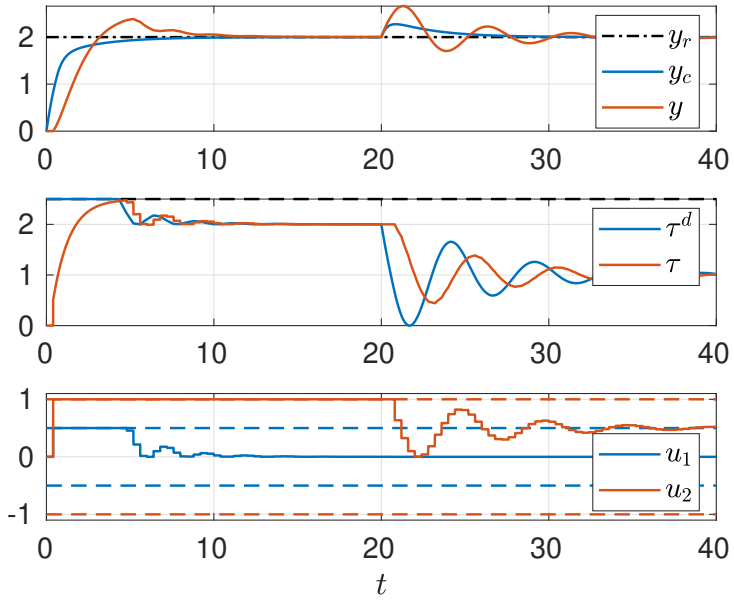

Figure 7.10: Simulation results obtained in the same context as the one of Ex. 7.1 but with $t_s = t_d = 0.4$ (instead of 0.2) and dynamical actuators, as described in Ex. 7.4 and for $\alpha = 1$. Compare each subplots with the ones of Fig. 7.9 and of Fig. 7.11 to appreciate how dynamical actuators combined with inefficient solvers impact accuracy of the CAM.

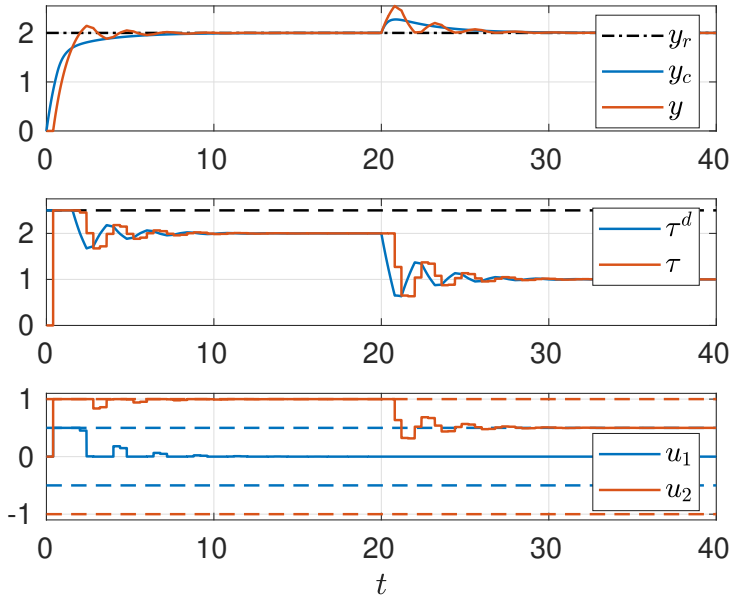

Figure 7.11: Simulation results obtained in the same context as the one of Ex. 7.1 but with $t_s = t_d = 0.4$ (instead of 0.2 as on Fig. 7.6).

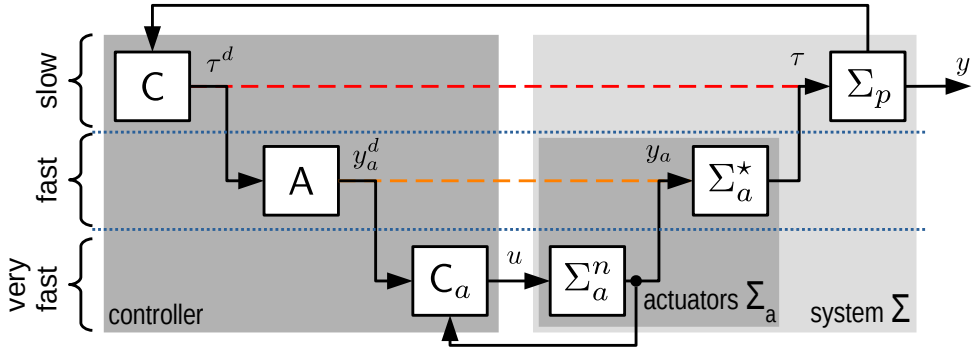

Figure 7.12: Dealing with the slow actuators by inverting their dynamics on a sufficiently large bandwidth.

Example 7.5 (Ex. 7.4 continued)**.** The mapping $\Sigma_a^\star$ is defined by $y_a \mapsto \tau = \begin{bmatrix} 1 & 2 \end{bmatrix} y_a$. The quadruple of Σ_a^n and the corresponding transfer function matrix G_a^n read:

$$\Sigma_a^n : \left[\begin{array}{c|cc} -\alpha & 0 & \alpha \\ \hline 0 & 1 & 0 \\ 1 & 0 & 0 \end{array}\right], \qquad G_a^n(s) = \begin{bmatrix} 1 & 0 \\ 0 & \dfrac{\alpha}{s+\alpha} \end{bmatrix}.$$

One can check that Σ_a is indeed the cascade of Σ_a^n feeding $\Sigma_a^\star$.

The key point is that if C_a succeeds in sufficiently accelerating the actuator responses, then the following equality can be considered an accurate approximation on which the allocator can rely:

$$y_a^d = y_a.$$

In other words, C_a aims to invert Σ_a^n. Consequently, Σ_a behaves as $\Sigma_a^\star$ *from the perspective of* A. This discussion leads to the following redefinition of the optimization part of the allocator, which is simply derived from (7.9) by replacing u by y_a^d:

$$\Xi_b : \tau^d(t) \mapsto y_a^d(t) \in \underset{\check{y}_a \in \mathcal{U}}{\arg\min}\, J(\check{y}_a) \quad \text{s.t.} \quad \tau^d(t) = \Sigma_a^\star(\check{y}_a) \tag{7.10}$$

Just as the high-level controller C ignores how τ^d is effectively produced, the allocator A disregards how actuators are driven by C_a, provided that $y_a = y_a^d$ is a reasonable assumption.

In practice, $y_a^d = y_a$ is often an unrealistic assumption, though, since they is no C_a that sufficiently accelerates the actuators. Ensuring the validity of the following equality for all $k \in \mathbb{N}$ is more reasonable:

$$y_a(kt_s) = y_a^d((k-1)t_s)$$

This equality means that the interconnection of C_a with Σ_a^n behaves as a time delay t_s.[5] In this case, τ and τ^d are not equal, but rather are related via the following relationship:

$$\tau(kt_s) = \tau^d((k-2)t_s).$$

To see this, first note that (7.3) and (7.4) read $y_a^d(kt_s) = \Xi_b(\tau^d((k-1)t_s))$ and $\Sigma_a^\star(\Xi_b(\tau^d(kt_s))) = \tau^d(kt_s)$, respectively, in this context. Then, bearing those relationships in mind, one gets

$$\tau(kt_s) = \Sigma_a^\star\left(y_a(kt_s)\right) = \Sigma_a^\star\left(y_a^d((k-1)t_s)\right) = \Sigma_a^\star\left(\Xi_b\left(\tau^d\left((k-2)t_s\right)\right)\right) = \tau^d((k-2)t_s).$$

This fact shall be taken into account in the design of C, by modelling the two lower control layers as a pure time delay $2t_s$, instead of the identity mapping.

The two continous-time approaches

The inversion of Σ_a^n can be implemented in continuous-time either via an open-loop or via a feedback strategy, as suggested by Fig. 7.12, the latter being often preferable for actuators whose model is poorly known. In the following, different controllers C_a are derived, disregarding the actuator limits. Their ability to impose equality $y_a = y_a^d$ is assessed on the same benchmark. The results are shown in Fig. 7.13 and Fig. 7.14 and briefly commented below.

Open-loop design Inverting Σ_a^n via an open-loop strategy amounts to designing C_a in such a way that the left multiplication of its transfer function matrix by Σ_a^n gives $\mathbf{I}$. One drawback of this approach is that non proper C_a arises when Σ_a^n is strictly proper. As shown in the next example, an approximated inverse can be designed, though.

[5] Note that enlarging t_s helps in achieving such a purpose.

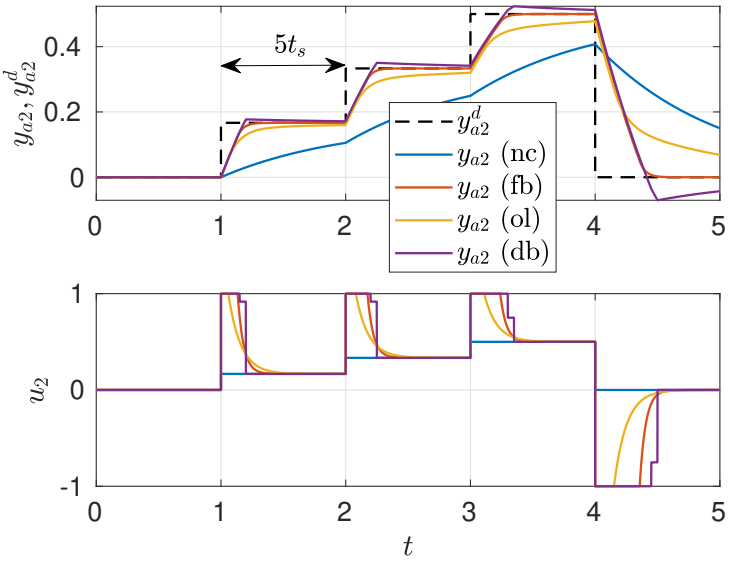

Figure 7.13: Simulation results obtained for the second dynamical actuator (see Ex. 7.4), taking its saturation into account and for different controllers, C_a: Without compensation (nc), by open-loop inversion for $\beta = 10$ (ol), with compensation by feedback for $k_a = 20$ (fb), and via a dead-beat controller (db). Observe the ability of those controllers to track y_a^d.

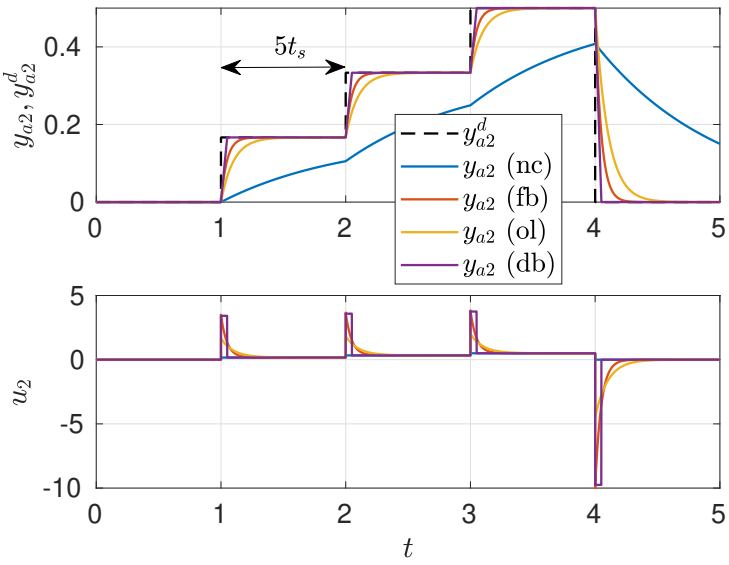

Figure 7.14: Simulation results analogous to the ones of Fig. 7.13, but in a context where the actuator is not affected by saturation limits.

Example 7.6 (Ex. 7.4 continued)**.** Let us focus on the second actuator because the first one is static. The following proper transfer function can be selected as the part of C_a that controls the dynamics of this second actuator:

$$\frac{\beta}{\alpha} \times \frac{s+\alpha}{s+\beta}$$

Indeed, for large $\beta > 0$, this lead-lag compensator can be regarded as an approximate inverse of the strictly proper transfer function $\alpha/(s+\alpha)$ of the second actuator.

It is well known that this apparently simple inversion problem hides other major shortcomings. First, this strategy is inherently fragile to uncertainties, like any open-loop control. Second, it is prone to saturate the actuators during transient, since the above statement implicitly neglects saturations by merely characterizing Σ_a^n in terms of transfer function. Third, unstable zeros of Σ_a^n lead to internal instability of C_a, unless a non-robust zero/pole cancellation is performed.

Closed-loop design Each of the drawbacks of the open-loop design listed above can be overcome (up to a certain limit) via an appropriate closed-loop control strategy.

Example 7.7 (Ex. 7.4 continued)**.** The second actuator can be controlled using the following mapping:

$$(y_{a2}^d, y_{a2}) \mapsto u_2 = \frac{k_a}{\alpha}(y_{a2}^d - y_{a2}) + y_{a2}^d$$

where $k_a > 0$ is a tuning parameter. It can be interpreted as a gain k_a/α on the output error, together with a unitary feedforward gain on y_a^d correcting the static error.

The discrete-time dead-beat strategy

In discrete-time, a popular strategy for inversion is the so-called dead-beat control. In the SISO case, recall that this design imposes on the closed-loop to behave as a finite impulse response (FIR), that is, the transfer function of the closed-loop system is a polynomial in z^{-1}. The minimal order is sought for this polynomial.

Note that the sampling time $t_a > 0$ associated with C_a may be different from t_s used by A. Typically, $t_a \ll t_s$ allows C_a to react faster than A.

Example 7.8 (Ex. 7.4 continued)**.** If u is the output of zero-order hold processing at period $t_a > 0$, then integration of the continuous dynamical equation governing the second actuator gives rise to the following difference equations:

$$\Sigma_{a2}^n : \quad y_{a2}(t) = e^{-\alpha t_a} y_{a2}(t - t_a) + (1 - e^{-\alpha t_a}) u_2(t - t_a). \tag{7.11}$$

The corresponding discrete-time transfer function reads:[a]

$$G_{a2}^n(z) = \frac{1-a}{z-a}$$

where $a = e^{-\alpha t_a} \in [0, 1[$. In this case, a deadbeat controller can be obtained using the following transfer function fed by the output error:

$$\frac{z-a}{(1-a)(z-1)}.$$

From the observation that the cascade of this transfer function with $G^n_{a2}(z)$ reads $(z-1)^{-1}$, the resulting closed-loop system reads

$$\frac{(z-1)^{-1}}{1+(z-1)^{-1}} = z^{-1}.$$

[a] With slight abuse of notations, both discrete-time and continuous-time transfer functions share the same name G^n_a. The variable s or z should resolve the ambiguity.

7.2.2 Coding the model of the actuators in the constraint of the allocator

In a nutshell, the strategy exposed in the previous subsection consists of speeding up the internal dynamics of the actuators as much as possible, and then adjusting t_s for $y_a(kt_s) = y^d_a((k-1)t_s)$ to be an accurate model of the fastest layer depicted in Fig. 7.12.

In this framework, the slowest actuator dictates the value of t_s. This approach can be regarded as conservative because the fastest actuators might very well compensate for the lag induced by the slowest actuators during the transient. In this case, the overall actuation subsystem reacts faster, and t_s is kept larger.

To implement such a control strategy, the allocator should be designed differently. The core of the methodology is exposed via the following example, which considers Fig. 7.2 instead of Fig. 7.12, i.e. the fastest control unit C_a is removed so that the allocator directly feeds the actuators, leading to equality $u = y^d_a$.

Example 7.9. Consider Fig. 7.2. The following discrete-time mapping from u to τ at the period t_s is derived by substituting t_a by t_s in (7.11) for $t = kt_s$ and bearing in mind that $y_{a1} = u_1$:

$$\begin{aligned}\tau(kt_s) &= \begin{bmatrix}1 & 2\end{bmatrix}\begin{bmatrix}y_{a1}(kt_s)\\ y_{a2}(kt_s)\end{bmatrix}\\ &= \left(\begin{bmatrix}0 & 0\\ 0 & e^{-\alpha t_s}\end{bmatrix} y_a((k-1)t_s) + \begin{bmatrix}1 & 0\\ 0 & 0\end{bmatrix} u(kt_s) + \begin{bmatrix}0 & 0\\ 0 & 1-e^{-\alpha t_s}\end{bmatrix} u((k-1)t_s)\right).\end{aligned}$$

To keep things simple, this relationship is further simplified by artificially introducing a time delay t_s in the control of the first static actuator. In this case, one gets:

$$\tau(kt_s) = \begin{bmatrix}1 & 2\end{bmatrix}\left(\begin{bmatrix}0 & 0\\ 0 & e^{-\alpha t_s}\end{bmatrix} y_a((k-1)t_s) + \begin{bmatrix}1 & 0\\ 0 & 1-e^{-\alpha t_s}\end{bmatrix} u((k-1)t_s)\right)$$

Then, the optimizing part of A is naturally redefined as follows, where the previous equation is directly treated as the constraint of the optimization problem:

$$(\tau^d(t), y_a(t)) \mapsto u(t) \in \underset{\breve{u}\in\mathcal{U}}{\arg\min}\, J(\breve{u}) \quad \text{s.t.} \quad \tau^d(t) = \begin{bmatrix}0 & 2e^{-\alpha t_s}\end{bmatrix} y_a(t) + \begin{bmatrix}1 & 2(1-e^{-\alpha t_s})\end{bmatrix}\breve{u} \tag{7.12}$$

Note that the state y_a of Σ_a must now be fed back to A.

Consider the more general case where the set of actuators is governed by the following discrete-time state-space model:

$$\begin{aligned}\xi_a((k+1)t_s) &= f(\xi_a(kt_s), u(kt_s))\\ \tau(kt_s) &= h(\xi_a(kt_s))\end{aligned}$$

which gives

$$\tau(kt_s) = (h\circ f)\left(\xi_a((k-1)t_s), u((k-1)t_s)\right). \tag{7.13}$$

In this case, the optimization problem solved by A reads:[6]

$$\Xi_c : (\xi_a(t), \tau^d(t)) \mapsto u(t) \in \underset{\breve{u}\in\mathcal{U}}{\arg\min}\, J(\breve{u}) \quad \text{s.t.} \quad \tau^d(t) = (h \circ f)\,(\xi_a(t), \breve{u}) \tag{7.14}$$

It should be emphasized that the state vector $\xi_a(t)$ of the actuators must now be fed back to the optimizer.

Let us now illustrate the crucial difference between Ξ_a and Ξ_c on the previous example.

Example 7.10. The allocator (7.12) obtained in Ex. 7.9 is now compared with the one using (7.9), where the dynamics of the actuators are neglected. The simulation results are shown in Fig. 7.15. The signal τ^d is defined as an arbitrary repeating stair sequence. It feeds both allocators as reference signals to be tracked by τ.
Let us focus on the second stair of τ^d starting at $t_1 = 10$. Bearing in mind that the cost function aims to penalize the first actuators, (7.9) puts all the effort into the second actuators because this choice complies with the actuator limits, that is,

$$u(t_1) = \Xi_a(\tau^d(t_1) = 2) = \begin{bmatrix} 0 & 2 \end{bmatrix}^\intercal \in \mathcal{U}.$$

As clearly shown by the first subplot, this distribution leads to poor tracking of τ^d by τ since the dynamics of the second actuator is neglected, see the fourth subplot.
The constraint of (7.9) reads $\tau^d(t) = \Sigma_a^\star \breve{u}$. Let us rewrite the one of (7.12) as follows:

$$\tau^d(t) = \Sigma_a^\star \begin{bmatrix} \breve{u}_1 \\ \breve{u}_2 - \delta \end{bmatrix}$$

with $\delta = e^{-\alpha t_s}(\breve{u}_2 - y_{a2}(t)) \in \mathbb{R}$. Comparing the two expressions reveals that if $u_2(t)$ is kept constant over one period t_s (as it is set by A), then the actual contribution of this actuator at the end of this period of time equals $\breve{u}_2 - \delta$ instead of $\breve{u}_2$, the value of the steady-state contribution. The scalar δ affecting the contribution of the second actuator originates from the non-zero settling time of this second actuator. This is confirmed by the observation that δ is a decreasing function of t_s; the larger t_s is, the closer the second actuator is from its steady-state behavior.
Using (7.12) instead of (7.9) informs the allocator about the dynamic nature of the second actuator. This observation has the following crucial consequence: (7.12) can transfer the missing term δ from the second dynamical actuator to the first static one. This makes the first actuator compensate for the lag in the response of the second actuator. This phenomenon can be observed in Fig. 7.15 during the transient regime starting at $t = 5$. Not only is the second actuator somehow overdriven to compensate for its own dynamics (see the third subplot), but the first actuator is also asked to contribute to the overall control effort (see the second subplot) since $u_2(t)$ hits its boundaries. For other stairs of τ^d, the same phenomena can also be observed.

As a summary of the discussion proposed in this section, let us now compare the different versions of the allocator A obtained so far. Tab. 7.2 is offered for this purpose. The following comments can be made:

- As opposed to Ξ_a, the allocation strategy using Ξ_b takes the dynamical nature of the actuators into account by delivering y_a^d instead of u. Using the auxiliary control unit C_a, this dynamics is accelerated up to a point where $y_a^d \mapsto y_a$ can be regarded as a pure time delay t_s. This allows to preserve the original allocation strategy: From Ξ_a to Ξ_b, u has simply been replaced by y_a.

[6] For the sake of simplicity, assume that $u \mapsto (h \circ f)(\xi_a, u)$ is a function of each component of u for all ξ_a, that is, the relative degree of Σ_a equals one with respect to all inputs. This ensures that each actuator contributes to τ after a dead-time of t_s.

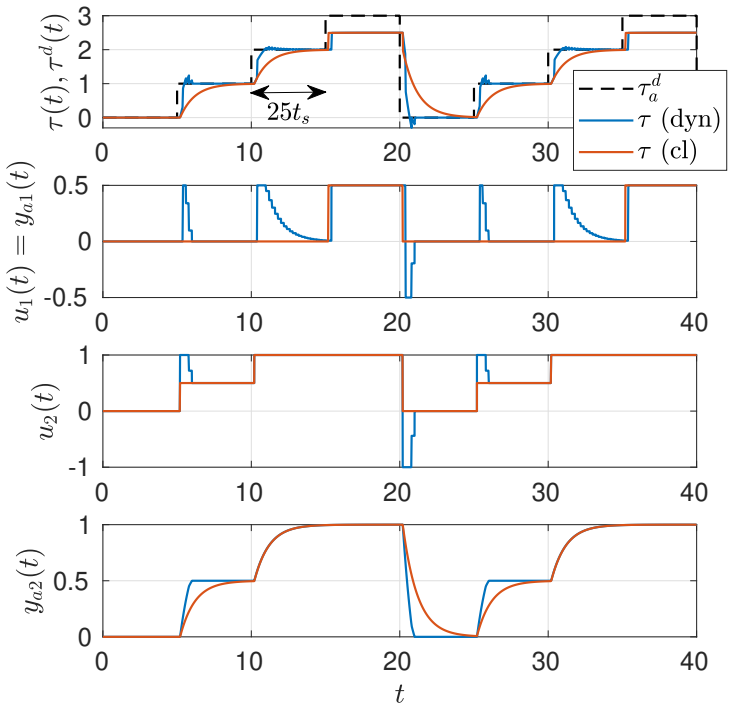

Figure 7.15: Simulation results comparing the achievement of the classical allocator using (7.9) ("cl" in red) and the one using (7.12) ("dyn" in blue). The first subplot shows the reference τ^d to be tracked by the output τ of the actuation subsystem. Differences between the two strategies can be analyzed via the input/output chronographs of the first static actuator (second subplot) and of the second dynamical actuator (third and fourth subplots).

Table 7.2: Comparison of the different allocators A. First line reads as follows: The allocator defined via (7.9) considers Fig. 7.2; it delivers the signal u; the synthesis of the control unit relies on the assumption that mapping $u \mapsto \tau$ is static; *under this assumption*, $\tau^d \mapsto \tau$ reduces to a pure time-delay t_s.

Optimizer	Related figure	Output	Assumption	$\tau^d \mapsto \tau$
Ξ_a, cf. (7.9)	Fig. 7.2	u	$u \mapsto \tau$ is static	time-delay t_s
Ξ_b, cf. (7.10)	Fig. 7.12	y_a	$y_a^d \mapsto y_a$ is a time-delay t_s	time-delay $2t_s$
Ξ_c, cf. (7.14)	Fig. 7.2	u	None	See Rem. 7.11

- When considering Ξ_b, the standing assumption is that the cascade of C_a and Σ_a^n behaves as the time-delay t_s *for all actuators*. If the natural settling times of the actuators are significantly different, it is necessary to rush the slowest actuators at a level that might be unacceptable. In other words, the value of t_s must be increased to remain within the limits of the slowest actuator. Otherwise, the difference between $y_a^d(kt_s)$ and $y_a((k+1)t_s)$ is too large.

- Dealing with the previous issue can be seen as the main justification for the introduction of Ξ_c. The architecture of the controller using the last optimizer discards C_a. The fact that the actuators are dynamical is somehow directly handled via the constraint of Ξ_c, which can be interpreted as $\tau = \Sigma_a(u)$ where Σ_a is the input-output operator of the actuation system. This allows the allocator to compute the optimal distribution of the overall control effort by taking into account the fact that the actual contribution of each actuator might differ from the steady-state one, due to non-zero settling time.

- When comparing Ξ_b and Ξ_c, first observe that $\tau(kt_s) = \tau^d((k-2)t_s)$ can be made valid in both cases, see forthcoming Rem 7.11. As opposed to Ξ_c, such a result is achieved *indirectly* by Ξ_b by letting C_a impose $y_a(t_s) = y_a^d((k-1)t_s)$ and by controlling y_a^d via the allocator. The key point is that $y_a(kt_s) = y_a^d((k-1)t_s)$ is not necessary for $\tau^d(kt_s) = \tau((k-2)t_s)$ to hold, the former being an equality constraint for all actuators, whereas the latter considers the overall contribution of the actuation subsystem. This observation can be regarded as the origin of the design of Ξ_c, where $\tau^d(kt_s) = \tau((k-2)t_s)$ is handled directly without the need to introduce C_a.

Remark 7.11 (A modified version Ξ_c). In this remark, notations are lightened by removing t_s, that is, $x(k)$ means $x(kt_s)$. Consider Ξ_c. At first glance, one expects that τ and τ^d are related by the following relationship:

$$\tau(k) = \tau^d(k-2). \tag{7.15}$$

Indeed, along the path from τ^d to τ in Fig. 7.2, two time delays are crossed over. The first one models the computational effort required by A to solve Ξ_c. This can be captured via the following relationship, which is analogous to (7.3):

$$u(k) = \Xi_c(\xi_a(k-1), \tau^d(k-1)) \tag{7.16}$$

The second time delay is related to the intrinsic dead time associated with the discrete-time model of Σ_a, see (7.13).

For $\tau(k) = \tau^d(k-2)$ to hold, the definition of Ξ_c must be modified as follows:

$$\hat{\Xi}_c : (\xi_a(t), \tau^d(t)) \mapsto u(t) \in \underset{\check{u}\in\mathcal{U}}{\arg\min}\, J(\check{u}) \quad \text{s.t.} \quad \tau^d(t) = (h \circ f)\,(f(\xi_a(t), \check{u}), \check{u}) \tag{7.17}$$

To see this, first observe that (7.4) reads as follows in the current context:

$$(h \circ f)(\xi_a(k), \Xi_c(\xi_a(k), \tau^d(k))) = \tau^d(k) \tag{7.18}$$

Indeed, the constraint $\tau^d(k) = (h \circ f)\,(\xi_a(k), u(k))$ of the optimization problem of Ξ_c holds true for its solution $u(k) = \Xi_c(\xi_a(k), \tau^d(k))$. Then, one gets:

$$\tau(k) \overset{(7.13)}{=} (h \circ f)\,(\xi_a(k-1), u(k-1)) \overset{(7.16)}{=} (h \circ f)\left(\xi_a(k-1), \Xi_c(\xi_a(k-2), \tau^d(k-2)\right)$$

From this relationship, the key observation is that $\tau(k)$ is not equal to $\tau^d(k-2)$, in general. Indeed, one needs $\xi_a(k-1)$ to be replaced by $\xi_a(k-2)$ in the last term for (7.18) to be used and,

in turn, gives $\tau^d(k-2)$. This issue originates from the fact that the constraint of Ξ_c considers $\xi_a(k)$, whereas the state of the actuator is $\xi_a(k+1)$ when the output of Ξ_c reaches Σ_a owing to the time delay (7.16).

A workaround to this issue consists of predicting the state of the actuator in the constraint of the allocator, as is done in $\hat{\Xi}_c$. The following equation confirms this assertion:

$$\tau(k) \overset{(7.13)}{=} (h \circ f)\left(\xi_a(k-1), u(k-1)\right) = (h \circ f)\left(\xi_a(k-1), \hat{\Xi}_c(\xi_a(k-2), \tau^d(k-2))\right) = \tau^d(k-2)$$

where (7.16) with $\hat{\Xi}_c$ in place of Ξ_c is used for the second equality, and the following identity justifies the third one:

$$(h \circ f)(\xi_a(k+1), \hat{\Xi}_c(\xi_a(k), \tau^d(k))) = \tau^d(k)$$

This last relationship is analogous to (7.18) when using $\hat{\Xi}_c$ in place of Ξ_c. It derives from the observation that the constraint $\tau^d(k) = (h \circ f)\left(f(\xi_a(k), u(k)), u(k)\right)$ of the optimization problem of $\hat{\Xi}_c$ holds true for its solution $u(k) = \hat{\Xi}_c(\xi_a(k), \tau^d(k))$, i.e.

$$\tau^d(k) = (h \circ f)\left(f(\xi_a(k), u(k)), u(k)\right) = (h \circ f)\left(\xi_a(k+1), u(k)\right).$$

•

Remark 7.12 (Mixing up the two strategies). The last two strategies can be merged. First, the control unit C_a can be designed to accelerate each actuator individually as much as possible. Then, an optimizer that ressembles to Ξ_c can be implemented. In this case, the equality constraint of Ξ_c considers the interconnection of C_a with Σ_a, instead of Σ_a itself. •

Remark 7.13 (An implicit optimal dead-beat controller). By imposing $\tau(kt_s) = \tau^d((k-2)t_s)$, the optimizer $\hat{\Xi}_c$ acts as a dead-beat controller formulated in an implicit way allowing for optimality, i.e. $\hat{\Xi}_c$ can be regarded as an online mechanism seeking for the optimal dead-beat controller at each instant time. Saying it differently, this control strategy is a particular MPC considering the terminal constraint on the output of Σ_a and using a horizon length equal to one. Note that this length is naturally chosen as the minimal number of sampling periods associated with the dead-beat control. In footnote 6 on p. 104, it is assumed that this quantity equals one, but is generally larger depending on the relative degree of Σ_a^n. •

7.3 Beyond the CAM in the case of dynamical actuators

Let us now gather the set of actuators and the plant into the single system

$$\Sigma = \Sigma_p \circ \Sigma_a.$$

Around 2010, two strikingly different approaches that could handle Σ directly were presented in (i) [Zac09] and (ii) [Ser12]. This section introduces these two new approaches. Both are illustrated in Ex. 7.1 and Ex. 7.4. Tab. 7.3 offers a summary of the controllers obtained in the different cases.

7.3.1 A common framework

Fig. 7.16 exhibits a common control framework which allows both methodologies to be exposed. The design process assumes the existence of a controller C_c stabilizing Σ, but not necessarily in an optimal way with respect to the distribution of the control effort among the actuators. Then, control units $\mathsf{C}_\perp$ and C_η are inserted between C_c and Σ with the aim of modifying the input u_c by adding the signal $u_\perp$. This last signal is shaped to meet the following two specifications:

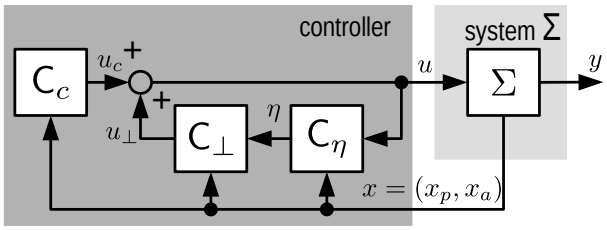

(a) Feedback form.

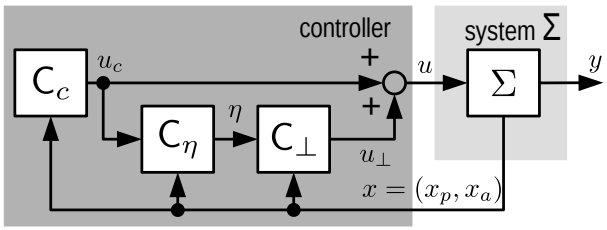

(b) Feedforward form.

Figure 7.16: The two versions of the common framework for the control strategies exposed in Sec. 7.3. x_p and x_a refer to the state of the plant and the actuators, respectively. Note that all control units C_c, $\mathsf{C}_\perp$ and C_η are modeled via a continuous-time system. The internal feedback in Fig. 7.16a is used most of the time. When turning this feedback over, one gets the feedforward loop shown by Fig. 7.16b.

(a) $u_\perp$ should be invisible from the output y, as much as possible;

(b) The input $u = u_c + u_\perp$ should minimize a given cost function $u \mapsto J(u) \in \mathbb{R}$ at the steady-state, i.e. $u_\perp$ asymptotically solves the following problem:

$$\min_{u_\perp} J(u(u_\perp)) \quad \text{s.t.} \quad u(u_\perp) = u_c + u_\perp$$

Importantly, those competing objectives are ordered: (a) is addressed as well as possible, and then the remaining degrees of freedom (if any) are used to treat (b). This hierarchy is handled by imposing that $u_\perp$ is produced via an annihilator denoted by $\mathsf{C}_\perp$, which is specifically designed to meet (a). Then, (b) is treated by selecting the appropriate input η of $\mathsf{C}_\perp$, so that the previous optimization problem reads as follows:

$$\min_{\eta} J(u(\eta)) \quad \text{s.t.} \quad u(\eta) = u_c + \mathsf{C}_\perp(\eta) \tag{7.19}$$

The control unit C_η is devoted to asymptotically solving this optimization problem.

In the following, different control strategies are proposed based on different constructions of the annihilator $\mathsf{C}_\perp$. First, the Input-to-State Annihilator (ISA) satisfying

$$\text{ISA}: \quad \Sigma_x \circ \mathsf{C}_\perp = \mathbf{0}$$

where Σ_x is the input-to-state mapping of Σ. Second, the asymptotic Input-to-Output Annihilator (a-IOA) satisfying

$$\text{a-IOA}: \quad \Sigma^\star \circ \mathsf{C}_\perp = \mathbf{0}$$

where $\Sigma^\star$ denotes the DC gain of Σ. Third, the Input-to-Output Annihilator (IOA) satisfying

$$\text{IOA}: \quad \Sigma \circ \mathsf{C}_\perp = \mathbf{0}$$

Table 7.3: Definition of the control signals of Fig. 7.16 for the different control strategies, and in the case of Ex. 7.1 and Ex. 7.4. Scalar k must be strictly positive in all cases and sufficiently small for the a-IOA case. Scalar k_η must satisfies $k_\eta < 1$.

$\mathsf{C}_\perp$	Σ_a	u_c	$u_\perp$	$\dot{\eta}$
ISA	static	$\begin{bmatrix} 1/3 \\ 1/3 \end{bmatrix} \tau^d$	$\begin{bmatrix} 1 \\ -1/2 \end{bmatrix} \eta$	$-ku_1$
a-IOA	dynamic	$\begin{bmatrix} 1 \\ 0 \end{bmatrix} \tau^d$	$\begin{bmatrix} 1 \\ -1/2 \end{bmatrix} \eta$	$-ku_1$
IOA	dynamic	$\begin{bmatrix} 1 \\ 0 \end{bmatrix} \tau^d$	$\begin{bmatrix} -2x_2 \\ \eta \end{bmatrix}$	$k_\eta x_2 + (1-k_\eta)\varphi$ with $\dot{\varphi} = k(\tau^d - 2\varphi)$

Remark 7.14 (Analytical solution of (7.19)). Assume that the annihilator is the linear map $\eta \mapsto u_\perp = N\eta$. Then, an analytical solution of the problem (7.19) can be obtained by solving the following equation, where η is the unknown vector:

$$\frac{\mathrm{d}J(u(\eta))}{\mathrm{d}\eta} = J'(u(\eta))u'(\eta) = J'(u_c + N\eta)N = \mathbf{0} \tag{7.20}$$

In particular, if $J(u) = u^\intercal W u$ holds with $W \succ \mathbf{0}$ and N is full rank, one can check that

$$\eta = -(N^\intercal W N)^{-1} N^\intercal W u_c$$

solves the previous equation. Note that if such an analytical solution is available, the control scheme naturally adopts the feedforward form shown in Fig. 7.16b. For reasons that are discussed in the conclusive discussion, online solving of (7.19) is preferred to the analytical solution. •

Remark 7.15 (Continuous-time solver of (7.19)). In the case where J is strictly convex, u_c is constant, and $\mathsf{C}_\perp$ maps η to $u_\perp = N\eta$ with N a full rank matrix, the problem (7.19) can be solved in continuous time by defining the dynamics of η as follows:

$$\mathsf{C}_\eta : \dot{\eta}(t) = -KN^\intercal \nabla J(u(t)) \tag{7.21}$$

where $K \succ \mathbf{0}$ is arbitrary. Indeed, the following derivative of $J \circ u$ along the trajectory of η is strictly negative for all $\eta(t)$, but the unique minimizer $\eta^\star$ of $J \circ u$:

$$\frac{\mathrm{d}J(u(\eta(t)))}{\mathrm{d}t} = J'(u(\eta(t)))u'(\eta(t))\dot{\eta}(t) \overset{(7.21)}{=} -(\nabla J(u(\eta(t))))^\intercal NKN^\intercal \nabla J(u(\eta(t)))$$

This proves that η converges asymptotically to $\eta^\star$. Besides, note that the internal feedback in Fig. 7.16a originates from (7.21), where $u(t)$ is used to compute $\dot{\eta}(t)$. •

Remark 7.16 (A simplified framework). To facilitate the comparison in a general context between the different approaches exposed in this section, a simplified framework is retained. Namely, (i) the cost function associated with the input preferences is quadratic and strictly convex and (ii) the input limits are ruled out, i.e.

$$\mathcal{U} = \mathbb{R}^m.$$

We return to the second point in the concluding remarks of this chapter. In addition, the attention is restricted to strictly proper systems, for which $\Sigma = C\Sigma_x$ holds, so that any ISA is also an IOA, a fortiori.
Clearly, Ex.7.1 does not feet into this context, because $J(u) = u_1^2$ is not strictly convex. This example thus illustrates how applicability of the general results can be enlarged. •

7.3.2 Input-to-State Annihilator (ISA)

Let us begin with the continued version of Ex. 7.1 where the actuators are all static.

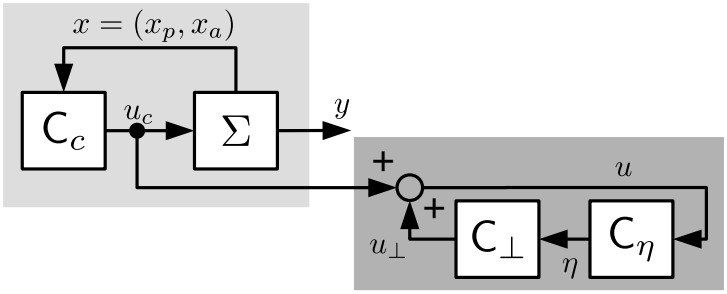

(a) $\mathsf{C}_\perp$ is the Input-to-State Annihilator (ISA) $\eta \mapsto u_\perp = N\eta$ with $\mathrm{Im}\{N\} = \mathrm{Ker}\{B\}$.

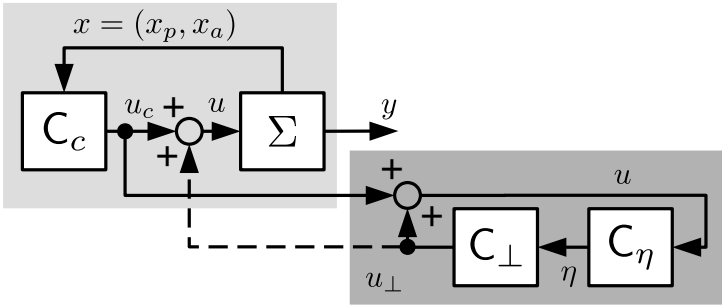

(b) $\mathsf{C}_\perp$ is the asymptotically Input-to-Output Annihilator (a-IOA) $\eta \mapsto u_\perp = N\eta$ with $\mathrm{Im}\{N\} = \mathrm{Ker}\{\Sigma^\star\}$.

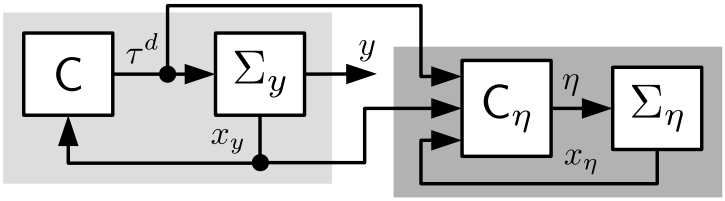

(c) $\mathsf{C}_\perp$ is the Input-to-Output Annihilator (IOA) $(\eta, x) \mapsto u_\perp = Fx + N\eta$ with $\mathrm{Im}\{N\} = B^{-1}\mathcal{R}^*$ and $(A + BF)\mathcal{R}^* \subset \mathcal{R}^* \subset \mathrm{Ker}\{C\}$.

Figure 7.17: Cascaded and quasi-cascaded reformulation of Fig. 7.16a.

Example 7.17 (Ex. 7.1 continued)**.** Consider Ex. 7.1 under the assumption that $\Sigma_a = \Sigma_a^\star$. In this case, Σ reads as follows:

$$\Sigma = \Sigma_p \circ \Sigma_a^\star = \left[\begin{array}{c|cc} -1 & 1 & 2 \\ \hline 1 & 0 & 0 \end{array}\right]$$

Let us first define the control unit C_c via to the following relationship

$$\mathsf{C}_c : u_c = \begin{bmatrix} 1/3 \\ 1/3 \end{bmatrix} \tau_d \tag{7.22}$$

with

$$\tau_d(t) = k_p(y_r - y(t)) + k_i \int_0^t y_r - y(s)\mathrm{d}s \tag{7.23}$$

where $k_p = 2$, $k_i = 1$ and $y_r = 2$. This controller derives from the PI controller C introduced earlier and used to compute $\tau_d(t)$ from $y(t)$. Here, C_c equally distributes the control effort between the two actuators. Gains are selected in such a way that the closed-loop equation governing y is the same equation as in the case where $\tau = \tau^d$ was assumed, i.e.

$$\dot{y} = -y + k_p(y^r - y) + k_i \int (y^r - y) \tag{7.24}$$

From the previous sections of this chapter, $y^\star = y^r$ is a stable equilibrium for this dynamics.
Define $u_\perp$ as follows:

$$\mathsf{C}_\perp : u_\perp = N\eta \quad \text{with} \quad N = \begin{bmatrix} 1 \\ -1/2 \end{bmatrix} \tag{7.25}$$

where η is an internal signal to be defined. The key observation is that $BN = \mathbf{0}$ holds true. This implies that x and, in turn, y are independent of $u_\perp$. Thus, this last signal structurally satisfies (a), that is, $u_\perp$ is invisible from the output, whatever is η.
The structure of the control problem resulting from the above definitions of u_c and $u_\perp$ can be exhibited via the following quadruple of Σ using (τ^d, η) as the new inputs instead of $u = u_c + N\eta$:

$$\left[\begin{array}{c|cc} -1 & 1 & 0 \\ \hline 1 & 0 & 0 \end{array}\right]$$

Clearly, η has no impact on either x or y.
Now, let us address (b). Recall that $J(u) = u_1^2/2$ so that the minimum of (7.19) is reached when

$$u_1 = 0 \overset{(7.25)}{\Longleftrightarrow} u_{c1} + \eta = 0 \tag{7.26}$$

holds because u equals $u_c + u_\perp$. One can simply impose $\eta = -u_{c1}$, by proceeding as in Rem. 7.14. Here, we follow Rem. 7.15 (and get Fig. 7.16a) and merely seek asymptotic optimality by letting η be governed by the following differential equation:

$$\mathsf{C}_\eta : \dot{\eta}(t) = -ku_1(t) \overset{(7.25)}{=} -k(u_{c1}(t) + \eta(t)) \tag{7.27}$$

where $k > 0$ acts as a tuning parameter. One can check that (7.27) is nothing but (7.21) particularized to the context of this example.
If $u_\perp$ is completely invisible from the output, then feeding Σ with $u_c + u_\perp$ or simply u_c is equivalent. Thus, Fig. 7.16a can be equivalently transformed into Fig. 7.17a. Observe that the latter exhibits a cascaded form, which can be exploited to formally prove the stability of the closed-loop equilibrium. Indeed, the two subsystems being linear, stability derives from the internal stability of the upstream subsystem and 0-stability of the downstream one.[a] The former follows from the definitions of u_c and τ^d. The latter was proven by Rem. 7.15 when η is governed by (7.27).
The simulation results are shown in Fig. 7.18. It is shown that the actuation effort is redistributed between the two actuators to asymptotically reach the optimal regime characterized by $u_1(t) = 0 \Leftrightarrow u_{c1}(t) = -\eta(t)$, see (7.26). The speed of this redistribution can be adjusted using k. Observe that the output dynamics is completely independent of this redistribution, which can be arbitrarily fast.

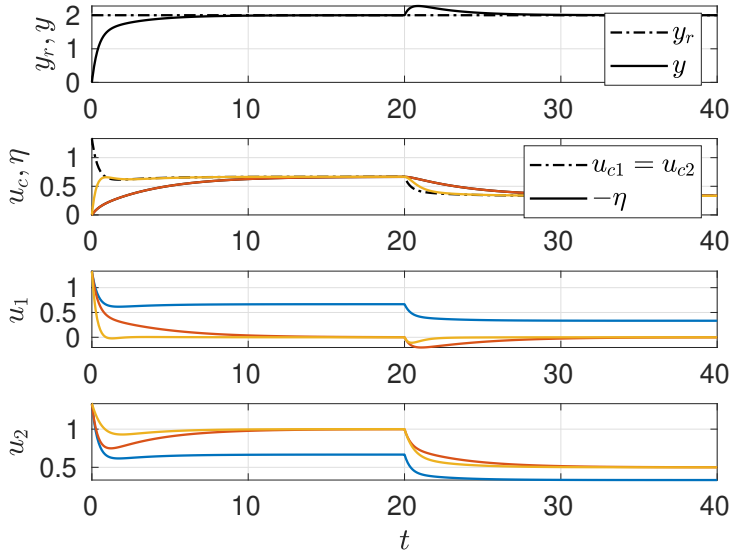

Figure 7.18: Simulation results when $\mathsf{C}_\perp$ is an ISA and for the *unsaturated* static actuators of Ex. 7.1. The signals of the controller in Fig. 7.16a are defined by (7.22), (7.25) and (7.27). Different controller parameters, leading to different chronographs of $u_\perp$, are used to appreciate the impact of this signal. The red lines correspond to $k = 0.3$ and the yellow lines to $k = 2$. The blue lines are obtained by imposing $u_\perp = \mathbf{0}$ (note that η is useless in this case and is therefore not depicted in the second subplot). When all curves coincide, the black color is used, as on the first and second subplots showing that the output y and the components of u_c are both independent of $u_\perp$. In the legend of the second subplot, the generic black color indicates that the continuous lines of all colors correspond to $-\eta$.

[a] In this manuscript, 0-stability is to be understood in the broad sense of "stability of the downstream system when the upstream one is at its equilibrium", which is not necessarily zero.

The previous example can be easily generalized by defining $u_\perp$ as follows:

$$C_\perp : u_\perp = N\eta \quad \text{with} \quad \mathrm{Im}\{N\} = \mathrm{Ker}\{B\}$$

In this case, $\mathsf{C}_\perp$ is an Input-to-State Annihilator (ISA) because η is invisible from the state. Using (7.21) with $K \succ \mathbf{0}$, specifications (a) and (b) are satisfied, provided that the interconnection of the linear controller C_c and Σ is internally stable for $u_\perp = \mathbf{0}$.

7.3.3 Asymptotic Input-to-Output Annihilator (a-IOA)

Once again, let us start with the running example.

Example 7.18 (Ex. 7.4 continued)**.** Consider the case where the second actuator is dynamic. The cascade of Σ_a and Σ_p now reads as follows:

$$\Sigma := \Sigma_p \circ \Sigma_a = \left[\begin{array}{cc|cc} -1 & 2 & 1 & 0 \\ 0 & -\alpha & 0 & \alpha \\ \hline 1 & 0 & 0 & 0 \end{array}\right] \tag{7.28}$$

The control unit C_c is defined via

$$\mathsf{C}_c : u_c = \begin{bmatrix} 1 \\ 0 \end{bmatrix} \tau^d \tag{7.29}$$

where τ^d reads as in (7.23), with the same control parameters as before. For later needs, let us already analyze how the resulting closed-loop behaves in the case where $u_\perp$ is constant. Observe that y is governed by (7.24), with $2x_2$ as an additional term on the right-hand side of this equation. Since $\dot{x}_2 = -\alpha(x_2 - u_\perp)$ holds, this term $2x_2$ asymptotically converges to $2u_\perp$ and is then rejected by the integral action in τ^d so that y converges to y_r whatever is $u_\perp$.
Let us now define $\mathsf{C}_\perp$ and address (a). Clearly, the kernel of B reduces to $\{\mathbf{0}\}$. Hence, there is no matrix N such that $u_\perp = N\eta$ can be made invisible from the state. The following strategy is proposed as a workaround: If $u_\perp$ inevitably impacts x, it could at least let the steady state of the output remain unchanged. Denoting by $\Sigma^\star$ the DC gain of Σ

$$\Sigma^\star := \lim_{s\to 0^+} C(s\mathbf{I} - A)^{-1}B \tag{7.30}$$

this is equivalent to saying that $\Sigma^\star u_\perp = \mathbf{0}$. This can be naturally achieved by defining $\mathsf{C}_\perp$ as follows

$$\mathsf{C}_\perp : u_\perp = N\eta \quad \text{with} \quad N = \begin{bmatrix} 1 \\ -1/2 \end{bmatrix} \tag{7.31}$$

since columns of N form a basis of $\mathrm{Ker}\left\{\Sigma^\star = \begin{bmatrix} 1 & 2 \end{bmatrix}\right\}$.[a] In this case, the asymptotic input-output relationship reads $y^\star = \Sigma^\star(u_c^\star + u_\perp^\star) = \Sigma^\star u_c^\star$.
In this context, note that the quadruple of Σ using (τ^d, η) as the new input instead of $u = u_c + N\eta$ reads as follows:

$$\left[\begin{array}{cc|cc} -1 & 2 & 1 & 1 \\ 0 & -\alpha & 0 & -\alpha/2 \\ \hline 1 & 0 & 0 & 0 \end{array}\right]$$

Observe that η now affects $x_1 = y$ directly, as well as indirectly via x_2.
Let us now address (b). Consider for the time being that Σ is at the steady state, so that it behaves like $\Sigma^\star$ and u_c is constant. In this case, Rem. 7.15 ensures that if η satisfies (7.21) (or equivalently (7.27) for this example), then the optimization problem (7.19) is solved asymptotically. Note that because N has the same expression as in the static case, the optimality condition (7.26) remains unchanged.
Let us summarize the intermediate results obtained so far. The forthcoming discussion is supported by Fig. 7.17b which is an equivalent reformulation of Fig. 7.16a. (i) If $u_\perp$, which is associated with the dashed line, is constant, then the output of Σ is well driven by the feedback involving u_c. (ii) Conversely, if the upstream subsystem is at the steady-state, then (7.27) implies that η and, in turn, $u_\perp$ converges to the optimal solution of (7.19), i.e. the downstream subsystem reaches the optimal state. These apparently conflicting conclusions can be resolved by using two different time scales. Scalar k is instrumental for that purpose because it determines the bandwidth of η and, in turn, of the downstream subsystem. In particular, if k is sufficiently small, $u_\perp$ is quasi-constant from the perspective of the upstream system. Saying differently, from the point of view of $u_\perp$, this upstream subsystem evolves fast enough for being always at the steady state, so that Σ behaves as $\Sigma^\star$. Therefore, one can enjoy the benefits of (i) and (ii) by selecting k small enough, so that the slow downstream subsystem will slowly push the fast upstream subsystem toward the optimal steady state.
Fig. 7.19 depicts the simulation results obtained in this context. Key observations are now offered. (i) In contrast to the case of static actuators, signal $u_\perp$ impacts both y and u_c as shown in the first and second subplots. (ii) The parameter k determines the speed of the convergence to the optimal regime characterized by $u_1 = 0 \Leftrightarrow u_{c1} = -\eta$, see (7.26). (iii) Stability and asymptotic optimality are preserved for the two selected values of k.

[a] For the considered example, $\Sigma^\star = \Sigma_a^\star$ holds accidentally because Σ_p is SISO with unitary DC gain. This fact implies that N can be defined as in (7.25), even in the current context of dynamical actuators, because $\mathrm{Im}\{N\} = \mathrm{Ker}\{\Sigma_a^\star\} = \mathrm{Ker}\{\Sigma^\star\}$ holds. Let us stress that the last equality is by no means valid in the general case.

The discussion on the previous example can be generalized by defining $u_\perp$ as follows,

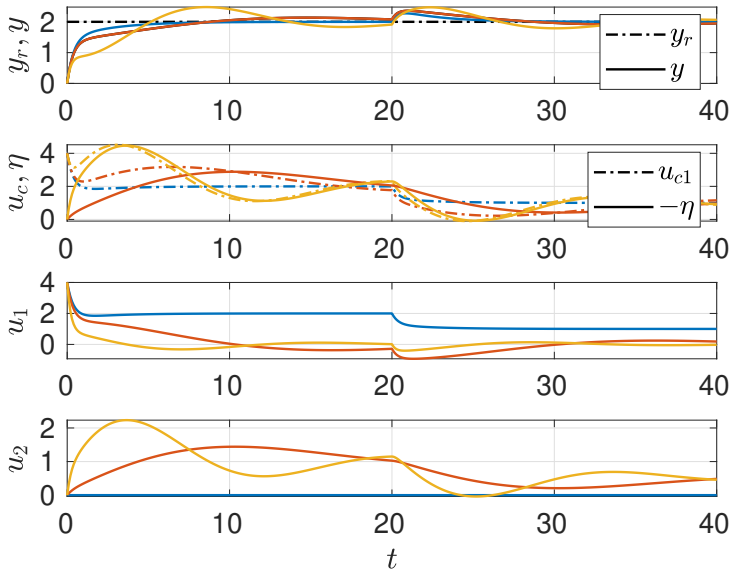

Figure 7.19: Simulation results with $\mathsf{C}_\perp$ as an a-IOA and for the *unsaturated* dynamical actuators of Ex. 7.4. The implemented controller is defined via Fig. 7.16a, (7.23), (7.27), (7.29) and (7.31). The blue, red, and yellow lines correspond to $u_\perp = \mathbf{0}$, $k = 0.3$ and $k = 2$, respectively. In the legend of the first and second subplots, the generic black color indicates that the continuous lines of all colors correspond to y on the first subplot and to $-\eta$ on the second one. In the same vein, the dashdotted lines of the second subplot are chronographs of u_{c1} in the different simulation contexts.

provided that $\Sigma^\star$ exists and is finite:

$$C_\perp : u_\perp = N\eta \quad \text{with} \quad \mathrm{Im}\,\{N\} = \mathrm{Ker}\,\{\Sigma^\star\}\,.$$

In this case, $\mathsf{C}_\perp$ is an asymptotically Input-to-Output Annihilator (a-IOA) because the invisibility of η (from the output) is ensured only at the steady state. The direct use of (7.21) to define the dynamics of η may lead to bad interactions between the dynamics of the two subsystems of Fig. 7.17b, though. This originates from the fact that BN is no longer zero, so $u_\perp$ impacts $\dot{x}$ as shown by the dashed line in Fig. 7.17b. The two-timescale strategy exposed earlier can be implemented by simply multiplying K in (7.21) by a sufficiently small scalar $\epsilon > 0$. A formal proof can be established using standard arguments on two time-scale systems, see e.g. [KKO99], provided that C_c is selected in such a way that the upper subsystem of Fig. 7.17b admits a stable equilibrium for any constant $u_\perp$.

7.3.4 Input-to-Output Annihilator (IOA)

If B admits a non-trivial kernel, imposing $u_\perp(t) \in \mathrm{Ker}\,\{B\}$ makes this signal invisible from the state and, in turn, from the output. This strategy leads to the ISA $\eta \mapsto N\eta$ with $\mathrm{Im}\,\{N\} = \mathrm{Ker}\,\{B\}$, which is also an IOA because Σ is strictly proper. Yet, there might also exist some signal $u_\perp$ that impacts x while remaining invisible from y. In this case, the set in which $u_\perp$ can be selected is larger than $\mathrm{Ker}\,\{B\}$. This remark suggests that one should look for an IOA directly instead of a mere ISA.

Let us show how to construct such an annihilator for the running example in the case of dynamic actuators.

Example 7.19 (Ex. 7.4 continued)**.** When the second actuator is dynamic, recall that the cascade of Σ_a and Σ_p is described by (7.28). The main signals of the controller are now defined as follows:

$$\mathsf{C}_c : u_c = \begin{bmatrix} 1 \\ 0 \end{bmatrix} \tau^d \tag{7.32}$$

and

$$\mathsf{C}_\perp : u_\perp = \begin{bmatrix} 0 & -2 \\ 0 & 0 \end{bmatrix} x + \begin{bmatrix} 0 \\ 1 \end{bmatrix} \eta \tag{7.33}$$

In this context, the quadruple of Σ using (τ^d, η) as the new input reads as follows:

$$\left[\begin{array}{cc|cc} -1 & 0 & 1 & 0 \\ 0 & -\alpha & 0 & \alpha \\ \hline 1 & 0 & 0 & 0 \end{array}\right] \tag{7.34}$$

The structure of this quadruple reveals the existence of two *uncoupled* subdynamics related to signals (i) $y = x_1$ driven by τ^d and (ii) x_2 which only depends on η. In the sequel, the first subsystem is denoted by Σ_y whereas Σ_η refers to the second one.

Let us now define τ^d and η by exploiting the above uncoupling. First, let τ^d be as in (7.23), so that the output is governed by the differential (7.24), for which $y^\star = y^r$ is an asymptotically stable equilibrium. Then, η is shaped to achieve the optimal regime. As an initial step toward this objective, observe that the asymptotic value of x_2 can also be optimized since it is invisible from the output, just like η. Bearing in mind that x_2 and η are related at the (stationary) steady state by the relationship $x_2 = \eta$ derived from (7.34), the optimization problem (7.19) is substituted by the following one:

$$\min_{x_2,\eta} J(u_c + u_\perp) \quad \text{s.t.} \quad (7.32), (7.33), x_2 = \eta \tag{7.35}$$

Unlike η, the state x_2 of Σ_η cannot be assigned instantaneously. Yet, any (x_2^r, η^r) can be tracked by defining η as follows:

$$\eta = k_\eta(x_2 - x_2^r) + \eta^r$$

for any $k_\eta < 1$. Indeed, (7.34) implies that $\dot{\tilde{x}}_2 = \alpha(k_\eta - 1)\tilde{x}_2$ with $\tilde{x}_2 = x_2 - x_2^r$ for any constant (x_2^r, η^r) satisfying $x_2^r = \eta^r$. Thus, if $k_\eta - 1 < 0$ holds, then (x_2, η) tends to (x_2^r, η^r). It remains to assign to (x_2^r, η^r) the argument of the optimization problem (7.35). In the same vein as in Rem. 7.15, this can be performed asymptotically. Bearing in mind that $J(u) = u_1^2$ holds, observe that (7.35) can be equivalently rewritten

$$\min_{\varphi} J\left(\begin{bmatrix} \tau^d - 2\varphi \\ \varphi \end{bmatrix}\right) = (\tau^d - 2\varphi)^2$$

with $\varphi = x_2 = \eta$. Thus, if φ is governed by the following differential equation:

$$\dot{\varphi} = k(\tau^d - 2\varphi)$$

then this signal converges to the minimizer of the optimization problem for any $k > 0$ and constant τ^d. Hence, letting

$$(x_2^r, \eta^r) = (\varphi, \varphi)$$

makes (x_2^r, η^r) converge to the minimizer of (7.35). To sum up, if C_η is governed as follows

$$\mathsf{C}_\eta : \eta = k_\eta x_2 + (1 - k_\eta)\varphi \quad \text{with} \quad \dot{\varphi} = k(\tau^d - 2\varphi) \tag{7.36}$$

then (x_2, η) asymptotically converges to the minimizer of (7.35), provided that τ^d is constant.

The resulting interconnection is depicted in Fig. 7.17c where C is defined by (7.23). This figures exhibits a cascaded structure originating from the fact that τ^d depends neither on x_2 nor on η. Once again, asymptotic stability of the overall system derives from this cascaded structure and the properties established earlier in the construction of each control unit.

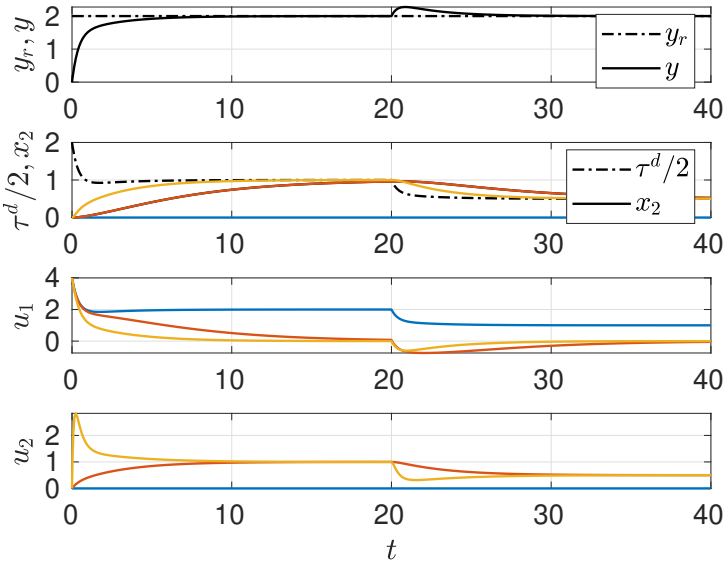

Figure 7.20: Simulation results with $\mathsf{C}_\perp$ as an IOA for the *unsaturated* dynamical actuators of Ex. 7.4. The implemented controller is defined in Fig. 7.16b, (7.23), (7.32), (7.33) and (7.36). The blue, red, and yellow lines correspond to $u_\perp = \mathbf{0}$, $k = 0.1$ and $k = 5$, respectively, whereas k_η is always equal to -1. As for Fig. 7.19, the legend indicates that (i) the continuous lines of all colors correspond to y on the first subplot and to x_2 on the second one and (ii) the dashdotted line of the second subplot is the chronograph of $\tau^d/2$, which is identical for the three simulations.

Fig. 7.20 shows the simulation results obtained in this context. The key observations are as follows. (i) Output y does not depend on $u_\perp$. (ii) Both parameters k and k_η determine the speed of convergence to the optimal regime characterized by $u_1 = 0 \Leftrightarrow x_2 = \tau^d/2$. (iii) Stability and asymptotic optimality are independent of the values of $k > 0$ and $k_\eta < 1$.

Remark 7.20 (A feedforward formulation). The control scheme associated with (7.42) adopts the feedforward form shown in Fig. 7.16b and not the feedback form of Fig. 7.16a. Indeed, C_η depends on τ^d, which defines u_c, and not on u. Alternatively, one can define $\dot{\varphi}$ as ku_1, but this may challenge the stability since u_1 equals $\tau^d - 2\varphi$ only at the steady state, where $\varphi = x_2 = \eta$ holds. •

Denote by $\mathcal{R}^*$ the controllable part of the largest controlled invariant subspace contained in $\mathrm{Ker}\,\{C\}$. Let F be any matrix that satisfies $(A + BF)\mathcal{R}^* \subset \mathcal{R}^* \subset \mathrm{Ker}\,\{C\}$. Define invertible matrices $H = \begin{bmatrix} N & H_y \end{bmatrix}$ and $T = \begin{bmatrix} T_\eta & T_y \end{bmatrix}$ satisfying $\mathrm{Im}\,\{N\} = B^{-1}\mathcal{R}^*$ and $\mathrm{Im}\,\{T_\eta\} = \mathcal{R}^*$. Then, let $u = u_c + u_\perp$ reads[7]

$$\mathsf{C}_c : u_c = H_y \tau^d \tag{7.37a}$$

$$\mathsf{C}_\perp : u_\perp = Fx + N\eta \tag{7.37b}$$

In this case, $\mathsf{C}_\perp$ is an Input-to-Output Annihilator (IOA) because η is invisible from the output *at all times*. The following quadruple of Σ using (η, τ^d) as the input and $(x_\eta, x_y) = T^{-1}x$ as the state highlights this fact:

$$\left[\begin{array}{cc|cc} A_{11} & A_{12} & B_{11} & B_{12} \\ \mathbf{0} & A_{22} & \mathbf{0} & B_{22} \\ \hline \mathbf{0} & C_2 & \mathbf{0} & \mathbf{0} \end{array}\right] \tag{7.38}$$

[7] Note that the mapping $(\tau^d, \eta) \mapsto u$ is a diffeomorphism (parameterized by x) and, hence, a well-defined change of variable.

The structure of this quadruple reveals the existence of unilateral coupling, where subsystem $\Sigma_y : (A_{22}, B_{22}, C_2, \mathbf{0})$ of state x_y and input τ^d feeds subsystem $\Sigma_\eta : (A_{11}, B_{11}, \mathbf{0}, \mathbf{0})$ of state x_η and input η by adding the term $A_{12}x_y + B_{12}\tau^d$ to its state equation. In this context, control unit C delivering τ^d is naturally selected as a stabilizer of Σ_y (see Fig. 7.17c).

Such a structure reveals that not only η but also x_η are invisible from the output. This suggests that substate x_η can enrich the set of decision variables of the optimization problem (7.19). The relevance of this proposition is enforced by the fact that x_η directly impacts u, as confirmed by the following expression of $u = u_c + u_\perp$ derived from (7.37):

$$u(x_\eta, \eta) = H_y\tau^d + F(T_\eta x_\eta + T_y x_y) + N\eta = \begin{bmatrix} FT_\eta & N \end{bmatrix} \begin{bmatrix} x_\eta \\ \eta \end{bmatrix} + \begin{bmatrix} FT_y & H_y \end{bmatrix} \begin{bmatrix} x_y \\ \tau^d \end{bmatrix} \tag{7.39}$$

Bearing in mind that η and x_η are coupled via (7.38), which imposes

$$\begin{bmatrix} A_{11} & B_{11} \end{bmatrix} \begin{bmatrix} x_\eta \\ \eta \end{bmatrix} + \begin{bmatrix} A_{12} & B_{12} \end{bmatrix} \begin{bmatrix} x_y \\ \tau^d \end{bmatrix} = \mathbf{0} \tag{7.40}$$

at the stationary steady state, the optimization problem reads:

$$\min_{\eta, x_\eta} J(u(\eta, x_\eta)) \quad \text{s.t.} \quad (7.39), (7.40) \tag{7.41}$$

In the spirit of Rem. 7.15, we consider the following continuous-time optimizer:

$$\dot{\varphi}(t) = -K \begin{bmatrix} A_{11} & B_{11} \end{bmatrix}_\perp^\intercal \begin{bmatrix} FT_\eta & N \end{bmatrix}^\intercal \nabla J \left(\begin{bmatrix} FT_\eta & N \end{bmatrix} \begin{bmatrix} x_\eta \\ \eta \end{bmatrix} (\varphi(t)) + \begin{bmatrix} FT_y & H_y \end{bmatrix} \begin{bmatrix} x_y \\ \tau^d \end{bmatrix} \right) \tag{7.42a}$$

$$\begin{bmatrix} x_\eta \\ \eta \end{bmatrix} (\varphi) = \begin{bmatrix} A_{11} & B_{11} \end{bmatrix}_\perp \varphi + M \begin{bmatrix} x_y \\ \tau^d \end{bmatrix} \tag{7.42b}$$

where $K \succ \mathbf{0}$ holds and M is any matrix satisfying $\begin{bmatrix} A_{11} & B_{11} \end{bmatrix} M = -\begin{bmatrix} A_{12} & B_{12} \end{bmatrix}$. It can be proved that this optimizer asymptotically reaches the optimal regime for any constant signals x_y and τ^d, provided that $\begin{bmatrix} A_{11} & B_{11} \end{bmatrix}_\perp^\intercal \begin{bmatrix} FT_\eta & N \end{bmatrix}$ is full rank and J is strictly convex.[8]

Because the pair (A_{11}, B_{11}) is controllable, signals η and x_η can be driven to the minimizer (x_η^r, η^r) of (7.41) by simply defining η as follows:

$$\eta = K_\eta(x_\eta - x_\eta^r) + \eta^r \tag{7.43}$$

where K_η is such that $A_{11} + B_{11}K_\eta$ is Hurwitz. Indeed, one can easily prove that $\dot{\tilde{x}}_\eta = (A_{11} + B_{11}K)\tilde{x}_\eta$ holds with $\tilde{x}_\eta = x_\eta - x_\eta^r$ so that $\tilde{x}_\eta$ tends to $\mathbf{0}$ which implies that (x_η, η) converges to (x_η^r, η^r).

From the above discussion, C_η is defined by (7.43) and (7.42), with (x_η^r, η^r) in place of (x_η, η). The output η of C_η serves as the input to Σ_η, see Fig. 7.17c. As in the case of the ISA, the overall closed-loop system admits a cascaded structure. It should be noted that the downstream subsystem shown in Fig. 7.17c corresponding to the interconnection of Σ_η and C_η can be itself formulated as a cascade where the lower subsystem is governed by $\dot{\tilde{x}}_\eta = (A_{11} + B_{11}K)\tilde{x}_\eta$, see the above discussion. This allows us to prove asymptotic stability and asymptotic optimality.

[8] The feasible set of (7.41) is explicitly parametrized by φ by solving analytically (7.40). An alternative strategy is to construct the Lagrangian of (7.41) and to design a dynamical system asymptotically converging to the solution of (7.41), in the spirit of the approach exposed in Sec. 7.1.4. Proceeding in this way allows us to avoid analytical solving of (7.40). Note that in this case, length of the state vector of this system is larger than the dimension of φ, since it includes the Lagrange multipliers.

7.3.5 A conclusive remark

Remark 7.21 (Rem. 7.14 continued). For the example treated in this subsection, it is always possible to analytically solve the optimization problem. In the cases of the ISA and a-IOA, the minimizer of (7.19) is $\eta = -u_{c1}$. This equation leads to an alternative definition of C_η. For the IOA, the minimum of (7.35) is reached at $x_2 = u_{c1}/2$, so it suffices to drive x_2 to this optimum by setting e.g. $\eta = u_{c1}/2$ as a new definition of C_η.

Out of the class of linear systems associated with the quadratic cost function, the analytical solution of the optimization problem is seldom available. This is true for the constrained case a fortiori. This obstruction is a clear motivation for using an online solver. In view of the beginning of this chapter, the case of input constraints for which $u(t) \in \mathcal{U}$ must be satisfied at all times is of particular interest. It can be handled using a continous-time solver by embedding the geometry of $\mathcal{U}$ into the cost function J via smooth barrier functions and implementing a gradient descent controller. •

7.4 Conclusions

Let us summarize the core ideas of the different contributions outlined in this chapter using a chronological exposition:

- CAM :
  - Split the system Σ in $\Sigma_p \circ \Sigma_a$, where Σ_a is a static mapping, and decompose the controller symmetrically in $\mathsf{A} \circ \mathsf{C}$, see Fig. 7.2.
  - Define A implicitely via an optimal problem ensuring $\tau = \tau^d$, that is solved online, frequently enough, see (7.1).
- [Joh04]:
  - Implement the allocator A as a continuous-time control unit achieving asymptotic optimality, so that (i) less demanding computational ressources are required and (ii) formal proof of stability of the overall closed-loop system can be established via standard theory.
- [Zac09]:
  - Insert an annihilator post-processing the input produced by some predesigned controller, so that the signal feeding the annihilator is invisible from the output.
  - Do not restrict the attention to ISA, but enlarge the scope of the analysis to incorporate a-IOA allowing for slow input signals impacting the states while remaining invisible from the output at the steady-state.[a]
- [Ser12]:
  - Use geometrical control theory to compute (exact) IOA delivering signal $u_\perp$ that can evolves arbitrarily fast.

[a] As discussed in the bibliographical notes ending this chapter, this idea actually already appears in [BE96].

7.5 Bibliographical notes

Existing works

Pioneer works and characteristic of the literature on control allocation

Historically, mechanical devices have been designed to distribute the desired control effort among different actuators, see [ODB11, Sec. 8.2] for an example on an aircraft equipped with multiple control surfaces that are mechanically constrained to move in concert via cables and pulleys. If such a solution is suitable under nominal conditions, it may not take full advantage of all available actuators when one of them is damaged. Post-fault reconfiguration is not optimal. In addition, for systems equipped with many unconventional actuators, the appropriate manner to make them work in concert becomes less obvious [Bod02, §1].

This was the original motivation for introducing the two-stage control scheme of Fig. 7.2, which already appear in [Cun83, p.78 and the figure p.79] where it is proposed to specified the control commands "in terms of forces, moments, and rates, instead of actual surface positions". Note also that this two-step procedure was already implemented in essence in [Che64], in the context of optimal control for rocket-propelled spaceflight.

Since the earliest contributions come from practitioners, control allocation can legitimately be qualified as an application-driven field. Formalization on this topic was only proposed afterwards, as an attempt to support ad-hoc solutions with a solid and unifying mathematical foundation. Such a situation is not without reminding the historical development of studies devoted to anti-windup, as outlined in e.g. [TT09].

From the above discussion, the first contributions to allocation control probably come from the field of aerospace and aeronautics, which perhaps attracts most of the efforts of the control community dedicated to the control allocation problem. As mentioned at the end of Chap. 6, the allocation problem is also used in the context of ship and underwater control. Another application field often cited for control allocation is automotive and ground vehicles. According to a survey [JF13], classical control problems include yaw stability control and rollover prevention for automotive parts. Other applications include mobile robots and electrical propulsion vehicles equipped with in-wheel electric motors combining drive and regenerative brake functions.

Selected list of contributions on control allocation

Let us outline a selection of important research directions without any claim of being exhaustive.

- Appart from G. Cherry and T. Cunningham [Che64; Cun83] cited above, F. Lallman who was with NASA proposes a control scheme for aircraft control where the two high-level inputs (called "pseudo control variables") are distributed among the five actual components of u via a matrix whose gains are scheduled according to flight conditions and relying on a modal analysis [Lal85b; Lal85a].
- A few years later, J. Paradiso from the Draper Laboratory was probably the first to formulate the allocation problem using the optimization vocabulary [Par89; Par91]. Specifically, the problem was cast as a linear problem where constraints translate actuator magnitude limits, and the objective function aims to discourage large aerosurface deflections and minimize drag, among other objectives.
- In the nineties, another line of research was conducted by W. Durham from Virginia Polytechnic Institute, and culminates in the book [DBB17]. As outlined in the bibliographical

notes ending Chapter 6, the contributions of this researcher and his former students, R. Grogan [Gro94], K. Bordignon [Bor96] and R. Beck [Bec02] are all about (7.1), in the special case where $\mathcal{U}$ is a hyperrectangle and Σ_a is a linear static mapping. Note that the input set $\mathcal{U}$ is denoted by Ω and the feasibility set $B\Omega = \Phi$ is referred to as the attainable moment set [Dur93; BD95b].

- In the last decades of the 20th century, D. Enns, who was with Honeywell Technology Center, his former phd student J. Buffington [Buf96] and co-author A. Teel put valuable effort into setting the ground for rigorous analysis of the CAM implementation issues. Instead of focusing on (7.1), the scope of the analysis has been enlarged to the overall closed-loop, where the allocator is only part of the controller. The starting point is an ad-hoc controller for the flight control of a supermaneuverable aircraft [SEG92]. Sequential dynamic inversion is performed, and redundancy is treated via a pseudoinverse. The stability of the overall scheme is then proved using a two-time scale argument. Note that the actuator limits are disregarded in this study. In [BE96; BET98], the authors enlarge the scope to an arbitrary linear system of the following form:

$$\begin{bmatrix} \dot{z} \\ \dot{y} \end{bmatrix} = \begin{bmatrix} A_{zz} & A_{zy} \\ A_{yz} & A_{yy} \end{bmatrix} \begin{bmatrix} z \\ y \end{bmatrix} + \begin{bmatrix} B_z \\ B_y \end{bmatrix} u \tag{7.44}$$

  where $\text{rank}\{B_y\} = p > m$.[9] It is shown that when this type of system is inverted, the zero-dynamic is affected by the allocator and may become unstable. Sufficient conditions for asymptotic stability of the zero dynamics are then proposed via a small-gain argument and a Lur'e reformulation of this dynamics, leading to asymptotic stability. This condition is specialized for three kinds of allocation: the pseudoinverse, the daisy chain and the direct allocation (see bibliographical notes of Chapter 6). Rephrased in the words of this chapter, the contribution is to highlight that the control unit C_η in Fig. 7.17c can destabilize internal dynamics, if not carefully designed. To investigate how the allocator impacts the zero-dynamic, the authors changed the focus from input-to-state to input-to-output mapping. From our personal view, this is a major contribution of this line of research, which has not received the attention that is deserved.

- O. Härkegård's pdh thesis [Här03], conducted under the supervision of T. Glad at Linköpings University, also adopt this enlarged scope where the focus is put on the entire closed-loop, rather than simply on the allocation algorithm. This gives rise to a theoretical contribution to control allocation with application to flight control [HG01]. Backstepping was proposed as a relevant tool for designing C. An important discussion is also offered on the comparison between the CAM and classical single-step optimal design [HG05]. Specifically, it is shown that if the Hamilton–Jacobi equation admits a continuously differentiable solution, then the two designs lead to the same optimal solution. Note that the input constraint was discarded in this analysis.

- Important contributions have been proposed by T. Fossen and T. Johansen, and the former phd students P. Tøndel [Tøn03], J. Tjønnås [Tjø08], J. Spjøtvold [Spj08] and M. Hanger [Han11] on both the theoretical and practical sides (marine, automotive, blending process, etc.). The core of the main contribution (from our personal viewpoint) is outlined in Subsec. 7.1.4, based on [Joh04], which generalizes the early works of [JS03; JS05] with

[9] Clearly, this formulation can be derived from the standard triple (C, A, B) if $\text{rank}\{C\} = p$ by performing the change of state variable $\left[\begin{smallmatrix} z \\ y \end{smallmatrix}\right] = Tx$ where T is any invertible matrix for which the last p lines correspond to C. In this case, B_y corresponds to the last p lines of $T^{-1}B$. Let us emphasize that the rank of B_y is not necessarily equal to p in general.

applications to nonlinear blending processes. Extensions of this research direction are (i) [TJ05; TJ08] to deal with uncertain parameters via an adaptive strategy and by applying set-stability analysis to also conclude on asymptotic stability of the optimal solution set [Tjo+06], and (ii) [TJ07b; TJ07a] to consider actuator dynamics. See also the applications of (i) on the yaw stabilization of an automotive vehicle using brakes [TJ06]. Besides, note that those researchers have often immersed the control allocation into the more general real-time optimization-based control, so that MPC is often treated together with control allocation. This explains the particular attention that they have paid to the software complexity of the proposed control law, motivating the work for the explicit solution of (7.1) [JFT05; Tøn03; Spj08]. The tools offered in Chap. 6 serves the same purpose.

- More recently, a stream of the literature supported by A. Cristofaro (University of Rome Sapienza), S. Galeani (University of Roma Tor Vergata), M. Sassano (University of Roma Tor Vergata), A. Serrani (Ohio State University), L. Zaccarian (LAAS-CNRS and University of Trento) and their co-authors offers a fresh point of view on the allocation problem. The essential papers [Zac09] and [Ser12] are outlined in Sec. 7.3, based on preliminary references [Zac07] and [Sig+06; SS06a; Sig+09] respectively.
  The proposed control scheme was applied to several technological fields, including tokamak [De +11; Bon+12], propeller platforms [Nai+17; Fur+20] and hypersonic aircraft [Sig+06; Sig+09].
  The fact that any allocator incorporates an annihilator fed by an optimizer was clarified in [CG14], even though it was already implicit in [Zac09] and [Ser12]. Note that the annihilators discussed in [CG14] are ISA and IOA, not a-IOA.
  The case of nonlinear dynamics was considered in [PSZ12; PSZ16]. The focus is on Σ_a, and thus the tracking of τ^d is the control goal. The existence of a linearizing state-feedback is assumed, leading to the closed-loop system $\dot{x}_a = \tilde{u}$, $y = h(x_a)$ where $\tilde{u}$ is the new input. One gets $\dot{y} = \nabla h^\intercal(x_a)\tilde{u}$. In this context, the core idea is to use an input-space basis adapted to $\nabla h(x_a)$. The direction of $\tilde{u}$ along $\nabla h(x_a)$ is responsible for output tracking, whereas the other direction addresses the optimality requirement. In the case where x_a is not measured, an open-loop observer for the actuator dynamics is proposed. A hydrodynamic dynamometer is considered as an application. Instead of performing feedback linearization, the authors of [CGS17] assumed the existence of a special normal form, from which an ISA is exhibited. Subsequently, three different optimizer designs are proposed. One of them comes from [Joh04].
  Output regulation problem is the topic of many papers written by those authors, e.g. [SS06a; Gal+15; ZCS17] to cite a few. See the bibliographical notes in Chap. 9 for more details.

How to deal with dynamical actuators ?

Often, the dynamics of the actuators have been negleted, see e.g. [HG05, Sec.6] among many others. Such an approximation is motivated by the gap existing between the time-scale of the plant and that of the actuators.

Dynamic inversion The importance of taking actuator dynamics into account has been acknowledged as early as in [VB94; Ber+96]. To tackle this issue, the first simple idea of inverting the dynamics of individual actuators can be traced back to [Bol97], where a feed-forward strategy was implemented on first-order dynamical scalar actuators. An analogous feedback strategy was also proposed in [VD01]. In [JF13], this additional control layer in charge of in-

verting the actuator dynamics is called "low-level actuation control". The two lowest control layers in Fig. 7.12 are analogous to [Här04, Fig.3].

Frequency-based design By compensating for the actuator dynamics, the control scheme using C_a destroys the complementarity of the set of actuators. This advocates for a strategy that optimizes control inputs to take full advantage of different dynamics. Heuristic methods addressing the problem of rate saturation were used in [PGH97; RBG96; DLB01] by making the allocator frequency dependent. The idea is to distribute the total actuation effort in the frequency domain and let the actuators operate in different parts of the frequency spectrum. Assume that the actuators are gathered into two groups, according to their bandwidth, and such that the first group assembles the slowest actuators. Then, the input vector in the Laplace domain reads $u(s) = B_1^+ L(s)\tau(s) + B_2^+(1 - L(s))\tau(s)$, where $L(s)$ is a low-pass filter to be designed and $B_{1,2}^+$ are weighted (right) pseudo-inverses of B selected such that B_k^+ gives priority to k-th group. It can be verified that $Bu(s) = \tau(s)$ holds for all s and that the low (resp. high) frequencies of τ are affected to the first and slowest (resp. second and fastest) group. According to [Bor96], a similar approach was already proposed in 1988 by P.D. Shaw. If this frequency-apportioned strategy is appealing, many questions remain open: How to shape $L(s)$? How can the boundary between the two groups of actuators be defined? How to treat actuator magnitude limits ? How can the frequency response of the actuators be incorporated a priori into the allocator ?

An analogous rationale is used in [BF97] where ships equipped with rotatable thrusters are considered. It is proposed to control the azimuth angles via the low-frequency component of the total thrust before computing the force to be produced by each thruster via a standard optimization problem.

Aside from the literature on control allocation, an inversion-based feedforward controller for non-square LTI systems was proposed in [BD00]. In the case of a fat system (more input than output), redundancy is resolved via an optimal problem formulated *in the frequency domain*, allowing for a trade-off between the control effort and output tracking. This allows different actuator bandwidths and ranges to be considered. If the use of the frequency domain for the design of the controller is appealing, this strategy falls short in treating actuation magnitude limits. In addition, this approach has the inherent lack of robustness of the feedforward controller.

Bounding the input rate Another idea for indirectly considering the inertia of the actuators is to impose the inequality $|\dot{u}(t)| \leq \overline{\delta}_u$ at all times via the controller. Here, $\overline{\delta}_u$ is the "rate limit " vector of the actuators. In discrete time, $\dot{u}(t)$ is often approximated via a forward Euler method (assuming that t_s is small) to obtain bounds on $u((k+1)t_s)$ that read $[u(kt_s) - \overline{\delta}_u t_s, u(kt_s) + \overline{\delta}_u t_s]$ [BM02, p.793]. This interval is then intersected with $\mathcal{U}$, which codes the magnitude limits of the actuators, and finally embedded in the constraints of (7.1) as a rough model of the actuation dynamics; see [PS00, p.4] and [PS02; OD04] for second-order dynamical actuators. Note that discretization of $\dot{u}(t)$ via analytical integration can also be implemented to obtain a more precise discrete-time model $u((k+1)t_s) = A_d u(kt_s) + B_d u^d(kt_s)$ where u^d is the desired input, as in **[Kre+21b]**. Then, $u((k+1)t_s)$ should be enforced to belong to the one-step reachable set $\mathcal{U} \cap (\{A_d u(kt_s)\} + B_d \mathcal{U})$.

In the same vein, the following equation is often regarded as yet another standard way to model the dynamical limitation of a first-order dynamical actuator with time constant $\alpha > 0$:

$$\dot{u} = \mathrm{sat}_{[-\overline{\delta}_u, \overline{\delta}_u]}\{(u^d - u)/\alpha\} \tag{7.45}$$

see [Ber+96] for a reference in the control allocation field and [SS99] for a more general treatment of this question. This last equation clarifies that the rate limits are actually saturation of the *state* of the actuator model.

In [Här04], another strategy was presented. The CAM is slightly modified by letting A depend on its past output $u((k-1)t_s)$ to penalize a weighted norm of $u(kt_s) - u((k-1)t_s)$ by redefining the cost function J. This promotes the use of fast actuators during transients. The method remains heuristic, however, since no stability certificate is offered and it is unclear how to derive the most appropriate norm from the actuator dynamical model.

Coding the dynamics of the actuator as a constraint of A The common limit of the references in the above paragraph "Bounding the input rate" is that the only model of the actuators considered in the allocator is the rough approximation (7.45). Hence, explicitly including a more precise version of these actuator dynamics in the design of A is highly desirable. This was the motivation for implementing an MPC philosophy *at the allocator level*. As shown in this chapter, this amounts to directly coding the dynamical model of the actuators as a constraint of the optimization problem (7.1) of the allocator, so that one can avoid using C_a as in [Luo+04, Fig.1]. Following pioneering works [PCM95; VOD04], the authors of [Luo+04] were perhaps the first to implement this MPC strategy in a standard way, considering a set of discretized second-order dynamical actuators subject to magnitude input constraints. In [Luo+05; Luo+07], the same authors dig in the same direction. It is worth noting that the predictive allocator requires the signal $\tau^d(\cdot)$ over a finite horizon to compute the input vector $u(kt_s)$, see [Luo+04, (5)]. For this reason, C is equipped with a prediction control unit constructing this desired trajectory of τ^d. The assumption of a constant desired trajectory considered in [Luo+04] is relaxed in [Luo+05]. Fed by this trajectory, the allocator is composed of a target calculation module that computes a feasible inverse of Σ_a and a model-predictive tracking controller solving the receding-horizon optimal control problem. The allocator is reformulated as a sequential two-step quadratic programming problem with dynamic constraints, which is further cast into a linear complementarity problem.

The obtained stability certificates merely apply to the inner loop made of A and Σ_a, i.e. there is no guarantee that the overall closed-loop system is stable. This was the motivation of the authors of [VSB07]. In this reference, a small gain condition was proposed for this purpose. From the expression of C, the first allocator is obtained under the constraint that the ISS property is ensured for a subsystem of the closed-loop. This (not necessarily optimal) controller is instrumental in defining the additional constraint for the ultimate MPC allocator. Using a frequency-based analysis, a small gain argument, and a scheme that ressembles to [VSB07, Fig.2], it is proposed in [Wu15] to quantify the level of robustness of the direct interconnection of C and Σ_p with respect to $\tau^d - \tau$. Then, this serves as a bound for the allocator design. However, if actuators are explicitly considered, the magnitude limits are beyond the scope of this study. Note also [Han+11] which is concerned with the investigation of using the software system CVXGEN to implement a standard MPC-based control allocation method.

The need for a trajectory of τ^d is in contrast with the approach proposed in this chapter, where $u(kt_s)$ is computed by A from $\tau^d(t_k)$ solely, see (7.14), where an assumption is made on the relative degree of Σ_a. As discussed in Rem. 7.13, our proposal can be interpreted as a one-step MPC with a terminal constraint on the output of Σ_a. It generalizes the result of [OD04], where only first- and second-order actuators are considered. In general, this receding horizon can be larger than one. In addition to being much simpler, this approach allows A to directly optimize the intermediate trajectory of Σ_a between two references τ^d delivered by C. Implicitly, this means that C works at a lower frequency than A. This has pros and cons: Less computational resources need to be affected to C, but a larger dead-time is required for this

control unit to react in case of change of reference or disturbance. Note that in [PS02, p.4], it is also recognized that deadbeat controller is an attractive solution, even if it is not ultimately retained "to avoid unnecessary oscillations ("ringing") of the actuators".

Taking the dynamics of the actuator into account amounts to changing the focus from the static mapping $\Sigma_a^* : y_a \mapsto \tau$ to the dynamical mapping $\Sigma_a : u \mapsto \tau$, see Fig. 7.12. The annihilator of the former can be simply obtained via a basis of Ker $\{\Sigma_a^*\}$. Defining the annihilator of the latter is more involved (see Chap. 8), so that implementation of the CAM has sometimes even be regarded as impossible if Ker $\{B_a\}$ is trivial [Här03, p.112]. Perhaps this explains why the MPC was first proposed as a way to treat redundancy: No explicit annihilator is required. Even if no annihilator is used in [TJ07b], this study considers the dynamics of the actuators by incorporating them in the overall system.

However, tools to construct annihilators of any input-to-output mapping have been proposed [Zac09] and [Ser12], as briefly shown in this chapter and analyzed in detail in the next two chapters. They can be readily applied to the mapping Σ_a and may lead to an annihilator even if Ker $\{B_a\}$ is trivial.

Designing C in the case of dynamic actuators It is shown in Tab. 7.2 that the cascade $\Sigma_a \circ \mathsf{A}$ should be modeled as pure time delays from the point of view of C. Let us stress that even in the case of static actuators, this sentence remains valid owing to the computational time required by the allocator. If a comprehensive discussion on this topic is missing, elements have been offered in [PS02; VSB07].

Rephrased existing works

The goals of this chapter are twofold. First, we identify and articulate the main ingredients toward a solid mathematical foundation of the CAM; see Sec. 7.1. Second, we bring closer the literature dedicated to CAM in Sec. 7.2, and those devoted to input redundancy, whose founding papers are outlined in Sec. 7.3. On both aspects, the added-value of this study is to rearrange existing, but disconnected and therefore quite misunderstood[10] pieces of the literature. By making use of a single running academic example, the aim is to provide an ambitious and (hopefully) neutral review of the literature, which is enlarged and deepened in the bibliographical notes continued in the forthcoming Sec. 7.6.

In completing this picture, missing (or seldom acknowledged) facts and arguments are identified and taylored, e.g. (i) $\Sigma = \Sigma_p \circ \Sigma_a$ should be treated directly and [Zac09; Ser12] offer tools to this purpose; (ii) Fig. 7.17; (iii) Both feedback and feedforward forms of Fig. 7.16 exist; (iv) Subsec. 7.2 on how to handle dynamical actuators in a general context; (v) The output of C should be saturated, out of $\Sigma_a(\mathcal{U})$.

7.6 Discussion on some trends of the literature

This chapter is closed with personal questions on some streams of the literature. Some of them opens perspectives for further works, that are outlined in the last chapter.

7.6.1 On modular design and the design requirements for C

Attaignability of τ^d Many papers treat the case of unattainable τ^d, leading to the "error minimization" problem outlined in e.g. [JF13, Sec. 2]. As an example, recall "direct allocation"

[10] See the bibliographical notes ending with Chap. 8 and Chap. 9, where, in particular, samples of confusing pieces of literature on the relationships between the a-IOA of [Zac09] and the IOA of [Ser12].

proposes scaling down τ^d while preserving its direction, in the case where τ^d does not belong to $\Sigma_a(\mathcal{U})$ [Dur93].

We believe that the relevance of this problem is questionable, though. As discussed in this chapter, we indeed firmly believe that $\tau^d \in \Sigma_a(\mathcal{U})$ must be a specification for the design of C, that is, this control unit must only deliver attainable τ^d to A. The rationale behind this rule comes from the observation that CAM is a particular case of hierarchical control. Such a control structure hinges on the fact that a controller of level N can disregard how level $N-1$ is implemented. Clearly, this strategy is legitimate only if the reference signal delivered at level N to drive $N-1$ is feasible. Violating this principle destroys the hierarchy and makes convoluted any formal rational on e.g. stability. In this case, the benefits of implementing a hierarchical structure become questionable. Indeed, if such modular schemes are inevitably more complex, they are primarily motivated by the quest to propose structures that are more amenable to formal proofs.

It is worth noting that once the CAM was settled in the literature in the early 90's, an important part of it was devoted to solving (7.1) *for its own*. For this task, the only relevant model is Σ_a. Signal τ^d is considered exogenous, forgetting about C from which it originates [DB96]. Perhaps this explains why arbitrary τ^d have been considered, even unattainable signals. In improving the design process of the allocator, one has forgotten the context in which this control unit is immersed.

Design requirements of C The quest for a fully independent design steps is hopeless. The key idea implicitly promoted in this chapter is that CAM can only bear fruit as a modular design if the following minimal dependencies are accepted between the designs of C and A. First, constraint $\mathcal{U}$, related to A, must be propagated through Σ_a to obtain the appropriate constraint on $\tau^d(t)$. The consequence of this rule is that if some actuators become faulty, the post-fault set $\mathcal{U}'$ must be used to update the expression of the set $\Sigma_a(\mathcal{U}')$ where $\tau^d(t)$ is to be selected. Along this line, it is incorrect to say that C is independent of the health of the set of actuators. Note that the tools offered in Chap. 6 are just intended for the computation of $\Sigma_a(\mathcal{U})$. Second, the design of C must be carefully tailored to the retained control unit A. Otherwise, the inevitable time delays (see Tab. 7.2) induced by the cascade $\Sigma_a \circ$ A might destabilize the closed loop. Similarly as the one exposed in [VSB07] and in [Joh04] (see Rem. 7.3), the design methodology promoted by this discussion is sequential rather than based on two independent tasks. However, as opposed to [VSB07], we advocate here to start with the design of A, and then continue with that of C.

See [**Kre+21b**] and, in particular its Fig. 6, for the implementation of those guidelines. Note that the main contributions of this reference are outlined in Subsec. 10.5.1 at p.192.

7.6.2 On the separation of Σ as $\Sigma_p \circ \Sigma_a$ and the optimal allocation of τ^d

A systemic way to perform this separation When implementing the CAM, the separation between the actuator subsystem Σ_a and the plant Σ_p is often performed based on technological considerations. Over-actuation is then regarded as a property of Σ_a. However, for some systems Σ, such a separation is considered difficult to identify. For instance, it is rarely acknowledged that parallel interconnection of DC/DC converters is an overactuated system, even if it can be viewed as such, see Chap. 10. Given Σ, the two questions to be addressed are: Is this system separable ? If so, how to split it or, saying it differently, how to identify τ in the causal chain from u to y ? A systemic way to answer these questions is desirable. In particular, formal methods leading to optimal separation would answer the second question throughout. By optimal, it is meant that the size of τ is minimized. This is expected to maximize the fea-

sible set of the optimization problem (7.1). Saying it differently, it would unveil all degrees of freedom associated with the control of the output. The methodology employed to design the IOA in this chapter is just one of the methods achieving such a purpose, see Chap. 8 for more details.

Is this separation and tracking of τ^d relevent ? Once τ has been identified, according to most of the cited references in the above literature review, the next step is to solve (7.1) and, in particular, to validate its constraint $\tau = \tau^d$ (modulo some time delay between those two signals). This equality is to be satisfied instantaneously (for static actuator), over a finite receding horizon (for MPC strategy with a reference trajectory for τ^d), after a finite number of sampling times (for MPC with terminal constraint), or asymptotically (for the optimum-seeking strategy). However, this subproblem is only an intermediate step toward controlling the input-to-output relationship. Thus, if the control of Σ can be tackled head-on, as in the approaches discussed in Sec. 7.3, there are no reasons to track τ^d with τ and, in turn, to separate Σ as $\Sigma_p \circ \Sigma_a$.

Recall that incorporation of the dynamics of the actuators amounts to enlarging the scope of the allocator from $\Sigma_a^* : y_a \mapsto \tau$ to $\Sigma_a : u \mapsto \tau$. Here, we propose to move a step forward by considering $\Sigma : u \mapsto y$. In this case, the distinction between the actuation subsystem Σ_a and plant Σ_p becomes irrelevant. After the authors of [Zac09; Ser12] (from our interpretation of their contributions), our conviction is that one should forget about control allocation (that is, tracking of τ^d) and instead keep digging toward the most appropriate treatment of the redundancy of Σ. It seems to us that this idea can be traced back to [BE96; BM02].

Are rate limits relevent ? Let us now introduce a related topic via the following quote: "Rate limits are of particular importance in mechanical systems where the inertia in various components of the actuator prevents it from moving very fast, thereby limiting the rate of the control signal that it can pass to the plant." [Tar+11, Sec.7-6-1]. Among many others, this sentence suggests that the inequality $|\dot{u}(t)| \leq \bar{\delta}_u$, or its refined version (7.45), should be regarded as a rough model of the actuators, capturing the limits to its intrinsic dynamics. This has two consequences, which makes the relevance of this modeling questionnable. (i) The above constraints on $\dot{u}$ shall be discarded as soon as the dynamics of the actuators can be incorporated directly, i.e. let Σ model the plant *and* actuation subsystem. However, many publications consider a model with actuator dynamics *and* the above rate limits, for example [VOD04; Här04]. (ii) As soon as a dynamical model comes with rate-limit saturation, as in [Luo+07; Zac09], one can legitimately understand that the input of such a model is y_a, the output of the actuator, rather than u, its input. However, in that case, the above guideline (incorporating the dynamics of the actuators into Σ) is not followed. Therefore, the question is why not gather the dynamics of both the actuators and the plant into Σ, and then discard the rate limits ?

7.6.3 On the substitution of standard solvers by continuous-time systems to solve the optimization problem

Benefits of continuous-time solvers In stark contrast with the CAM, but in the spirit of the results presented in Sec. 7.1.4, the approach proposed in Sec. 7.3 relies on a continuous-time dynamical subsystem to solve the optimization problem (7.19) or (7.41). In such a case, the resulting closed loop is a continuous-time dynamical system that can be analyzed using standard tools. This differs from the CAM, where the inevitable sample and hold mechanism illustrated in Fig. 7.3 induces a mix of continuous-time and discrete-time dynamics, which complexifies

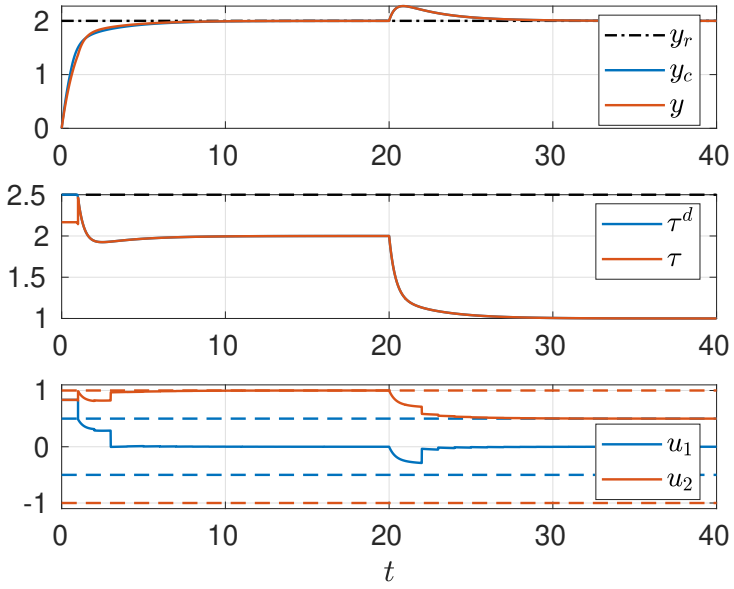

Figure 7.21: Simulation results obtained for Ex. 7.1 and using design (b) of Subsec. 7.6.3. Compare this picture with Fig. 7.7 where analogous results are displayed for design (a) of Subsec. 7.6.3. See the caption of Fig. 7.6 for a description of the different signals.

the analysis. The lack of an explicit expression of A defined by (7.1) is also a source of difficulty. Perhaps these are the reasons why ultimate proofs of stability considering the overall closed-loop system are seldom offered in this context.

Closed-loop is ultimately hybrid However, the standard implementation of the control law uses digital computational devices. As a result, the ultimate step of each strategy is the discretization of the control law via a sample-and-hold mechanism, even for the approaches proposed in Sec. 7.3. Dynamical closed-loop models for ultimate stability analysis are thus inevitably hybrid. This comment might weaken the benefits of using the continuous-time optimizer. However, it might also stimulate the combination of the two approaches.

Toward hybrid controllers As an illustration of the sentence closing the last paragraph, if there exists an ISA, then any traditional solver (implemented as in Fig. 7.3) for (7.19) can be used as the definition for the optimizer C_η. Compared with CAM, this drastically reduces the requirement for computational resources. To see this, consider the following two control schemes, which are implemented in the case of static actuators Σ_a for which the ISA reads $\eta \mapsto u_\perp = N\eta$ with $\Sigma_a N = \mathbf{0}$:

(a) Fig. 7.2 where A solves (7.1);

(b) Fig. 7.16b where C_η solves the enriched version of (7.19) taking the input constraints into account. For a fair comparison, signal u_c is defined such that $\tau = \tau^d$, which is equivalent to $u_c = L\tau^d$ with $\Sigma_a L = \mathbf{I}$ because $\tau = \Sigma_a(u_c + N\eta) = \Sigma_a u_c$.

In both cases, the solvers are surrounded by a sample and hold mechanism like the one depicted in Fig. 7.3.

To illustrate the results obtained using both designs, we consider Ex. 7.1 *with the input constraints* and we use a sampling period of $t_s = t_d = 1$ to model the computational effort of the solvers, see Fig. 7.3. The signal τ^d reads as in (7.7). The results of the first design are shown

in Fig. 7.7. The second design leads to the same control units C_c and $\mathsf{C}_\perp$ as in Sec. 7.3.2; see (7.22) and (7.25). In this context, the expression for C_η is as follows:

$$\mathsf{C}_\eta : u_c \mapsto \arg\min_{\check{\eta}} J(u_c + N\check{\eta}) = (u_{c1} + \check{\eta})^2 \quad \text{s.t.} \quad u_c + N\check{\eta} \in \mathcal{U} = [-0.5, 0.5] \times [-1, 1]$$

The simulation results are reported in Fig. 7.21. Comments are as follows. (i) Unlike $u_\perp = N\eta$ generated via the solver C_η, the signal $u = u_c + u_\perp$ is not piecewise constant since $u_c = L\tau^d$ is continuous. (ii) Output trajectory is very close to the reference y_c shapped by τ^d, and much more satisfactory than in the case of the first design, see Fig. 7.7. (iii) u_1 converges to zero after a short transient so that asymptotic optimality is achieved. (iv) When $t \in [0, 1]$, $u_1(t)$ slightly exceeds its limits, even if it is saturated by Σ_a. This phenomenon can indeed occur because C_η only ensures that $u_c((k-1)t_s) + N\eta(kt_s)$ belongs to $\mathcal{U}$ whereas $u(t) = u_c(t) + N\eta(kt_s)$ can escape from the input set very well, that is, C_η does not guarantee that the constraints $u(t) \in \mathcal{U}$ are satisfied during transients. We conjecture that this mismatch on u_1 cannot destabilize the closed-loop because τ^d has been already saturated in such a way that the optimization problem solved by C_η is feasible, so that $\tau = \tau^d$ is valid modulo short transients that are asymptotically vanishing.

The bottom line of this discussion is that the mixture of the two approaches proposed in the design (b) is much less demanding in terms of computational resources. Indeed, an inefficient solver parameterized by $t_s = 1$ leads to an almost perfect output trajectory for the design (b), whereas it destabilizes the closed-loop for the first design. Those differences can be explained via careful observations on the first design: When substituting u by its decomposition $L\tau^d + N\eta$ in the equality constraint of (7.1), one gets

$$\tau = \Sigma_a(L\tau^d + N\eta) = \tau^d$$

Therefore, this equality constraint imposes a value of τ^d and allows η to be freely optimized. The key point is that when implementing (7.1), as in the first design, these two input components are not separated. However, the time delay due to the computational effort affects η and τ^d, even if the ultimate value of the latter could have been predicted solely on the basis of the above equality constraint. This time delay on τ^d may challenge the stability, as shown in Fig. 7.7 because τ^d is the part of u that controls the output. The design (b) somehow discriminates the part of u that is imposed by the equality constraint and removes it from the optimization process, not to introduce unnecessary and dangerous time delay on this crucial component of the input that governs the output trajectory. In the unconstrained case, the remaining part η of the input can then be freely optimized as it is invisible from the output. When input constraints exist, then the above discussion on Ex. 7.1 suggests promising research directions.

A nice illustration of this line of thought is offered in [Zho+13; ZCS16]: In the context of output regulation, reference trajectories are selected via an MPC strategy among a *preselected set of suitable trajectories* constructed beforehand, on the basis of geometric decomposition of the system.

7.6.4 On the input space decomposition perspective

In Sec. 7.3, the "signal injection perspective" is implicitly adopted, i.e. given *arbitrary* u_c, the problem is to shape $u_\perp$ in such a way that u_c and $u_c + u_\perp$ generate the same output y, see Fig. 7.16. Following the discussion in the introduction and in the last paragraph, another perspective is to (i) decompose the input space into some direct sum $\mathcal{N} \oplus \mathcal{L}$ where $\mathcal{N}$ is the set of

all signals that are invisible from the output and (ii) impose that $u_\perp$ and u_c belong identically to $\mathcal{N}$ and $\mathcal{L}$, respectively.

However, owing to the linearity of Σ and the lack of constraints, the two points of view are equivalent in the sense that any result obtained from one perspective can be equivalently reformulated in the other. As an illustration, consider the case where $u_c(t)$ is arbitrary and $u_\perp(t)$ equals $N\eta(t)$ where the columns of N is a basis matrix of $\mathcal{N}$. This complies with the "signal injection perspective". Following the "input space decomposition perspective", one has rather restrict the set of admissible $u_c(t)$ to $\mathrm{Im}\{L\}$, where L is any matrix such that $\begin{bmatrix} N & L \end{bmatrix}$ is invertible. This can be imposed without loss of generality since it holds:

$$\forall u(t) \in \mathbb{R}^m, \exists \hat{u}_c(t) \in \mathrm{Im}\{L\}, \exists \hat{\eta}(t) : u(t) = \hat{u}_c(t) + N\hat{\eta}(t).$$

Therefore, any input $u(t) = u_c(t) + N\eta(t)$ can be equivalently rewritten as $\hat{u}_c(t) + N\hat{\eta}(t)$ for some $\hat{u}_c(t) \in \mathrm{Im}\{L\}$ and $\hat{\eta}(t)$. Roughly speaking, the part of $u_c(t)$ that lies in $\mathrm{Im}\{N\}$ can be transferred to $\eta(t)$, so that the rest belongs to $\mathrm{Im}\{L\}$. Observe that Ex. 7.1 has been treated in this manner in the case of the ISA. Indeed, $u_c(t) \in \mathrm{Im}\{L\}$ with $L = \begin{bmatrix} 1/3 & 1/3 \end{bmatrix}^\intercal$ has been imposed and $\begin{bmatrix} N & L \end{bmatrix}$ is invertible, see Subsection 7.3.2.

In the "signal injection perspective", the *given* controller C_c is post-processed by $\mathsf{C}_\perp$ and C_η as in Fig. 7.16. In essence, this strategy resembles the model recovery anti-windup design [Gal+09]. In both cases, the added control unit prostprocesses the control signal computed via a given controller with the aim of decreasing the norm of the input signal (via the annihilator) or enlarging the basin of attraction of the closed-loop equilibrium (via the antiwindup). In both cases, the output trajectory is preserved by post-processing as much as possible. The most attractive advantage of such two-step designs is perhaps their ability to incorporate an already existing controller.

However, when the control design is to be performed from scratch, it could be preferable to rely on geometrical decomposition. In this case, the input design can be divided into two independent steps. First, shape the part of u that belongs to $\mathcal{N}$ and is invisible from the output. Second, shape the part of u that belongs to $\mathcal{L}$. The key argument here is that this second step is a well-defined problem, as the domain restriction of Σ to $\mathcal{L}$ is left-invertible, that is, to any admissible output trajectory corresponds a unique input trajectory in $\mathcal{L}$, see the introduction.

Chapter 8

Input redundancy: Definitions, characterizations and taxonomy

Contents

From the previous chapter, it should be clear that Σ can be qualified as Input Redundant (IR) if it admits an input-output annihilator (IOA).[1] The purpose of this chapter is to provide a mathematical framework for this central idea. Henceforth, "annihilator" is used as a short for IOA. In addition, we aim to relate IR to the concept of inversion, as in the introduction.

Let us emphasize that efforts toward an appropriate definition of IR, together with tractable characterizations, not only help qualifying systems for which the control strategy applies, but also underpins the control architecture. The message is that suitable definitions lead to appropriate decomposition and, thereby, to a relevant control scheme. In accordance with this statement, this chapter and the next one show the core of the differences between the control schemes exposed in Chap. 7 originates from non-equivalent definitions of IR.

This chapter also shows how the proposed framework can cope with input and state constraints. This feature is indeed of major importance since IR has been historically regarded as a way to handle input limitations. Thus, this chapter aims to explore how constraints can challenge IR.

8.1 Introduction

This chapter is concerned with the linear, proper and time-invariant dynamical system Σ governed by the following equations

$$\dot{x}(t) = Ax(t) + Bu(t),\ x(0) =: x_0, \tag{8.1a}$$
$$y(t) = Cx(t) + Du(t), \tag{8.1b}$$

for some quadruple (A, B, C, D) of appropriate dimensions and with state-space

$$\mathcal{X} = \mathbb{R}^n.$$

From (8.1a), the input-to-state relationship is concisely captured via $\mathrm{H}_x[x_0; \cdot]$ which maps an input trajectory $u(\cdot)$ to the state trajectory $x(\cdot)$ produced by the system when excited by $u(\cdot)$ with an initial condition $x(0) = x_0 \in \mathcal{X}$. The corresponding input-to-output mapping $\mathrm{H}[x_0; \cdot] : u \mapsto C\mathrm{H}_x[x_0; u] + Du$ is defined by (8.1b).

Let $\mathbf{C}$ and $\mathbf{PC}$ be the set of causal continuous and causal piecewise continuous vector-valued signals, respectively. Input u is assumed to belong to $\mathbf{U} = \mathbf{PC}$. State x and, in turn, output y, are also assumed to be causal. From (8.1), we can define $\mathbf{X} := \mathbf{C}$ and $\mathbf{Y} := \mathbf{PC}$ as the codomains of $\mathrm{H}_x[x_0; \cdot]$ and $\mathrm{H}[x_0; \cdot]$, respectively. The set of triples (u, x, y) (resp. pairs (u, y)) *compatible for* $x_0 \in \mathcal{X}$ is denoted by $\mathbf{Q}(x_0)$ (resp. $\mathbf{W}(x_0)$), i.e.

$$\mathbf{Q}(x_0) := \{(u, x, y) \in \mathbf{U} \times \mathbf{X} \times \mathbf{Y} \mid \mathrm{H}_x[x_0; u] = x,\ \mathrm{H}[x_0; u] = y\},$$
$$\mathbf{W}(x_0) := \{(u, y) \in \mathbf{U} \times \mathbf{Y} \mid \exists x : (u, x, y) \in \mathbf{Q}(x_0)\}.$$

Owing to the linearity of the dynamics of Σ, recall that the following well-known relationships hold for all $x_0, \tilde{x}_0 \in \mathcal{X}$, $u, \tilde{u} \in \mathbf{U}$ and $\alpha \in \mathbb{R}$:

$$\mathrm{H}_x[x_0; u] + \mathrm{H}_x[\tilde{x}_0; \tilde{u}] = \mathrm{H}_x[x_0 + \tilde{x}_0; u + \tilde{u}],$$
$$\mathrm{H}_x[\alpha x_0; \alpha u] = \alpha \mathrm{H}_x[x_0; u].$$

Clearly, the same two properties hold for H instead of H_x.

[1] The case of a-IOA is also interesting. An in-depth comparison between the two concepts is one of the goals of Chap. 9.

8.2 Input redundancy

This concept of redundancy is now defined, characterized, and discussed.

8.2.1 Definition

Definition (Left-invertible)**.** System Σ is said *left-invertible* if identical output trajectories can only originate from identical input trajectories, i.e. the following implication[a]

$$(y_1 = y_2) \quad \Rightarrow \quad (u_1 = u_2). \tag{8.2}$$

holds for all $x_0 \in \mathcal{X}$ and for all $(u_1, y_1), (u_2, y_2) \in \mathbf{W}(x_0)$.

[a] Signals u_1, u_2 are said equal if $|\{u_1, u_2\}| = 1$ so that $u_1(t) = u_2(t)$ holds for almost all t.

Definition (Input redundant)**.** System Σ is *input redundant* (IR) if it is not left-invertible, i.e. there exists $x_0 \in \mathcal{X}$ such that

$$\exists (u_1, y_1), (u_2, y_2) \in \mathbf{W}(x_0) : u_1 \neq u_2, y_1 = y_2. \tag{8.3}$$

To prove that Σ is IR, it suffices to find a single output that admits at least two distinct preimages by $\mathrm{H}[x_0; \cdot]$ for some $x_0 \in \mathcal{X}$. This means that the system Σ is IR if and only if $\mathrm{H}[x_0; \cdot]$ is *not* injective for some $x_0 \in \mathcal{X}$. From the linearity of H, one immediately obtains

$$\exists x_0 \in \mathcal{X} : (8.3) \Leftrightarrow \exists \tilde{u} \in \mathbf{U} \setminus \{\mathbf{0}\} : \mathrm{H}[\mathbf{0}; \tilde{u}] = \mathbf{0}. \tag{8.4}$$

The independence of this condition wrt both x_0 and y highlights that this singularity actually occurs *for all* admissible outputs and *for all* initial states.[2]

Proposition 8.1 (**[KT21]**)**.** *If system Σ is IR, then it holds:*

$$\forall x_0 \in \mathcal{X}, \forall (u_1, y_1) \in \mathbf{W}(x_0), \exists (u_2, y_2) \in \mathbf{W}(x_0) : u_1 \neq u_2, y_1 = y_2.$$

8.2.2 Characterization

Let us now equipped the proposed definition of IR with tractable characterizations. Different tools exist for this purpose, e.g. the system matrix

$$P_\Sigma(s) := \begin{bmatrix} s\mathbf{I} - A & -B \\ C & D \end{bmatrix}, \tag{8.5}$$

the transfert function matrix

$$G(s) = C(s\mathbf{I} - A)^{-1}B + D$$

or a suitable geometrical decomposition of the input and state spaces are some of them.[3] As shown by the following theorem, any of these tools leads to distinct but equivalent characterizations of IR.

[2] It will be shown in the sequel that this property hinges not only on the linearity of H but also on that of the input and state spaces, see Prop.8.14.

[3] Recall that Appendix A provides essential concepts on geometric control theory.

Theorem 8.2 ([KT21]). *Define $\rho \in \mathbb{N}$ and $\mathcal{N} \subset \mathbb{R}^m$ as follows:*

$$\rho := \dim \operatorname{Ker} \left\{ \begin{bmatrix} B \\ D \end{bmatrix} \right\}, \tag{8.6}$$

$$\mathcal{N} := B^{-1}\mathcal{V}^* \cap \operatorname{Ker} \{D\}. \tag{8.7}$$

Then, the following statements are equivalent:

(i) System Σ is IR;

(ii) $\dim(\mathcal{R}^*) > 0$ or $\rho > 0$;

(iii) $\dim(\mathcal{N}) > 0$;

(iv) Transfer matrix $G(s)$ of Σ is not left-invertible, i.e. there exists a non-zero polynomial vector q such that $G(s)q(s) = \mathbf{0}$ for all $s \in \mathbb{C}$;

(v) System matrix of $P_\Sigma(s)$ is not left-invertible.

The next lemma offers an efficient way to compute $\dim \mathcal{N}$.

Lemma 8.3 ([KT21]). *It holds*

$$\dim \mathcal{N} = n + m - \operatorname{nrank} \{P_\Sigma\}. \tag{8.8}$$

Remark 8.4 (On (i)⇔(ii)). Bearing in mind the definition of $\mathcal{R}^*$ (see Appendix A), the equivalence between (i) and (ii) can be obtained via the following insightful chain of equivalences:

$$\begin{aligned}
\Sigma \text{ is IR} &\overset{(8.4)}{\iff} \exists \tilde{u} \in \mathbf{U} \setminus \{\mathbf{0}\} : \mathrm{H}[\mathbf{0}; \tilde{u}] = \mathbf{0} \\
&\overset{\text{def. of } \mathcal{R}^*}{\iff} \exists \tilde{u} \in \mathbf{U} \setminus \{\mathbf{0}\} : \mathrm{H}_x[\mathbf{0}; \tilde{u}](t) \in \mathcal{R}^*, \forall t \geq 0 \\
&\iff \left| \begin{array}{ll} \rho > 0, & (\text{since } \mathcal{R}^* = \{\mathbf{0}\} \Rightarrow \left[\begin{smallmatrix} B \\ D \end{smallmatrix}\right] \tilde{u} = \mathbf{0}) \\ \quad \text{or} & \\ \dim \mathcal{R}^* > 0, & (\text{since } \rho = 0 \Rightarrow \left[\begin{smallmatrix} B \\ D \end{smallmatrix}\right] \tilde{u} \neq \mathbf{0}) \end{array} \right.
\end{aligned}$$

•

Remark 8.5 (Normal rank of P_Σ and G). Given a matrix $T(s)$ parameterized by $s \in \mathbb{C}$. Its *normal rank* is defined as follows:

$$\operatorname{nrank} \{T\} := \max_{s \in \mathbb{C}} \operatorname{rank} \{T(s)\}.$$

It can be observed that (iv) and (v) of Th. 8.2 are equivalent to $\operatorname{nrank} \{G\} < m$ and $\operatorname{nrank} \{P_\Sigma\} < n + m$, respectively. •

8.2.3 Can IR be deduced from system dimensions?

Remark 8.6 (IR $\not\Rightarrow m > p$). The condition $m > p$ is often understood as a necessary condition for IR. Let us already provide a counterexample of this assertion. Consider the following square system, for which $m = p = 2$ holds:

$$\begin{aligned}
\dot{x} &= \begin{bmatrix} -1 & 0 & 0 \\ 0 & -1 & 0 \\ 0 & 0 & -1 \end{bmatrix} x + \begin{bmatrix} 1 & 0 \\ 1 & 0 \\ 0 & 1 \end{bmatrix} u \\
y &= \begin{bmatrix} 1 & 0 & 0 \\ 0 & 1 & 0 \end{bmatrix} x.
\end{aligned}$$

Then, IR follows from the observation that distinct input trajectories $u_1 : t \mapsto \mathbf{0}$ and $u_2 : t \mapsto \left[\begin{smallmatrix} 0 \\ 1 \end{smallmatrix}\right]$ produce the same output $y = \mathbf{0}$ for $x_0 = \mathbf{0}$. •

Right-invertibility can be characterized by $\operatorname{nrank}\{P_\Sigma\} = n + p$ [TSH12, Th. 8.13]. This statement leads to the following corollary of Th. 8.2 and Lem. 8.3.

Corollary 8.7 ([**KT21**]). *Assume that Σ is right-invertible. It holds*

$$\dim \mathcal{N} = m - p, \tag{8.9}$$

so that Σ is IR iff $m > p$ holds.

8.3 Annihilator

Referring to the introduction of this manuscript, let us turn our attention from the inversion perspective adopted so far to the signal injection perspective.

8.3.1 Definition

Referring to (8.3), define the incremental input $\tilde{u} := u_1 - u_2$. By means of this signal and renaming (u_2, y_2) by (u, y), observe that (8.3) can be equivalently rewritten as follows:

$$\exists (u, y) \in \mathbf{W}(x_0), \exists \tilde{u} \neq \mathbf{0} : (u + \tilde{u}, y) \in \mathbf{W}(x_0). \tag{8.10}$$

From a control point of view, this reformulation is of utmost importance. Indeed, it highlights that $\tilde{u}$ can be used as an increment to any input u which let the output unaffected. Therefore, $\tilde{u}$ can be shaped to serve a secondary control goal unrelated to the output trajectory.

Given $x_0 \in \mathcal{X}$ and $(u, y) \in \mathbf{W}(x_0)$. By definition of $\mathbf{W}$, there exists $\tilde{u}$ satisfying $(u + \tilde{u}, y) \in \mathbf{W}(x_0)$ iff $\tilde{u} \in \mathbf{U}_\Sigma$ and $\mathrm{H}[\mathbf{0}; \tilde{u}] = \mathbf{0}$ hold, see (8.4). These two conditions are concisely captured by $(\tilde{u}, \mathbf{0}) \in \mathbf{W}(\mathbf{0})$. Equation $\mathrm{H}[\mathbf{0}; \tilde{u}] = \mathbf{0}$ means that $\tilde{u}$ has to be selected as an input inducing zero output from the zero initial state, i.e. $\tilde{u}$ lies in the kernel of $\mathrm{H}[\mathbf{0}; \cdot]$. This is the motivation for calling "annihilator of Σ" the operator introduced by the following definition and illustrated by Fig. 8.1.

Definition (Annihilator of Σ)**.** The nonzero causal operator $\mathsf{C}_\perp$, associated with the mapping $\mathrm{H}_\perp[x_{a0}; \cdot] : v \mapsto \tilde{u}$ parametrized by the initial state x_{a0}, is an *annihilator of* Σ if:

$$\exists x_{a0}, \forall v(\cdot) \in \mathbf{PC} : \ (\tilde{u}, \mathbf{0}) \in \mathbf{W}(\mathbf{0}), \tag{8.11}$$

where $\tilde{u} := \mathrm{H}_\perp[x_{a0}; v]$.

8.3.2 Construction of an annihilator of Σ

The fact that Σ is IR is necessary for the existence of an annihilator of Σ, by definition. The next theorem shows that it is also sufficient.

Theorem 8.8. *Assume that Σ is IR. Select any F in $\mathbb{F}(\mathcal{R}^*)$. Let $N : \mathcal{N} \to \mathbb{R}^m$ be the natural embedding. Then, the quadruple*

$$(A_a, B_a, C_a, D_a) = ((A + BF)|\mathcal{R}^*, \mathcal{R}^*|B|\mathcal{N}, F|\mathcal{R}^*, N), \quad x_{a0} = \mathbf{0}, \tag{8.12}$$

characterizing $\mathrm{H}_\perp$ defines an annihilator of Σ.

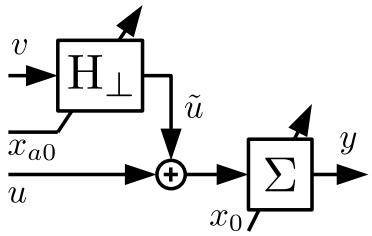

Figure 8.1: For all v and for all x_0, there exists x_{a0} such that signal $\tilde{u}$ is invisible from the output, i.e. both u and $u + \tilde{u}$ produces y.

Remark 8.9 (On $\sigma(A_a)$). The spectrum of A_a can be assigned arbitrarily using F. In particular, A_a can be made Hurwitz. •

Remark 8.10 (Maximal range). The annihilator of Th. 8.8 has maximal range in the following sense: For all $\tilde{u}$ such that $(\tilde{u}, \mathbf{0}) \in \mathbf{W}(\mathbf{0})$, there exist x_{a0} and $v \in \mathbf{PC}$ such that $\mathrm{H}_\perp[x_{a0}; v] = \tilde{u}$. •

Remark 8.11 (On the transfert function of $\mathsf{C}_\perp$). The transfer function matrix $G_\perp$ of $\mathsf{C}_\perp$ satisfies:

$$G(s)G_\perp(s) = \mathbf{0}$$

for all $s \in \mathbb{C}$. •

Remark 8.12 (The case $\mathbf{0} \in \mathbb{F}(\mathcal{R}^*)$). If the zero map belongs to $\mathbb{F}(\mathcal{R}^*)$, then selecting $F = \mathbf{0}$ makes $\tilde{u}$ independent of x_a so that the input-output mapping of $\mathrm{H}_\perp$ can be captured by the static mapping $v \mapsto Nv$. •

8.4 How constraints impact input redundancy ?

So far, it has been assumed that Σ is free from input or state constraints. However, from the very beginning, IR has been considered as a way to deal with input constraints by redistributing the overall control effort among actuators to avoid saturation, see Chap. 7. Motivated by this observation, let us now consider the more general case where constraints are imposed, not only on $u(t)$ but also on $x(t)$, so that the following conditions hold for all $t \geq 0$:

$$u(t) \in \mathcal{U}, \tag{8.13a}$$
$$x(t) \in \mathcal{X}, \tag{8.13b}$$

where $\mathcal{U} \subset \mathbb{R}^m$ and $\mathcal{X} \subset \mathbb{R}^n$ are *arbitrary* given sets.

In the unconstrained context where $\mathcal{U} = \mathbb{R}^m$ and $\mathcal{X} = \mathbb{R}^n$ hold, it is shown in this chapter that if one can find $x_0 \in \mathcal{X}$ and y generated by two distinct inputs $u_1, u_2 \in \mathbf{U}$, then such a redundancy occurs for any other (x_0, y), see Prop. 8.1. An immediate question is whether this uniform (wrt to (x_0, y)) non-uniqueness of the input remains valid in the constrained context. The following example explicitly shows that the answer can be negative, so constraints may challenge the redundancy.

Example 8.13. Consider the following system

$$\dot{x} = -x + \begin{bmatrix} 1 & 1 \end{bmatrix} u, \quad y = x + \begin{bmatrix} 1 & 0 \end{bmatrix} u,$$

for which each input is enforced to be non-negative, whereas state trajectory is unconstrained, i.e. $u(t) \in \mathcal{U} = \mathbb{R}^2_{\geq 0}$ and $x(t) \in \mathcal{X} = \mathbb{R}$ for all $t \in \mathbb{R}_{\geq 0}$. Observe that input-to-output mapping is fully captured via the following equation, where y acts as a parameter and $u =: [u_a, u_b]^\intercal$ are

unknown functions:

$$\dot{y} + y - u_b = \dot{u}_a + 2u_a, \tag{8.14}$$

with $u_a(0) = y(0) - x(0)$. Consider the following cases:

(i) Define $x_{0,1} := -1$ and $y_1 : t \mapsto -e^{-t}$. In this case, $u_1 =: [u_{1,a}, u_{1,b}]^\intercal = \mathbf{0}$ is the unique input satisfying $u(t) \in \mathcal{U}$ leading to y_1 when $x(0) = x_{0,1}$. Indeed, (8.14) reduces to $-u_b = \dot{u}_a + 2u_a$ with $u_a(0) = 0$, so that a strictly positive value of $u_b(t)$ induces a violation of constraint $u_a(t) \geq 0$. Hence, $u_1(t)$ must equal $\mathbf{0}$ at all times.

(ii) Keep $x(0) = x_{0,1}$ and choose $y_2 = \mathbf{0}$. Clearly, either $u_2 : t \mapsto [e^{-2t}, 0]^\intercal$ or $u_3 : t \mapsto [e^{-3t}, e^{-3t}]^\intercal$ produces y_2 and is compatible with the constraints.

(iii) Define $x_{0,2} = 0$ and let $y_2 = \mathbf{0}$ unchanged. For the same reason as in (i), output y_2 can only be produced by $u_1 = \mathbf{0}$ for $x(0) = x_{0,2}$.

To sum up, when $x(0) = x_{0,1}$, output y_2 can be produced by multiple inputs. In contrast, substituting the initial state by $x_{0,2}$ or the output by y_1 makes the input unique. Therefore, the ability to design different inputs giving rise to the same output depends on both the output trajectory y and the initial condition x_0.

This example shows that constraints give rise to unseen phenomena when instantaneous values of input and state vectors are free.

8.4.1 An enriched framework

To allow a detailed analysis of the phenomenology highlighted by Ex.8.13, let us enrich our framework by new notations and definitions.

From Σ to $\mathfrak{S}$

Let dynamical system $\mathfrak{S}$ be derived from Σ by imposing input and state constraints. Sets of signals associated with these two systems should be distinguished. For this reason, $\mathbf{U}$, $\mathbf{X}$, $\mathbf{Q}$ and $\mathbf{W}$ are henceforth renamed $\mathbf{U}_\Sigma$, $\mathbf{X}_\Sigma$, $\mathbf{Q}_\Sigma$ and $\mathbf{W}_\Sigma$, respectively. This allows us to associate the sets $\mathbf{U}$ and $\mathbf{X}$ with $\mathfrak{S}$ and redefine them as follows:

$$\mathbf{U} := \{u : \mathbb{R} \to \mathbb{R}^m \mid t \geq 0 \Rightarrow u(t) \in \mathcal{U}\} \cap \mathbf{U}_\Sigma,$$
$$\mathbf{X} := \{x : \mathbb{R} \to \mathbb{R}^n \mid t \geq 0 \Rightarrow x(t) \in \mathcal{X}\} \cap \mathbf{X}_\Sigma.$$

Accordingly, the set $\mathbf{Q}(x_0)$ of triple (u, x, y) compatible for x_0 with $\mathfrak{S}$ is derived from $\mathbf{Q}_\Sigma(x_0)$ by excluding trajectories that violate constraints, that is,

$$\mathbf{Q}(x_0) := \mathbf{Q}_\Sigma(x_0) \cap (\mathbf{U} \times \mathbf{X} \times \mathbf{Y}). \tag{8.15}$$

Thus, $(u, x, y) \in \mathbf{Q}(x_0)$ implies that $(u(t), x(t)) \in \mathcal{U} \times \mathcal{X}$ holds for all non-negative t. Similarly, denote by $\mathbf{W}(x_0)$ the set of input-to-output pairs compatible for x_0 with $\mathfrak{S}$, that is, $(u, y) \in \mathbf{W}(x_0)$ if there exists x such that $(u, x, y) \in \mathbf{Q}(x_0)$.

Qualifying pairs (x_0, y) and the definition of IR in the constrained context

In view of Ex. 8.13, IR should be associated to a pair (x_0, y) rather than to the system $\mathfrak{S}$.

Definition (IR pair)**.** A pair $(x_0, y) \in \mathcal{X} \times \mathbf{Y}$ is *IR* if output y can be produced by (at least)

two distinct inputs for the initial condition x_0, i.e.

$$\exists (u_1, y_1), (u_2, y_2) \in \mathbf{W}(x_0) : \; u_1 \neq u_2, \; y_1 = y_2 = y. \tag{8.16}$$

The set $\mathbf{S} \subset \mathcal{X} \times \mathbf{Y}$ of IR pairs reads:

$$\mathbf{S} := \{(x_0, y) \in \mathcal{X} \times \mathbf{Y} : (8.16)\}.$$

$\mathfrak{S}$ is IR iff $\mathbf{S}$ is non empty. Besides, define also the set of admissible pair (x_0, y).[4]

Definition (Admissible pair)**.** Let $\mathbf{A}$ be the set of *admissible pairs* $(x_0, y) \in \mathcal{X} \times \mathbf{Y}$:

$$\mathbf{A} := \{(x_0, y) \in \mathcal{X} \times \mathbf{Y} \mid \exists u : (u, y) \in \mathbf{W}(x_0)\}.$$

Observe that the following inclusion chain holds:

$$\mathbf{S} \subset \mathbf{A} \subset (\mathcal{X} \times \mathbf{Y}).$$

The definition of IR applies verbatim in the constrained context.

8.4.2 Sufficient condition for IR to be preserved

In addition to being part of the description of $\mathfrak{S}$, system Σ can be regarded as the unconstrained version of $\mathfrak{S}$. Therefore, comparison of the set of signals associated with these two systems allows evaluation of how constraints impact IR. This is the goal of this subsection.

The linear case

Let us first consider the case where both $\mathcal{U}$ and $\mathcal{X}$ are linear. Next proposition generalized Prop. 8.1 in this context.

Proposition 8.14 (**[TK24]**)**.** *Let sets $\mathcal{U} \subset \mathbb{R}^m$ and $\mathcal{X} \subset \mathbb{R}^n$ be linear over the field $\mathbb{R}$. If $\mathfrak{S}$ admits an IR pair $(x_0, y) \in \mathcal{X} \times \mathbf{Y}$, then $\mathfrak{S}$ is uniformly IR in the sense that every admissible pair is IR, i.e. $\mathbf{A} = \mathbf{S} \neq \{\varnothing\}$.*

The general case of arbitrary constraint sets

Via Ex. 8.13, it has been observed that constraints can destroy IR of a pair (x_0, y), in the sense that (x_0, y) can be IR for Σ but not for $\mathfrak{S}$. The following theorem offers a sufficient condition to prevent this situation from occurring, that is, for IR to be preserved in the constrained context.

Theorem 8.15 (**[TK24]**)**.** *Define the following relationships:*

$$u(t) \in \mathrm{int}(\mathcal{U}), \tag{8.17a}$$
$$x(t) \in \mathrm{int}(\mathcal{X}), \tag{8.17b}$$

parameterized by $t \in \mathbb{R}_{\geq 0}$, $u \in \mathbf{U}$ and $x \in \mathbf{X}$. Assume that the unconstrained system Σ is IR. Then, the admissible pair $(x_0, y) \in \mathbf{A}$ is IR (for $\mathfrak{S}$) if there exist (u, x) and $0 \leq t_0 < t_f$ such that $(u, x, y) \in \mathbf{Q}(x_0)$ holds and:

- *if $\rho > 0$,* (8.17a) *holds for all $t \in]t_0, t_f[$;*

[4] Unless otherwise specified, admissibility shall be understood "*with* $\mathfrak{S}$".

- *if* $\rho = 0$, (8.17a) *and* (8.17b) *hold for all* $t \in]t_0, t_f[$.

where ρ *is defined in* (8.6).

When $\mathcal{U}$ is open, (8.17a) (resp. (8.17b)) is valid for all $u \in \mathbf{U}$ (resp. for all $x \in \mathbf{X}$), and for all $t \in \mathbb{R}_{\geq 0}$. This leads to the following corollary.

Corollary 8.16 (**[TK24]**). *Assume that the unconstrained system* Σ *is IR. If one of the following conditions is valid:*

- $\rho > 0$ *and* $\mathcal{U}$ *is open,*
- $\rho = 0$ *and both* $\mathcal{U}$ *and* $\mathcal{X}$ *are open,*

then, $\mathfrak{S}$ *is uniformly IR in the sense that every admissible pair is IR, i.e.* $\mathbf{A} = \mathbf{S} \neq \{\varnothing\}$.

Contraposition of Th. 8.15 is also of major importance. In the context of Th. 8.15, assume that $\rho > 0$ (resp. $\rho = 0$) holds, and that (x_0, y) is admissible but *not* IR, so that there is a unique pair (u, x) satisfying $(u, x, y) \in \mathbf{Q}(x_0)$. Then, for all non-empty $]t_0, t_f[\subset \mathbb{R}_{\geq 0}$, condition (8.17a) (resp. (8.17a) and (8.17b)) is violated for some $t = t_i \in]t_0, t_f[$, i.e. $u(t_i) \in \mathcal{U} \setminus \text{int}(\mathcal{U})$ holds (resp. either $u(t_i) \in \mathcal{U} \setminus \text{int}(\mathcal{U})$ or $x(t_i) \in \mathcal{X} \setminus \text{int}(\mathcal{X})$ holds). This observation, together with the piecewise continuity of u and continuity of x leads to the following corollary.

Corollary 8.17 (**[TK24]**). *Define the following relationships:*

$$u(t) \in \mathcal{U} \setminus \text{int}(\mathcal{U}), \tag{8.18a}$$
$$x(t) \in \mathcal{X} \setminus \text{int}(\mathcal{X}), \tag{8.18b}$$

parametrized by $t \in \mathbb{R}_{\geq 0}$, $u \in \mathbf{U}$ *and* $x \in \mathbf{X}$. *Assume that the unconstrained system* Σ *is IR. Then, the admissible pair* $(x_0, y) \in \mathbf{A}$ is not IR (for $\mathfrak{S}$) only if *the unique* (u, x) *satisfying* $(u, x, y) \in \mathbf{Q}(x_0)$ *is such that:*

- *if* $\rho > 0$, *then* (8.18a) *holds for all* $t \in \mathcal{C}$;
- *if* $\rho = 0$, *then* (8.18a) *or* (8.18b) *holds for all* $t \in \mathcal{C}$,

where $\mathcal{C}$ *is the largest open subset of* $\mathbb{R}_{\geq 0}$ *where* u *is continuous.*

If $\mathcal{U}$ and $\mathcal{X}$ are closed and Σ is IR, then Cor. 8.17 proves that admissible pairs (x_0, y) which are not IR are necessarily associated with input and state trajectories that lie alternatively on the boundary of $\mathcal{U}$ and $\mathcal{X}$ for all t where u is continuous.

Example 8.18 (Ex. 8.13 continued)**.** Case (ii) proves that $\mathfrak{S}$ and, in turn, Σ are IR. For cases (i) and (iii), the unique input $u_1 = \mathbf{0}$ making pairs $(x_{0,1}, y_1), (x_{0,2}, y_2)$ admissible satisfies $u_1(t) \in \mathcal{U} \setminus \text{int}(\mathcal{U}) = (\{0\} \oplus \mathbb{R}_{\geq 0}) \cup (\mathbb{R}_{\geq 0} \oplus \{0\})$ for all $\mathcal{C} = \mathbb{R}_{\geq 0}$, as predicted by Cor. 8.17.

Remark 8.19 (Constraints might destroy IR). Constraints can completely eliminate redundancy. A trivial two inputs example is the case where quadruple of Σ is $(1, \begin{bmatrix} 1 & 1 \end{bmatrix}, 1, \mathbf{0})$, with $\mathcal{U} = \text{span}\left\{\begin{bmatrix} 1 \\ 0 \end{bmatrix}\right\}$ and $\mathcal{X} = \mathbb{R}$. •

8.4.3 Construction of an annihilator of $\mathfrak{S}$ when $\mathbf{0} \in \mathbb{F}(\mathcal{R}^*)$ and $\mathcal{X} = \mathbb{R}^n$

Extending the concept of annihilator

Given x_0 and $(u, y) \in \mathbf{W}(x_0)$, recall that the annihilator aims to shape $\tilde{u}$ under the constraint that $(u + \tilde{u}, y)$ belongs to $\mathbf{W}(x_0)$, see (8.10). In the general case where $\mathcal{U}$ and $\mathcal{X}$ are not linear, the equivalence between $(u + \tilde{u}, y) \in \mathbf{W}(x_0)$ and $(\tilde{u}, \mathbf{0}) \in \mathbf{W}(\mathbf{0})$ may not hold depending on x_0 and (u, y). From this observation, let us now enlarge the applicability of the concept of annihilator from Σ to $\mathfrak{S}$.

Definition (Annihilator of $\mathfrak{S}$)**.** The nonzero causal operator $\mathsf{C}_\perp$, associated with the mapping $\mathrm{H}_\perp[x_{a0}; \cdot] : v \mapsto \tilde{u}$ parametrized by the initial state x_{a0}, is an *annihilator of* $\mathfrak{S}$ if:

$$\forall x_0, \forall (u, y) \in \mathbf{W}(x_0), \exists x_{a0}, \forall v \in \mathbf{PC} : \ (u + \tilde{u}, y) \in \mathbf{W}(x_0), \tag{8.19}$$

where $\tilde{u} := \mathrm{H}_\perp[x_{a0}; v]$.

The expression of the annihilator in closed-form

Given x_0 and $(u, y) \in \mathbf{W}(x_0)$. If $\mathbf{0}$ is a friend of $\mathcal{R}^*$ and $\mathcal{X} = \mathbb{R}^n$ holds, then $(u + \tilde{u}, y) \in \mathbf{W}(x_0)$ reduces to $u + \tilde{u} =: \vartheta \in \mathbf{U}_\Sigma \Leftrightarrow \tilde{u} \in \mathbf{U}_\Sigma$ and

$$\vartheta(t) \in (u(t) + \mathcal{N}) \cap \mathcal{U} \tag{8.20}$$

for all $t \geq 0$. Condition (8.20) is treated as in Chap. 6. To see this, pick any $P_1 \in \mathbb{R}^{m \times (m - \dim \mathcal{N})}$ such that $P = [P_1, N] \in \mathbb{R}^{m \times m}$ is orthogonal. Then, note that $\vartheta(t) \in \mathcal{N} + u(t)$ is equivalent to $P_1^\mathsf{T} \vartheta(t) = P_1^\mathsf{T} u(t) =: u_\mathcal{L}(t)$, so that solving (8.20) is equivalent to solving $P_1^\mathsf{T} \vartheta(t) = u_\mathcal{L}(t)$ under constraints $\vartheta(t) \in \mathcal{U}$. Exploiting the results of Chap. 6 (see Fig. 6.4 where v is the output of the block "Opt"), the following proposition solves this problem and summarizes the above discussion.

Lemma 8.20. *Assume that (i) $\mathfrak{S}$ is IR, (ii) $\mathbf{0} \in \mathbb{F}(\mathcal{R}^*)$ and (iii) $\mathcal{X} = \mathbb{R}^n$ hold. Pick any $\mathcal{L}$ such that $\mathcal{L} \oplus \mathcal{N} = \mathbb{R}^m$ and any orthogonal matrix $P = [P_1, N] \in \mathbb{R}^{m \times m}$ whose columns form a basis that is adapted to $\mathcal{L} \oplus \mathcal{N}$. Let $r := \dim \mathcal{L} = m - \dim \mathcal{N}$. Define*

$$\hat{\mathcal{U}}_{1:r} := \left\{ \hat{u}_{1:r} \in \mathbb{R}^r : \exists \hat{u}_{r+1:m} \in \mathbb{R}^{\dim \mathcal{N}}, \hat{u} \in P^\mathsf{T} \mathcal{U} \right\}$$
$$\hat{\mathcal{U}}_{r+1:m}(\hat{u}_{1:r}) := \left\{ \hat{u}_{r+1:m} \in \mathbb{R}^{\dim \mathcal{N}} : \hat{u} \in P^\mathsf{T} \mathcal{U} \right\}$$

and the mapping $H_\perp : \mathbb{R}^m \times \mathbb{R}^{\dim \mathcal{N}} \to \mathbb{R}^m$

$$H_\perp : (u, v) \mapsto \tilde{u} = \begin{cases} N(\mathrm{sat}_{\hat{\mathcal{U}}_{r+1:m}(P_1^\mathsf{T} u)}(v) - N^\mathsf{T} u), & (\textit{if } P_1^\mathsf{T} u \in \hat{\mathcal{U}}_{1:r}) \\ \mathbf{0}, & (\textit{otherwise}) \end{cases} \tag{8.21}$$

If $t \mapsto H_\perp(u(t), v(t))$ belongs to **PC** *for all $u, v \in$* **PC**, *then $\mathrm{H}_\perp$ defines a (static) annihilator of $\mathfrak{S}$.*

Remark 8.21 (Maximal range). The above annihilator has maximal range in the following sense: For all $x_0 \in \mathcal{X}$, $(u, y) \in \mathbf{W}(x_0)$ and $\tilde{u}$ satisfying $(u + \tilde{u}, y) \in \mathbf{W}(x_0)$, there exists v such that $\tilde{u}(t) = H_\perp(u(t), v(t))$ holds for all $t \geq 0$. Note that this condition is weaker than that of Rem. 8.10 since $v \in$ **PC** is not required here. •

8.5 Taxonomy and degree of input redundancy

8.5.1 Classifying the IR pair

The ability of distinct inputs to produce not only identical outputs but also identical state trajectories is instrumental in classifying different species of IR. Let us introduce state trajectories into (8.16): Given a pair $(x_0, y) \in \mathcal{X} \times \mathbf{Y}$, define the following relationships

$$\exists (u_1, x_1, y_1), (u_2, x_2, y_2) \in \mathbf{Q}(x_0) : \; u_1 \neq u_2, x_1 = x_2, y_1 = y_2 = y, \tag{8.22}$$

$$\exists (u_1, x_1, y_1), (u_2, x_2, y_2) \in \mathbf{Q}(x_0) : \; u_1 \neq u_2, x_1 \neq x_2, y_1 = y_2 = y. \tag{8.23}$$

Observe that if (x_0, y) is IR, then at least one of the above relationships holds.

Making use of (8.22) and (8.23), instead of (8.16), allows for investigating the origin of IR. This gives rise to a taxonomy that distinguishes IR pairs.

Definition (IR pair of the k-th kind)**.** Let $(x_0, y) \in \mathcal{X} \times \mathbf{Y}$ be an IR pair. It is of:

- The *1st kind* if (8.22) holds but (8.23) does not, i.e. if the following implication

$$\left.\begin{array}{r} u_1 \neq u_2 \\ y = y_1 = y_2 \end{array}\right\} \Rightarrow x_1 = x_2 \tag{8.24}$$

  holds for all $(u_1, x_1, y_1), (u_2, x_2, y_2) \in \mathbf{Q}(x_0)$;

- The *2nd kind* if (8.22) does not hold but (8.23) does, i.e. the following implication

$$\left.\begin{array}{r} u_1 \neq u_2 \\ y = y_1 = y_2 \end{array}\right\} \Rightarrow x_1 \neq x_2 \tag{8.25}$$

  holds for all $(u_1, x_1, y_1), (u_2, x_2, y_2) \in \mathbf{Q}(x_0)$;

- The *3rd kind* if both (8.22) and (8.23) hold, i.e. neither (8.24) nor (8.25) is valid for all $(u_1, x_1, y_1), (u_2, x_2, y_2) \in \mathbf{Q}(x_0)$.

The different kinds of pairs are mutually exclusive: No pair (x_0, y) can be simultaneously of different kinds. This motivates the partitioning of $\mathbf{S}$ as follows:

$$\mathbf{S} = \mathbf{S}_1 \cup \mathbf{S}_2 \cup \mathbf{S}_3,$$

where $\mathbf{S}_k$ gathers IR pairs of the k-th kind and satisfies $\mathbf{S}_k \cap \mathbf{S}_j = \{\varnothing\}$ for all $k \neq j$.

8.5.2 Linearity implies uniformity

Focusing on the linear case, the next proposition enriches Prop. 8.14 by indicating that linearity implies uniformity not only of IR but also of the kind of IR.

Proposition 8.22 (**[TK24]**)**.** *Let sets $\mathcal{U} \subset \mathbb{R}^m$ and $\mathcal{X} \subset \mathbb{R}^n$ be linear over the field $\mathbb{R}$. If $\mathfrak{S}$ admits an IR pair $(x_0, y) \in \mathcal{X} \times \mathbf{Y}$ of the k-th kind, then $\mathfrak{S}$ is uniformly IR of the k-th kind in the sense that every admissible pair is IR of the k-th kind, i.e. $\mathbf{A} = \mathbf{S} = \mathbf{S}_k \neq \{\varnothing\}$.*

8.5.3 Characterization of the kind of IR and degree of IR

This subsection is concerned with the unconstrained context, so that Σ (and not $\mathfrak{S}$) is considered.

Characterization of the kind of IR Prop. 8.22, together with Th. 8.2 and Rem. 8.4, allow to characterize the kind of uniform redundancy of Σ.

Corollary 8.23 ([**KT21**]). *System Σ is uniformly IR of:*

- *The 1st kind iff $\rho > 0 = \dim \mathcal{R}^*$ holds;*
- *The 2nd kind iff $\rho = 0 < \dim \mathcal{R}^*$ holds;*
- *The 3rd kind iff $\rho > 0 < \dim \mathcal{R}^*$ holds.*

Degree of IR Recall that $\dim \mathcal{N}$ corresponds to the dimension of the input v of the annihilator of Th. 8.8. Hence, it is the number of independent input directions (after regular state-feedback with any friend of $\mathcal{V}^*$) that do not affect the output. To better understand the role played by each directions, let us define ν as the codimension of $\mathrm{Ker}\left\{\left[\begin{smallmatrix} B \\ D \end{smallmatrix}\right]\right\}$ in $\mathcal{N}$ i.e.[5]

$$\nu := \dim\left(\mathcal{N} / \mathrm{Ker}\left\{\left[\begin{smallmatrix} B \\ D \end{smallmatrix}\right]\right\}\right) \tag{8.26}$$

This leads to the following decomposition:

$$\dim \mathcal{N} = \rho + \nu \tag{8.27}$$

where ρ is defined as the dimension of $\mathrm{Ker}\left\{\left[\begin{smallmatrix} B \\ D \end{smallmatrix}\right]\right\}$. The above sum indicates that among the $\dim \mathcal{N}$ input directions letting the output unchanged, ρ of them do not affect the state, whereas ν of them impact the state. This motivates the use of these two integers to quantify the degree of IR.

> **Definition** (Degree of IR)**.** The pair (ρ, ν), defined by (8.6) and (8.26), is called the *degree of input redundancy* of the system Σ.

Remark 8.24 (Degree of IR and kind of IR). From (8.27), note that the following equivalence follows readily by rewriting item (ii) of Th. 8.2 as $\rho + \dim(\mathcal{R}^*) > 0$:

$$\dim \mathcal{R}^* > 0 \;\Leftrightarrow\; \nu > 0. \tag{8.28}$$

This relationship, together with Cor. 8.23, allow to easily relate the degree of IR with the kind of IR: Just replace $\dim \mathcal{R}^*$ by ν in the statement of Cor. 8.23. Let us emphasize that $\dim \mathcal{R}^*$ and ν are by no means equal, in general. •

Remark 8.25 (The right-invertible case). In the case where Σ is right-invertible, combining (8.27) with Cor. 8.7 yields $(\rho, \nu) = (\rho, m - p - \rho)$. •

8.5.4 How constraints impact the taxonomy ?

Assume that the unconstrained system Σ is (uniformly) IR of the k-th kind. Given an IR pair $(x_0, y) \in \mathbf{S}$.[6] Then, a natural question is: Does (x_0, y) belong to $\mathbf{S}_k$? Saying it differently, can the constraints modify the kind of IR of a pair ? For $k \in \{1, 2\}$, the answer to the last question is always negative, i.e. constraints cannot change IR of the 1st or of the 2nd kind.[7]

[5] Observe that $\mathrm{Ker}\,\{B\} \cap \mathrm{Ker}\,\{D\}$ is indeed included in $\mathcal{N}$, so that ν is well-defined.

[6] Recall that $\mathbf{S}$ and $\mathbf{S}_{1,2,3}$ are associated to $\mathfrak{S}$, and not to Σ.

[7] To see this, let $(x_0, y) \in \mathbf{S}$. Assume that Σ is IR of the 1st (resp. 2nd) kind. Then $u_1 \neq u_2$ together with $y_1 = y_2 = y$ implies $x_1 = x_2$ (resp. $x_1 \neq x_2$) for all $(u_1, x_1, y_1), (u_2, x_2, y_2) \in \mathbf{Q}_\Sigma(x_0)$. Since $\mathbf{Q}(x_0) \subset \mathbf{Q}_\Sigma(x_0)$, this proves that (x_0, y) belongs to $\mathbf{S}_1$ (resp. to $\mathbf{S}_2$).

Lemma 8.26 ([TK24]). *Let Σ be IR of the k-th kind, with $k \in \{1,2\}$. If $\mathfrak{S}$ is IR, then $\mathfrak{S}$ is uniformly IR of the k-th kind in the sense that $\mathbf{S} = \mathbf{S}_k \neq \{\varnothing\}$ holds.*

If Σ is IR of the 3rd kind, then not only $\mathfrak{S}$ can be of the 1st or 2nd kind (see **[TK24**, Ex.15]), but IR pairs of different kinds can also coexist for $\mathfrak{S}$, as shown by the following example.

Example 8.27. Let Σ be defined as follows:

$$\begin{aligned}\dot{x}(t) &= \begin{bmatrix}1 & 0\\ 0 & 1\end{bmatrix} x(t) + \begin{bmatrix}1 & 0 & 0\\ 0 & 1 & 1\end{bmatrix} u(t)\\ y(t) &= \begin{bmatrix}0 & 1\end{bmatrix} x(t).\end{aligned}$$

Constrained system $\mathfrak{S}$ is derived from Σ by imposing $\mathcal{U} = [-1;+\infty[^3$ and $\mathcal{X} = [0;1] \times [0;2]$. Let us show that $\mathfrak{S}$ admits IR pairs of each kind:

- Pair $(x_{0,1}, y_1) := (\left[\begin{smallmatrix}1\\0\end{smallmatrix}\right], \mathbf{0})$ is of the 1st kind. Indeed, the first input necessarily equals $t \mapsto -1$ for the first state not to escape from $[0;1]$. Together with $y = \mathbf{0}$, this implies that x is constant and equal $t \mapsto x_{0,1}$. Thus, y_1 can be produced by any input $u \in \mathbf{U}_\Sigma$ that satisfies $u(t) \in \{-1\} \times (\mathrm{Ker}\,\{[1,1]\} \cap [-1;+\infty[^2)$ for all $t \in \mathbb{R}_{\geq 0}$.
- Pair $(x_{0,2}, y_2) := (\left[\begin{smallmatrix}0.5\\2\end{smallmatrix}\right], t \mapsto 2)$ is of the 2nd kind. This time, the last two inputs must equal $t \mapsto -1$ for $y(t) = 2$ to hold for all $t \in \mathbb{R}_{\geq 0}$. Thus, y_2 originates from any input $u \in \mathbf{U}_\Sigma$ such that (i) $u(t)$ belongs to $[-1;+\infty[\times \{-1\}^2$ for all $t \in \mathbb{R}_{\geq 0}$ and (ii) the first state belongs to $[0;1]$. In particular, $\eta_\alpha : t \mapsto -\alpha e^{(1-\alpha)t}/2$ is a suitable trajectory for the first input, whatever is $\alpha \in [1;2]$. To see this more easily, note that η_α can be interpreted as the feedback of gain $-\alpha$ between the first state and first input. Furthermore, any of these input candidates leads to distinct state trajectories.
- Pair $(x_{0,3}, y_3) := (\left[\begin{smallmatrix}0.5\\0\end{smallmatrix}\right], \mathbf{0})$ is of the 3rd kind. This can be proved by constructing triples (u_4, x_4, y_4), (u_5, x_5, y_5), $(u_6, x_6, y_6) \in \mathbf{Q}(x_{0,3})$ satisfying $y_4 = y_5 = y_6 = y_3$, $x_4 = x_5 \neq x_6$ and $u_k, (k \in \{4,5,6\})$, all distinct. Using distinct $\alpha_1, \alpha_2 \in [1;2]$, it can be verified that $u_4 = [\eta_{\alpha_1}, \mathbf{0}, \mathbf{0}]^\intercal$, $u_5 = (t \mapsto [\eta_{\alpha_1}(t), 1, -1]^\intercal)$ and $u_6 = [\eta_{\alpha_2}, \mathbf{0}, \mathbf{0}]^\intercal$ comply with those constraints.

8.6 Conclusions

As a summary of this chapter, let us recall its essential messages:

- IR is ¬LI, which coincides with $m > p$ in the right-invertible case.
- Σ is IR iff Ker $\{\left[\begin{smallmatrix}B\\D\end{smallmatrix}\right]\}$ or $\mathcal{R}^*$ is non trivial, see Th. 8.2.
- IR is equivalent to the existence of an annihilator generating inputs $\tilde{u}$ inducing zero output of Σ *for zero initial state*, see Th. 8.8.
- If $\mathcal{U}$ and $\mathcal{X}$ are linear, then the taxonomy of IR pairs is uniform, see Prop. 8.22.
- Input and state constraints can challenge IR only if input and state trajectories alternatively lie on the boundary of $\mathcal{U}$ and $\mathcal{X}$ for all t where u is continuous, see Cor. 8.17.
- By exploiting results of Chap. 6, an annihilator with maximal range can be constructed in the input constraint context if $F = \mathbf{0}$ is a friend of $\mathcal{R}^*$, see Lem. 8.20.

8.7 Bibliographical notes

This chapter combines extractions from [**KT21**] (for the unconstrained context) and [**TK24**] (dealing with input and state constraints) with unpublished materials on the annihilator that are exposed in Sec. 8.3 and Sec. 8.4.3.

Existing works

Definitions of IR When examining literature on control allocation and IR, one might be puzzled by the proliferation of distinct definitions and characterizations of IR and its taxonomy.[8] Let us quote a few of them:

1) Conditions on the input-to-state mapping: Referring to the constraint of (7.1), namely $\tau = \Sigma_a(u)$, and under the assumption that $\Sigma_a(\cdot)$ is linear and static, early definitions read: The system is over-actuated if Σ_a *has more columns than rows*, see e.g. [FS91, p.400], [Dur93, p.718], [BF97], [Joh04], [ODB11], [BE96] to cite a few.

2) Conditions on the input-to-output mapping: In [BET98, p.458], over-actuation is related to *more controls than commanded states*, what can be translated as $p < m$. See also [Luo+04], [VSB07] and [Sig+09] for analogous statements.

3) Control problem oriented: "A characteristic feature of the over-actuated control problem is that *for a given reference output $y^\star$ the corresponding equilibrium point is not unique.*" [JS03].

4) Informal definitions: Over-actuated systems have "*more effectors than strictly needed to meet the motion control objectives*" [JF13].

5) Formal characterizations:

[Zac09] : System Σ is said *strongly IR* if $\rho > 0$ and *weakly IR* if $G^\star := \lim_{s\to 0} G(s)$ is finite and satisfies $\mathrm{Ker}\,\{G^\star\} \neq \{\mathbf{0}\}$.

[Ser12] : Under the following assumption that Σ is minimal, strictly proper and right-invertible, *strong IR* means $m > \mathrm{rank}\,\{B\} = p$ whereas *weak IR* means $m \geq \mathrm{rank}\,\{B\} > p$.

[GP14]-a) : Σ is said *strongly IR* if $\rho = m - p$ and *weakly IR* if $\rho = 0$.

[GP14]-b) : In the context of output regulation (see Chap. 9), and assuming that $\lambda \notin \sigma(A)$ and $\mathrm{rank}\,\{P_\Sigma(\lambda)\} = n + p$ hold for all $\lambda \in \sigma(S)$, then Σ is *IR at frequency ω if* $\mathrm{Ker}\,\{P(j\omega)\}$ *is non trivial*.[9]

[DO19] : Under the assumption that Σ is minimal and strictly proper, the system is said *strongly IR* if $\rho > 0$ hold and *weakly IR* if $\dim \mathrm{Ker}\,\{G(s)\} > 0$ holds for all $s \in \mathbb{C}$.

The comparison of the definitions of this chapter with:

- 1), 2), [Ser12], [GP14]-a) and [DO19] follows from the material of this chapter;
- 3), 4), [GP14]-b) and [Zac09] can be performed using results in Chap. 9.

[8] Sometimes, these definitions are not explicitly exposed, so the reader is left to identify them with the conditions under which the proposed control law is relevant.

[9] We deduce this definition from the following statement: "For some ω, a matrix N_ω satisfying $\mathrm{Im}\,\{N_\omega\} = \mathrm{Ker}\,\{P(j\omega)\}$ is called IR matrix basis at frequency ω", [GP14].

See Subsec. 9.6.1 of Chap. 9 for in-depth comparisons between [Zac09] and [Ser12].

A comparison between these definitions is not always trivial, so that seemingly distinct (even if they are actually the same) as well as apparently identical (whereas they are distinct) statements coexist. This strongly impacts the literature stream, which has become increasingly sliced into hermetic rooms due to the lack of a common framework everyone can refer to. We believe that this lack of homogeneity is a harsh obstruction to the recent attempts toward formalization of the research field.[10] Besides, scrupulous analysis of the literature reveals that this heterogeneity introduces not only confusion but also fallacies.[11]

Among the existing works, [Ser12] is the closest to the framework presented in [**KT21**] and in this chapter. Yet, there is a number of issues that prevent the very important study to receive the audience that it deserves.[12] (i) Analysis is conducted under the assumption of right-invertibility, minimality and strict properness.[13] Not only does this make the study less general, but also does this not help in fighting against widespread misconceptions that are only valid in this context. The main one is that $m > p$ is a necessary condition for LTI system to be IR, see Rem. 8.6 and example **(a)** at the end of Chap. 9. (ii) In the context of right-invertible, minimal, and strictly proper systems, the analysis hinges on the claim that $\dim \mathcal{N}$ equals $m - p$. Right invertibility alone is indeed a necessary and sufficient condition for this equality to hold, as stated in Cor. 8.7 that is formally proven in [**KT21**]. Note that without this assumption of right-invertibility, $\dim \mathcal{N}$, and in turn, IR (see Th. 8.2) cannot be inferred from m, p and ρ in general.

Annihilator The concept of annihilator was first defined in [CG14, p.4248], even though it was already introduced in essence in [Zac09]. In the constructive part of [CG14], the offered algorithm leading to an annihilator is deduced from the material of [Ser12] and coincides with that of Th. 8.8 in the case where F is such that $A + BF$ is Hurwitz and for a strictly proper system. Building on [Ser12], another definition of an annihilator is offered in [CSZ18, p.216]. As the context of [CSZ18] is the output regulation problem, a comparison with this annihilator is discussed in the next chapter, which is concerned with this control problem.

The construction of the annihilator proposed in this chapter uses standard result of geometric control theory, see Appendix A. The commutative diagram [Ser12, Fig.1] nicely illustrates this construction for strictly proper systems.

As investigated in [CG14] , an annihilator can also be constructed from $G(s)$, see also [Wol74, Sec.5.5] on the left-inverse of $G(s)$ or [CLS04, Sec.8] for factorizations of $G(s)$.

[10] Hopefully, the work presented in this manuscript will be regarded as a valuable step toward such a unifying framework, rather than yet another set of definitions of existing concepts.

[11] As an illustration, it is claimed in [DO19] that weak IR (defined as $\dim \mathrm{Ker}\,\{G(s)\} > 0$ for all $s \in \mathbb{C}$) "can also be defined by a larger number of inputs compared to outputs". If this statement is valid *under the assumption of right-invertibility*, it is false in general: This condition on $G(s)$ does not imply $m > p$, see e.g. example **(a)** at the end of Chap. 9. In addition, the definitions of this paper are introduced in a quite ambiguous way by suggesting that this study is a continuation of [Zac09], whereas it is much more in line with [Ser12] and the definitions proposed in this chapter. As shown at the end of Chap. 9, [Zac09] and [Ser12] use distinct notions of IR.
Another example is [GP14] where it is said that "the central idea in [Zac09] (as coded in [Zac09, Def.1]) consists in classifying [...] a plant as strongly redundant if it admits exactly $m - p$ linearly independent strongly redundant input directions, and weakly redundant otherwise.". Using the terms of this chapter, this sentence can be rephrased as follows: A plant is strongly IR as in [Zac09] if $m - p = \rho$ holds, and weakly IR as in [Zac09] otherwise. This is incorrect. Example **(c)** at the end of Chap. 9 is a counter-example: This system is strongly IR as in [Zac09] (and right-invertible), but $m - p = 2 \neq \rho = 1$ holds.

[12] See also the end of Chap. 9 for additional facts on [Ser12].

[13] Note that minimality was already dismissed in [Zho+13].

The constrained context From the very beginning, IR has been considered as a way to deal with input constraints by redistributing the overall control effort among actuators to avoid saturation, see the bibliographical notes of Chap. 7. Thus, IR and input constraints are intrinsically related research fields. Although the former is still in its infancy in many aspects, the latter benefits from solid results on classical notions of control theory. Together with stabilizability, the concept of controllability has probably monopolized most of the attention of the control community working on input-constrained dynamical systems; see [Bra72] and most of the standard textbooks on this topic, such as [Tar+11; HL01; Sab+00]. Roughly speaking, this notion is related to the existence of a suitable input trajectory. On the contrary, IR deals with the uniqueness of this input. The key point is that the question of existence has received much more attention than that of uniqueness, by far.

In recent literature devoted to IR systems, several attempts to deal with constraints can be found. In [Zac09], the natural embedding $H_\perp : \operatorname{Ker}\{B\} \cap \operatorname{Ker}\{D\} \to \mathbb{R}^m$ is used as a (non-maximal range) annihilator to inject $\tilde{u}$ in such a way that $\tilde{u} + u$ remains within the saturation limits, see Fig. 8.1. The authors of [VG13; GV13] offer methods for the computation of the zero-error steady-state solutions of the regulation problem under input constraints. For the same problem, an online optimizer scheme is proposed in [Gal+15], with the goal of promoting steady-state inputs with the smallest infinity norm. In the discrete-time case, a model predictive control scheme is offered in [ZCS17] to ensure that the internal dynamics comply with state and input constraints.

All these contributions are valuable attempts toward control design handling input and state constraints. They share the following common pattern, though: First, IR is defined by referring to the *unconstrained* context, and second, the control methodology is exposed and implemented when input constraints affect the system. Consequently, it cannot be ensured that the proposed methods apply to the class of IR systems characterized beforehand.

Works never seen elsewhere in those terms ($\approx$ new)

It should be noted that one of the contributions of this manuscript is that it addresses the concept of IR outside the context of output regulation. This concept indeed deserves separate consideration. This point is reflected in the structure of the manuscript, in which the content of Chap. 8 and Chap. 9 is kept separate.

Definitions of IR The definition of IR as non-left invertibility was first proposed in [**KT21**].[14] We believe that adopting this open-loop signal-oriented formulation has several advantages. In addition to being intuitive, such a formulation is intended for direct extension out of the class of unconstrained LTI systems. The discussion of how input and state constraints impact IR illustrates this potentiality. This also allows us to connect two parts of the literature. Among other things, this achievement readily leads to a comprehensive set of equivalent characterizations of IR by exploiting the well-established literature of system inversions; see, for example,

[14] Note that this fact was sometimes approached, but to the best of our knowledge, no clear and rigorous statement can be found in the literature. The closest quotes to this intuition are "IR with full-rank input operators constitutes an intrinsic redundancy in the system, as multiple independently controllable state-trajectories exist that are compatible with a given reference output." [Ser12, p.4871]; "Weakly IR systems are characterized by multiple independently controllable state trajectories that are compatible with a given output" [Gal+15, p.346]; "Obviously, system (1) [an over-actuated system] is not left-invertible." [Gal+11, p. 4771]. See also the definition of an annihilator in [CG14]. If these quotations translate insightful intuitions, they can be seen as ambiguous. Indeed, they acknowledge that the two notions are closely related, but they do not explicitly say that they can be defined (and they are sometimes actually defined) as opposite to each other. This, in turn, suggests that the relationship between the two notions is more involved, whereas it is not.

[TSH12, Chap.8] and [NP07] for geometric results on this topic.

The existing taxonomy of IR in this chapter comes from [**KT21**]. It revisits and enriches the ones existing in the literature, see the end of Chap. 9 for an in-depth comparison with those presented in [Zac09] and [Ser12]. The reader is referred to [**KT21**] for a discussion of the definition proposed in [GP14].

Annihilator The (unpublished) definition of the annihilator introduced in this chapter simplifies that of [CG14] by removing the requirements of ISS and "asymptotically-constant-input asymptotically-constant-state". In [CG14], an extra requirement for the annihilator is introduced: The invertibility of its DC gain. Perhaps this assumption can be satisfied as a byproduct of the minimality of the annihilator. This chapter also clearly states (i) that IR is a necessary and sufficient condition for the existence of an annihilator and (ii) that the proposed annihilator has maximal range. These two facts are also unpublished. Finally, the proposed annihilator enlarges the constructive part of [CG14] by removing the assumption of strict properness.

The constrained context To the best of our knowledge, IR is defined and (partially) characterized for systems subject to input or state constraints for the first time in [**TK24**]. This challenge is tackled head-on, by exploiting *verbatim* the definition of IR introduced in [**KT21**]. By doing so, it brings closer the literature dedicated to IR and that devoted to input and state constraints.

Chapter 9

Exploiting input redundancy in the output regulation problem

Contents

This chapter discusses the output regulation problem. Our aim is to unveil and exploit all degrees of freedom related to IR in the design of the problem solution. The analysis starts within the classical framework, where suitable reference trajectories are constructed from the solution of the regulator equations. A key example shows that these equations can admit a unique solution, even if distinct reference trajectories exist. This proves that these equations are not an appropriate tool for investigating the non-uniqueness of the steady state. This motivates an extensive study on the "shapability" of the steady state, a characterization of this property, and the derivation of a control scheme allowing full exploitation of this redundancy. Remarkably, definitions of IR, coins as "weak IR" and "bounded persistent weak IR", emerges from this discussion.

9.1 Background on the output regulation problem

9.1.1 Problem statement

The output regulation problem deals with the exogenous bounded and persistent signal w feeding the system Σ_w, which is derived from Σ as follows:

$$\dot{x}(t) = Ax(t) + Bu(t) + Pw(t) \tag{9.1a}$$
$$e(t) = Cx(t) + Du(t) + Qw(t) \tag{9.1b}$$

where $e(t) \in \mathbb{R}^p$ and $w(t) \in \mathbb{R}^q$. The signal w represents either a disturbance to be rejected or a reference to be tracked; both control objectives correspond to regulating $e(t)$ to $\mathbf{0}$. The following equation governs the dynamics of w delivered by the exosystem E:

$$\dot{w}(t) = Sw(t) \tag{9.2}$$

In the so-called full-information framework illustrated in Fig. 9.1, both x and w are assumed to be signals available to the control law. The corresponding problem reads as follows.

Problem 9.1. Find a causal mapping from (w, x) to u such that the following two conditions are satisfied:

(a) State of the system as well as that of the controller (if the controller is dynamic) remain bounded at all time;

(b) Output error signal e asymptotically converges to zero;

for all initial conditions of the system, of the controller (if the controller is dynamic), and of the exosystem.

As customary, solutions of the above problem are derived under the following standing assumption, which is not recalled in the sequel.

Assumption 9.2. Pair (A, B) is stabilizable. Matrix S is semi-simple and such that $\sigma(S) \subset \mathbb{C}^0$.

In contrast with many existing works, note that the following so-called "non resonance condition" is *not* assumed to be valid in this chapter.[1]

[1] Since this hypothesis is related to robustness w.r.t. to parametric uncertainties [Fra77], a detailed discussion on this topic is offered in Chap. 11.

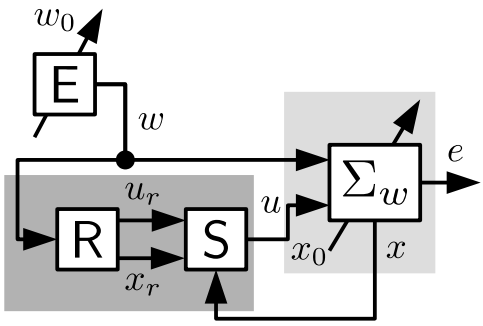

Figure 9.1: The feedback loop of the full information output regulation problem.

Assumption 9.3 (Non resonance condition)**.** System Σ is right-invertible and the set $\mathcal{Z}$ of invariant zero is disjoint from the spectrum of S, i.e. $\mathcal{Z} \cap \sigma(S) = \{\varnothing\}$.

9.1.2 Problem solution

The classical controller solving the above problem is decomposed into two control units: (i) a reference trajectory generator $\mathsf{R} : w \mapsto (u_r, x_r)$ and (ii) a state-feedback stabilizer $\mathsf{S} : (u_r, x_r, x) \mapsto u$, see Figure 9.1.

- R shapes (u_r, x_r) in such a way that this pair solves (9.1) as well as satisfies (b) at all time, i.e.

$$\dot{x}_r(t) = Ax_r(t) + Bu_r(t) + Pw(t) \tag{9.3a}$$
$$\mathbf{0} = Cx_r(t) + Du_r(t) + Qw(t) \tag{9.3b}$$

- S ensures that (a) as well as $u(t) \to u_r(t)$ and $x(t) \to x_r(t)$ hold. If (9.3) is satisfied, then S can be simply defined as follows:[2]

$$\mathsf{S} : (u_r, x_r) \mapsto u = K(x - x_r) + u_r \tag{9.4}$$

  for any K such that $A + BK$ is Hurwitz. Such a matrix K exists if (A, B) is stabilizable.

9.1.3 Scope of this chapter and notations

In this chapter, neither input nor state constraints are considered, i.e. $\mathcal{U} = \mathbb{R}^m$ and $\mathcal{X} = \mathbb{R}^n$ hold. Thus, the original definition of function spaces $\mathbf{U}, \mathbf{X}$ applies, see the beginning of Chap. 8. In view of Prop. 8.22, the adjective "uniform" can be dropped in this context when qualifying IR of Σ.

If the concept of IR, as defined in the previous chapter, is fully relevant for the construction of S, it is proved in this chapter that this is not the case when dealing with R. For this reason, our focus in this chapter is on R.[3] For this control unit, our goal is (i) to define the appropriate notion of IR, (ii) to characterize it, and (iii) to address the associated degrees of freedom via a suitable annihilator. To this end, the following set is of utmost importance:

$$\mathbf{R}(w) := \{(u_r, x_r) : (9.3), u_r \in \mathbf{U}, x_r \in \mathbf{X}\}$$

[2]Let us emphasize that notations referring to the stabilizer S and the matrix S of the exosystem are closed but distinct, see the general formatting rules at the beginning of this manuscript.

[3]See the bibliographical notes ending this chapter for a discussion on how redundancy shall be exploited in each control unit, i.e. not only S but also R should be equipped with appropriate (and distinct) annihilators.

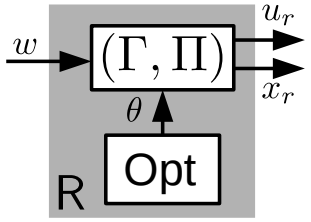

Figure 9.2: Reference trajectories generator in the classical paradigm, where θ parametrizes $\mathcal{F}$ and is used to select the optimal pair (Γ, Π).

which is parameterized by a solution w of $\dot{w} = Sw$.

To easily manipulate $\mathbf{R}(w)$, we define the input-to-state operator H_x^w associated with (9.1). It maps an input trajectory $u(\cdot)$ to the state trajectory $x(\cdot)$ produced by the system when excited by $u(\cdot)$ and $w(\cdot)$ with an initial condition $x(0) = x_0 \in \mathcal{X}$. Observe that the following relationship holds for all $x_0, \tilde{x}_0 \in \mathcal{X}$ and $u, \tilde{u} \in \mathbf{U}$:

$$\mathrm{H}_x^w[x_0 + \tilde{x}_0; u + \tilde{u}] = \mathrm{H}_x^w[x_0; u] + \mathrm{H}_x[\tilde{x}_0; \tilde{u}] \tag{9.5}$$

9.2 Comprehensive treatment in the classical paradigm

In the classical paradigm, the reference trajectory generator is defined as follows:

$$\mathsf{R} : w \mapsto (u_r, x_r) = (\Pi w, \Gamma w) \tag{9.6}$$

where $(\Pi, \Gamma) \in \mathbb{R}^{n \times q} \times \mathbb{R}^{m \times q}$ solves the following so-called "regulator equations", see [Fra77]:

$$\Pi S = A\Pi + B\Gamma + P, \tag{9.7a}$$
$$\mathbf{0} = C\Pi + D\Gamma + Q. \tag{9.7b}$$

Let us introduce the set $\mathcal{F}$ of solutions to the regulator equations:

$$\mathcal{F} := \left\{ \begin{bmatrix} \Pi \\ \Gamma \end{bmatrix} \in \mathbb{R}^{(n+m) \times q} : (9.7) \right\}.$$

We are interested in the case where $\mathcal{F}$ does not contain a single element, so that distinct steady states solving the regulator problem exist. Clearly, this under-determined situation is related to some redundancy. In this subsection, two questions are addressed:

- How to parametrize $\mathcal{F}$ and relate its dimension to some characteristics of Σ?
- How to proceed to on-line selection of the most appropriate element of $\mathcal{F}$, i.e. how to handle the time-dependency of $\left[\begin{smallmatrix} \Pi \\ \Gamma \end{smallmatrix}\right]$ on the output error e and on the internal stability of Σ_w?

Fig. 9.2 illustrates how the online selection of (Γ, Π) can be implemented via a parametrization of $\mathcal{F}$ by θ, which is computed via an optimization process.

9.2.1 Exhaustive parametrization of the solutions of the regulator equations

Define the linear operator $\mathrm{H_F} : \mathbb{R}^{(n+m)\times q} \to \mathbb{R}^{(n+p)\times q}$ as follows:

$$\mathrm{H_F} : \begin{bmatrix} \Pi \\ \Gamma \end{bmatrix} \mapsto \begin{bmatrix} A\Pi - \Pi S + B\Gamma \\ C\Pi + D\Gamma \end{bmatrix}.$$

This allows us to equivalently rewrite (9.7) as follows:

$$\mathrm{H_F} \begin{bmatrix} \Pi \\ \Gamma \end{bmatrix} = - \begin{bmatrix} P \\ Q \end{bmatrix} \tag{9.8}$$

This highlights that $\mathcal{F}$ is the affine space $\begin{bmatrix} \Pi_0 \\ \Gamma_0 \end{bmatrix} + \mathrm{Ker}\,\{\mathrm{H_F}\}$ where $\begin{bmatrix} \Pi_0 \\ \Gamma_0 \end{bmatrix} \in \mathcal{F}$ is any particular solution. Parametrization of $\mathcal{F}$ thus amounts to computing a basis of $\mathrm{Ker}\,\{\mathrm{H_F}\}$. This is the technical challenge associated with the following proposition.

Proposition 9.4. *Define:*

$$\begin{aligned} \{\lambda_1, \ldots, \lambda_q\} &\coloneqq \sigma(S) \\ \gamma_i &\coloneqq \dim \mathrm{Ker}\,\{P_\Sigma(\lambda_i)\} \\ \mathcal{I} &\coloneqq \{i \in [\![1, q]\!] : \gamma_i > 0\} \\ \mathcal{J} &\coloneqq \{(i, j) : i \in \mathcal{I},\, j \in [\![1, \gamma_i]\!]\} \end{aligned}$$

Define $\Pi_{i,j}, \Gamma_{i,j}, ((i,j) \in \mathcal{J})$ *as in Appendix C.1. The set*

$$\left(\begin{bmatrix} \Pi_{i,j} \\ \Gamma_{i,j} \end{bmatrix} \right)_{(i,j)\in\mathcal{J}}$$

forms a basis of $\mathrm{Ker}\,\{\mathrm{H_F}\}$.

Proof. See Appendix C.1.3. □

Corollary 9.5. *It holds:*

$$\mathcal{F} = \left\{ \begin{bmatrix} \Pi_0 \\ \Gamma_0 \end{bmatrix} + \sum_{(i,j)\in\mathcal{J}} \theta_{i,j} \begin{bmatrix} \Pi_{i,j} \\ \Gamma_{i,j} \end{bmatrix} : \theta_{i,j} \in \mathbb{R} \right\} \tag{9.9}$$

where $\begin{bmatrix} \Pi_0 \\ \Gamma_0 \end{bmatrix} \in \mathcal{F}$ *is any particular solution to* (9.7).

Prop. 9.4 provides the dimensions of $\mathcal{F}$. Interestingly, one can relate $\dim \mathcal{F}$ with some properties of Σ, such as left and right invertibility or the set of invariant zeros.

Corollary 9.6. *It holds:*

$$\dim \mathcal{F} = \sum_{i\in\mathcal{I}} \gamma_i = \kappa|\mathcal{I}| + \sum_{i\in\mathcal{I}} \delta_i, \tag{9.10}$$

where δ_i *is the number of additional dimensions of* $\mathrm{Ker}\,\{P_\Sigma(\lambda_i)\}$ *w.r.t. the normal case:*

$$\delta_i \coloneqq \gamma_i - \kappa \tag{9.11}$$

and κ *is the normal dimension of* $\mathrm{Ker}\,\{P_\Sigma\}$*:*

$$\kappa \coloneqq \min_{\lambda\in\mathbb{C}} \dim \mathrm{Ker}\,\{P_\Sigma(\lambda)\} = (n+m) - \mathrm{nrank}\,\{P_\Sigma\}.$$

Besides, it holds:

1. *If Σ is IR (Σ is not left invertible), then $\gamma_i > 0$ holds for all $i \in [\![1, q]\!]$, so that $|\mathcal{I}| = q$.*
2. *If Σ is not IR (Σ is left invertible), then $\kappa = 0$ holds.*
3. *If Σ is right invertible, then $\kappa = m - p$ holds.*
4. *If $\sigma(S)$ and $\mathcal{Z}$ are disjoint, then $\delta_i = 0$ holds for all $i \in [\![1, q]\!]$.*

Let us emphasize how the above corollary relates $\dim \mathcal{F}$ to IR. (i) If Σ is IR, then $\dim \mathcal{F}$ is strictly positive, i.e. there is an infinite number of solutions to the regulator equations. (ii) The converse implication is false, i.e. $\dim \mathcal{F} > 0$ does not imply IR. Indeed, as shown by the forthcoming Ex. 9.11, there exist systems Σ that are *not* IR (so that $\kappa = 0$) but such that $\delta_i = \gamma_i$ is strictly positive for some i, i.e. the eigenvalue λ_i of S is also an invariant zero of Σ.[4] This means that the property of IR does not capture all degrees of freedom related to the definition of the steady state.

Remark 9.7 (The non resonance assumption). Assume that ASM 9.3 is valid, so that $m \geq p$ holds. Particularization of Cor. 9.6 gives $\dim \mathcal{F} = (m - p)q$, see Appendix C.1.5. •

Remark 9.8 (Interpretation of κ). From (8.8), it holds $\kappa = \dim \mathcal{N}$. •

9.2.2 Online selection of (Γ, Π)

Sometimes, online selection of the most suitable $\left[\begin{smallmatrix}\Pi\\ \Gamma\end{smallmatrix}\right] \in \mathcal{F}$ might be desirable to adapt the references to the operating conditions. Next theorem shows how resulting time-dependency of $\left[\begin{smallmatrix}\Pi\\ \Gamma\end{smallmatrix}\right]$ can be handled, by relating each term of the basis of $\operatorname{Ker}\{\mathrm{H_F}\}$ to the weakly unobservable subspace $\mathcal{V}^*$, its "good" part $\mathcal{V}^*_g$ and its controllable part $\mathcal{R}^*$ (see Prop. C.5).

Theorem 9.9. *Given any bounded differentiable signal $\theta_{i,j} \in \mathbf{D} \cap \mathbf{B}, ((i,j) \in \mathcal{J})$ satisfying $\dot{\theta}_{i,j} \in \mathbf{PC}$. Let $\theta(t) \in \mathbb{R}^{\dim \mathcal{F}}$ gathers every signal $\theta_{i,j}(t)$. Select any $F \in \mathbb{R}^{m \times n}$ such that $A + BF$ is Hurwitz and define the control law*

$$(w, x) \mapsto u = \Gamma(\theta)w + F(x - \Pi(\theta)w) \tag{9.12}$$

parametrized by θ where $\theta \mapsto \Pi(\theta)$ and $\theta \mapsto \Gamma(\theta)$ are given by

$$\Pi(\theta) := \Pi_0 + \sum_{(i,j)\in\mathcal{J}} \theta_{i,j}\Pi_{i,j}$$
$$\Gamma(\theta) := \Gamma_0 + \sum_{(i,j)\in\mathcal{J}} \theta_{i,j}\Gamma_{i,j}$$

where $\Pi_{i,j}$ and $\Gamma_{i,j}$ are defined as in Appendix C.1.2. Consider the following two conditions parameterized by $\mathcal{G} \subset \mathcal{I} \times [\![1, n+m]\!]$:

$$\lim_{t\to 0} \sum_{(i,j)\in\mathcal{G}} \dot{\theta}_{i,j}(t)\Pi_{i,j}w(t) = \mathbf{0} \tag{9.13a}$$
$$\sum_{(i,j)\in\mathcal{G}} \dot{\theta}_{i,j}(t)\Pi_{i,j}w(t) = \mathbf{0} \tag{9.13b}$$

and define the following set via Prop. C.5:

$$\mathcal{J}_g := \{(i,j) \in \mathcal{J} : \operatorname{Im}\{\Pi_{i,j}\} \subset \mathcal{V}^*_g\}.$$

[4] This is just one the situations that is ruled out by the non-resonance condition.

(a) *If* (9.13a) *holds for* $\mathcal{G} = \mathcal{J}$, *then* (9.12) *solves Problem 9.1.*

(b) *If (i)* (9.13a) *holds for all* $\mathcal{G} = \mathcal{J} \setminus \mathcal{J}_g$ *and (ii)* $F \in \mathbb{F}(\mathcal{V}_g^*)$, *then* (9.12) *solves Problem 9.1.*

(c) *If* (9.13b) *holds for* $\mathcal{G} = \mathcal{J}$ *and* $x(0) = \Pi(\theta(0))w(0)$ *holds, then* (9.12) *solves Problem 9.1* exactly *in the sense that* $e(t)$ *is identically zero.*

(d) *If (i)* (9.13b) *holds for all* $\mathcal{G} = \mathcal{J} \setminus \mathcal{J}_g$, *(ii)* $F \in \mathbb{F}(\mathcal{V}_g^*)$ *and (iii)* $x(0) \in \Pi(\theta(0))w(0) + \mathcal{V}_g^*$, *then* (9.12) *solves Problem 9.1* exactly.

Proof. See Appendix C.1.4. □

Remark 9.10 (Rem. 9.7 continued). Consider the only non-trivial case where $\dim \mathcal{F} > 0 \Leftrightarrow m > p$. In this situation, $\mathcal{J}$ equals $\mathcal{J}_g$ so that assertions (i) of both (b) and (d) of Th. 9.9 are vacuously true. Besides, item (ii) of (b) in the same theorem can be replaced by $F \in \mathbb{F}(\mathcal{R}^*)$. See Appendix C.1.5. •

9.3 Shortfalls of the classical paradigm

The above section suggests that the existence of degrees of freedom in the definition of the reference trajectories (u_r, x_r) is directly related to the non-uniqueness of the regulator equations (9.7). A counterexample of this statement is now offered. Specifically, it is shown that $\mathcal{F}$ can contain a single element, even if distinct reference trajectories (u_r, x_r) solving (9.3) exist, i.e. even if $\mathbf{R}(w)$ contains more than one element.

9.3.1 An under-determined steady-state

Example 9.11. Consider the following quadruple

$$\left[\begin{array}{ccc|c} -2 & -1 & 1 & 0 \\ 1 & 0 & 0 & 0 \\ 0 & 0 & -1 & 1 \\ \hline -2 & 0 & 1 & 0 \end{array}\right]. \tag{9.14}$$

The control objective is to impose the value of output y to an arbitrary given $y_r \in \mathbb{R}$. This problem can be formulated as a standard output regulation problem by defining e as $y - y_r$ and identifying y_r with w, i.e. (9.1) and (9.2) hold with $S = 0$, $P = \mathbf{0}_3$ and $Q = -1$. Here, we are concerned with the construction of a steady state that achieves $y = y_r \Leftrightarrow e = \mathbf{0}$. Specifically, we aim to construct trajectories (u_r, x_r) in $\mathbf{R}(w)$, that is, $(u_r, x_r) \in \mathbf{U} \times \mathbf{X}$ solving (9.3).
Following the classical paradigm, let us solve (9.7):

$$\left[\begin{array}{c} 0 \\ 0 \\ 0 \\ \hline 1 \end{array}\right] = \left[\begin{array}{ccc|c} -2 & -1 & 1 & 0 \\ 1 & 0 & 0 & 0 \\ 0 & 0 & -1 & 1 \\ \hline -2 & 0 & 1 & 0 \end{array}\right] \left[\begin{array}{c} \Pi \\ \hline \Gamma \end{array}\right] \Longleftrightarrow \left[\begin{array}{c} \Pi \\ \hline \Gamma \end{array}\right] = \left[\begin{array}{c} 0 \\ 1 \\ 1 \\ \hline 1 \end{array}\right]$$

The above unique solution (Γ, Π) gives rise to the following reference trajectories:

$$(u_{r1}(t), x_{r1}(t)) = (\Gamma w(t), \Pi w(t)) = \left(w(t),\ w(t) \begin{bmatrix} 0 \\ 1 \\ 1 \end{bmatrix} \right)$$

One can check that $(u_{r1}(t), x_{r1}(t))$ belongs to $\mathbf{R}(w)$ for all signals w solving $\dot{w} = Sw$, see the left hand-side column of Fig. 9.3. In particular, it is clear that $e(t) = Cx_{r1}(t) + Qw(t) = 0 \Leftrightarrow y(t) =$

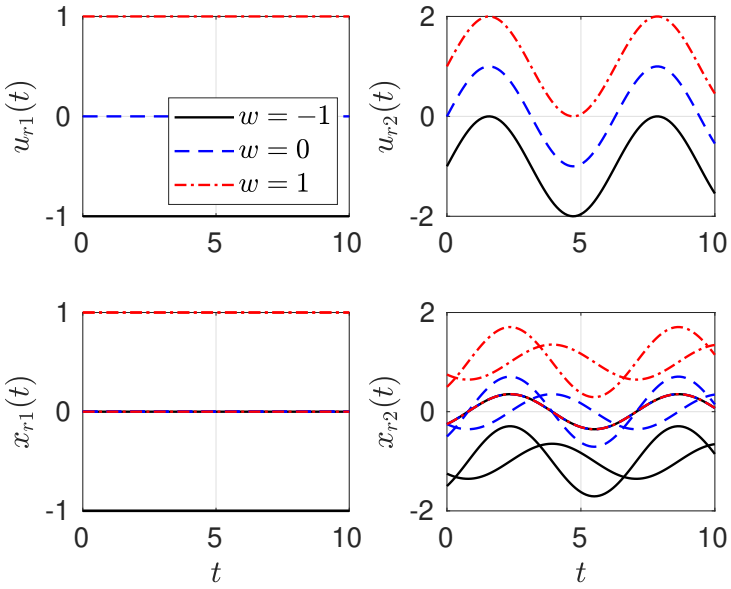

Figure 9.3: Left and right columns gives two distinct reference trajectories $(u_r, x_r) \in \mathbf{R}(w)$ for different values of $w = y_r$.

y_r for all t. Let us define another pair of reference trajectories as follows:

$$(u_{r2}(t), x_{r2}(t)) = (u_{r1}(t), x_{r1}(t)) + \left(\sin(t),\ -\frac{\sqrt{2}}{4} \begin{bmatrix} \cos(t+\pi/4) \\ \sin(t+\pi/4) \\ 2\cos(t+\pi/4) \end{bmatrix} \right)$$

Once again, it can be verified that $(u_{r2}(t), x_{r2}(t)) \in \mathbf{R}(w)$ holds for all $w \in \{w : \dot{w} = Sw\}$, see the right hand-side column of Fig. 9.3.
The key point is $(u_{r2}(t), x_{r2}(t))$ is distinct from $(u_{r1}(t), x_{r1}(t))$, whereas the latter is the unique pair of reference trajectories that can be constructed via the regulator equations. Thus, the uniqueness of the solution of the regulator equations is not a suitable test to detect uniqueness of the reference trajectory. IR is neither a suitable characterization of this situation, since one can show that Σ is not IR.

9.3.2 The pitfall of the regulator equations for non uniqueness of reference trajectories

The regulator equations (9.7) are derived by plugging $(u_r, x_r) = (\Gamma w, \Pi w)$ in (9.3). Thus, this strategy implicitly restricts the scope of the study to reference trajectories that are both time-invariant and linear wrt w, i.e. one focuses on the set $\mathbf{L}(w)$:

$$\mathbf{L}(w) := \left\{ (\Gamma w, \Pi w) : \Gamma \in \mathbb{R}^{m \times q}, \Pi \in \mathbb{R}^{n \times q} \right\}.$$

Saying it differently, by focusing on $\mathbf{L}(w)$ instead of $\mathbf{R}(w)$, the classical paradigm dismisses the reference trajectories in $\mathbf{R}(w) \setminus \mathbf{L}(w)$. This set can be non empty, as shown by Ex. 9.11.

The merit of the strategy relying on $\mathbf{L}(w)$ is to transform the search for signals (u_r, x_r) into a finite-dimensional algebraic problem, leading to matrices (Γ, Π). This is fully relevant for investigating the solvability (but not uniqueness !) of the problem, as shown by the following lemma.

Lemma 9.12. *Let* $\mathbf{E} := \{w : \dot{w} = Sw\}$. *It holds:*

$$\big(\forall w \in \mathbf{E} : \mathbf{R}(w) \neq \{\varnothing\}\big) \Leftrightarrow \big(\forall w \in \mathbf{E} : \mathbf{L}(w) \cap \mathbf{R}(w) \neq \{\varnothing\}\big) \Leftrightarrow \big(\mathcal{F} \neq \{\varnothing\}\big)$$

Proof. See Appendix C.2. □

9.4 Strong annihilator and weak input redundancy

Recall that our goal is to detect when reference trajectories are non-unique. Two deadlocks have already been exhibited. First, IR of Σ is not a suitable characterization of this situation.[5] Second, the uniqueness of the solution of the regulator equations is not a suitable test either, as shown by Ex. 9.11.

These observations suggest that the problem of parameterizing $\mathbf{R}(w)$ should be tackled head-on. This is the goal of this section. The algebraic structure of $\mathbf{R}(w)$ is first exhibited. Then, the input injection point of view is adopted to construct a reference trajectory generator made of a copy of the system Σ_w and a suitable annihilator. Finally, an extensive analysis of the existence of this annihilator gives rise to a weaker definition of IR.

9.4.1 The structure of $\mathbf{R}(w)$

Assume that there exists w solving $\dot{w} = Sw$ such that $\mathbf{R}(w) \neq \{\varnothing\}$ holds. Pick any particular (u_r^p, x_r^p) in $\mathbf{R}(w)$. Any other $(u_r, x_r) \in \mathbf{R}(w)$ can then be defined *relative* to (u_r^p, x_r^p) as follows:

$$(u_r, x_r) = (u_r^p, x_r^p) + (\tilde{u}_r, \tilde{x}_r) \tag{9.15}$$

where $(\tilde{u}_r, \tilde{x}_r) := (u_r, x_r) - (u_r^p, x_r^p)$ holds, see Fig. 9.4b. From this reformulation and making use of (9.5) with H_x in place of H, one proves the first one of the following equivalences:

$$(u_r, x_r) \in \mathbf{R}(w) \Leftrightarrow (\tilde{u}_r, \tilde{x}_r) \in \mathbf{R}(\mathbf{0}) \Leftrightarrow (\tilde{u}_r, \mathbf{0}) \in \mathbf{W}(\tilde{x}_r(0)) \tag{9.16}$$

The second equivalence is just another way to write $(\tilde{u}_r, \tilde{x}_r) \in \mathbf{R}(\mathbf{0})$, that is introduced here for further references. By the definition of $\mathbf{R}(w)$, $(\tilde{u}_r, \tilde{x}_r) \in \mathbf{R}(\mathbf{0})$ means that input $\tilde{u}_r$ generates zero output when exerted on Σ from $\tilde{x}_r(0)$. $\tilde{x}_r$ is the corresponding state trajectory. We have just proved the next lemma.

Lemma 9.13. *Choose any w solving $\dot{w} = Sw$ such that $\mathbf{R}(w) \neq \{\varnothing\}$ holds. Select any $(u_r^p, x_r^p) \in \mathbf{R}(w)$. It holds:*

$$\mathbf{R}(w) = (u_r^p, x_r^p) + \mathbf{R}(\mathbf{0}) \tag{9.17}$$

Set $\mathbf{R}(\mathbf{0})$ is linear and can be equivalently written as follows:

$$\mathbf{R}(\mathbf{0}) = \{(\tilde{u}_r, \tilde{x}_r) : (\tilde{u}_r, \tilde{x}_r, \mathbf{0}) \in \mathbf{Q}(\tilde{x}_r(0))\}$$

Hence, $\mathbf{R}(w)$ is affine.

[5] It will be shown in the sequel that other definitions existing in the literature like e.g. [Zac09; Ser12] are not appropriate tools either.

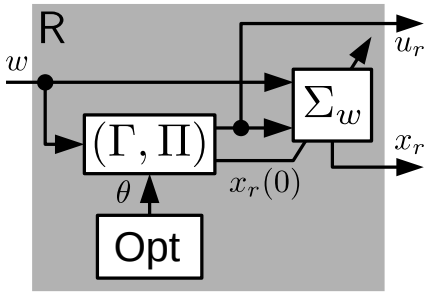

(a) The state trajectory x_r is generated by an embedded copy of Σ_w fed by w, $u_r = \Gamma w$ and $x_r(0) = \Pi w(0)$.

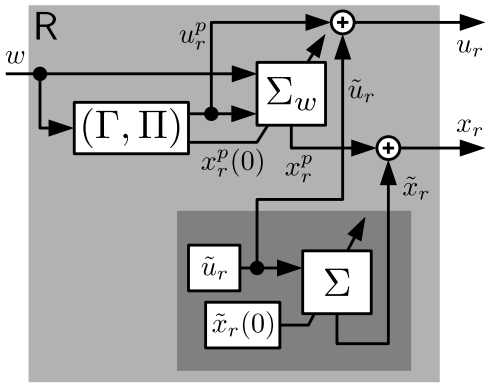

(b) Implementation of the exhaustive parametrization of $\mathbf{R}(w)$ via (9.15), see Lem. 9.13.

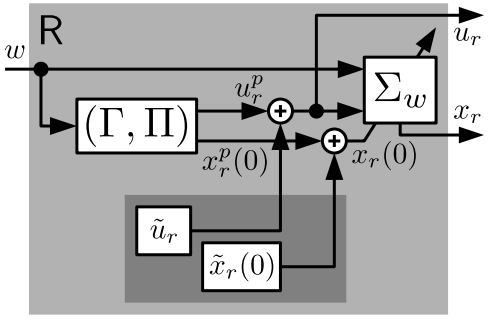

(c) Implementation of (9.5) to move $\tilde{x}_r(0)$ and $\tilde{u}_r$ ahead of Σ_w and getting rid of the copy of the system Σ.

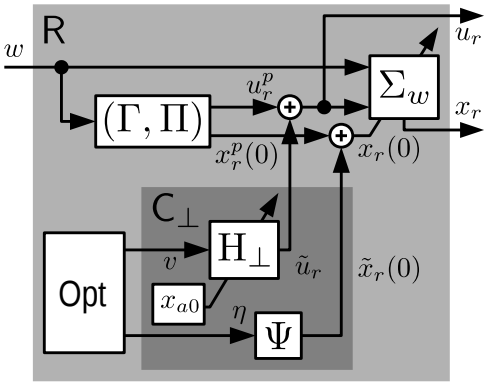

(d) Introduction of the two mappings $\mathrm{H}_\perp$ and Ψ composing the strong annihilator $\mathsf{C}_\perp$.

Figure 9.4: Gradual construction of the incremental reference trajectory generator R equipped with a strong annihilator driven by $v(\cdot)$ and η. Note the parameterization of R by $(u_r^p, x_r^p(0))$ where $(u_r^p, x_r^p) = (\Gamma w, \Pi w)$ are particular reference trajectories in $\mathbf{R}(w)$ because $\left[\begin{smallmatrix}\Pi\\ \Gamma\end{smallmatrix}\right] \in \mathcal{F}$ holds.

9.4.2 Strong annihilator: definition

Our goal is now to design the reference trajectory generator R allowing for online selection of some suitable pair (u_r, x_r) in $\mathbf{R}(w)$. This is achieved via Fig. 9.4, which is now discussed.

- Fig. 9.4a: The starting point is the equivalent reformulation of Fig. 9.2, that is obtained by letting the state trajectory x_r be computed via a copy of the system Σ_w.
- Fig. 9.4b: The conclusions drawn from Ex. 9.11 are implemented by substituting the (non-exhaustive) parametrization of $\mathbf{R}(w)$ via (Γ, Π) (and θ) with the (exhaustive) parametrization of $\mathbf{R}(w)$ via $(\tilde{u}_r, \tilde{x}_r) \in \mathbf{R}(\mathbf{0})$, see Lem. 9.13. This leads to Fig. 9.4b where, without loss of generality (see Lem. 9.12), the particular solution $(u_r^p, x_r^p) \in \mathbf{R}(w)$ is computed using an arbitrary $\left[\begin{smallmatrix}\Pi\\ \Gamma\end{smallmatrix}\right] \in \mathcal{F}$. In this figure, the state trajectory $\tilde{x}_r$ is obtained using a copy of Σ and exploiting the relationship $\tilde{x}_r = \mathrm{H}_x[\tilde{x}_r(0); \tilde{u}_r]$. Note that this amounts to parameterizing $\mathbf{R}(\mathbf{0})$ via $\tilde{x}_r(0)$ and $\tilde{u}_r$, which can be selected independently. Note that the optimizer delivering θ in Fig. 9.4a have been removed. Indeed, what is to be optimized in Fig. 9.4b is $\tilde{u}_r$ and $\tilde{x}_r(0)$, *under the constraint* that this pair leads to reference trajectories $(\tilde{u}_r, \tilde{x}_r)$ that belong to $\mathbf{R}(\mathbf{0})$.
- Fig. 9.4c: The next step is to somehow factorize Σ and Σ_w so that the increments $\tilde{x}_r(0)$ and $\tilde{u}_r$ are added ahead of Σ_w. This manipulation is supported by (9.5).
- Fig. 9.4d: As a final step, the dynamical mapping $\mathrm{H}_\perp[x_{a0}; \cdot]$, parameterized by the initial state x_{a0}, and the static map Ψ are introduced. They are responsible for computing $\tilde{u}_r$ and $\tilde{x}_r(0)$ from signal v and constant vector η, respectively. Specifically, those mappings should be tailored to code the constraint $(\tilde{u}_r, \tilde{x}_r) \in \mathbf{R}(\mathbf{0})$ (where $\tilde{x}_r$ derives from $\tilde{u}_r$ and $\tilde{x}_r(0)$), that is, for any $v(\cdot)$ and η, condition $(\tilde{u}_r, \tilde{x}_r) \in \mathbf{R}(\mathbf{0})$ must hold.

These two mappings $\mathrm{H}_\perp$ and Ψ are the ingredients of a new kind of annihilator $\mathsf{C}_\perp$ that is now defined by making use of the last term of (9.16).

Definition (Strong annihilator)**.** The nonzero causal operator $\mathsf{C}_\perp$, associated with the mappings $\Psi : \eta \mapsto \tilde{x}_r(0)$ and $\mathrm{H}_\perp[x_{a0}; \cdot] : v \mapsto \tilde{u}_r$ parametrized by the initial state x_{a0}, is an *strong annihilator of* Σ if

$$\forall \eta, \exists x_{a0}, \forall v(\cdot) \in \mathbf{PC} : \ (\tilde{u}_r, \mathbf{0}) \in \mathbf{W}(\tilde{x}_r(0)), \tag{9.18}$$

where $\tilde{x}_r(0) := \Psi(\eta)$ and $\tilde{u}_r := \mathrm{H}_\perp[x_{a0}; v]$ hold true.

Pick any w that solves $\dot{w} = Sw$ and any $(\tilde{u}_r^p, \tilde{x}_r^p)$ in $\mathbf{R}(w)$. If Ψ and $\mathrm{H}_\perp[x_{a0}; \cdot]$ define a strong annihilator, then the output (u_r, x_r) of R depicted in Fig. 9.4d belongs to $\mathbf{R}(w)$, whatever is $v \in \mathbf{PC}$ or η. In this context, these two variables can be freely optimized, as illustrated in Fig. 9.4d.

From the (simple) annihilator in Fig. 8.1 to the strong annihilator in Fig. 9.4d, the key modification is the introduction of an additional mapping Ψ that delivers the increment $\tilde{x}_r(0)$ of the initial condition $x_r(0)$ of the copy of Σ_w. This is just the essential difference that motivates the introduction of this new kind of annihilator that is tailored for the reference trajectory generator R, whereas the (simple) annihilator of Chap. 8 is to be used as a subsystem of the stabilizer S.

Remark 9.14 (Strong annihilator $\Rightarrow$ (simple) annihilator). By definition, if Σ is IR, then a (simple) annihilator of Σ can be derived from any strong annihilator of Σ by setting $\Psi = \mathbf{0}$, provided that the strong annihilator has maximal range (see Rem. 9.20). •

9.4.3 Strong annihilator: existence and WIR

The next step is to ask when a strong annihilator of Σ exists, or equivalently, when two distinct reference trajectories can be selected in $\mathbf{R}(w)$. From (9.16), it comes out that a non-trivial pair $(\tilde{u}_r, \tilde{x}_r) \neq (\mathbf{0}, \mathbf{0})$ can be constructed in $\mathbf{R}(\mathbf{0})$ iff one of the two following cases occur:

(a) $\tilde{u}_r = \mathbf{0}$: Equality $(\mathbf{0}, \mathbf{0}) \in \mathbf{W}(\tilde{x}_r(0))$ is equivalent to saying that $\tilde{x}_r(t)$ identically belongs to the unobservable subspace $\langle \mathcal{K} | A \rangle$. Because the pair $(\tilde{u}_r, \tilde{x}_r)$ is nonzero, this subspace is necessarily nontrivial.

(b) $\tilde{u}_r \neq \mathbf{0}$: If $\tilde{x}_r(0) = \mathbf{0}$ holds, then Σ is input redundant (IR), by definition. To the best of our knowledge, the case $\tilde{x}_r(0) \neq \mathbf{0}$ has been neglected in the literature. However, this is also of interest. Ex. 9.11 indeed exhibits a non-IR and observable system for which $(\tilde{u}_r, \mathbf{0}) \in \mathbf{W}(\tilde{x}_r(0))$ and $\tilde{u}_r \neq \mathbf{0}$ implies $\tilde{x}_r(0) \neq \mathbf{0}$. Therefore, distinct reference trajectories can be constructed for non-IR or observable systems.

Point (b) motivates the introduction of a new kind of input redundancy.

Definition (WIR)**.** System Σ is *weakly input redundant* (WIR) if there exists an output y which can be produced by (at least) two distinct inputs u_1 and u_2 from possibly distinct initial states, i.e. there exist $x_{0,1}, x_{0,2} \in \mathcal{X}$ such that

$$\exists (u_1, y_1) \in \mathbf{W}(x_{0,1}),\ \exists (u_2, y_2) \in \mathbf{W}(x_{0,2}) : u_1 \neq u_2,\ y_1 = y_2. \tag{9.19}$$

Two immediate comments can be made from this definition:

- IR implies WIR since IR corresponds to the particular case where $x_{0,1}$ and $x_{0,2}$ are identical;
- Σ is WIR iff there exists $\tilde{x}_0$ and $\tilde{u} \neq \mathbf{0}$ such that $(\tilde{u}, \mathbf{0}) \in \mathbf{W}(\tilde{x}_0)$, by linearity of H and by defining $\tilde{x}_0 = x_{0,1} - x_{0,2}$ and $\tilde{u} = u_1 - u_2$ from the definition of WIR.

The following theorem is now in order. It summarizes the discussion in this subsection by exploiting (9.16) and the definition of WIR. Tractable conditions of the considered situation are also given by anticipating the forthcoming Prop. 9.16 where WIR is characterized. Recall the definition of integer $\rho \in \mathbb{N}$ given by (8.6):

$$\rho := \dim(\mathrm{Ker}\,\{B\} \cap \mathrm{Ker}\,\{D\})$$

and bear in mind the definition of $\mathcal{Z}$ given by (A.17) in p.235.

Theorem 9.15. *Choose any w solving $\dot{w} = Sw$ and such that $\mathbf{R}(w) \neq \{\varnothing\}$ holds. The following statements are equivalent:*

(i) *There exists $(u_{r1}, x_{r1}), (u_{r2}, x_{r2}) \in \mathbf{R}(w)$ such that $(u_{r1}, x_{r1}) \neq (u_{r2}, x_{r2})$;*

(ii) *There exists $(\tilde{u}_r, \tilde{x}_r) \in \mathbf{R}(\mathbf{0}) \setminus \{(\mathbf{0}, \mathbf{0})\}$;*

(iii) *There exists $(\tilde{u}_r, \tilde{x}_r(0)) \neq (\mathbf{0}, \mathbf{0})$ such that $(\tilde{u}_r, \mathbf{0}) \in \mathbf{W}(\tilde{x}_r(0))$ holds;*

(iv) *Σ is WIR or $\dim \langle \mathcal{K} | A \rangle > 0$ holds;*

(v) *$\rho > 0$ or $\dim(\mathcal{V}^*) > 0$;*

(vi) *$\mathrm{nrank}\,\{P_\Sigma\} < n + m$ or $\mathcal{Z} \neq \{\varnothing\}$;*

(vii) $\exists z \in \mathbb{C}$ *such that* $\operatorname{rank}\{P_\Sigma(z)\} < n + m$.

Proof. See Appendix C.6. □

Let us now associate tractable conditions with the definition of WIR. To this end, define the subspace $\mathcal{M} \subset \mathbb{R}^m$:

$$\mathcal{M} := \begin{bmatrix} B \\ D \end{bmatrix}^{-1} \left(\mathcal{V}^* \oplus \{0\} + \begin{bmatrix} A \\ C \end{bmatrix} \mathcal{V}^* \right) \tag{9.20}$$

and recall that the set of output decoupling zeros reads:

$$\mathcal{Z}_{\text{od}} := \sigma(A|\,\langle \mathcal{K}|A\rangle) \tag{9.21}$$

Proposition 9.16. *The following statements are equivalent:*

(i) *System* Σ *is WIR;*

(ii) $\rho > 0$ *or* $\dim(\mathcal{R}^*) > 0$ *or* $\dim(\mathcal{V}^*/(\mathcal{R}^* + \langle \mathcal{K}|A\rangle)) > 0$*;*

(iii) $\dim(\mathcal{M}) > 0$*;*

(iv) $\operatorname{nrank}\{P_\Sigma\} < n + m$ *or* $\mathcal{Z} \setminus \mathcal{Z}_{\text{od}} \neq \{\varnothing\}$.

Proof. See Appendix C.5. □

9.4.4 Strong annihilator: construction

Each equivalent item of Th. 9.15 is a necessary and sufficient condition for the existence of a strong annihilator of Σ, by definition. The constructive part of this result is offered by the following theorem.

Theorem 9.17. *Assume that one of the equivalent items of Th. 9.15 is valid. Let* $N : \mathcal{N} \to \mathbb{R}^m$ *be the natural embedding. Select any matrix in* $\mathbb{F}(\mathcal{V}^*)$*. Then, together with* $\Psi : \mathcal{V}^* \to \mathcal{X}$ *the natural embedding, the quadruple*

$$(A_a, B_a, C_a, D_a) = ((A + BF)|\mathcal{V}^*, \mathcal{V}^*|B|\mathcal{N}, F|\mathcal{V}^*, N)\,, \quad x_{a0} = \eta = \Psi^{-1}\tilde{x}_r(0) \tag{9.22}$$

characterizing $\mathrm{H}_\perp$ *defines a strong annihilator of* Σ.

Proof. See Appendix C.9. □

Remark 9.18 (The case $\mathbf{0} \in \mathbb{F}(\mathcal{V}^*)$). If the zero map belongs to $\mathbb{F}(\mathcal{V}^*)$, then selecting $F = \mathbf{0}$ makes $\tilde{u}_r$ independent of x_a so that the input-output mapping of $\mathrm{H}_\perp$ can be captured by the static mapping $v \mapsto Nv$. •

Remark 9.19 (The case $\mathcal{V}^* = \{\mathbf{0}\}$). If $\mathcal{V}^*$ is trivial, then $\mathcal{N}$ reduces to $\operatorname{Ker}\{B\} \cap \operatorname{Ker}\{D\}$ and the strong annihilator of Th. 9.17 degenerates into the static mapping $v \mapsto Nv$. •

Remark 9.20 (Maximal range). The strong annihilator of Th. 9.17 has maximal range in the sense that for all $\tilde{x}_r(0)$ and for all $\tilde{u}_r$ such that $(\tilde{u}_r, \mathbf{0}) \in \mathbf{W}(\tilde{x}_r(0))$, there exist x_{a0}, v and η satisfying $\mathrm{H}_\perp[x_{a0}; v] = \tilde{u}_r$ and $\tilde{x}_r(0) = \Psi(\eta)$. See Appendix C.9 for the proof of this statement. •

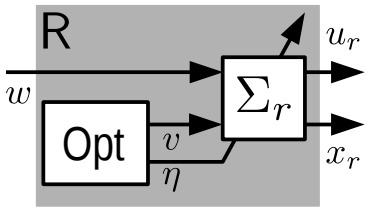

Figure 9.5: Equivalent reformulation of Fig. 9.4d, see Rem. 9.21.

Remark 9.21 (Reformulation of R). From Fig. 9.4d, one gets

$$x_r = \mathrm{H}_x^w[x_r^p(0) + \tilde{x}_r(0); u_r^p + \tilde{u}_r] \overset{(9.5)}{=} \mathrm{H}_x^w[x_r^p(0); u_r^p] + \mathrm{H}_x[\tilde{x}_r(0); \tilde{u}_r].$$

The first term $\mathrm{H}_x^w[x_r^p(0); u_r^p]$ equals Πw because $x_r^p(0) = \Pi w(0)$ and $u_r^p = \Gamma w$ hold. Using the notations of Th. 9.17, the second term $\mathrm{H}_x[\tilde{x}_r(0); \tilde{u}_r]$ reads Ψx_a with x_a solving $\dot{x}_a = A_a x_a + B_a v$ with $x_a(0) = \eta$, see the proof of Th. 9.17 in Appendix C.9. Bearing in mind that u_r equals $u_r^p + \tilde{u}_r = \Gamma w + C_a x_a + D_a v$, one concludes that (u_r, x_r) are the output of the linear dynamical system Σ_r fed by (w, v), initialized by η and characterized by the following quadruple:

$$\left(A_a, \begin{bmatrix} \mathbf{0} & B_a \end{bmatrix}, \begin{bmatrix} C_a \\ \Psi \end{bmatrix}, \begin{bmatrix} \Gamma & D_a \\ \Pi & \mathbf{0} \end{bmatrix} \right), \tag{9.23}$$

Fig. 9.5 illustrates this conclusion. •

9.5 Bounded persistent weak input redundancy

Pick any (u_r^p, x_r^p) in $\mathbf{R}(w)$. From the previous section, selecting another pair of reference trajectories $(u_r, x_r) \neq (u_r^p, x_r^p)$ in $\mathbf{R}(w)$ amounts to choosing $(\tilde{u}_r, \tilde{x}_r)$ in $\mathbf{R}(\mathbf{0}) \setminus \{(\mathbf{0}, \mathbf{0})\}$ and adding it to (u_r^p, x_r^p). In doing so, each of the following two situations might occur. (i) (u_r, x_r) grows unbounded. (ii) Both (u_r, x_r) and (u_r^p, x_r^p) share the same steady state. In this section, it is argued that these two situations are undesirable. This motivates the construction of tractable tests to rule them out, as well as the construction of a new kind of annihilator.

9.5.1 Motivation

Without loss of generality, assume that (u_r^p, x_r^p) equals $(\Gamma w, \Pi w)$ for some $(\Gamma, \Pi) \in \mathcal{F}$ solving the regulator equations (9.7), see Lem. 9.12. Let us comment on the two previous situations.

(i) Since (u_r^p, x_r^p) is bounded, unbounded growth of $(u_r, x_r) = (u_r^p, x_r^p) + (\tilde{u}_r, \tilde{x}_r)$ must originate from $(\tilde{u}_r, \tilde{x}_r)$. Therefore, avoiding (i) is equivalent to impose that $(\tilde{u}_r, \tilde{x}_r)$ remains bounded.

(ii) Recall that $(u(t), x(t))$ asymptotically converges to $(u_r(t), x_r(t))$, thanks to the stabilizer S. Hence, if (u_r, x_r) and (u_r^p, x_r^p) share the same steady state, then any of those two reference trajectories leads to an identical permanent regime; that is, even if (u_r, x_r) and (u_r^p, x_r^p) are distinct, they shape the steady state in the same way. From the reference trajectory generator point of view, there are no benefits to choose (u_r, x_r) in place of (u_r^p, x_r^p) in this case. Clearly, this situation is captured by the condition $(\tilde{u}_r(t), \tilde{x}_r(t)) \to \mathbf{0}$.

The bottom line of this discussion is that relevant redundancy for the reference trajectory generator R is related to signals $(\tilde{u}_r, \tilde{x}_r) \in \mathbf{R}(\mathbf{0})$ that are both bounded and persistent. By persistent signal, we mean a non-vanishing signal. The set of causal and persistent signals reads:

$$\mathbf{P} = \{x(\cdot) \text{ causal} : \text{if } x^\star = \lim_{t\to+\infty} x(t) \text{ exists, then } x^\star \neq \mathbf{0}\}$$

In the sequel, bp is used as a short for "bounded persistent".

9.5.2 On $\mathbf{R}(\mathbf{0})$ and bp-WIR

Let us now describe the subset of $\mathbf{R}(\mathbf{0})$ gathering $(\tilde{u}_r, \tilde{x}_r)$ that are bp (and hence non-trivial).[6] The following two situations arise:

(a) $\tilde{u} = \mathbf{0}$: In this case, $\tilde{x}_r = \mathrm{H}_x[\tilde{x}_r(0); \mathbf{0}]$ must be bp, so that $\tilde{x}_r(0)$ is necessarily distinct from zero. Such a situation occurs iff Σ admits bp unobservable modes, whose characteristic exponents are hence on the imaginary axis of the complex plane.

(b) $\tilde{u} \neq \mathbf{0}$: If $\tilde{u}$ is bounded but vanishing, then $\tilde{x}_r = \mathrm{H}_x[\tilde{x}_r(0); \tilde{u}]$ must be bp. It is shown in the sequel that such a situation is similar to the case (a), modulo a vanishing transient, i.e. boundedness and persistency are due to bp unobservable modes. The last case, where $\tilde{u}$ is bp, motivates the introduction of the following subclass of WIR systems.

Definition (bp-WIR)**.** System Σ is *bounded persistent weakly input redundant* (bp-WIR) if there exists an output y which can be produced by (at least) two inputs u_1 and u_2 whose difference is bp from possibly distinct initial states, i.e. there exist $x_{0,1}, x_{0,2} \in \mathcal{X}$ such that:

$$\exists (u_1, y_1) \in \mathbf{W}(x_{0,1}),\ \exists (u_2, y_2) \in \mathbf{W}(x_{0,2}) : u_1 - u_2 \in \mathbf{B} \cap \mathbf{P},\ y_1 = y_2. \tag{9.24}$$

By virtue of the linearity of H, it comes out that Σ is bp-WIR iff there exists $\tilde{x}_0$ and $\tilde{u}$ such that $\mathrm{H}[\tilde{x}_0; \tilde{u}] = \mathbf{0}$ holds and $\tilde{u}$ is bp. As shown in Subsec. C.3, this allows to prove that IR implies bp-WIR.

Relying on these observations, the next proposition summarizes the discussion of this subsection. By anticipating the forthcoming Prop. 9.23 characterizing bp-WIR, it also provides the conditions for all relevant situations when treating redundancy at the level of the reference trajectory generator R. For that purpose, the two following subspaces are defined:[7]

- the *bounded persistent subspace* $\mathcal{X}_{bp} \subset \mathcal{X}$ is the largest subspace $\mathcal{V}$ such that (i) $A\mathcal{V} \subset \mathcal{V}$ holds, (ii) $\sigma(A|\mathcal{V}) \subset \mathbb{C}^0$ is valid and (iii) $A|\mathcal{V}$ is semi-simple;[8]
- the *bounded persistent weakly unobservable subspace* $\mathcal{V}^*_{bp} \subset \mathcal{X}$ is the largest subspace $\mathcal{V}$ for which there exists F such that (i) $(A+BF)\mathcal{V} \subset \mathcal{V} \subset \mathrm{Ker}\,\{C+DF\}$ holds, (ii) $\sigma(A+BF|\mathcal{V}) \subset \mathbb{C}^0$ is valid and (iii) $(A+BF)|\mathcal{V}$ is semi-simple.

It can be proved that $\mathcal{R}^* \subset \mathcal{V}^*_{bp} \subset \mathcal{V}^*$ holds, see Lem. C.19 and Lem. C.20. Among other things, this allows to introduce the following set

$$\mathcal{Z}_{bp} := \sigma((A+BF)|\mathcal{V}^*_{bp}/\mathcal{R}^*) \tag{9.25}$$

[6] Let us emphasize that $(\tilde{u}_r, \tilde{x}_r) \in \mathbf{B} \cap \mathbf{P}$ is equivalent to (a) both $\tilde{u}$ and $\tilde{x}$ are bounded, and (b) $\tilde{u}$ *or* $\tilde{x}$ is persistent.
[7] See Appendix C for a formal proof that the following subspaces are well-defined supremums.
[8] Recall that a linear map M is semi-simple iff it is diagonalizable over the complex field $\mathbb{C}$.

where $F \in \mathbb{F}(\mathcal{V}^*)$. As proved in Subsec. C.3, this set is well defined for arbitrary $F \in \mathbb{F}(\mathcal{V}^*)$ in the sense that (i) $\mathcal{V}^*_{bp}/\mathcal{R}^*$ is $(A+BF)$-invariant and (ii) $\mathcal{Z}_{bp}$ is independent of $F \in \mathbb{F}(\mathcal{V}^*)$, that is, for any $F_1, F_2 \in \mathbb{F}(\mathcal{V}^*)$, one has $\sigma((A+BF_1)|\mathcal{V}^*_{bp}/\mathcal{R}^*) = \sigma((A+BF_2)|\mathcal{V}^*_{bp}/\mathcal{R}^*)$. Note also that $\mathcal{Z}_{bp} \subset \mathcal{Z}$ holds true.

Theorem 9.22. *Choose any w solving $\mathcal{W} = S\mathcal{W}$ and such that $\mathbf{R}(w) \neq \{\varnothing\}$ holds. The following statements are equivalent:*

(i) There exists $(u_{r1}, x_{r1}), (u_{r2}, x_{r2}) \in \mathbf{R}(w)$ such that $(u_{r1} - u_{r2}, x_{r1} - x_{r2})$ is bp;

(ii) There exists $(\tilde{u}_r, \tilde{x}_r) \in \mathbf{R}(\mathbf{0})$ such that $(\tilde{u}_r, \tilde{x}_r)$ is bp;

(iii) There exist $\tilde{x}_0$ and $(\tilde{u}, \tilde{x}, \tilde{y}) \in \mathbf{Q}(\tilde{x}_0)$ such that (a) $\tilde{y} = \mathbf{0}$ holds and (b) $(\tilde{u}, \tilde{x})$ is bp;

(iv) Σ is bp-WIR or $\dim(\mathcal{X}_{bp} \cap \langle \mathcal{K}|A\rangle) > 0$ holds;

(v) $\rho > 0$ or $\dim(\mathcal{V}^*_{bp}) > 0$;

(vi) $\operatorname{nrank}\{P_\Sigma\} < n + m$ or $\mathcal{Z}_{bp} \neq \{\varnothing\}$.

Proof. See Appendix C.8. □

Tractable conditions allowing to test if Σ is bp-WIR are now offered. One of them uses the subspace $\mathcal{M}_{bp} \subset \mathbb{R}^m$ defined as follows:

$$\mathcal{M}_{bp} := \begin{bmatrix} B \\ D \end{bmatrix}^{-1} \left(\mathcal{V}^*_{bp} \oplus \{0\} + \begin{bmatrix} A \\ C \end{bmatrix} \mathcal{V}^*_{bp} \right) \tag{9.26}$$

Proposition 9.23. *The following statements are equivalent:*

(i) System Σ is bp-WIR;

(ii) $\rho > 0$ or $\dim(\mathcal{R}^*) > 0$ or $\dim(\mathcal{V}^*_{bp}/(\mathcal{R}^* + \langle \mathcal{K}|A\rangle \cap \mathcal{V}^*_{bp})) > 0$;

(iii) $\dim(\mathcal{M}_{bp}) > 0$;

(iv) $\operatorname{nrank}\{P_\Sigma\} < n + m$ or $\mathcal{Z}_{bp} \setminus \sigma(A|\mathcal{X}_{bp} \cap \langle \mathcal{K}|A\rangle) \neq \{\varnothing\}$.

Proof. See Appendix C.7. □

9.5.3 bp-strong annihilator: definition, existence and construction

Let us now introduce the concept of bp-strong annihilator, corresponding to a specific strong annihilator (so that Fig. 9.4 still applies), inducing bp signals $(\tilde{u}_r, \tilde{x}_r)$. To this end, let the state trajectory $\tilde{x}_r$ appear in the following equivalent reformulation of (9.18), which is used to define a strong annihilator:

$$\forall \eta, \exists x_{a0}, \forall v(\cdot) \in \mathbf{PC} : \ (\tilde{u}_r, \tilde{x}_r, \mathbf{0}) \in \mathbf{Q}(\tilde{x}_r(0)). \tag{9.27}$$

This condition is modified in three directions. First, it is imposed that $(\tilde{u}_r, \tilde{x}_r)$ is either bp or zero.[9] Second, cases in which the annihilator input v is unbounded are ruled out. Third, ensuring that either $\tilde{u}_r$ or $\tilde{x}_r$ is persistent induces an interplay between the selection of η and v. This is handled via sequential selection of η and v, where the latter is chosen based on the former via the set-valued mapping $\mathbf{V}(\cdot)$. This leads to the following definition.

[9] The case $(\tilde{u}_r, \tilde{x}_r) = \mathbf{0}$ is allowed in the same way as $\tilde{u} = \mathbf{0}$ is not excluded by (8.19).

Definition (bp-strong annihilator of Σ)**.** The nonzero causal operator $\mathsf{C}_\perp$, associated with the set-valued mapping $\mathbf{V} : x_{a0} \mapsto \mathbf{V}(x_{a0}) \subset \mathbf{PC} \cap \mathbf{B}$ and the mappings $\Psi_{bp} : \eta \mapsto \tilde{x}_r(0)$ and $\mathrm{H}_\perp^{bp}[x_{a0}; \cdot] : v \mapsto \tilde{u}_r$ parametrized by the initial state x_{a0}, is an *bp-strong annihilator of* Σ if:

$$\forall \eta, \exists x_{a0}, \forall v(\cdot) \in \mathbf{V}(x_{a0}) : \begin{cases} (\tilde{u}_r, \tilde{x}_r, \mathbf{0}) \in \mathbf{Q}(\tilde{x}_r(0)), \\ (\tilde{u}_r, \tilde{x}_r) \in (\mathbf{B} \cap \mathbf{P}) \cup \{\mathbf{0}\}, \end{cases} \tag{9.28}$$

with $\tilde{x}_r(0) := \Psi_{bp}(\eta)$, $\tilde{u}_r := \mathrm{H}_\perp^{bp}[x_{a0}; v]$, and where $\tilde{x}_r$ is uniquely defined from $\tilde{u}_r$ and $\tilde{x}_r(0)$ by $(\tilde{u}_r, \tilde{x}_r, \mathbf{0}) \in \mathbf{Q}(\tilde{x}_r(0))$.

All the equivalent items of Th. 9.22 is a necessary condition for the existence of a bp-strong annihilator of Σ, by definition. These equivalent conditions are also sufficient, as shown in the following theorem.

Theorem 9.24. *Assume that one of the equivalent items of Th. 9.22 is valid. Let $N : \mathcal{N} \to \mathbb{R}^m$ be the natural embedding. Select any matrix in $\mathbb{F}(\mathcal{V}^*)$ such that $\sigma((A + BF)|\mathcal{R}^*) \subset \mathbb{C}^-$. Then, together with $\Psi_{bp} : \mathcal{V}_{bp}^* \to \mathcal{X}$ the natural embedding, the quadruple*

$$(A_a, B_a, C_a, D_a) = \left((A + BF)|\mathcal{V}_{bp}^*, \mathcal{V}_{bp}^*|B|\mathcal{N}, F|\mathcal{V}_{bp}^*, N\right), \quad x_{a0} = \eta = \Psi_{bp}^{-1}\tilde{x}_r(0) \tag{9.29}$$

characterizing $\mathrm{H}_\perp^{bp}$, define a bp-strong annihilator of Σ if $\mathbf{V}$ reads:

$$\mathbf{V}(x_{a0}) = \begin{cases} (\mathbf{B} \cap \mathbf{P} \cap \mathbf{PC}) \cup \{\mathbf{0}\}, & (\textit{if } x_{a0} = \mathbf{0}), \\ \mathbf{B} \cap \mathbf{P} \cap \mathbf{PC}, & (\textit{if } \Psi_{bp} x_{a0} \in \mathcal{R}^* \setminus \{\mathbf{0}\}), \\ \mathbf{B} \cap \mathbf{PC}, & (\textit{otherwise}). \end{cases} \tag{9.30}$$

Proof. See Appendix C.9. □

Remark 9.25 (The case $\mathbf{0} \in \mathbb{F}(\mathcal{V}_{bp}^*)$). The comment of Rem. 9.18 applies mutatis mutandis, i.e. if possible, the selection $F = \mathbf{0} \in \mathbb{F}(\mathcal{V}^*)$ simplifies $\mathrm{H}_\perp$ to the static mapping $v \mapsto Nv$. •

Remark 9.26 (The case $\mathcal{V}_{bp}^* = \{\mathbf{0}\}$). Under the conditions of Th. 9.24, if $\mathcal{V}_{bp}^*$ is trivial, then $\mathcal{N}$ reduces to $\mathrm{Ker}\,\{B\} \cap \mathrm{Ker}\,\{D\}$ and the bp-strong annihilator of Th. 9.24 degenerates into the static mapping $v \mapsto Nv$. •

Remark 9.27 (Maximal range). The bp-strong annihilator of Th. 9.24 has maximal range in the sense that for all $(\tilde{u}_r, \tilde{x}_r) \in (\mathbf{B} \cap \mathbf{P}) \cup \{\mathbf{0}\}$ satisfying $(\tilde{u}_r, \tilde{x}_r, \mathbf{0}) \in \mathbf{Q}(\tilde{x}_r(0))$, there exist $\eta = x_{a0}$ and $v \in \mathbf{V}(x_{a0}) \subset \mathbf{PC} \cap \mathbf{B}$ satisfying $\mathrm{H}_\perp^{bp}[x_{a0}; v] = \tilde{u}_r$ and $\tilde{x}_r(0) = \Psi_{bp}(\eta)$. See Appendix C.9 for the proof of this statement. •

Remark 9.28 (bp-strong annihilator ⇒ strong annihilator). By definition, any bp-strong annihilator of Σ is also a strong annihilator of Σ. In general, the converse relationship does not hold, though, i.e. given a strong annihilator of Σ, setting $\Psi_{bp} = \Psi$ and $\mathrm{H}_\perp^{bp} = \mathrm{H}_\perp$ does not lead to a bp-strong annihilator of Σ, irrespective of the definition of $\mathbf{V}$. The origin of this fact is that $\dim \mathcal{V}^* > 0$ does not imply that $\mathcal{V}_{bp}^*$ is nontrivial. •

9.6 Miscellaneous

9.6.1 Comparison with existing definitions of IR and WIR

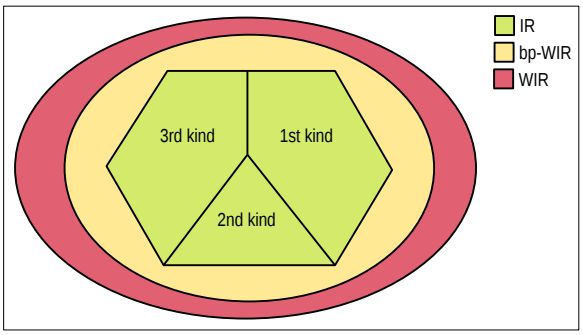

(a) Proposed taxonomy.

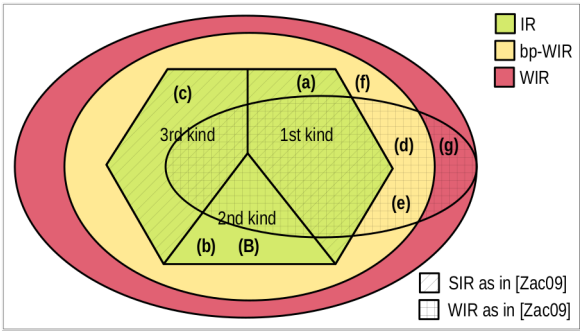

(b) Taxonomy of [Zac09].

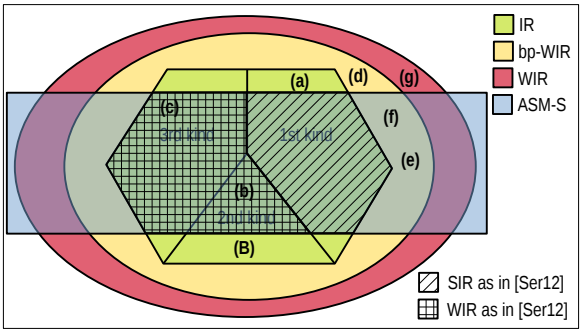

(c) Taxonomy of [Ser12].

Figure 9.6: Comparison of the proposed taxonomy with the ones of [Zac09] and [Ser12].

Table 9.1: Examples of Fig. 9.6. Ex. **(f)** corresponds to Ex. 9.11. Ex. **(B)** is the parallel interconnection of bucks, see Chap. 10.

Ex.	$\left[\begin{array}{c\|c} A & B \\ \hline C & D \end{array}\right]$	$G(s)$	$\mathrm{Ker}\left\{\left[\begin{smallmatrix} B \\ D \end{smallmatrix}\right]\right\}$	$\mathcal{R}^*$	$\mathcal{V}^*_{bp}$	$\mathcal{V}^*$	Taxonomy		
							Proposed	[Zac09]	[Ser12]
(a)	$\left[\begin{array}{c\|cc} 0 & 1 & 1 \\ \hline 1 & 0 & 0 \\ 1 & 0 & 0 \end{array}\right]$	$\frac{1}{s}\begin{bmatrix} 1 & 1 \\ 1 & 1 \end{bmatrix}$	$\mathrm{span}\left\{\begin{bmatrix} 1 \\ -1 \end{bmatrix}\right\}$	$\{\mathbf{0}\}$			IR 1st kind	SIR not WIR	inapplicable (not right. inv.)
(b)	$\left[\begin{array}{cc\|cc} 0 & 0 & 1 & 0 \\ 0 & -1 & 0 & 1 \\ \hline 1 & 1 & 0 & 0 \end{array}\right]$	$\begin{bmatrix} \frac{1}{s} & \frac{1}{s+1} \end{bmatrix}$	$\{\mathbf{0}\}$	$\mathrm{span}\left\{\begin{bmatrix} 1 \\ -1 \end{bmatrix}\right\}$			IR 2nd kind	–	WIR not SIR
(c)	$\left[\begin{array}{cc\|ccc} 0 & 0 & 1 & 0 & 0 \\ 0 & -1 & 0 & 1 & 1 \\ \hline 1 & 1 & 0 & 0 & 0 \end{array}\right]$	$\begin{bmatrix} \frac{1}{s} & \frac{1}{s+1} & \frac{1}{s+1} \end{bmatrix}$	$\mathrm{span}\left\{\begin{bmatrix} 0 \\ 1 \\ -1 \end{bmatrix}\right\}$	$\mathrm{span}\left\{\begin{bmatrix} 1 \\ -1 \end{bmatrix}\right\}$			IR 3rd kind	SIR not WIR	WIR not SIR
(d)	$\left[\begin{array}{c\|c} -1 & 1 \\ \hline -1 & 1 \end{array}\right]$	$\frac{s}{s+1}$	$\{\mathbf{0}\}$	$\{\mathbf{0}\}$	$\mathbb{R}$		bp-WIR	WIR	inapplicable ($D \neq \mathbf{0}$)
(e)	$\left[\begin{array}{cc\|c} -1 & 1 & 0 \\ 0 & -1 & 1 \\ \hline -1 & 1 & 0 \end{array}\right]$	$\frac{s}{(s+1)^2}$	$\{\mathbf{0}\}$	$\{\mathbf{0}\}$	$\mathrm{span}\left\{\begin{bmatrix} 1 \\ 1 \end{bmatrix}\right\}$		bp-WIR	WIR	–
(f)	$\left[\begin{array}{ccc\|c} -2 & -1 & 1 & 0 \\ 1 & 0 & 0 & 0 \\ 0 & 0 & -1 & 1 \\ \hline -2 & 0 & 1 & 0 \end{array}\right]$	$\frac{s^2+1}{(s+1)^3}$	$\{\mathbf{0}\}$	$\{\mathbf{0}\}$	$\mathrm{span}\left\{\begin{bmatrix} 1 & 0 \\ 0 & 1 \\ 2 & 0 \end{bmatrix}\right\}$		bp-WIR	–	–
(g)	$\left[\begin{array}{ccc\|c} 0 & 1 & 0 & 0 \\ 0 & -1 & 1 & 0 \\ 0 & 0 & -1 & 1 \\ \hline 0 & -1 & 1 & 0 \end{array}\right]$	$\frac{s}{(s+1)^2}$	$\{\mathbf{0}\}$	$\{\mathbf{0}\}$	$\mathrm{span}\left\{\begin{bmatrix} 1 \\ 0 \\ 0 \end{bmatrix}\right\}$	$\mathrm{span}\left\{\begin{bmatrix} 1 & 0 \\ 0 & 1 \\ 0 & 1 \end{bmatrix}\right\}$	WIR	WIR	inapplicable (not observ.)
(B)	See Chap. 10						IR 2nd kind	WIR	inapplicable (not observ.)

In the last two decades, several definitions, characterizations, and taxonomies of IR have been proposed in the literature in the unconstrained context. Let us quote two important studies in this respect:

- [Zac09]: "System Σ is said *strongly IR* (SIR) if $\rho > 0$ and *weakly IR* (WIR) if $G^\star := \lim_{s\to 0} G(s)$ is finite and satisfies Ker $\{G^\star\} \neq \{\mathbf{0}\}$."
- [Ser12]: "Under the following assumption:

  ASM-S: Σ is minimal, strictly proper, and right-invertible.

  strong IR (SIR) means $m >$ rank $\{B\} = p$ whereas *weak IR* (WIR) means $m \geq$ rank $\{B\} > p$."

These concepts are now related to our definitions via the Venn diagrams of Fig. 9.6. Hereafter, without further details, IR (of the k-th kind), bp-WIR, and WIR refer to the definitions proposed in this chapter and in the previous one.

Letters on Fig. 9.6 identify examples offered in Tab. 9.1 and serve as counter-examples of hypothetical inclusions. Comments on Fig. 9.6b are as follows:

- SIR as in [Zac09] is equivalent to IR of the 1st kind or IR of the 3rd kind;
- SIR as in [Zac09] does not imply WIR as in [Zac09], see examples **(a)** and **(c)**;
- WIR as in [Zac09] implies WIR, see Appendix C.10, but not bp-WIR, see example **(g)**;
- bp-WIR does not imply WIR as in [Zac09], see example **(f)**;
- IR of the 2nd kind implies neither SIR as in [Zac09] nor WIR as in [Zac09], see example **(b)**.

Fig. 9.6c illustrates that:

- If ASM-S is valid, then SIR as in [Ser12] (respectively WIR as in [Ser12]) is equivalent to IR of the 1st kind (resp. IR of the 2nd kind or 3rd kind);
- If ASM-S is not valid, those concepts are not equivalent any more, see examples **(a)** and **(B)**;
- SIR as in [Ser12] does not imply WIR as in [Ser12];
- bp-WIR and, a fortiori, WIR imply neither SIR as in [Ser12] nor WIR as in [Ser12], see examples **(d)**, **(e)**, **(f)** and **(g)**.

9.6.2 On IR and left-invertibility

Recall that Σ is left-invertible (LI) if the implication

$$(y_1 = y_2) \Rightarrow (u_1 = u_2) \tag{9.31}$$

holds for all $x_0 \in \mathcal{X}$ and for all $(u_1, y_1), (u_2, y_2) \in \mathbf{W}(x_0)$. By definition, system Σ is IR iff it is *not* LI.

Similarly, both bp-WIR and WIR concepts can be related to some variations around the notion of LI. The first one is *strong left invertibility* (SLI): Σ is SLI if (9.31) is valid for all $x_{0,1}, x_{0,2} \in \mathcal{X}$ and for all $(u_1, y_1) \in \mathbf{W}(x_{0,1}), (u_2, y_2) \in \mathbf{W}(x_{0,2})$. By definition, it holds:

$$\text{WIR} \Leftrightarrow \neg\text{SLI} \tag{9.32}$$

To go further, let us introduce yet another notion of left invertibility. Σ is said *asymptotically strongly left invertibility* (as-LI) if the implication

$$(y_1 = y_2) \Rightarrow (u_1(t) \to u_2(t))$$

holds for all $x_{0,1}, x_{0,2} \in \mathcal{X}$ and for all $(u_1, y_1) \in \mathbf{W}(x_{0,1}), (u_2, y_2) \in \mathbf{W}(x_{0,2})$. This definition is related to bp-WIR as follows:

$$\text{bp-WIR} \Rightarrow \neg\text{as-LI}.$$

However, $\neg$as-LI does not imply bp-WIR because $u_1 - u_2$ can grow unbounded.

The next table summarizes this discussion and can be obtained by inspection:

$$\begin{array}{ccccc} \text{IR} & \Rightarrow & \text{bp-WIR} & \Rightarrow & \text{WIR} \\ \text{LI} & \Leftarrow & \neg\text{bp-WIR} & \Leftarrow & \text{SLI} \\ & \nwArr & \Uparrow & \swArr & \\ & & \text{as-LI} & & \end{array}$$

The first line is illustrated in Fig. 9.6. The second line is the contraposition of the first one. Note that Σ is not bp-WIR if the implication

$$(y_1 = y_2) \Rightarrow (u_1(t) - u_2(t)) \to \{0, \pm\infty\}$$

holds for all $x_{0,1}, x_{0,2} \in \mathcal{X}$ and for all $(u_1, y_1) \in \mathbf{W}(x_{0,1}), (u_2, y_2) \in \mathbf{W}(x_{0,2})$.

9.7 Conclusions

As a summary of this chapter, let us recall its essential messages:

- A basis of the set $\mathcal{F}$ of solutions of the regulator equations can be constructed from the system matrix $P_\Sigma(s)$, see Cor. 9.5. This allows to predict $\dim \mathcal{F}$ on the basis of the invertibility properties of Σ and its zero structure, see Cor. 9.6. This also leads to sufficient conditions for online selection of elements of $\mathcal{F}$, see Th. 9.9.
- The regulator equations parametrize the subset of the reference trajectories that are linear wrt w. For this reason, there exists output regulation problem for which the regulator equations admit a unique solution, even if distinct reference trajectories exist, see Ex. 9.11.
- There exists distinct reference trajectories (resp. bounded and asymptotically distinct reference trajectories) for the regulation problem iff there exists a strong annihilator (resp. a bp-strong annihilator). Thus, a suitable annihilator for the copy of Σ_w embedded in the reference trajectory generator R is a bp-strong annihilator. As a strong annihilator, it delivers not only $\tilde{u}$ but also $\tilde{x}_0$ such that the corresponding output is zero. It also has a specific feature, in that $(\tilde{u}, \tilde{x})$ is bp.
- A strong annihilator (resp. a bp-strong annihilator) with maximal range can be explicitly constructed, see Th. 9.17 and Th. 9.24. Its state space is $\mathcal{V}^*$ (resp. $\mathcal{V}^*_{bp}$). In general, the (simple) annihilator of Th. 8.8 leads neither to a strong annihilator with maximal range nor to a bp-strong annihilator with maximal range, regardless of the selection of Ψ.
- For the output regulation problem, throughout exploitation of the existing degrees-

of-freedom requires to equip the stabilizer S and the reference trajectory generator R with a (simple) annihilator and a bp-strong annihilator, respectively.

- There exists a strong annihilator (resp. a bp-strong annihilator) iff (i) Σ is WIR (resp. bp-WIR) or (ii) $\langle \mathcal{K}|A\rangle$ is nontrivial (resp. $\mathcal{X}_{bp} \cap \langle \mathcal{K}|A\rangle$ is non-trivial), see Th. 9.15 and Th. 9.22.
- It holds IR$\Rightarrow$bp-WIR$\Rightarrow$WIR$\Leftrightarrow \neg$SLI. In general, the converse implications are false.
- Σ is WIR (resp. bp-WIR) iff $\mathrm{Ker}\left\{\left[\begin{smallmatrix} B \\ D \end{smallmatrix}\right]\right\}$ or $\mathcal{R}^*$ or $\mathcal{V}^*/(\mathcal{R}^* + \langle \mathcal{K}|A\rangle)$ is nontrivial (resp. $\mathrm{Ker}\left\{\left[\begin{smallmatrix} B \\ D \end{smallmatrix}\right]\right\}$ or $\mathcal{R}^*$ or $\mathcal{V}^*_{bp}/(\mathcal{R}^* + \langle \mathcal{K}|A\rangle \cap \mathcal{V}^*_{bp})$ is non-trivial), see Prop. 9.16 and Prop. 9.23.

9.8 Bibliographical notes

Existing works

Output regulation

Classical references to the output regulation problem include [Dav72; FW75a; Fra77; DW80; IB90]. The vast majority of studies devoted to this problem neglect the non-uniqueness of reference trajectories. Notable exceptions have now been listed. As shown in this chapter, the reference trajectories can be constructed in two different ways: compare [Ser12, Fig.2] and [Gal+15, Fig.1] (and the associate definitions) to appreciate the distinctions between the following two lines of research.

1. The *classical paradigm* amounts to selecting a solution (Γ, Π) of the regulator equations (9.7), and then setting (u_r, x_r) to $(\Gamma w, \Pi w)$, as in Sec. 9.2.

2. Starting from any particular trajectories $(u_r^p, x_r^p) \in \mathbf{R}(w)$, the *incremental perspective* consists of adding any $(\tilde{u}_r, \tilde{x}_r) \in \mathbf{R}(0)$ to (u_r^p, x_r^p), as in Sec. 9.4.

The classical paradigm In [Joh04; JS05], the authors design a continuous-time optimum-seeking control unit. In [Sig+06], this idea is immersed in the classical output regulation framework discussed in this chapter, where the exosystem model is not restricted to pure integrators as in [JS05]. The system considered in [Sig+06] is a hypersonic vehicle with more inputs than the regulated outputs. As in Th. 9.9, the reference trajectory generator exploits redundancy by selecting the optimal solution in the regulator equations (9.7). See also [SS06a] for a direct exposition of this result in a more general context. This line of research, culminating in [Gal+15], is pursued in [Gal+11]. Note that in [Sig+09], these results are extended to the LPV case. However, regulator equations in this context are generally untractable. For this reason, a "frozen" LPV regulator problem is considered to derive approximate solutions corresponding to the true LPV setup. As is customary, the stabilizing controller is decomposed into an LPV state feedback and an LPV reduced-order observer.

On the set of solutions of the regulator equations The regulator equations (9.7) can be found in [Fra77, (27)]. A standard reference for matrix equations is [Gan00; Gan09], see also [TSH12, Sec.9.3] for a concise introduction and [Ant05a]. The tractable condition for the existence of solutions of the regulator equations was first offered in [Hau83a], and is now reported as a

classical result in textbooks such as [Sab+00, Corollary 2.5.2] and [TSH12, Th.9.9] for an algebraic statement and [BM92, Chap.5-6] for the geometric treatment of this problem. Uniqueness is also implicitly characterized in [Hau83a], see also [Sab+00, Lemma 2.5.1] stating that "The regulator equations has at most one solution iff Σ is left-invertible and $\sigma(S) \cap \mathcal{Z} = \{\varnothing\}$ holds." Only recently, deeper investigations on the case where many solutions exist have been conducted, under the assumption that $m > p$ holds and that the non-resonance condition is valid. In this context, the characterization of the set of all solutions is obtained. Following the terminology of [Ant05b, Chap.6], the Kronecker product method (relying on vectorization of unknown matrices) was implemented in [Sig+06]. The dimension of the space of the solution is also given in [Sig+06, (31)]. Quite implicitly, a more informative parametrization of the set of solutions is obtained in [Gal+15, Proof of Prop.2] via the invariant subspace method, under the additional assumption that $\rho = 0$ holds.

The existence of solution of the regulator equations is also investigated in the context where input constraints affect an over-actuated system. The mapping $w \mapsto (x_r, u_r)(w)$ is considered piecewise linear in [GV13], where the focus is on a purely integrator exosystem, and polynomial in [VG13], when sum-of-square techniques are utilized to derive a tractable tool to construct the trajectories. The problem of the existence of a solution is interpreted as the maximization of the set of exogenous signals for which regulation can be achieved.

The incremental perspective The second line of research, first proposed in [Ser12], dismisses the regulator equations and considers the direct synthesis of the reference trajectories $(u_r, x_r) \in \mathbf{R}(w)$. In this paper, a trajectory generator called the "extended reference model" or "extended servomechanism" is introduced. This subsystem is driven by (w, v). As in Sec. 9.4, v is used to shape (u_r, x_r). In this framework, the implementation of an MPC strategy to accommodate the input and state constraints was proposed in [Zho+13; ZCS15; ZCS16; ZCS17]. To this end, a discrete-time formulation of the setup in [Ser12] is adopted. Starting from the case of turbocharged internal combustion engines for automotive [Zho+13], this analysis is getting deeper in [ZCS15], [ZCS16] and [ZCS17]. In the last paper, a distinction is introduced between non-intrusive actions, when the reference trajectories are compatible with the output to be tracked, and intrusive actions, where the requirement of perfect output tracking is relaxed. Obviously, the controller is parameterized to promote the former over the latter. To achieve this purpose, the range of the subsystem producing the reference trajectories (u_r, x_r) is enlarged: [ZCS16, (5) and Prop.1] can be recovered from [ZCS17, (6), (8)] by setting $\xi_2(0) = \mathbf{0}$ and $v_2 = \mathbf{0}$, thus excluding intrusive actions.

Note that the robust counterpart of the regulation problem is tackled in [CSZ16; CSZ18]. The plant is affected by uncertainties, and the regulated error is the only measured quantity. Structural stability is ensured. Asymptotic optimality is also achieved in the case where $w = \mathbf{0}$ holds.

Annihilator for the output regulation problem In [CSZ18, p.216], an annihilator is extracted from the "extended reference model" defined in [Ser12]. Note that this annihilator is distinct in nature not only from the original definition of an annihilator offered in [CG14] but also from the one offered in this chapter. Indeed, the annihilator in [CG14] is related to a (simple) annihilator (see Chap. 8), whereas that of [CSZ18] ressembles to a strong annihilator because its initial state can be adjusted, see below for a detailed comparison.

Exploitation of system zeros The role played by the zeros in the output regulation problem, and its robust counterpart, has already been investigated in [DW74; DW77; FW75b]. Once

again, those results are on the existence of solution. The uniqueness is beyond the scope of these studies. Recently, the importance of zeros for non-uniqueness has been acknowledged. As shown in the bibliographical notes in Chap. 8, the literature on IR navigates between (i) zero-based definitions, as e.g. in [Zac09], and (ii) zero-free definitions, as e.g. in [DO19; Ser12]. See also [GP14, Def.2] and [GS18, Def.1] for pioneering works on the exploitation of system zeros to select the optimal steady state.

Left-inversion

The concept of left-inversion is standard in control theory, see e.g. [Wol74, Sec.5.5] and [TSH12, Chap.8]. The term strong left-invertibility (SLI) is borrowed from [LE23], where it is coined in accordance with the terminology "strong detectability" introduced in [Hau83b]. See also [LE23, below Def.6] for other synonyms of SLI existing in the literature such as "time-domain left-invertibility" used in [EGM04; Bon+07]. A characterization of SLI in geometric terms is offered in [Bon+07, Th.10], but only for strictly proper systems.

Never seen elsewhere in this term ($\approx$ new)

Output regulation

Comprehensive treatment in the classical paradigm The material of Sec. 9.2 is unpublished, namely the exhaustive parametrization of the set $\mathcal{F}$ of the solutions of the regulator equations, its dimension, and the sufficient conditions for online selection of (Γ, Π). These results extend those of [Sig+06; Gal+15] in the following directions:

- Under the only assumption of semi-simplicity of the exogenous matrix S and stabilizability of (A, B), any proper system can be handled, i.e ρ might be strictly positive and the non resonance assumption ASM 9.3 is not required. This gives rise to new solutions that emerge whenever some eigenvalues of S are invariant zeros of Σ.

- A basis of $\mathcal{F}$ is explicitly constructed by making use of the system matrix P_Σ, see Cor. 9.5.[10] This pivotal tool in linear system analysis allows for insightful connexion with systemic properties, like left or right invertibility and the invariant zero structure, see Cor. 9.6.[11] Compared to the Kronecker product method of [Sig+06] which typically involves large sparse matrices, this feature is also computationally attractive. In addition, no change of basis is required, unlike the parametrization offered in [Gal+15].

- Sufficient conditions allow for online selection of (Π, Γ), see Th. 9.9. Whenever it is possible, conditions of [Gal+15, Th.1] have been weaken (i) by considering (9.13a) in place of (9.13b) and (ii) by enlarging the set of initial conditions leading to exact solving of the output regulation problem from $\{\Pi(\theta(0))w(0)\}$ to $\Pi(\theta(0))w(0) + \mathcal{V}_g^*$.[12]

[10] Following the terminology of [Ant05b, Chap.6], this achievement is obtained by implementing a mixture of the invariant subspace and eigenvalue methods.

[11] Note that the equality $\dim \mathcal{F} = (m-p)q$ in [Gal+15, Prop.1] is recovered from Cor. 9.6 as a special case, see Rem. 9.7.

[12] Adopting the non-hybrid context of this chapter, [Gal+15, Th.1] can be rephrased as follows: Let F make $A + BF$ Hurwitz. Let $\mathcal{G} = \mathcal{J}$. (a′) If (9.13b) holds, then (9.12) solves Problem 9.1; (b′) If $F \in \mathbb{F}(\mathcal{R}^*)$, then (9.12) solves Problem 9.1; (c′) If (9.13b) and $x(0) = \Pi(\theta(0))w(0)$ hold, then (9.12) solves Problem 9.1 exactly. (d′) If $F \in \mathbb{F}(\mathcal{R}^*)$ and $x(0) = \Pi(\theta(0))w(0)$ holds, then (9.12) solves Problem 9.1 exactly. These conditions are now compared with those of Th. 9.9, bearing in mind that the non-resonance condition is assumed in [Gal+15] so that Rem. 9.10 applies. From (a′) to (a), the condition (9.13b) of (a′) is relaxed to (9.13a). Conditions (b) and (c) are equal to (b′) and (c′), respectively. From (d′) to (d), the condition $x(0) = \Pi(\theta(0))w(0)$ of (d′) has been relaxed

The shortfall of the classical paradigm The discussion in Sec. 9.3 and that related to the affine structure of $\mathbf{R}(w)$ are unpublished. Note that the existing literature navigates (sometimes in the same paper) between the *nonequivalent* two perspectives, where either (i) $\mathbf{R}(w)$ or simply (ii) its linear subset $\mathbf{R}(w) \cap \mathbf{L}(w)$ is considered. Using chronological ordering, perspective (i) is retained in e.g. [Ser12, Def.3.1 and Prop.4.1], [ZCS15, (5) and Def.1], [ZCS16, (5) and Def.1], [ZCS17, (6) and (8)], and [CSZ18, (5) and Def.1]; whereas perspective (ii) is used in e.g. [Ser12, Sec.5.A], [Gal+15, (6)], [ZCS15, ASM2], [ZCS16, ASM2], and [ZCS17, Sec.V.A]. We believe that this might be a source of confusion, and sometimes even fallacies.[13]

Strong annihilator and the output regulation problem The entire Sec. 9.4 is unpublished. Recall that it includes (i) the definition of a strong annihilator, (ii) the conditions of its existence, (iii) the relationship of this concept with the output regulation problem and the associated control schemes, (iv) the construction of this annihilator, and (v) the proof that it has maximal range. Among the existing concepts available in the literature, the annihilator (An) in [CSZ18, p.216] is the closest to the strong annihilator (SAn) proposed in this chapter. The differences between (An) and (SAn), and their respective properties, are now outlined:

(i) Definitions: First, linearity and strict properness of $\mathrm{H}_\perp$ is assumed in the definition of (An), unlike in (SAn). Second, the output of (An) is $(\tilde{u}_r, \tilde{x}_r)$, whereas (SAn) produces $\tilde{u}_r$ and $\tilde{x}_r(0)$. Clearly, $\tilde{x}_r = \mathrm{H}[\tilde{x}_r(0); \tilde{u}]$ can be reconstructed from $\tilde{u}_r$ and $\tilde{x}_r(0)$, so the two formulations are equivalent. The formulation retained in (SAn) is preferred for two reasons. First, it is closer to the definition of WIR: Just like the (simple) annihilator is obtained by following the definition of IR and decomposing the input of Σ as $u^p + \tilde{u}$, the definition of (SAn) can be viewed as the result of decomposing not only the input of Σ_w as $u^p + \tilde{u}$ (written $u_{\mathrm{reg}} + u_{\mathrm{rd}}$ in [CSZ18, (7)]) but also its initial state as $x_0^p + \tilde{x}_0$. Second, it mimics the interconnection of the (simple) annihilator introduced in Chap. 8: A cascade is used to interconnect (SAn) with Σ_w, just like the (simple) annihilator feeds Σ (compare Fig. 9.4d and Fig. 8.1).

(ii) Existence: The existence of (An) is implicitly characterized by the set of assumptions made in [CSZ18]. Among them, right-invertibility and $m > p$ shall be thought of as the key hypotheses, see Cor. 8.7 proving that this context corresponds to IR. Several equivalent characterizations of the existence of (SAn) are explicitly offered in Th. 9.15. In view of item (iv) of this theorem, (SAn) enlarges the scope of (An) from IR to WIR or unobservable systems.

(iii) Relationship with the output regulation problem: (SAn) is specifically designed for this control problem, with the aims of capturing all the degrees-of-freedom offered by the redundancy, see Th. 9.15. If (An) is designed in the context of output regulation, its features are related to IR (not WIR), as shown in Chap. 8.

---

to $x(0) \in \Pi(\theta(0))w(0) + \mathcal{V}_g^*$ at the price of substituting $F \in \mathbb{F}(\mathcal{R}^*)$ by the stronger condition $F \in \mathbb{F}(\mathcal{V}_g^*)$. Note, however, that if $\mathbb{F}(\mathcal{R}^*) \not\subset \mathbb{F}(\mathcal{V}_g^*)$ holds in general, it is always possible to select $F \in \mathbb{F}(\mathcal{V}_g^*)$ such that $A + BF$ is Hurwitz, i.e. from (d′) to (d), the set of acceptable F is reduced but the scope of the theorem remains unaffected.

Finally, note that [Gal+15] allows for a discontinuous signal $\theta(\cdot)$, whereas the current version of Th. 9.9 does not. We expect low technical difficulties in extending Th. 9.9 in this direction.

[13] In [GS18], it is said "whenever $m = p$, and provided that Assumption 2 [stabilizability, detectability, and non-resonnance assumption] is verified, the correct steady-state input achieving output regulation is uniquely determined, as entailed also by the existence of a unique solution Π, Γ to the well-known Francis Equations". By exhibiting a minimal system for which the non-resonance assumption is valid, Ex. 9.11 is a counter-example of this statement because multiple suitable reference trajectories exist, even if the regulator equations admit a unique solution.

(iv) Construction: The state-space of (SAn) is $\mathcal{V}^*$, see Th. 9.17, whereas that of (An) is $\mathcal{R}^*$.

(v) Maximality: By considering $\mathcal{V}^*$ instead of $\mathcal{R}^*$, maximal range of (SAn) can be proved, see Rem. 9.20.[14]

Extended reference model Following the terminology introduced in [Ser12, Def.3], note that the subsystem Σ_r depicted in Fig. 9.5 (together with a copy of the exogenous system E) is an extended reference model. In view of the above items (i) and (iv), it differs from that of [Ser12] for two reasons. First, Σ_r is driven by not only $v(\cdot)$ but also η, which is instrumental in setting (or resetting) the initial state of Σ_r. Second, observe that using in (9.23) the definition of the quadruple (A_a, B_a, C_a, D_a) *of the (simple) annihilator* (as in Th. 8.8 and not as in Th. 9.17), one arrives at the extended reference model of [Ser12, Def.3 and Prop.4].

bp-strong annihilator and the output regulation problem The whole Sec. 9.5 is unpublished. Recall that it replicates Sec. 9.4 in the bp context, namely it includes (i) the definition of bp-strong annihilator, (ii) the condition of its existence, see Th. 9.22, (iii) the relationship of this concept with the output regulation problem and the associated control scheme, see Th. 9.22, (iv) the construction of this annihilator, see Th. 9.24, and (v) the proof that it has maximal range, see Rem. 9.27.

Left-inversion, definitions of IR and WIR and associated taxonomy

The zero structure Together with Chap. 8, this chapter clarifies that the zero structure is related to WIR (and $\mathcal{V}^*/\mathcal{R}^*$), but not to IR (and $\mathcal{R}^*$), see Th. 8.2, Prop. 9.16 and the bibliographical note at the end of Chap. 8 showing that this point is ambiguous in the existing literature.

IR, WIR, bp-WIR and annihilators The unpublished material of Sec. 9.6.2 summarizes the relationship of the existing concepts around the notion of left-invertibility with those related to IR. This clarifies that the definitions and characterizations of WIR (see Prop. 9.16), and bp-WIR (see Prop. 9.23) can serve as characterizations for ¬WIR=SLI and ¬bp-WIR. In particular, ¬(ii) and ¬(iii) of Prop. 9.16 are geometric characterizations of SLI that are distinct (yet equivalent, but hopefully more insightful) than those available in [Bon+07, Th.10] and whose scope is restricted to strictly proper systems. Note also that the algebraic condition ¬(iv) coincides with [LE23, Th.12], even if completely different paths are used to obtain this result.

Comparative framework Along with the end of Chap. 8, this chapter offers a framework allowing an in-depth comparison between the two most important definitions of IR existing in the literature, see Sec.9.6.1 where pieces of [**KT21**] have been collected and enriched with unpublished materials like Fig. 9.6 and Tab. 9.1. Compared with [Zac09], the proposed taxonomy introduced in [**KT21**] refines the study by distinguishing: (i) IR of the 1st kind from IR of the 3rd kind, which are different in nature, (ii) IR of the 2nd kind from WIR, which are distinct concepts, and (iii) bp-WIR from WIR, the former already capturing all relevant cases

[14] In [CSZ18, p.216], one reads "Roughly speaking, an annihilator is a dynamical system whose outputs parametrize all the possible inputs and state trajectories that are invisible from the output e." This suggests that (An) has maximal range. This is incorrect even under the assumption of the [CSZ18], that are right-invertibility and strict properness. Indeed, in this context (An) exists iff $m > p$ holds. Ex. 9.11 exhibits a right-invertible, strictly proper system and square system for which distinct reference trajectories exist, even if (An) is the zero system in this case. This is in contrast to (SAn), which can be constructed in this case via Th. 9.17, and that can produce $(\tilde{u}_r, \tilde{x}_r(0)) \neq \mathbf{0}$ like $(u_{r2}, x_{r2}(0)) - (u_{r1}, x_{r1}(0))$ defined in Ex. 9.11.

from the control point of view. Besides, the scope of [Zac09] is enlarged: (i) By removing the requirement that $G^\star$ is finite and (ii) by considering non-constant bp steady-state, i.e. the entire imaginary axis is taken into account to characterize bp-WIR. For a comparison between the materials of this chapter and the definitions proposed in [GP14], the reader is referred to [**KT21**].

Contributions wrt [Ser12]

Let us continue the discussion started at the end of Chap. 8 on how this chapter and the previous one contribute to strengthen and enhance the framework exposed in the pionner and seminal paper [Ser12], then completed by [CSZ18] where this setting is equipped with a new definition of annihilator. Recall that the study of IR offered in [Ser12] is immediately immersed in the output regulation problem and implicitly uses an annihilator whose state space is $\mathcal{R}^*$.

- The proposed taxonomy aims refining the study by distinguishing IR of the 2nd kind from IR of the 3rd kind, which are different in nature, see Fig. 9.6c.

- Studying IR for its own, and exploiting this feature for the output regulation problem, call for distinct treatments making use of distinct concepts. The division of the material of the two chapters is meant to establish a clear distinction between those two studies. In particular, the concept of (simple) annihilator (resp. strong annihilator) emerges as the natural control tool for exploiting IR of Σ (resp. for exploiting WIR and unobservability for Σ_w). In doing so, dealing with the input redundancy in the context of output regulation calls for equipping (i) the stabilizer with a (simple) annihilator and (ii) the reference trajectory generator with a strong annihilator. Note that the resulting modular control scheme fits into the classical framework where the reference trajectory generator deals with the steady state, whereas the duty of the stabilizer is related to the transient, see Sec. 9.1.

- From the (simple) annihilator to the strong annihilator, the state space is enlarged from $\mathcal{R}^*$ to $\mathcal{V}^*$. Besides, the strong annihilator has the unique feature of producing the increment $\tilde{x}_r(0)$ to the initial state $x_r(0)$ to be used to initialize (or reinitialize) the copy of the system Σ_w. These two features of the strong annihilator are essential to prove maximality of its range. Indeed, for this property to be achieved, it must be possible to drive the state x_r of Σ_w out of $\mathcal{R}^*$ while preserving $e(t) = \mathbf{0}$, i.e. $x_r(t)$ has to reach $\mathcal{V}^* \setminus \mathcal{R}^*$. This scenario requires that x_r be directly manipulable because acting on Σ_w via v does not offer enough control authority. As a result, as soon as the state space of the annihilator becomes $\mathcal{V}^*$, the set of decision variables to be used when optimizing (x_r, u_r) must include not only $v(\cdot)$ but also $\tilde{x}_r(0)$.[15]

- The bp-strong annihilator and the bp-WIR concept highlight that the suitable conceptual tools for the reference trajectory generator is actually in between IR and WIR. The roots of this statement can be traced back to [Zac09], where both the boundedness and

[15]Note that for the (simple) annihilator, manipulating $\tilde{x}_r(0)$ can still be useful for cancelling (or shortening) the transient regime of x_r. In [Ser12, p.4873], this point is clearly made: "the selection of the trajectory $\xi(\cdot)$, which is the available degree of freedom in (8), is accomplished by setting appropriately the initial condition $\xi(0)$ in the extended servomechanism and by controlling the evolution of $\xi(t)$ via the control $v(\cdot)$". A similar statement can be found in [ZCS17, below (6)]. Other references are more ambiguous, though. It is unclear why $\xi(0)$ is not included in the decision variable set of [Zho+13, (12)] and not mentioned in the sentence "the selection of the assignable trajectory $\xi(\cdot)$ through the input $v(\cdot)$" [ZCS15, p.4569]. Analogous comments can be made in [CSZ18, below (7) and above (9)] .

persistency of the incremental input were already sought by focusing on $G(0)$. From this point of view, the bp-strong annihilator could be conceived of as the outcome of a fruitful mixture of [Zac09] and [Ser12].

Chapter 10

Control of a modular DC/DC converter

Contents

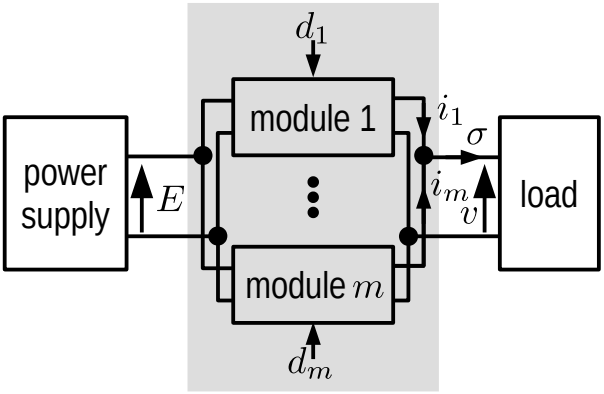

Figure 10.1: Input Parallel Output Parallel modular DC/DC converter.

This chapter deals with the output regulation of a parallel interconnection of buck DC/DC converters, for which control specifications are intrinsically ordered. This topic is relevant from the power electronics research field [TV98; Shi+99; HT07]. From the control point of view, it is not only illustrative of the material exposed in the previous chapters but also inspiring. It serves as a realization of the discussion of the introduction, enriched by the materials of the two previous chapters. In particular, an "input space decomposition perspective" to this problem is offered. This chapter goes beyond Chap. 9 by also addressing the robustness issue, paving the way for extending the materials of the previous chapters in that direction.

10.1 Parallel modular DC/DC converters

DC/DC power converters are electronic devices that aim to adapt the output voltage level of a DC power supply to the input voltage level of a load. Modular DC/DC power converters are built by combining several DC/DC power converters. The Input Parallel Output Parallel interconnection depicted in Fig. 10.1 is one of the possible assembling topologies of power modules.

10.1.1 Context and control problem statement

Why parallelling modules ? An essential feature offered by parallel interconnection of converters is the possibility to distribute the load current over the different modules, also called "current-sharing". Therefore, each module handles only a fraction of the total power delivered from the supply to the load. This technical solution has several advantages. It increases both the overall system efficiency and reliability owing to redundancy. Each of the following items contributes to the latter: (i) distribution of stresses of components, (ii) ease of maintenance and repair, and (iii) improved thermal management. In addition, the reduction of output ripple by interleaving phase of Pulse Width Modulation (PWM) is yet another benefit of this solution.

Main physical variables The output voltage is denoted by v [V], and the current flowing from the k-th power module is referred to as i_k [A]. The magnitude of the voltage source E [V] is supposed to be known and constant. The m power modules are composed of passive electrical components and one controlled leg. It is assumed that a PWM strategy is implemented for each leg so that the duty cycle $d_k \in [0, 1]$ plays the role of the control variable of the k-th leg,

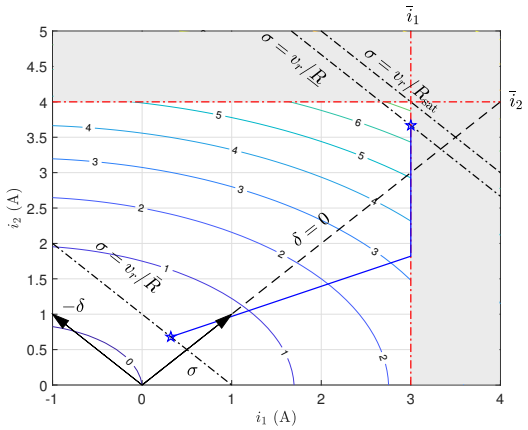

(a) Colored thin lines are level set of J. The white area is the subset where the current constraint $\mathbf{0}_2 \leq i \leq \bar{i}$ is valid.

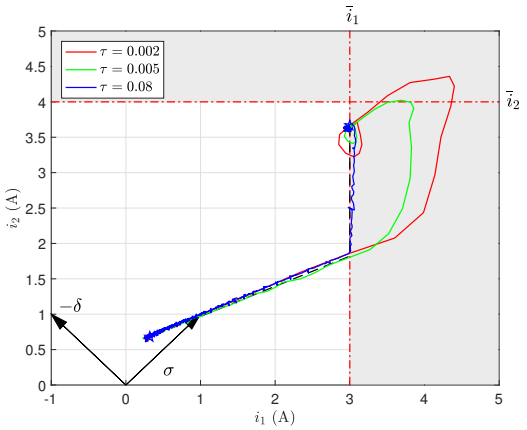

(b) Three experiments obtained by letting $R(t)$ describes its interval: The larger is τ, the slower $R(t)$ moves from $\underline{R}$ to $\overline{R}$.

Figure 10.2: Example of load-dependent optimal steady-state current locus (Fig. 10.2a) that is made stable by the controller of Th. 10.7 so that experimental closed-loop current trajectories track this locus (Fig. 10.2b) in the current plan for $m = 2$.

instead of the binary input in $\{0, 1\}$, see Chap. 6 and Fig. 10.1. Thus, the input set reads:

$$\mathcal{D} = [0, 1]^m \tag{10.1}$$

Defining the current distribution The current-sharing policy over the modules is indirectly defined via a cost function J that penalizes the undesirable steady state. Typically, J equals $\sum_k J_k$ where J_k expresses, for the k-th module, the power losses, thermal state, or stresses of the electrical components, see Fig. 10.2a for an illustration in which J models the overall power losses. The current-sharing strategy is also defined via some constraints such as the upper bound on the current i_k. These limits are captured via the set $\mathcal{I}$ to which the steady-state current must belong:

$$\mathcal{I} = [0, \bar{i}_1] \times \ldots \times [0, \bar{i}_m] \tag{10.2}$$

where $0 \leq \bar{i}_k$ holds for all $k \in [\![1, m]\!]$, see Fig. 10.2a for an illustration. Note that the introduction of $\mathcal{I}$ makes it possible to engage or disengage modules while supplying the load continuously by temporarily setting i_k to zero by adjusting $\mathcal{I}$. This discussion suggests a possible time-dependency of the optimization problem defining the steady state, either by letting J depend on the online measurement (like the thermal state of the modules) or by allowing $\mathcal{I}$ to be changed by the user during the operating phase. Finally, note that this framework encompasses balanced current sharing (uniform current distribution) as a particular case.

Unknown load In most of practical situations, the dynamical behavior of the load is not fully known. Typically, it is modeled via a capacitor connected in parallel with an electrical component having a known algebraic current-voltage relationship, for example, $v = Ri_L$ or $vi_L = c$, where i_L is the current flowing through the load, and R [Ω] and c [W] are used for purely resistive and constant power loads, respectively. Let us stress that the magnitude of the constants R or c appearing in those mathematical models are unknown.

Table 10.1: Description of parallel DC/DC converter as an over-actuated system.

Parallel DC/DC converter	Σ_i	Σ_σ	d	v	σ
Over-actuated system (see Chap. 7)	Σ_a	Σ_p	u	y	τ

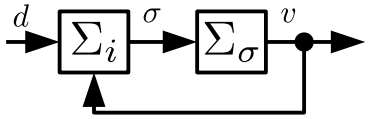

Figure 10.3: Coupling between current and voltage dynamics.

An over-actuated system point of view Following Chap. 7, the overall system mapping d to v can be decomposed into two subsystems, as shown in Fig. 10.3. Each module can be identified with a (dynamic) actuator. In this figure, Σ_i is the dynamical system associated with the set of actuators. It maps d to the total current σ corresponding to the current feeding the load, see Fig. 10.1. The load is assimilated to the plant Σ_σ mapping σ to v. Tab. 10.1 summarizes the elements of this analogy.

Control problem From the above discussion, distinct control objectives are of interest:
(CC) Current Constraints: $i \in \mathcal{I}$;
(VR) Voltage Regulation: $v = V_r$;
(OC) Optimal Current: $i \mapsto J(i)$ is minimal.
As stated below, the control engineering problem hinges on these control goals.

Problem 10.1. Design a control law computing the duty cycle d from the measurement of (i, v) and achieving asymptotic **(OC)** under the constraint of **(CC)** and **(VR)**. This control law must be independent of the unknown load parameters.

Remark 10.2 (**(CC)** during transient). For a solution of Prob. 10.1, $i(t) \in \mathcal{I}$ can be violated during the transient because **(CC)** is only achieved asymptotically. This is motivated by the fact that the upper bounds $\bar{i}_k$ translate thermal capacity of electrical components, so that overtaking those limits for a short period of time will not dramatically change the temperature of the devices and, hence, is fully acceptable. This suggests that imposing $i(t) \in \mathcal{I}$ at all times is not only useless but also conservative, in the sense that performance could be lowered by this restriction. •

Hierarchy of competing control goals In general, the control objectives are competing. Typically, satisfying **(OC)** alone leads to $i = \mathbf{0}$. This prevents **(VR)** from being achieved for standard practical cases, see e.g. Fig. 10.2a. In Prob. 10.1, this conflit is resolved by formulating the desired steady state as the solution of an optimization problem, where **(OC)** is the criterion to be optimized, and both **(CC)** and **(VR)** are the constraints. This prioritizes **(CC)** and **(VR)** over **(OC)**, so that the goals are (partially) hierarchically ordered. Accommodating this hierarchy is the real challenge for the control design.

Coupled dynamics From Fig. 10.3, the dynamics of v governed by Σ_σ is affected by σ and the dynamics of σ described by Σ_i depends on v. Therefore, even if the control goals are ordered, addressing them reintroduces a bilateral coupling, for example, regulating v to address **(VR)** can only be achieved indirectly through the control of σ, driven by duty cycle d.

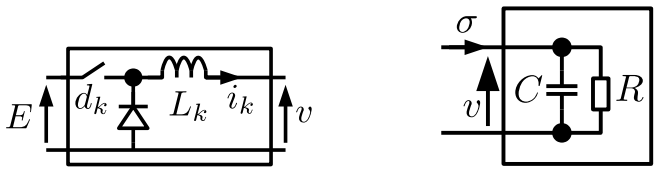

(a) k-th power module. (b) Load.

Figure 10.4: Considered electrical circuit of the load and the power modules.

10.1.2 The case of buck converters and resistive load

Considered system The load results from the parallel interconnection of capacitor C [F] with resistive load R, as depicted in Fig. 10.4b. Magnitude of R is supposed to be constant and to satisfy

$$R \in [\underline{R}, \overline{R}] \subset \mathbb{R}_{>0}.$$

The bounds of this interval are known, unlike the value of R. The power modules are buck (step-down) DC/DC converters so that the output voltage is lower than the input voltage E. Their electrical circuit is depicted in Fig. 10.4a. The inductance of the k-th leg is denoted by L_k [H]. Let us stress that the magnitudes of these inductances are not assumed to be identical.

Model It is assumed that the power modules operate in continuous conduction. Electrical components and switches are ideals, i.e. parasitic elements (resistances, losses) can be neglected. The switching frequency of the PWM is supposed to be sufficiently large for the dynamics to be approximated by an average model. In this context, the load dynamics is captured by the following equations:

$$C\frac{\mathrm{d}}{\mathrm{d}t}v = \sigma - v/R, \tag{10.3a}$$

whereas the following relationships govern the dynamics of the set of power modules:

$$\forall k \in [\![1, m]\!],\ L_k\frac{\mathrm{d}}{\mathrm{d}t}i_k = -v + E_k d_k. \tag{10.3b}$$

$$\sigma = \sum_{k=1}^{m} i_k = \mathbf{1}_m^\intercal\, i, \tag{10.3c}$$

Observe the internal feedback of v in the last equation, see Fig. 10.3.[1] Those equations can be gathered in the following state-space equation

$$\begin{bmatrix} \mathrm{diag}\,\{L\} & \mathbf{0} \\ \mathbf{0} & C \end{bmatrix} \frac{\mathrm{d}}{\mathrm{d}t}\begin{bmatrix} i \\ v \end{bmatrix} = \begin{bmatrix} \mathbf{0} & -\mathbf{1}_m \\ \mathbf{1}_m^\intercal & -1/R \end{bmatrix}\begin{bmatrix} i \\ v \end{bmatrix} + \begin{bmatrix} E\mathbf{I}_m \\ \mathbf{0}_m^\intercal \end{bmatrix} d, \tag{10.4}$$

where the state vector reads:

$$\mathbb{R}^{m+1} \ni x(t) := \begin{bmatrix} i(t) \\ v(t) \end{bmatrix}$$

The expressions of the state and input matrices $A(R)$ and B can be deduced from (10.4).

Problem statement We are now ready to formalize Prob. 10.1.

[1] As an averaged model, (10.3) refers to mean value of the signals. However, for the sake of simplicity, we do not distinguish the instantaneous value from the mean value in the notations, as in Chap. 6. Henceforth, mean value is implicit.

Problem 10.3. Given any J and any $V_r \in [0, E]$, design a (possibly dynamical) causal state-feedback control law $(i, v) \mapsto d$ such that, for all $R \in [\underline{R}, \overline{R}]$, the closed-loop system admits an asymptotically stable equilibrium (i_r, v_r) for which there exists d_r satisfying:

$$(d_r, i_r, v_r) \in \underset{(d,i,v)\in\mathcal{D}\times\mathcal{I}\times\mathbb{R}}{\arg\min} J(i) \quad \text{s.t.} \quad A(R)\begin{bmatrix} i \\ v \end{bmatrix} + Bd = \mathbf{0},\ v = V_r \tag{10.5}$$

The control law must be independent of R and $d(t)$ must identically belong to $\mathcal{D}$.

For further reference, let

$$(d_r(\cdot), i_r(\cdot), v_r(\cdot)) : [\underline{R}, \overline{R}] \to \mathbb{R}^m \times \mathbb{R}^m \times \mathbb{R} \tag{10.6}$$

be the argument of the optimization problem (10.5) parametrized by the value of the load R, i.e. the load-dependent to be stabilized by the controller. It is assumed that this profile is known via offline computation. The blue segments in Fig. 10.2a is an example of the locus of $i_r(R)$ when R describes $[\underline{R}, \overline{R}]$, so that the blue stars correspond to $i_r(\underline{R})$ and $i_r(\overline{R})$.

Remark 10.4 (About state-feedback). As shown in the sequel, Σ is not observable (and not even detectable) from the output voltage measurement. This motivates the use of state feedback in Prob. 10.1. •

10.2 Solution to Prob. 10.3 for $m = 2$

Henceforth, let us focus on the case of $m = 2$ modules. This choice is expected to enforce the didactic purpose of this chapter.[2] In this case, the model description is recalled.

$$\frac{\mathrm{d}}{\mathrm{d}t}\begin{bmatrix} i_1 \\ i_2 \\ v \end{bmatrix} = \begin{bmatrix} 0 & 0 & -1/L_1 \\ 0 & 0 & -1/L_2 \\ 1/C & 1/C & -1/(CR) \end{bmatrix}\begin{bmatrix} i_1 \\ i_2 \\ v \end{bmatrix} + \begin{bmatrix} E/L_1 & 0 \\ 0 & E/L_2 \\ 0 & 0 \end{bmatrix}\begin{bmatrix} d_1 \\ d_2 \end{bmatrix} \tag{10.7}$$

Let us also make the following assumption:

$$L_1 < L_2 \tag{10.8}$$

to emphasize the added value of this chapter wrt to the literature where $L_1 = L_2$ is almost always assumed.[3]

10.2.1 Decomposition of the input-space and the state-space

In view of (10.3a), the voltage dynamics does not depend on each current i_k individually but rather on the total current σ. In order to better exhibit this dependency, let us introduce the new state coordinates $(\delta, \sigma, v) \in \mathbb{R} \times \mathbb{R} \times \mathbb{R}$ where σ explicitly appears:

$$\begin{bmatrix} \delta \\ \sigma \\ v \end{bmatrix} = \begin{bmatrix} 1 & -1 & 0 \\ 1 & 1 & 0 \\ 0 & 0 & 1 \end{bmatrix}\begin{bmatrix} i_1 \\ i_2 \\ v \end{bmatrix} \iff \begin{bmatrix} i_1 \\ i_2 \\ v \end{bmatrix} = \frac{1}{2}\begin{bmatrix} 1 & 1 & 0 \\ -1 & 1 & 0 \\ 0 & 0 & 2 \end{bmatrix}\begin{bmatrix} \delta \\ \sigma \\ v \end{bmatrix} \tag{10.9}$$

[2] See the bibliographical notes at the end of this chapter for references on the results for arbitrary value of m.

[3] Note that the case $L_1 = L_2$ can be also be treated using the same philosophy, see the bibliographical notes for references.

The new coordinate $\delta \in \mathbb{R}$ represents the difference between the two currents. This quantity reflects the current distribution, an information that is indeed missing in $\sigma = i_1 + i_2$. Fig. 10.2 depicts the axis related to these new variables. Let us also proceed to the following change of input coordinates

$$\begin{bmatrix} \lambda \\ \mu \end{bmatrix} = \begin{bmatrix} L_\delta/L_1 & -L_\delta/L_2 \\ L_\sigma/L_1 & L_\sigma/L_2 \end{bmatrix} \begin{bmatrix} d_1 \\ d_2 \end{bmatrix} \iff \begin{bmatrix} d_1 \\ d_2 \end{bmatrix} = \frac{1}{2} \begin{bmatrix} L_1/L_\delta & L_1/L_\sigma \\ -L_2/L_\delta & L_2/L_\sigma \end{bmatrix} \begin{bmatrix} \lambda \\ \mu \end{bmatrix} \tag{10.10}$$

where

$$\frac{1}{L_\sigma} := \frac{1}{L_1} + \frac{1}{L_2}, \qquad \frac{1}{L_\delta} := \frac{1}{L_1} - \frac{1}{L_2}. \tag{10.11}$$

Physically, λ and μ are related to the difference and sum of the two duty cycles, respectively, after scaling by L_1 and L_2. For instance, if $L_2 = 2L_1$, one gets:

$$\begin{bmatrix} \lambda \\ \mu \end{bmatrix} = \begin{bmatrix} 2 & -1 \\ 2/3 & 1/3 \end{bmatrix} \begin{bmatrix} d_1 \\ d_2 \end{bmatrix}.$$

The axis related to those new input variables is represented in Fig. 10.8.

10.2.2 The feasible set of the optimisation problem

When equating $\dot{v}$ to zero, one obtains $\sigma = v/R$. Setting the derivative of i to zero imposes $d = (v/E)\mathbf{1}_2$, which belongs to $\mathcal{D}$ if $v \in [0, E]$ holds. As a result, the feasibility set of (10.5) reads:

$$\left\{ \frac{V_r}{E} \begin{bmatrix} 1 \\ 1 \end{bmatrix} \right\} \times \left\{ \frac{1}{2} \begin{bmatrix} 1 & 1 \\ -1 & 1 \end{bmatrix} \begin{bmatrix} \delta \\ \sigma \end{bmatrix} : \sigma = \frac{V_r}{R}, \delta \in \mathbb{R} \right\} \cap \mathcal{I} \times \{V_r\} \tag{10.12}$$

Assignment $v = V_r$ thus imposes σ and d but let current distribution δ free. In other words, rewriting problem (10.5) in the new coordinates leaves us with an optimization problem for which the set of decision variables reduces to $\{\delta\}$, as equality constraints assign values of σ, v and d. Referring to (10.6), this gives:

$$d_r(R) = \frac{V_r}{E} \begin{bmatrix} 1 \\ 1 \end{bmatrix}, \quad \sigma_r(R) = \frac{V_r}{R}$$

where σ_r refers to the coordinate σ of i_r. Observe that $d_r(\cdot)$ is independent of R. Fig. 10.2a allows us to visualize $\{i : i_1 + i_2 = V_r/R\}$ via the dash-dotted black line, which translates from the top right to the bottom left when R increases. The intersection of this line with the white rectangle represents the coordinates i of the feasibility set. This set is non-empty iff $R \geq R_{\text{sat}}$ where R_{sat} is related to the case in which the intersection of the dash-dotted black line with the white rectangle reduces to a unique point.

Assumption 10.5. The following inequality holds:

$$V_r/(\bar{i}_1 + \bar{i}_2) =: R_{\text{sat}} \leq \underline{R} \tag{10.13}$$

This assumption simply states that the magnitude of the total current is limited by $\bar{i}_1 + \bar{i}_2$ so that $[\underline{R}, \overline{R}]$ must be bounded from below.

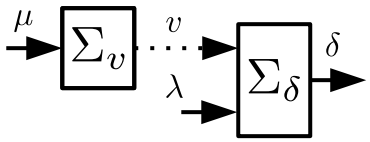

Figure 10.5: New cascaded open-loop model.

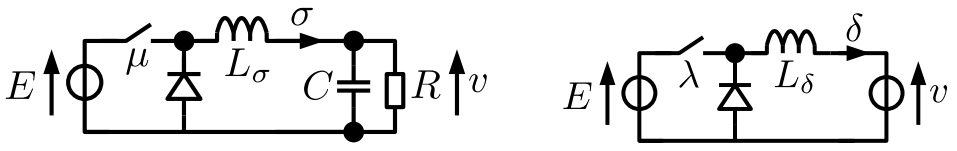

(a) Σ_v (b) Σ_δ

Figure 10.6: Circuit theory interpretation of Σ in the new coordinates.

10.2.3 Open-loop reformulation of Σ

State space in the new coordinates In this new basis, (10.7) becomes

$$\frac{\mathrm{d}}{\mathrm{d}t}\left[\begin{array}{c}\delta\\ \hline \sigma\\ v\end{array}\right] = \left[\begin{array}{c|cc}\mathbf{0} & \mathbf{0} & -1/L_\delta\\ \hline \mathbf{0} & 0 & -1/L_\sigma\\ \mathbf{0} & 1/C & -1/(RC)\end{array}\right]\left[\begin{array}{c}\delta\\ \hline \sigma\\ v\end{array}\right] + \left[\begin{array}{cc}E/L_\delta & 0\\ \hline 0 & E/L_\sigma\\ 0 & 0\end{array}\right]\left[\begin{array}{c}\lambda\\ \hline \mu\end{array}\right], \tag{10.14}$$

where the state matrices admit a block triangular structure. This allows us to interpret the system as a cascade of two dynamic blocs. The upper-subsystem Σ_v governs voltage dynamics through total current σ controlled by input μ

$$\Sigma_v : \begin{bmatrix}L_\sigma & 0\\ 0 & C\end{bmatrix}\frac{\mathrm{d}}{\mathrm{d}t}\begin{bmatrix}\sigma\\ v\end{bmatrix} = \begin{bmatrix}0 & -1\\ 1 & -1/R\end{bmatrix}\begin{bmatrix}\sigma\\ v\end{bmatrix} + \begin{bmatrix}E\\ 0\end{bmatrix}\mu, \tag{10.15}$$

and perturbs the lower-subsystem Σ_δ corresponding to dynamics of δ driven by control signal λ

$$\Sigma_\delta : L_\delta\frac{\mathrm{d}}{\mathrm{d}t}\delta = -v + E\lambda. \tag{10.16}$$

This cascaded structure originates from the independence of the dynamics of (σ, v) from δ, so that the upper subsystem impacts the lower one but there is no signal in the other way around. Fig. 10.5 illustrates this structure. Compare it with Fig. 10.3 and note that the dynamics of σ is associated with Σ_v in Fig. 10.5 and with Σ_σ in Fig. 10.3.

Circuit theory interpretation From its dynamical equation (10.15), the upper subsystem Σ_v can be physically interpreted as the averaged model of the buck converter illustrated in Fig. 10.6a. The duty cycle of this virtual device corresponds to μ and the current flowing through its coils is nothing but σ. It is connected to the same load as the original system. Its inductance and voltage input are equal to L_σ and E, respectively. Note also that L_σ is nothing but the equivalent inductor resulting from the parallel interconnection of the two coils L_1 and L_2. Hence, the inertia of this virtual buck is smaller than that of each of the two original bucks because $L_\sigma < \min\{L_1, L_2\}$ holds.

As far as Σ_δ is concerned, its dynamics can be interpreted as yet another electrical circuit, as depicted in Fig. 10.6b, where $E\lambda$ acts as a controllable voltage source that affects the current δ flowing through the coil L_δ. In this circuit, v acts as a time-varying voltage source that disturbs the current dynamics.

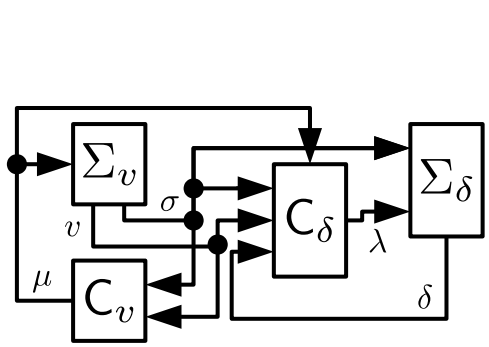

(a) Conceptual scheme.

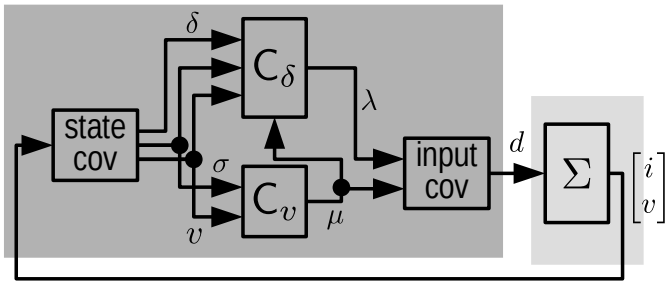

(b) Implementation scheme.
("cov" means "change of variables", see (10.9) and (10.10)).

Figure 10.7: Proposed control scheme, deriving from Fig. 10.5.

Significance of the new formulation for control purpose The previous change of variables, leading to Fig. 10.5, facilitates the control design for reasons that are now exposed. The forthcoming discussion is supported by Fig. 10.7a, which can be viewed as the natural control counterpart of Fig. 10.5.

1) From the previous subsection, it comes out that λ parameterizes the part of d that is invisible to σ and hence v, whereas μ is the remaining part by which σ can be affected. As a result, regulation of v boils down to the design of the controller

$$\mathsf{C}_v : \quad (\sigma, v) \mapsto \mu,$$

which is actually nothing but a voltage regulation problem for a single buck converter.

2) The new formulation allows for sequential modular design. Provided that all trajectories are bounded, once C_v has been defined (step 1), it suffices for

$$\mathsf{C}_\delta : \quad (\delta, \sigma, v) \mapsto \lambda,$$

to ensure zero stability (step 2), that is stability of the down stream system $\mathsf{C}_\delta \star \Sigma_\delta$ when the upper stream $\mathsf{C}_v \star \Sigma_v$ is at the equilibrium, see the next subsection.[4]

3) The ordering of the cascade complies with the hierarchy of control objectives. Indeed, **(VR)** dominates **(OC)** in the control objective hierarchy. This is consistent with the fact that $\mathsf{C}_v \star \Sigma_v$ is unaffected by $\mathsf{C}_\delta \star \Sigma_\delta$. As shown in the next subsection, this cascade and, in turn, this hierarchy can be preserved even when the input constraints come into play.

10.2.4 Problem solution

A procedure leading to subcontrollers C_v and C_δ is now offered, together with a theoretical certificate that the overall resulting controller solves Prob. 10.3, see Th. 10.7. What is highlighted is the potential offered by the design framework rather than a definite answer to each step. Therefore, what follows is expected to be sufficiently simple to fulfill the didactic purpose, yet leaving large room for improvement.

Control design without input constraints Exploiting the cascaded structure depicted in Fig. 10.7a, the proof of stability of the reference can be established using classical tools for such an interconnection. For this purpose, the stability and 0-stability of $\mathsf{C}_v \star \Sigma_v$ and $\mathsf{C}_\delta \star \Sigma_\delta$, respectively, are the key ingredients. This allows us to cope with non-linearities that are introduced by load estimation as well as input constraints.

[4]The operator $\star$ interconnects its arguments.

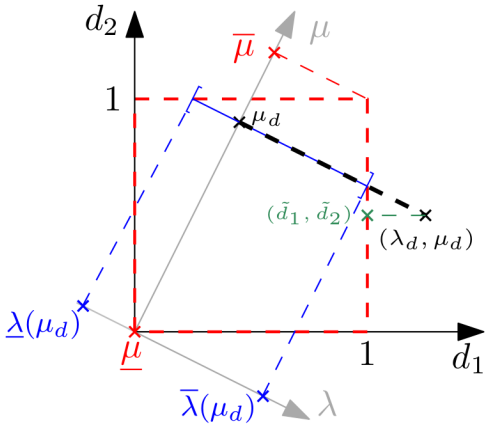

Figure 10.8: Input space $\mathbb{R}^2$ with the set $\mathcal{D}$ (delimited by the red dashed lines) and the axes of the new coordinates λ and μ (grey arrows).

- The interconnection $\mathsf{C}_v \star \Sigma_v$ can be robustly stabilized via the following state-feedback with integrator on voltage deviation:

$$\mathsf{C}_v : \quad \begin{cases} \dot{z} &= (V_r - v)/C \\ \mu &= -k_i z - k_p(V_r - v) - k_d \sigma. \end{cases} \tag{10.17}$$

- Controller C_δ has to ensure 0-stability of $\delta = \delta_r(R)$. Remarking that the equilibrium must verify $v = R\sigma$, the computation of V_r/σ can serve as a simple load estimator that asymptotically converges to R provided that $v \to V_r$. By saturating the quantity V_r/σ outside $[\underline{R}, \overline{R}]$ to prevent division by zero, we obtain the following estimator $\hat{R} : \mathbb{R} \to [\underline{R}, \overline{R}]$:

$$\hat{R}(\sigma) := \mathrm{sat}_{[\underline{R},\overline{R}]}(V_r/\sigma)$$

  The following static map is thus a simple suitable candidate for C_δ:

$$\mathsf{C}_\delta : \quad \lambda = \frac{1}{E}\left(k_\delta(\delta_r(\hat{R}(\sigma)) - \delta) + V_r\right) \tag{10.18}$$

  whenever $k_\delta > 0$.

Under the following technical assumption, this leads to a solution for Prob. 10.3.

Assumption 10.6. The map $\delta_r(\cdot)$ is Lipschitz continuous.

Theorem 10.7 ([TD19]). *Under ASM. 10.5 and ASM. 10.6, the map $(i, v) \mapsto d$ described in Fig. 10.7b and* (10.9), (10.10), (10.17), *and* (10.18), *solves Prob. 10.3 if $k_\delta > 0$ holds and (k_p, k_i, k_d) makes $\mathsf{C}_v \star \Sigma_v$ robustly stable.*

The experimental results obtained via the control law are reported in Fig. 10.2b. It can be seen that the optimal steady state is tracked when R is time-varying, all the more precisely as $\dot{R}(t)$ (related to $1/\tau$) is small.

Dealing with input constraints Fig. 10.7a depicts the conceptual scheme that guides control design. The implementation of the controller is illustrated in Fig. 10.7b. In this last subfigure,

input constraints can be modeled by saturating the output of the controller to enforce d to remain within $\mathcal{D}$. Let d_d be the desired input vector *before* this saturation, and denote by (λ_d, μ_d) its expression in the new coordinates. As on Fig. 10.8, assume that $d_d \notin \mathcal{D}$ holds because d_{d1} is larger than 1, whereas $0 \leq d_{d2} \leq 1$ holds. Thus, the effective duty cycle impacting the system is $(\bar{d}_1, \bar{d}_2) = (1, d_{d2})$, as identified by the green cross in Fig. 10.8. Clearly, both λ and μ coordinates of this last point are distinct from (λ_d, μ_d), so that not only δ but also (σ, v) are impacted. Saturations restore a bilateral coupling between the dynamics of σ and δ.

The key point is that the coordinate μ_d can be preserved. Indeed, the subset of $\mathcal{D}$ for which $\mu = \mu_d$ is non-empty. It corresponds to the continuous blue segment in Fig. 10.8. In this segment, it seems natural to select the point that serves **(OC)** at best, that is, the point of the segment closest to d_d. In contrast to the first naive choice, this second choice complies with the hierarchy of the control objectives, where **(VR)**, related to μ, is prioritized. Mere unilateral coupling is achieved.

From Fig. 10.8, the above strategy is applicable as soon as the continuous blue segment is non-empty, that is, if μ_d belongs to $[\underline{\mu}, \overline{\mu}]$. This is the motivation for imposing the following constraint on the design of C_v:

$$\mu \in [\underline{\mu}, \overline{\mu}] =: [0, 1] \tag{10.19a}$$

Then, it suffises to apply the following μ-dependent saturation to the output of C_δ:

$$\lambda \in \left[\underline{\lambda}(\mu), \overline{\lambda}(\mu)\right] =: \left[\max\left\{-\frac{L_\delta}{L_\sigma}\mu, \frac{L_\delta}{L_\sigma}\mu - 2\frac{L_\delta}{L_2}\right\}, \min\left\{2\frac{L_\delta}{L_1} - \frac{L_\delta}{L_\sigma}\mu, \frac{L_\delta}{L_\sigma}\mu\right\}\right] \tag{10.19b}$$

In order to preserve the cascade, the proposed methodology amounts to embedding the saturation directly into C_v and C_δ, after back propagation of the saturation mapping from the output of the controller through the input change of variables, see Fig. 10.7b. As for proving Th. 10.7, the stability certificate can be obtained by exploiting the cascade, provided that $\mathsf{C}_v \star \Sigma_v$ is robustly stable when the saturation of μ applies, see (10.19a).

10.3 The underling output regulation problem and its geometry

In the remainder of this chapter, our goal is to review the design framework for solving Prob. 10.3 offered in the previous section by adopting the under-determined output regulation point of view used in Chap. 9. Standard solutions for Prob. 10.3 are also exposed, in order to highlight the benefits of the proposed approach.

10.3.1 An output regulation reformulation

By adding the (fairly reasonable) requirement of the internal stability of the controller, Prob. 10.3 can be recast into an output regulation problem (i) by defining v as the output y of Σ and (ii) by letting the regulated output e be the voltage deviation with respect to V_r, which is assimilated to the exosignal w, that is,

$$y \coloneqq v, \quad w \coloneqq V_r, \quad e \coloneqq y - w$$

This leads to the following matrices that complete the definition of Σ_w, see (9.3):

$$C = \begin{bmatrix} 0 & 0 & 1 \end{bmatrix}, \quad D = \mathbf{0}, \quad P = \mathbf{0}, \quad Q = -1$$

Setting $S = 0$ implies that V_r is constant.

From the discussion above, this output regulation problem is (i) under-determined, because there exists more than one stationary steady state satisfying $e = 0$, (ii) uncertain, owing

to the unknown load R and (iii) subjected to constraints, because the current must belong to $\mathcal{I} \times \mathbb{R}$ at the steady state and the input d is confined to $\mathcal{D}$ at all times. As in Chap. 8, $\mathfrak{S}$ derives from Σ by taking $\mathcal{D}$ into account, but letting the state freely evolve in $\mathbb{R}^3$, see Rem. 10.2.

10.3.2 The geometric structure of Σ

Fundamental subspaces The geometric structure of Σ is now unveiled by computing some of its fundamental subspaces:

$$\langle A|\mathcal{B}\rangle = \mathbb{R}^3 \tag{10.20}$$

$$\text{Ker}\,\{B\} \cap \text{Ker}\,\{D\} = \{\mathbf{0}\} \tag{10.21}$$

$$\mathcal{R}^* = \mathcal{V}^*_{bp} = \mathcal{V}^* = \langle \mathcal{K}|A\rangle = \text{Ker}\left\{\begin{bmatrix}1 & 1\end{bmatrix}\right\} \oplus \{0\} \tag{10.22}$$

$$\mathcal{N} = \text{diag}\,\{L\}\,\text{Ker}\left\{\begin{bmatrix}1 & 1\end{bmatrix}\right\} \tag{10.23}$$

Thus, one concludes that:

- Σ is IR of the 2nd kind and of degree $(\rho, \nu) = (0, 1)$;
- $\mathbf{0} \in \mathbb{F}(\mathcal{V}^*)$ since $\mathcal{V}^* = \langle \mathcal{K}|A\rangle$ holds;
- ASM 9.2 is satisfied, i.e. (A, B) is stabilizable, and the semi-simple matrix S satisfies $\sigma(S) \subset \mathbb{C}^0$.

Remark 10.8. The transfer function matrix is as follows:

$$G(s) = \frac{ER}{CL_1L_2Rs^2 + L_1L_2s + (L_1 + L_2)R}\begin{bmatrix}L_2 & L_1\end{bmatrix}$$

so that $G(0) = \frac{E}{L_1+L_2}\begin{bmatrix}L_2 & L_1\end{bmatrix}$ admits a non trivial kernel. As a result, this non-minimal system is WIR in the sense of [Zac09]. •

The roots of the changes of variables Let Ψ be the first column of $(\delta, \sigma, v) \mapsto (i, v)$, see (10.9), and let N and L_μ be the columns of the matrix of $(\lambda, \mu) \mapsto d$, see (10.10):

$$\Psi := \frac{1}{2}\begin{bmatrix}1\\-1\\0\end{bmatrix}, \quad \begin{bmatrix}N & L_\mu\end{bmatrix} := \frac{1}{2}\begin{bmatrix}L_1/L_\delta & L_1/L_\sigma\\ -L_2/L_\delta & L_2/L_\sigma\end{bmatrix}. \tag{10.24}$$

A key observation is that the matrix of $(\delta, \sigma, v) \mapsto (i, v)$ is adapted to $\mathcal{R}^* = \mathcal{V}^*_{bp}$, i.e. Ψ is a basis of $\mathcal{R}^*$. This means that δ is nothing but the coordinate of x in $\mathcal{R}^*$, whereas (σ, v) are those in a complementary subspace $\mathcal{L}_v$ of $\mathcal{R}^*$ in $\mathbb{R}^3$ spanned by the last two columns of this matrix. Similarly, $\begin{bmatrix}N & L_\mu\end{bmatrix}$ is adapted to $\mathcal{N}$. Hence, λ and μ are the coordinates of d in $\mathcal{N}$ and $\text{Im}\left\{L_\mu\right\} =: \mathcal{L}_\mu$, respectively, which is a complementary subspace of $\mathcal{N}$ in $\mathbb{R}^2$. Note that $\mathcal{L}_\mu$ has been defined to satisfy

$$\begin{bmatrix}B\\D\end{bmatrix}\mathcal{L}_\mu \subset \mathcal{L}_v \oplus \{0\} \tag{10.25}$$

to separate the contribution of d to each subspace of $\mathcal{R}^* \oplus \mathcal{L}_v$.

10.3.3 Revisiting the problem solution in the known load subproblem

As a preliminary step, let us tackle the subproblem where the magnitude of the load R is known. For the time being, let us also allow the input $d(t)$ to take values outside $\mathcal{D}$.

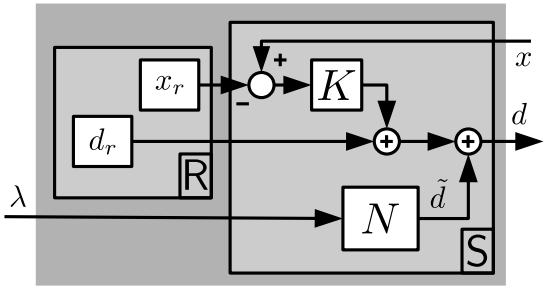

Figure 10.9: Standard problem solution equipped with the annihilator introduced in Chap. 8.

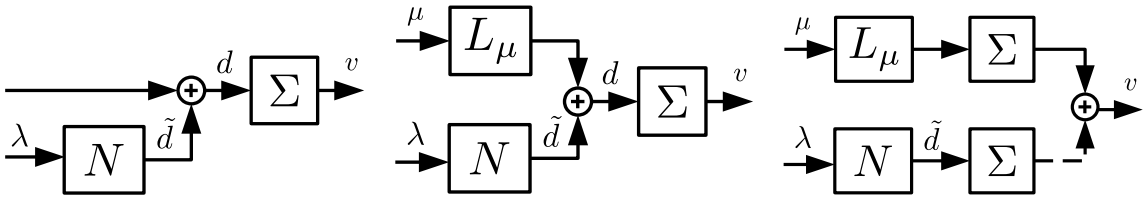

Figure 10.10: As in Chap. 8, an annihilator adds $\tilde{d}$ to the input of Σ, see Fig. 10.10a. The input space is then decomposed according to $\mathcal{N} \oplus \mathcal{L}_\mu = \mathbb{R}^2$ which leads to Fig. 10.10b from which Fig. 10.10c is derived by moving Σ ahead of the sum. Note that the dashed line conveys the zero signal. The open-loop decomposition of Fig. 10.5 then derives from Fig. 10.10c by exploiting (10.26).

Standard problem solution The answer to this simplified problem can be easily obtained via a two-step procedure corresponding to the classical treatment of the output regulation problem, see the beginning of Chap. 9:

1. Compute the optimal reference trajectories (u_r, x_r), i.e. the solution of the optimisation problem (10.5).

2. Define a stabilizer which makes this equilibrium stable for the closed-loop system. Because Σ is controllable, the existence of K ensuring that $A + BK$ is Hurwitz is guaranteed, so that the standard stabilizer $x \mapsto d = K(x - x_r) + d_r$ can be used.

Direct implementation of the methology of Chap. 8 If the hierarchy of the control objectives is satisfied at the steady state, this might not be the case during the transient regime, though: There is no guarantee that satisfying **(OC)** will not perturbe the optimal **(VR)** transient.

This is the motivation of implementing the methodology introduced in Chap. 8. This boils down to add an annihilator $\mathsf{C}_\perp$ of Σ to the standard problem solution, see Fig. 10.9. From $\mathbf{0} \in \mathbb{F}(\mathcal{R}^*)$, it comes out that $\lambda \mapsto \tilde{d} = N\lambda$ is a suitable annihilator. Given an arbitrary trajectory $y = v$, any transient of Σ inducing the same output can be imposed by way of the appropriate use of λ, since $\mathsf{C}_\perp$ has maximal range. In this sense, full exploitation of the degrees of freedom is ensured *during the transient regime*. By addressing **(OC)** only through $\mathsf{C}_\perp$ via λ, one ends up with a "priority-aware" controller that strictly meet the hierarchy of the control goals.

Comparative analysis It is now shown that adding this annihilator is equivalent to decomposing the system, as shown in Fig. 10.5, i.e. Fig. 10.9 and Fig. 10.7a are equivalent up to a

change of variables. To see this, let us focus on Fig. 10.10a where Fig. 10.9 have been partially reported. From the caption of Fig. 10.10, one ends up with Fig. 10.10c. First, observe that the cascade of N with Σ in Fig. 10.10c corresponds to Σ_δ^0, that is Σ_δ for $v = 0$:

$$\Sigma_\delta^0 : (A|\mathcal{R}^*, \mathcal{R}^*|B|\mathcal{N}, \mathbf{0}, \mathbf{0}) \tag{10.26a}$$

The output of this subsystem is zero. Specifically, Σ_δ^0 is the largest subdynamic of Σ that is invisible from the output $y = v$. Second, note that the cascade of L_μ with Σ in Fig. 10.10c corresponds to Σ_v. This subsystem is derived from Σ using the canonical projection associated with $\mathbb{R}^m/\mathcal{R}^*$:

$$\Sigma_v : (A|(\mathbb{R}^n/\mathcal{R}^*), B|(\mathbb{R}^m/\mathcal{N}), C|(\mathbb{R}^n/\mathcal{R}^*), \mathbf{0}) \tag{10.26b}$$

This corresponds to Σ disregarding the invisible dynamics. Saying it differently, it isolates the smallest part of the dynamics that impacts the output. This discussion leads to Fig. 10.5, where Σ_δ is also fed by v. This last observation originates from the fact that $\mathcal{L}_v \simeq \mathbb{R}^n/\mathcal{R}^*$ is not A-invariant, unlike $\mathcal{R}^*$.

As a last comment, note that stabilizer $x \mapsto K(x - x_r) + d_r$ in Fig. 10.9 can be split into two parts, namely $\mathsf{C}_\delta : \delta \mapsto \lambda = K_\delta(\delta_r - \delta) + \lambda_r$ to control Σ_δ and $\mathsf{C}_v : \left[\begin{smallmatrix}\sigma\\ v\end{smallmatrix}\right] \mapsto \mu = K_\mu(\left[\begin{smallmatrix}\sigma_r\\ v_r\end{smallmatrix}\right] - \left[\begin{smallmatrix}\sigma\\ v\end{smallmatrix}\right]) + \mu_r$ to stabilize Σ_v. The resulting scheme is analogous to Fig. 10.7.

Remark 10.9 (On the dependency of Σ_δ wrt v). If $\mathcal{L}_v$ is not A-invariant, it is controlled invariant, considering $A\mathcal{L}_v \subset \mathcal{L}_v + \mathrm{Im}\,\{B\}$. Hence, there exists a matrix F such that the (σ, v) dynamics can be made invariant via regular state-feedback. This fact has already been highlighted by the dotted line in Fig. 10.5. With such feedback, and bearing in mind (10.25), the subsystem Σ_v^F reads:

$$\Sigma_v^F : ((A + BF)|\mathcal{L}_v, \mathcal{L}_v|B|\mathcal{L}_\mu, C|\mathcal{L}_v, \mathbf{0})$$

Without this feedback, Σ_v feeds Σ_δ, as shown in Fig. 10.5. •

Remark 10.10 (From signal injection to input space decomposition). The annihilator on Fig. 10.10a takes the λ coordinates of the effective input. Hence, the λ coordinate of the signal entering on the sum by the left-hand side is eventually ignored. This motivates the introduction of Fig. 10.10b where only the μ coordinate is retained. •

Handeling the input constraints Remarkably, a priority-aware controller can even be designed in the input-constrained context. Indeed, it suffices to use the annihilator $\mathsf{C}_\perp$ of Σ by an annihilator $\mathsf{C}_\perp$ to $\mathfrak{S}$ with maximal range. Using Lem. 8.20, this annihilator reads:[5]

$$\begin{aligned}
&\mathsf{C}_\perp : \mathbb{R}^2 \times \mathbb{R} \to \mathbb{R}^2 \\
&\left(\begin{bmatrix}\lambda_d\\ \mu_d\end{bmatrix}, \lambda\right) \mapsto \tilde{d} = \begin{cases} N\left(\mathrm{sat}_{[\underline{\lambda}(\mu_d), \overline{\lambda}(\mu_d)]}(\lambda) - \lambda_d\right), & (\text{if } \mu_d \in [\underline{\mu}, \overline{\mu}]) \\ \mathbf{0}_2, & (\text{otherwise}) \end{cases}
\end{aligned}$$

Indeed, sets $\hat{\mathcal{U}}_{1:r}$ and $\hat{\mathcal{U}}_{r+1:m}(\hat{u}_{1:r})$ defined in Lem. 8.20 correspond to the two following sets

$$\left\{\mu \in \mathbb{R} : \exists \lambda \in \mathbb{R}, \begin{bmatrix} N & L_\mu \end{bmatrix} \begin{bmatrix}\lambda\\ \mu\end{bmatrix} \in \mathcal{D}\right\} = [\underline{\mu}, \overline{\mu}]$$

$$\left\{\lambda \in \mathbb{R} : \begin{bmatrix} N & L_\mu \end{bmatrix} \begin{bmatrix}\lambda\\ \mu\end{bmatrix} \in \mathcal{D}\right\} = [\underline{\lambda}(\mu), \overline{\lambda}(\mu)]$$

respectively, see (10.19). One recovers the strategy illustrated in Fig. 10.8.

[5] Unlike in Lem. 8.20, note that the first argument d_d of $\mathsf{C}_\perp$ is given directly in the new coordinates.

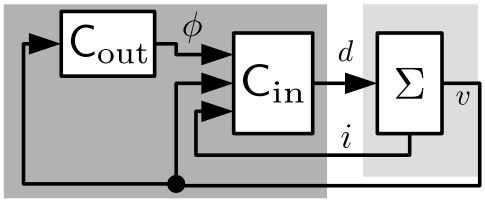

Figure 10.11: The ubiquitous two nested control scheme.

10.4 Comparison with a standard problem solution

The fact that R is unknown is expected to challenge not only the stability of the desired equilibrium but also its location in the state-space. The stabilizer is in charge of the former, whereas the latter is related to the reference trajectory generator.

10.4.1 Standard problem solution

Owing to the unknown operating conditions, the standard solution to solve Prob. 10.1 is to resort to a sequential design procedure leading to two nested control layers consisting of (i) a stabilizing inner controller C_{in} working in concert with (ii) an outer controller C_{out} driving the inner closed-loop toward the optimal equilibrium. The challenge of avoiding bad interaction between the two layers is addressed by imposing that the two loops operate at different time scales. Typically, the outer layer is slower than the inner layer.

Inner controller design Let the inner controller C_{in} be as follows:

$$(\phi_k, i_k, v) \mapsto d_k = (\alpha_k(V_{\text{ref}} + \phi_k) - (\alpha_k - 1)v - \beta_k i_k) \,/\, E, \tag{10.27}$$

for all $k \in [\![1, 2]\!]$. Scalars α_k and β_k are the tuning parameters. The signal ϕ_k is fed by the outer controller, see Fig. 10.11. This signal can be interpreted as a voltage reference shift, which is distinct from one module to another.

Outer controller design Recall that a load-dependent solution $(d_r, x_r(R))$ of the optimization problem is available. Thus, identifying the desired equilibrium amounts to estimating the load. This can be achieved via an integrator on the voltage deviation. When J is quadratic, the following outer controller C_{out} can generate ϕ from the integrator output:

$$\dot{z} = \epsilon(V_{\text{ref}} - v), \tag{10.28a}$$
$$\phi = Fz + H. \tag{10.28b}$$

For a suitable selection of F and H, signal ϕ drives the inner loop to the optimal steady state if $\epsilon > 0$ is sufficiently small. This scalar allows to slow down the time-scale of ϕ, which is equivalent to saying that ϵ can increase the time-scale separation of the two loops. Selecting a sufficiently small ϵ allows the exploitation of the steady-state model of the inner loop to design the outer loop. The expressions of F and H can be obtained by inverting this model.

Problem solution Next statement summarizes this discussion, see the bibliographical note for references on how to compute the controller parameters.

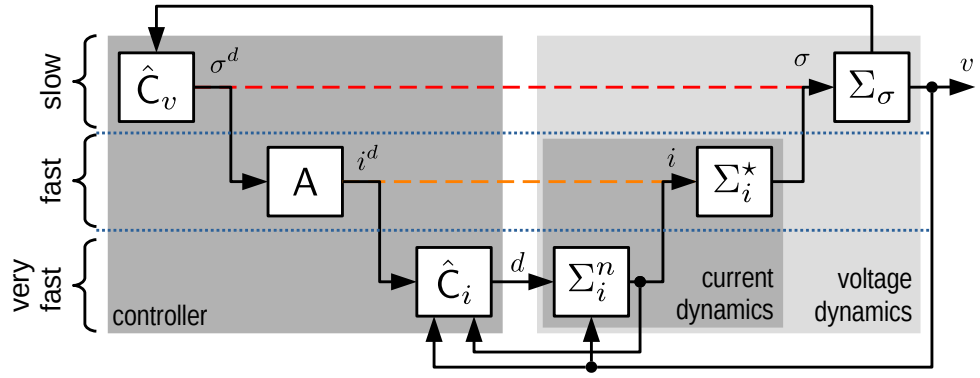

Figure 10.12: Control scheme resulting from implementation of the CAM.

Theorem 10.11 ([Del+19]). *If J is quadratic and $\mathcal{I} = \mathbb{R}^2$, then the map $(i, v) \mapsto d$ described in Fig. 10.11,* (10.27) *and* (10.28) *solve Prob. 10.3 for some $\alpha, \beta, \epsilon, F$ and H.*

10.4.2 The priority-aware controller of Subsec. 10.2

In the general robust context, the direct implementation of the methodology outlined in Chap. 9, and devoted to the reference trajectory generator R, is impossible. Indeed, every subsystem of R depends on the system parameters, see Fig. 9.4d on p. 158.

On solution of Subsec. 10.2 For bucks, not only the annihilator but also the input and state change of variables are independent of the load. Therefore, the decomposition of Σ as in Fig. 10.5 can be performed even if R is unknown. This allows the use of the control structure depicted in Fig. 10.7 in the robust context. This leads to the solution being exposed in Subsec. 10.2: C_v is augmented by an integrator, which serves not only to regulate v but also as a load estimator. From this estimation, C_δ can drive δ to the optimal current distribution.

Comparison with Th. 10.11 Recall that the standard problem solution relies on time scale separation as the key feature to achieve stability. If this strategy offers tractability, it also unavoidably lowers performance: The transient of the outer loop must be sufficiently slow not to destabilize the inner one. In stark contrast, the approach described in Subsec. 10.2 does not require any time scale separation. Indeed, interactions between dynamics are handled via *geometric* decoupling.

10.5 Miscellaneous

Before concluding, three additional solutions to Prob. 10.1 are outlined, and a discussion on the conditioning of matrices is proposed.

10.5.1 The CAM solution

Outline of the solution Relying on the analogy highlighted in Tab. 10.1, the strict implementation of the CAM (see Subsec. 7.2.1 on p. 97) gives rise to yet another solution for Prob. 10.1. The core idea of this strategy is captured by Fig. 10.12, built on the decomposition of Σ proposed in Fig. 10.3. Compare Fig. 10.12 and Fig. 7.12 on p. 99, and observe how the dependency

of Σ_i wrt to v (see Fig. 10.3) is implemented. On Fig. 10.12, the static mapping $\Sigma_i^\star$ sums the entries of its input.[6]

In accordance with the CAM, the control law is structured as follows:

- $\hat{\mathsf{C}}_v$ is designed to address **(VR)** by computing a desired global effort σ^d in order to control the output v;
- A takes the total effort reference σ^d as an input and delivers suitable desired current vector i^d such that (i) the total current σ tracks σ^d and (ii) **(OC)** is met;
- $\hat{\mathsf{C}}_i$ aims stabilizing the response of the power modules and delivers the duty cycle d by an internal feedback on i and v.

The design of $\hat{\mathsf{C}}_v$ is based on deadbeat control. This makes it possible to include the duty cycle constraints in the control allocator A. For a quadratic J corresponding to the power losses, the allocator computes the desired current i^d via an active set quadratic optimization method. Signal i^d allows the tracking of the desired total current while ensuring the feasibility of d and addressing **(OC)** as a secondary objective.

Comparitive analysis Compared to the solution of Th. 10.7, this new approach allows us to comply with current constraints $i(t) \in \mathcal{I}$ at all times, *modulo a short transient* owing to the response of $\hat{\mathsf{C}}_i \star \Sigma_i^n$. In view of Rem. 10.2, the relevance of this feature is questionable. In addition, this new solution is much more demanding in terms of computational resources, as the implementation of A amounts to solving an optimization problem online and at each time step.

10.5.2 An Hamiltonian point of view

Outline of the solution Introducing the energy variables in the model is the first step to adopt the energy-based point of view characterizing the Hamiltonian framework, i.e. the capacitor charge $Q = Cv$ and the magnetic fluxes $\varphi_k = L_k i_k$ of the inductors. Using $x := (\varphi_1, \varphi_2, Q)$ as the state variable allows us to rewrite (10.7) as the following Hamiltonian system:

$$\dot{x} = (\mathcal{J} - \mathcal{R})\nabla_x H(x) + Bd \tag{10.29}$$

where $H : \mathbb{R}^3 \to \mathbb{R}$ is the total energy stored by the circuit:

$$H(x) = \frac{1}{2}(\varphi_1^2/L_1 + \varphi_2^2/L_2 + v^2/C) \tag{10.30}$$

Energy dissipation is characterized by $\mathcal{R}$, whereas $\mathcal{J}$ together with B describe the interconnection structure:

$$\mathcal{R} = \mathcal{R}^\intercal = \begin{bmatrix} 0 & 0 & 0 \\ 0 & 0 & 0 \\ 0 & 0 & 1/R \end{bmatrix}, \quad \mathcal{J} = -\mathcal{J}^\intercal = \begin{bmatrix} 0 & 0 & -1 \\ 0 & 0 & -1 \\ 1 & 1 & 0 \end{bmatrix}, \quad B = E \begin{bmatrix} 1 & 0 \\ 0 & 1 \\ 0 & 0 \end{bmatrix}.$$

Define $\mathcal{C} : (\varphi_1, \varphi_2, v) \mapsto \varphi_1 - \varphi_2$. Observe that, for $d = \mathbf{0}$ and for all t, one has:

$$\frac{\mathrm{d}}{\mathrm{d}t}\mathcal{C}(x(t)) = \frac{\partial \mathcal{C}}{\partial x}(x(t))\dot{x}(t) = \begin{bmatrix} 1 & -1 & 0 \end{bmatrix}(\mathcal{J} - \mathcal{R})\nabla H(x(t)) = 0$$

[6] Unlike in Chap. 7, $\Sigma_i^\star$ cannot be defined as the DC gain matrix of Σ_i. Indeed, this gain is not a well-defined mapping because the state matrix of Σ_i has an eigenvalue at zero. Instead, $\Sigma_i^\star$ should be viewed as the DC gain of $\hat{\mathsf{C}}_i \star \Sigma_i$.

This relationship is valid for all H, which proves that $\mathcal{C}$ is a Casimir function, by definition, see [Van17, p. 87]. From $\mathcal{C}$, we define the following change of variables, where φ_T is introduced:

$$\begin{bmatrix} \mathcal{C} \\ \varphi_T \\ Q \end{bmatrix} = \begin{bmatrix} 1 & -1 & 0 \\ L_\sigma/L_1 & L_\sigma/L_2 & 0 \\ 0 & 0 & 1 \end{bmatrix} \begin{bmatrix} \varphi_1 \\ \varphi_2 \\ Q \end{bmatrix} \tag{10.31}$$

Physically, $\mathcal{C}$ reflects the flux distribution, and φ_T is the total flux. Let us also proceed to the following change of input coordinates:

$$\begin{bmatrix} \vartheta \\ \mu \end{bmatrix} = \begin{bmatrix} 1 & -1 \\ L_\sigma/L_1 & L_\sigma/L_2 \end{bmatrix} \begin{bmatrix} d_1 \\ d_2 \end{bmatrix} \tag{10.32}$$

The use of these new input and state variables leads to a new Hamiltonian system, characterized by the same matrices B and $\mathcal{R}$ but modifying H and $\mathcal{J}$ as follows:

$$H' = \frac{1}{2}(\mathcal{C}^2/(L_1+L_2) + \varphi_T^2/L_\sigma + v^2/C), \quad \mathcal{J}' = \begin{bmatrix} 0 & 0 & 0 \\ 0 & 0 & -1 \\ 0 & 1 & 0 \end{bmatrix}$$

The obtained system consists of two fully disconnected subsystems. The state and input of the first one $\Sigma_\mathcal{C}$ are $\mathcal{C}$ and ϑ, respectively, whereas the analogous variables for the second one Σ_Q are (φ_T, Q) and μ. The second subsystem can be physically interpreted as a buck converter. From this structure, the stabilizing controller can be easily found if the load is known. Otherwise, a strategy analogous to that of Subsec. 10.2 can be implemented: Design a PI controller for the second subsystem and feed the controller of the first subsystem with signals containing sufficient information to define the optimal equilibrium. The stability of the whole system can then be proved by exploiting the resulting cascade.

Comparitive analysis Compared to the solution of Th. 10.7, this new approach leads to an open-loop decomposition of Σ characterized by *disconnected* subsystems and obtained via a completely different path.[7] However, the benefit of this feature is reduced by the necessary reintroduction of a unilateral coupling from Σ_Q to $\Sigma_\mathcal{C}$ to identify the optimal flux distribution. Besides, note that input constraints are not treated in this new approach.

10.5.3 A robust cooperative distributed control approach

Outline of the solution In statement of Prob. 10.1, it is implicitly assumed that d can be computed in a centralized manner using the measurement of the voltage and of all currents. A less demanding problem is the one where d_k is delivered by a local controller using only the local current and neighboring currents made available by a communication network. The following controller provides an example of such an alternative solution:

$$\dot{z}_k = V_{\text{ref}} - v - \gamma \sum_{j=1}^{m} \varrho_{k,j}(i_k - i_j), \tag{10.33a}$$

$$d_k = \alpha_k v + \beta_k i_k + F_k z + G_k \sum_{j=1}^{m} \varrho_{k,j}(i_k - i_j). \tag{10.33b}$$

[7] See Rem. 10.9 where it is shown that fully disconnected subsystems can also be obtained for the solution of Th. 10.7, but using regular feedback.

for all $k \in [\![1, m]\!]$. The scalars $\varrho_{k,j}$ satisfy

$$\varrho_{k,j} = \begin{cases} 1, & (\text{if } |k-j| \in \{1, m-1\}), \\ 0, & (\text{otherwise}). \end{cases}$$

They determine the communication among the power modules. This choice corresponds to a connected, undirected communication network topology. The other parameters of (10.33) are gains to be selected offline. In this context, it can be shown that **(VR)** and balanced current sharing is asymptotically achieved. Note that the control design requires neither the magnitude of R nor the number m of power modules.

Compared to the two-layer controller of Th. 10.11, observe that each local controller embeds its own integrator, which is fed not only by the voltage deviation but also by the imbalance of the local current i_k wrt the neighboring currents i_j.

Note that the controller (10.33) can cop with unknown false data injection Δd_k added to the input channel d_k. It can be shown that if Δd_k is bounded, then both **(VR)** and balanced current sharing can be arbitrarily accurate via suitable controller gain selection.

Comparitive analysis The distribution of the control computation has important advantages in terms of reliability and plug-and-play features. However, compared to Th. 10.7, the proposed solution considers neither **(CC)** nor input constraint into account. **(OC)** is also only achieved for the particular case of balanced current sharing. Finally, there is no guarantee that the hierarchy between **(VR)** and **(OC)** is met.

10.5.4 Enhancing matrix conditioning via appropriate change of variable

Numerical tools are often used for gain synthesis. Matrix conditioning is essential for this task to be accurate. This is problematic for the considered system. As an example, the design of C_v relies on the following matrices of Σ_v, which are typically poorly conditioned owing to the difference in magnitude between inductances L_σ and C:

$$A = \begin{bmatrix} 0 & -1/L_\sigma \\ 1/C & -1/(RC) \end{bmatrix}, \quad B = \begin{bmatrix} E/L_\sigma \\ 0 \end{bmatrix}$$

However, performing a suitable time-scale, state, and input change of variables gives to those matrices the following expression:

$$A' = \begin{bmatrix} 0 & -1 \\ 1 & -1/(RQ_C) \end{bmatrix}, \quad B' = \begin{bmatrix} 1 \\ 0 \end{bmatrix}$$

where $Q_C = \sqrt{C/L_\sigma}$. It also transforms Σ_δ into a set of disconnected integrators that are no longer affected by v (as in the Hamiltonian framework), that is, $\dot{\delta} = \lambda$ holds.

Then, one can use those better-conditioned new models to design a controller, from which C_v can be deduced via the inverse transformation.

10.6 Conclusions

Recall the most remarkable features of the controller presented in Sec. 10.2:

- The lack of time-scale separation requirement which limits the achievable transient performances and complicates controller gains synthesis since the bounds on ϵ is

often hard to compute;

- The ability of the control law to strictly met the hierarchy of the specifications. Note that this feature is related to the existence of a cascade, see Fig. 10.5 which allows for standard tools related to this structure to be used and, in turn, formal stability proofs to be more easily derived;
- The electrical circuit interpretation of the subsystems of the cascade, which not only allows to reuse existing results for the control of single power module but also facilitates the spread of the framework out of the control community;
- The universality of the solution since every control scheme solving the control problem can be reformulated into the proposed framework, due to the fact that the decomposition of Σ is performed by manipulating open-loop equations, instead of some precompensated model like in the two-nested loop framework.

The key features of the system enabling these achievements are as follows:

- $\mathcal{R}^* = \mathcal{V}^*_{bp}$ which implies that the bp-strong annihilator for the reference trajectories generator R and the (simple) annihilator of the stabilizer S coincide;
- $F = \mathbf{0} \in \mathbb{F}(\mathcal{R}^* = \mathcal{V}^*_{bp})$ which induces that this annihilator degenerates into a static mapping for which maximality of its range can be achieved even when facing input constraints;
- Neither $\mathcal{N}$ nor $\mathcal{R}^* = \mathcal{V}^*_{bp}$ is affected by the uncertainties, so that the geometric decomposition of the system can be performed even in the uncertain context.

10.7 Bibliographical notes

Existing works

For technological motivations and general considerations on the parallel interconnection of DC/DC converters, see [TV98; Shi+99; HT07] and other references cited in the next chapter.

The vast majority of existing results on this topic have been derived in the context of the same converters (the same class of converters sharing identical electrical components). In this context, balanced-current sharing is fully justified by the fact that it equally distributes stress among the converters. However, several papers have demonstrated that making non-identical converters work in concert would improve the unloading transient response and reduce the output voltage overshoot [MZY10; STT14; Švi+13]. In the patent [Rep+17], asymmetric inductors in multiphase DC/DC converters are proposed to achieve a fast transient response and to optimize efficiency over the load range. In this case, a uniform current distribution is no longer optimal.

Existing solutions to achieve nonuniform current sharing relies on "virtual droop resistors" which can be interpreted as a low-frequency negative feedback (the feedback gain is the so-called "droop resistor") on current which aims adjusting equilibrium current [Ham+15; SK15]. Then, a rule of thumb is to fix the droop resistor magnitude for bus voltage to remain into allowed bounds when the converter injects its maximum power [Gue+11; Ham+15]. As noted in [SK15], this strategy maintains a constant current ratio between converters, whereas optimal current sharing requires a load-dependent current ratio. In addition, this approach deals with current distribution and voltage regulation as competing objectives. If priority is given to

voltage regulation, the current distribution deteriorates, and vice versa. As a result, an optimal current distribution can only be obtained by allowing a static error on the output voltage (see [MTA08]), see also [Bar+19] for an extension of such a method for a DC microgrid, and [BSL94].

Other methods fall into the category of "active current-sharing mechanisms", that is, feedback-based methods. Literature in this area is well surveyed in [Shi+99; HT07] for identical converters. Remarkably, almost all existing solutions use the two-nested-loop scheme depicted in Fig. 10.11. Many solutions exist, depending on how ϕ acts on the inner loop, e.g. as a voltage or current reference shift, and how it is produced, e.g. "master/slave" and "democratic" strategies. However, theoretical proof of the existence of some attractive equilibrium for *the overall interconnection* is seldom provided, even for the inner loop alone and under the assumption that ϕ is constant.

If this strategy offers tractability, it also unavoidably lowers performance: The transient of the outer loop must be sufficiently slow not to destabilize the inner loop. Relying on models with complex impedances, interesting research directions have been opened to go beyond this frequency separation: In [TV98] arbitrary number of identical converters are considered, whereas the case of two different converters is treated in [Sun+05]. However, theoretical stability certificates of the overall system are not formally provided. Furthermore, control schemes (the so-called "master/slave" and "democratic") are *a priori* imposed even if discussions about their intrinsic conservatisms seem hard to handle. Moreover, the variability of the load must also be taken into account. In addition, generalization to an arbitrary number of non-identical converters along those lines leads to a calculus burden.

We believe that the limitations of most of those existing results are inherent to the retained methodology, which heavily relies on the interconnection of single-input single-output (SISO) transfer functions.

Rephrased existing works

The interested reader can consulte [**TD19**, Sec.3] for an extensive analysis of the classical literature, the ubiquitous two nested loops, and the highlight that time-scale separation is the fundamental tool for achieving closed-loop stability (even if it is seldom acknowledged).

Never seen elsewhere in this term ($\approx$ new)

For all cited contributions below, an arbitrary large set of *heterogeneous* converters can be handled, that is, power modules must not share the same value of L_k. Furthermore, *load-dependent* current distribution is treated either after off-line computation of the reference profile $(d_r(\cdot), x_r(\cdot))$ as in [**Del+19**; **TD19**] or by on-line implementation of a continuous time gradient descent controller [**Kre+21a**]. Finally, the constants E_k are not necessarily identical. Note that this makes the proposed solution applicable to DC microgrids, where each power module connects a generator/storage unit to the DC bus.

Literature on over-actuation were inspiring for those contributions, even if is rarely (never ?) acknowledged that parallel interconnection of buck converters is an overactuated system.

The two nested loops framework A comprehensive statement and proof of Th. 10.11 can be found in [**Del+19**], where the preliminary study [**TDG16**] was extended. In particular, explicit expressions of F and H are provided, together with guidelines to select suitable gains α, β and ϵ. In those two papers, however, neither the input constraint nor the current saturation are taken into account. It is also proved in [**Del+19**], both theoretically and experimentally,

that the constant-current ratio is not always optimal. Considering an example of $m = 2$ non-identical buck converters, it is shown that for low output power, most of the power should be conveyed by one converter, whereas the opposite ordering should be preferred for higher output power.

Note that the time-scale separation rationale makes those results close in spirit with the approach offered in [Zac09]. They all rely on the idea that the inner-loop equilibrium (d, x) can be slowly shifted to its optimal location. However, the strategy of [Zac09] consisting of optimizing u is inapplicable to bucks. Indeed, all inner-loop equilibria share the same input irrespective of the expression of C_{in}, see (10.12). The quantity to be optimized is x (not u). This makes this system beyond the scope of [Zac09].

The geometric approach Based on [**TD17**], the proof of Th. 10.7 can be found in [**TD19**]. If the strategy to handle the saturations was already outlined in [**TD19**], a throughout treatment of this solution is offered in [**Kre+19**].

Other approaches The implementation of the CAM is exposed in [**Kre+21b**]. Note that the proposed design methodology notably differs from the classical one: When constructing $\hat{\mathsf{C}}_v$, both the limits of σ and the time delay induced by the internal loop $\mathsf{A} \star \hat{\mathsf{C}}_i \star \Sigma_i$ are formally taken into account, see the end of Subsec. 7.6.1 in Chap. 7.

In [**Kre+21a**], the Hamiltonian point of view is adopted. This work was inspiring to develop the change of variables offered in [**Ndo+22**, Lem.18], which improves conditioning of the model and decouples the two subsystems. This result can be regarded as an extension of the modular converters of the normalization proposed in [SS06b, p.15] for single converters. The distributed controller is offered in [**Sad+22**], see Lem.3 of this paper for the controller gain tuning.

Chapter 11

Perspectives

Contents

This chapter introduces new research avenues and intends to explore existing ones more thoroughly. The first one aims to build a universal framework for the control of modular power electronics converters. In this sense, it extends the results obtained on parallel buck converters and the 3-phases inverter. The challenges identified justify a series of research directions around IR and its exploitation in control, that aimed at completing and extending the results of this manuscript. Finally, the expected benefits of co-designing the system, its control and the specifications are highlighted. To this end, the importance of inversion in the context of constrained dynamic systems is emphasized.

11.1 A universal framework for the control of modular power converters

Modular Power Converters (PC) are made of power modules that are connected via a certain topology to let them serve a common goal by working in concert. Chap. 10 provides an example of such a device, namely, the input-parallel-output-parallel connection of buck converters feeding a common load. The star-connected inverter in Fig. 5.1 in Chap. 5 can be seen as yet another modular PC for which the positive pins of three modulated voltage sources (corresponding to the power modules in this specific case) are linked to the positive pins of the loads, whereas all negative pins of the loads are connected to the neutral node.

Let us review the main arguments in favor of the modular approach in PC design:

- Enabling technical solutions (1/2): Input series-connected (resp. input parallel-connected) modular PC can reduce the voltage exerted at the input of the power modules (resp. the current flowing through the power modules) by distributing the input voltage (resp. input current) among the modules; see [LDT18] and [Che+09, Tab.1]. This feature not only reduces stress on the electrical components, but also enables technical solutions that cannot be realized with standard non-modular solutions [MCR20]. For instance, the topology of modular multilevel converters allows the distribution of the input voltage among power modules such that each of them merely withstands a part of this voltage, which typically has a very large magnitude [Per+21].
- Enabling technical solutions (2/2): Modular PC can also be used to reduce the output voltage/current ripples by interleaving the currents of each power modules, at a level that is unreachable via a single module for the same switching frequency [Tha+09; Cid+11].
- Standardisation of the production and design: By using functional building blocks that can be used for multiple applications, the modular approach results "in high volume production and reduced engineering effort, design testing, onsite installation and maintenance work for specific customer applications" [CKK09].
- Increase reparability: By using standard modules, this kind of power converters are expected to be more easily reparable. This, in turn, is expected to reduce the ecological impact of such devices, when measured over the entire life-cycle.

11.1.1 Background on model and control of modular power converters

Control of modular PC

Existing control laws for modular PC often result from ad hoc developments. In [Gat+02], the case of a 3-cells flying capacitors PC is treated via input-output linearization. In [GCG17],

a standard matrix converter is considered using binary control. Interestingly, an arbitrary number of modules are sometimes considered see e.g. [HDD16] for flying capacitor PC using binary control, [**Sim+23a**; **Sim+23b**] for modular power flow controller in the context of electrical microgrids using forwarding and singular perturbation theory, [De +12; Mes+23] for parallel boost converters using linearization and LMI techniques, and flatness-based control, respectively, to cite a few. If these results are valuable, it seems difficult to generalize them out of the considered PC.

Besides, let us emphasize that formal analysis of the closed-loop is missing or unconvincing in most of the study (unlike in the above mentioned studies), see [TV98; Sun+05; Gir+06; He+14; HT07; Shi+99] to cite a few and the literature review in [**TD19**, Sec.3].[1]

Least but not the least, very few existing control schemes comply with the hierarchy of the control specification as the one in Chap. 10 does. As valuable exceptions to this statement, Marc Bodson and its co-authors have successfully implemented the CAM on modular PC. The case of 3-phases multilevel flying capacitor PC is treated in [BBF17]. The four-leg inverter is the topic of [BBF18]. A modular multilevel converter is considered in [LFB22a; LFB22b]. As outlined in Chap. 7, these solutions hinge on online optimization. Such an implementation requirement is a real challenge for electrical engineering applications because the typically involved dynamics can be extremely fast and in turn requires a demanding computational setup.

As shown in Chap. 10, the inversion approach proposed in Chap. 8 and Chap. 9 requires fewer resources for implementation. They are also scalable in the sense that increasing the number of power modules does not lead to an explosion of the computation burden. This should be confirmed by generalizing these approaches out of the context of Chap. 10.

> The development of a comprehensive framework for the control of modular PC represents a highly significant research direction, which still offers substantial opportunities to enhance existing findings.

Model of modular PC

The lack of a general model of modular PC is certainly an obstruction to the increase in the level of generality of the control counterpart. For this task, rigorous mathematical formalization is a major requirement because modular PC typically have a large number of inputs and outputs with coupled dynamics. In this context, gain selection by intuition is hopeless.

The models that are useful for modular PCs are diverse and depend on their intended use.

- Design-oriented models: In the field of circuit design, the models usually considered as relevant should provide information on the efficiency and thermal behavior of the circuit, *at the steady-state* [Wan+09]. To this end, the challenge is to obtain current waveforms and accurate loss functions, possibly via a frequency-domain approach [MD25]. To account

[1] (i) Generally, formal proofs of stability (if any) very often reduce to the (local) analysis of a SISO model represented by a transfer function derived from linearization and linear circuit theory using impedances rather than linear differential equations [TV98; Sun+05]. If eigenvalue analysis of the state-matrix is sometimes performed [Gir+06], nonlinear analysis is very often out of the scope of the studies. In particular, this prevents the impact of duty cycle saturations from being analyzed. (ii) Control law structures are often derived from mono-dimensional nested loops [Sun+05; He+14]. This makes the analysis and guidelines for gain selection (if any) convoluted. This is particularly concerning when stability actually relies on some hidden time-scale decoupling, whose validity just hinges on the gain selection, see [HT07] and the analysis of [**TD19**, Sec.3]; (iii) Discussions of the results are sometimes hazardous, since they often attribute the obtained performance to the structure of the control law, without demonstrating that the proposed gain selection is optimal [Shi+99].

for power losses, including the parasitic elements of the electrical components is a common approach, see [Kaz08]. Note that if dynamical models are used, the complexity of the model is not as concerning as that of the control-oriented model. Indeed, the former are used for numerical simulations, whereas the latter often supports the construction of formal stability certificates for a whole range of initial conditions.

- Controlled-oriented models: For control, on the other hand, what is expected of a model is to be able to account for the dynamic behavior of the system, particularly in transient regime. To achieve tractability, these models often ignore parasitic elements, as advised by [SS06b, p.53]. Although we fully agree with this point of view *for the transient regime*, we believe that these parasitic elements reflecting the power losses must be considered when it comes to steady-state selection. This last subproblem is indeed part of the control specifications in the case of a modular PC, as shown by Chap. 9 and Chap. 10. The contradictions raised by this discussion are only apparent. As illustrated in Chap. 10, steady-state selection can be made by taking parasitic elements into account via the J cost function, as in Prob. 10.3 on p.182, whereas the dynamic equations discard those elements given the closed-loop natural robustness properties.

Let us restrict our analysis to PC models that are useful for control purposes. In order to obtain a universal version of these models, a wide variety of design choices and phenomena must be taken into account. Let us list some examples.

- Different systems: There is virtually an infinite number of distinct modular PC, depending on the type of power modules (different type and sizing of electrical components; different topology of interconnection within the module) and the considered topology of interconnection of these modules; See [MCR20] for power modules made of submodules; See [Per+21, Fig.2] for an example of the variety of topology of power module for modular multilevel converters. As an example, Fig. 11.1 shows the classical four possible combinations of input-output connections of two modules. This diversity is mainly motivated by the variety of applications, that is, the type of loads and sources that the PC is intended to connect, see e.g. [Per+21, Sec.IV] for a review of applications of modular multilevel converters.
  In addition to the model of each physical electrical component, mutual inductances can also induce non-negligible additional dynamics. This phenomenon can be intentionally induced or be the consequence of the undesirable effect of the placement.

- Different state of health: The post-fault circuit can be distinct from any commonly used topology. This dramatically enlarges the number of circuits to be considered.

- Different operating modes of the power modules: In Chap. 10, each power module is assumed (i) to remain on and (ii) to permanently operate in Continuous Conduction Mode (CCM). Improvement of the overall efficiency of the system is expected by allowing different operating modes, i.e. some power modules could be switched off or allowed to operate in Discontinuous Conduction Mode (DCM) [Kaz08].

- Different loads: Purely restive load is considered in Chap. 10 as the most common and simple choice. A constant power load is another more complex load behavior that is commonly considered [Gri+98; El +19]. In this case, the output voltage v equals the nonlinear function $i \mapsto p/i$ where $p > 0$ is the power constant. Another common load model is the ZIP load, which corresponds to the parallel interconnection of a constant impedance (Z), a constant current (I), and a constant power (P).

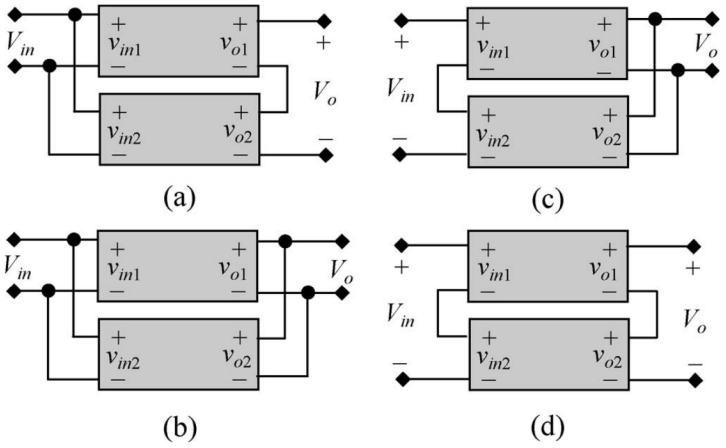

Figure 11.1: Possible combinations of input-output connections of two modules, [Gir+06, Fig.1].

- Different specifications: The specifications associated with modular PC are not uniform. A control-oriented model must account for them. Similar to a conventional PC, the input and output physical quantities may be either currents or voltages, and either sinusoidal or constant [MCR20]. In addition, the hierarchy of specification items may sometimes be reversed from those presented in Chap. 10, [MCR20].
- Different measurements: The types of measurements used by the control system also vary widely.
- Different previews on load variations: In some context, the controller can have access to some preview on the load trajectory, including transient magnitude and time of occurrence of the changes. Specifically, microprocessors, which are loads with fast transients, "can predict the energy requirement and time of code executions quite accurately" [STT14].

> A universal control-oriented model must accommodate various systems, states of health, operating modes of the power modules, loads, and preview scenarios on their trajectories, specifications, and measurements.

11.1.2 Toward a universal control-oriented model

Let us now give preliminary results on how to derive a universal control-oriented model for a module PC.

Remark 11.1. As in the previous chapters, every current and voltage is assumed to be averaged, unless explicitly stated otherwise, even if the notations do not explicitly mention this fact. •

General interconnection of healthy or faulty power modules

The electrical circuit of a modular PC can be very complex. The interconnection scheme can indeed involve a very large number of power modules. For example, modular multilevel converters used in a high-voltage DC system commonly have more than 200 submodules per arm [Per+21]. In addition, each module can itself be an intricate circuit.

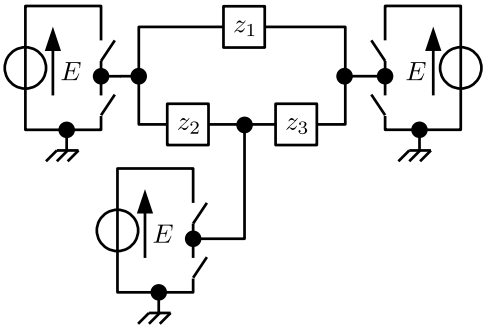

(a) Triangle 3-phases.

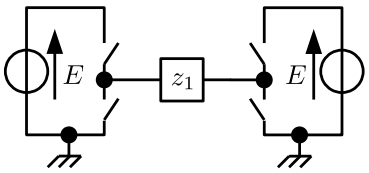

(b) H-bridge 1-phase.

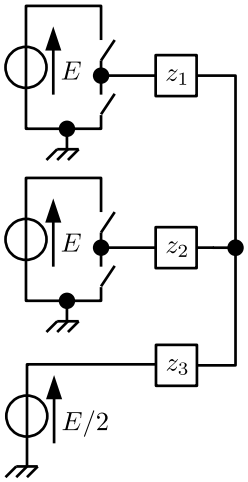

(c) 4-switches 3-phases.

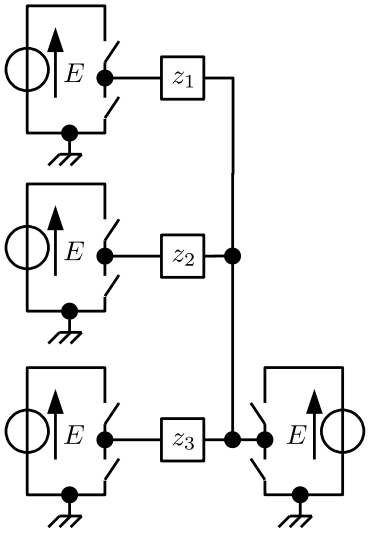

(d) 4-legs 3-phases.

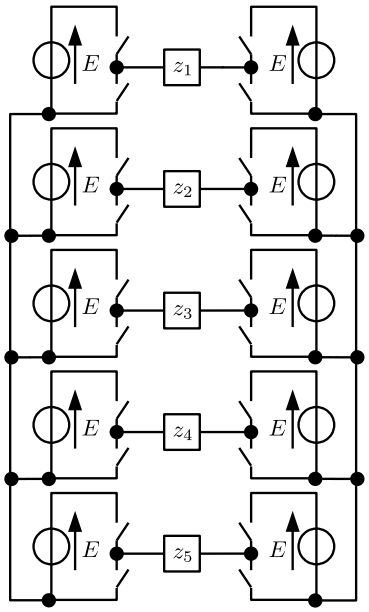

(e) Open-end winding 5-phases with isolated sources.

Figure 11.2: Examples of inverter that belong to the considered class of voltage source inverters.

Such complexity can be handled via graph theory. This subsection aims to illustrate this statement by treating the class of voltage source inverters made of two voltage level legs. Even in this case, it is worth noting that many different inverters can be found in the literature. They differ by the considered topology. As an illustration, a few of them are depicted in Fig. 11.2. The star-connected 3-phases inverter of Chap. 5 also belongs to this class, see Fig. 5.1.

The considered class of inverter The considered framework is as follows:[2]

- Arbitrary large number of loads z_k, $(k \in [\![1, p]\!])$, is considered, see Fig. 11.3a. These loads are not necessarily identical;
- These loads are fed by (i) g voltage sources, see Fig. 11.3c, and (ii) m modulated voltage sources, i.e. voltage generators connected in parallel with a two-level voltage leg, see Fig. 11.3b. Denote by E_k the magnitude of the k-th voltage source. Let d_k be the duty cycle of the k-th leg.

[2]Notations of Chap. 5 are reused, after renaming u as u_z.

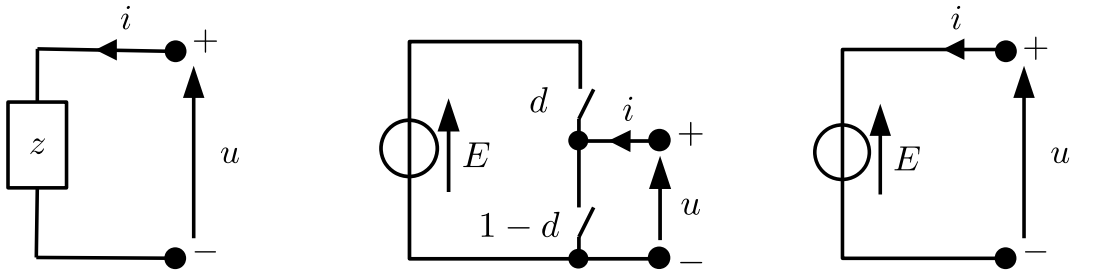

(a) Impedance (b) Inverter leg (c) Fixed voltage source

Figure 11.3: Elementary dipoles making up inverters.

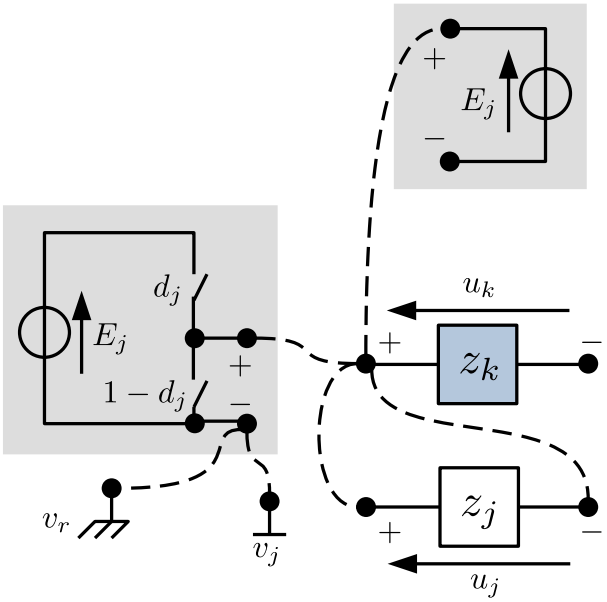

Figure 11.4: Circuit of the considered class of voltage source inverter. Dashed lines illustrate possible connection (i) of the positive pin of the k-th load and (ii) of the negative pin of the j-th modulated voltage source.

- Depending on the considered topology, the positive pin of the load z_k is linked either to the positive pin of a voltage source (modulated or not) or to some of the two pins of another load z_j, see Fig. 11.4. To take post-fault operation into account, the positive pin of z_k can even remain unconnected, leading to a floating potential. An analogous possibility of connection is offered for the negative pin of the load z_k.

- Negative pin of voltage sources E_j (modulated or not) can be connected either (i) to the absolute reference voltage v_r or (ii) to some local ground reference voltage v_j, see Fig. 11.3b. Hence, a non-zero voltage drop may exist between this negative pin and v_r.

It is straightforward to verify that any of the inverters depicted in Fig. 11.2 and Fig. 5.1 falls within the framework described above.

From the electrical circuit to the input/output model Based on the above discussion, each of the considered inverters is a collection of components selected from the set of devices depicted in Fig. 11.3. Since all of them can be viewed as dipoles, the digraph corresponding to the

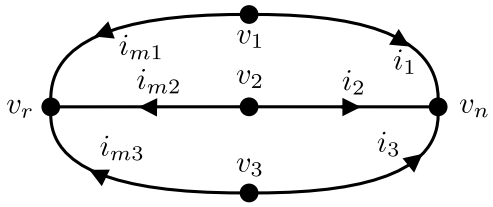

Figure 11.5: Digraph corresponding to the circuit of Fig. 5.1 in p. 52.

circuit is the result of the standard procedure described in e.g. [CDK87; DSB18]. For didactical purposes, this procedure is now outlined for the star-connected 3-phases inverter in Fig. 5.1.

1. Construction of the digraph: The digraph deriving from the circuit of this inverter, depicted on Fig. 5.1 and equipped with current arrows, as in Fig. 11.3, is proposed in Fig. 11.5. Observe the similarity between Fig. 5.1 and Fig. 11.5.

2. Defining the current and voltage vectors: The nodes and edges of the digraph are ordered to arrive at the following definition of the current and voltage vectors:

$$\begin{aligned} i &= \begin{bmatrix} i_1 & i_2 & i_3 & i_{m1} & i_{m2} & i_{m3} \end{bmatrix}^\intercal \\ v &= \begin{bmatrix} v_1 & v_2 & v_3 & v_n & v_r \end{bmatrix}^\intercal \\ u &= \begin{bmatrix} \underbrace{u_1 \quad u_2 \quad u_3}_{u_z} & E_0 d_1 & E_0 d_2 & E_0 d_3 \end{bmatrix}^\intercal \end{aligned}$$

3. A first model: The incidence matrix B of the digraph in Fig. 11.5 is specified as follows:

$$B = \left[\begin{array}{ccc|ccc} 1 & 0 & 0 & 1 & 0 & 0 \\ 0 & 1 & 0 & 0 & 1 & 0 \\ 0 & 0 & 1 & 0 & 0 & 1 \\ \hline -1 & -1 & -1 & 0 & 0 & 0 \\ 0 & 0 & 0 & -1 & -1 & -1 \end{array}\right]$$

   Exploiting the fact that Kirchoff's voltage law (KVL) reads $u = B^\intercal v$, direct algebraic manipulation leads to the following model:

$$u_z = E_0 d - (v_n - v_r)\mathbf{1}_3. \tag{11.1}$$

   In this simple case, the above equation is nothing but $u_k = E_0 d_k - (v_n - v_r)$, $(k \in [\![1,3]\!])$ derived from KVL.

4. Eliminating floating voltages: In (11.1), the output voltage u_z depends not only on d but also on the floating voltages v_n and v_r. Those voltages being unknown, the mapping $d \mapsto u_z$ is therefore not suitable for control purposes. This obstruction can be overcome by defining the natural projection $P : \mathbb{R}^3 \to \mathrm{Im}\,\{\mathbf{1}_3\}^\perp$, where $\mathrm{Im}\,\{\mathbf{1}_3\}^\perp$ is the orthogonal subspace of $\mathrm{Im}\,\{\mathbf{1}_3\}$ in $\mathbb{R}^3$. Projecting (11.1) via P gives the largest part of u_z which is always independent of $v_n - v_r$. This corresponds to the only physical quantity that can be assigned via d. This can be interpreted as the $\alpha\beta$ coordinates of u_z, which means that the 0 coordinate of u_z remains out of control.

Fortunately, in the balanced load case, it appends that u_z belongs to $\mathrm{Im}\,\{\mathbf{1}_3\}^\perp$, so that u_z is actually intrinsically independent of $v_n - v_r$. Exploiting this fact in the last step of the above procedure allows to recover the equation $u_z = Hd$, given at the beginning of Chap. 5 and where u_z is indeed independent $v_n - v_r$.

Post-fault model The proposed framework can easily cop with post-fault control. To see this, suppose that a short-circuit damages the leg of the inverter leg of Fig. 11.3b. Then, the corresponding voltage u becomes either floating or equal to 0 or E. The above methodology can readily handle any of these cases. Thus, a new model can be automatically generated.

> Graph theory automatically considers all the different interconnection topologies of power modules, regardless of their state of health.

Switched non linear models for elementary power modules

Power modules are usually dynamic systems Unlike in the above class of inverters, the causal path from the duty cycle to the output voltages/currents usually involves a differential relationship, so that the resulting input-output is captured by a *dynamic* model. As shown in Fig. 10.3 on p. 180, the modular PC of Chap. 10 illustrates this fact: The output voltage only depends on the duty cycle indirectly via the total current. In this case, the suitable mathematical framework is closer to the contents of Chap. 8 and Chap. 9 than that of Chap. 6.

Even when focusing on the above class of inverters, note that the following two observations suggest that dynamical model is the appropriate tool to extend the previous discussion further.

- The control of voltage vector u_z considered in the above discussion is usually a mere intermediate step toward the control of the currents flowing through the loads. The discussion opening Chap. 7 illustrates this statement by recalling that a possible use of the voltage-source inverter considered in Chap. 5 is the control of the currents flowing into the phases of the AC motors. The causal path between the duty cycles and these currents is captured using a differential map.

- Appropriate treatment of the criteria to be optimized when handling the degrees-of-freedom in the inversion procedure call for dynamic systems. Recall that power loss is a criterion for selecting a suitable homopolar duty cycle d_0 in Chap. 5; see the bibliographical notes ending Chap. 5. Among others, switching losses motivate the use of a current model, and hence a dynamic model, because switching losses depend on the current value at the switching instant [Kaz08].

Power modules should switch between operating modes To reach the optimal steady-state in any operating condition, power modules should be (i) turned off and on, and (ii) switched from Continuous Conduction Mode (CCM) to Discontinuous Conduction Modes (DCM).

Let us consider these two points. (i) To allow a transition between on/off modes, a new binary control input should be introduced for each power module. (ii) If the legs are made of a controlled switch and diode, as in Fig. 10.4a, the rule governing the transition between DCM and CCM depends on the magnitude of the current. In contrast, if two controlled switches are used for the same leg, as shown in Fig. 11.3b, they can be driven in a complementary manner or not [Kaz08]. This induces CCM or DCM *when the average value of the current is sufficiently small*. As a result, the transition between these two modes can also be (partially) controlled via yet another binary control input per power module. Let us emphasize that this kind of binary input is non-standard: In the vast majority of the literature, binary inputs directly drive the state of the controlled switched, whereas, here, the proposed binary input enables or disables the lower controlled switch, while *remaining within in the PWM framework*.

The CCM and DCM averaged current models are distinct. As an example, the following equation is proposed in [Jia+01] as a dynamical current model for the single buck converter in

DCM:

$$\frac{\mathrm{d}}{\mathrm{d}t} i = \frac{E}{L} d - \frac{2iv}{dT_s(E-v)} \tag{11.2}$$

where T_s [s] is the switching frequency and E [V] is the input voltage. Compare (11.2) with (10.3b), where CCM is considered. Note the nonlinearity of (11.2) wrt to $(d, \left[\begin{smallmatrix} i \\ v \end{smallmatrix}\right])$.

Bilinear models capture the dynamic behavior of most of power modules in CCM The most common types of DC/DC converters are well reviewed in [SS06b, Chap.2], namely buck, boost, buck-boost, non-inverting buck-boost, Ćuk, sepic, zeta, quadratic buck, boost-boost, and double buck-boost converters. For any of them, it is shown that the implementation of the PWM strategy leads to a dynamic averaged model that belongs to the class of bilinear systems, *provided that the load is purely resistive and the converter operates permanently in CCM*.

> The switched nonlinear model captures the relevant dynamics for the control purposes of most of the power modules of interest. Bilinear models are a suitable class for capturing the dynamics of power modules operating permanently in CCM.

11.1.3 Toward a robust, priority aware, and constraints compliant universal control-law

Consider any member of the class of voltage-source inverters considered in Sec. 11.1 for any state of health. Based on the above discussion, the mapping from the manipulable duty cycles d to the load voltages u_z can be captured via a static affine system. Consequently, the inversion-based tools of Chap. 6 apply, verbatim. They lead to a controller that is relevant during both the transient and permanent regimes and in any faulty condition. Because this procedure can be entirely reduced to an algorithm, any faults of this type can be handled automatically, that is, post-fault reconfiguration is at hand, provided that the fault can be appropriately detected. In addition, the control framework is universal in the sense that any controller can be viewed as the implementation of a particular policy for dealing with the degrees-of-freedom. Finally, remark that the incidence matrix of the digraph is the only ingredient used in the construction of the model. Unlike system parameters, this matrix is not subjected to uncertainties, so robustness is not expected to be an issue in this case.

The ultimate goal is to achieve analogous results for a universal (dynamic) model of modular PC. To this end, preliminary investigations are outlined. They are intended to complete the material for Chap. 8, Chap. 9 and Chap. 10.

Change of variables to isolate the dynamic induces by complex load behavior

The framework of Chap. 10 not only complies with the hierarchy of the specifications but also greatly simplifies the treatment of nonlinearity in the load model. Indeed, the decoupling introduced in this chapter can be achieved regardless of the load model. This implies that nonlinearities in the load model are confined to subsystem Σ_v with a single virtual module, which can be treated via any results of the literature devoted to standard nonmodular PC, for example, see [KK07; He+18; El +19] for buck, buck-boost, and boost converters, respectively. It is expected that the same decoupling approach can be achieved for some other parallel modular PC, and perhaps other interconnection topologies.

The changes of input and state variables, similar to those discussed in Chap. 10, could be employed to address nonlinear load models by allowing the use of standard results for nonmodular PC on the same type of load.

Hyperrectangles for duty cycle, current and voltage constraints

For any PC, the set $\mathcal{D}$ to which the duty cycle vector d belongs is the hypercube $[0,1]^m$. Hence, the specific case where the input set is a hyperrectangle already encompasses any case of interest when a PWM strategy is implemented.

Guarantying that both the current and voltage limits are not overtaken is also of utmost importance. Overvoltages can indeed destroy submodules in modular multilevel converters [Per+21; Mar18], just like overcurrents can damage the coils in the modular PC considered in Chap. 10.[3] Importantly, these limits are also decentralized saturations and can therefore be captured by the class of hyperrectangles.

The simple class of hyperrectangles already allows the modeling of the duty cycle, current, and voltage constraints.

Control of modular PC is an under-determined output regulation problem

General control problem of PC is an output regulation problem Any control problem associated with a PC can be coded as an output regulation problem. It suffices to associate the input and output references of the PC to a component of the exogenous signal w. Depending on the considered problem, these components can be made constant (DC) or sinusoidal (AC) by defining matrix S accordingly. Recall that treating robustness against parametric uncertainties, including parametric load variation and output feedback, is the standard second-step topic following the full information problem considered in Chap. 10, see [Isi17].

Controlling current/voltage sharing dynamics in a robust and optimal way As in Chap. 10, the steady-state power flow through the modules must be optimized. To this end, essential tools can be found in Chap. 9. Besides, this optimization should be performed despite the load variations.

Let us review the answer to this requirement offered in Chap. 10. In the output regulation problem paradigm, the integrator of C_v in Chap. 10 plays the role of an internal model of the exosystem. By embedding such a model, this enables robustness of the closed-loop voltage deviation dynamics wrt uncertainties of the model, like load variation. In contrast, the current distribution deviation (wrt the optimal one) has been computed by solving an offline model-based optimization problem. This approach is intrinsically fragile to modelling uncertainties.

To enhance the robustness of the optimal current distribution, one can perform an online computation of the optimal current sharing problem. Implementing an extremum-seeking strategy *on the δ dynamic* is one way to proceed. As customary, bad interactions of this additional control layer with the δ dynamic should be easily prevented by resorting to a time-scale separation strategy [AK04]. Let us stress that this extremum seeking strategy does not affect voltage regulation at all.

Note that another motivation for solving the optimal steady-state problem online is the difficulty in computing the analytical solution, see Sec. 7.6.3 in Chap. 7 for insights into how to

[3] As far as the current constraints are concerned, recall that distinct limit values should be used depending on whether the transient or permanent regime is considered; see Rem. 10.2.

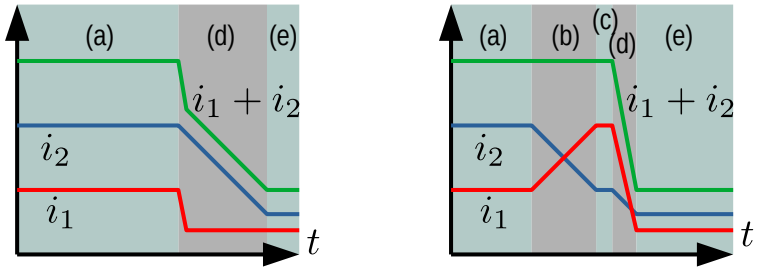

(a) Without preview (b) With preview

Figure 11.6: Impact on the transient of preview on load trajectory. Observe that phase (d) can be made shorter by reconfigure the steady-state in phase (b) before the disturbance changes.

implement this online optimization. Finally, recall that in the most general context, selecting the operating modes (on/off and DCM/CCM) should be part of the optimization process.

Taking advantage of preview on load variations Let us outline another motivation for solving the steady-state optimization problem online. Consider the case of two power modules connected in parallel to a common resistive load, as in Chap. 10. Assume that the load suddenly increases, so that the total current must quickly decrease to regulate the output voltage. Assume further that the controller has some preview on this load variation. In this case, we claim that the transient can be enhanced by taking advantage of the heterogeneity between the two modules. To see this, assume that the first module has a lower inertia than the second one, as in Chap. 10.

- Consider first the scenario where the controller has no preview, as illustrated in Fig. 11.6a. In this case, when the load changes, each power module decreases its current as fast as possible (the duty cycles hit their lower bound, that is 0), individually. In general, the transient duration in phase (d) is determined by the slowest power module.

- If the controller know in advance how the load will vary, as in Fig. 11.6b, more current can flow into the first module than in the second module before the load variation, as illustrated in phase (b). Let us emphasize that this can be achieved in an invisible way from the output by reconfiguring the current sharing and letting the total current unchanged. When the load increases, then the slowest module is already close to its new reference, so that the transient is shorter, as in phase (d). This opposite observation can be made for the other module. This strategy allows for the reduction of the overall transient.
  Note that low inertia typically comes with high steady-state losses, so that the steady-state reconfiguration before load variation should be performed at the last moment, i.e. phase (c) in Fig. 11.6b should be as short as possible.

> The control of modular PC is an under-determined output regulation problem for which the steady state, related to the power flow through the modules, can be optimized online for e.g. avoiding complex analytical solving, improving robustness, and taking advantage of preview on load variations.

11.2 Perspectives on the control of IR systems

Each of the research directions outlined in the previous section for modular power converters can be related to gaps in the control literature. Some existing results that partially fill these gaps are now discussed. Each of them can be seen as perspectives of the previous chapters.

11.2.1 Nonlinear spaces

Reference trajectories compliant with the constraints Unlike Chap. 9, Chap. 8 includes result for the constrained case. Extending the results of Chap. 9 in this direction is to be done. The first step is to enlarge the scope of the incremental analysis developed in [**TK24**] which enabled the derivation of the result in Chap. 8. This results in expressing (u_r, x_r) relative to any $(u_r^p, x_r^p) \in \mathbf{R}(w)$. As stated in Lem. 9.13, the resulting incremental trajectories $(\tilde{u}_r, \tilde{x}_r)$ lie in $\mathbf{R}(\mathbf{0})$, i.e. $y = \mathbf{0}$ is induced by $(\tilde{u}_r, \tilde{x}_r)$. In the constrained context, $(\tilde{u}_r, \tilde{x}_r)$ must also belong to some time-dependent sets. It is anticipated that a result similar to that of Th. 8.15 holds true: The trajectories for which redundancy is destroyed by the constraints are singularities.

Generally, the generation of optimal trajectories satisfying some given constraints can be seen as an optimal control problem. The time horizon corresponds to the period of the periodic exosignal. The initial conditions $w(0)$ and $x(0)$ parametrize the problem and define the terminal constraints to impose the continuity of the periodic trajectories. This topic is closely related to what is often called motion/path planning in robotics [LaV06; Mal+22; Ioa+21] and guidance in the aerospace field [Lu21]. For IR systems subjected to input constraints, the sum-of-square tools used in [VG13] is an interesting starting point for constructive results.

Dealing with the state set Set invariance theory is the traditional framework used to handle state constraints [BM08]. Control barrier function has also be proposed as a tool to achieve constructive results [Ame+19]. See also projected dynamical systems, for which set invariance is ensured by redirecting the vector field at the boundary of the set [HT23].

Particularization to specific type of sets The main results in Chap. 8 on the characterization of IR in the context of input and state constraints are general because they apply to any set. Particularization of Th. 8.15 to some class of sets of interest could strengthen these results with a low loss of generality from the control practitioner point of view. The case of convex sets or even polytopic sets is of particular interest. In the context of convex sets, a suitable characterization of the set $\mathbf{S}$ of IR pairs (x_0, y) may be achieved by leveraging the extremal trajectories. This would mimic the analysis of the null controllable region performed for LTI systems subjected to input saturation, as discussed in [HL01, Chap.2].

Preserving the classical architecture of output regulation One of the aims of this manuscript is to propose an treatment of IR that preserves the classical architecture illustrated in Fig. 9.1 and where the reference trajectories generator R feeds the stabilizer S. Without constraints, it is shown in Chap. 9 that the use of this architecture is not conservative, i.e. any controller solving the output regulation problem can be reformulated in this framework.

Perhaps, this architecture can be exploited to handle nonlinear input and state constraints. The obtained solution will differ from that in [ZCS17]. In this last study, R is indeed allowed to generate reference trajectories for which $e \neq 0$ by allowing what are called intrusive actions. This relaxation is meant to help the stabilizer ensure compliance with the input and state constraints in the transient. In line with Chap. 9, what is envisioned here is to rather make a clear distinction in the roles played by each subsystem: The transient is handled by S, whereas

R only accounts for the steady state and therefore only delivers trajectories compatible with $e = \mathbf{0}$. Equipping both stages with appropriate annihilators is expected to be beneficial for addressing these constraints.

> How can constructive results be derived to handle the input and state constraints? For the output regulation problem, is the classical architecture helpful for this purpose?

11.2.2 Nonlinear dynamics

First results on IR have been obtained for linear systems and linear input and state sets. Very often, dealing with nonlinear dynamics is envisioned as the next step. In this manuscript, we rather tackle the case of nonlinear sets. Let us now give a few references containing insights for the case of nonlinear systems.

Considering the flavor in this manuscript, differential geometry seems to be the natural tool to extend the analysis to a nonlinear vector field. In the control community, standard references on this topic are [NV90; Isi95]; See also [Res90] for results on left and right invertibility.

Perhaps dealing with a less general problem as an initial treatment would yield valuable insights.

- Given the importance of bilinear systems for modular PC, this class of nonlinear systems is of particular interest; See [PY10, Chap.1, Sec.7.3] on left-invertibility of bilinear systems.
- LPV or quasi-LPV systems could be used to enable a linear treatment to nonlinear dynamics [MB04].[4] Results on IR for LPV systems can be found in [KJ22; VKJ24c; VKJ24b]. In [KJ22, Def.1], robust IR is defined by the following condition:

  $$\exists x_0, \exists u_1 \neq u_2, \forall \theta : y_1 = y_2$$

  This definition is close to the treatment of uncertainties proposed in [BM87; CPM91], where a *constant* subspace is said to be a robust controlled invariant if it is controlled invariant for all parameter values. A less restrictive perspective is adopted in [VKJ24c] where adaptive IR means that $\Sigma(\theta)$ is IR for some θ, i.e.

  $$\exists \theta, \exists x_0, \exists u_1 \neq u_2 : y_1 = y_2$$

  Note that, $\theta(\cdot)$ is allowed to be time-varying in [VKJ24c].
  It is expected that IR of (i) the electropneumatic system discussed in [Abr+16] and (ii) the permanent magnet synchronous motor [**Kre+18b**] can be treated via LPV systems. Physically, IR for these systems originates (i) from the independence of the piston position wrt to the sum of the pressure of each chamber, and (ii) the independence of the torque wrt to the current in the d-axis.
- The above discussion highlights that the case of parallel buck converters feeding a constant power load is an example where the nonlinear model is actually an nonlinear SISO mapping surrounded by SIMO and MISO linear maps, i.e. a sandwich system [SSS12, Chap.10]. This feature allows for a linear treatment, effectively confining the nonlinearity to a low-dimensional subsystem, which is merely unilaterally coupled with the remaining linear systems. This kind of combination of linear and nonlinear methods is expected to give elegant constructive results in other cases.

[4] See also [Ilc89] and, in particular, the discussion in the introduction on the advantages of treating nonlinear systems as linear time-varying systems when possible.

How can constructive results be obtained in the case of nonlinear dynamics?

11.2.3 Resolving under-determination of the steady-state

If an exhaustive parametrization of the acceptable steady states is offered in Chap. 9, the computation of the optimal solution was not discussed. Even in the constraint-free context, some remarks can be made on this topic. First, the relevant application can require a non-trivial setup such as a mix integer or non-smooth optimization, even for a set-point steady state. The optimal power flow in modular power converters is an example: Recall that binary inputs should be associated with each module to identify its operating modes (on/of and DCM/CCM). In addition, the cost function (typically, the overall losses) could be non-smooth owing to possible non-differentiability at the transition between the CCM and DCM. We now make two further remarks.

Disturbance rejection with preview Inspired by the above discussion on parallel power modules, we believe that disturbance preview can be exploited for many other systems.[5] The discussion supported by Fig. 11.6 can be generalized as follows: Before an abrupt change in the operating condition, the zero dynamics can be reconfigured by driving the slowest subsystems closer to their expected post-perturbation new set-point. In general, the states of the other subsystems are also modified to make this internal reconfiguration invisible from the output. However, their ability to move faster to the new set point could make the direction of this pre-motion insignificant. Such a strategy could be seen as an *internal* energy redistribution ahead of the disturbance strike.

An additional application of previews is to increase the overall energy of the system, thereby reducing its sensitivity to external disturbances. As an illustration, consider the pneumatic cylinder shown in Fig. 11.7. Assume that the control goal is to regulate the position y of the mass to a constant value. Suppose that a hammer strikes the mass when the system is at rest. The magnitude of the resulting motion of the mass depends on the intrinsic stiffness of the system, which is closely related to the sum of the pressure. Thus, increasing the total pressure ahead of the strike is expected to decrease the post-strike motion. Importantly, this variation in the total pressure can be performed in such a way that the mass does not move. It suffices to preserve the difference in pressures in the two chambers. We emphasize that these conclusions are independent of the aggressiveness of the feedback control law. Indeed, the impulsive nature of the strike prevents the servovalves from modifying the pressure in both chambers fast enough to reject the perturbation, i.e. both servovalves are at their full capacity in the first post-strike phase.

A similar third example is studied in **[Kre+18b]**. A permanent-magnet electrical motor is considered. An abrupt torque demand is assumed so that the manipulable inputs hit their bounds in the immediate post-demand phase. Depending on the direction of torque demand, it is shown that the total energy can be increased or decreased beforehand by adjusting the current in the d-direction. If this current has no impact on the electrical torque, it can be related to its maximal derivative. Because this preloading is energy consuming and must comply with both input voltage and current limits, an optimization problem is formulated to let the user adjust the level of preloading.

[5] The preview scenario over a short horizon could be seen as a realistic tradeoff between the too pessimistic H_∞ case (where nothing is known on w) and the too optimistic one, where w is known on the entire time axis. Note that knowledge of the model of the exosystem, which is commonly assumed in the output regulation framework, is yet another tradeoff of this kind.

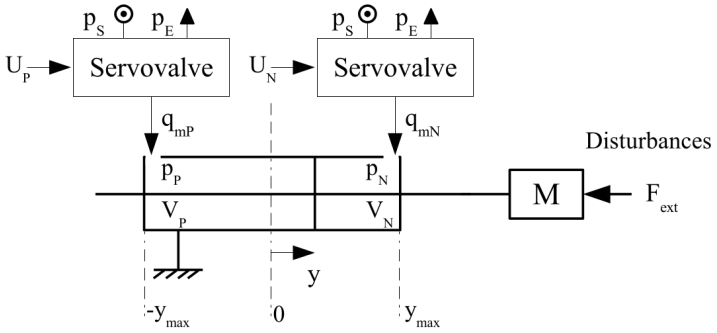

Figure 11.7: Pneumatic cylinder, [Abr+16, Fig.2].

The problem of disturbance rejection with preview is considered in [Tom75; MNZ05; MM06]. In [MNZ05; MM06], the optimality of the rejection is measured via the H_2 norm of the system mapping the disturbance to the output. An explicit connection between this problem and IR has not been reported in any of those papers. In fact, assumption A2 of [MM06] implies left-invertibility, i.e. not IR. In this case, the pre-strike reconfiguration necessarily affects the output. In addition, no input limitations were considered in those studies.

Non stationary permanent regime Most of the times, "optimizing the permanent regime" is thought as "selecting the best input and state *constant* set-point". According to the following quote, in many cases, the search should be enlarged to a nonstationary regime and, in particular, to a periodic steady state.

> "The fact that a periodic operation may be advantageous is well-known to mankind since time immemorial. All farmers know that it is not advisable to always grow the same crop over the same field since the yield can be improved by adopting a crops rotation criterion. So, cycling is good." [BC09, p.x]

It has been shown that some uncertain systems can only be robustly stabilized by resorting to periodic control [KPT85]. This type of control can also improve the closed-loop performance. For instance, "waste production may be suppressed by cycling" [Bai74]. See pioneering applications of this idea in the area of chemical and aerospace engineering fields, see references [1-5] in [BC09]. Furthermore, periodic control has been proposed to stabilize some under-actuated systems [Fre+08; Mor+95; Shi+06]. PWM control of power converters are obviously relevant examples of this kind, considering that binary inputs are nothing but a particular kind of under-actuation; see, for example, [Ben+16] for the construction of an optimal periodic steady state with binary control for multilevel converters. Finally, obstruction to stability via time-invariant control is a strong argument in support of periodic control. One can cite the stabilization in SO(3) [CSM11] and the control of non-holomonic systems [BMZ05; Cor92].

In the output regulation framework, periodicity is induced by the types of trajectories that the exosystem is capable of producing. For suitable control, these persistent oscillations lead to an internal periodic motion of the closed-loop system. Thus, a non-stationary permanent regime is commonly thought to be the (unavoidable) consequence of the periodic reference to be tracked and/or a periodic disturbance to be rejected. Out of the two situations, many examples suggest that periodicity is also desirable. To illustrate this point, consider the orbital station-keeping problem, that is, keeping a spacecraft at a specified distance from, for instance, Earth. The deviation with respect to this distance is the regulated output. In this context, set-point stabilization means that the spacecraft is maintained at a constant location. This, in turn,

requires that a constant force is produced to counteract gravity. Such a scenario is unrealistic, considering the induced energy consumption of the actuators. The well-known solution is to induce an orbital motion while keeping the altitude of the spacecraft constant. In other words, it creates an *internal* periodic regime while maintaining output regulation at zero. A spin stabilization spacecraft is yet another example where a periodic steady state is created by setting the spacecraft spinning (just like a spinning top) in order to use the gyroscopic action of the rotating spacecraft mass as a stabilizing mechanism and, in turn, to decrease the sensitivity to external perturbation. In view of the above discussion, it seems that *intentionally* creating an internal periodic regime can improve the achieved performance in some cases. This scenario is more easily induced on IR system, because the dimension of the zero dynamics is typically larger.

> "Unfortunately, as pointed out in [15], periodic control was still considered "too advanced" in the scenario of industrial control, in that "the steady-state operation is the norm and unsteady process behavior is taboo"."[BC09, p.x]

In this quote, reference [15] dates back to 1972. Has this perception fundamentally changed? The material of Chap. 9, and in particular, the concept of bp-strong annihilator, is a suitable tool to induce a periodic regime and then optimize it, because it allows an exhaustive parametrization of the set of admissible steady states for the output regulation problem, hence including periodic motion.

> How can IR be used for the disturbance rejection problem? An internal periodic steady state can be more easily induced if the system is IR. How can this feature be exploited?

11.2.4 On robustness

The entire manuscript relies on the concept of inversion, that is, feedforward. Not feedback. This approach is usually considered as fragile.[6] We agree with this statement to a certain extent, as indicated by the following observations.

- Inversion can be (sometimes) successfully implemented in practice: The inversion strategy discussed in Chap. 5 for the voltage source inverter has been implemented in practice for years. And it works. Similarly, successful experimental results implementing inversion-based control of the parallel bucks of Chap. 10 were reported in [**TD19**].

- Choosing between feedback and feedforward is not the question: It seems to us that a suitable control scheme is an ingenious blend of inversion and feedback. As a general guideline, we suggest to "inverse what is known by feedforward, and tune the rest online by feedback", see [Dev02] on this topic.

- Fragility is not an absolute concept, because not everything needs to be precise: Generally speaking, control specifications can be classified into two categories: Stability and optimality (of the transient and/or the steady-state). Stability issue is rightly considered very crucial. No compromise should be accepted regarding this. The optimality is different. It seems that in many practical cases, near-optimality is fully acceptable. As an illustration, consider the case of output feedback in an SISO dynamical system. Provided

[6] One should rather say that it is *periodically* considered fragile, in view of the following quote: "Feedback is a very powerful tool, but, maybe because of its simplicity, it often gets overlooked and forgotten, and it seems that its advantages need to be rediscovered every 20 years or so." [Sko09, p.149].

that stability is at hand, the closed-loop performance achieved by a simple proportional controller can be considered satisfactory, even if a small output deviation remains at the steady state. Equipping the controller with an integral part to reach perfect/optimal steady state could sometimes be seen as an unnecessary complication and even irrelevant if, for example, the basin of attraction is reduced. As in the introduction, the message is that the specification list is ordered. If robustness is required for the foremost control goals, near-optimality can be accepted for less important goals. Perhaps our efforts as a control scientist should be allocated in accordance with these lines.

Bearing these generalities in mind, the issue of the robustness of IR systems is discussed.

Necessity of the Non Resonance condition (NRC) is about modelling, not control

NRC is necessary for structural stability Consider that ASM 9.2 on p.150 holds true. In this context, the NRC ASM. 9.3 on p.151 is necessary if structural stability is required, that is, preservation of both closed-loop stability and assumptotic regulation in a neighborhood of the nominal case in the parametric space [Fra77, p.487]. The key point is that, in [Fra77], this parametric space is related to every matrix of the system. In other words, structural stability is related to the robustness wrt *any matrix entries* of the systems. In general, this requirement is too demanding, because some system parameters are known, for example, for a SISO system in the observability canonical form, a single column of the A matrix is parameter-dependent.

The above comment suggests that there exist systems for which the NRC is not valid, but the output regulation problem can be solved robustly, i.e. for any *relevant* parametric variation. Next example is just an illustration of this statement.[7]

Example 11.2. Consider the following system

$$\dot{x} = -\alpha x + u + w \tag{11.3}$$
$$e = \beta\dot{x} = -\alpha\beta x + \beta u + \beta w \tag{11.4}$$

parameterized by $\alpha > 0$ and $\beta \neq 0$, where w is driven by the exosystem $\dot{w} = 0$.
In this case, observe that:

$$\det P_\Sigma(s) = \det \begin{bmatrix} -\alpha - s & 1 \\ -\alpha\beta & \beta \end{bmatrix} = -\beta s \tag{11.5}$$

so that

$$\text{rank}P_\Sigma(0) < \text{nrank}P_\Sigma = 2 \tag{11.6}$$

is valid for all $(\alpha, \beta) \in \mathbb{R} \times \mathbb{R}^*$. This proves that 0 is an invariant zero of the system (as well as an eigenvalue of S) whatever are $(\alpha, \beta) \in \mathbb{R} \times \mathbb{R}^*$, i.e. the NRC is valid nowhere in the parametric space.
However, the output regulation problem is indeed solved if $u = -ke + u_p$, $k > -1$ and u_p is an arbitrary constant. This can be easily seen from the transfer function matrix of $(u_p, w) \mapsto e$:

$$\frac{s}{(1+k)s + \alpha} \begin{bmatrix} 1 & 1 \end{bmatrix}$$

As a last comment, note that the set $\mathbf{R}(w)$ of reference trajectories for which $e = 0$ reads $\mathbf{R}(w) = \{(u_r, x_r) : -\alpha x_r + u_r + w = 0, \dot{u}_r = \dot{x}_r = 0\}$. For all constant w and all $\alpha \in \mathbb{R}$, this set does not reduce to a singleton, i.e. the steady-state is under-determined.

[7] Note that the less trivial system $\dot{w} = 0, \dot{x}_1 = -\gamma x_1 + \alpha x_2 + \alpha u, \dot{x}_2 = \alpha x_2 + \alpha u + \beta w, e = \gamma x_1 + \beta w$ parametrized by $\alpha, \beta, \gamma \in \mathbb{R}^*$ leads to an analogous conclusion.

NRC is necessary for universal solvability of the regulator equations The same conclusions can be drawn by focusing on the regulator equations. Under ASM 9.2, recall that the solvability of these equations is necessary and sufficient for the non-robust problem to admit a solution; see Lem. 9.12. The NRC is necessary and sufficient for the regulator equations to be *universally/generically solvable*, that is, to be solvable for any small enough variation of any entries in the data of the problem; see [Hau83a] reported in [TSH12, Th. 9.10]. This is indeed a well-known fact that robust solvability of algebraic problem is easier to handle than individual solvability, i.e. solvability for given parameter values.[8] Rem. 9.7 of p. 154 can be seen as an illustration of this statement.

Structural analysis for the output regulation problem An intermediary point between universal and individual solvability pertains to structural analysis [DCV03; RAP22]. Recall that the data of structural analysis are merely the identification of which parameters are identically zero, the others being free. For LTI dynamical systems in state space form, it corresponds to the location of fixed zeros in the matrices of the quadruple. From these information, structural analysis investigate systemic properties (like controllability, invertibility, the finite and infinite zero structure) which are true for almost any value of the free parameters (not fixed zero).[9] Structural analysis can be seen as more realistic than the two extreme cases where *all* parameters are assumed (i) to be perfectly known or (ii) to be subjected to uncertainties. Based on this discussion, solving the output regulation problem for structured systems is desirable. This strategy would enable us to leverage a more accurate model that clearly differentiates between elements that are genuinely uncertain and those that are definitively known.

> By focusing on super-robustness, that is, structural stability or universal solvability, the non-resonance condition could be too pessimistic. Adopting the point of view of structural analysis when solving the output regulation problem would be more realistic.

An internal model approach

Robust output regulation for IR systems has already been tackled in the literature. We interpret the approach proposed in [CSZ18] as an adaptive strategy where the dynamics of the input of the *nominal* annihilateur is defined via gradient descent flow dynamics, see [CSZ18, (17)]. References [CPM91; CP93; KJ22; VKJ24b; VKJ24a; VKJ24c] already cited for the LPV case could be used as an essential ingredient to treat the robust case by following the standard strategy of designing an adaptive control law fed by an observer of the uncertainties.

The above strategies share a common characteristic: They do not apply the internal model principle, saying that the internal model of the exogenous system must be embedded to achieve the "super robust" structural stability. We believe that there is potential for further enhancement in the effective application of this principle to IR systems. The following example illustrates the potential results that can be obtained by applying this idea.

Example 11.3 (Ex. 7.4 of Chap. 7 continued)**.** Consider the case in which the second actuator is

[8] As an example, $Ax = b$ is universally solvable in x iff A is full row rank. This condition does not depend on b, unlike the more involved individual solvability condition $b \in \mathrm{Im}\,\{A\}$.

[9] Note that terms in the literature are quite confusing: Structural analysis as in [Fra77] is about non-structured systems as in [DCV03].

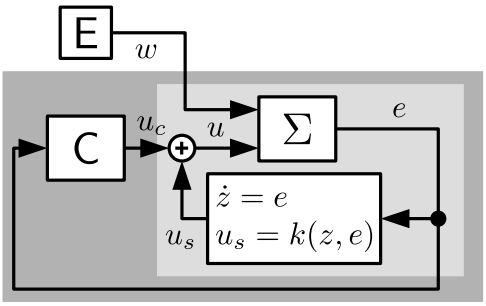

Figure 11.8: An internal approach for the robust case.

dynamic. Recall that the quadruple of the cascade of Σ_a and Σ_p reads as follows:

$$\left[\begin{array}{c|c} A & B \\ \hline C & D \end{array}\right] = \left[\begin{array}{cc|cc} -1 & \beta & 1 & 0 \\ 0 & -\alpha & 0 & \alpha \\ \hline 1 & 0 & 0 & 0 \end{array}\right]$$

The system parameters and their nominal values are $\alpha = 1$ and $\beta = 2$. Define $e = y - w$ with $\dot{w} = 0$. The set of admissible steady-state trajectories

$$\mathbf{R}(w) = \left\{ \left(\begin{bmatrix} w - \beta x_2 \\ u_2 \end{bmatrix}, \begin{bmatrix} w \\ x_2 \end{bmatrix} \right) : \dot{x}_2 = -\alpha x_2 + u_2, u_2 \in \mathbf{B} \cap \mathbf{PC} \right\}$$

can be parametrized by u_2 which is assumed to be bounded and piecewise constant. Let us denote by $\mathbf{R}_i(w) \subset \mathbf{R}(w)$ its subset that gathers the time-invariant trajectories:

$$\mathbf{R}_i(w) = \left\{ \left(t \mapsto u_r^i, t \mapsto x_r^i \right) : \begin{bmatrix} u_r^i \\ x_r^i \end{bmatrix} \in \mathcal{I} := \begin{bmatrix} w(0) \\ 0 \\ w(0) \\ 0 \end{bmatrix} + \text{span} \left\{ \begin{bmatrix} -\beta \\ \alpha \\ 0 \\ 1 \end{bmatrix} \right\} \right\}$$

Recall that the standard problem solution is obtained by selecting *beforehand* the optimal steady-state (u_r, x_r) in $\mathbf{R}_i(w)$ and then implement an internal model strategy, that is, adding the integrator $\dot{z} = e$ and computing a robust stabilizing output controller $u = k(z, e)$ for the augmented system. The closed-loop system then converges asymptotically to the desired steady state. This strategy would be entirely satisfactory if (i) it ensured that the steady state remains optimal, even in the face of unpredictable disturbances, and if (ii) (u_r, x_r) were optimal wrt to $\mathbf{R}(w)$, and not its subset $\mathbf{R}_i(w)$.
We propose retaining the advantages achieved here without questioning the existence of the internal model. In the absence of an accurate plant model, optimality would be pursued by exploring $\mathbf{R}(w)$ via an extra term u_c added to u. As an initial discussion, let us replace $\mathbf{R}(w)$ with $\mathcal{I}$ in the previous sentence. The corresponding picture is shown in Fig. 11.8 where the output of the stabilizer has been renamed u_s. The crucial point here is that this exploration of $\mathcal{I}$ is significantly facilitated by the super-robust inner and outer stability of $\mathcal{I}$. Indeed, this feature ensures that the necessarily partially blind exploration of $\mathcal{I}$ to achieve optimality does not undermine its stability. The foremost control goal $e = \mathbf{0}$ is satisfied in a super-robust manner, whereas optimality *in* $\mathcal{I}$ is treated via a best-effort approach and achieved asymptotically.

Let us comment on the above example.

- Exploration of $\mathcal{I}$: Perhaps an extremum seeking strategy can be implemented to explore $\mathcal{I}$ [AK04], provided that the cost function can be measured (or estimated). Note that the perturbations on e induced by the persistent signal used to locally estimate the gradient of the cost function can be easily rejected within the output regulation framework: It suf-

fices to equip the robust stabilizer with an internal model of this persistant signal. The performance of this rejection is related to the aggressiveness of this stabilizer and can, therefore, be easily tuned.
Perhaps an adaptive strategy can be implemented for this exploration. Recall that the fragility of this approach is not an issue because output regulation and closed-loop stability are at hand.

- A well-known two loops control scheme? Fig. 11.8 ressembles to the classical control scheme, where a slow external loop drives a fast internal one toward the suitable equilibrium; see the bibliographical note of Chap. 10. Let us stress that the two approaches are fundamentally different by the fact that the output regulation is achieved here via the *inner* loop. As this loop is typically the fastest one, the foremost control loop is not artificially slow down by the secondary objective.

- Comparison with [Zac09]: In a way, the proposed approach can be seen as a robustification of the solution in [Zac09], where the role of the annihilator in the WIR case is played here by the combinaison of the stabilizer with the internal model. They become a super-robust dynamic annihilator so that u_c becomes asymptotically invisible on e.

- Reconstruction of the annihilator: From Sec. 7.3.4 in Chap. 7, recall that the Input-to-Output annihilator reads:

$$\mathsf{C}_\perp : u_\perp = \begin{bmatrix} 0 & -\beta \\ 0 & 0 \end{bmatrix} x + \begin{bmatrix} 0 \\ 1 \end{bmatrix} \eta$$

  If such an annihilator is known, then $\mathbf{R}(w)$ could be entirely explored. Perhaps $\mathsf{C}_\perp$ can be reconstructed online by perturbating Σ. Roughly speaking, the idea is to define $\dot{\mathsf{C}}_\perp$ in such a way that the cascade of $\Sigma \circ \mathsf{C}_\perp$ converges to the null operator. A suitable excitation via the input channel u_c may be the solution.

Let us make the following final comment: The entire manuscript can be read as elements for answering the question: How to define a control strategy that decouples distinct dynamics that are related to distinct control purposes? At least how to induce a cascade between them. Two fundamental tools exist to achieve this purpose. The first is time scale separation [Sim62]. This was the central idea in [Zac09]. The second is geometric decomposition. This is at the core of the underlying solution [Ser12]. Perhaps the incertain context is an invitation for control scientists to take advantage of both ideas.

> Time-scale separation is robust but slow. Nominal geometric decomposition is fragile, but there is nothing faster than it because it computes the inverse of the model. How can geometric decomposition be made robust by suitably exploiting time-scale separation?

11.2.5 Miscellaneous

A degree of WIR and bp-WIR

In Chap. 9, the following chain of inclusions has been obtained:

$$(\mathrm{Ker}\,\{B\} \cap \mathrm{Ker}\,\{D\}) \subset \mathcal{N} \subset \mathcal{M}_{bp} \subset \mathcal{M}. \tag{11.7}$$

This allows to decompose the dimension of $\mathcal{M} \subset \mathbb{R}^m$ as the sum of four integers:

$$\dim \mathcal{M} = \rho + \nu + \mu_{bp} + \mu, \tag{11.8}$$

where $\mu_{bp} := \dim(\mathcal{M}_{bp}/\mathcal{N})$ and $\mu := \dim(\mathcal{M}/\mathcal{M}_{bp})$. Each of these integers contributes to the dimension of $\mathcal{M}$ and, in turn, makes Σ WIR. Thus, μ_{bp} and μ could be associated with the degree of WIR and bp-WIR, respectively. As for (ρ, ν), it would be interesting to relate μ_{bp} and μ to the number of some particular input directions, just as it is for ρ and ν at the end of Chap. 8.

> How can we relate μ_{bp} and μ to some input directions?

Computer-aided control design for IR systems

The development of a software environment supporting Chap. 6, Chap. 8 and Chap. 9 could help disseminate their results. Examples include:

- Chap. 6: Automate the computation of $\mathcal{Y}$ and $(\mathrm{H}|\mathcal{U})^+(y)$ when $\mathcal{U}$ is polyhedral. In the LPV case, this leads to a symbolic implementation of the Fourrier-Motzkin algorithm, a less frequent (existing?) feature of existing software solutions;
- Chap. 8: Automate the evaluation of characterizations of IR and the related taxonomy by computing the degree (ρ, ν) of IR. Compute the expression for the matrices of the annihilator of Th. 8.8. Compute the matrices of input and state change of variables associated with the decomposition of Σ.
- Chap. 9: Automate the computation of (i) a basis of the set $\mathcal{F}$ of solutions of the regulator equations, (ii) the characterizations of bp-WIR and the conditions of Th. 9.22, and (iii) the quadruple of Σ_r in Rem. 9.21 in the case of the bp-strong annihilator of Th. 9.24.

A useful starting point for the numerical (non-symbolic) part of these computations is the software developed by G. Basile and G. Marro in the context of geometric control theory [Mar04]. L. Ntogramatzidis and its co-authors also developed many results to compute bases of fundamental spaces in a non recursive way [NS14; PN18; NPF24]. This is an interesting path for more numerically robust algorithms. A symbolic computation of these results would also be highly beneficial, notably for the computation of a basis of $\mathcal{V}^*_{bp}$, for which a Jordan normal form needs to be constructed, a task generally considered numerically fragile.

> A software environment supporting Chap. 6, Chap. 8 and Chap. 9 could help disseminate their results.

An input space decomposition point of view in the dynamic case

Among the three points of view on IR outlined in the introduction (inversion, annihilator, and input space decomposition), implementation of the last one for dynamic systems requires additional developments that are neither included in Chap. 8 nor in Chap. 9. The goal is to construct a suitable decomposition of dynamic systems, from which the controller is directly derived by "mirror construction", just like Fig. 6.4 is obtained from Fig. 6.3 in Chap. 6. In the non-constrained case, this amounts to rephrasing the commutative diagram [Ser12, Fig.1] and extending it to the non-strictly proper case. Block diagrams being a more common tools than commutative diagrams in the control community, this is expected to enlarge the audience of this study.

> Providing an input space decomposition point of view for dynamic systems by constructing a suitable block diagram could enlarge the audience of studies on IR.

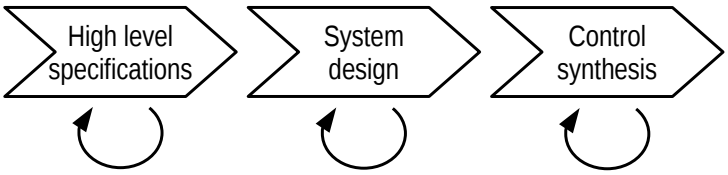

Figure 11.9: Archetype of the design procedure.

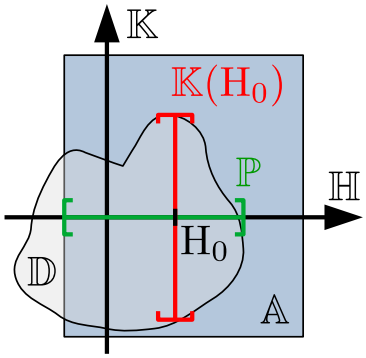

Figure 11.10: Design procedure rephrased as an optimisation problem.

11.3 Co-design

This section provides an overview of the closed-loop system design. The intention is to offer a broad understanding. For this reason, the discussion does not prioritize tractability and deliberately omits explicit consideration of constraints and parametric uncertainties.

11.3.1 An overview of the overall closed-loop system design

A sequential design

A classical view of the closed-loop system design is sketched in Fig. 11.9. The process starts with high-level specifications, which can be roughly thought of as a description of some prescribed behavior in specific case studies. Subsequently, the designer constructs a system by effectively integrating personal skills with professional expertise and established methodologies. In some cases (not always), the control engineer comes into play at the last step to allow an increase of performance of the system, that is confer/improve the ability of the controlled system "to react to changes in demand, specifications, feedstock, and the environment in an economical and safe manner" [PI92, p.3].

In this process, control synthesis comes at the very end, when the system is already fully designed and sometimes even built. Based on a synthesis model and control-oriented specifications, his duty is to synthesize the control law to ensure that these specifications are fulfilled by the closed-loop system.

In practice, this procedure is not strictly linear. Iterations frequently occur within each of the three stages, as shown in Fig. 11.9. Nevertheless, the organization of the primary stages of the overall approach often mirrors this sequential process.

Rephrasing the overall closed-loop system design as an optimization problem

Let us use "optimization grammar" to describe this process. Fig. 11.10 supports this discussion. Let $\mathbb{H}$ and $\mathbb{K}$ be the sets of all (open-loop) systems and controllers, respectively. Denote

by $\mathrm{H} \star K \in \mathbb{H} \times \mathbb{K}$ the closed-loop system resulting from the interconnection of the controller $K \in \mathbb{K}$ and the open-loop system $\mathrm{H} \in \mathbb{H}$.[10] Let $\mathbb{A} \subset \mathbb{H} \times \mathbb{K}$ be the subset of closed-loop systems that are achievable and technologically feasible. Define $\mathbb{D} \subset \mathbb{H} \times \mathbb{K}$ as the set of closed-loop system that meet the specifications.[11] Then, the overall design process can be translated as follows:

$$\min_{\mathrm{H},K} J(\mathrm{H} \star K) \quad \text{s.t.} \quad \mathrm{H} \star K \in \mathbb{D} \cap \mathbb{A} \tag{11.9}$$

where $J : \mathbb{H} \times \mathbb{K} \to \mathbb{R}_{\geq 0}$ denotes a suitable real-valued cost function.

The optimization problem (11.9) does not correctly model the procedure in Fig. 11.9, because it is not sequential, i.e. both H and K are computed simultaneously. To capture the process shown in Fig. 11.9, let us introduce the following projection:

$$\mathbb{P} := \{\mathrm{H} \in \mathbb{H} : \exists K \in \mathbb{K},\ \mathrm{H} \star K \in \mathbb{D} \cap \mathbb{A}\}$$

Set $\mathbb{P}$ gathers all systems for which a suitable controller exists. Note how "$\exists K$" anticipates the control synthesis step. The control synthesis step then involves selecting K in the following set:

$$\mathbb{K}(\mathrm{H}) := \{K \in \mathbb{K} : \mathrm{H} \star K \in \mathbb{D} \cap \mathbb{A}\}$$

Fig. 11.10 illustrates these sets. Problem (11.9) can be *equivalently* reformulated as follows:

$$\min_{\mathrm{H} \in \mathbb{P}} \min_{K \in \mathbb{K}(\mathrm{H})} J(\mathrm{H} \star K) \tag{11.10}$$

> Control synthesis can be anticipated at the system design step via suitable projection of the set of admissible closed-loop systems.

On control synthesis

Let us now provide a more precise formulation of the set $\mathbb{D}$, which is related to the appropriate behavior of the closed-loop system. For this purpose, the following quote is helpful:

> "At least conceptually, one can distinguish two types of requirements: flexibility, i.e., the ability of the system to handle a new situation at steady state, and controllability, i.e., the ability of the system to accomplish the dynamic transition between the operating states in an acceptable manner." [PI92, p.4]

Let us retain this terminology in this section.[12] This leads to the following reformulation of $\mathbb{D}$:

$$\mathbb{D} = \mathbb{D}_f \cap \mathbb{D}_c$$

where $\mathbb{D}_f$ and $\mathbb{D}_c$ capture the set of closed-loop systems that are flexible and controllable, respectively.

The next quote is useful to go further in the formalisation of $\mathbb{D}$:[13]

[10] For simplicity, assume that any controller can be interconnected with any open-loop system so that the set of closed-loop systems is $\mathbb{H} \times \mathbb{K}$.

[11] Following [BB91, p.48], a specification is thought of as a boolean function or test on the closed-loop model. If the latter behaves appropriately, the function gives true, and false otherwise.

[12] It is important to note that the definitions of these concepts are inconsistent across the literature. This observation is particularly valid for the notion of controllability; see [SP05, p.162] for a discussion on this topic.

[13] In [SP05], this is the definition of what is called "(Input-output) controllability".

> "The ability to achieve acceptable control performance; that is, to keep the outputs (y) within specified bounds or displacements from their references (r), in spite of unknown but bounded variations, such as disturbances (w) and plant changes (including uncertainty), using available inputs (u) and available measurements (y_m or d_m)." [SP05, p.160]

This definition seems effective for both flexibility and controllability. Let us formalize this definition by considering that the closed-loop system $\mathrm{H} \star K$ maps the disturbance w and the initial state of the augmented system $x_a(0)$ to the regulated output $e = r - y$. For clarity of the exposition, let us discarding the "plant changes" due to uncertainty. In this case, the concept of controllability is coded as follows:

$$\forall w, \forall x_a(0) : \|e\| \leq \epsilon_c \quad \text{with} \quad e = (\mathrm{H} \star K)[w, x_a(0)] \tag{11.11}$$

for a given $\epsilon_c \geq 0$. A more precise definition of $\mathbb{D}_c$ can now be given:

$$\mathbb{D}_c = \{(\mathrm{H}, K) \in \mathbb{H} \times \mathbb{K} : (11.11)\}$$

An analogous definition can be obtained to model the concept of flexibility by substituting $\forall x_a(0)$ by $\exists x_a(0)$:

$$\mathbb{D}_f = \{(\mathrm{H}, K) \in \mathbb{H} \times \mathbb{K} : (11.12)\}$$

with

$$\forall w, \exists x_a(0) : \|e\| \leq \epsilon_f \quad \text{with} \quad e = (\mathrm{H} \star K)[w, x_a(0)] \tag{11.12}$$

for a given $\epsilon_f \geq 0$.

Note that $\mathbb{D}_c$ and $\mathbb{D}_f$ are parameterized by ϵ_c and ϵ_f, respectively. These scalars reflect the strength of the requirements.

Remark 11.4 (Light notational framework). To keep the discussion fluent, this section retains a light notational framework. In particular, it is implicite that signals w in (11.11) and (11.12) are to be selected in some set $\mathbf{W}$ whose definition is part of the specifications modelling. Similarly, the dependencies with respect to the scalars ϵ_c and ϵ_f remain implicit. •

Remark 11.5 (On the modeling of specifications). The retained formulations of the specifications in both (11.11) and (11.12) are very close to that of the output regulation problem. Specification modeling is a research topic on its own, so we do not pretend to any exhaustiveness. The reader is referred to e.g. [BB91] and [And+19] for the standard specifications. Some of less classical formulations can be found in e.g. [BJV19; SVB23] for a contract formulation that was originally developed in computer science and [BM08] for set-invariance formulation. •

Remark 11.6 (Limitations of performance). We emphasize that the framework chosen here to model the performance limits of the closed loop differs from what is classically discussed in the literature in the context of "limitations on performance", see e.g. [SP05, Sec.5-6]. The existing discussions are often general in the sense that they do not assume any particular control architecture, but they are often specific because they focus on a particular class of controllers, typically LTI controllers. It is known that enlarging this class can enhance performance, see e.g. [Zha+19]. •

The control configuration

From the above discussion, the data for the control synthesis are the model H and the levels $\epsilon_{c,f}$ of the required closed-loop performance. This implies that the outcomes of the following tasks are already set:

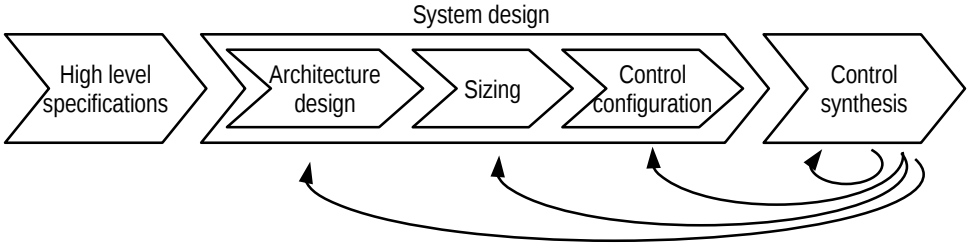

Figure 11.11: Sequential design, with feedbacks.

- model the control-oriented specifications, which includes:
  - modelling of noises or disturbances that may act on the system, i.e. define **W** in which admissible w belong to;
  - modelling desirable or required qualities of the closed-loop system, i.e. select the value of ϵ;
  - decide which variables are to be controlled, i.e. define the regulated output map associated with e;
- select and place the actuators and sensors, i.e. define the input and measured output maps;
- deriving a mathematical model that is suitable for control synthesis, i.e define H.

The outcomes of these tasks constitue what we call the "control configuration". Note that many textbooks on control focus exclusively on controller synthesis and closed-loop analysis. Thus, the control configuration is implicitly out of their scope. However, after others, we believe that this task is very important to control engineers. They should be involved in it and not just provided with the data listed above. The control configuration is indeed a "middle area" between the system design and the control synthesis.

Recognizing the point regarding the control engineer's role in shaping the control configuration, let us nevertheless consider this step as a part of the system design to ensure that the discussion remains coherent; see Fig. 11.11.

11.3.2 Toward co-design: a paradigm shift

What is wrong with the sequential procedure?

It is now argued that this sequential design is not always satisfactory. In particular, it may fail in practice to produce a closed loop that meets the specifications. Note that the closed-loop performance can only be entirely assessed once the ultimate step of the control synthesis is completed.

- $\mathbb{K}(\mathrm{H})$ is poorly known. Indeed, control theory is limited, as are control engineers and scientists. Consequently, in the case where control synthesis fails, the control engineer is left with two alternatives. First, reconsider the control synthesis by, for example, changing the control architecture and the gain synthesis method. Second, give up, following the conviction that a suitable controller does not exist, i.e. $\mathbb{K}(\mathrm{H})$ is empty. Deciding the right options between these two is a difficult task because an explicit expression of $\mathbb{K}(\mathrm{H})$ is usually not available.

- Control limitations are not always correctly anticipated at the design step, so that $\mathbb{P}$ is poorly known too. As a result, control synthesis may be very well implemented on corrompt data for which H does not belong to $\mathbb{P}$, i.e. $\mathbb{K}(\mathrm{H})$ is empty. By definition, this means that control synthesis becomes an unsolvable problem in this case.

Not surprisingly for control scientists, we feel that the answer to uncertainties is feedback. In the present case, this amounts to providing the engineer in charge of the upstream tasks with information related to the failure. Fig. 11.11 illustrates this process. With this representation in mind, if something goes wrong at the control synthesis step, then it seems natural to start by reconsidering the control configuration. Specifically, the specifications can be weakened. Adding new actuators or sensors is another option.

Modifying the system itself

As indicated by Fig. 11.11, the control configuration is established for a specific system. In cases where control synthesis is unsuccessful, one can look beyond the control configuration itself. It may be necessary to "reconstruct" the sequential pathway depicted in Fig. 11.9 to evaluate the system design critically. The challenge lies in determining whether the origin of the fail can be attributed to H or K.

Viewing the design of plant and control laws as a unified entity is not a novel idea, as evidenced by the following quote from a paper by Ziegler and Nichols published in 1943:

> "In the application of automatic controllers, it is important to realize that controller and process form a unit; credit or discredit for results obtained are attributable to one as much as the other. A poor controller is often able to perform acceptably on a process that is easily controlled. The finest controller made, when applied to a miserably designed process, may not deliver the desired performance. True, on badly designed processes, advanced controllers are able to eke out better results than older models, but on these processes, there is a definite end point which can be approached by instrumentation and it falls short of perfection." [ZN42]

Just like control synthesis can be decomposed into control structure selection and gain computation, system design can be split into (i) system architecture design and (ii) sizing of components, as illustrated in Fig. 11.11. Typically, the decision variables of (i) are integers, whereas those of (ii) are real numbers. To account for this distinction, the set of systems is decomposed as follows:

$$\mathbb{H} = \mathrm{H}_1(\mathcal{M}_1) \cup \ \ldots \ \cup \mathrm{H}_I(\mathcal{M}_r)$$

where H_k is the system corresponding to the k-th architecture and $\mathcal{M}_k$ is the set to which the continuous variables for this architecture belong.

Integrate sizing and control synthesis Sizing is the problem of selecting suitable continuous parameters for a given system architecture, i.e. find H in $\mathrm{H}_k(\mathcal{M}_k)$, where k is given. The following quote clearly highlights the interplay between sizing and control synthesis:

> "To reduce the effects of a disturbance one may in process control consider changing the size of a buffer tank, or in automotive control one might decide to change the properties of a spring. In other situations, the speed of response of a measurement device might be an important factor in achieving acceptable control." [SP05, p.160]

To account for this coupling, the following subproblem is derived from (11.10) by substituting $\mathbb{H}$ with $\mathrm{H}_k(\mathcal{M}_k)$ as follows:

$$\min_{\mathrm{H}\in\mathrm{H}_k(\mathcal{M}_k)} \min_{K\in\mathbb{K}(\mathrm{H})} J(\mathrm{H}\star K) \tag{11.13}$$

In general, $\mathrm{H}_k(\mathcal{M}_k)$ is a proper subset of $\mathbb{H}$ so that the minimum of (11.13) is greater or equal than the minimum (11.10).

Integrate architecture design and control synthesis If the achievable performance for a given architecture is unsatisfactory, one can go further than the sizing adjustment by reconsidering the system architecture itself. In this case, the value of k can be modified via an additional optimization layer, so that one obtains

$$\min_{k\in[\![1,I]\!]} \min_{\mathrm{H}\in\mathrm{H}_k(\mathcal{M}_k)} \min_{K\in\mathbb{K}(\mathrm{H})} J(\mathrm{H}\star K) \tag{11.14}$$

Unlike (11.13), problem (11.14) is equivalent to (11.10). The added value of (11.14) is to highlight the two-stage problem better, where the architecture is selected before seeking for optimal sizing.

Remark 11.7. Structural analysis serves as an effective tool for distinguishing between architectural design and sizing [DCV03; RAP22]. Although it is primarily an analytical method, it can also be employed as a design tool in this context. •

11.3.3 How can control community contribute?

An open-loop perspective

It is now demonstrated that inversion tools can be helpful for computing $\mathbb{P}$. Recall that this set gathers open-loop systems H such that there exists a controller K for which the closed-loop $\mathrm{H}\star K$ is achievable and meets the specifications. Let us focus on the specifications and treat flexibility and controllability separately by way of the following sets:

$$\mathbb{P}^c_{\mathbb{D}} := \{\mathbb{H}\in\mathbb{H} : \exists K\in\mathbb{K},\ \mathrm{H}\star K\in\mathbb{D}_c\} \supset \mathbb{P}$$
$$\mathbb{P}^f_{\mathbb{D}} := \{\mathbb{H}\in\mathbb{H} : \exists K\in\mathbb{K},\ \mathrm{H}\star K\in\mathbb{D}_f\} \supset \mathbb{P}$$

Clearly, there is a suitable controller for the controllability task only if, for all w, there exists a suitable input for the open-loop system $(w, x(0), u) \mapsto e = \mathrm{H}^w[x(0); u]$, i.e. the following condition is necessary for the existence of such a controller:

$$\forall w, \forall x(0), \exists u : \|e\| \le \epsilon_c \quad \text{with} \quad e = \mathrm{H}^w[x(0); u] \tag{11.15}$$

It is also sufficient, as open-loop controller must not be excluded.[14] Hence, $\mathbb{P}^c_{\mathbb{D}}$ is the set of $\mathrm{H}\in\mathbb{H}$ for which (11.15) holds. Similarly, flexibility can be treated by substituting $\forall x(0)$ by $\exists x(0)$ in (11.15), i.e.

$$\forall w, \exists x(0), \exists u : \|e\| \le \epsilon_f \quad \text{with} \quad e = \mathrm{H}^w[x(0); u] \tag{11.16}$$

Hence, $\mathbb{P}^f_{\mathbb{D}}$ is the set of $\mathrm{H}\in\mathbb{H}$ for which (11.16) holds. The idea of this discussion is to remove K from (11.11) and (11.12): Both conditions (11.16) and (11.15) depend only on H. This reformulation is just what is required at the design step.

[14] For simplicity, we implicitly assume that w is known, so that open-loop strategy is implementable.

For simplicity, assume that the achievability of the design only depends on H, i.e. there exists $\mathbb{A}_H \subset \mathbb{H}$ such that $\mathbb{A} = \mathbb{A}_H \times \mathbb{K}$. Then, $\mathbb{P}$ reads:

$$\mathbb{P} = \{\mathrm{H} \in \mathbb{A}_H : (11.15), (11.16)\}$$

Thus, the system design step can be implemented by testing (11.15) and (11.16) to validate achievable open-loop candidates in the sense that the existence of a suitable controller is ensured.

Our point is that (11.15) and (11.16) are about the inversion of dynamical systems. A topic on which the control community has recognized expertise. Therefore, control engineers have suitable tools to help system designers.

> Obstruction to the existence of a satisfactory controller can be anticipated by inversion at the system design step.

How the tools of this manuscript are related to this discussion?

IR is super controllability Assume that (11.15) holds, so that there exists u such that $\|e\| \leq \epsilon_c$ holds, given arbitrary w and $x(0)$. Then, this input u inducing this e is non-unique iff there exists $\tilde{u}$ satisfying $\mathrm{H}[\mathbf{0}; \tilde{u}] = \mathbf{0}$.[15] This situation is just one of the key characterizations of IR. An exhaustive parameterization of all u leading to output e can be obtained via the (simple) annihilator given in Chap. 8 in view of the maximality of its range.

Therefore, if an IR model H is controllable in the sense of (11.11), then it is somehow super-controllable. We emphasize that this discussion does not depend on ϵ_c.

"WIR or unobservability" is super flexibility Similarly, assume that (11.16) holds, so that there exist $x(0)$ and u such that $e = \mathrm{H}^w[x(0); u]$ is satisfied, given an arbitrary w. This pair $(x(0), u)$ inducing this e is non-unique iff there exist $\tilde{x}_0$ and $\tilde{u}$ such that $\mathrm{H}[\tilde{x}_0; \tilde{u}] = \mathbf{0}$ holds true, which is just the situation characterized by Th. 9.15. An exhaustive parametrization of the pairs $(u, x(0))$ leading to the same e can also be obtained, this time via the strong annihilator of Chap. 9.[16]

Therefore, if a model H satisfies any of the equivalent items of Th. 9.15 (like "WIR or unobservability") and is also flexible, in the sense of (11.12), then it is somehow super-flexible. The discussion does not depend on ϵ_f.

Remark 11.8. The tools in Chap. 6 give rise to analogous results when the system is static and affine. •

This manuscript focuses on success analysis From the outset of this section, it is suggested that a comprehensive analysis is essential when a design fails. This is indeed true. However, success requires an equally detailed analysis. Generally, failure results in the weakening of high-level specifications or over-dimensioning, whereas success necessitates just the opposite: strengthening specifications and/or downsizing to be as close as possible to the optimal design. In both scenarios, determining the appropriate actions requires a thorough analysis.

As discussed earlier, the tools presented in this manuscript facilitate the analysis of success. For a given model H, sufficient conditions are available to predict at the design step whether the controller demonstrating flexibility or controllability is unique. Furthermore, a subset of such satisfactory controllers can be parameterized. Consequently, the tools developed allow us

[15] This follows from (9.5), which is valid with H^w in place of H^w_x.

[16] Recall that Chap. 9 also offers tools to treat the case in which bp of $(\tilde{u}, \tilde{x})$ is also required, with $\tilde{x} = \mathrm{H}_x[\tilde{x}_0; \tilde{u}]$.

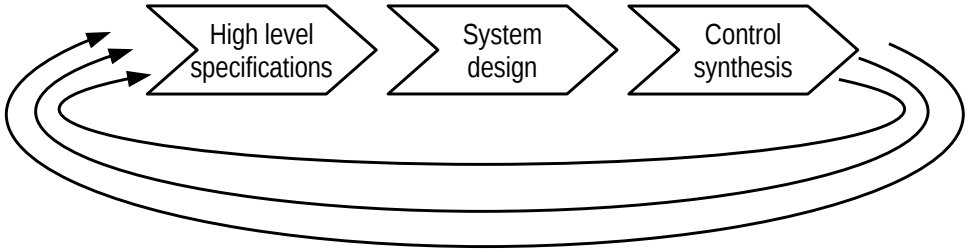

Figure 11.12: Sequential design, encapsulated within iterations.

to analyze the successes by identifying the directions where degrees of freedom exist. These tools can then be applied to address new specifications *without altering those that are already considered*. The list of specifications constructed in this manner is ordered naturally, as in the introduction of this manuscript.

11.3.4 Discussion

On tractability This discussion demonstrates that the design process can be equivalently reformulated as a sequential process by utilizing projections. Additionally, a controlled synthesis step can be anticipated through inversion.

The discussion is conducted at the conceptual level, discarding about tractability issues of the considered optimization problem.[17] In this context, the hierarchy of solving methods follows a traditional approach. First, prioritize an analytical solution, although it is seldom attainable outside the realm of affine sets and mappings. Second, look for convexity, as it typically results in a problem that can be solved numerically.

Is successes more frequent than fails? Our review of the literature apparently suggests that the majority of efforts have concentrated on analyzing failures rather than successes. This focus is reminiscent of the disparity in attention the control community has paid to issues of under-actuation compared with those of over-actuation. This focus in the literature is entirely justified if the design approach is too optimistic. If the iterative process shown in Fig. 11.9 with demanding high-level specifications, then the failure will most probably be encountered, so that specifications will have to be weakened.

However, an alternative approach is possible. Begin a design with rudimentary specifications, reduce to the essentials, and then enrich it through successive iterations in specific directions that are determined by analysis conducted at each stage. Start with a vague idea of what the system can achieve and refine the specifications as the design progresses. Our feeling is that this way to proceed can be more easily implemented. When facing a complex design, one often starts with the foremost goal of the design, *and nothing else*. Analysis of the expected success then certainly reveals that additional specification can be incorporated in some specific directions.

Beetween formal optimization, heuristict and engineering expertize A perfect plug-and-play algorithm for solving the universal engineering problem is obviously hopeless. The goal of this section is to employ the language of optimization to offer an overview of the analy-

[17] There are two reasons for this decision. First, untractability is a vanishing horizon owing to computational and methodological progress. Second, the aim is to provide a general picture of the problem, discarding the implementation details.

sis, thereby facilitating interdisciplinary collaboration and distinguishing between steps where mathematical optimization is feasible and those where the designer's expertise is essential.

How can this process be performed? We firmly believe that control scientists should be involved in the design discussion as soon as possible. Preferably, even at the step of defining high-level specifications. The goal is to reach a mutual understanding of the challenges associated with making specific design choices and using particular control configurations. Common tools are essential for such a discussion. One such method is structural analysis. Output regulation can also serve as another one, in the way it captures various control-oriented specifications.

In line with the previous discussion, the next step involves formulating an initial rough specification. Maintaining a sequential process is not necessarily disadvantageous, provided that it is encapsulated within iterations, as illustrated in Fig. 11.12. This approach allows for the introduction of models that start simple and gradually increase in complexity. An idea that is very familiar to control scientists who are used to play with models of distinct accuracy.

In concluding this chapter, let us clearly outline the following research direction, which can serve as a unifying theme for the entire manuscript.

> How can we design a methodology for the co-design of modular power converters, that is, the design of the topology (system architecture), sizing of components, control architecture, and gain synthesis?

Appendix A

Background on geometric control theory

This manuscript heavily relies on geometric control theory that was pioneered by G. Marro and G. Basile [BM69], on one side (of the Atlantic), and A. Morse, W. Wonham [WM70], on the other side. The useful concepts for our purpose in this research field are now briefly outlined. For broader treatment, the reader is referred to standard monographs [Won85; BM92; TSH12] and, in particular, to [Won85, Chap. 0] or [TSH12, Sec. 2.2] for the notational background. See also the tutorial paper [Mar+10] for a concise introduction to this topic or [**TK23**, Appendix A] for a personal note pursuing a similar goal, but focusing on the material related to the topic of this manuscript.

A.1 State trajectories of autonomous system

Define $\mathcal{X}_g$ as follows:

$$\mathcal{X}_g \coloneqq \sup\{\mathcal{V} : A\mathcal{V} \subset \mathcal{V}, \sigma(A|\mathcal{V}) \subset \mathbb{C}^-\}. \tag{A.1}$$

and recall the definition of $\mathcal{X}_{bp}$, see p.163:

$$\mathcal{X}_{bp} \coloneqq \sup\{\mathcal{V} : A\mathcal{V} \subset \mathcal{V}, \sigma(A|\mathcal{V}) \subset \mathbb{C}^0, A|\mathcal{V} \text{ is semi-simple}\}$$

The intersection $\mathcal{X}_g \cap \mathcal{X}_{bp}$ is trivial.[1] Thus, there exists a subspace $\mathcal{X}_b \subset \mathbb{R}^n$ such that:

$$\mathbb{R}^n = \mathcal{X}_g \oplus \mathcal{X}_{bp} \oplus \mathcal{X}_b \tag{A.2}$$

holds.

This decomposition can be related to the classical state-space decomposition into the stable subspace $\mathcal{X}_s$, the center subspace $\mathcal{X}_c$ and the unstable subspace $\mathcal{X}_u$, which are now defined, following [Per01, Sec. 1.9]. Let $w_j = u_j + iv_j$ with $u_j, v_j \in \mathbb{R}^n$ be a generalized eigenvector of A corresponding to an eigenvalue $\lambda_j \in \sigma(A)$. Assume that the first $\iota \in \mathbb{N}$ eigenvalues are real, so that $v_j = \mathbf{0}, (j \in [\![1, \iota]\!])$. Define $\varpi \in \mathbb{N}$ via $2\varpi - \iota = n$ and let

$$\{u_1, \ldots, u_\iota, u_{\iota+1}, v_{\iota+1}, \ldots, u_\varpi, v_\varpi\} \tag{A.3}$$

be a basis of $\mathbb{R}^n$. Then, it holds:

$$\begin{aligned}
\mathcal{X}_s &\coloneqq \operatorname{span}\left\{u_j, v_j : \lambda_j \in \mathbb{C}^-\right\}, \\
\mathcal{X}_c &\coloneqq \operatorname{span}\left\{u_j, v_j : \lambda_j \in \mathbb{C}^0\right\}, \\
\mathcal{X}_u &\coloneqq \operatorname{span}\left\{u_j, v_j : \lambda_j \in \mathbb{C}^+\right\},
\end{aligned}$$

[1] By convention, the trivial A-invariant subspace $\{\mathbf{0}\}$ belongs to both $\mathcal{X}_g$ and $\mathcal{X}_{bp}$.

From [Per01, Th.1, p.55], those subspaces are all A-invariant and satisfy

$$\mathbb{R}^n = \mathcal{X}_s \oplus \mathcal{X}_c \oplus \mathcal{X}_u. \tag{A.4}$$

Lemma A.1. *It holds $\mathcal{X}_s = \mathcal{X}_g$ and $\mathcal{X}_{bp} \subset \mathcal{X}_c$.*

Proof. To prove that $\mathcal{X}_s$ equals $\mathcal{X}_g$, pick any $\mathcal{V}$ satisfying $\mathcal{X}_s \subset \mathcal{V} \subset \mathcal{X}_g$. Note that $\mathcal{V} \subset \mathcal{X}_g$ implies that $\mathcal{V}$ is A-invariant. From $\mathcal{X}_s \subset \mathcal{V}$ and (A.4), there exists an A-invariant subspace $\mathcal{V}_{cu} \subset \mathcal{X}_{cu} := \mathcal{X}_c \oplus \mathcal{X}_u$ such that $\mathcal{V} = \mathcal{X}_s \oplus \mathcal{V}_{cu}$ by virtue of Fact. A.12. Hence, one gets $\sigma(A|\mathcal{V}) = \sigma(A|\mathcal{X}_s) \uplus \sigma(A|\mathcal{V}_{cu})$. From $\mathcal{V} \subset \mathcal{X}_g$, this spectrum must be included in $\mathbb{C}^-$ which implies $\sigma(A|\mathcal{V}_{cu}) \subset \mathbb{C}^-$. Since $\sigma(A|\mathcal{V}_{cu}) \subset \sigma(A|\mathcal{X}_{cu}) \subset \mathbb{C}^0 \cup \mathbb{C}^+$, this implies that $\mathcal{V}_{cu}$ is trivial, so that $\mathcal{V} = \mathcal{X}_s$ holds. This proves that $\mathcal{X}_s$ is the largest A-invariant subspace $\mathcal{V}$ such that $\sigma(A|\mathcal{V}) \subset \mathbb{C}^-$, i.e. $\mathcal{X}_s$ equals $\mathcal{X}_g$.

Similarly, one can prove that $\mathcal{X}_c$ is the largest A-invariant subspace $\mathcal{V}$ such that $\sigma(A|\mathcal{V}) \subset \mathbb{C}^0$. This implies $\mathcal{X}_{bp} \subset \mathcal{X}_c$. □

Remark A.2 (The two decompositions of $\mathcal{X}$). From Lem. A.1, there exists $\mathcal{X}_{u0}$ such that $\mathcal{X}_{u0} \oplus \mathcal{X}_{bp} = \mathcal{X}_c$. This leads to:

$$\underbrace{\mathcal{X}_s}_{\mathcal{X}_g} \oplus \overbrace{\mathcal{X}_{bp} \oplus \underbrace{\mathcal{X}_{u0}}_{\mathcal{X}_b}}^{\mathcal{X}_c} \oplus \mathcal{X}_u$$

which relates the different decompositions of $\mathbb{R}^n$. •

The set of x_0 such that $\mathrm{H}_x[x_0; \mathbf{0}]$ is bp is not a subspace, since $x_0 = \mathbf{0}$ does not belong to this set. However, it can be related to $\mathcal{X}_g$ and $\mathcal{X}_{bp}$ as shown by the next lemma, by exploiting classical results on state trajectories initiated in the stable, centered, or unstable subspaces.

Lemma A.3. *It holds:*

$$\{x_0 : \mathrm{H}_x[x_0; \mathbf{0}] \textit{ is bp}\} = (\mathcal{X}_g + \mathcal{X}_{bp}) \setminus \mathcal{X}_g \tag{A.5}$$

$$\{\mathbf{0}\} \cup \{x_0 : \mathrm{H}_x[x_0; \mathbf{0}] \textit{ is bp}\} \supset \mathcal{X}_{bp} \tag{A.6}$$

$$\{x_0 : \mathrm{H}_x[x_0; \mathbf{0}] \textit{ is periodic}\} = \mathcal{X}_{bp} \tag{A.7}$$

Proof. Eq. (A.2) allows to decompose x_0 as $x_{0,g} + x_{0,bp} + x_{0,b}$. From the linearity of $\mathrm{H}_x[\cdot; \mathbf{0}]$, $x := \mathrm{H}_x[x_0; \mathbf{0}]$ equals $x_g + x_{bp} + x_b$ with $x_a := \mathrm{H}_x[x_{0,a}; \mathbf{0}]$ for all $a \in \{g, bp, b\}$. In view of e.g. [CC97, Th.3.11, p.75], $\|x_b(t)\|$ tends to infinity iff $x_{0,b} \neq \mathbf{0}$; $x_g(t)$ tends to zero for all $x_{0,g}$; x_{bp} is bp iff $x_{0,bp} \neq \mathbf{0}$. Thus, x is bp iff $x_{bp}(0) \neq \mathbf{0}$ and $x_b(0) = \mathbf{0}$. This proves both (A.5) and (A.6). (A.7) follows from the fact that x is periodic iff $x_b = \mathbf{0}$ and $x_g = \mathbf{0}$. □

A.2 The unobservable subspace

- Let $\mathcal{K} := \mathrm{Ker}\,\{C\}$. The unobservable subspace $\langle \mathcal{K}|A \rangle \subset \mathbb{R}^n$ reads

$$\langle \mathcal{K}|A \rangle := \{x_0 \in \mathbb{R}^n : \mathrm{H}[x_0; \mathbf{0}] = \mathbf{0}\}.$$

- As suggested by the standard notation $\langle \cdot|\cdot \rangle$, $\langle \mathcal{K}|A \rangle$ coincides with the largest A-invariant subspace contained in $\mathcal{K}$, i.e. the largest subspace $\mathcal{V}$ satisfying:

$$\begin{bmatrix} A \\ C \end{bmatrix} \mathcal{V} \subset \mathcal{V} \oplus \{\mathbf{0}\}$$

- Alternatively, $\langle \mathcal{K}|A \rangle$ can be characterized as follows:

$$\langle \mathcal{K}|A \rangle = \bigcap_{i=0}^{n-1} A^{-i}\mathcal{K}.$$

A.3 Output nulling controlled invariant subspace

A.3.1 Definition, characterizations and general statements

- A subspace $\mathcal{V} \subset \mathbb{R}^n$ is *output nulling controlled invariant* if, for all $x_0 \in \mathcal{V}$, there exists $u : \mathbb{R}_{\geq 0} \to \mathbb{R}^m$ satisfying $\mathrm{H}[x_0; u] = \mathbf{0}$ and $\mathrm{H}_x[x_0; u](t) \in \mathcal{V}$ for all $t \geq 0$;
- $\mathcal{V}$ is output nulling controlled invariant iff it holds:

$$\begin{bmatrix} A \\ C \end{bmatrix} \mathcal{V} \subset \mathcal{V} \oplus \{\mathbf{0}\} + \mathrm{Im} \left\{ \begin{bmatrix} B \\ D \end{bmatrix} \right\} \tag{A.8}$$

- Equivalently, $\mathcal{V}$ is output nulling controlled invariant if there exists $F : \mathbb{R}^n \to \mathbb{R}^m$ satisfying:

$$(A + BF)\mathcal{V} \subset \mathcal{V} \subset \mathrm{Ker}\,\{C + DF\} \tag{A.9}$$

  so that

$$(\text{A.8}) \Leftrightarrow \exists F : (\text{A.9}) \tag{A.10}$$

- A matrix F satisfying (A.9) is called a friend of $\mathcal{V}$ and the set of such matrices is denoted by $\mathbb{F}(\mathcal{V})$, i.e.

$$\mathbb{F}(\mathcal{V}) \coloneqq \{F : (\text{A.9})\}$$

A.3.2 Instrumental results

Lemma A.4. *Given any subspaces $\mathcal{V} \subset \mathcal{W}$ such that $\mathbb{F}(\mathcal{V})$ and $\mathbb{F}(\mathcal{W})$ are distinct from $\{\varnothing\}$. Pick any $F_v \in \mathbb{F}(\mathcal{V})$. Then, there exists $F \in \mathbb{F}(\mathcal{W}) \cap \mathbb{F}(\mathcal{V})$ such that $F|\mathcal{V} = F_v|\mathcal{V}$ holds.*

Proof. Let $V \coloneqq \begin{bmatrix} V_1 & V_2 \end{bmatrix}$ be a matrix whose columns form a basis of $\mathcal{W}$ that is adapted to $\mathcal{V} \subset \mathcal{W}$, i.e. the columns of V_1 form a basis of $\mathcal{V}$. From $F_v \in \mathbb{F}(\mathcal{V})$ and (A.9), one deduces that there exists W_1 satisfying $\mathrm{Im}\,\{W_1\} \subset \mathcal{V}$ and:

$$\begin{bmatrix} A \\ C \end{bmatrix} V_1 = \begin{bmatrix} W_1 \\ \mathbf{0} \end{bmatrix} + \begin{bmatrix} B \\ D \end{bmatrix} U_1 \tag{A.11}$$

with $U_1 = -F_v V_1$ holds. Pick any $F_w \in \mathbb{F}(\mathcal{W})$. Similarly, one proves that there exists $W \coloneqq \begin{bmatrix} W_1' & W_2 \end{bmatrix}$ such that $\mathrm{Im}\,\{W\} \subset \mathcal{W}$ and satisfying:

$$\begin{bmatrix} A \\ C \end{bmatrix} \begin{bmatrix} V_1 & V_2 \end{bmatrix} = \begin{bmatrix} W_1' & W_2 \\ \mathbf{0} & \mathbf{0} \end{bmatrix} + \begin{bmatrix} B \\ D \end{bmatrix} \begin{bmatrix} U_1' & U_2 \end{bmatrix} \tag{A.12}$$

and $U = \begin{bmatrix} U_1' & U_2 \end{bmatrix} = -F_w \begin{bmatrix} V_1 & V_2 \end{bmatrix}$. Combining (A.11) and the second column of (A.12) gives:

$$\begin{bmatrix} A \\ C \end{bmatrix} \begin{bmatrix} V_1 & V_2 \end{bmatrix} = \begin{bmatrix} W_1 & W_2 \\ \mathbf{0} & \mathbf{0} \end{bmatrix} + \begin{bmatrix} B \\ D \end{bmatrix} \begin{bmatrix} U_1 & U_2 \end{bmatrix} \tag{A.13}$$

Define $F \coloneqq -\begin{bmatrix} U_1 & U_2 \end{bmatrix} (V^\intercal V)^{-1} V^\intercal$, so that

$$F \begin{bmatrix} V_1 & V_2 \end{bmatrix} = -\begin{bmatrix} U_1 & U_2 \end{bmatrix} \tag{A.14}$$

holds, yielding $\left[\begin{smallmatrix} A+BF \\ C+DF \end{smallmatrix}\right] V = \left[\begin{smallmatrix} W_1 & W_2 \\ \mathbf{0} & \mathbf{0} \end{smallmatrix}\right]$. This proves $F \in \mathbb{F}(\mathcal{W})$. Equality $F|\mathcal{V} = F_v|\mathcal{V}$ follows from $FV_1 = -U_1 = F_v V_1$ and implies $F \in \mathbb{F}(\mathcal{V})$. □

Lemma A.5. *Given any $\mathcal{V}$ and F satisfying* (A.9)*. Define*

$$\mathcal{R} := \langle A + BF | \mathcal{V} \cap B\mathrm{Ker}\,\{D\}\rangle.$$

Then, it holds:

(i) $\mathcal{R} \subset \mathcal{V}$;

(ii) $\mathbb{F}(\mathcal{V}) \subset \mathbb{F}(\mathcal{R})$;

(iii) For any $\hat{F} \in \mathbb{F}(\mathcal{V})$*, it holds* $(A + BF)|\mathcal{V}/\mathcal{R} = (A + B\hat{F})|\mathcal{V}/\mathcal{R}$;

(iv) Given any real monic polynomial q *with* $\deg q = \dim \mathcal{R}$*, there exists* $F \in \mathbb{F}(\mathcal{V})$ *such that the characteristic polynomial of* $(A + BF)|\mathcal{R}$ *equals* q;

(v) For any $\hat{F} \in \mathbb{F}(\mathcal{V})$*, it holds* $\mathcal{R} = \langle A + B\hat{F}|\mathcal{R} \cap \mathrm{Im}\,\{B\}\rangle$;

(vi) Subspace

$$\mathcal{N}_v := B^{-1}\mathcal{V} \cap \mathrm{Ker}\,\{D\} \subset \mathbb{R}^m$$

equals $B^{-1}\mathcal{R} \cap \mathrm{Ker}\,\{D\}$ *and the pair* $((A + BF)|\mathcal{R}, \mathcal{R}|B|\mathcal{N}_v)$ *is controllable;*

(vii) It holds:

$$\begin{bmatrix} A + BF \\ C + DF \end{bmatrix} \mathcal{Y} + \begin{bmatrix} B \\ D \end{bmatrix} \mathcal{N} \subset \mathcal{Y} \oplus \{\mathbf{0}\}$$

for all $\mathcal{Y} \in \{\mathcal{R}, \mathcal{V}\}$.

A.4 The weakly unobservable subspace

A.4.1 Definition, characterizations and general statements

- The *weakly unobservable subspace* $\mathcal{V}^* \subset \mathcal{X}$ reads

  $$\mathcal{V}^* := \{x_0 \in \mathbb{R}^n \mid \exists u : \mathbb{R}_{\geq 0} \to \mathbb{R}^m : \mathrm{H}[x_0; u] = \mathbf{0}\}.$$

  It can be proven that $\mathcal{V}^*$ is a linear subspace of $\mathbb{R}^n$.

- $\mathcal{V}^*$ is the largest output nulling controlled invariant subspace.

- $\mathcal{V}^*$ satisfies:

  $$\mathcal{V}^* = \sup\{\mathcal{V} \mid \mathbb{F}(\mathcal{V}) \neq \{\varnothing\}\} \tag{A.15}$$

- One has $\langle \mathcal{K}|A\rangle \subset \mathcal{V}^*$ and $\mathbf{0} \in \mathbb{F}(\langle \mathcal{K}|A\rangle)$.

- The *stabilizable weakly unobservable subspace* $\mathcal{V}_g^* \subset \mathcal{V}^*$ reads:

  $$\mathcal{V}_g^* := \sup\{\mathcal{V} \mid \exists F \in \mathbb{F}(\mathcal{V}),\ \sigma(A + BF|\mathcal{V}) \subset \mathbb{C}^-\}$$

- The *controllable weakly unobservable subspace* reads[2]

  $$\mathcal{R}^* := \{x_f \in \mathbb{R}^n \mid \exists T > 0,\ \exists (u : [0, T] \to \mathbb{R}^m) : \mathrm{H}[\mathbf{0}; u] = \mathbf{0},\ \mathrm{H}_x[\mathbf{0}; u](T) = x_f\}.$$

  see [TSH12, p.170]. It can be proven that $\mathcal{V}^*$ is a linear subspace of $\mathbb{R}^n$ that is included in $\mathcal{V}^*$.

- For any $\mathbb{F}(\mathcal{V}^*)$, it holds:

  $$\mathcal{R}^* := \langle A + BF|\mathcal{V}^* \cap B\mathrm{Ker}\,\{D\}\rangle.$$

[2] By definition, $\mathcal{R}^*$ gathers output-nulling *reachable* states, that is "controllable-from-the-origin". Equivalently, one can defined $\mathcal{R}^*$ as the set of initial states which are output-nulling "controllable-to-the-origin", i.e. x_0 belongs to $\mathcal{R}^*$ iff there exist $T > 0$ and $u : [0, T] \to \mathbb{R}^m$ such that $\mathrm{H}[x_0; u] = \mathbf{0}$ and $\mathrm{H}_x[x_0; u](T) = \mathbf{0}$, see [TSH12, p.163].

A.4.2 Instrumental results

Lemma A.6. *There exists $F \in \mathbb{F}(\mathcal{V}^*)$ that satisfies $F|\langle \mathcal{K}|A\rangle = \{\mathbf{0}\}$.*

Proof. Bearing in mind that both $\mathbb{F}(\langle \mathcal{K}|A\rangle)$ and $\mathbb{F}(\mathcal{V}^*)$ are non empty, by definition of $\langle \mathcal{K}|A\rangle$ and from (A.15), it suffices to invoke Lem. A.4 with $\mathcal{V} = \langle \mathcal{K}|A\rangle$, $\mathcal{W} = \mathcal{V}^*$ and $F_v = \mathbf{0} \in \mathbb{F}(\langle \mathcal{K}|A\rangle)$. □

Lemma A.7. *Choose any $F \in \mathbb{F}(\mathcal{V}^*)$. Let $N : \mathcal{N} \to \mathcal{X}$ the natural embedding. Given $x_0 \in \mathcal{X}$ and $(u, x, y) \in \mathbf{Q}(x_0)$. It holds*

$$y = \mathbf{0} \Leftrightarrow \begin{cases} x_0 \in \mathcal{V}^* \\ \exists v : u = Fx + Nv \end{cases} \tag{A.16}$$

Proof. (A.16) derives from [TSH12, Th.7.11]. □

A.5 System zeros

A.5.1 Definition, characterizations and general statements

- Given any $F \in \mathbb{F}(\mathcal{V}^*)$, the set $\mathcal{Z} \subset \mathbb{C}$ of *invariant zeros* reads:

$$\mathcal{Z} := \sigma(A + BF|\mathcal{V}^*/\mathcal{R}^*) \tag{A.17}$$

  This set is independent of $F \in \mathbb{F}(\mathcal{V}^*)$.

- The set $\mathcal{Z}_{\text{od}} \subset \mathbb{C}$ of *output decoupling zeros* reads:

$$\mathcal{Z}_{\text{od}} := \sigma(A|\langle \mathcal{K}|A\rangle)$$

- The following inclusions hold:

$$\mathcal{Z} \supset \{z \in \mathbb{C} : \text{rank}\,\{P_\Sigma(z)\} < \text{nrank}\,\{P_\Sigma\}\} \tag{A.18}$$

$$\mathcal{Z}_{\text{od}} \supset \{z \in \mathbb{C} : \text{rank}\left\{\begin{bmatrix} z\mathbf{I} - A \\ C \end{bmatrix}\right\} < n\} \tag{A.19}$$

A.5.2 Instrumental results

Lemma A.8. *If $\mathcal{R}^*$ is trivial, then $\mathcal{Z}_{\text{od}} \subset \mathcal{Z}$ holds true.*

Proof. Choose $F \in \mathbb{F}(\mathcal{V}^*)$ as in Lem. A.6, so that $(A + BF)|\langle \mathcal{K}|A\rangle = A|\langle \mathcal{K}|A\rangle$ which proves that $\langle \mathcal{K}|A\rangle$ is $(A + BF)$-invariant. Bearing in mind that $\langle \mathcal{K}|A\rangle \subset \mathcal{V}^*$, $\mathcal{R}^* = \{\mathbf{0}\}$ implies $\mathcal{Z} = \sigma((A + BF)|\mathcal{V}^*) \supset \sigma((A + BF)|\langle \mathcal{K}|A\rangle) = \sigma(A|\langle \mathcal{K}|A\rangle) = \mathcal{Z}_{\text{od}}$. □

Lemma A.9. *If $\text{rank}\,\{P_\Sigma(z)\} = \text{nrank}\,\{P_\Sigma\}$ for all $z \in \mathbb{C}$, then $\mathcal{V}^* = \mathcal{R}^*$ holds true.*

Proof. The invariant factors of the polynomial matrix P_Σ are all trivial, i.e. equal to 0 or 1. In view of [TSH12, Th.7.19] and picking any $F \in \mathbb{F}(\mathcal{V}^*)$, this implies that the invariant factors of $s\mathbf{I} - (A + BF)|\mathcal{V}^*/\mathcal{R}^*$ are all trivial as well. Thus, $\mathcal{V}^* = \mathcal{R}^*$ holds. □

A.6 Instrumental facts of general purpose

Fact A.10. *The family of A-invariant subspaces is a lattice, relative to $\subset$, $+$, and $\cap$, i.e. the intersection and the sum of A-invariant subspaces is A-invariant.*

Fact A.11. *Given two A-invariant finite-dimensional vector spaces $\mathcal{V}, \mathcal{W}$ such that $\mathcal{V} \subset \mathcal{W}$ holds. It holds:*

$$\sigma(A|\mathcal{V}) = \sigma(A|\mathcal{W}) \Leftrightarrow \mathcal{V} = \mathcal{W} \tag{A.20}$$

Proof. Equality $\sigma(A|\mathcal{V}) = \sigma(A|\mathcal{W})$ implies $\dim \mathcal{V} = \dim \mathcal{W}$, so that $\mathcal{V} = \mathcal{W}$ holds. The other implication is trivial. □

Fact A.12. *Given two A-invariant finite-dimensional vector spaces $\mathcal{X}_1, \mathcal{X}_2$ such that $\mathcal{X}_1 \cap \mathcal{X}_2 = \{\mathbf{0}\}$. For any A-invariant vector space $\mathcal{V}$ that satisfies $\mathcal{X}_1 \subset \mathcal{V} \subset \mathcal{X}_1 \oplus \mathcal{X}_2$, there exists an A-invariant vector space $\mathcal{V}_2 \subset \mathcal{X}_2$ such that $\mathcal{V} = \mathcal{X}_1 \oplus \mathcal{V}_2$.*

Proof. Consider an arbitrary basis $\{v^j\}$ of $\mathcal{V}$. Let us decompose v^j as $v_1^j + v_2^j$ according to $\mathcal{X}_1 \oplus \mathcal{X}_2$ so that $\mathcal{V} = \sum_j \mathrm{Span}\{v_1^j + v_2^j\}$. Adding $\mathcal{X}_1 = \mathcal{X}_1 + \sum_j \mathrm{Span}\{v_1^j\}$ on both sides of this equality leads to:

$$\begin{aligned}\mathcal{V} &= \sum_j \mathrm{Span}\{v_1^j + v_2^j, v_1^j\} + \mathcal{X}_1 \\ &= \sum_j \mathrm{Span}\{v_2^j, v_1^j\} + \mathcal{X}_1 \\ &= \mathcal{V}_2 + \mathcal{X}_1\end{aligned}$$

where $\mathcal{V}_2 \coloneqq \sum_j \mathrm{Span}\{v_2^j\} \subset \mathcal{X}_2$. The sum is direct because $\mathcal{V}_2 \cap \mathcal{X}_1 \subset \mathcal{X}_2 \cap \mathcal{X}_1 = \{\mathbf{0}\}$ holds.

Let us prove that $\mathcal{V}_2$ is A-invariant. $A\mathcal{V} \subset \mathcal{V}$ reads $A\mathcal{X}_1 + A\mathcal{V}_2 \subset \mathcal{X}_1 \oplus \mathcal{V}_2$. By intersecting both sides by $\mathcal{X}_2$ and exploiting A-invariance of $\mathcal{X}_2$ inducing $A\mathcal{V}_2 \subset A\mathcal{X}_2 \subset \mathcal{X}_2$, one obtains $\mathcal{X}_2 \cap (A\mathcal{X}_1 + A\mathcal{V}_2) = A\mathcal{V}_2 + \mathcal{X}_2 \cap (A\mathcal{X}_1) \subset \mathcal{X}_2 \cap (\mathcal{X}_1 \oplus \mathcal{V}_2) = \mathcal{V}_2$. This proves A-invariance of $\mathcal{V}_2$ since A-invariance of $\mathcal{X}_1$ implies $\mathcal{X}_2 \cap (A\mathcal{X}_1) \subset \mathcal{X}_2 \cap \mathcal{X}_1 = \{\mathbf{0}\}$. □

Fact A.13. *Given any finite-dimensional vector spaces $\mathcal{V}, \mathcal{W}$ and any linear injective mapping i. If $\mathcal{V} \cap \mathcal{W}$ is trivial, then $i\mathcal{V} \cap i\mathcal{W} = \{\mathbf{0}\}$ holds true.*

Proof. Let $\mathcal{J} \coloneqq i\mathcal{V} \cap i\mathcal{W}$. On the one hand, one has $i^{-1}\mathcal{J} = (i^{-1}i\mathcal{V}) \cap (i^{-1}i\mathcal{W}) = (\mathcal{V} + \mathrm{Ker}\,\{i\}) \cap (\mathcal{W} + \mathrm{Ker}\,\{i\}) = \mathcal{V} \cap \mathcal{W}$. On the other hand, observe that $\dim(i^{-1}\mathcal{J}) = \dim \mathrm{Ker}\,\{i\} + \dim(\mathcal{J} \cap \mathrm{Im}\,\{i\}) = \dim \mathcal{J}$ holds because $\mathcal{J} \subset \mathrm{Im}\,\{i\}$ and i are injective. □

Fact A.14. *Given any finite-dimensional vector space $\mathcal{V}, \mathcal{W}$ such that $\mathcal{V} \cap \mathcal{W}$ is trivial and any linear injective mapping i. It holds:*

$$i(\mathcal{V} \oplus \mathcal{W}) = i\mathcal{V} \oplus i\mathcal{W}$$

Proof. Direct consequences of Fact A.13. □

Fact A.15. *Given any sets $\mathcal{A}, \mathcal{B}$ and any injective mapping i. Then, $i(\mathcal{A} \setminus \mathcal{B}) = (i\mathcal{A}) \setminus (i\mathcal{B})$.*

Proof. $i(\mathcal{A} \setminus \mathcal{B})$ reads $i\{a : a \in \mathcal{A}, a \notin \mathcal{B}\}$. $(i\mathcal{A}) \setminus (i\mathcal{B})$ reads $\{ia : a \in \mathcal{A}, ia \notin i\mathcal{B}\}$. Hence, it is sufficient to prove that $a \notin \mathcal{B}$ is equivalent to $ia \notin i\mathcal{B}$. First, note that $ia \notin i\mathcal{B} \Leftrightarrow \neg(\exists b \in \mathcal{B} : ia = ib)$ holds. Owing to the injectivity of i, $ia = ib$ is equivalent to $a = b$. Thus, the previous condition is equivalent to $\neg(\exists b \in \mathcal{B} : a = b) \Leftrightarrow a \notin \mathcal{B}$. □

Lemma A.16. *Given a vector space $\mathcal{W}$ that is A_1-invariant and A_2-invariant. Given $\mathcal{V} \subset \mathcal{W}$ an A_1-invariant vector space. If $A_1|\mathcal{W} = A_2|\mathcal{W}$ holds, then (i) $\mathcal{V}$ is A_2-invariant, and (ii) $A_1|\mathcal{V} = A_2|\mathcal{V}$ holds.*

Proof. By definition, recall that $A_1|\mathcal{W} : \mathcal{W} \to \mathcal{W}, w \mapsto A_1 w$, see [TSH12, p.17]. Pick any $v \in \mathcal{V} \subset \mathcal{W}$. It holds

$$A_1 v = (A_1|\mathcal{W})v = (A_2|\mathcal{W})v = A_2 v.$$

Because $A_1 v \in \mathcal{V}$, this proves that $\mathcal{V}$ is A_2-invariant. This also proves that mapping $A_1|\mathcal{V} : \mathcal{V} \to \mathcal{V}, v \mapsto A_1 v$ coincides with mapping $A_2|\mathcal{V} : \mathcal{V} \to \mathcal{V}, v \mapsto A_2 v$. □

Lemma A.17. *Given a map A and A-invariant vector space $\mathcal{R}$. For any $\mathcal{V} \supset \mathcal{R}$, it holds:*

$$A(\mathcal{V}/\mathcal{R}) \subset \mathcal{V}/\mathcal{R} \Leftrightarrow A\mathcal{V} \subset \mathcal{V} \tag{A.21}$$

Proof. Recall that $A(\mathcal{V}/\mathcal{R}) \subset \mathcal{V}/\mathcal{R}$ reads:

$$\{A(v + \mathcal{R}) : v \in \mathcal{V}\} \subset \{v + \mathcal{R} : v \in \mathcal{V}\}. \tag{A.22}$$

$\Leftarrow$ Pick any $v \in \mathcal{V}$ and let $v_a := Av \in \mathcal{V}$. Observe that $A(v + \mathcal{R}) = v_a + A\mathcal{R} \subset v_a + \mathcal{R}$.
$\Rightarrow$ Pick any $v \in \mathcal{V}$. From (A.22), there exists $v_a \in \mathcal{V}$ such that $A(v + \mathcal{R}) = v_a + \mathcal{R}$. From $v_a + \mathcal{R} \subset \mathcal{V}$, one concludes that $A(v + \mathcal{R})$ and, in turn, Av belong to $\mathcal{V}$.. □

Appendix B

Proofs associated with Chap. 6

B.1 Proof of Lem. 6.7

Without loss of generality, assume that $\theta_r = 0$ because any other case can be recovered via a simple change of origin. Our attention can be further restricted to the case where $\theta \in [-\pi/6, \pi/6[$. Indeed, from this specific situation, we will show later on how the general case where

$$\theta \in \Theta \coloneqq [0, 2\pi[- \pi/6$$

can be recovered by exploiting the symmetry of $\mathcal{U}$ as well as the periodicity of $A(\cdot)$.

The output being a scalar, one can simply choose $Q(\theta) = 1$. Therefore, the first step reduces to the computation of the change of input variables. The orthogonal matrix $P(\theta)$ given by (6.24) and defined in the inverter context, achieves this purpose. Indeed, in this case, it holds:

$$Q^{-1}(\theta)A(\theta)P(\theta) = \begin{bmatrix} 1 & 0 & 0 \end{bmatrix},$$

so that $R(\theta) = 1$, $r(\theta) \coloneqq \operatorname{rank}\{A(\theta)\} = 1$ and $\hat{u}_1(\hat{y}) = \hat{y}$ hold. The output set $\mathcal{Y}(\theta) = \hat{\mathcal{Y}}(\theta)$ equals $\hat{\mathcal{U}}_1(\theta)$, see (6.13). Let us now implement the Fourier-Motzkin algorithm to compute $\hat{\mathcal{U}}_1(\theta)$. The first step corresponds to rewriting $\hat{\mathcal{U}}(\theta)$ as follows:

$$\hat{\mathcal{U}}(\theta) = \left\{\hat{u} : \hat{u}_3 \in [\underline{\hat{u}}_3(\theta, \hat{u}_{1:2}), \overline{\hat{u}}_3(\theta, \hat{u}_{1:2})]\right\},$$

with

$$\underline{\hat{u}}_3(\theta, \hat{u}_{1:2}) \coloneqq \sqrt{3}\max\left\{\mathbf{1}_3\underline{u} - P_{1:2}(\theta)\hat{u}_{1:2}\right\}, \tag{B.1}$$

$$\overline{\hat{u}}_3(\theta, \hat{u}_{1:2}) \coloneqq \sqrt{3}\min\left\{\mathbf{1}_3\overline{u} - P_{1:2}(\theta)\hat{u}_{1:2}\right\}, \tag{B.2}$$

so that

$$\hat{\mathcal{U}}_{1:2}(\theta) = \left\{\hat{u}_{1:2} : \exists \hat{u}_3, \hat{u} \in \hat{\mathcal{U}}(\theta)\right\} = \left\{\hat{u}_{1:2} : \underline{\hat{u}}_3(\theta, \hat{u}_{1:2}) \leq \overline{\hat{u}}_3(\theta, \hat{u}_{1:2})\right\}.$$

Next step starts with the following reformulation

$$\hat{\mathcal{U}}_{1:2}(\theta) = \left\{\hat{u}_{1:2} : \hat{u}_2 \in [\underline{\hat{u}}_2(\theta, \hat{u}_1), \overline{\hat{u}}_2(\theta, \hat{u}_1)]\right\},$$

leading to

$$\hat{\mathcal{U}}_1(\theta) = \left\{\hat{u}_1 : \exists \hat{u}_2, \hat{u}_{1:2} \in \hat{\mathcal{U}}_{1:2}(\theta)\right\} = \left\{\hat{u}_1 : \underline{\hat{u}}_2(\theta, \hat{u}_1) \leq \overline{\hat{u}}_2(\theta, \hat{u}_1)\right\},$$

with

$$\underline{\hat{u}}_2(\theta, \hat{u}_1) \coloneqq -\min\left\{ \begin{bmatrix} \tan(\theta - \pi/3) \\ \tan(\theta + \pi/3) \\ \tan(\theta) \end{bmatrix} \hat{u}_1 + \frac{\overline{u} - \underline{u}}{\sqrt{2}} \begin{bmatrix} \cos(\theta - \pi/3) \\ \cos(\theta + \pi/3) \\ \cos(\theta) \end{bmatrix}^{-1} \right\}, \tag{B.3}$$

$$\overline{\hat{u}}_2(\theta, \hat{u}_1) \coloneqq -\max\left\{ \begin{bmatrix} \tan(\theta + \pi/3) \\ \tan(\theta - \pi/3) \\ \tan(\theta) \end{bmatrix} \hat{u}_1 - \frac{\overline{u} - \underline{u}}{\sqrt{2}} \begin{bmatrix} \cos(\theta + \pi/3) \\ \cos(\theta - \pi/3) \\ \cos(\theta) \end{bmatrix}^{-1} \right\}. \tag{B.4}$$

Ultimate step reads:

$$\hat{\mathcal{U}}_1(\theta) = \overline{\hat{u}}_1(\theta)[-1, 1] \quad \text{with} \quad \overline{\hat{u}}_1(\theta) = \sqrt{\frac{2}{3}}(\overline{u} - \underline{u})\cos(\theta).$$

Then, if $y = \hat{y} \in \mathcal{Y}(\theta) = \hat{\mathcal{U}}_1(\theta)$, the set of solutions reads as follows (see (6.14)):

$$(\hat{H}(\theta)|\hat{\mathcal{U}})^{-1}(\hat{y}) = \{y\} \times \hat{\mathcal{U}}_{2:3}(y) = \{y\} \times \left\{ \hat{u}_{2:3} : \hat{u}_1 = y,\ \hat{u} \in \hat{\mathcal{U}} \right\}$$

or, equivalently,

$$(H(\theta)|\mathcal{U})^{-1}(y) = P_1(\theta)y + P_{2:3}(\theta) \left\{ \hat{u}_{2:3} : \mathbf{1}_3 \underline{u} - P_1(\theta)y \leq P_{2:3}(\theta)\hat{u}_{2:3} \leq \mathbf{1}_3 \overline{u} - P_1(\theta)y \right\}.$$

Let us now investigate how to treat the general case, where $\theta \in \Theta$. To this end, pick any $\theta \in \Theta$. Then, define $k_\theta \in [\![0, 5]\!]$ and $r_\theta \in [-\pi/6, \pi/6[$ such that $\theta = r_\theta + k_\theta \pi/3$ holds, i.e. $r_\theta + \pi/6$ and k_θ are the rest and the quotient of the Euclidean division of $\theta + \pi/6$ by $\pi/3$, respectively. In addition to being 2π-periodic, observe that $A(\cdot)$ also satisfies the following identities for any $\theta \in \Theta$:

$$A(\theta + \frac{\pi}{3}) = A(\theta)C \quad \text{with} \quad C \coloneqq \begin{bmatrix} 0 & 0 & -1 \\ -1 & 0 & 0 \\ 0 & -1 & 0 \end{bmatrix}.$$

This induces:

$$A(\theta) = A(r_\theta + k_\theta \frac{\pi}{3}) = A(r_\theta)C^{k_\theta}. \tag{B.5}$$

Pick arbitrary $k \in \mathbb{N}$. Using identity $C^k = (-1)^k(-C)^k$ and the fact that $-C$ is a 3×3 permutation matrix, one concludes that (i) C^k is invertible and (ii) $(-C)^k\mathcal{U} = [\underline{u}, \overline{u}]^3 = \mathcal{U}$ so that it holds

$$C^k\mathcal{U} = (-1)^k\mathcal{U}. \tag{B.6}$$

Hence, one gets

$$\mathcal{Y}(\theta) = A(\theta)\mathcal{U} \overset{(B.5)}{=} A(r_\theta)C^{k_\theta}\mathcal{U} \overset{(B.6)}{=} (-1)^{k_0}A(r_\theta)\mathcal{U},$$

$$(H(\theta)|\mathcal{U})^{-1}(y) = \{u \in \mathcal{U} : y = A(\theta)u\} \overset{(B.5)}{=} \{C^{-k_\theta}C^{k_\theta}u \in \mathcal{U} : y = A(r_\theta)C^{k_\theta}u\} = C^{-k_\theta}\mathcal{S}(r_\theta, y).$$

The key observation is that both sets $A(r_\theta)\mathcal{U}$ and $\mathcal{S}(r_\theta, y)$ have already been expressed in closed form when considering $\theta \in [-\pi/6, \pi/6[\Leftrightarrow \theta = r_\theta$. From the expression of $\hat{\mathcal{U}}_1(\theta)$, note also that $-A(r_\theta)\mathcal{U} = -\mathcal{Y}(\theta) = -\hat{\mathcal{U}}_1(\theta) = \hat{\mathcal{U}}_1(\theta)$ holds, so that $\mathcal{Y}(\theta)$ equals $\hat{\mathcal{U}}_1(\theta)$ for all θ.

Appendix C

Proofs associated with Chap. 9

C.1 The classical paradigm

C.1.1 Technical preliminaries

The notations in this subsection are independent of the rest of Sec. C.1. In particular, the vectors v_i are not necessarily eigenvectors of S.

Definition (s-conformably ordered)**.** For $s \in \mathbb{N}^*$, a matrix $V = [v_1, \dots, v_m] \in \mathbb{C}^{p\times m}$ is said to be *s-conformably ordered* if the first $2\,s \leq m$ columns are pairwise complex conjugate, while the remaining are real, that is

$$\bar{v}_{2k-1} = v_{2k}, \forall k \in [\![1, s]\!] \tag{C.1}$$
$$v_i \in \mathbb{R}^p, \forall i \in [\![2s+1, m]\!] \tag{C.2}$$

The set of s-conformably ordered matrices (of all dimensions) is denoted by $\mathcal{C}_s$. This definition is naturally extended to the case $s = 0$ by letting $\mathcal{C}_0$ gather all matrices with real entries.

The following lemma follows by direct computation.

Lemma C.1. *Define invertible matrix $U \in \mathbb{C}^{2\times 2}$ as follows*

$$U \coloneqq \frac{1}{2}\begin{bmatrix} 1 & -i \\ 1 & i \end{bmatrix}.$$

For any $\alpha \in \mathbb{C}$, it holds

$$\begin{bmatrix} \alpha & 0 \\ 0 & \bar{\alpha} \end{bmatrix} = U \begin{bmatrix} \mathfrak{Re}(\alpha) & \mathfrak{Im}(\alpha) \\ -\mathfrak{Im}(\alpha) & \mathfrak{Re}(\alpha) \end{bmatrix} U^{-1}$$

Given $s, m \in \mathbb{N}$ satisfying $2s \leq m$. Define the invertible matrix $N_s \in \mathbb{C}^{m\times m}$ as follows

$$N_s \coloneqq \operatorname{diag}\left\{\mathbf{I}_s \otimes U, \mathbf{I}_{m-2s}\right\}.$$

where $\otimes$ denotes the Kronecker product. For any matrix $V = [v_1, \dots, v_m] \in \mathbb{C}^{n\times m}$ which is s-conformably ordered, equality

$$\mathbb{R}^{n\times m} \ni VN_s = \begin{bmatrix} \mathfrak{Re}(v_1) & \mathfrak{Im}(v_1) & \mathfrak{Re}(v_3) & \mathfrak{Im}(v_3) & \dots & \mathfrak{Re}(v_{2s-1}) & \mathfrak{Im}(v_{2s-1}) & v_{2s+1} & \dots & v_m \end{bmatrix}$$

holds.

Lemma C.2. *Given an matrix $V \in \mathbb{C}^{n\times m}$ that is s-conformably ordered for some $s \in \mathbb{N}$. Define the mapping $\mathrm{M_V} : \mathbb{R}^{p\times n} \to \mathbb{C}^{p\times m}, W \mapsto WV$. Then, the range of $\mathrm{M_V}$ reads*

$$\{WV : W \in \mathbb{R}^{p\times n}\} = \{Y \in \mathcal{C}_s \cap \mathbb{C}^{p\times m} \mid \mathrm{Ker}\,\{VN_s\} \cap \mathbb{R}^m \subset \mathrm{Ker}\,\{YN_s\} \cap \mathbb{R}^m\}.$$

Proof. The range of $\mathrm{M_V}$ is $\{Y = [y_1, \ldots, y_m] \in \mathbb{C}^{p\times m} : \exists W \in \mathbb{R}^{p\times n}, Y = WV\}$. Pick any $k \in [\![1, s]\!]$. In view of Lem C.1, observe that the columns $2k-1$ and $2k$ of the equation $YN_s = WVN_s$ read

$$\begin{bmatrix}\mathfrak{Re}(y_{2k-1}) & \mathfrak{Im}(y_{2k-1}) & \mathfrak{Re}(y_{2k}) & \mathfrak{Im}(y_{2k})\end{bmatrix} \begin{bmatrix}1 & 0\\ i & 0\\ 0 & 1\\ 0 & i\end{bmatrix} U = W \begin{bmatrix}v_{2k-1} & \bar{v}_{2k-1}\end{bmatrix} U,$$

$$\begin{bmatrix}\mathfrak{Re}(y_{2k-1}) & \mathfrak{Im}(y_{2k-1}) & \mathfrak{Re}(y_{2k}) & \mathfrak{Im}(y_{2k})\end{bmatrix} \frac{1}{2}\left(\begin{bmatrix}1 & 0\\ 0 & 1\\ 1 & 0\\ 0 & -1\end{bmatrix} + i \begin{bmatrix}0 & -1\\ 1 & 0\\ 0 & 1\\ 1 & 0\end{bmatrix}\right) = W \begin{bmatrix}\mathfrak{Re}(v_{2k-1}) & \mathfrak{Im}(v_{2k-1})\end{bmatrix}, \tag{C.3}$$

whereas the column $i \in [\![2s+1, m]\!]$ of the same equation reads

$$y_i = Wv_i. \tag{C.4}$$

The right-hand side of both (C.3) and (C.4) being real, it follows that $\bar{y}_{2k-1} = y_{2k}, (k \in [\![1, s]\!])$ (the imaginary part of the left-hand side of (C.3) is zero) and $y_i \in \mathbb{R}^p, (i \in [\![2s+1, m]\!])$. We have just proved that $Y \in \mathcal{C}_s$ is necessary for Y to belong to the range of $\mathrm{M_V}$.

Because N_s is invertible, this condition is also sufficient if, for any $Y \in \mathcal{C}_s$, the real matrix equation $YN_s = WVN_s$ admits a (real) solution W. This is true iff $\mathrm{Ker}\,\{VN_s\} \subset \mathrm{Ker}\,\{YN_s\}$ holds, where both kernels are subsets of $\mathbb{R}^m$. □

In the particular case where V is injective, $\mathrm{Ker}\,\{VN_s\} = \{\mathbf{0}\}$ is trivially included in $\mathrm{Ker}\,\{YN_s\}$, whatever is Y.

Corollary C.3. *Given an* injective *matrix $V \in \mathbb{C}^{n\times m}$ which is s-conformably ordered for some $s \in \mathbb{N}$. Then, the range of $\boldsymbol{M}_V$ is the set of s-conformably ordered matrices of dimension $p \times m$, i.e.*

$$\{WV : W \in \mathbb{R}^{p\times n}\} = \mathcal{C}_s \cap \mathbb{C}^{p\times m}.$$

The last technical lemma is as follows.

Lemma C.4. *Define $J := \left[\begin{smallmatrix}0 & 1\\ -1 & 0\end{smallmatrix}\right]$.*

(i) Given two real vectors v, w not all zeros. Matrices $\begin{bmatrix}v & w\end{bmatrix}$ and $\begin{bmatrix}-w & v\end{bmatrix}$ are linearly independent;

(ii) Given $z \in \mathbb{R}^2$. The matrix $\begin{bmatrix}Jz & z\end{bmatrix}$ is invertible iff $z \neq \mathbf{0}$.

Proof. To prove (ii), let $z = \begin{bmatrix}\beta & \alpha\end{bmatrix}^\intercal$ and compute $\det\left(\begin{bmatrix}Jz & z\end{bmatrix}\right) = \alpha^2 + \beta^2$ which is zero iff $z = \mathbf{0}$. Pick arbitrary $\alpha, \beta \in \mathbb{R}$. Observe that

$$\alpha \begin{bmatrix}v & w\end{bmatrix} + \beta \begin{bmatrix}-w & v\end{bmatrix} = \begin{bmatrix}\mathbf{0} & \mathbf{0}\end{bmatrix} \tag{C.5}$$

reads:

$$V(\alpha \mathbf{I}_2 + \beta J) = V \begin{bmatrix}Jz & z\end{bmatrix} = \begin{bmatrix}\mathbf{0} & \mathbf{0}\end{bmatrix} \tag{C.6}$$

with $V := \begin{bmatrix}v & w\end{bmatrix}$. If $z \neq \mathbf{0}$, the right multiplication by $\begin{bmatrix}Jz & z\end{bmatrix}^{-1}$ leads to $V = \mathbf{0}$ which contradicts the assumption of (i). Thus, $z = \mathbf{0}$ holds, which is equivalent to $\alpha = \beta = 0$, so that V and VJ are linearly independent. □

C.1.2 Expression of $\Pi_{i,j}$ and $\Gamma_{i,j}$

Under ASM 9.2, there exist q pairs $(\lambda_k, v_k) \in \mathbb{C}^0 \times \mathbb{C}^q$ such that $V = [v_1, \ldots, v_q]$ is invertible, and $\Lambda := V^{-1}SV = \operatorname{diag}\{\lambda_1, \ldots, \lambda_q\}$ holds. Without loss of generality, it is assumed that V is s-conformably ordered (see p.241) for some $s \in \mathbb{N}$. Define $V_r \in \mathbb{R}^{q\times q}$ as follows:

$$V_r := \begin{bmatrix} \mathfrak{Re}(v_1) & \mathfrak{Im}(v_1) & \mathfrak{Re}(v_3) & \mathfrak{Im}(v_3) & \ldots & \mathfrak{Re}(v_{2s-1}) & \mathfrak{Im}(v_{2s-1}) & v_{2s+1} & \ldots & v_q \end{bmatrix}. \tag{C.7}$$

Given any $(i,j) \in \mathcal{J}$. Let vectors $\phi_{i,j} \in \mathbb{C}^{n+m}$ be a basis of $\operatorname{Ker}\{P_\Sigma(\lambda_i)\}$, i.e.

$$\operatorname{Ker}\{P_\Sigma(\lambda_i)\} = \operatorname{span}\{\phi_{i,1}, \ldots, \phi_{i,\gamma_i}\}. \tag{C.8}$$

Define matrices $\Phi_{i,j} \in \mathbb{R}^{(n+m)\times q}$ as follows:

$$\Phi_{2k-1,j} = \begin{bmatrix} \mathbf{0}_{(n+m)\times(2k-2)} & \mathfrak{Re}(\phi_{2k-1,j}) & \mathfrak{Im}(\phi_{2k-1,j}) & \mathbf{0}_{(n+m)\times(q-2k)} \end{bmatrix} V_r^{-1}, \tag{C.9}$$

$$\Phi_{2k,j} = \begin{bmatrix} \mathbf{0}_{(n+m)\times(2k-2)} & -\mathfrak{Im}(\phi_{2k-1,j}) & \mathfrak{Re}(\phi_{2k-1,j}) & \mathbf{0}_{(n+m)\times(q-2k)} \end{bmatrix} V_r^{-1}, \tag{C.10}$$

if $k \in [\![1, s]\!]$ and $j \in [\![1, \gamma_{2k}]\!]$ hold and

$$\Phi_{i,j} = \begin{bmatrix} \mathbf{0}_{(n+m)\times(i-1)} & \phi_{i,j} & \mathbf{0}_{(n+m)\times(q-i)} \end{bmatrix} V_r^{-1}, \tag{C.11}$$

if $i \in [\![2s+1, q]\!]$ and $j \in [\![1, \gamma_i]\!]$ hold true.

For $(i,j) \in \mathcal{J}$, define

$$\Pi_{i,j} := \begin{bmatrix} \mathbf{I}_n & \mathbf{0} \end{bmatrix} \Phi_{i,j}, \tag{C.12}$$

$$\Gamma_{i,j} := \begin{bmatrix} \mathbf{0} & \mathbf{I}_m \end{bmatrix} \Phi_{i,j}. \tag{C.13}$$

C.1.3 Proof of Prop. 9.4

Let us extend $\mathrm{H_F} : \mathbb{C}^{(n+m)\times q} \to \mathbb{C}^{(n+p)\times q}$ while preserving its definition when its argument is non-real. Define $\mathrm{H_V} : \mathbb{C}^{(n+m)\times q} \to \mathbb{C}^{(n+p)\times q}$ as follows:

$$\mathrm{H_V} : \begin{bmatrix} \mathrm{Y} \\ \Psi \end{bmatrix} \mapsto \mathrm{H_F} \begin{bmatrix} \mathrm{Y}V^{-1} \\ \Psi V^{-1} \end{bmatrix} \times V = \begin{bmatrix} A\mathrm{Y} - \mathrm{Y}\Lambda + B\Psi \\ C\mathrm{Y} + D\Psi \end{bmatrix} \tag{C.14}$$

where the columns of V are eigenvectors of S. From the diagonal structure of Λ, observe that

$$\operatorname{Ker}\{\mathrm{H_V}\} = \left\{ \begin{bmatrix} v_1 & \cdots & v_q \\ w_1 & \cdots & w_q \end{bmatrix} : \begin{bmatrix} v_i \\ w_i \end{bmatrix} \in \operatorname{Ker}\{P_\Sigma(\lambda_i)\} \right\}$$

Define the isomorphism $\mathrm{M_V} : \mathbb{R}^{(n+p)\times q} \to \mathbb{C}^{(n+m)\times q}$ as $\left[\begin{smallmatrix} \Pi \\ \Gamma \end{smallmatrix}\right] \mapsto \left[\begin{smallmatrix} \Pi \\ \Gamma \end{smallmatrix}\right] V$. Observe that $\mathrm{H_V} = \mathrm{M_V} \circ \mathrm{H_F} \circ \mathrm{M_V}^{-1}$, so that $\operatorname{Ker}\{\mathrm{H_F}\} = \operatorname{Ker}\left\{\mathrm{M_V}^{-1} \circ \mathrm{H_V} \circ \mathrm{M_V}\right\} = \mathrm{M_V}^{-1}(\operatorname{Ker}\{\mathrm{H_V}\} \cap \operatorname{dom}(\mathrm{M_V}^{-1}))$. Since the domain of $\mathrm{M_V}^{-1}$ is the range of $\mathrm{M_V}$, Cor. C.3 ensures that $\operatorname{Ker}\{\mathrm{H_V}\} \cap \operatorname{dom}(\mathrm{M_V}^{-1})$ corresponds to elements of $\operatorname{Ker}\{\mathrm{H_V}\}$ which are s-conformably ordered, i.e. $\bar{v}_{2k-1} = v_{2k}$ and $\bar{w}_{2k-1} = w_{2k}$ hold for all $k \in [\![1, s]\!]$, and both v_i and w_i are real vectors for all $i \in [\![2s+1, q]\!]$. Bearing in mind that $\bar{\lambda}_{2k-1}$ equals λ_{2k}, so that $\operatorname{Ker}\{P_\Sigma(\lambda_{2k})\} = \{\bar{b} : b \in \operatorname{Ker}\{P_\Sigma(\lambda_{2k-1})\}\}$, one gets

$$\operatorname{Ker}\{\mathrm{H_V}\} \cap \operatorname{dom}(\mathrm{M_V}^{-1}) = \left\{ \begin{bmatrix} v_1 & \bar{v}_1 & v_3 & \bar{v}_3 & \cdots & v_{2s-1} & \bar{v}_{2s-1} & v_{2s+1} & \cdots & v_q \\ w_1 & \bar{w}_1 & w_3 & \bar{w}_3 & \cdots & w_{2s-1} & \bar{w}_{2s-1} & w_{2s+1} & \cdots & w_q \end{bmatrix} : \right.$$
$$\left. \begin{bmatrix} v_{2k-1} \\ w_{2k-1} \end{bmatrix} \in \operatorname{Ker}\{P_\Sigma(\lambda_{2k-1})\}, (k \in [\![1, s]\!]), \begin{bmatrix} v_i \\ w_i \end{bmatrix} \in \operatorname{Ker}\{P_\Sigma(\lambda_i)\} \cap \mathbb{R}^{n+p}, (i \in [\![2s+1, q]\!]) \right\}.$$

Bearing in mind the statement of Lem C.1 and using (C.8), observe that $\left[\begin{smallmatrix} v_{2k-1} \\ w_{2k-1} \end{smallmatrix}\right] \in \operatorname{Ker}\left\{P_\Sigma(\lambda_{2k-1})\right\}$, $(k \in [\![1, s]\!])$ holds iff there exists $\alpha_{2k-1,j} \in \mathbb{C}$, $(j \in [\![1, \gamma_{2k-1}]\!])$ such that:

$$\begin{aligned}
\begin{bmatrix} v_{2k-1} & \bar{v}_{2k-1} \\ w_{2k-1} & \bar{w}_{2k-1} \end{bmatrix} &= \sum_{j=1}^{\gamma_{2k-1}} \begin{bmatrix} \phi_{2k-1,j} & \bar{\phi}_{2k-1,j} \end{bmatrix} \begin{bmatrix} \alpha_{2k-1,j} & 0 \\ 0 & \bar{\alpha}_{2k-1,j} \end{bmatrix} \\
&= \sum_{j=1}^{\gamma_{2k-1}} \begin{bmatrix} \phi_{2k-1,j} & \bar{\phi}_{2k-1,j} \end{bmatrix} U \begin{bmatrix} \mathfrak{Re}(\alpha_{2k-1,j}) & \mathfrak{Im}(\alpha_{2k-1,j}) \\ -\mathfrak{Im}(\alpha_{2k-1,j}) & \mathfrak{Re}(\alpha_{2k-1,j}) \end{bmatrix} U^{-1} \\
&= \sum_{j=1}^{\gamma_{2k-1}} \begin{bmatrix} \mathfrak{Re}(\phi_{2k-1,j}) & \mathfrak{Im}(\phi_{2k-1,j}) \end{bmatrix} (\mathfrak{Re}(\alpha_{2k-1,j}) \begin{bmatrix} 1 & 0 \\ 0 & 1 \end{bmatrix} + \mathfrak{Im}(\alpha_{2k-1,j}) \begin{bmatrix} 0 & 1 \\ -1 & 0 \end{bmatrix}) U^{-1} \\
&= \sum_{j=1}^{\gamma_{2k-1}} \left(\mathfrak{Re}(\alpha_{2k-1,j}) \begin{bmatrix} \mathfrak{Re}(\phi_{2k-1,j}) & \mathfrak{Im}(\phi_{2k-1,j}) \end{bmatrix} + \mathfrak{Im}(\alpha_{2k-1,j}) \begin{bmatrix} -\mathfrak{Im}(\phi_{2k-1,j}) & \mathfrak{Re}(\phi_{2k-1,j}) \end{bmatrix}\right) U^{-}
\end{aligned}$$

Since $\begin{bmatrix} \mathfrak{Re}(\phi_{2k-1,j}) & \mathfrak{Im}(\phi_{2k-1,j}) \end{bmatrix}$ and $\begin{bmatrix} -\mathfrak{Im}(\phi_{2k-1,j}) & \mathfrak{Re}(\phi_{2k-1,j}) \end{bmatrix}$ are linearly independent for any $\phi_{2k-1,j} \neq \mathbf{0}$, by virtue of Lem. C.4, this proves Prop. 9.4, since Lem C.1 ensures that $N_s^{-1} V^{-1} = (V N_s)^{-1} = V_r^{-1}$ where $N_s \in \mathbb{C}^{q \times q}$ reads $\operatorname{diag}\left\{\mathbf{I}_s \otimes U, \mathbf{I}_{q-2s}\right\}$.

C.1.4 Proof of Th. 9.9

Before stating the proof, consider the following intermediate result.

Proposition C.5. *Define the subset $\mathcal{I}_z$ of $\mathcal{I}$ gathering the indices i for which the eigenvalue λ_i of S is also an invariant zero:*

$$\mathcal{I}_z \coloneqq \{i \in [\![1, q]\!] : \delta_i > 0, \gamma_i > 0\} \subset \mathcal{I},$$

together with its complement relatively to $\mathcal{I}$

$$\mathcal{I}_z^c \coloneqq \{i \in [\![1, q]\!] : \delta_i = 0, \gamma_i > 0\} \subset \mathcal{I}.$$

For all $i \in \mathcal{I}$ and for all $j \in [\![1, \gamma_i]\!]$, it holds:

(i) $\operatorname{Im}\left\{\Pi_{i,j}\right\} \subset \mathcal{V}^*$;

(ii) $\operatorname{Im}\left\{\Pi_{i,j}\right\} \subset \mathcal{R}^* \Leftrightarrow \left(i \in \mathcal{I}_z^c \vee (i \in [\![1, 2s]\!] \wedge \operatorname{rank}\left\{\Pi_{i,j}\right\} < 2) \vee (i \in [\![2s+1, q]\!] \wedge \Pi_{i,j} = \mathbf{0})\right)$;

(iii) $\operatorname{Im}\left\{\Pi_{i,j}\right\} \subset \mathcal{V}_g^* \Leftrightarrow \left(\operatorname{Im}\left\{\Pi_{i,j}\right\} \subset \mathcal{R}^* \vee (i \in \mathcal{I}_z \wedge \lambda_i \in \mathbb{C}^-)\right)$.

Proof. First, consider the case in which $i \in \mathcal{I} \cap [\![2s+1, q]\!]$. Select any $j \in [\![1, \gamma_i]\!]$. Define

$$\begin{bmatrix} X \\ U \end{bmatrix} \coloneqq \begin{bmatrix} \mathbf{I}_n & \mathbf{0} \\ \mathbf{0} & \mathbf{I}_m \end{bmatrix} \phi_{i,j},$$
$$\Delta \coloneqq \lambda_i.$$

From (C.8), one has $P_\Sigma(\lambda_i) \left[\begin{smallmatrix} X \\ U \end{smallmatrix}\right] = \mathbf{0}$ which can be rewritten as follows:

$$\begin{bmatrix} A \\ C \end{bmatrix} X = \begin{bmatrix} X \\ \mathbf{0} \end{bmatrix} \Delta - \begin{bmatrix} B \\ D \end{bmatrix} U. \tag{C.15}$$

If $X = \mathbf{0}$, then $\Pi_{i,j}$ is a null matrix, so that $\operatorname{Im}\left\{\Pi_{i,j}\right\} \subset \mathcal{R}^*$ trivially holds. Otherwise, let $F = U(X^\intercal X)^{-1} X^\intercal \in \mathbb{R}^{m \times n}$ so that $FX = U$ holds. Substituting this last expression in (C.15) gives

$$\begin{bmatrix} A + BF \\ C + DF \end{bmatrix} X = \begin{bmatrix} X \\ \mathbf{0} \end{bmatrix} \Delta, \tag{C.16}$$

which proves that $\mathrm{Im}\{X\} = \mathrm{Im}\{\Pi_{i,j}\} \subset \mathcal{V}^*$. This equation also implies that $\sigma(A+BF|X) = \sigma(\Delta)$. Thus, $\mathrm{Im}\{X\} \subset \mathcal{R}^*$ holds iff $\sigma(\Delta) \cap \mathcal{Z}$ is empty, which is equivalent to saying that i belongs to $\mathcal{I}_z^c$, by definition of this last set. Besides, since $\mathcal{R}^* \subset \mathcal{V}_g^*$ holds, one has

$$\mathrm{Im}\{X\} \subset \mathcal{V}_g^* \Leftrightarrow (\mathrm{Im}\{X\} \subset \mathcal{R}^*) \vee (\sigma(\Delta) \subset \mathcal{Z} \cap \mathbb{C}^-). \tag{C.17}$$

and $\sigma(\Delta) = \{\lambda_i\} \subset \mathcal{Z} \cap \mathbb{C}^-$ is equivalent to $i \in \mathcal{I}_z \wedge \lambda_i \in \mathbb{C}^-$ by the definition of $\mathcal{I}_z$. We have proved (i)-(iii) for any $i \in \mathcal{I} \cap [\![2s+1, q]\!]$.

Select any even $i = 2k \in \mathcal{I} \cap [\![1, 2s]\!]$ and observe that $i-1$ also belongs to $\mathcal{I} \cap [\![1, 2s]\!]$. Select any $j \in [\![1, \gamma_i]\!]$. From (C.8), one has $P_\Sigma(\lambda_{i-1})\phi_{i-1,j} = \mathbf{0}$ which also implies $\overline{P_\Sigma(\lambda_{i-1})\phi_{i-1,j}} = P_\Sigma(\bar{\lambda}_{i-1})\bar{\phi}_{i-1,j} = \mathbf{0}$. By combining these two equations, one obtains

$$\begin{bmatrix} A & B \\ C & D \end{bmatrix} \begin{bmatrix} \phi_{i-1,j} & \bar{\phi}_{i-1,j} \end{bmatrix} = \begin{bmatrix} \mathbf{I}_n & \mathbf{0} \\ \mathbf{0} & \mathbf{0} \end{bmatrix} \begin{bmatrix} \phi_{i-1,j} & \bar{\phi}_{i-1,j} \end{bmatrix} \begin{bmatrix} \lambda_{i-1} & 0 \\ 0 & \bar{\lambda}_{i-1} \end{bmatrix}.$$

Right multiply this equation by U (see Lem. C.1) and insert $UU^{-1} = \mathbf{I}$ before the last matrix. Using Lem. C.1 and bearing in mind that $\lambda_{i-1} \in \mathbb{C}^0$ holds, one then arrives at (C.15) by redefining X, U and Δ as follows:

$$\begin{bmatrix} X \\ U \end{bmatrix} = \begin{bmatrix} \mathbf{I}_n & \mathbf{0} \\ \mathbf{0} & \mathbf{I}_m \end{bmatrix} \begin{bmatrix} \mathfrak{Re}(\phi_{i-1,j}) & \mathfrak{Im}(\phi_{i-1,j}) \end{bmatrix},$$
$$\Delta = \mathfrak{Im}(\lambda_{i-1}) \begin{bmatrix} 0 & 1 \\ -1 & 0 \end{bmatrix}.$$

Once again, if $X = \mathbf{0}$ holds, then $\mathrm{Im}\{\Pi_{i-1,j}\} = \{\mathbf{0}\} \subset \mathcal{R}^*$ holds trivially. Now, assume that $X \in \mathbb{R}^{n\times 2}$ is full rank. Let $F = U(X^\intercal X)^{-1}X^\intercal$ so that U can be substituted by FX holds in (C.15) to arrive at (C.16), which proves that $\mathrm{Im}\{X\} \subset \mathcal{V}^*$. In addition, $\mathrm{Im}\{X\} \subset \mathcal{R}^*$ holds iff $i-1 \in \mathcal{I}_z^c$ because (C.16) implies $\sigma(A+BF|X) = \sigma(\Delta) = \{\lambda_{i-1}, \bar{\lambda}_{i-1}\}$. Also, (iii) is valid in the current context, since (C.17) applies. Since $i-1 \in \mathcal{I}_z^c$ is equivalent to $i \in \mathcal{I}_z^c$ (recall that $\lambda_{i-1} = \bar{\lambda}_i$) and because

$$\mathrm{Im}\{\Pi_{i-1,j}\} = \mathrm{Im}\{\Pi_{i,j}\} = \mathrm{Im}\{X\},$$

holds, this completes the proof for any even i such that $i, i-1 \in [\![1, 2s]\!]$ and X is zero or full rank. This first part of the proof was inspired by [NS14, Th.4.1].

Keeping the same value of i, let us consider the last case, where X is neither full rank nor zero. Define $T := \begin{bmatrix} T_1 & T_2 \end{bmatrix} \in \mathbb{R}^{2\times 2}$ as a orthogonal matrix which is adapted to $\mathrm{Ker}\{X\}$, so that $\mathrm{Ker}\{X\} = \mathrm{span}\{T_1\}$ is non trivial. Right multiplication of (C.15) by T gives

$$\begin{bmatrix} A \\ C \end{bmatrix} \begin{bmatrix} \mathbf{0} & XT_2 \end{bmatrix} = \begin{bmatrix} \mathbf{0} & XT_2 \\ \mathbf{0} & \mathbf{0} \end{bmatrix} T^\intercal \Delta T - \begin{bmatrix} B \\ D \end{bmatrix} \begin{bmatrix} UT_1 & UT_2 \end{bmatrix}. \tag{C.18}$$

Because XT_2 is injective, one can define $F = UT_2((XT_2)^\intercal XT_2)^{-1}(XT_2)^\intercal$ so that $FXT_2 = UT_2$ holds. Substituting the last expression into (C.18) yields (C.16) with XT_2 and $T_2^\intercal \Delta T_2$ in place of X and Δ, respectively. This proves that $\mathrm{span}\{XT_2\} = \mathrm{Im}\{XT\} = \mathrm{Im}\{X\} \subset \mathcal{V}^*$. Now, the right multiplication of (C.15) by $T_1 \neq \mathbf{0}$ leads to:

$$\begin{bmatrix} X \\ \mathbf{0} \end{bmatrix} \Delta T_1 = \begin{bmatrix} B \\ D \end{bmatrix} UT_1 \tag{C.19}$$

This proves that $UT_1 \in \mathrm{Ker}\{D\}$, so that the vector $X\Delta T_1$ belongs not only to $\mathcal{V}^*$ but also to $B\mathrm{Ker}\{D\}$. As a result, $X\Delta T_1 \in \mathcal{V}^* \cap (B\mathrm{Ker}\{D\}) \subset \mathcal{R}^*$ holds, see e.g. [TSH12, Th.7.14]. Besides, from the expression of Δ and the fact that $\mathfrak{Im}(\lambda_{i-1}) \neq 0$, Lem. C.4 ensures that $\begin{bmatrix} \Delta T_1 & T_1 \end{bmatrix}$ is invertible. Thus, one has

$$\mathrm{Im}\{X\} = \mathrm{Im}\{X \begin{bmatrix} \Delta T_1 & T_1 \end{bmatrix}\} = \mathrm{span}\{X\Delta T_1\} \subset \mathcal{R}^*$$

In summary, if $i = 2k \in \mathcal{I} \cap [\![1, 2s]\!]$ holds, then $\mathrm{Im}\left\{\Pi_{i-1,j}\right\} = \mathrm{Im}\left\{\Pi_{i,j}\right\} = \mathrm{Im}\left\{X\right\}$ is included in $\mathcal{V}^*$ for all i, j whereas $\mathrm{Im}\left\{X\right\} \subset \mathcal{R}^*$ holds iff (a) $X = \mathbf{0}$ or (b) $i \in \mathcal{I}_z^c$ and X is full rank or (c) X is not full rank. □

Th. 9.9 can now be proven.

Proof. (Boundedness of the solutions). The dynamical equation of the closed loop of (9.1a) and (9.12) reads as follows:

$$\dot{x}(t) = (A + BF)x(t) + f(\theta(t), w(t)) \tag{C.20}$$

where $f(\theta, w) = (B\Gamma(\theta) - BF\Pi(\theta) + P)w$. From the linearity of $\Pi(\cdot)$ and $\Gamma(\cdot)$, the boundedness of $\theta(\cdot)$, and the boundedness of w (recall that S is semi-simple), one proves that $t \mapsto f(\theta(t), w(t))$ is bounded. Therefore, x is bounded as $(A + BF)$ is Hurwitz.

(Relative coordinates) Define $x_r(t) := \Pi(\theta(t))w(t)$ and $u_r(t) := \Gamma(\theta(t))w(t)$. Using (9.7) and (9.2), one can prove that

$$\dot{x}_r(t) = \sum_{(i,j)\in\mathcal{J}} \dot{\theta}_{i,j}(t)\Pi_{i,j}w(t) + \Pi(\theta(t))Sw(t)$$

so that

$$\begin{aligned} f(\theta(t), w(t)) &= \left(A\Pi(\theta(t)) - A\Pi(\theta(t)) + B\Gamma(\theta(t)) - BF\Pi(\theta(t)) + P\right) w(t) \\ &\overset{(9.7a)}{=} \Pi(\theta(t))Sw(t) - (A + BF)x_r(t) = \dot{x}_r(t) - (A + BF)x_r(t) - \sum_{(i,j)\in\mathcal{J}} \dot{\theta}_{i,j}(t)\Pi_{i,j}w(t) \end{aligned}$$

is valid. By injecting the previous expression in (C.20), this proves

$$\dot{\tilde{x}}(t) = (A + BF)\tilde{x}(t) - \sum_{(i,j)\in\mathcal{J}} \dot{\theta}_{i,j}(t)\Pi_{i,j}w(t) \tag{C.21a}$$

where $\tilde{x} := x - x_r$. In addition, subtracting (9.3b) from (9.1b) yields $e = C\tilde{x} + D\tilde{u}$. Remark that (9.12) reads $\tilde{u} = F\tilde{x}$, so that

$$e(t) = (C + DF)\tilde{x}(t) \tag{C.21b}$$

holds.

(a): In view of (C.21), the sum of the terms $\dot{\theta}_{i,j}(t)\Pi_{i,j}w(t)$ acts as a vanishing piecewise continuous perturbation on LTI dynamics with a Hurwitz state matrix. Thus, $\tilde{x} \to \mathbf{0}$ holds and, in turn, $e(t)$ tends to $\mathbf{0}$.

(b): The stable outer dynamics of the $(A + BF)$-invariant subspace $\mathcal{V}_g^*$ is driven by a vanishing piecewise continuous perturbation. This implies that $\tilde{x}(t) \to \mathcal{V}_g^*$ so that $e(t) \to (C + DF)\mathcal{V}_g^* = \{\mathbf{0}\}$.

(c): The linear dynamics is unperturbed and initialized at $\tilde{x}(0) = \mathbf{0} \Leftrightarrow x(0) = \Pi(\theta(0))w(0)$. This implies $e = \mathbf{0}$.

(d): The outer dynamics of $\mathcal{V}_g^*$ is identically zero because it is unperturbed and $\tilde{x}(0) \in \mathcal{V}_g^* \Leftrightarrow x(0) \in \Pi(\theta(0))w(0) + \mathcal{V}_g^*$ holds. This implies $e = \mathbf{0}$. □

C.1.5 Proofs of Rem. 9.7 and Rem. 9.10

Proof of Rem. 9.7:

Proof. Assume that ASM 9.3 is valid. Particularization of Cor. 9.6 to this particular case yields $\kappa = m - p \geq 0$ and $\delta_i = 0, (i \in [\![1, q]\!])$, so that $\dim \mathcal{F} = (m - p)|\mathcal{I}|$ holds. Besides, $\gamma_i = m - p$ holds. In this context, $\dim \mathcal{F}$ equals $(m - p)q$ if $m > p$ is valid and 0 if $m = p$ holds. □

Proof of Rem. 9.10:

Proof. Recall that ASM 9.3 is valid. One can check that $\gamma_i = m - p > 0$ implies $\mathcal{I} = \mathcal{I}_z^c = [\![1, q]\!]$ and, in turn, $\mathrm{Im}\left\{\Pi_{i,j}\right\} \subset \mathcal{R}^*, ((i,j) \in \mathcal{J})$ are valid, see (ii) of Prop. C.5. In this context, $\mathcal{J}$ equals $\mathcal{J}_g$, and in turn, item (b) of Th. 9.9 reads: If $F \in \mathbb{F}(\mathcal{V}_g^*)$, then (9.12) solves Problem 9.1. Following the proof of Th. 9.9, the condition $F \in \mathbb{F}(\mathcal{V}_g^*)$ can be relaxed to $F \in \mathbb{F}(\mathcal{R}^*)$ since, in the latter case, the *unperturbed* stable outer dynamics of the $(A + BF)$-invariant subspace $\mathcal{R}^*$ converges to $\mathbf{0}$, so that $e(t) \to (C + DF)\mathcal{R}^* = \{\mathbf{0}\}$. □

C.2 Proof of Lem. 9.12

As a preliminary step, consider the following instrumental lemma.

Lemma C.6. *Given linear spaces* $\mathbf{X}, \mathbf{Y}, \mathbf{W}$ *and linear operators* $\mathrm{A} : \mathbf{X} \to \mathbf{Y}$ *and* $\mathrm{B} : \mathbf{W} \to \mathbf{Y}$*. Assume that there exists a mapping* $\mathrm{C} : \mathbf{W} \to \mathbf{X}$ *(possibly non linear) satisfying* $\mathrm{A} \circ \mathrm{C} = \mathrm{B}$ *as illustrated by the following commutative diagram:*

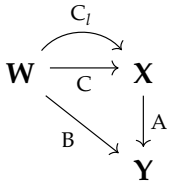

Then, there exists a linear *operator* $\mathrm{C}_l : \mathbf{W} \to \mathbf{X}$ *that satisfies* $\mathrm{A} \circ \mathrm{C}_l = \mathrm{B}$*.*

Proof. From $\mathrm{A} \circ \mathrm{C} = \mathrm{B}$, we can deduce that $\mathrm{Im}\,\{\mathrm{B}\}$ is included in $\mathrm{Im}\,\{\mathrm{A}\}$. Let $\underline{\mathrm{A}} \coloneqq \mathrm{Im}\,\{\mathrm{B}\}\,|\mathrm{A}|\mathrm{A}^{-1}\mathrm{Im}\,\{\mathrm{B}\}$ be the co-domain restriction to $\mathrm{Im}\,\{\mathrm{B}\}$ of the domain restriction of A to $\mathrm{A}^{-1}\mathrm{Im}\,\{\mathrm{B}\}$. By construction and from $\mathrm{Im}\,\{\mathrm{B}\} \subset \mathrm{Im}\,\{\mathrm{A}\}$, the mapping $\underline{\mathrm{A}} : \mathrm{A}^{-1}\mathrm{Im}\,\{\mathrm{B}\} \to \mathrm{Im}\,\{\mathrm{B}\}$ is surjective. Hence, it admits a right-inverse $\underline{\mathrm{A}}^+ : \mathrm{Im}\,\{\mathrm{B}\} \to \mathrm{A}^{-1}\mathrm{Im}\,\{\mathrm{B}\}$, i.e. $\underline{\mathrm{A}}\,\underline{\mathrm{A}}^+$ is the identity of $\mathrm{Im}\,\{\mathrm{B}\}$. Let $i_B : \mathrm{Im}\,\{\mathrm{B}\} \to \mathbf{Y}$ and $i_x : \mathrm{A}^{-1}\mathrm{Im}\,\{\mathrm{B}\} \to \mathbf{X}$ be the natural embeddings. Define the linear operator $\mathrm{C}_l : \mathbf{W} \to \mathbf{X}$ as $\mathrm{C}_l \coloneqq i_x \underline{\mathrm{A}}^+ i_B^{-1}\mathrm{B}$. From the following commutative diagram

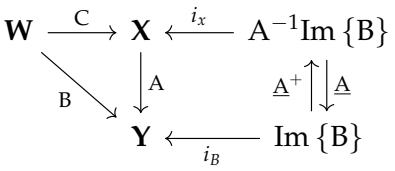

one can check that

$$\mathrm{A} \circ \mathrm{C} = \mathrm{A} \circ \mathrm{C}_l$$

is valid. □

The proof of Lem. 9.12 is now offered.

Proof. The first equivalence follows by applying Lem. C.6 with linear spaces $\mathbf{W} = \mathbf{E} \subset \mathbf{C}$, $\mathbf{X} = \mathbf{PC} \times \mathbf{PD}$ and $\mathbf{Y} = \mathbf{PC} \times \mathbf{PC}$ and the linear operators:

$$\mathrm{A} : (u_r, x_r) \mapsto (Ax_r + Bu_r - \dot{x}_r, Cx_r + Du_r)$$
$$\mathrm{B} : w \mapsto (-Pw, -Qw)$$

Indeed, using those notations, the left-hand side of the first equivalence means that there exists an operator $\mathrm{C} : \mathbf{W} \to \mathbf{X}$ solving $\mathrm{A} \circ \mathrm{C} = \mathrm{B}$. By virtue of Lem. C.6, this implies the existence of a *linear* operator $\mathrm{C}_l : \mathbf{W} \to \mathbf{X}$ satisfying $\mathrm{A} \circ \mathrm{C}_l = \mathrm{B}$, i.e. $\mathbf{L}(w) \cap \mathbf{R}(w)$ is non-empty for all $w \in \mathbf{E}$. The second equivalence can be proved by plugging $(u_r, x_r) = (\Gamma w, \Pi w)$ into (9.3), which gives (9.7). □

C.3 On $\mathcal{Z}_{bp}$ and the implication IR $\Rightarrow$ bp-WIR

C.3.1 $\mathcal{Z}_{bp}$ is well-defined and independent on $F \in \mathbb{F}(\mathcal{V}^*)$

Applying Lem. A.4 with $(\mathcal{V}, \mathcal{W}) = (\mathcal{V}^*_{bp}, \mathcal{V}^*)$ guarantees the existence of $F_{bp} \in \mathbb{F}(\mathcal{V}^*) \cap \mathbb{F}(\mathcal{V}^*_{bp})$. Since $\mathbb{F}(\mathcal{V}^*) \subset \mathbb{F}(\mathcal{R}^*)$, see Lem. A.5, this implies that both $\mathcal{V}^*_{bp}$ and $\mathcal{R}^*$ are $(A + BF_{bp})$-invariant, so that $(A + BF_{bp})|\mathcal{V}^*_{bp}/\mathcal{R}^*$ is a well-defined mapping.

Choose any $F \in \mathbb{F}(\mathcal{V}^*) \subset \mathbb{F}(\mathcal{R}^*)$. Recall that $(A + BF)|\mathcal{V}^*/\mathcal{R}^*$ equals $(A + BF_{bp})|\mathcal{V}^*/\mathcal{R}^*$, see Lem. A.5. Thus, using Lem. A.16 with $(A_1, A_2, \mathcal{V}, \mathcal{W}) = (A + BF_{bp}, A + BF, \mathcal{V}^*_{bp}/\mathcal{R}^*, \mathcal{V}^*/\mathcal{R}^*)$, one proves $(A + BF)$-invariance of $\mathcal{V}^*_{bp}/\mathcal{R}^*$ and $(A + BF)|\mathcal{V}^*_{bp}/\mathcal{R}^* = (A + BF_{bp})|\mathcal{V}^*_{bp}/\mathcal{R}^*$, i.e. $(A + BF)|(\mathcal{V}^*_{bp}/\mathcal{R}^*)$ and, in turn, $\mathcal{Z}_{bp}$ is independent of the choice of $F \in \mathbb{F}(\mathcal{V}^*)$.

C.3.2 IR $\Rightarrow$ bp-WIR

Assume that Σ is IR. Let us prove that it is also bp-WIR by constructing a bp signal $\tilde{u}$ that induces $\tilde{y} := \mathrm{H}[\tilde{x}_0; \tilde{u}] = \mathbf{0}$ for some initial condition $\tilde{x}_0$.

If $\rho > 0$, any bp signal $\tilde{u} : \mathbb{R}_{\geq 0} \to \mathrm{Ker}\,\{B\} \cap \mathrm{Ker}\,\{D\}$ associated with $\tilde{x}_0 = \mathbf{0}$ achieves that purpose and, in turn, proves that $\rho > 0$ implies Σ bp-WIR.

Henceforth, assume $\rho = 0$. By virtue of Th. 8.2, both $\mathcal{R}^*$ and $\mathcal{N}$ are nontrivial. This allows to build a matrix F in $\mathbb{F}(\mathcal{R}^*)$ satisfying $\sigma((A + BF)|\mathcal{R}^*) \subset \mathbb{C}^-$, see Lem. A.5, and to pick a non-zero vector v in $\mathcal{N}$. Note that $\rho = 0$ implies $Bv \neq \mathbf{0}$. Define the input

$$\tilde{u} := F\tilde{x} + wv,$$

with $w : t \mapsto \sin(\omega t)$ and $\tilde{x} := \mathrm{H}_x[\tilde{x}_0; \tilde{u}]$ and where ω is a strictly positive scalar, to be defined later on. Let $T := 2\pi/\omega$.

From Lem. A.5, recall that:

$$\begin{bmatrix} A + BF \\ C + DF \end{bmatrix} \mathcal{R}^* + \begin{bmatrix} B \\ D \end{bmatrix} \mathcal{N} \subset \mathcal{R}^* \oplus \{\mathbf{0}\}$$

holds. For any $\tilde{x}_0 \in \mathcal{R}^*$, this proves that $\tilde{x}(t)$ identically belongs to $\mathcal{R}^*$ and $\tilde{y}$ equals zero. This allows to consider the system $\dot{\tilde{x}} = A\tilde{x} + B\tilde{u}$ with state space $\mathcal{R}^*$, i.e.

$$\dot{\tilde{x}}_r = A_r\tilde{x}_r + b_r w \tag{C.22}$$

where $A_r := (A + BF)|\mathcal{R}^*$ and $b_r := \mathcal{R}^*|Bv \neq \mathbf{0}$. By construction, for any $x_0 \in \mathcal{R}^*$, the signal $\tilde{x}$ can be related to $\tilde{x}_r$ in a bijective manner. In fact, $i\tilde{x}_r = \tilde{x}$ holds with $i : \mathcal{R}^* \to \mathbb{R}^n$ the natural embedding.

If $\tilde{x}_0 \in \mathcal{R}^*$, then $\tilde{x}$ asymptotically converges to some T-periodic steady-state $\tilde{x}^\star : \mathbb{R}_{\geq 0} \to \mathcal{R}^*$ solving the state equation, i.e.

$$\lim_{t \to +\infty} \tilde{x}(t) - \tilde{x}^\star(t) = \mathbf{0}, \tag{C.23a}$$

$$\forall t \geq 0,\ \tilde{x}^\star(t + T) = \tilde{x}^\star(t), \tag{C.23b}$$

$$A\tilde{x}^\star + B\tilde{u}^\star = \dot{\tilde{x}}^\star, \tag{C.23c}$$

with

$$\tilde{u}^\star := F\tilde{x}^\star + wv.$$

Let us now prove this assertion. First, remark that w can be rewritten as $\begin{bmatrix} 1 & 0 \end{bmatrix} w^e$ for the T-periodic signal w^e solving $\dot{w}^e = Sw^e$ with $S := \left[\begin{smallmatrix} 0 & \omega \\ -\omega & 0 \end{smallmatrix}\right]$ and for some $w^e(0)$. Second, by

substituting $\tilde{x}_r$ by Πw^e in (C.22), one arrives at the Sylvester equation $\Pi S = A_r \Pi + b_r \begin{bmatrix} 1 & 0 \end{bmatrix}$. This equation admits a non-zero solution Π in view of $\sigma(A_r) \cap \sigma(S) = \{\varnothing\}$ and $b_r \neq \mathbf{0}$, [Gan00, p.225]. This proves that there exists a linear mapping $\Pi \neq \mathbf{0}$ that satisfies $\tilde{x}_r = \Pi w^e$. Let $\tilde{x}^\star := i\tilde{x}_r$ and observe that (C.23b) and (C.23c) are valid. To prove (C.23a), it suffices to remark that $\varepsilon := i^{-1}\tilde{x} - \tilde{x}_r$ solves $\dot{\varepsilon} = A_r \varepsilon$ in view of (C.23c) and to recall that A_r is Hurwitz.

Let us now prove that $\tilde{u}$ is bp if $\omega \in \mathbb{R}$ is chosen in such a way that T is not a multiple of the period of some purely imaginary mode of A, that is,

$$T \notin \{kT_a : k \in \mathbb{N} \setminus \{0\}, i2\pi/T_a \in \sigma(A)\} \tag{C.24}$$

First observe that $\tilde{u}^\star$ inherits continuity and T-periodicity from those of $\tilde{x}^\star$ and w. Since $\tilde{u}$ tends to $\tilde{u}^\star$, the former is bp if the latter is. Let us prove that $\tilde{u}^\star$ is indeed bp. By contradiction, first assume that $\tilde{u}^\star$ is zero. In this case, it holds $\dot{\tilde{x}}^\star = A\tilde{x}^\star$. This contradicts the fact that $\tilde{x}^\star$ is a T-periodic signal with ω satisfying (C.24). Thus, $\tilde{u}^\star$ is a nonzero signal. Since it is also periodic and continuous, this proves that it is bp.

C.4 Technical results on input and state trajectories related to $\mathcal{V}_g^*$ and $\mathcal{V}_{bp}^*$

Define the two properties $\mathbf{P}_g$ and $\mathbf{P}_{bp}$ that apply to a square matrix E:

- $\mathbf{P}_g(E)$ is valid if $\sigma(E) \subset \mathbb{C}^-$ holds;
- $\mathbf{P}_{bp}(E)$ is valid if $\sigma(E) \subset \mathbb{C}^0$ holds and E is semi-simple.

To keep things general and factorize the forthcoming mathematical developments, we introduce the (abstract) property $\mathbf{P}$. Our goal is to study the largest invariant subspace and the largest output nulling controlled invariant subspace where $\mathbf{P}$ is valid, i.e.

$$\mathcal{X}(\mathbf{P}) := \sup \mathfrak{V}_x(\mathbf{P})$$
$$\mathcal{V}^*(\mathbf{P}) := \sup \mathfrak{V}_v(\mathbf{P})$$

where

$$\mathfrak{V}_x(\mathbf{P}) := \{\mathcal{V} \mid A\mathcal{V} \subset \mathcal{V}, \mathbf{P}(A|\mathcal{V}) \text{ is valid}\} \tag{C.25a}$$
$$\mathfrak{V}_v(\mathbf{P}) := \{\mathcal{V} \mid \exists F \in \mathbb{F}(\mathcal{V}), \mathbf{P}((A+BF)|\mathcal{V}) \text{ is valid}\} \tag{C.25b}$$

For $\mathcal{X}(\mathbf{P})$ and $\mathcal{V}^*(\mathbf{P})$ to be well defined, it suffices to prove that both $\mathfrak{V}_x(\mathbf{P})$ and $\mathfrak{V}_v(\mathbf{P})$ possess at least one member and are upper semilattices with respect to inclusion and subspace addition. Next assumption translates this requirement.

Assumption C.7. $\mathbf{P}$ is such that (i) both $\mathfrak{V}_x(\mathbf{P})$ and $\mathfrak{V}_v(\mathbf{P})$ contain $\{\mathbf{0}\}$ and (ii) the following implications hold:

$$\mathcal{V}, \mathcal{W} \in \mathfrak{V}_x(\mathbf{P}) \Rightarrow \mathcal{V} + \mathcal{W} \in \mathfrak{V}_x(\mathbf{P}),$$
$$\mathcal{V}, \mathcal{W} \in \mathfrak{V}_v(\mathbf{P}) \Rightarrow \mathcal{V} + \mathcal{W} \in \mathfrak{V}_v(\mathbf{P}),$$

for all subspaces $\mathcal{V}$ and $\mathcal{W}$.

We also need to make the following assumption:

Assumption C.8. **P** is such that the following implication holds:

$$\left.\begin{array}{r} \mathcal{W} \in \mathfrak{V}_x(\mathbf{P}) \\ A\mathcal{V} \subset \mathcal{V} \subset \mathcal{W} \end{array}\right\} \Rightarrow \mathcal{V} \in \mathfrak{V}_x(\mathbf{P}),$$

for all subspaces $\mathcal{W}$.

Remark C.9 (Existing definitions captured by $\mathcal{X}(\cdot)$ and $\mathcal{V}^*(\cdot)$). By definition, it holds:

$$\begin{array}{ll} \mathcal{X}_g = \mathcal{X}(\mathbf{P}_g), & \mathcal{V}_g^* = \mathcal{V}^*(\mathbf{P}_g) \\ \mathcal{X}_{bp} = \mathcal{X}(\mathbf{P}_{bp}), & \mathcal{V}_{bp}^* = \mathcal{V}^*(\mathbf{P}_{bp}) \end{array}$$

The validity of ASM C.7 and ASM C.8 for $\mathbf{P} = \mathbf{P}_g$ is well known. Analogous results for $\mathbf{P} = \mathbf{P}_{bp}$ are offered in Subsec. C.4.2. •

Remark C.10 ($\mathcal{X}_a$ as a short for $\mathcal{X}_a(A)$). In the sequel, when there is a risk of confusion, the notation $\mathcal{X}_a(A), (a \in \{g, bp, b, s, c, u\})$ is used in place of $\mathcal{X}_a$ to make explicit the state matrix involved in the definition of $\mathcal{X}_a$. •

C.4.1 The largest invariant subspace of $\mathbb{R}^n$ and $\mathcal{V}^*$ where P is valid

Throughout this subsection, it is assumed that both ASM C.7 and ASM C.8 hold.

By the definition of $\mathcal{X}(\mathbf{P})$ and $\mathcal{V}^*(\mathbf{P})$, the following relationships immediately follow:

$$\mathcal{X}(\mathbf{P}) \cap \langle \mathcal{K}|A\rangle \subset \mathcal{V}^*(\mathbf{P}) \subset \mathcal{V}^*. \tag{C.26}$$

The first inclusion can be derived from

$$A(\mathcal{X}(\mathbf{P}) \cap \langle \mathcal{K}|A\rangle) \subset \mathcal{X}(\mathbf{P}) \cap \langle \mathcal{K}|A\rangle \subset \langle \mathcal{K}|A\rangle \subset \operatorname{Ker}\{C\}$$

which proves $F = \mathbf{0} \in \mathbb{F}(\mathcal{X}(\mathbf{P}) \cap \langle \mathcal{K}|A\rangle)$ and the validity of $\mathbf{P}((A+BF)|(\mathcal{X}(\mathbf{P}) \cap \langle \mathcal{K}|A\rangle))$, in view of ASM C.8 used with $(\mathcal{V}, \mathcal{W}) = (\mathcal{X}(\mathbf{P}) \cap \langle \mathcal{K}|A\rangle, \mathcal{X}(\mathbf{P}))$. The second one can be deduced from $\mathcal{V}^* = \sup\{\mathcal{V} : \mathbb{F}(\mathcal{V}) \neq \{\varnothing\}\}$.

In the following, we focus on the case whichere $\mathcal{R}^*$ is trivial. In this context, our main goal is to characterize the case where the first inclusion of (C.26) is actually an equality, see the forthcoming Lem. C.13. To this end, several intermediate statements are first established.

Lemma C.11. *Assume that $\mathcal{R}^*$ is trivial. Given any $F_0 \in \mathbb{F}(\mathcal{V}^*)$. Given any $\mathcal{V}$ and $F \in \mathbb{F}(\mathcal{V})$. Then, (i) $F_0 \in \mathbb{F}(\mathcal{V})$ and (ii) $(A+BF)|\mathcal{V} = (A+BF_0)|\mathcal{V}$ hold.*

Proof. Since $\mathcal{V} \subset \mathcal{V}^*$ holds, Lem. A.4 applies and ensures that there exists $F^e \in \mathbb{F}(\mathcal{V}^*) \cap \mathbb{F}(\mathcal{V})$ satisfying:

$$(A+BF^e)|\mathcal{V} = (A+BF)|\mathcal{V} \tag{C.27}$$

For any subspace $\mathcal{W}$, one can identify $\mathcal{W}/\mathcal{R}^*$ with $\mathcal{W}$ since $\mathcal{R}^*$ is trivial.. This allows to use Lem. A.16 with $(A_1, A_2, \mathcal{V}, \mathcal{W}) = (A+BF^e, A+BF_0, \mathcal{V}/\mathcal{R}^*, \mathcal{V}^*/\mathcal{R}^*)$ since $(A+BF^e)|\mathcal{V}^*/\mathcal{R}^* = (A+BF_0)|\mathcal{V}^*/\mathcal{R}^*$ by virtue of Lem. A.5. This proves that (a) $\mathcal{V}/\mathcal{R}^*$ is $(A+BF_0)$-invariant, and (b) $(A+BF^e)|\mathcal{V}/\mathcal{R}^* = (A+BF_0)|\mathcal{V}/\mathcal{R}^*$ holds.

Item (a) is equivalent to $(A+BF_0)\mathcal{V} \subset \mathcal{V}$ and, in turn, to (i) because $\mathcal{V} \subset \mathcal{V}^* \subset \operatorname{Ker}\{C+DF_0\}$ holds. Item (b) equivalently reads $(A+BF^e)|\mathcal{V} = (A+BF_0)|\mathcal{V}$ which is nothing but (ii) since (C.27) holds. □

Lemma C.12. *Assume that $\mathcal{R}^*$ is trivial. Given any $F_0 \in \mathbb{F}(\mathcal{V}^*)$. Then, $\mathcal{V}^*(\mathbf{P})$ is the largest subspace $\mathcal{V} \subset \mathcal{V}^*$ such that (i) $\mathcal{V}$ is $(A+BF_0)$-invariant, and (ii) $\mathbf{P}((A+BF_0)|\mathcal{V})$ is valid. Besides, $(A+BF_0)|\mathcal{V}^*(\mathbf{P})$ is independent of the selection of F_0 in $\mathbb{F}(\mathcal{V}^*)$.*

Proof. Define the following set:

$$\tilde{\mathfrak{V}}_v(\mathbf{P}, F_0) := \{\mathcal{V} \mid F_0 \in \mathbb{F}(\mathcal{V}), \mathbf{P}((A+BF_0)|\mathcal{V}) \text{ is valid}\}$$

Given any $F_0 \in \mathbb{F}(\mathcal{V}^*)$. It holds $\mathfrak{V}_v(\mathbf{P}) = \tilde{\mathfrak{V}}_v(\mathbf{P}, F_0)$: On the one hand, one has $\mathfrak{V}_v(\mathbf{P}) \supset \tilde{\mathfrak{V}}_v(\mathbf{P}, F_0)$, by definition. On the other hand, for any $\mathcal{V}$ that is proven to belong to $\mathfrak{V}_v(\mathbf{P})$ via F, Lem. C.11 ensures that $F_0 \in \mathbb{F}(\mathcal{V})$ and $(A+BF)|\mathcal{V} = (A+BF_0)|\mathcal{V}$ hold so that $\mathcal{V} \in \tilde{\mathfrak{V}}_v(\mathbf{P}, F_0)$, i.e. $\mathfrak{V}_v(\mathbf{P}) \subset \tilde{\mathfrak{V}}_v(\mathbf{P}, F_0)$.

As a result, $\mathcal{V}^*(\mathbf{P})$ is the largest subspace $\mathcal{V}$ in $\mathfrak{V}_v(\mathbf{P}) = \tilde{\mathfrak{V}}_v(\mathbf{P}, F_0)$, i.e. the largest $\mathcal{V}$ such that (a) $\mathcal{V}$ is $(A+BF_0)$-invariant, (b) $(C+DF_0)\mathcal{V}$ is trivial, and (c) $\mathbf{P}((A+BF_0)|\mathcal{V})$ is valid. One can freely add the new item (d) $\mathcal{V} \subset \mathcal{V}^*$ to this list, since $\mathcal{V}^*(\mathbf{P}) \subset \mathcal{V}^*$ holds. In this case, item (b) can be dropped since $\mathcal{V} \subset \mathcal{V}^* \subset \mathrm{Ker}\,\{C+DF_0\}$ holds.

Finally, the fact that $(A+BF_0)|\mathcal{V}^*(\mathbf{P})$ is independent of the selection of F_0 in $\mathbb{F}(\mathcal{V}^*)$ follows (A) by invoking Lem. A.5 to prove that $(A+BF_0)|\mathcal{V}^*/\mathcal{R}^*$ does not depend of $F_0 \in \mathbb{F}(\mathcal{V}^*)$, (B) by using the identity $\mathcal{V}^*(\mathbf{P})/\mathcal{R}^* \subset \mathcal{V}^*/\mathcal{R}^*$ and (C) by identifying $\mathcal{V}^*(\mathbf{P})/\mathcal{R}^*$ as $\mathcal{V}^*(\mathbf{P})$. □

Given any $F_0 \in \mathbb{F}(\mathcal{V}^*)$. If $\mathcal{R}^*$ is trivial, then Lem. C.12 ensures that the following set is well defined and does not depend on the choice of F_0 in $\mathbb{F}(\mathcal{V}^*)$:

$$\mathcal{Z}(\mathbf{P}) := \sigma(A+BF_0|\mathcal{V}^*(\mathbf{P})) \tag{C.28}$$

By choosing $F_0 \in \mathbb{F}(\mathcal{V}^*)$ as in Lem. A.6, one also derives the following relationship

$$\sigma(A|\mathcal{X}(\mathbf{P}) \cap \langle \mathcal{K}|A\rangle) \subset \mathcal{Z}(\mathbf{P}). \tag{C.29}$$

Indeed, $\mathcal{J} := \mathcal{X}(\mathbf{P}) \cap \langle \mathcal{K}|A\rangle$ inherits A-invariance from those of $\mathcal{X}(\mathbf{P})$ and $\langle \mathcal{K}|A\rangle$. Since, $F_0\mathcal{J} \subset F_0 \langle \mathcal{K}|A\rangle = \{\mathbf{0}\}$ implies $(A+BF_0)\mathcal{J} = A\mathcal{J} \subset \mathcal{J}$, this gives (C.29) from (C.26).

Lemma C.13. *Assume that $\mathcal{R}^*$ is trivial. The following statement are equivalent:*

(i) $\mathcal{V}^*(\mathbf{P}) \subset \langle \mathcal{K}|A\rangle$

(ii) $\mathcal{V}^*(\mathbf{P}) = \mathcal{X}(\mathbf{P}) \cap \langle \mathcal{K}|A\rangle$

(iii) $\mathcal{Z}(\mathbf{P}) = \sigma(A|\mathcal{X}(\mathbf{P}) \cap \langle \mathcal{K}|A\rangle)$

Proof. Let us choose $F_0 \in \mathbb{F}(\mathcal{V}^*)$ as in Lem. A.6, so that $\langle \mathcal{K}|A\rangle \subset \mathrm{Ker}\,\{F_0\}$ holds. Bear in mind that $\mathcal{V}^*(\mathbf{P})$ is $(A+BF_0)$-invariant by virtue of Lem. C.12.
(i)⇔(ii): In view of (C.26), it suffices to prove that (i) implies $\mathcal{V}^*(\mathbf{P}) \subset \mathcal{X}(\mathbf{P})$. From (i), one deduces $F_0\mathcal{V}^*(\mathbf{P}) \subset F_0 \langle \mathcal{K}|A\rangle = \{\mathbf{0}\}$ and, in turn, $A\mathcal{V}^*(\mathbf{P}) = (A+BF_0)\mathcal{V}^*(\mathbf{P}) \subset \mathcal{V}^*(\mathbf{P})$ and $A|\mathcal{V}^*(\mathbf{P}) = (A+BF_0)|\mathcal{V}^*(\mathbf{P})$. Hence, $\mathbf{P}(A|\mathcal{V}^*(\mathbf{P}))$ is equal to $\mathbf{P}((A+BF_0)|\mathcal{V}^*(\mathbf{P}))$, which is proven to be valid in Lem. C.12. This implies that $\mathcal{V}^*(\mathbf{P})$ is included in $\mathcal{X}(\mathbf{P})$ by the definition of $\mathcal{X}(\mathbf{P})$.
(ii)⇔(iii): Recall that both $\mathcal{J} := \mathcal{X}(\mathbf{P}) \cap \langle \mathcal{K}|A\rangle$ and $\mathcal{V}^*(\mathbf{P})$ are $(A+BF_0)$-invariant. In view of (C.26), this allows to apply Fact A.11 with $(\mathcal{V}, \mathcal{W}, A)$ corresponding to $(\mathcal{J}, \mathcal{V}^*(\mathbf{P}), A+BF_0)$. This proves (ii)⇔(iii) since $\sigma((A+BF_0)|\mathcal{J}) = \sigma(A|\mathcal{J})$ holds. □

C.4.2 Proof that ASM C.7 and ASM C.8 are valid for $\mathbf{P} = \mathbf{P}_{bp}$

Our primary goal in this subsection is to prove the following lemma.

Lemma C.14. *ASM C.7 holds true for* $\mathbf{P}_{bp}$.

Both $\mathfrak{V}_x(\mathbf{P}_{bp})$ and $\mathfrak{V}_v(\mathbf{P}_{bp})$ contain $\{\mathbf{0}\}$.[1] Therefore, it suffices to prove that these classes are closed under the operation of subspace addition. Before tackling this problem, preliminary results for $\mathbf{P}_{bp}$ are established. One of these results proves that ASM C.8 is valid for $\mathbf{P} = \mathbf{P}_{bp}$.

Preliminary results about $\mathbf{P}_{bp}$

$\mathbf{P}_{bp}(A|\mathcal{V})$ is valid iff $A|\mathcal{V}$ is $\mathbb{C}$-diagonalizable and its spectrum lies on $\mathbb{C}^0$. An alternative characterization is now offered using the geometric language.

Fact C.15. *Given an A-invariant subspace $\mathcal{V}$. $\mathbf{P}_{bp}(A|\mathcal{V})$ is valid iff there exist A-invariant subspaces $\mathcal{V}_k, (k \in [\![1, q]\!])$ such that $\mathcal{V} = \mathcal{V}_1 \oplus \ldots \oplus \mathcal{V}_q$, where for all k, it holds:*

$$A\mathcal{Y} \subset \mathcal{Y} \subset \mathcal{V}_k \Rightarrow \mathcal{Y} \in \{\{\mathbf{0}\}, \mathcal{V}_k\} \tag{C.30}$$

as well as $\sigma(A|\mathcal{V}_k) \subset \mathbb{C}^0$. Besides, if $\mathbf{P}_{bp}(A|\mathcal{V})$ is valid, then it holds:

$$A\mathcal{Y} \subset \mathcal{Y} \subset \mathcal{V} \Rightarrow \exists S \subset [\![1, k]\!] : \mathcal{Y} = \sum_{j \in S} \mathcal{V}_j \tag{C.31}$$

Proof. From a geometric point of view, computing the real Jordan form of $A|\mathcal{V}$ corresponds to decomposing $\mathcal{V}$ into the direct sum of A-invariant subspaces $\mathcal{V}_k$ where the matrices of $A|\mathcal{V}_k$ are similar to one of the two following real elementary Jordan blocks, depending on whether the eigenvalue $a_k + ib_k$ associated with $A|\mathcal{V}_k$ is real:

$$\begin{bmatrix} a_k & 1 & & \\ & a_k & \ddots & \\ & & \ddots & 1 \\ & & & a_k \end{bmatrix}, \quad \begin{bmatrix} E_k & \mathbf{I}_2 & & \\ & E_k & \ddots & \\ & & \ddots & \mathbf{I}_2 \\ & & & E_k \end{bmatrix}$$

where $E_k = \left[\begin{smallmatrix} a_k & b_k \\ -b_k & a_k \end{smallmatrix}\right] \in \mathbb{R}^{2\times 2}$, see e.g. [Per01, Sec.1.8]. By definition, $\mathbf{P}_{bp}(A|\mathcal{V})$ is valid iff (i) it is $\mathbb{C}$-diagonalizable and (ii) $\sigma(A|\mathcal{V}) \subset \mathbb{C}^0$ holds. On the one hand, (ii) is equivalent to $\sigma(A|\mathcal{V}_k) \subset \mathbb{C}^0$ for all k since $\sigma(A|\mathcal{V}) = \biguplus_k \sigma(A|\mathcal{V}_k)$ holds. On the other hand, (i) is equivalent to (C.30). To see this, pick any k and observe that, in general, other subspaces must be added to the class on the right-hand side of (C.30). One of them is the eigenspace related to the first column (the first and second columns, respectively) in the real case (in the imaginary case, respectively) of the elementary Jordan block associated with $A|\mathcal{V}_k$. Thus, (C.30) holds iff those subspaces coincide with $\mathcal{V}_k$ itself, i.e. the elementary Jordan blocks are either $[a_k]$ or E_k. This condition is necessary and sufficient for $A|\mathcal{V}_k$ to be $\mathbb{C}$-diagonalizable. This concludes the proof, since $A|\mathcal{V}$ is $\mathbb{C}$-diagonalizable iff each $A|\mathcal{V}_k$ enjoys this property.

To prove (C.31), recall that the class of A-invariant subspaces included in $\mathcal{W}$ is a lattice relative to $\subset$, $+$, and $\cap$. From (C.30), the nontrivial subspace of the smallest dimension of this lattice is $\mathcal{V}_k$s. Thus, A-invariance of $\mathcal{Y} \subset \mathcal{V}$ implies that $\mathcal{Y}$ equals $\sum_{j\in S} \mathcal{V}_j$ for some $S \subset [\![1, k]\!]$. □

[1] See footnote 1 on p.231.

By exploiting this characterization of $\mathbf{P}_{bp}$, the following fact gathers several statements establishing how property $\mathbf{P}_{bp}$ can be transmitted from one map to another.

Fact C.16. *Given two A-invariant finite dimensional vector spaces $\mathcal{V}$ and $\mathcal{W}$.*

(i) If $\mathcal{V}$ and $\mathcal{W}$ are isomorphic, then $\mathbf{P}_{bp}(A|\mathcal{V})$ is valid iff $\mathbf{P}_{bp}(A|\mathcal{W})$ is valid.

(ii) If $\mathcal{V} \subset \mathcal{W}$ holds, then validity of $\mathbf{P}_{bp}(A|\mathcal{W})$ implies the existence of an A-invariant subspace $\mathcal{J}$ satisfying $\mathcal{J} \oplus \mathcal{V} = \mathcal{W}$ and such that both $\mathbf{P}_{bp}(A|\mathcal{V})$ and $\mathbf{P}_{bp}(A|\mathcal{J})$ are valid.

(iii) If $\mathcal{V} \subset \mathcal{W}$ holds, then validity of $\mathbf{P}_{bp}(A|\mathcal{W})$ implies validity of $\mathbf{P}_{bp}(A|\mathcal{W}/\mathcal{V})$.

(iv) If $\mathcal{V} \cap \mathcal{W}$ is trivial, then $\mathbf{P}_{bp}(A|(\mathcal{V} \oplus \mathcal{W}))$ is valid iff both $\mathbf{P}_{bp}(A|\mathcal{V})$ and $\mathbf{P}_{bp}(A|\mathcal{W})$ are valid.

Proof. (i): If $\mathcal{V}$ and $\mathcal{W}$ are isomorphic, then $A|\mathcal{V}$ and $A|\mathcal{W}$ are similar maps and $\mathbf{P}_{bp}$ is preserved by similarity transformation.
(ii): From Fact C.15, A-invariance of $\mathcal{V} \subset \mathcal{W}$ together with the validity of $\mathbf{P}_{bp}(A|\mathcal{W})$ implies that $\mathcal{V}$ equals $\sum_{i\in S} \mathcal{W}_i$ for some $S \subset [\![1, q]\!]$, where the A-invariant subspaces $\mathcal{W}_k$ satisfy $\mathcal{W} = \mathcal{W}_1 \oplus \ldots \oplus \mathcal{W}_q$ and the properties defined in Fact C.15. Therefore, $\mathcal{W}$ equals $\mathcal{V} \oplus \mathcal{J}$ where $\mathcal{J} := \bigoplus_{j\in[\![1,q]\!]\setminus S} \mathcal{W}_j$. By construction, and in view of Fact C.15, $\mathbf{P}_{bp}(A|\mathcal{J})$ is valid.
(iii): Use (ii) and the fact that $\mathcal{J}$ and $\mathcal{W}/\mathcal{V}$ are isomorphic so that (i) applies.
(iv): Validity of both $\mathbf{P}_{bp}(A|\mathcal{V})$ and $\mathbf{P}_{bp}(A|\mathcal{W})$ implies the existence of A-invariant subspaces $\mathcal{V}_k$ and $\mathcal{W}_k$ such that $\mathcal{V} = \mathcal{V}_1 \oplus \ldots \oplus \mathcal{V}_r$ and $\mathcal{W} = \mathcal{W}_1 \oplus \ldots \oplus \mathcal{W}_q$ holds, where $\mathcal{V}_k, (k \in [\![1, r]\!])$ and $\mathcal{W}_k, (k \in [\![1, q]\!])$ satisfy the properties defined in Fact C.15. Since $\mathcal{V} \cap \mathcal{W}$ is trivial, this proves that $\mathbf{P}_{bp}(A|(\mathcal{V} \oplus \mathcal{W}))$ is valid since $\mathcal{V} \oplus \mathcal{W} = \mathcal{V}_1 \oplus \ldots \oplus \mathcal{V}_r \oplus \mathcal{W}_1 \oplus \ldots \oplus \mathcal{W}_q$ holds. Conversely, (ii) and the validity of $\mathbf{P}_{bp}(A|(\mathcal{V} \oplus \mathcal{W}))$ ensure the existence of an A-invariant subspace $\mathcal{J}$ such that both $\mathbf{P}_{bp}(A|\mathcal{V})$ and $\mathbf{P}_{bp}(A|\mathcal{J})$ are valid and $\mathcal{J} \oplus \mathcal{V} = \mathcal{V} \oplus \mathcal{W}$ holds. This last equality proves that $\mathcal{W}$ and $\mathcal{J}$ are isomorphic, so that (i) induces that $\mathbf{P}_{bp}(A|\mathcal{W})$ is valid. □

ASM C.8 is valid for $\mathbf{P} = \mathbf{P}_{bp}$

Lemma C.17. *ASM C.8 holds true for $\mathbf{P}_{bp}$.*

Proof. Just use item ((ii)) of Fact. C.16. □

Closure property on $\mathfrak{V}_x(\mathbf{P}_{bp})$

Lemma C.18. *$\mathfrak{V}_x(\mathbf{P}_{bp})$ is closed under the operation of subspace addition.*

Proof. Pick any $\mathcal{V}, \mathcal{W} \in \mathfrak{V}_x(\mathbf{P}_{bp})$. Since $\mathcal{V} + \mathcal{W}$ is A-invariant, as the sum of A-invariant subspaces, it suffices to prove that $\mathbf{P}_{bp}(A|(\mathcal{V} + \mathcal{W}))$ is valid. Fact C.15 proves the existence of A-invariant subspaces $\mathcal{V}_k$ satisfying $\mathcal{V} = \mathcal{V}_1 \oplus \ldots \oplus \mathcal{V}_q$, and for all k, $\sigma(A|\mathcal{V}_k) \subset \mathbb{C}^0$ and (C.30). An analogous argument proves the existence of a similar decomposition of $\mathcal{W}$ as $\mathcal{W}_1 \oplus \ldots \oplus \mathcal{W}_r$. For all k, $\mathcal{V}_k \cap \mathcal{W}$ is A-invariant as the intersection of A-invariant subspaces. From (C.30), if this subspace is not trivial, then it is equal to $\mathcal{V}_k$, so that $\mathcal{V}_k \subset \mathcal{W}$. Hence, the sum $\mathcal{V}_k + \mathcal{W}$ is either direct or equal to $\mathcal{W}$. This proves

$$\mathcal{W} + \mathcal{V} = \bigoplus_{k\in[\![1,r]\!]} \mathcal{W}_k \oplus \bigoplus_{k\in\mathcal{I}} \mathcal{V}_k$$

where $\mathcal{I} := \{k \in [\![1, q]\!] : \mathcal{V}_k \cap \mathcal{W} = \{\mathbf{0}\}\}$. By the definition of $\mathcal{V}_k$ and $\mathcal{W}_k$, this relationship implies that $\mathcal{V} + \mathcal{W}$ is A-invariant and that $\sigma(A|(\mathcal{V} + \mathcal{W})) = \uplus_{k\in[\![1,r]\!]} \sigma(A|\mathcal{V}_k) \uplus \uplus_{k\in\mathcal{I}} \sigma(A|\mathcal{W}_k) \subset \mathbb{C}^0$ holds. This proves that $\mathbf{P}_{bp}(A|(\mathcal{V} + \mathcal{W}))$ is valid by virtue of Fact C.15. □

Closure property on $\mathfrak{V}_v(\mathbf{P}_{bp})$

Lemma C.19. *Given any $\mathcal{V}$ and $F \in \mathbb{F}(\mathcal{V})$. Define*

$$\mathcal{R} := \langle A + BF | \mathcal{V} \cap B\mathrm{Ker}\,\{D\} \rangle.$$

There exists a mapping F_0 and a subspace $\mathcal{J}$ such that (i) $F_0 \in \mathbb{F}(\mathcal{J}) \cap \mathbb{F}(\mathcal{R}) \cap \mathbb{F}(\mathcal{V})$, (ii) $\mathcal{V} = \mathcal{J} \oplus \mathcal{R}$ and (iii) $\mathbf{P}_{bp}((A + BF_0)|\mathcal{R})$ is valid. In addition, if $\mathbf{P}_{bp}((A + BF)|\mathcal{V})$ is valid, then (iv) $\mathbf{P}_{bp}((A + BF_0)|\mathcal{J})$ is also valid.

Proof. First, recall that $\mathcal{R}$ is $(A + BF)$-invariant and contained in $\mathcal{V}$, see Lem. A.5. This lemma also ensures that $\mathbb{F}(\mathcal{V}) \subset \mathbb{F}(\mathcal{R})$, so that (i) is equivalent to $F_0 \in \mathbb{F}(\mathcal{J}) \cap \mathbb{F}(\mathcal{V})$.

Assume that $\mathbf{P}_{bp}((A + BF)|\mathcal{V})$ is valid. In this context, Fact C.16 can be invoked to prove the existence of an $(A + BF)$-invariant subspace $\mathcal{J}$ satisfying $\mathcal{V} = \mathcal{J} \oplus \mathcal{R}$, such that both $\mathbf{P}_{bp}((A + BF)|\mathcal{R})$ and $\mathbf{P}_{bp}((A + BF)|\mathcal{J})$ are valid. Because $\mathcal{V} \subset \mathrm{Ker}\,\{C + DF\}$, this implies $F \in \mathbb{F}(\mathcal{J})$ which proves (i), (ii), (iii), and (iv) for $F_0 = F$.

Henceforth, let us remove the assumption that $\mathbf{P}_{bp}((A + BF)|\mathcal{V})$ is valid. Let $r \in \mathbb{N}$ be the quotient of the division of $\dim \mathcal{R}$ by 2. Choose distinct strictly positive reals $\omega_1, \ldots, \omega_r$ such that

$$\{\pm i\omega_1, \ldots, \pm i\omega_r\} \cap \sigma((A + BF)|\mathcal{V}/\mathcal{R}) = \{\varnothing\}. \tag{C.32}$$

Define the polynomials $q_e(s)$ and $q(s)$ as follows:

$$q_e(s) = \prod_{k=1}^{r} (s^2 + \omega_k^2),$$

$$q(s) = \begin{cases} q_e(s), & \text{if } \dim \mathcal{R} \text{ is even,} \\ s\, q_e(s), & \text{otherwise.} \end{cases}$$

Lem. A.5 guarantees the existence of $F_0 \in \mathbb{F}(\mathcal{V})$ such that the characteristic polynomial of $(A + BF_0)|\mathcal{R}$ equals $q(s)$. This implies (iii) by the construction of $q(s)$.

To end the proof, it suffices to prove that $\mathcal{R}$ is complementable (in $\mathcal{V}$), i.e. that there exists an $(A + BF_0)$-invariant subspace $\mathcal{J} \subset \mathcal{V}$ satisfying (ii). Indeed, in such a case, $F_0 \in \mathbb{F}(\mathcal{J})$ holds since $\mathcal{V} \subset \mathrm{Ker}\,\{C + DF_0\}$. If $\mathcal{R} = \mathcal{V}$ holds, $\mathcal{J} = \{\mathbf{0}\}$ proves that $\mathcal{R}$ is trivially complementable. Besides, if $\dim \mathcal{R}$ is even or if $0 \notin \sigma((A + BF)|\mathcal{V}/\mathcal{R})$ holds, then $(A + BF)|\mathcal{R}$ and $(A + BF_0)|\mathcal{V}/\mathcal{R}$ have a disjoint spectrum so that $\mathcal{R}$ is also complementable.

Let us investigate the remaining case: Henceforth, assume that $\mathcal{R} \subsetneq \mathcal{V}$ and $0 \in \sigma((A + BF_0)|\mathcal{V}/\mathcal{R})$ hold and $\dim \mathcal{R}$ is odd, so that $\sigma((A + BF_0)|\mathcal{R}) = \{0, \pm i\omega_1, \ldots, \pm i\omega_r\}$. By splitting this spectrum, one proves the existence of $\mathcal{R}_0, \mathcal{R}_\omega$ satisfying (a) $\mathcal{R}_0 \oplus \mathcal{R}_\omega = \mathcal{R}$, (b) $\sigma((A + BF_0)|\mathcal{R}_0) = \{0\}$ and (c) $\sigma(A_\omega) = \{\pm i\omega_1, \ldots, \pm i\omega_r\}$ with $A_\omega := (A + BF_0)|\mathcal{R}_\omega$. Similarly, all the zeros in the spectrum of $\sigma((A + BF_0)|\mathcal{V}/\mathcal{R})$ can be separated from the rest to prove the existence of $\mathcal{V}_N$ satisfying (d) $\mathcal{R} \subsetneq \mathcal{V}_N \subset \mathcal{V}$, (e) $(A + BF_0)(\mathcal{V}_N/\mathcal{R}) \subset \mathcal{V}_N/\mathcal{R}$ and (f) $\sigma(N) = \{0, \ldots, 0\}$ with $N := (A + BF_0)|\mathcal{V}_N/\mathcal{R}$. Consider a basis P of $\mathcal{V}$ that is adapted to $\mathcal{R}_\omega \oplus \mathcal{R}_0 \subset \mathcal{V}_N \subset \mathcal{V}$. In P, the map $(A + BF_0)|\mathcal{V}$ reads:

$$\left[\begin{array}{cc|cc} A_\omega & \mathbf{0} & A_{13} & A_{14} \\ \mathbf{0} & 0 & A_{23} & A_{24} \\ \hline \mathbf{0} & \mathbf{0} & N & \mathbf{0} \\ \mathbf{0} & \mathbf{0} & \mathbf{0} & A_{44} \end{array}\right] \tag{C.33}$$

From (C.32), (c) and (f), it holds

$$\sigma(A_\omega) \cap \sigma(N) = \{\varnothing\} \tag{C.34a}$$

$$\sigma(A_{44}) \cap (\sigma(A_\omega) \cup \{0\}) = \{\varnothing\} \tag{C.34b}$$

$\mathcal{R}$ is complementable iff the following Sylvester equation admits solution, see e.g. [BM92, p.132]:

$$\begin{bmatrix} A_\omega & \mathbf{0} \\ \mathbf{0} & 0 \end{bmatrix} X - X \begin{bmatrix} N & \mathbf{0} \\ \mathbf{0} & A_{44} \end{bmatrix} = - \begin{bmatrix} A_{13} & A_{14} \\ A_{23} & A_{24} \end{bmatrix} \tag{C.35}$$

By splitting the unknown matrix X as follows

$$X =: \begin{bmatrix} X_{11} & X_{12} \\ X_{21} & X_{22} \end{bmatrix}$$

equation (C.35) can be decomposed in the following way:

$$A_\omega X_{11} - X_{11} N = -A_{13} \tag{C.36a}$$
$$A_\omega X_{12} - X_{12} A_{44} = -A_{14} \tag{C.36b}$$
$$-X_{21} N = -A_{23} \tag{C.36c}$$
$$-X_{22} A_{44} = -A_{24} \tag{C.36d}$$

Both Sylvester equations (C.36a) and (C.36b) are solvable in view of (C.34a) and (C.34b). Because (C.34b) also implies that A_{44} is invertible, (C.36d) is also solvable. Therefore, there exists X solving (C.35) iff (C.36c) admits solution. This condition is equivalent to $A_{23}Q = \mathbf{0}$ where columns of Q form a basis of $\mathrm{Ker}\,\{N\}$.

Assume that $A_{23}Q$ is distinct from zero. It is now shown that $A_{23}Q = \mathbf{0}$ can be imposed by tuning F, i.e. there exists F_1 such that $A'_{23}Q = \mathbf{0}$ holds, where A'_{23} is obtained from $A + B(F_0 + F_1)$ in the same way as A_{23} has been derived from $A + BF_0$. To see this, let $\mathcal{N}_v := B^{-1}\mathcal{V} \cap \mathrm{Ker}\,\{D\}$. Observe that the map $\mathcal{V}|B|\mathcal{N}_v$ is well defined and reads as follows in the basis P of $\mathcal{V}$:

$$\begin{bmatrix} B_1 \\ B_2 \\ \mathbf{0} \\ \mathbf{0} \end{bmatrix} \tag{C.37}$$

This lemma also ensures that the following pair is controllable:

$$\begin{bmatrix} A_\omega & \mathbf{0} \\ \mathbf{0} & 0 \end{bmatrix}, \begin{bmatrix} B_1 \\ B_2 \end{bmatrix}$$

This proves that the single-line matrix B_2 is nonzero and, in turn, full row rank. Consider some mapping $F_1 : \mathcal{V} \to \mathcal{N}_v$. From Lem. A.5, one obtains

$$\begin{bmatrix} A + B(F_0 + F_1) \\ C + D(F_0 + F_1) \end{bmatrix} \mathcal{V} \subset \begin{bmatrix} A + BF_0 \\ C + DF_0 \end{bmatrix} \mathcal{V} + \begin{bmatrix} B \\ D \end{bmatrix} \mathcal{N}_v \subset \mathcal{V} \oplus \{\mathbf{0}\}$$

which proves $(F_0 + F_1) \in \mathbb{F}(\mathcal{V})$. Without loss of generality, assume that $F_1|\mathcal{V}$ in the basis P reads $\begin{bmatrix} \mathbf{0} & \mathbf{0} & F_{13} & \mathbf{0} \end{bmatrix}$. By construction, the matrix of $(A + B(F_0 + F_1))|\mathcal{V}$ in this basis reads as in (C.33) with $A_{13} + B_1 F_{13}$ and $A_{23} + B_2 F_{13} =: A'_{23}$ in place of A_{13} and A_{23}, respectively. This proves $(A + B(F_0 + F_1))|\mathcal{R} = (A + BF_0)|\mathcal{R}$ so that $\mathbf{P}_{bp}((A + B(F_0 + F_1))|\mathcal{R})$ inherits the validity of $\mathbf{P}_{bp}((A + BF_0)|\mathcal{R})$. Thus, it remains to be proven that $\mathcal{R}$ is complementable in $\mathcal{V}$ and w.r.t. $A + B(F_0 + F_1)$. In this context, the previous necessary and sufficient condition for the solvability of the equation analogous to (C.35) reads as follows:

$$A'_{23}Q = \mathbf{0} \Leftrightarrow (A_{23} + B_2 F_{13})Q = \mathbf{0} \Leftrightarrow A_{23}Q + B_2 F'_{13} = \mathbf{0} \tag{C.38}$$

where $F'_{13} := F_{13}Q$. Since B_2 is full rank, there exists F'_{13} satisfying (C.38). Bearing in mind that Q is a full column rank so that there exists $Q^\dagger$ satisfying $Q^\dagger Q = \mathbf{I}$, this leads to $F_{13} = F'_{13}Q^\dagger$ solving (C.38). In summary, if $A_{23}Q$ is distinct from zero, then there exists F_1 such that $A'_{23}Q = \mathbf{0}$ holds, which proves that $\mathcal{R}$ is complementable. □

Lemma C.20. *$\mathfrak{V}_v(\mathbf{P}_{bp})$ is closed under the operation of subspace addition.*

Proof. Pick any $\mathcal{V}$ in $\mathfrak{V}_v(\mathbf{P}_{bp})$, i.e. there exists $F \in \mathbb{F}(\mathcal{V})$ such that $\mathbf{P}_{bp}((A+BF)|\mathcal{V})$ is valid. For further references, let us already define

$$\mathcal{R}_v \coloneqq \langle A+BF|\mathcal{V} \cap B\mathrm{Ker}\,\{D\}\rangle.$$

Similarly, pick any $\mathcal{W}$ in $\mathfrak{V}_v(\mathbf{P}_{bp})$ and define $\mathcal{R}_w$ in an analogous manner.

Recall the equivalence (A.10), that is valid for any subspace $\mathcal{V}$. This allows to conclude that

$$\begin{bmatrix} A \\ C \end{bmatrix}(\mathcal{V}+\mathcal{W}) = \begin{bmatrix} A \\ C \end{bmatrix}\mathcal{V} + \begin{bmatrix} A \\ C \end{bmatrix}\mathcal{W} \subset (\mathcal{V}+\mathcal{W}) \oplus \{\mathbf{0}\} + \mathrm{Im}\left\{\begin{bmatrix} B \\ D \end{bmatrix}\right\}$$

holds, which in turn proves that there exists $F_0 \in \mathbb{F}(\mathcal{V}+\mathcal{W})$. This allows to define:

$$\mathcal{R}_{vw} \coloneqq \langle A+BF_0|(\mathcal{V}+\mathcal{W}) \cap B\mathrm{Ker}\,\{D\}\rangle.$$

By virtue of Lem. C.19, there exists a mapping F_{vw} and a subspace $\mathcal{J}_{vw}$ such that (i) $F_{vw} \in \mathbb{F}(\mathcal{J}_{vw}) \cap \mathbb{F}(\mathcal{R}_{vw}) \cap \mathbb{F}(\mathcal{V}+\mathcal{W})$, (ii) $\mathcal{V}+\mathcal{W} = \mathcal{J}_{vw} \oplus \mathcal{R}_{vw}$ and (iii) $\mathbf{P}_{bp}((A+BF_{vw})|\mathcal{R}_{vw})$ is valid. In view of item ((iv)) of Fact C.16, to prove that $\mathcal{V}+\mathcal{W}$ belongs to $\mathfrak{V}_v(\mathbf{P}_{bp})$, it suffices to ensure the validity of $\mathbf{P}_{bp}((A+BF_{vw})|\mathcal{J}_{vw})$. Since $\mathcal{J}_{vw}$ and

$$\mathcal{A} \coloneqq (\mathcal{V}+\mathcal{W})/\mathcal{R}_{vw}$$

are isomorphic, this is equivalent to the validity of $\mathbf{P}_{bp}((A+BF_{vw})|\mathcal{A})$, in view of item ((i)) of Fact C.16. Note that $(A+BF_{vw})$-invariance of both $\mathcal{V}+\mathcal{W}$ and $\mathcal{R}_{vw}$ ensures that $(A+BF_{vw})|\mathcal{A}$ is indeed well-defined.

It is proved in the sequel that $\mathcal{A}$ can be decomposed as follows

$$\mathcal{A} \coloneqq \underbrace{(\mathcal{J}_v+\mathcal{R}_{vw})/\mathcal{R}_{vw}}_{\mathcal{A}_v} + \underbrace{(\mathcal{J}_w+\mathcal{R}_{vw})/\mathcal{R}_{vw}}_{\mathcal{A}_w} \tag{C.39}$$

for some $\mathcal{J}_v$ and $\mathcal{J}_w$ for which both $\mathcal{A}_v$ and $\mathcal{A}_w$ are $(A+BF_{vw})$-invariant and such that

$$\mathbf{P}_{bp}((A+BF_{vw})|\mathcal{A}_v) \text{ is valid} \tag{C.40}$$

$$\mathbf{P}_{bp}((A+BF_{vw})|\mathcal{A}_w) \text{ is valid} \tag{C.41}$$

In such a case, $\mathbf{P}_{bp}((A+BF_{vw})|\mathcal{A})$ is valid since the class $\{\mathcal{Q} \subset (\mathcal{V}+\mathcal{W})/\mathcal{R}_{vw} : (A+BF_{vw})\mathcal{Q} \subset \mathcal{Q}, \mathbf{P}_{bp}((A+BF_{vw})|\mathcal{Q}) \text{ is valid}\}$ is closed under the operation of subspace addition, as proved via direct extension of Lem. C.18.

The existence of such a subspace $\mathcal{J}_v$ is ensured by Lem. C.19. Indeed, this lemma proves the existence of a mapping F_v and of a subspace $\mathcal{J}_v$ such that (i) $F_v \in \mathbb{F}(\mathcal{J}_v) \cap \mathbb{F}(\mathcal{V})$, (ii) $\mathcal{V} = \mathcal{J}_v \oplus \mathcal{R}_v$ and (iii) $\mathbf{P}_{bp}((A+BF_v)|\mathcal{J}_v)$ is valid. In view of Lem. A.4, there exists F_v^e such that $F_v^e \in \mathbb{F}(\mathcal{V}) \cap \mathbb{F}(\mathcal{V}+\mathcal{W})$ and $(A+BF_v^e)|\mathcal{V} = (A+BF_v)|\mathcal{V}$ hold. Since $\mathcal{J}_v$ is included in $\mathcal{V}$ and $F_v \in \mathbb{F}(\mathcal{J}_v)$ holds, this implies that $\mathcal{J}_v$ is $(A+BF_v^e)$-invariant and that

$$\mathbf{P}_{bp}((A+BF_v^e)|\mathcal{J}_v) \text{ is valid.} \tag{C.42}$$

The proof of (C.40) is derived from (C.42) as follows:

$$\text{(C.42)} \overset{1}{\Rightarrow} \mathbf{P}_{bp}((A+BF_v^e)|\mathcal{J}_v/(\mathcal{R}_{vw} \cap \mathcal{J}_v)) \text{ i.v.} \overset{2}{\Leftrightarrow} \mathbf{P}_{bp}((A+BF_v^e)|\mathcal{A}_v) \text{ i.v.} \overset{3}{\Leftrightarrow} \text{(C.40)} \tag{C.43}$$

where "i.v." means "is valid" and implication as well as equivalences are numbered for further references. Before proving (C.43), note that every restriction of $(A+BF_v^e)$ involved in

those identities is well defined if $\mathcal{R}_{vw}$ is $(A + BF_v^e)$-invariant. In view of Lem. A.5, this is indeed the case since $F_v^e \in \mathbb{F}(\mathcal{V} + \mathcal{W})$ holds. Implication 1 of (C.43) can be proven by invoking item ((iii)) of Fact C.16. Equivalence 2 of (C.43) follows from item ((i)) of Fact C.16 and $\mathcal{A}_v \simeq \mathcal{J}_v/(\mathcal{R}_{vw} \cap \mathcal{J}_v)$, see e.g. [Won85, p.11]. Equivalence 3 of (C.43) derives from $(A + BF_v^e)|\mathcal{A}_v = (A + BF_{vw})|\mathcal{A}_v$ which can be proved via Lem. A.16 with $(\mathcal{V}, \mathcal{W}, A_1, A_2) = (\mathcal{A}_v, (\mathcal{V} + \mathcal{W})/\mathcal{R}_{vw}, A + BF_v^e, A + BF_{vw})$, which applies by virtue of Lem. A.5.

Similarly, one proves the existence of $\mathcal{J}_w$ satisfying (C.41) and $\mathcal{W} = \mathcal{J}_w \oplus \mathcal{R}_w$.

It remains to prove (C.39). This follows from $\mathcal{R}_v, \mathcal{R}_w \subset \mathcal{R}_{vw}$ and $\mathcal{R}_{vw} \subset \mathcal{V} + \mathcal{W} = \mathcal{J}_v + \mathcal{R}_v + \mathcal{J}_w + \mathcal{R}_w$ which induce:

$$\mathcal{A} = (\mathcal{J}_v + \mathcal{J}_w + \mathcal{R}_{vw})/\mathcal{R}_{vw} = \mathcal{A}_v + \mathcal{A}_w$$

To conclude, let us prove $\mathcal{R}_v \subset \mathcal{R}_{vw}$. The inclusion $\mathcal{R}_w \subset \mathcal{R}_{vw}$ follows in a similar manner. On the one hand, one has $\mathcal{R}_{vw} \supset (\mathcal{V} + \mathcal{W}) \cap B\mathrm{Ker}\,\{D\} \supset \mathcal{V} \cap B\mathrm{Ker}\,\{D\}$ by definition of $\mathcal{R}_{vw}$. Intersecting by $\mathrm{Im}\,\{B\}$ yields $\mathcal{R}_{vw} \cap \mathrm{Im}\,\{B\} \supset \mathcal{V} \cap B\mathrm{Ker}\,\{D\}$. On the other hand, $\mathcal{R}_v$ can be written $\langle A + BF_v^e|\mathcal{V} \cap B\mathrm{Ker}\,\{D\}\rangle$ because $\mathcal{R}_v \subset \mathcal{V}$ holds. This implies $\mathcal{R}_v \subset \mathcal{R}_{vw}$ because $\mathcal{R}_{vw} = \langle A + BF_v^e|\mathcal{R}_{vw} \cap \mathrm{Im}\,\{B\}\rangle$ holds by virtue of Lem. A.5. □

C.4.3 Decomposition of $\mathcal{V}^*$

This subsection is devoted to the analysis of state trajectories that identically belong to $\mathcal{V}^*$ in the case where $\mathcal{R}^*$ is trivial. To this end, let us first particularize Lem. C.13 for $\mathbf{P} = \mathbf{P}_{bp}$.

Corollary C.21. *Assume that $\mathcal{R}^*$ is trivial. The following statement are equivalent:*

(i) $\mathcal{V}_{bp}^* \subset \langle \mathcal{K}|A\rangle$

(ii) $\mathcal{V}_{bp}^* = \mathcal{X}_{bp} \cap \langle \mathcal{K}|A\rangle$

(iii) $\mathcal{Z}_{bp} = \sigma(A|\mathcal{X}_{bp} \cap \langle \mathcal{K}|A\rangle)$

The use of $\mathbf{P}_g$ and $\mathbf{P}_{bp}$, together with (A.2), also allows the decomposition of $\mathcal{V}^*$ when $\mathcal{R}^*$ is trivial, as shown in the next lemma.

Lemma C.22. *Assume that $\mathcal{R}^*$ is trivial. Given any $F \in \mathbb{F}(\mathcal{V}^*)$. Then, $\mathcal{V}_g^*$ and $\mathcal{V}_{bp}^*$ are $(A + BF)$-invariant, and there exists a subspace $\mathcal{V}_b^* \subset \mathbb{R}^n$ such that:*

$$\mathcal{V}^* = \mathcal{V}_g^* \oplus \mathcal{V}_{bp}^* \oplus \mathcal{V}_b^* \tag{C.44}$$

holds. Besides, both $(A + BF)|\mathcal{V}_g^*$ and $(A + BF)|\mathcal{V}_{bp}^*$ are independent of the selection of F in $\mathbb{F}(\mathcal{V}^*)$.

Proof. To prove that both $\mathcal{V}_g^*$ and $\mathcal{V}_{bp}^*$ are $(A + BF)$-invariant, it suffices to invoke Lem. C.12 with $\mathbf{P} = \mathbf{P}_g$ and then $\mathbf{P} = \mathbf{P}_{bp}$. This also proves that $(A + BF)|\mathcal{V}_g^*$ and $(A + BF)|\mathcal{V}_{bp}^*$ do not depend on $F \in \mathbb{F}(\mathcal{V}^*)$. Define $E := (A + BF)|\mathcal{V}^*$. Exploiting (A.2) on E allows to decompose $\mathbb{R}^{\dim \mathcal{V}^*}$ into $\mathcal{X}_g(E) \oplus \mathcal{X}_{bp}(E) \oplus \mathcal{X}_b(E)$. Define the natural embedding $i : \mathcal{V}^* \to \mathbb{R}^n$. From Fact A.14, one gets

$$\mathcal{V}^* = i\mathbb{R}^{\dim \mathcal{V}^*} = i(\mathcal{X}_g(E) \oplus \mathcal{X}_{bp}(E) \oplus \mathcal{X}_b(E)) = i\mathcal{X}_g(E) \oplus i\mathcal{X}_{bp}(E) \oplus i\mathcal{X}_b(E)$$

Clearly, $i\mathcal{X}_g(E)$ corresponds to the largest $(A + BF)$-invariant subspace $\mathcal{V} \subset \mathcal{V}^*$ such that $\sigma(A + BF|\mathcal{V}) \subset \mathbb{C}^-$, i.e. $i\mathcal{X}_g(E)$ equals $\mathcal{V}_g^*$ in view of Lem. C.12. Similarly, one concludes that $i\mathcal{X}_{bp}(E) = \mathcal{V}_{bp}^*$. This yields (C.44), with $\mathcal{V}_b^* := i\mathcal{X}_b(E)$. □

C.4.4 Input and state trajectories when Σ is not IR

The following lemma exploits (C.44) to decompose the state trajectories associated with zero output in the case where Σ is not IR.

Lemma C.23. *Assume that Σ is not IR. Choose any $F \in \mathbb{F}(\mathcal{V}^*)$. Given $x_0 \in \mathcal{X}$ and $(u, x, y) \in \mathbf{Q}(x_0)$. It holds*

$$y = \mathbf{0} \Leftrightarrow \begin{cases} x_0 \in \mathcal{V}^* \\ u = Fx \end{cases} \tag{C.45}$$

In addition, if (C.45) *holds, then x can be uniquely decomposed as follows:*

$$x = x_g + x_{bp} + x_b$$

where for all $a \in \{g, bp\}$:

- *x_a satisfies $x_a(0) \in \mathcal{V}_a^*$ and:*

$$\dot{x}_a = (A + BF)x_a, \tag{C.46a}$$
$$\mathbf{0} = (C + DF)x_a, \tag{C.46b}$$

- *x_a and Fx_a identically belong to $\mathcal{V}_a^*$ and $\mathcal{M}_a$, respectively, where $\mathcal{M}_{bp}, \mathcal{M}_g \subset \mathbb{R}^m$ are defined by* (9.26) *and the following equation:*

$$\mathcal{M}_g := \begin{bmatrix} B \\ D \end{bmatrix}^{-1} \left(\mathcal{V}_g^* \oplus \{0\} + \begin{bmatrix} A \\ C \end{bmatrix} \mathcal{V}_g^* \right). \tag{C.47}$$

Proof. First, note that if Σ is not IR, then both $\mathcal{N}$ and $\mathcal{R}^*$ are trivial, as proved in [**KT21**, Th.3.1]. In this context, (C.45) is a corollary of Lem. A.7. Assume that (C.45) holds. Because $\mathcal{R}^* = \{\mathbf{0}\}$ holds, Lem. C.22 applies. It allows us to uniquely decompose x_0 according to (C.44) and, in turn, x in the same way, because $u = Fx$ and by the linearity of $x_0 \mapsto e^{t(A+BF)}x_0$. This yields (C.46a). For all $a \in \{g, bp\}$, Lem. C.22 also proves that $\mathcal{V}_a^*$ is $(A + BF)$-invariant, so that x_a identically belongs to $\mathcal{V}_a^* \subset \mathcal{V}^* \subset \operatorname{Ker}\{C + DF\}$. This proves that (C.46b) and $Fx_a(t) \in \mathcal{M}_a$, $(t \geq 0)$, as in the proof of Prop. 9.16. □

Combining Lem. A.3 with Lem. C.23 gives the following lemma.

Lemma C.24. *Assume that Σ is not IR. Given $x_0 \in \mathcal{X}$ and $(u, x, y) \in \mathbf{Q}(x_0)$. Assume that $y = \mathbf{0}$ holds true. Then:*

(i) x is bp iff $x_0 \in (\mathcal{V}_g^* + \mathcal{V}_{bp}^*) \setminus \mathcal{V}_g^*$ hold.

(ii) u is bp only if $\mathcal{M}_{bp}$ is non trivial;

(iii) If "x bp" implies "u not bp" (for all x_0 such that $y = \mathbf{0}$ holds), then $\mathcal{V}_{bp}^* = \mathcal{X}_{bp} \cap \langle \mathcal{K} | A \rangle$ holds.

Proof. Let us use the notation of Lem. C.23. Choose any $F \in \mathbb{F}(\mathcal{V}^*)$.
(i): From (C.45), $\dot{x} = (A + BF)x$ holds with $x_0 \in \mathcal{V}^*$. Define the natural embedding $i : \mathcal{V}^* \to \mathbb{R}^n$. One can focus on the reduced dynamic associated with $x = ix_E$ and governed by $\dot{x}_E = Ex_E$ with

$$E := A + BF|\mathcal{V}^*.$$

From the injectivity of i, $x = ix_E$ is bp iff x_E is bp. From Lem. A.3 and Fact A.15, this is equivalent to $x_0 \in i((\mathcal{X}_g(E) + \mathcal{X}_{bp}(E)) \setminus \mathcal{X}_g(E)) = (i\mathcal{X}_g(E) + i\mathcal{X}_{bp}(E)) \setminus i\mathcal{X}_g(E) = (\mathcal{V}_g^* + \mathcal{V}_{bp}^*) \setminus \mathcal{V}_g^*$

since $i\mathcal{X}_g(E) = \mathcal{V}_g^*$ and $i\mathcal{X}_{bp}(E) = \mathcal{V}_{bp}^*$ hold, as shown in the proof of Lem. C.22.
(ii): $Fx_g(t)$ tends to zero and $\|Fx_b(t)\|$ either is zero or tends to infinity. Because $u = F(x_{bp} + x_g + x_b)$ holds, owing to (C.45), this implies that u is bp only if Fx_{bp} is non-zero. From Lem. C.23, $\mathcal{M}_{bp} \neq \{\mathbf{0}\}$ is a necessary condition for this to append.
(iii): Consider any $x(0)$ such that $x = x_g + x_{bp} + x_b$ is bp. From (i), this is equivalent to saying that $x_b(0) = \mathbf{0}$ holds, and $x_{bp}(0)$ is arbitrary in $\mathcal{V}_{bp}^* \setminus \{\mathbf{0}\}$. Hence, x_b is zero so that u equals $F(x_{bp} + x_g)$ which tends to Fx_{bp}. Assume that u is not bp. This implies $x_{bp}(t) \to \operatorname{Ker}\{F\}$ which is equivalent to $x_{bp}(0) \in \operatorname{Ker}\{F\}$ because x_{bp} is periodic. Therefore, $\mathcal{V}_{bp}^* \subset \operatorname{Ker}\{F\}$ holds because $x_{bp}(0)$ is arbitrary in $\mathcal{V}_{bp}^* \setminus \{\mathbf{0}\}$. As a result, and in view of Lem. C.22 and $\mathcal{V}_{bp}^* \subset \mathcal{V}^* \subset \operatorname{Ker}\{C + DF\}$, one gets:

$$\begin{bmatrix} A \\ C \end{bmatrix} \mathcal{V}_{bp}^* = \begin{bmatrix} A + CF \\ C + DF \end{bmatrix} \mathcal{V}_{bp}^* \subset \mathcal{V}_{bp}^* \oplus \{\mathbf{0}\}$$

which proves that $\mathcal{V}_{bp}^*$ is an A-invariant subspace contained in $\operatorname{Ker}\{C\}$, i.e. $\mathcal{V}_{bp}^* \subset \langle \mathcal{K}|A\rangle$, and in turn, $\mathcal{V}_{bp}^* = \mathcal{X}_{bp} \cap \langle \mathcal{K}|A\rangle$ holds by virtue of Cor. C.21. □

C.5 Proof of Prop. 9.16

Let us first assume that Σ is IR. Referring to [**KT21**, Th. 3.1], all conditions are valid (and therefore equivalent) in this case, namely (i) since IR implies WIR, (ii) because IR is equivalent to $\dim(\mathcal{R}^*) > 0$ or $\rho > 0$, (iii) due to the fact that IR is equivalent to $\dim \mathcal{N} > 0$ and $\mathcal{N} \subset \mathcal{M}$ holds in view of the following reformulation of $\mathcal{N}$, see (8.7):

$$\mathcal{N} = \begin{bmatrix} B \\ D \end{bmatrix}^{-1} (\mathcal{V}^* \oplus \{\mathbf{0}\}) \tag{C.48}$$

and (iv) since IR is equivalent to $\operatorname{nrank}\{P\} < n + m$.

Henceforth, assume that Σ is not IR, so that $\rho = \dim \mathcal{R}^* = \dim \mathcal{N} = 0$ holds, as well as $\operatorname{nrank}\{P\} = n + m$.

As a first step, let $\mathcal{V}^*$ be trivial. In this context, all conditions are false (and therefore equivalent), namely (i) since $\mathrm{H}[\tilde{x}_0; \tilde{u}] = \mathbf{0}$ implies $\tilde{x}_0 = \mathbf{0}$ (see (C.45) for $\mathcal{V}^* = \{\mathbf{0}\}$) and therefore $\tilde{u} = \mathbf{0}$ because Σ is not IR, i.e. left-invertible, (ii) by inspection, (iii) since $\mathcal{M}$ reduces to $\operatorname{Ker}\left\{\left[\begin{smallmatrix} B \\ D \end{smallmatrix}\right]\right\}$ and $\rho = 0$ and (iv) because $\mathcal{V}^* = \{\mathbf{0}\}$ implies $\mathcal{Z} = \{\varnothing\}$.

The rest of the proof is devoted to the case where $\mathcal{V}^*$ is non-trivial (and Σ is not IR). In this context, the negation of the conditions reads as follows. ¬(i): The implication $\mathrm{H}[\tilde{x}_0; \tilde{u}] = \mathbf{0} \Rightarrow \tilde{u} = \mathbf{0}$ holds for all $\tilde{x}_0 \in \mathbb{R}^n$. ¬(ii): $\mathcal{V}^* = \langle \mathcal{K}|A\rangle$. ¬(iii): $\mathcal{M}$ is trivial. ¬(iv): $\mathcal{Z} \subset \mathcal{Z}_{\mathrm{od}}$. It is now proven that the negation of all conditions is equivalent.

¬(i)⇒ ¬(ii): This follows from the definition of $\langle \mathcal{K}|A\rangle$.

¬(ii)⇒ ¬(iii): $\mathcal{V}^* = \langle \mathcal{K}|A\rangle$ implies that $\left[\begin{smallmatrix} A \\ C \end{smallmatrix}\right] \mathcal{V}^* \subset \mathcal{V}^* \oplus \{\mathbf{0}\}$, so that $\mathcal{M}$ reduces to $\mathcal{N}$ which is trivial, see (C.48).

¬(iii)⇒ ¬(i): Pick arbitrary $\tilde{x}_0$ and $\tilde{u}$, such that $\mathrm{H}[\tilde{x}_0; \tilde{u}] = \mathbf{0}$ holds. This equality is equivalent to $\mathrm{H}_x[\tilde{x}_0; \tilde{u}](t) \in \mathcal{V}^*$ for all $t \geq 0$, see (C.45). As a result, $\left[\begin{smallmatrix} A \\ C \end{smallmatrix}\right] \tilde{x}(t) + \left[\begin{smallmatrix} B \\ D \end{smallmatrix}\right] \tilde{u}(t) = \left[\begin{smallmatrix} \dot{\tilde{x}}(t) \\ y(t) \end{smallmatrix}\right]$ belongs to $\mathcal{V}^* \oplus \{\mathbf{0}\}$ for all $t \geq 0$. This implies that $\tilde{u}(t)$ belongs identically to $\mathcal{M}$. Thus, if $\mathcal{M}$ is trivial, then $\tilde{u} = \mathbf{0}$ holds.

¬(ii)⇔ ¬(iv): Choose $F \in \mathbb{F}(\mathcal{V}^*)$ as in Lem. A.6, so that $\langle \mathcal{K}|A\rangle$ is $(A + BF)$-invariant and $(A + BF)|\langle \mathcal{K}|A\rangle = A|\langle \mathcal{K}|A\rangle$ holds. Applying Fact A.11 with $(\mathcal{V}, \mathcal{W}, A) = (\langle \mathcal{K}|A\rangle, \mathcal{V}^*, A + BF)$ proves that ¬(ii) is equivalent to $\mathcal{Z}_{\mathrm{od}} = \sigma((A + BF)|\langle \mathcal{K}|A\rangle) = \sigma((A + BF)|\mathcal{V}^*) = \mathcal{Z}$. This is equivalent to ¬(iv) since $\mathcal{R}^* = \{\mathbf{0}\}$ implies $\mathcal{Z} \supset \mathcal{Z}_{\mathrm{od}}$ by virtue of Lem. A.8.

C.6 Proof of Th. 9.15

Equivalence between the first four items has already been proven in the discussion above the statement of Th. 9.15.

Let us focus on conditions (iv) to (vi) for the time being. First observe that if Σ is WIR, then those conditions are valid (and therefore equivalent) in view of items (ii) and (iv) of Prop. 9.16. Assume now that Σ is not WIR and, in turn, not IR, so that $\rho = \dim \mathcal{R}^* = 0$ holds, as well as $\operatorname{nrank}\{P_\Sigma\} = n + m$, $\mathcal{V}^* = \langle \mathcal{K}|A\rangle$ and $\mathcal{Z} \subset \mathcal{Z}_{\text{od}}$, see Prop. 9.23. Note that $\mathcal{Z} \subset \mathcal{Z}_{\text{od}}$ is equivalent to $\mathcal{Z} = \mathcal{Z}_{\text{od}}$ by virtue of Lem. A.8. In this context, the conditions are as follows: (iv) $\dim \langle \mathcal{K}|A\rangle > 0$, (v) $\dim \mathcal{V}^* > 0$ and (vi) $\mathcal{Z} \neq \{\varnothing\}$. Clearly, they are all equivalent.

Let us prove (vi)$\Leftrightarrow$(vii). From (A.18), (vii) implies (vi). Conversely, let us prove $\neg$(vii)$\Rightarrow$ $\neg$(vi). This implication can be reformulated as follows: If $\operatorname{rank}\{P_\Sigma(z)\} = n + m = \operatorname{nrank}\{P_\Sigma\}$ for all $z \in \mathbb{C}$, then $\mathcal{Z} = \{\varnothing\}$ holds. This follows from Lem. A.9.

C.7 Proof of Prop. 9.23

Let us first assume that Σ is IR. Referring to [**KT21**, Th. 3.1], all conditions are valid (and therefore equivalent) in this case, namely (i) since IR implies bp-WIR, see Sec. C.3, (ii) because IR is equivalent to $\dim(\mathcal{R}^*) > 0$ or $\rho > 0$, (iii) due to the fact that IR is equivalent to $\dim \mathcal{N} > 0$ and

$$\mathcal{N} = \begin{bmatrix} B \\ D \end{bmatrix}^{-1} (\mathcal{R}^* \oplus \{\mathbf{0}\}) \subset \begin{bmatrix} B \\ D \end{bmatrix}^{-1} (\mathcal{V}_{bp}^* \oplus \{\mathbf{0}\}) \subset \mathcal{M}_{bp}$$

holds in view of the identities $\mathcal{R}^* \subset \mathcal{V}_{bp}^*$ and $\mathcal{N} = B^{-1}\mathcal{R}^* \cap \operatorname{Ker}\{D\}$ and (iv) since IR is equivalent to $\operatorname{nrank}\{P\} < n + m$.

Henceforth, assume that Σ is not IR, so that $\rho = \dim \mathcal{R}^* = \dim \mathcal{N} = 0$ holds as well as $\operatorname{nrank}\{P\} = n + m$. If, in addition to that, $\mathcal{V}_{bp}^*$ is trivial, then one can verify that all conditions are false (and therefore equivalent), namely (ii) by inspection, (iii) since $\mathcal{M}_{bp}$ reduces to $\operatorname{Ker}\left\{\left[\begin{smallmatrix} B \\ D \end{smallmatrix}\right]\right\}$ and $\rho = 0$, (i) due to item (ii) of Lem. C.24 and $\mathcal{M}_{bp} = \{\mathbf{0}\}$ and (iv) because $\mathcal{Z}_{bp} = \{\varnothing\}$ holds if $\mathcal{V}_{bp}^*$ is trivial.

The rest of the proof is devoted to the case where $\mathcal{V}_{bp}^*$ is non-trivial (and Σ is not IR). In this context, the negation of the conditions reads as follows. $\neg$(i): The implication $(\mathrm{H}[\tilde{x}_0; \tilde{u}] = \mathbf{0} \Rightarrow \tilde{u}$ not bp) holds for all $\tilde{x}_0 \in \mathbb{R}^n$. $\neg$(ii): $\mathcal{V}_{bp}^* \subset \langle \mathcal{K}|A\rangle$. $\neg$(iii): $\mathcal{M}_{bp}$ is trivial. $\neg$(iv): $\mathcal{Z}_{bp} = \sigma(A|\mathcal{X}_{bp} \cap \langle \mathcal{K}|A\rangle)$. Note that the expression of $\neg$(iv) follows from (C.29) with $\mathbf{P} = \mathbf{P}_{bp}$. It is now proven that these conditions are equivalent.

$\neg$(i)$\Rightarrow$ $\neg$(ii): Pick any $\tilde{x}_0$ and any $(\tilde{u}, \tilde{x}, \tilde{y}) \in \mathbf{Q}(\tilde{x}_0)$ such that $\tilde{y} = \mathbf{0}$ holds. $\tilde{u}$ not bp due to $\neg(i)$. In this context, item (iii) of Lem. C.24 applies and proves that $\mathcal{V}_{bp}^* \subset \langle \mathcal{K}|A\rangle$, in view of Cor. C.21.

$\neg$(ii)$\Rightarrow$ $\neg$(iii): From $\mathcal{V}_{bp}^* \subset \langle \mathcal{K}|A\rangle$, one obtains $\mathcal{V}_{bp}^* \oplus \{\mathbf{0}\} + \left[\begin{smallmatrix} A \\ C \end{smallmatrix}\right] \mathcal{V}_{bp}^* \subset \langle \mathcal{K}|A\rangle \oplus \{\mathbf{0}\} + \left[\begin{smallmatrix} A \\ C \end{smallmatrix}\right] \langle \mathcal{K}|A\rangle = \langle \mathcal{K}|A\rangle \oplus \{\mathbf{0}\} \subset \mathcal{V}^* \oplus \{\mathbf{0}\}$. Hence, $\mathcal{M}_{bp}$ is included in $\left[\begin{smallmatrix} B \\ D \end{smallmatrix}\right]^{-1} (\mathcal{V}^* \oplus \{\mathbf{0}\}) = \mathcal{N}$ which is trivial since Σ is IR.

$\neg$(iii)$\Rightarrow$ $\neg$(i): See item (ii) of Lem. C.24.

$\neg$(ii)$\Leftrightarrow$ $\neg$(iv): See Cor. C.21.

C.8 Proof of Th. 9.22

Equivalence between the first three items has already been proven in the discussion above the statement of Th. 9.22.

First, observe that if Σ is bp-WIR, then all remaining conditions are valid (and therefore equivalent). Indeed, Prop. 9.23 ensures $\rho > 0$ or $\dim(\mathcal{R}^*) > 0$ or $\dim(\mathcal{V}_{bp}^*/(\mathcal{R}^* + \langle \mathcal{K}|A\rangle \cap \mathcal{V}_{bp}^*)) > 0$, which implies $\rho > 0$ or $\dim(\mathcal{V}_{bp}^*) > 0$ because $\mathcal{R}^* \subset \mathcal{V}_{bp}^*$ holds.

Henceforth, assume that Σ is not bp-WIR and, in turn, not IR (see Sec. C.3), so that $\rho = \dim \mathcal{R}^* = 0$ holds as well as $\operatorname{nrank}\{P_\Sigma\} = n + m$ and $\mathcal{V}_{bp}^* \subset \langle \mathcal{K}|A\rangle$, see Prop. 9.23. In view of Cor. C.21, this implies $\mathcal{V}_{bp}^* = \mathcal{X}_{bp} \cap \langle \mathcal{K}|A\rangle$ and $\mathcal{Z}_{bp} = \sigma(A|\mathcal{X}_{bp} \cap \langle \mathcal{K}|A\rangle)$.

In this context, the conditions are as follows: (iii) $\exists \tilde{x}_0, \exists(\tilde{u}, \tilde{x}, \tilde{y}) \in \mathbf{Q}(\tilde{x}_0) : \tilde{y} = \mathbf{0}, \tilde{x}$ bp, (iv) $\dim \mathcal{X}_{bp} \cap \langle \mathcal{K}|A\rangle > 0$, (v) $\dim \mathcal{V}_{bp}^* > 0$ and (vi) $\mathcal{Z}_{bp} \neq \{\varnothing\}$. Clearly, (iv), (v), and (vi) are all equivalent. Equivalence (iii)$\Leftrightarrow$(v) follows from item (i) of Lem. C.24 because $\dim \mathcal{V}_{bp}^* > 0 \Leftrightarrow (\mathcal{V}_g^* + \mathcal{V}_{bp}^*) \setminus \mathcal{V}_g^* \neq \{\varnothing\}$, in view of (C.44).

C.9 Proofs related to the construction of annihilators

C.9.1 Strong annihilators

Proof of Th. 9.17

From $F \in \mathbb{F}(\mathcal{V}^*)$, one obtains $(A + BF)\mathcal{V}^* \subset \mathcal{V}^*$ which proves that A_a is well defined. Matrix B_a is also well-posed because $B\mathcal{N} \subset \mathcal{V}^*$ holds.

Pick any $\eta = x_{a0} = x_a(0)$ and any v. Denote by x_a the corresponding state trajectory of the strong annihilator. Define $\tilde{x}_r := \Psi x_a$ and observe that this relationship is valid for $t = 0$ by definition of the annihilator. By construction of the quadruple (9.22), it holds $\dot{\tilde{x}}_r = (A + BF)\tilde{x}_r + BNv$ or, equivalently, $\dot{\tilde{x}}_r = A\tilde{x}_r + B\tilde{u}_r$ since $\tilde{u}_r = F\tilde{x}_r + Nv$ holds. This implies that $(\tilde{u}_r, \tilde{x}_r, \tilde{y}_r) \in \mathbf{Q}(\tilde{x}_r(0))$ holds for some $\tilde{y}_r$ because $v \in \mathbf{PC}$ induces $\tilde{x}_r \in \mathbf{C}$ and, in turn, $\tilde{u}_r = F\tilde{x}_r + Nv \in \mathbf{PC}$. From $\tilde{x}_r(0) \in \mathcal{V}^*$ and the definition of $\tilde{u}_r$, it is ensured by Lem. A.7 that $\tilde{y}_r$ is zero.

Since both $\eta \in \mathbb{R}^{\dim \mathcal{N}}$ and $v \in \mathbf{PC}$ are arbitrary, this proves that the mapping associated with (9.22) is a strong annihilator of Σ, by definition. Indeed, one of the items in Th. 9.15 states that $\rho > 0$ or $\dim(\mathcal{V}^*) > 0$ holds, which proves that the annihilator is non-zero, that is, there exists v and η such that $(\tilde{x}_r(0), \tilde{u}_r) \neq \mathbf{0}$.

Proof of maximal range

Pick any $\tilde{x}_r(0)$ and any $\tilde{u}_r$ satisfying $(\tilde{u}_r, \mathbf{0}) \in \mathbf{W}(\tilde{x}_r(0))$. By virtue of Lem. A.7, $\tilde{x}_r(0) \in \mathcal{V}^*$ holds, so that there exists η satisfying $\tilde{x}_r(0) = \Psi\eta$, and there exists v satisfying $\tilde{u}_r = F\tilde{x}_r + Nv$ where $\tilde{x}_r$ solves $\dot{\tilde{x}}_r = A\tilde{x}_r + B\tilde{u}_r = (A + BF)\tilde{x}_r + BNv$. As in the proof of Th. 9.17, one establishes that the state trajectory x_a of the strong annihilator fed by v and initialized at $x_a(0) = \eta$ is equal to $\Psi^{-1}\tilde{x}_r$. This proves $\tilde{u}_r = \mathrm{H}_\perp[x_{a0}; v]$.

Let us prove $v \in \mathbf{PC}$. First, note that $\tilde{u}_r \in \mathbf{PC}$ is implied by $(\tilde{u}_r, \mathbf{0}) \in \mathbf{W}(\tilde{x}_r(0))$. Then, observe that $\mathrm{H}_x[\tilde{x}_0; \mathbf{PC}] \subset \mathbf{C}$ holds for all $\tilde{x}_0$ so that $\tilde{x}_r \in \mathbf{C}$ holds. Since $\mathbf{PC} \supset \mathbf{C}$ is linear then $Nv = \tilde{u}_r - F\tilde{x}_r$ and, in turn, v belongs to $\mathbf{PC}$, due to injectivity of N.

C.9.2 bp-strong annihilators

Preliminaries

Lemma C.25. *Assume that $\mathcal{V}_{bp}^*$ is nontrivial. It holds $\mathbb{F}(\mathcal{V}^*) \subset \mathbb{F}(\mathcal{V}_{bp}^*)$.*

Proof. First, note that both $\mathbb{F}(\mathcal{V}^*)$ and $\mathbb{F}(\mathcal{V}_{bp}^*)$ are non-empty because $\mathcal{V}_{bp}^* \subset \mathcal{V}^*$ are non-trivial. Choose any $F \in \mathbb{F}(\mathcal{V}^*)$. Since $\mathcal{V}_{bp}^* \subset \mathcal{V}^* \subset \operatorname{Ker}\{C + DF\}$ holds, one should prove that $\mathcal{V}_{bp}^*$

is $(A+BF)$-invariant. Applying Lem. A.4 with $(\mathcal{V},\mathcal{W}) = (\mathcal{V}^*_{bp},\mathcal{V}^*)$ proves the existence of $F^v_{bp} \in \mathbb{F}(\mathcal{V}^*) \cap \mathbb{F}(\mathcal{V}^*_{bp})$. This leads to the following equivalences:

$$(A+BF^v_{bp})\mathcal{V}^*_{bp} \subset \mathcal{V}^*_{bp} \overset{1}{\Leftrightarrow} (A+BF^v_{bp})(\mathcal{V}^*_{bp}/\mathcal{R}^*) \subset (\mathcal{V}^*_{bp}/\mathcal{R}^*)$$
$$\overset{2}{\Leftrightarrow} (A+BF)(\mathcal{V}^*_{bp}/\mathcal{R}^*) \subset (\mathcal{V}^*_{bp}/\mathcal{R}^*) \overset{3}{\Leftrightarrow} (A+BF)\mathcal{V}^*_{bp} \subset \mathcal{V}^*_{bp}$$

Bearing in mind that $F^v_{bp}, F \in \mathbb{F}(\mathcal{V}^*) \subset \mathbb{F}(\mathcal{R}^*)$ holds, equivalences 1 and 3 follow from Lem. A.17, whereas equivalence 2 is due to

$$(A+BF^v_{bp})|(\mathcal{V}^*_{bp}/\mathcal{R}^*) = (A+BF)|(\mathcal{V}^*_{bp}/\mathcal{R}^*). \tag{C.49}$$

This last equality can be proven by invoking Lem. A.16 with $(\mathcal{V},\mathcal{W},A_1,A_2) = (\mathcal{V}^*_{bp}/\mathcal{R}^*, \mathcal{V}^*/\mathcal{R}^*, A+BF^v_{bp}, A+BF)$ which applies because $(A+BF^v_{bp})|(\mathcal{V}^*/\mathcal{R}^*) = (A+BF)|(\mathcal{V}^*/\mathcal{R}^*)$ holds, in view of Lem. A.5. □

Lemma C.26. *Assume that $\mathcal{V}^*_{bp}$ is non trivial. Let $\tilde{x}_r(0) \in \mathcal{V}^*_{bp}$. Choose any $(\tilde{u}_r,\tilde{x}_r)$ such that $(\tilde{u}_r,\tilde{x}_r,\mathbf{0}) \in \mathbf{Q}(\tilde{x}_r(0))$ and any $F \in \mathbb{F}(\mathcal{V}^*)$. By virtue of Lem. A.7, there exists v satisfying*

$$\tilde{u}_r = F\tilde{x}_r + Nv \tag{C.50}$$

where $N : \mathcal{N} \to \mathcal{X}$ is the natural embedding. It holds:

$$(\tilde{u}_r,\tilde{x}_r) \in (\mathbf{B}\cap\mathbf{P}) \cup \{\mathbf{0}\} \Leftrightarrow v \in \mathbf{V}(\Psi^{-1}_{bp}\tilde{x}_r(0)) \tag{C.51}$$

where $\Psi_{bp} : \mathcal{V}^*_{bp} \to \mathcal{X}$ is the natural embedding.

Proof. Pick any $\tilde{x}_r(0) \in \mathcal{V}^*_{bp}$ and any $(\tilde{u}_r,\tilde{x}_r)$ such that $(\tilde{u}_r,\tilde{x}_r,\mathbf{0}) \in \mathbf{Q}(\tilde{x}_r(0))$. First, observe that $(\tilde{u}_r,\tilde{x}_r) \in \mathbf{PC}\times\mathbf{C}$ is implied by $(\tilde{u}_r,\tilde{x}_r,\mathbf{0}) \in \mathbf{Q}(\tilde{x}_r(0))$ so that Nv and, in turn, v are in $\mathbf{PC}$, in view of (C.50) and because N is injective.

Let $x_a(0) \coloneqq \Psi^{-1}_{bp}\tilde{x}_r(0)$. In view of Lem. C.25, using $(A+BF)\mathcal{V}^*_{bp} + B\mathcal{N} \subset \mathcal{V}^*_{bp} + \mathcal{R}^* = \mathcal{V}^*_{bp}$ and similarly as in the proof of Th. 9.17, one proves that $\tilde{x}_r(t)$ identically belongs to $\mathcal{V}^*_{bp}$ and that $x_a \coloneqq \Psi^{-1}_{bp}\tilde{x}_r$ solves the equation governing the bp-strong annihilator for some v satisfying (C.50). Let us consider a basis of the state space of this quadruple that is adapted to $\Psi^{-1}_{bp}\mathcal{R}^*$. In this basis, one gets

$$\left[\begin{array}{c|c} A_a & B_a \end{array}\right] = \left[\begin{array}{cc|c} A_{11} & A_{12} & B_1 \\ \mathbf{0} & A_{22} & \mathbf{0} \end{array}\right]$$

since (i) $F \in \mathbb{F}(\mathcal{V}^*) \subset \mathbb{F}(\mathcal{R}^*)$ so that $\mathcal{R}^*$ is $(A+BF)$-invariant and (ii) $B\mathcal{N} \subset \mathcal{R}^*$. Besides, $A_{11} = (A+BF)|\mathcal{R}^*$ is Hurwitz and $A_{22} = (A+BF)|\mathcal{V}^*_{bp}/\mathcal{R}^*$ is a semi-simple matrix satisfying $\sigma(A_{22}) \subset \mathbb{C}^0$, recall that $(A+BF)|\mathcal{V}^*/\mathcal{R}^*$ and, in turn, A_{22} is independent of $F \in \mathbb{F}(\mathcal{V}^*)$, see Lem. A.5. Let us decompose x_a as $\left[\begin{smallmatrix} x_1 \\ x_2 \end{smallmatrix}\right]$ according to the above basis. In this context (in particular, recall that $v \in \mathbf{PC}$ holds), observe that:

$$v \in \mathbf{B} \Rightarrow x_a \in \mathbf{B} \tag{C.52}$$

$$x_a(0) \in \Psi^{-1}_{bp}\mathcal{R}^* \Rightarrow (x_a \in \mathbf{B}\cap\mathbf{P} \Leftrightarrow B_1v \in \mathbf{B}\cap\mathbf{P}) \tag{C.53}$$

To prove (C.52), observe that x_2 solves $\dot{x}_2 = A_{22}x_2$ so that x_2 is bounded, whatever is $x_2(0)$. Besides, x_1 solves $\dot{x}_1 = A_{11}x_1 + A_{12}x_2 + B_1v$. Thus, x_1 is bounded for all $v \in \mathbf{B}$ because A_{11}

is Hurwitz. To prove (C.53), note that $x_a(0) \in \Psi_{bp}^{-1}\mathcal{R}^* \Leftrightarrow x_2(0) = \mathbf{0} \Leftrightarrow x_2 = \mathbf{0}$ implies $\dot{x}_1 = A_{11}x_1 + B_1 v$. Therefore, x_a and, in turn, x_1 are bp iff $B_1 v$ is bp because A_{11} is Hurwitz.

Let us now prove the equivalence of (C.51), bearing in mind that $v \in \mathbf{PC}$ holds:

$$x_a(0) \in \Psi_{bp}^{-1}\mathcal{R}^* \Leftrightarrow \Psi_{bp}x_a(0) = \tilde{x}_r(0) \in \mathcal{R}^*$$

and that $v \in \mathbf{PC}$ holds.

$\Rightarrow$ First, observe that if $(\tilde{u}_r, \tilde{x}_r)$ is bounded, then Nv and, in turn, v are bounded, in view of (C.50) and because N is injective. Second, note that $(\tilde{u}_r, \tilde{x}_r) = \mathbf{0}$ implies $\Psi_{bp}^{-1}\tilde{x}_r(0) = \mathbf{0}$ and $v = \mathbf{0}$ for analogous reasons. Thus, $v \in \mathbf{V}(\Psi_{bp}^{-1}\tilde{x}_r(0))$ is valid in this case. As a third and last step, let us prove that if $(\tilde{u}_r, \tilde{x}_r)$ is bp and $\tilde{x}_r(0)$ belongs to $\mathcal{R}^*$, then v is persistent. To see this, observe that if $\tilde{x}_r$ is bp, then so does $x_a = \Psi_{bp}^{-1}\tilde{x}_r$, which implies $B_1 v \in \mathbf{B} \cap \mathbf{P}$, in view of (C.53), and, in turn, $v \in \mathbf{B} \cap \mathbf{P}$. On the contrary, if $\tilde{x}_r$ is not bp, so that $\tilde{u}_r$ enjoys this property, then the bounded signal $\tilde{x}_r$ vanishes, so that $\tilde{u}_r$ converges to Nv in view of (C.50). This proves that v is bp.

$\Leftarrow$ Assume that $v \in \mathbf{V}(\Psi_{bp}^{-1}\tilde{x}_r(0))$ holds. First, observe that x_a is bounded, in view of (C.52) and because $\mathbf{V}(\Psi_{bp}^{-1}\tilde{x}_r(0)) \subset \mathbf{B}$ holds for all $\tilde{x}_r(0)$. This implies that $(\tilde{u}_r, \tilde{x}_r)$ is bounded because $\tilde{x}_r = \Psi_{bp}x_a \in \mathbf{B}$ which implies $\tilde{u}_r \in \mathbf{B}$ owing to (C.50). Second, $v = \mathbf{0}$ and $\tilde{x}_r(0) = \mathbf{0}$ render $v \in \mathbf{V}(\Psi_{bp}^{-1}\tilde{x}_r(0))$ valid. In this case, one obtains $(\tilde{u}_r, \tilde{x}_r) = \mathbf{0}$ because $x_a = \mathbf{0}$ which implies $\tilde{x}_r = \mathbf{0}$ and, in turn, $\tilde{u}_r = \mathbf{0}$ in view of (C.50). As a third and last step, let us prove that if v is bp and $\tilde{x}_r(0)$ belongs to $\mathcal{R}^*$, then $(\tilde{u}_r, \tilde{x}_r)$ is persistent. To see this, observe that if $B_1 v$ is bp, then so is x_a in view of (C.53). This implies $\tilde{x}_r = \Psi_{bp}x_a \in \mathbf{B} \cap \mathbf{P}$. On the contrary, if $B_1 v$ is not bp, then the bounded signal x_a and, in turn, $\tilde{x}_r$ are either zero or vanishing, see (C.53). Thus, $\tilde{u}_r$ converges to Nv in view of (C.50). This proves that $\tilde{u}_r$ is bp since N is injective. □

Proof of Th. 9.24

From $F \in \mathbb{F}(\mathcal{V}^*) \subset \mathbb{F}(\mathcal{V}_{bp}^*)$, see Lem. C.25, one gets $(A + BF)\mathcal{V}_{bp}^* \subset \mathcal{V}_{bp}^*$ which proves that A_a is well defined. Matrix B_a is also well-posed because $B\mathcal{N} \subset \mathcal{R}^* \subset \mathcal{V}_{bp}^*$ holds.

Pick any $\eta = x_{a0} = x_a(0)$ and any $v \in \mathbf{V}(x_{a0})$. Denote by x_a the corresponding state trajectory of the bp-strong annihilator. Similarly, as in the proof of Th. 9.17, one proves that $\tilde{x}_r := \Psi_{bp}x_a$ satisfies $(\tilde{u}_r, \tilde{x}_r, \mathbf{0}) \in \mathbf{Q}(\tilde{x}_r(0))$ with $\tilde{u}_r = F\tilde{x}_r + Nv$. By virtue of Lem. C.26, $v \in \mathbf{V}(x_{a0})$ implies $(\tilde{u}_r, \tilde{x}_r) \in (\mathbf{B} \cap \mathbf{P}) \cup \{\mathbf{0}\}$.

Proof of maximal range

Pick any $(\tilde{x}_r(0), \tilde{u}_r)$ satisfying $(\tilde{u}_r, \mathbf{0}) \in \mathbf{W}(\tilde{x}_r(0))$ and outside the range of the bp-strong annihilator of Th. 9.24, i.e. at least one of the following conditions is valid:

$$(\forall \eta, \tilde{x}_r(0) \neq \Psi_{bp}\eta) \Leftrightarrow \tilde{x}_r(0) \notin \mathcal{V}_{bp}^*, \tag{C.54}$$

$$\forall \eta, \forall v \in \mathbf{V}(\eta), \tilde{u}_r \neq \mathrm{H}_{\perp}^{bp}[\eta; v]. \tag{C.55}$$

Recall that $(\tilde{u}_r, \mathbf{0}) \in \mathbf{W}(\tilde{x}_r(0))$ implies the existence of $\hat{v} \in \mathbf{PC}$ satisfying

$$\tilde{u}_r = \mathrm{H}_{\perp}[\hat{\eta}; \hat{v}], \tag{C.56}$$

with $\hat{\eta} := \Psi^{-1}\tilde{x}_r(0)$, due to the fact that the strong annihilator of Th. 9.17 has maximal range, see Th. 9.17 for the definitions of Ψ and $\mathrm{H}_{\perp}$.

Assume that (C.54) does not hold, i.e. $\tilde{x}_r(0) \in \mathcal{V}_{bp}^*$, so that (C.55) is valid. In this case, where $\tilde{x}_r(0) \in \mathcal{V}_{bp}^*$, it holds $\mathrm{H}_\perp[\eta; v] = \mathrm{H}_\perp^{bp}[\eta; v]$ for all η and for all v, in view of Lem. C.25 and the expressions of the quadruples associated with $\mathrm{H}_\perp^{bp}$ and $\mathrm{H}_\perp$. Thus, (C.56) yields that $\tilde{u}_r = \mathrm{H}_\perp^{bp}[\hat{\eta}; \hat{v}]$. From (C.55), this implies $\hat{v} \notin \mathbf{V}(\hat{\eta})$. Let $\tilde{x}_r$ be such that $(\tilde{u}_r, \tilde{x}_r, \mathbf{0}) \in \mathbf{Q}(\tilde{x}_r(0))$. In such a case, $(\tilde{u}_r, \tilde{x}_r)$ is neither zero nor bp by virtue of Lem. C.26.

Summarizing, we have proved that for all $\tilde{x}_r(0)$ and for all $(\tilde{u}_r, \tilde{x}_r)$ satisfying $(\tilde{u}_r, \tilde{x}_r, \mathbf{0}) \in \mathbf{Q}(\tilde{x}_r(0))$, if $(\tilde{x}_r(0), \tilde{u}_r)$ is out of the range of the bp-strong annihilator, then $(\tilde{u}_r, \tilde{x}_r)$ is neither bp nor zero. The contraposition of this statement proves that the bp-strong annihilator has maximal range.

C.10 Proof that WIR as in [Zac09] implies WIR

Assume that Σ is WIR as in [Zac09], i.e.

$$0 \in \mathcal{Z}_z \coloneqq \{s : \lim_{s \to +\infty} G(s) \text{ is finite, } \operatorname{rank}\{G(s)\} < \operatorname{nrank}\{G\}\}.$$

First, observe that if Σ is IR, then it is also WIR. Henceforth, assume that Σ is not IR, so that $\rho = \dim \mathcal{R}^* = 0$ and $\operatorname{nrank}\{G\} = m$ hold, see Th. 8.2. In this context, WIR is equivalent to $\mathcal{V}^* \neq \langle \mathcal{K} | A \rangle$, see Prop. 9.16. By contradiction, assume that $\mathcal{V}^* = \langle \mathcal{K} | A \rangle$. In this case, one gets

$$\langle \mathcal{K} | A \rangle = \mathcal{R}^* + \langle \mathcal{K} | A \rangle = \mathcal{V}^* \cap (\langle \mathcal{K} | A \rangle + \langle A | \mathcal{B} \rangle)$$

so that the set $\mathcal{Z}_{tr}$ of transmission zeros is empty, in view of the following characterization:

$$\mathcal{Z}_{tr} = \sigma(A_0 | (\mathcal{V}^* \cap (\langle \mathcal{K} | A \rangle + \langle A | \mathcal{B} \rangle)) \,/\, (\mathcal{R}^* + \langle \mathcal{K} | A \rangle))$$

where A_0 is a state matrix resulting from specific regular feedback and output injection, see [AS84, Cor.1]. This leads to a contradiction because $\mathcal{Z}_z \subset \mathcal{Z}_{tr}$ holds. Note that this last inclusion is derived from the definition of $\mathcal{Z}_{tr}$, that is, the zeros of the numerator polynomials of the non-trivial entries (i.e. not equal to zero) of the Smith-McMillan form of $G(s)$.

Bibliography

Personal bibliography

In journal

[Del+19] Romain Delpoux, Jean-François Trégouët, Jean-Yves Gauthier, and Cyril Lacombe. "New Framework for Optimal Current Sharing of Nonidentical Parallel Buck Converters". In: *IEEE Transactions on Control Systems Technology* 27.3 (May 2019), pp. 1237–1243.

[Kre+21a] Jeremie Kreiss, Jean-François Trégouët, Damien Eberard, Romain Delpoux, Jean-Yves Gauthier, and Xuefang Lin-Shi. "Hamiltonian Point of View on Parallel Interconnection of Buck Converters". In: *IEEE Transactions on Control Systems Technology* 29.1 (Jan. 2021), pp. 43–52.

[Kre+21b] Jérémie Kreiss, Marc Bodson, Romain Delpoux, Jean-Yves Gauthier, Jean-François Trégouët, and Xuefang Lin-Shi. "Optimal Control Allocation for the Parallel Interconnection of Buck Converters". In: *Control Engineering Practice* 109 (Apr. 2021), p. 104727.

[KT21] Jérémie Kreiss and Jean-François Trégouët. "Input Redundancy: Definitions, Taxonomy, Characterizations and Application to over-Actuated Systems". In: *Systems & Control Letters* 158 (Dec. 2021), p. 105060.

[Ndo+22] Aboubacar Ndoye, Romain Delpoux, Jean-François Trégouët, and Xuefang Lin-Shi. "Switching Control Design for LTI System with Uncertain Equilibrium: Application to Parallel Interconnection of DC/DC Converters". In: *Automatica* 145 (Nov. 2022), p. 110522.

[NT24] Aboubacar Ndoye and Jean-François Trégouët. "Robust Switching Control Design Using Lur'e Lyapunov Functions". In: *International Journal of Robust and Nonlinear Control* 34.7 (May 2024), pp. 4626–4649.

[Nto+16b] Lorenzo Ntogramatzidis, Jean-François Trégouët, Robert Schmid, and Augusto Ferrante. "Globally Monotonic Tracking Control of Multivariable Systems". In: *IEEE Transactions on Automatic Control* 61.9 (Sept. 2016), pp. 2559–2564.

[Sad+22] Mahdieh S. Sadabadi, Nenad Mijatovic, Jean-François Trégouët, and Tomislav Dragičević. "Distributed Control of Parallel DC–DC Converters Under FDI Attacks on Actuators". In: *IEEE Transactions on Industrial Electronics* 69.10 (Oct. 2022), pp. 10478–10488.

[Sim+23a] Tanguy Simon, Mattia Giaccagli, Jean-François Trégouët, Daniele Astolfi, Vincent Andrieu, Hervé Morel, and Xuefang Lin-Shi. "Robust Regulation of a Power Flow Controller via Nonlinear Integral Action". In: *IEEE Transactions on Control Systems Technology* 31.4 (July 2023), pp. 1636–1648.

[Sim+23b] Tanguy Simon, Jean-François Trégouët, Xuefang Lin-Shi, and Hervé Morel. "Robust Nonlinear Control of a Power Flow Controller for Meshed DC Grids". In: *Control Engineering Practice* 131 (Feb. 2023), p. 105389.

[TD19] Jean-François Trégouët and Romain Delpoux. "New Framework for Parallel Interconnection of Buck Converters: Application to Optimal Current-Sharing with Constraints and Unknown Load". In: *Control Engineering Practice* 87 (June 2019), pp. 59–75.

[TK24] Jean-François Trégouët and Jérémie Kreiss. "Input Redundancy under Input and State Constraints". In: *Automatica* 159 (Jan. 2024), p. 111344.

[Tré+13b] Jean-François Trégouët, Dimitri Peaucelle, Denis Arzelier, and Yoshio Ebihara. "Periodic Memory State-Feedback Controller: New Formulation, Analysis, and Design Results". In: *IEEE Transactions on Automatic Control* 58.8 (Aug. 2013), pp. 1986–2000.

[Tré+15] Jean-François Trégouët, Denis Arzelier, Dimitri Peaucelle, Christelle Pittet, and Luca Zaccarian. "Reaction Wheels Desaturation Using Magnetorquers and Static Input Allocation". In: *Control Systems Technology, IEEE Transactions on* 23.2 (2015), pp. 525–539.

[TSD16] Jean-François Trégouët, Alexandre Seuret, and Michaël Di Loreto. "A Periodic Approach for Input-delay Problems: Application to Network Controlled Systems Affected by Polytopic Uncertainties". In: *International Journal of Robust and Nonlinear Control* 26.3 (Feb. 2016), pp. 385–400.

[Zha+21] Xiaokang Zhang, Jean-Yves Gauthier, Xuefang Lin-Shi, Romain Delpoux, and Jean-François Trégouët. "Modeling, Control, and Experimental Evaluation of Multifunctional Converter System". In: *IEEE Transactions on Industrial Electronics* 68.9 (Sept. 2021), pp. 7747–7756.

In proceedings

[Dar+24] Justin Darnet, Éric Bideaux, Jean-François Trégouët, and Yohann Brunel. "Model Predictive Speed Control of a Digital Hydraulic Drive". In: *BATH/ASME 2024 Symposium on Fluid Power and Motion Control*. 2024, V001T01A007.

[DBT23] Justin Darnet, Éric Bideaux, and Jean-François Trégouët. "Projection Method for Hydraulic Piston Motor Torque Control". In: *ASME/BATH 2023 Symposium on Fluid Power and Motion Control*. 2023, V001T01A025.

[Jav+17] S. Javanmardi, Éric Bideaux, Jean-François Trégouët, R. Trigui, H. Tattegrain, and E. Nicouleau Bourles. "Driving Style Modelling for Eco-driving Applications". In: *IFAC-PapersOnLine*. Vol. 50. 20th IFAC World Congress. Toulouse, France, July 2017, pp. 13866–13871.

[Kre+18a] Jeremie Kreiss, Jean-François Trégouët, Romain Delpoux, Jean-Yves Gauthier, and Xuefang Lin-Shi. "A Geometric Point of View on Parallel Interconnection of Buck Converters". In: *2018 European Control Conference (ECC)*. Limassol: IEEE, June 2018, pp. 70–75.

[Kre+18b] Jérémie Kreiss, Jean-François Trégouët, Romain Delpoux, Jean-Yves Gauthier, and Xuefang Lin-Shi. "Flux Weakening of PMSM for Enhancing Torque Tracking". In: *17th European Control Conference (ECC)*. Limassol, Cyprus, 2018, pp. 2665–2670.

[Kre+19] Jeremie Kreiss, Jean-François Trégouët, Romain Delpoux, Jean-Yves Gauthier, and Xuefang Lin-Shi. "A New Framework for Dealing with Input Constraints on Parallel Interconnection of Buck Converters". In: *2019 18th European Control Conference (ECC)*. Naples, Italy: IEEE, June 2019, pp. 429–434.

[Lin+21] Xuefang Lin-Shi, Tanguy Simon, Jean-François Trégouët, and Hervé Morel. "Flatness-Based Control of an m-Branch Power Flow Controller for Meshed DC Microgrids". In: *2021 IEEE 1st International Power Electronics and Application Symposium (PEAS)*. Nov. 2021, pp. 1–6.

[Ndo+19] Aboubacar Ndoye, Romain Delpoux, Lorentiu Hetel, Alexandre Kruszewski, Jean-François Trégouët, and Xuefang Lin-Shi. "Robust Relay Control for Buck Converters : Experimental Application". In: *Proceedings of the 58th IEEE Conference on Decision and Control (CDC)*. Nice, France, 2019, pp. 8124–8129.

[Nto+16a] Lorenzo Ntogramatzidis, Jean-François Trégouët, Robert Schmid, and Augusto Ferrante. "A Tutorial on the Globally Monotonic Tracking Control Problem with Geometric Techniques". In: *2016 IEEE 55th Conference on Decision and Control (CDC)*. Dec. 2016, pp. 4913–4918.

[Sim+21a] Tanguy Simon, Mattia Giaccagli, Jean-François Trégouët, Daniele Astolfi, Vincent Andrieu, Xuefang Lin-Shi, and Hervé Morel. "Robust Output Set-Point Tracking for a Power Flow Controller via Forwarding Design". In: *2021 60th IEEE Conference on Decision and Control (CDC)*. Dec. 2021, pp. 6385–6390.

[Sim+21b] Tanguy Simon, Jean-François Trégouët, Herve Morel, and Xuefang Lin-Shi. "Modelling and Control of a Power Flow Controller for DC Microgrids". In: *2021 23rd European Conference on Power Electronics and Applications (EPE'21 ECCE Europe)*. Ghent, Belgium: IEEE, Sept. 2021, P.1–P.10.

[TD17] Jean-François Trégouët and Romain Delpoux. "Parallel Interconnection of Buck Converters Revisited". In: *IFAC-PapersOnLine*. Vol. 50. Toulouse, France, July 2017, pp. 15792–15797.

[TDG16] Jean-François Trégouët, Romain Delpoux, and Jean-Yves Gauthier. "Optimal Secondary Control for DC Microgrids". In: *2016 IEEE 25th International Symposium on Industrial Electronics (ISIE)*. June 2016, pp. 510–515.

[Tré+11a] Jean-François Trégouët, Denis Arzelier, Dimitri Peaucelle, Yoshio Ebihara, Christelle Pittet, and Alexandre Falcoz. "Periodic FIR Controller Synthesis for Discrete-Time Uncertain Linear Systems". In: *IEEE Conference on Decision and Control and European Control Conference*. Orlando, FL, USA: IEEE, Dec. 2011, pp. 1367–1372.

[Tré+11b] Jean-François Trégouët, Denis Arzelier, Dimitri Peaucelle, Yoshio Ebihara, Christelle Pittet, and Alexandre Falcoz. "Periodic H2 Synthesis for Spacecraft Attitude Control with Magnetorquers and Reaction Wheels". In: *IEEE Conference on Decision and Control and European Control Conference*. Orlando, FL, USA: IEEE, Dec. 2011, pp. 6876–6881.

[Tré+12a] Jean-François Trégouët, Denis Arzelier, Dimitri Peaucelle, Yoshio Ebihara, Christelle Pittet, and Alexandre Falcoz. "Robust $\mathfrak{H}\infty$ Performance of Periodic Systems with Memory: New Formulations, Analysis and Design Results". In: *2012 IEEE 51st IEEE Conference on Decision and Control (CDC)*. Dec. 2012, pp. 7781–7786.

[Tré+12b] Jean-François Trégouët, Yoshio Ebihara, Denis Arzelier, Dimitri Peaucelle, Christelle Pittet, and Alexandre Falcoz. "Robust Stability of Periodic Systems with Memory: New Formulations, Analysis and Design Results". In: *IFAC Proceedings Volumes*. Vol. 45. Aalborg, Denmark, Jan. 2012, pp. 684–689.

[Tré+13a] Jean-François Trégouët, Denis Arzelier, Dimitri Peaucelle, and Luca Zaccarian. "Static Input Allocation for Reaction Wheels Desaturation Using Magnetorquers". In: *IFAC Proceedings Volumes*. Vol. 46. 19th IFAC Symposium on Automatic Control in Aerospace. Würzburg, Germany, Jan. 2013, pp. 559–564.

Thesis

[Tré09] Jean-François Trégouët. "Modélisation, Identification et Commande Du Satellite de Laboratoire LABSAT". MA thesis. Université de Sherbrooke, 2009.

[Tré12] Jean-François Trégouët. "Synthèse de Correcteurs Robustes Périodiques à Mémoire et Application Au Contrôle d'attitude de Satellites Par Roues à Réaction et Magnéto–Coupleurs". PhD thesis. Toulouse, ISAE, 2012.

Others

[RST20a] Hervé Rivano, Nicolas Stouls, and Jean-François Trégouët. "Le Numérique Menace-t-Il La Transition Énergétique ?" In: *Pop'sciences Mag* 7 (Nov. 2020), pp. 22–27.

[RST20b] Hervé Rivano, Nicolas Stouls, and Jean-François Trégouët. "Transitions Énergétiques et Numériques, Éléments d'une Démocratie Technique Informée". In: *AOC* (Nov. 2020).

General bibliography

[Abr+16] Frederic Abry, Xavier Brun, Sylvie Sesmat, Eric Bideaux, and Christophe Ducat. "Electropneumatic Cylinder Backstepping Position Controller Design With Real-Time Closed-Loop Stiffness and Damping Tuning". In: *IEEE Transactions on Control Systems Technology* 24.2 (Mar. 2016), pp. 541–552.

[Ada+94] Richard J. Adams, James M. Buffington, Andrew G. Sparks, and Siva S. Banda. *Robust Multivariable Flight Control*. Advances in Industrial Control. London: Springer London, 1994.

[AF09] Jean-Pierre Aubin and Hélène Frankowska. *Set-Valued Analysis*. Boston: Birkhäuser Boston, 2009.

[AK04] Kartik B. Ariyur and Miroslav Krstic. *Real-Time Optimization by Extremum-Seeking Control*. Hoboken, NJ: Wiley-Interscience, 2004.

[Ame+19] Aaron D. Ames, Samuel Coogan, Magnus Egerstedt, Gennaro Notomista, Koushil Sreenath, and Paulo Tabuada. "Control Barrier Functions: Theory and Applications". In: *2019 18th European Control Conference (ECC)*. IEEE, 2019, pp. 3420–3431.

[And+19] James Anderson, John C. Doyle, Steven H. Low, and Nikolai Matni. "System Level Synthesis". In: *Annual Reviews in Control* 47 (Jan. 2019), pp. 364–393.

[Ant05a] Athanasios C. Antoulas. "6. Sylvester and Lyapunov Equations". In: *Approximation of Large-Scale Dynamical Systems*. Advances in Design and Control. Society for Industrial and Applied Mathematics, Jan. 2005, pp. 173–204.

[Ant05b] Athanasios C. Antoulas. *Approximation of Large-Scale Dynamical Systems*. Advances in Design and Control 6. Philadelphia, Pa: Society for Industrial and Applied Mathematics (SIAM, 3600 Market Street, Floor 6, Philadelphia, PA 19104), 2005.

[AS84] H. Aling and J. M. Schumacher. "A Nine-Fold Canonical Decomposition for Linear Systems". In: *International Journal of Control* 39.4 (Apr. 1984), pp. 779–805.

[ASB10] Matthias Althoff, Olaf Stursberg, and Martin Buss. "Computing Reachable Sets of Hybrid Systems Using a Combination of Zonotopes and Polytopes". In: *Nonlinear Analysis: Hybrid Systems* 4.2 (May 2010), pp. 233–249.

[Bai74] J. E. Bailey. "Periodic Operation of Chemical Reactions: A Review". In: *Chemical Engineering Communications* 1 (Jan. 1974).

[Bai85] J. Baillieul. "Kinematic Programming Alternatives for Redundant Manipulators". In: *1985 IEEE International Conference on Robotics and Automation Proceedings*. Vol. 2. Mar. 1985, pp. 722–728.

[Bar+19] Mayank Baranwal, Alireza Askarian, Srinivasa Salapaka, and Murti Salapaka. "A Distributed Architecture for Robust and Optimal Control of DC Microgrids". In: *IEEE Transactions on Industrial Electronics* 66.4 (Apr. 2019), pp. 3082–3092.

[BB91] Stephen P. Boyd and Craig H. Barratt. *Linear Controller Design: Limits of Performance*. Prentice Hall Information and System Sciences Series. Englewood Cliffs, N.J: Prentice Hall, 1991.

[BBF17] Abdelkader Bouarfa, Marc Bodson, and Maurice Fadel. "A Fast Active-Balancing Method for the 3-Phase Multilevel Flying Capacitor Inverter Derived from Control Allocation Theory". In: *IFAC-PapersOnLine* 50.1 (July 2017), pp. 2113–2118.

[BBF18] Abdelkader Bouarfa, Marc Bodson, and Maurice Fadel. "An Optimization Formulation of Converter Control and Its General Solution for the Four-Leg Two-Level Inverter". In: *IEEE Transactions on Control Systems Technology* 26.5 (Sept. 2018), pp. 1901–1908.

[BC09] Sergio Bittanti and Patrizio Colaneri. *Periodic Systems*. Communications and Control Engineering. London: Springer London, 2009.

[BD00] Rob Brinkerhoff and Santosh Devasia. "Output Tracking for Actuator Deficient/Redundant Systems: Multiple Piezoactuator Example". In: *Journal of Guidance, Control, and Dynamics* 23.2 (Mar. 2000), pp. 370–373.

[BD95a] Kenneth Bordignon and Wayne Durham. "Null-Space Augmented Solutions to Constrained Control Allocation Problems". In: *Guidance, Navigation, and Control Conference*. Baltimore, MD, U.S.A.: American Institute of Aeronautics and Astronautics, 1995.

[BD95b] Kenneth A. Bordignon and Wayne C. Durham. "Closed-Form Solutions to Constrained Control Allocation Problem". In: *Journal of Guidance, Control, and Dynamics* 18.5 (1995), pp. 1000–1007.

[BE96] James M. Buffington and Dale F. Enns. "Lyapunov Stability Analysis of Daisy Chain Control Allocation". In: *Journal of Guidance, Control, and Dynamics* 19.6 (1996), pp. 1226–1230.

[Bec02] Roger Ezekiel Beck. "Application of Control Allocation Methods to Linear Systems with Four or More Objectives". Doctoral thesis. Virginia Polytechnic Institute and State University, June 2002. HDL: 10919/28088.

[Ben+16] M. Benmiloud, A. Benalia, M. Defoort, and M. Djemai. "On the Limit Cycle Stabilization of a DC/DC Three-Cell Converter". In: *Control Engineering Practice* 49 (Apr. 2016), pp. 29–41.

[Ber+96] J.M. Berg, K.D. Hammett, C.A. Schwartz, and S.S. Banda. "An Analysis of the Destabilizing Effect of Daisy Chained Rate-Limited Actuators". In: *IEEE Transactions on Control Systems Technology* 4.2 (Mar. 1996), pp. 171–176.

[BET98] James M. Buffington, Dale F. Enns, and Andrew R. Teel. "Control Allocation and Zero Dynamics". In: *Journal of Guidance, Control, and Dynamics* 21.3 (1998), pp. 458–464.

[BF97] Svein P. Berge and Thor I. Fossen. "Robust Control Allocation of Overactuated Ships; Experiments with a Model Ship". In: *IFAC Proceedings Volumes* 30.22 (Sept. 1997), pp. 193–198.

[BG05] Keith Burns and Marian Gidea. *Differential Geometry and Topology: With a View to Dynamical Systems*. Studies in Advanced Mathematics. Boca Raton, [Florida]: CRC Press, 2005.

[BJV19] Bart Besselink, Karl H. Johansson, and Arjan Van Der Schaft. "Contracts as Specifications for Dynamical Systems in Driving Variable Form". In: *2019 18th European Control Conference (ECC)*. June 2019, pp. 263–268.

[BM02] J.D. Boskovic and R.K. Mehra. "Control Allocation in Overactuated Aircraft under Position and Rate Limiting". In: *Proceedings of the 2002 American Control Conference (IEEE Cat. No.CH37301)*. Vol. 1. May 2002, 791–796 vol.1.

[BM08] Franco Blanchini and Stefano Miani. *Set-Theoretic Methods in Control*. Systems & Control. Boston, Mass: Birkhäuser, 2008.

[BM69] G. Basile and G. Marro. "Controlled and Conditioned Invariant Subspaces in Linear System Theory". In: *Journal of Optimization Theory and Applications* 3.5 (May 1969), pp. 306–315.

[BM87] G Basile and G Marro. "On the Robust Controlled Invariant". In: *Systems & Control Letters* 9.3 (Sept. 1987), pp. 191–195.

[BM92] Giuseppe Basile and Giovanni Marro. *Controlled and Conditioned Invariants in Linear System Theory*. Englewood Cliffs, N.J: Prentice Hall, 1992.

[BMZ05] Anthony M. Bloch, Jerrold E. Marsden, and Dmitry V. Zenkov. "Nonholonomic Dynamics". In: *Notices of the AMS* 52.3 (2005), pp. 320–329.

[BO98] Egon Balas and Maarten Oosten. "On the Dimension of Projected Polyhedra". In: *Discrete Applied Mathematics* 87.1-3 (Oct. 1998), pp. 1–9.

[Bod02] Marc Bodson. "Evaluation of Optimization Methods for Control Allocation". In: *Journal of Guidance, Control, and Dynamics* 25.4 (2002), pp. 703–711.

[Bol97] John Glenn Bolling. "Implementation of Constrained Control Allocation Techniques Using an Aerodynamic Model of an F-15 Aircraft". MA thesis. Virginia Polytechnic Institute and State University, 1997.

[Bon+07] Moisés Bonilla Estrada, Maricela Figueroa Garcia, Michel Malabre, and Juan Carlos Martínez García. "Left Invertibility and Duality for Linear Systems". In: *Linear Algebra and its Applications* 425.2-3 (Sept. 2007), pp. 345–373.

[Bon+12] Luca Boncagni, Sergio Galeani, Gustavo Granucci, Gianluca Varano, Vincenzo Vitale, and Luca Zaccarian. "Plasma Position and Elongation Regulation at FTU Using Dynamic Input Allocation". In: *IEEE Transactions on Control Systems Technology* 20.3 (May 2012), pp. 641–651.

[Bor96] Kenneth A. Bordignon. "Constrained Control Allocation for Systems with Redundant Control Effectors". Doctoral Thesis. Virginia Polytechnic Institute and State University, Dec. 1996. HDL: 10919/28570.

[Bou22] Adrien Bourgeade. "PWM Control Optimization of a Two-Level Inverter : Application to Electric and Hybrid Vehicles". PhD thesis. École centrale de Nantes, Oct. 2022.

[Bra72] Robert F. Brammer. "Controllability in Linear Autonomous Systems with Positive Controllers". In: *SIAM Journal on Control* 10.2 (May 1972), pp. 339–353.

[BSL94] I. Batarseh, K. Siri, and H. Lee. "Investigation of the Output Droop Characteristics of Parallel-Connnected DC-DC Converters". In: *Proceedings of 1994 Power Electronics Specialist Conference - PESC'94*. Vol. 2. June 1994, 1342–1351 vol.2.

[BT97] Dimitris Bertsimas and John N. Tsitsiklis. *Introduction to Linear Optimization*. Athena Scientific Series in Optimization and Neural Computation. Belmont, Mass: Athena Scientific, 1997.

[Buf96] James Michael Buffington. "Control Design and Analysis for Systems with Redundant Limited Controls". PhD thesis. University of Minnesota, 1996.

[Bur88] J. W. Burdick. "Kinematic Analysis and Design of Redundant Manipulators". PhD thesis. Stanford University, 1988.

[Bur89] Joel W. Burdick. "On the Inverse Kinematics of Redundant Manipulators: Characterization of the Self-Motion Manifolds". In: *Advanced Robotics: 1989*. Ed. by Kenneth J. Waldron. Berlin, Heidelberg: Springer, 1989, pp. 25–34.

[BV04] Stephen P. Boyd and Lieven Vandenberghe. *Convex Optimization*. Cambridge, UK ; New York: Cambridge University Press, 2004.

[BY97] S.R. Bowes and Yen-Shin Lai. "The Relationship between Space-Vector Modulation and Regular-Sampled PWM". In: *IEEE Transactions on Industrial Electronics* 44.5 (Oct. 1997), pp. 670–679.

[CC97] Earl A. Coddington and Robert Carlson. *Linear Ordinary Differential Equations*. Philadelphia: Soc. for Industrial and Applied Mathematics, 1997.

[CDK87] Leon O. Chua, Charles A. Desoer, and Ernest S. Kuh. *Linear and Nonlinear Circuits*. McGraw-Hill Series in Electrical Engineering. New York: McGraw-Hill, 1987.

[CG14] Andrea Cristofaro and Sergio Galeani. "Output Invisible Control Allocation with Steady-State Input Optimization for Weakly Redundant Plants". In: *53rd IEEE Conference on Decision and Control*. Los Angeles, CA, USA: IEEE, Dec. 2014, pp. 4246–4253.

[CGS17] Andrea Cristofaro, Sergio Galeani, and Andrea Serrani. "Output Invisible Control Allocation with Asymptotic Optimization for Nonlinear Systems in Normal Form". In: *2017 IEEE 56th Annual Conference on Decision and Control (CDC)*. Melbourne, Australia: IEEE, Dec. 2017, pp. 2563–2568.

[Che+09] Wu Chen, Xinbo Ruan, Hong Yan, and Chi K. Tse. "DC/DC Conversion Systems Consisting of Multiple Converter Modules: Stability, Control, and Experimental Verifications". In: *IEEE Transactions on Power Electronics* 24.6 (June 2009), pp. 1463–1474.

[Che64] G. Cherry. "A General, Explicit, Optimizing Guidance Law for Rocket-Propelled Spaceflight". In: *Astrodynamics Guidance and Control Conference*. American Institute of Aeronautics and Astronautics, 1964.

[Cid+11] Angel Cid-Pastor, Roberto Giral, Javier Calvente, V. I. Utkin, and Luis Martinez-Salamero. "Interleaved Converters Based on Sliding-Mode Control in a Ring Configuration". In: *IEEE Transactions on Circuits and Systems I: Regular Papers* 58.10 (Oct. 2011), pp. 2566–2577.

[CKK09] Sudipta Chakraborty, Bill Kramer, and Benjamin Kroposki. "A Review of Power Electronics Interfaces for Distributed Energy Systems towards Achieving Low-Cost Modular Design". In: *Renewable and Sustainable Energy Reviews* 13.9 (Dec. 2009), pp. 2323–2335.

[CLS04] Ben M. Chen, Zongli Lin, and Yacov Shamash. *Linear Systems Theory*. Boston, MA: Birkhäuser Boston, 2004.

[Cor92] Jean -Michel Coron. "Global Asymptotic Stabilization for Controllable Systems without Drift". In: *Mathematics of Control, Signals, and Systems* 5.3 (Sept. 1992), pp. 295–312.

[CP93] G. Conte and A.M. Perdon. "Robust Disturbance Decoupling Problem for Parameter Dependent Families of Linear Systems". In: *Automatica* 29.2 (Mar. 1993), pp. 475–478.

[CPM91] G. Conte, A.M. Perdon, and G. Marro. "Computing the Maximum Robust Controlled Invariant Subspace". In: *Systems & Control Letters* 17.2 (Aug. 1991), pp. 131–135.

[CSE94] Stefano Chiaverini, Bruno Siciliano, and Olav Egeland. "Review of the Damped Least-Squares Inverse Kinematics with Experiments on an Industrial Robot Manipulator". In: *IEEE Transactions on control systems technology* 2.2 (1994), pp. 123–134.

[CSM11] Nalin A. Chaturvedi, Amit K. Sanyal, and N. Harris McClamroch. "Rigid-Body Attitude Control". In: *IEEE Control Systems Magazine* 31.3 (June 2011), pp. 30–51.

[CSZ16] Matteo Cocetti, Andrea Serrani, and Luca Zaccarian. "Dynamic Input Allocation for Uncertain Linear Over-Actuated Systems". In: *2016 American Control Conference (ACC)*. Boston, MA, USA: IEEE, July 2016, pp. 2906–2911.

[CSZ18] Matteo Cocetti, Andrea Serrani, and Luca Zaccarian. "Linear Output Regulation with Dynamic Optimization for Uncertain Linear Over-Actuated Systems". In: *Automatica* 97 (Nov. 2018), pp. 214–225.

[Cun83] Thomas B. Cunningham. "Robust Reconfiguration for High Reliability and Survivability for Advanced Aircraft". In: *Restructurable Controls*. NASA Conference Publication 2277, ed. Montoya, R.J., Hampton, VA, 1983, pp. 43–80.

[Dav72] E. Davison. "The Output Control of Linear Time-Invariant Multivariable Systems with Unmeasurable Arbitrary Disturbances". In: *IEEE Transactions on Automatic Control* 17.5 (Oct. 1972), pp. 621–630.

[DB96] Wayne C. Durham and Kenneth A. Bordignon. “Multiple Control Effector Rate Limiting”. In: *Journal of Guidance, Control, and Dynamics* 19.1 (1996), pp. 30–37.

[DBB17] Wayne Durham, Kenneth A. Bordignon, and Roger Beck. *Aircraft Control Allocation*. Chichester, West Sussex, United Kingdom: Wiley, 2017.

[DCV03] Jean-Michel Dion, Christian Commault, and Jacob Van Der Woude. “Generic Properties and Control of Linear Structured Systems: A Survey”. In: *Automatica* 39.7 (July 2003), pp. 1125–1144.

[De +08] Mark De Berg, Otfried Cheong, Marc Van Kreveld, and Mark Overmars. *Computational Geometry: Algorithms and Applications*. Berlin, Heidelberg: Springer Berlin Heidelberg, 2008.

[De +11] Gianmaria De Tommasi, Sergio Galeani, Alfredo Pironti, Gianluca Varano, and Luca Zaccarian. “Nonlinear Dynamic Allocator for Optimal Input/Output Performance Trade-off: Application to the JET Tokamak Shape Controller”. In: *Automatica* 47.5 (2011), pp. 981–987.

[De +12] Ricardo De Castro, Rui Esteves Araujo, João Pedro F. Trovao, Paulo G. Pereirinha, Pedro Melo, and Diamantino Freitas. “Robust DC-Link Control in EVs With Multiple Energy Storage Systems”. In: *IEEE Transactions on Vehicular Technology* 61.8 (Oct. 2012), pp. 3553–3565.

[Dev02] S. Devasia. “Should Model-Based Inverse Inputs Be Used as Feedforward under Plant Uncertainty?” In: *IEEE Transactions on Automatic Control* 47.11 (Nov. 2002), pp. 1865–1871.

[DLB01] John Davidson, Frederick J. Lallman, and W. Bundick. “Integrated Reconfigurable Control Allocation”. In: *AIAA Guidance, Navigation, and Control Conference and Exhibit*. Montreal,Canada: American Institute of Aeronautics and Astronautics, Aug. 2001.

[DO19] Molong Duan and Chinedum E. Okwudire. “Connections between Control Allocation and Linear Quadratic Control for Weakly Redundant Systems”. In: *Automatica* 101 (Mar. 2019), pp. 96–102.

[DSB18] Florian Dorfler, John W. Simpson-Porco, and Francesco Bullo. “Electrical Networks and Algebraic Graph Theory: Models, Properties, and Applications”. In: *Proceedings of the IEEE* 106.5 (May 2018), pp. 977–1005.

[DSB96] Carlos Canudas De Wit, Bruno Siciliano, and Georges Bastin, eds. *Theory of Robot Control*. Communications and Control Engineering. London: Springer London, 1996.

[Dur01] Wayne C. Durham. “Computationally Efficient Control Allocation”. In: *Journal of Guidance, Control, and Dynamics* 24.3 (May 2001), pp. 519–524.

[Dur93] Wayne C. Durham. “Constrained Control Allocation”. In: *Journal of Guidance, Control, and Dynamics* 16.4 (1993), pp. 717–725.

[Dur94] Wayne C. Durham. “Attainable Moments for the Constrained Control Allocation Problem”. In: *Journal of Guidance, Control, and Dynamics* 17.6 (Nov. 1994), pp. 1371–1373.

[DW74] E. J Davison and S. H Wang. “Properties and Calculation of Transmission Zeros of Linear Multivariable Systems”. In: *Automatica* 10.6 (Dec. 1974), pp. 643–658.

[DW77] E. J Davison and S. H Wang. “Properties and Calculation of Transmission Zeroes of Linear Multi-Variable Systems”. In: *Automatica* 13.3 (May 1977), p. 327.

[DW80] C. A. Desoer and Y. T. Wang. “Linear Time-Invariant Robust Servomechanism Problem: A Self-Contained Exposition*”. In: *Control and Dynamic Systems*. Ed. by C. T. Leondes. Vol. 16. Advances in Theory and Application. Academic Press, Jan. 1980, pp. 81–129.

[EGM04] Moisés Bonilla Estrada, Maricela Figueroa Garcia, and Michel Malabre. “Time Domain Left Invertibility: Application to Failure Detection”. In: *IFAC Proceedings Volumes* 37.21 (Dec. 2004), pp. 573–578.

[El +19] Abdelali El Aroudi, Blanca Areli Martínez-Treviño, Enric Vidal-Idiarte, and Angel Cid-Pastor. “Fixed Switching Frequency Digital Sliding-Mode Control of DC-DC Power Supplies Loaded by Constant Power Loads with Inrush Current Limitation Capability”. In: *Energies* 12.6 (Mar. 2019), p. 1055.

[EMW14] Adrien Escande, Nicolas Mansard, and Pierre-Brice Wieber. “Hierarchical Quadratic Programming: Fast Online Humanoid-Robot Motion Generation”. In: *The International Journal of Robotics Research* 33.7 (June 2014), pp. 1006–1028.

[Enn98] Dale Enns. “Control Allocation Approaches”. In: *Guidance, Navigation, and Control Conference and Exhibit*. Boston,MA,U.S.A.: American Institute of Aeronautics and Astronautics, Aug. 1998.

[FJ06] Thor I. Fossen and Tor A. Johansen. “A Survey of Control Allocation Methods for Ships and Underwater Vehicles”. In: *Control and Automation, 2006. MED '06. 14th Mediterranean Conference On*. June 2006, pp. 1–6.

[Fra77] Bruce A. Francis. “The Linear Multivariable Regulator Problem”. In: *SIAM Journal on Control and Optimization* 15.3 (May 1977), pp. 486–505.

[Fre+08] L. Freidovich, A. Robertsson, A. Shiriaev, and R. Johansson. “Periodic Motions of the Pendubot via Virtual Holonomic Constraints: Theory and Experiments”. In: *Automatica* 44.3 (Mar. 2008), pp. 785–791.

[FS91] Thor I. Fossen and Svein I. Sagatun. “Adaptive Control of Nonlinear Systems: A Case Study of Underwater Robotic Systems”. In: *Journal of Robotic Systems* 8.3 (1991), pp. 393–412.

[Fur+20] Michele Furci, Carlo Nainer, Luca Zaccarian, and Antonio Franchi. “Input Allocation for the Propeller-Based Overactuated Platform ROSPO”. In: *IEEE Transactions on Control Systems Technology* 28.6 (Nov. 2020), pp. 2720–2727.

[FW75a] B. A. Francis and W. M. Wonham. “The Internal Model Principle for Linear Multivariable Regulators”. In: *Applied Mathematics and Optimization* 2.2 (June 1975), pp. 170–194.

[FW75b] B. A. Francis and W.M. Wonham. “The Role of Transmission Zeros in Linear Multivariable Regulators”. In: *International Journal of Control* 22.5 (Nov. 1975), pp. 657–681.

[Gal+09] Sergio Galeani, Sophie Tarbouriech, Matthew Turner, and Luca Zaccarian. “A Tutorial on Modern Anti-windup Design”. In: *European Journal of Control* 15.3-4 (Jan. 2009), pp. 418–440.

[Gal+11] Sergio Galeani, Andrea Serrani, Gianluca Varano, and Luca Zaccarian. “On Linear Over-Actuated Regulation Using Input Allocation”. In: *IEEE Conference on Decision and Control and European Control Conference*. Orlando, FL, USA: IEEE, Dec. 2011, pp. 4771–4776.

[Gal+15] Sergio Galeani, Andrea Serrani, Gianluca Varano, and Luca Zaccarian. "On Input Allocation-Based Regulation for Linear over-Actuated Systems". In: *Automatica* 52 (Feb. 2015), pp. 346–354.

[Gal08] Jean Gallier. *Notes on Convex Sets, Polytopes, Polyhedra, Combinatorial Topology, Voronoi Diagrams and Delaunay Triangulations*. May 2008. arXiv: `0805.0292 [math]`.

[Gan00] Feliks Ruvimovič Gantmaher. *The Theory of Matrices*. Providence (R. I.): AMS Chelsea Publ, 2000.

[Gan09] Feliks R. Gantmacher. *The Theory of Matrices. Vol. 2*. Reprinted. Vol. 2. Providence, RI: American Mathematical Soc, 2009.

[Gat+02] G. Gateau, M. Fadel, P. Maussion, R. Bensaid, and T.A. Meynard. "Multicell Converters: Active Control and Observation of Flying-Capacitor Voltages". In: *IEEE Transactions on Industrial Electronics* 49.5 (Oct. 2002), pp. 998–1008.

[GCG17] Jeremy Van Gorp, Mohunparsad Caussy, and Cyrille Gillot. "Binary Signals Design to Control the Matrix Converter in the Context of Smart Grids". In: *IFAC-PapersOnLine*. Vol. 50. Toulouse, France, July 2017, pp. 2119–2124.

[GGL17] Martin Gendrin, Jean-Yves Gauthier, and Xuefang Lin-Shi. "A Predictive Hybrid Pulse-Width-Modulation Technique for Active-Front-End Rectifiers". In: *IEEE Transactions on Power Electronics* 32.7 (July 2017), pp. 5487–5496.

[Gir+06] R. Giri, V. Choudhary, R. Ayyanar, and N. Mohan. "Common-Duty-Ratio Control of Input-Series Connected Modular DC-DC Converters with Active Input Voltage and Load-Current Sharing". In: *IEEE Transactions on Industry Applications* 42.4 (July 2006), pp. 1101–1111.

[GJ] Ewgenij Gawrilow and Michael Joswig. *Polymake Wiki*. https://polymake.org/doku.php.

[GJ00] Ewgenij Gawrilow and Michael Joswig. "Polymake: A Framework for Analyzing Convex Polytopes". In: *Polytopes — Combinatorics and Computation*. Ed. by Gil Kalai and Günter M. Ziegler. DMV Seminar. Basel: Birkhäuser, 2000, pp. 43–73.

[Got86] D. Gottlieb. "Robots and Topology". In: *1986 IEEE International Conference on Robotics and Automation Proceedings*. Vol. 3. Apr. 1986, pp. 1689–1691.

[GP14] Sergio Galeani and Silvia Pettinari. "On Dynamic Input Allocation for Fat Plants Subject to Multi-Sinusoidal Exogenous Inputs". In: *53rd IEEE Conference on Decision and Control*. Los Angeles, CA, USA: IEEE, Dec. 2014, pp. 2396–2403.

[Gri+98] V. Grigore, J. Hatonen, J. Kyyra, and T. Suntio. "Dynamics of a Buck Converter with a Constant Power Load". In: *PESC 98 Record. 29th Annual IEEE Power Electronics Specialists Conference (Cat. No.98CH36196)*. Vol. 1. May 1998, 72–78 vol.1.

[Gro94] Robert L. Grogan. "A Thesis on the Application of Neural Network Computing to the Constrained Flight Control Allocation Problem". MA thesis. Virginia Tech, May 1994. HDL: `10919/44616`.

[GS18] Sergio Galeani and Mario Sassano. "Output Regulation for Redundant Plants via Orthogonal Moments". In: *2018 European Control Conference (ECC)*. June 2018, pp. 1945–1950.

[Gue+11] Josep M. Guerrero, Juan C. Vasquez, José Matas, Luis García De Vicuna, and Miguel Castilla. "Hierarchical Control of Droop-Controlled AC and DC Microgrids—A General Approach Toward Standardization". In: *IEEE Transactions on Industrial Electronics* 58.1 (Jan. 2011), pp. 158–172.

[GV13] Sergio Galeani and Giorgio Valmorbida. “Nonlinear Regulation for Linear Fat Plants: The Constant Reference/Disturbance Case”. In: *21st Mediterranean Conference on Control and Automation*. Platanias, Chania - Crete, Greece: IEEE, June 2013, pp. 683–690.

[Ham+15] Mohsen Hamzeh, Amin Ghazanfari, Yasser Abdel-Rady I. Mohamed, and Yaser Karimi. “Modeling and Design of an Oscillatory Current-Sharing Control Strategy in DC Microgrids”. In: *IEEE Transactions on Industrial Electronics* 62.11 (Nov. 2015), pp. 6647–6657.

[Han+11] Martin Hanger, Tor A. Johansen, Geir Kare Mykland, and Aage Skullestad. “Dynamic Model Predictive Control Allocation Using CVXGEN”. In: *2011 9th IEEE International Conference on Control and Automation (ICCA)*. Santiago, Chile: IEEE, Dec. 2011, pp. 417–422.

[Han11] Martin Bøgseth Hanger. “Model Predictive Control Allocation”. MA thesis. Institutt for teknisk kybernetikk, 2011.

[Här03] Ola Härkegård. “Backstepping and Control Allocation with Applications to Flight Control”. Doctoral Thesis. Linköpings universitet, 2003.

[Här04] Ola Härkegård. “Dynamic Control Allocation Using Constrained Quadratic Programming”. In: *Journal of Guidance, Control, and Dynamics* 27.6 (Nov. 2004), pp. 1028–1034.

[Hau83a] M.L.J. Hautus. “Linear Matrix Equations with Applications to the Regulator Problem”. In: *Outils et Modèles Mathématique Pour l’Automatique*. ed. CNRS. Paris, France, 1983, pp. 399–412.

[Hau83b] M.L.J. Hautus. “Strong Detectability and Observers”. In: *Linear Algebra and its Applications* 50 (Apr. 1983), pp. 353–368.

[HDD16] Laurenţiu Hetel, Michael Defoort, and Mohamed Djemaï. “Binary Control Design for a Class of Bilinear Systems: Application to a Multilevel Power Converter”. In: *IEEE Transactions on Control Systems Technology* 24.2 (Mar. 2016), pp. 719–726.

[He+14] Guofeng He, Min Chen, Wei Yu, Ning He, and Dehong Xu. “Design and Analysis of Multiloop Controllers With DC Suppression Loop for Paralleled UPS Inverter System”. In: *IEEE Transactions on Industrial Electronics* 61.12 (Dec. 2014), pp. 6494–6506.

[He+18] Wei He, Carlos Abraham Soriano-Rangel, Romeo Ortega, Alessandro Astolfi, Fernando Mancilla-David, and Shihua Li. “DC-DC Buck-Boost Converters with Unknown CPL: An Adaptive PBC”. In: *2018 Annual American Control Conference (ACC)*. Milwaukee, WI: IEEE, June 2018, pp. 6749–6754.

[Her+13] Martin Herceg, Michal Kvasnica, Colin N. Jones, and Manfred Morari. “Multi-Parametric Toolbox 3.0”. In: *2013 European Control Conference (ECC)*. Zurich: IEEE, July 2013, pp. 502–510.

[HG01] Ola Härkegård and S. Torkel Glad. “Flight Control Design Using Backstepping”. In: *IFAC Proceedings Volumes* 34.6 (2001), pp. 283–288.

[HG05] Ola Härkegård and S. Torkel Glad. “Resolving Actuator Redundancy—Optimal Control vs. Control Allocation”. In: *Automatica* 41.1 (Jan. 2005), pp. 137–144.

[HL01] Tingshu Hu and Zongli Lin. *Control Systems with Actuator Saturation: Analysis and Design*. Control Engineering. Boston: Birkhäuser, 2001.

[Hor09] Dariusz Horla. “On Directional Change and Anti-Windup Compensation in Multivariable Control Systems”. In: *International Journal of Applied Mathematics and Computer Science* 19.2 (June 2009), pp. 281–289.

[HT07] Yuehui Huang and Chi K. Tse. “Circuit Theoretic Classification of Parallel Connected DC-DC Converters”. In: *IEEE Transactions on Circuits and Systems I: Regular Papers* 54.5 (May 2007), pp. 1099–1108.

[HT23] W. P. M. H. Heemels and Aneel Tanwani. “Existence and Completeness of Solutions to Extended Projected Dynamical Systems and Sector-Bounded Projection-Based Controllers”. In: *IEEE Control Systems Letters* 7 (2023), pp. 1590–1595.

[IB90] A. Isidori and C.I. Byrnes. “Output Regulation of Nonlinear Systems”. In: *IEEE Transactions on Automatic Control* 35.2 (Feb. 1990), pp. 131–140.

[Ilc89] Achim Ilchmann. “Time-Varying Linear Control Systems: A Geometric Approach”. In: *IMA Journal of Mathematical Control and Information* 6.4 (1989), pp. 411–440.

[Ioa+21] Daniel Ioan, Ionela Prodan, Sorin Olaru, Florin Stoican, and Silviu-Iulian Niculescu. “Mixed-Integer Programming in Motion Planning”. In: *Annual Reviews in Control* 51 (Jan. 2021), pp. 65–87.

[Isi17] Alberto Isidori. *Lectures in Feedback Design for Multivariable Systems*. Advanced Textbooks in Control and Signal Processing. Cham: Springer International Publishing, 2017.

[Isi95] Alberto Isidori. *Nonlinear Control Systems*. Ed. by E. D. Sontag, M. Thoma, A. Isidori, and J. H. Van Schuppen. Communications and Control Engineering. London: Springer London, 1995.

[JF13] Tor A. Johansen and Thor I. Fossen. “Control Allocation—A Survey”. In: *Automatica* 49.5 (2013), pp. 1087–1103.

[JFT05] Tor A. Johansen, Thor I. Fossen, and Petter Tøndel. “Efficient Optimal Constrained Control Allocation via Multiparametric Programming”. In: *Journal of Guidance, Control, and Dynamics* 28.3 (2005), pp. 506–515.

[Jia+01] Jian Sun, D.M. Mitchell, M.F. Greuel, P.T. Krein, and R.M. Bass. “Averaged Modeling of PWM Converters Operating in Discontinuous Conduction Mode”. In: *IEEE Transactions on Power Electronics* 16.4 (July 2001), pp. 482–492.

[JKM08] C. N. Jones, E. C. Kerrigan, and J. M. Maciejowski. “On Polyhedral Projection and Parametric Programming”. In: *Journal of Optimization Theory and Applications* 138.2 (Aug. 2008), pp. 207–220.

[Joh04] T.A. Johansen. “Optimizing Nonlinear Control Allocation”. In: *43rd IEEE Conference on Decision and Control (CDC)*. Vol. 4. Nassau, Bahamas: IEEE, 2004, pp. 3435–3440.

[Jon05] Colin N Jones. “Polyhedral Tools for Control”. PhD thesis. University of Cambridge, 2005.

[JS03] Tor A. Johansen and Daniel Sbarbaro. “Optimizing Control of Over-Actuated Linear Systems with Nonlinear Output Maps via Control Lyapunov Functions”. In: *2003 European Control Conference (ECC)*. Cambridge, UK: IEEE, Sept. 2003, pp. 324–329.

[JS05] Tor A Johansen and Daniel Sbárbaro. “Lyapunov-Based Optimizing Control of Nonlinear Blending Processes”. In: *Control Systems Technology, IEEE Transactions on* 13.4 (2005), pp. 631–638.

[JT03] Michael Joswig and Nobuki Takayama, eds. *Algebra, Geometry and Software Systems*. Berlin, Heidelberg: Springer Berlin Heidelberg, 2003.

[JT13] Michael Joswig and Thorsten Theobald. *Polyhedral and Algebraic Methods in Computational Geometry*. Universitext. London: Springer London, 2013.

[Kar+83] Mark H. Karwan, Vahid Lotfi, Stanley Zionts, and Jan Telgen. *Redundancy in Mathematical Programming*. Ed. by M. Beckmann and W. Krelle. Vol. 206. Lecture Notes in Economics and Mathematical Systems. Berlin, Heidelberg: Springer, 1983.

[Kaz08] Marian K. Kazimierczuk. *Pulse-Width Modulated DC-DC Power Converters. Hauptbd.* 1. ed. Chichester: Wiley, 2008.

[KBL94] Prabha Kundur, Neal J. Balu, and Mark G. Lauby. *Power System Stability and Control*. The EPRI Power System Engineering Series. New York San Francisco Washington [etc.]: McGraw-Hill, 1994.

[KD02] Keliang Zhou and Danwei Wang. "Relationship between Space-Vector Modulation and Three-Phase Carrier-Based PWM: A Comprehensive Analysis [Three-Phase Inverters]". In: *IEEE Transactions on Industrial Electronics* 49.1 (Feb. 2002), pp. 186–196.

[Ker01] Eric C Kerrigan. "Robust Constraint Satisfaction : Invariant Sets and Predictive Control". PhD thesis. United Kingdom: University of Cambridge, 2001.

[KH83] Charles A. Klein and Ching-Hsiang Huang. "Review of Pseudoinverse Control for Use with Kinematically Redundant Manipulators". In: *IEEE Transactions on Systems, Man, and Cybernetics* SMC-13.2 (Mar. 1983), pp. 245–250.

[KJ22] Jérémie Kreiss and Marc Jungers. "Robust Input Redundancy for Uncertain Systems". In: *IFAC-PapersOnLine*. 10th IFAC Symposium on Robust Control Design ROCOND 2022 55.25 (Jan. 2022), pp. 157–162.

[KK07] A. Kwasinski and P. T. Krein. "Passivity-Based Control of Buck Converters with Constant-Power Loads". In: *2007 IEEE Power Electronics Specialists Conference*. Orlando, FL, USA: IEEE, 2007, pp. 259–265.

[KKO99] Petar V. Kokotović, Hassan K. Khalil, and John O'Reilly. *Singular Perturbation Methods in Control: Analysis and Design*. Classics in Applied Mathematics 25. Philadelphia: Society for Industrial and Applied Mathematics, 1999.

[KPT85] P. Khargonekar, K. Poolla, and A. Tannenbaum. "Robust Control of Linear Time-Invariant Plants Using Periodic Compensation". In: *IEEE Transactions on Automatic Control* 30.11 (Nov. 1985), pp. 1088–1096.

[Lal85a] Frederick J. Lallman. *Preliminary Design Study of a Lateral-Directional Control System Using Thrust Vectoring*. Tech. rep. 1985.

[Lal85b] Frederick J. Lallman. *Relative Control Effectiveness Technique with Application to Airplane Control Coordination*. Tech. rep. 1985.

[LaV06] Steven M. LaValle. *Planning Algorithms*. 1st ed. Cambridge University Press, May 2006.

[LDT18] Xiaolu Lucia Li, Zheng Dong, and Chi K. Tse. "Analysis of Basic Structures of Interconnected Converters for Single-Input Multiple-Output Applications". In: *2018 IEEE International Power Electronics and Application Conference and Exposition (PEAC)*. Shenzhen, China: IEEE, Nov. 2018, pp. 1–6.

[LE23] Michael Di Loreto and Damien Eberard. “Strong Left Inversion of Linear Systems and Input Reconstruction”. In: *IEEE Transactions on Automatic Control* 68.6 (June 2023), pp. 3612–3617.

[LFB22a] Grégoire Le Goff, Maurice Fadel, and Marc Bodson. “Scalable Control Allocation: Real-time Optimized Current Control in the Modular Multilevel Converter for Polyphase Systems”. In: *2022 International Symposium on Power Electronics, Electrical Drives, Automation and Motion (SPEEDAM)*. Sorrento, Italy: IEEE, June 2022, pp. 712–718.

[LFB22b] Grégoire Le Goff, Maurice Fadel, and Marc Bodson. “Scalable Optimal Control Allocation: Linear and Quadratic Programming Methods Applied to Active Capacitor Balancing in Modular Multilevel Converters”. In: *IFAC-PapersOnLine* 55.16 (2022), pp. 80–85.

[Lie77] Alain Liegeois. “Automatic Supervisory Control of the Configuration and Behavior of Multibody Mechanisms”. In: *IEEE transactions on systems, man, and cybernetics* 7.12 (1977), pp. 868–871.

[Lu21] “What Is Guidance?” In: *Journal of Guidance, Control, and Dynamics* 44.7 (July 2021). Ed. by Ping Lu, pp. 1237–1238.

[Luo+04] Yu Luo, Andrea Serrani, Stephen Yurkovich, David B. Doman, and Michael W. Oppenheimer. “Model Predictive Dynamic Control Allocation with Actuator Dynamics”. In: *Proceedings of the 2004 American Control Conference*. Vol. 2. IEEE, 2004, pp. 1695–1700.

[Luo+05] Yu Luo, A. Serrani, S. Yurkovich, D.B. Doman, and M.W. Oppenheimer. “Dynamic Control Allocation with Asymptotic Tracking of Time-Varying Control Input Commands”. In: *Proceedings of the 2005, American Control Conference, 2005.* June 2005, 2098–2103 vol. 3.

[Luo+07] Yu Luo, Andrea Serrani, Stephen Yurkovich, Michael W. Oppenheimer, and David B. Doman. “Model-Predictive Dynamic Control Allocation Scheme for Reentry Vehicles”. In: *Journal of Guidance, Control, and Dynamics* 30.1 (Jan. 2007), pp. 100–113.

[Mal+22] Danylo Malyuta, Taylor P. Reynolds, Michael Szmuk, Thomas Lew, Riccardo Bonalli, Marco Pavone, and Behçet Açıkmeşe. “Convex Optimization for Trajectory Generation: A Tutorial on Generating Dynamically Feasible Trajectories Reliably and Efficiently”. In: *IEEE Control Systems* 42.5 (Oct. 2022), pp. 40–113.

[Mar+10] Giovanni Marro, Fabio Morbidi, Lorenzo Ntogramatzidis, and Domenico Prattichizzo. “Geometric Control Theory for Linear Systems: A Tutorial”. In: *Proceedings of the 19th International Symposium on Mathematical Theory of Networks and Systems–MTNS*. Vol. 5. 2010.

[Mar04] Giovanni Marro. *The Geometric Approach Tools*. 2004.

[Mar18] Rainer Marquardt. “Modular Multilevel Converters: State of the Art and Future Progress”. In: *IEEE Power Electronics Magazine* 5.4 (Dec. 2018), pp. 24–31.

[May14] David Q. Mayne. “Model Predictive Control: Recent Developments and Future Promise”. In: *Automatica* 50.12 (Dec. 2014), pp. 2967–2986.

[MB04] Andrés Marcos and Gary J. Balas. “Development of Linear-Parameter-Varying Models for Aircraft”. In: *Journal of Guidance, Control, and Dynamics* 27.2 (Mar. 2004), pp. 218–228.

[MB76] R. Morris and R. Brown. “Extension of Validity of GRG Method in Optimal Control Calculation”. In: *IEEE Transactions on Automatic Control* 21.3 (June 1976), pp. 420–422.

[MCR20] Dajun Ma, Wu Chen, and Xinbo Ruan. “A Review of Voltage/Current Sharing Techniques for Series–Parallel-Connected Modular Power Conversion Systems”. In: *IEEE Transactions on Power Electronics* 35.11 (Nov. 2020), pp. 12383–12400.

[MD25] Ayan Mallik and Saikat Dey. “Generalized Modeling Methodologies for Modular Multiport Power Converters”. In: *Switching Modulator Optimization in Isolated Power Converters*. Springer, Cham, 2025, pp. 11–61.

[Mes+23] Souhir Messaoudi, Florentina Nicolau, Malek Ghanes, Lassaad Sbita, and Jean-Pierre Barbot. “Flatness-Based Control Strategy for n Parallel Connected Boost Choppers and n Sources With Differing Characteristics”. In: *IEEE Control Systems Letters* 7 (2023), pp. 3084–3089.

[Mic09] Yvan Michellod. “Overactuated Systems Coordination”. PhD thesis. Switzerland: École Polytechnique Fédérale de Lausanne, 2009.

[MM06] Agoes A. Moelja and Gjerrit Meinsma. “H2 Control of Preview Systems”. In: *Automatica* 42.6 (June 2006), pp. 945–952.

[MNZ05] G. Marro, Lorenzo Ntogramatzidis, and E. Zattoni. “H2-Optimal Rejection with Preview in the Continuous-Time Domain”. In: *Automatica* 41.5 (May 2005), pp. 815–821.

[Mor+95] P. Morin, C. Samson, J. -B. Pomet, and Z. -P. Jiang. “Time-Varying Feedback Stabilization of the Attitude of a Rigid Spacecraft with Two Controls”. In: *Systems & Control Letters* 25.5 (Aug. 1995), pp. 375–385.

[MTA08] Sudip K. Mazumder, Muhammad Tahir, and Kaustuva Acharya. “Master–Slave Current-Sharing Control of a Parallel DC–DC Converter System Over an RF Communication Interface”. In: *IEEE Transactions on Industrial Electronics* 55.1 (Jan. 2008), pp. 59–66.

[MUR07] Ned Mohan, Tore M. Undeland, and William P. Robbins. *Power Electronics: Converters, Applications, and Design*. Media enhanced 3. ed., [Nachdr.] Hoboken, NJ: Wiley, 2007.

[MZY10] E. Meyer, Zhiliang Zhang, and Yan-Fei Liu. “Controlled Auxiliary Circuit to Improve the Unloading Transient Response of Buck Converters”. In: *IEEE Transactions on Power Electronics* 25.4 (Apr. 2010), pp. 806–819.

[Nai+17] C. Nainer, M. Furci, A. Seuret, L. Zaccarian, and A. Franchi. “Hierarchical Control of the Over-Actuated ROSPO Platform via Static Input Allocation”. In: *IFAC-PapersOnLine* 50.1 (July 2017), pp. 12698–12703.

[Nen89] Dragomir N. Nenchev. “Redundancy Resolution through Local Optimization: A Review”. In: *Journal of Robotic Systems* 6.6 (1989), pp. 769–798.

[NL96] D. W. Novotny and T. A. Lipo. *Vector Control and Dynamics of AC Drives*. Monographs in Electrical and Electronic Engineering 41. Oxford : New York: Clarendon Press ; Oxford University Press, 1996.

[NP07] Lorenzo Ntogramatzidis and Domenico Prattichizzo. “Squaring down LTI Systems: A Geometric Approach”. In: *Systems & Control Letters* 56.3 (Mar. 2007), pp. 236–244.

[NPF24] Lorenzo Ntogramatzidis, Fabrizio Padula, and Augusto Ferrante. "New Results on Algorithms for the Computation of Output-Nulling and Input-Containing Subspaces". In: *International Journal of Control* 97.7 (July 2024), pp. 1586–1593.

[NS14] Lorenzo Ntogramatzidis and Robert Schmid. "Robust Eigenstructure Assignment in Geometric Control Theory". In: *SIAM Journal on Control and Optimization* 52.2 (Jan. 2014), pp. 960–986.

[NV90] Henk Nijmeijer and Arjan Van Der Schaft. *Nonlinear Dynamical Control Systems*. New York, NY: Springer New York, 1990.

[OD04] Michael W. Oppenheimer and David B. Doman. "Methods for Compensating for Control Allocator and Actuator Interactions". In: *Journal of Guidance, Control, and Dynamics* 27.5 (Sept. 2004), pp. 922–927.

[ODB11] Michael W Oppenheimer, David B. Doman, and Michael A. Bolender. "Control Allocation". In: *The Control Handbook: Control System Applications, Second Edition*. 2nd ed. The Electrical Engineering Handbook Series. Boca Raton: CRC Press, 2011, pp. 8.1–8.24.

[Par89] Joseph A. Paradiso. "A Highly Adaptable Method of Managing Jets and Aerosurfaces for Control of Aerospace Vehicles". In: *Guidance, Navigation and Control Conference*. American Institute of Aeronautics and Astronautics, 1989.

[Par91] Joseph A. Paradiso. "Adaptable Method of Managing Jets and Aerosurfaces for Aerospace Vehicle Control". In: *Journal of Guidance, Control, and Dynamics* 14.1 (1991), pp. 44–50.

[Pat15] Nicolas Patin. *Power Electronics Applied to Industrial Systems and Transports*. London, UK Oxford, UK: ISTE Press Elsevier, 2015.

[PCM95] M. Pachter, P. R. Chandler, and M. Mears. "Reconfigurable Tracking Control with Saturation". In: *Journal of Guidance, Control, and Dynamics* 18.5 (Sept. 1995), pp. 1016–1022.

[Per+21] Marcelo A. Perez, Salvador Ceballos, Georgios Konstantinou, Josep Pou, and Ricardo P. Aguilera. "Modular Multilevel Converters: Recent Achievements and Challenges". In: *IEEE Open Journal of the Industrial Electronics Society* 2 (2021), pp. 224–239.

[Per01] Lawrence Perko. *Differential Equations and Dynamical Systems*. Ed. by J. E. Marsden, L. Sirovich, and M. Golubitsky. Vol. 7. Texts in Applied Mathematics. New York, NY: Springer New York, 2001.

[PGH97] George Papageorgiou, Keith Glover, and Rick A. Hyde. "The H∞ Loop-Shaping Approach". In: *Robust Flight Control*. Ed. by Jean-François Magni, Samir Bennani, and Jan Terlouw. Berlin, Heidelberg: Springer, 1997, pp. 464–483.

[PI92] J. D. Perkins and International Federation of Automatic Control, eds. *Interactions between Process Design and Process Control: Preprints of the IFAC Workshop, London, UK, 7-8 September 1992*. 1st ed. Oxford ; New York: Published for the International Federation of Automatic Control by Pergamon Press, 1992.

[PN18] Fabrizio Padula and Lorenzo Ntogramatzidis. "On the Construction of Jordan Chains in the Eigenstructure Assignment for Output-Nulling Subspaces". In: *2018 European Control Conference (ECC)*. June 2018, pp. 2861–2866.

[PS00] Anthony Page and Marc Steinberg. "A Closed-Loop Comparison of Control Allocation Methods". In: *AIAA Guidance, Navigation, and Control Conference and Exhibit*. American Institute of Aeronautics and Astronautics, 2000.

[PS02] Anthony Page and Marc Steinberg. "High-Fidelity Simulation Testing of Control Allocation Methods". In: *AIAA Guidance, Navigation, and Control Conference and Exhibit*. American Institute of Aeronautics and Astronautics, 2002.

[PSZ12] T. E. Passenbrunner, M. Sassano, and L. Zaccarian. "Nonlinear Setpoint Regulation of Dynamically Redundant Actuators". In: *2012 American Control Conference (ACC)*. Montreal, QC: IEEE, June 2012, pp. 973–978.

[PSZ16] Thomas E. Passenbrunner, Mario Sassano, and Luca Zaccarian. "Optimality-Based Dynamic Allocation with Nonlinear First-Order Redundant Actuators". In: *European Journal of Control* 31 (Sept. 2016), pp. 33–40.

[PY10] Panos M. Pardalos and Vitaliy A. Yatsenko. *Optimization and Control of Bilinear Systems: Theory, Algorithms, and Applications*. Springer Optimization and Its Applications v.11. Dordrecht: Springer, 2010.

[RAP22] Guilherme Ramos, A. Pedro Aguiar, and Sérgio Pequito. "An Overview of Structural Systems Theory". In: *Automatica* 140 (June 2022), p. 110229.

[RBG96] Jacob Reiner, Gary J. Balas, and William L. Garrard. "Flight Control Design Using Robust Dynamic Inversion and Time-Scale Separation". In: *Automatica* 32.11 (Nov. 1996), pp. 1493–1504.

[Rep+17] Andrew Repton, Hidenori Kobayashi, Mark Childs, and Jindrich Svorc. "Asymmetric Inductors in Multi-Phase DCDC Converters". US 2015/0097542 A1. Sept. 2017.

[Res90] Witold Respondek. "Right and Left Invertibility of Nonlinear Control Systems". In: *Nonlinear Controllability and Optimal Control*. Vol. 24. Routledge, 1990, pp. 133–176.

[RLD99] M.J. Ryan, R.D. Lorenz, and R. De Doncker. "Modeling of Multileg Sine-Wave Inverters: A Geometric Approach". In: *IEEE Transactions on Industrial Electronics* 46.6 (Dec. 1999), pp. 1183–1191.

[Sab+00] Ali Saberi, Anton Stoorvogel, Peddapullaiah Sannuti, and Anton A. Stoorvogel. *Control of linear systems with regulation and input constraints*. Communications and control engineering. London Berlin Heidelberg New York Barcelona Hong Kong Milan Paris Santa Clara Singapore Tokyo: Springer, 2000.

[Sad+19] Edouard Sadien, Mathieu Carton, Christophe Grimault, Louis Emmanuel Romana, Clement Roos, Abderazik Birouche, and Michel Basset. "A Detailed Comparison of Control Allocation Techniques on a Realistic On-Ground Aircraft Benchmark". In: *2019 American Control Conference (ACC)*. Philadelphia, PA, USA: IEEE, July 2019, pp. 2891–2896.

[Sch11] Alexander Schrijver. *Theory of Linear and Integer Programming*. Nachdr. Wiley-Interscience Series in Discrete Mathematics and Optimization. Chichester Weinheim: Wiley, 2011.

[SEG92] S. Antony Snell, Dale F. Enns, and William L. Garrard. "Nonlinear Inversion Flight Control for a Supermaneuverable Aircraft". In: *Journal of Guidance, Control, and Dynamics* 15.4 (July 1992), pp. 976–984.

[Ser12] A. Serrani. "Output Regulation for Over-Actuated Linear Systems via Inverse Model Allocation". In: *2012 IEEE 51st IEEE Conference on Decision and Control (CDC)*. Maui, HI, USA: IEEE, Dec. 2012, pp. 4871–4876.

[Ser89] H. Seraji. "Configuration Control of Redundant Manipulators: Theory and Implementation". In: *IEEE Transactions on Robotics and Automation* 5.4 (Aug. 1989), pp. 472–490.

[Shi+06] A. Shiriaev, A. Robertsson, J. Perram, and A. Sandberg. "Periodic Motion Planning for Virtually Constrained Euler–Lagrange Systems". In: *Systems & Control Letters* 55.11 (Nov. 2006), pp. 900–907.

[Shi+99] Shiguo Luo, Zhihong Ye, Ray-Lee Lin, and F.C. Lee. "A Classification and Evaluation of Paralleling Methods for Power Supply Modules". In: *30th Annual IEEE Power Electronics Specialists Conference. Record. (Cat. No.99CH36321)*. Vol. 2. Charleston, SC, USA: IEEE, 1999, pp. 901–908.

[Sig+06] David Sigthorsson, Andrea Serrani, Stephen Yurkovich, Michael Bolender, and David Doman. "Tracking Control for an Overactuated Hypersonic Air-Breathing Vehicle with Steady State Constraints". In: *AIAA Guidance, Navigation, and Control Conference and Exhibit*. Keystone, Colorado: American Institute of Aeronautics and Astronautics, Aug. 2006.

[Sig+09] David Sigthorsson, Andrea Serrani, Michael Bolender, and David Doman. "LPV Control Design for Over-Actuated Hypersonic Vehicles Models". In: *AIAA Guidance, Navigation, and Control Conference*. Chicago, Illinois: American Institute of Aeronautics and Astronautics, Aug. 2009.

[Sim62] Herbert A. Simon. "The Architecture of Complexity". In: *Proceedings of the American Philosophical Society* 106.6 (1962), pp. 467–482. JSTOR: 985254.

[SK15] Mahesh Srinivasan and Alexis Kwasinski. "Autonomous Hierarchical Control of Dc Microgrids with Constant-Power Loads". In: *2015 IEEE Applied Power Electronics Conference and Exposition (APEC)*. IEEE, 2015, pp. 2808–2815.

[Sko09] S. Skogestad. "Feedback: Still the Simplest and Best Solution". In: *Modeling, Identification and Control: A Norwegian Research Bulletin* 30.3 (2009), pp. 149–155.

[Sør97] O. J. Sørdalen. "Optimal Thrust Allocation for Marine Vessels". In: *Control Engineering Practice* 5.9 (Sept. 1997), pp. 1223–1231.

[SP05] Sigurd Skogestad and Ian Postlethwaite. *Multivariable Feedback Control: Analysis and Design*. 2nd ed. Hoboken, NJ: John Wiley, 2005.

[Spj08] Jørgen Spjøtvold. "Parametric Programming in Control Theory". Doctoral Thesis. Fakultet for informasjonsteknologi, matematikk og elektroteknikk, 2008.

[SS06a] David O. Sigthorsson and Andrea Serrani. "Tracking with Steady-State Optimization: An Application to Air-Breathing Hypersonic Vehicle Control". In: *2006 14th Mediterranean Conference on Control and Automation*. Ancona, Italy: IEEE, June 2006, pp. 1–6.

[SS06b] Hebertt J. Sira Ramírez and Ramón Silva-Ortigoza. *Control Design Techniques in Power Electronics Devices*. Power Systems. London: Springer, 2006.

[SS99] Anton A Stoorvogel and Ali Saberi. "Output Regulation of Linear Plants with Actuators Subject to Amplitude and Rate Constraints". In: *Int. J. Robust Nonlinear Control* (1999).

[SSS12] Ali Saberi, Anton A. Stoorvogel, and Peddapullaiah Sannuti. *Internal and External Stabilization of Linear Systems with Constraints*. Systems & Control: Foundations & Applications. Boston, MA: Birkhäuser Boston, 2012.

[STT14] Zhenyu Shan, Chi K. Tse, and Siew-Chong Tan. "Classification of Auxiliary Circuit Schemes for Feeding Fast Load Transients in Switching Power Supplies". In: *IEEE Transactions on Circuits and Systems I: Regular Papers* 61.3 (Mar. 2014), pp. 930–942.

[Sun+05] J. Sun, Y. Qiu, B. Lu, M. Xu, F.C. Lee, and W.C. Tipton. "Dynamic Performance Analysis of Outer-Loop Current Sharing Control for Paralleled DC-DC Converters". In: *Twentieth Annual IEEE Applied Power Electronics Conference and Exposition, 2005. APEC 2005.* Vol. 2. Mar. 2005, 1346–1352 Vol. 2.

[SVB23] Brayan M. Shali, Arjan Van Der Schaft, and Bart Besselink. "Composition of Behavioural Assume–Guarantee Contracts". In: *IEEE Transactions on Automatic Control* 68.10 (Oct. 2023), pp. 5991–6006.

[Švi+13] V Šviković, P Alou, J A Oliver, O García, and J A Cobos. "Improvement of the Dynamic Performance of a Multiphase Current Controlled Buck Converter Using an Auxiliary Synchronous Buck Converter as an Additional Energy Path". In: *XX Seminario Anual de Automatica, Electronica Industrial e Instrumentacion SAAEI 2013*. Madrid, 2013.

[Tar+11] Sophie Tarbouriech, Germain Garcia, João Manoel Gomes Da Silva, and Isabelle Queinnec. *Stability and Stabilization of Linear Systems with Saturating Actuators*. London: Springer London, 2011.

[Tha+09] H. Dang Thai, O. Deleage, H. Chazal, Y. Lembeye, R. Rolland, and Jc Crebier. "Design of Modular Converters; Survey and Introduction to Generic Approaches". In: *2009 Twenty-Fourth Annual IEEE Applied Power Electronics Conference and Exposition*. Washington, DC, USA: IEEE, Feb. 2009, pp. 1427–1433.

[TJ05] Johannes Tjønnås and Tor A. Johansen. "Optimizing Nonlinear Adaptive Control Allocation". In: *IFAC Proceedings Volumes* 38.1 (2005), pp. 1160–1165.

[TJ06] Johannes Tjonnaas and Tor Arne Johansen. "Adaptive Optimizing Dynamic Control Allocation Algorithm for Yaw Stabilization of an Automotive Vehicle Using Brakes". In: *2006 14th Mediterranean Conference on Control and Automation*. IEEE, 2006, pp. 1–6.

[TJ07a] Johannes Tjonnas and Tor Arne Johansen. "Optimizing Adaptive Control Allocation with Actuator Dynamics". In: *2007 46th IEEE Conference on Decision and Control*. IEEE, 2007, pp. 3780–3785.

[TJ07b] Johannes Tjønnås and Tor A. Johansen. "On Optimizing Nonlinear Adaptive Control Allocation with Actuator Dynamics". In: *IFAC Proceedings Volumes* 40.12 (2007), pp. 852–857.

[TJ08] Johannes Tjønnås and Tor A. Johansen. "Adaptive Control Allocation". In: *Automatica* 44.11 (Nov. 2008), pp. 2754–2765.

[Tjo+06] Johannes Tjonnas, Antoine Chaillet, Elena Pantele, and Tor Arne Johansen. "Cascade Lemma for Set-Stable Systems". In: *Proceedings of the 45th IEEE Conference on Decision and Control*. San Diego, CA, USA: IEEE, 2006, pp. 338–342.

[Tjø08] Johannes Tjønnås. "Nonlinear and Adaptive Dynamic Control Allocation". Doctoral Thesis. Fakultet for informasjonsteknologi, matematikk og elektroteknikk, 2008.

[Tom75] M. Tomizuka. “Optimal Continuous Finite Preview Problem”. In: *IEEE Transactions on Automatic Control* 20.3 (June 1975), pp. 362–365.

[Tøn03] Petter Tøndel. “Constrained Optimal Control via Multiparametric Quadratic Programming”. PhD thesis. Trondheim, Norway: University of Science and Technology Trondheim, Norway, 2003.

[TSH12] Harry L Trentelman, Anton A Stoorvogel, and Malo Hautus. *Control Theory for Linear Systems*. Springer Science & Business Media, 2012.

[TT09] S. Tarbouriech and M. Turner. “Anti-Windup Design: An Overview of Some Recent Advances and Open Problems”. In: *IET Control Theory & Applications* 3.1 (Jan. 2009), pp. 1–19.

[TV98] V.J. Thottuvelil and G.C. Verghese. “Analysis and Control Design of Paralleled DC/DC Converters with Current Sharing”. In: *IEEE Transactions on Power Electronics* 13.4 (July 1998), pp. 635–644.

[Van17] Arjan Van Der Schaft. *L2-Gain and Passivity Techniques in Nonlinear Control*. Communications and Control Engineering. Cham: Springer International Publishing, 2017.

[VB94] John Virnig and David Bodden. “Multivariable Control Allocation and Control Law Conditioning When Control Effectors Limit”. In: *Guidance, Navigation, and Control Conference*. American Institute of Aeronautics and Astronautics, 1994.

[VD01] Ram Venkataraman and David B. Doman. “Control Allocation and Compensation for Over-Actuated Systems with Non-Linear Effectors”. In: *Proceedings of the 2001 American Control Conference.(Cat. No. 01CH37148)*. Vol. 3. IEEE, 2001, pp. 1812–1814.

[VG13] Giorgio Valmorbida and Sergio Galeani. “Nonlinear Output Regulation for Over-Actuated Linear Systems”. In: *52nd IEEE Conference on Decision and Control*. Firenze: IEEE, Dec. 2013, pp. 4485–4490.

[Vid+19] Paul-Étienne Vidal, Simon Cailhol, Frédéric Rotella, and Maurice Fadel. “Generic Pulse Width Modulation Model, Based on Generalized Inverses and Applied to Voltage Source Inverters”. In: *COMPEL - The international journal for computation and mathematics in electrical and electronic engineering* 38.2 (Mar. 2019), pp. 845–861.

[VKJ24a] V. V. Viana, J. Kreiss, and M. Jungers. “Input Redundancy of Switched Linear Systems via Polynomial Parameter-Dependent Systems”. In: *IEEE Control Systems Letters* 8 (2024), pp. 1066–1071.

[VKJ24b] Valessa V. Viana, Jérémie Kreiss, and Marc Jungers. “On the Computation of Controlled Invariant and Output Invisible Subspaces for Parameter-Dependent Systems”. In: *IEEE Transactions on Automatic Control* 69.7 (July 2024), pp. 4695–4701.

[VKJ24c] Valessa Valentim Viana, Jérémie Kreiss, and Marc Jungers. “Adaptive Input Redundancy of Polynomial Parameter-Dependent Systems”. In: *Preprint submitted on 26 Feb 2024* (2024).

[VOD04] R. Venkataraman, M. Oppenheimer, and D. Doman. “A New Control Allocation Method That Accounts for Effector Dynamics”. In: *2004 IEEE Aerospace Conference Proceedings (IEEE Cat. No.04TH8720)*. Vol. 4. Mar. 2004, 2710–2715 Vol.4.

[VSB07] Chris Vermillion, Jing Sun, and Ken Butts. “Model Predictive Control Allocation for Overactuated Systems - Stability and Performance”. In: *2007 46th IEEE Conference on Decision and Control*. New Orleans, LA, USA: IEEE, 2007, pp. 1251–1256.

[Wan+09] Fei Wang, Wei Shen, Dushan Boroyevich, Scott Ragon, Victor Stefanovic, and Michel Arpilliere. "Voltage Source Inverter". In: *IEEE Industry Applications Magazine* 15.2 (Mar. 2009), pp. 24–33.

[Whi69] Daniel E. Whitney. "Resolved Motion Rate Control of Manipulators and Human Prostheses". In: *IEEE Transactions on Man-Machine Systems* 10.2 (June 1969), pp. 47–53.

[WM70] W. M. Wonham and A. S. Morse. "Decoupling and Pole Assignment in Linear Multivariable Systems: A Geometric Approach". In: *SIAM Journal on Control* 8.1 (Feb. 1970), pp. 1–18.

[Wol74] William A. Wolovich. *Linear Multivariable Systems*. Applied Mathematical Sciences 11. New York: Springer-Verlag, 1974.

[Won85] W. Murray Wonham. *Linear Multivariable Control: A Geometric Approach*. 3rd ed. New York: Springer-Verlag, 1985.

[WS93] K. S. Walgama and J. Sternby. "Conditioning Technique for Multiinput Multioutput Processes with Input Saturation". In: *IEE Proceedings D (Control Theory and Applications)* 140.4 (July 1993), pp. 231–242.

[Wu15] Hao Wu. "Stratégie d'allocation de Contrôle Pour Les Systèmes Sur-Actionnés". MA thesis. Villeurbanne, France: INSA Lyon, 2015.

[Zac07] Luca Zaccarian. "On Dynamic Control Allocation for Input-Redundant Control Systems". In: *2007 46th IEEE Conference on Decision and Control*. New Orleans, LA, USA: IEEE, 2007, pp. 1192–1197.

[Zac09] Luca Zaccarian. "Dynamic Allocation for Input Redundant Control Systems". In: *Automatica* 45.6 (June 2009), pp. 1431–1438.

[ZCS15] Junqiang Zhou, Marcello Canova, and Andrea Serrani. "Stability and Feasibility of Predictive Inverse Model Allocation for Constrained Over-Actuated Linear Systems". In: *2015 American Control Conference (ACC)*. Chicago, IL, USA: IEEE, July 2015, pp. 4567–4572.

[ZCS16] Junqiang Zhou, Marcello Canova, and Andrea Serrani. "Predictive Inverse Model Allocation for Constrained Over-Actuated Linear Systems". In: *Automatica* 67 (May 2016), pp. 267–276.

[ZCS17] Junqiang Zhou, Marcello Canova, and Andrea Serrani. "Non-Intrusive Reference Governors for Over-Actuated Linear Systems". In: *IEEE Transactions on Automatic Control* 62.9 (Sept. 2017), pp. 4734–4740.

[Zha+19] Guanglei Zhao, Dragan Nešić, Ying Tan, and Changchun Hua. "Overcoming Overshoot Performance Limitations of Linear Systems with Reset Control". In: *Automatica* 101 (Mar. 2019), pp. 27–35.

[Zho+13] Zhou, Junqiang, Lisa Fiorentini, Marcello Canova, and Andrea Serrani. "Dynamic Steady-State Allocation for over-Actuated Turbocharged Diesel Engines". In: *52nd IEEE Conference on Decision and Control*. Firenze: IEEE, Dec. 2013, pp. 6843–6848.

[Zie95] Günter M. Ziegler. *Lectures on Polytopes*. Vol. 152. Graduate Texts in Mathematics. New York, NY: Springer New York, 1995.

[ZN42] J. G. Ziegler and N. B. Nichols. "Optimum Settings for Automatic Controllers". In: *Transactions of the American Society of Mechanical Engineers* 64.8 (Nov. 1942), pp. 759–765.

Summary

Replacing a single high-capacity actuator with several ones operating in concert is an increasingly popular technological trend. The aim is to increase not only the overall capacity of the actuation subsystem, but also its systemic robustness against the failure of one of its components.

The control specifications for such a system are naturally ordered, since component preferences must only be taken into account if their overall contribution to the control effort is preserved. Strict compliance with this hierarchy is closely related to the notion of Input Redundancy (IR). This property is redefined as the existence of distinct input trajectories giving rise to the same output trajectory. In other words, IR is the opposite of left-invertibility. In the case of linear systems associated with linear input and state spaces, IR is equivalent to the existence of an annihilator, whose output can be injected at the system input without modifying its output trajectory. Under the same assumptions, it is possible to isolate the part of the input that influences the output. These three points of view (inversion, annihilator, input decomposition) are illustrated by considering the case of the 3-phases star-connected inverter, then generalized to general static and affine systems subject to input constraints.

In the case of dynamic systems, the structure of the control law is traditionally based on control allocation. This strategy formulates the overall actuation effort distribution as an optimization problem, which is solved quasi-continuously, on-line. An in-depth analysis of the literature dedicated to this approach is proposed, adopting a historical point of view and illustrating the techniques presented on a single academic example.

This analysis naturally opens on the extension to dynamic systems of the discussion adopting the three previous points of view. IR is formally defined for this class of systems. Taking the state trajectory into account gives rise to a taxonomy of input-redundant systems, in the linear case. Under the latter assumption, characterizations of IR and its taxonomy are proposed. The existence, construction and implementation of an annihilator are also discussed, as well as the impact of input and state constraints on IR.

The central problem of output regulation is also re-examined through the lens of IR. The inadequacy of the regulator equations to take advantage of the degrees of freedom offered by IR is highlighted. On the contrary, equipping the trajectories generator with an annihilator specifically designed for this purpose enables exhaustive parameterization of acceptable steady-state. This in turn offers the possibility of making an optimal choice of permanent regime, on-line. In so doing, the notion of IR is weakened, then shaped into a version specifically adapted to output control: the bounded and persistent weak IR. The resulting framework enables an in-depth comparison of existing definitions of IR, which are also linked to several notions of left-invertibility.

The problem of output regulation of a parallel interconnection of buck converters is addressed. In addition to its relevance to power electronics research, this problem is inspiring for control theory. It allows us to concretize and enrich the discussions on the three previous points of view, in the case of dynamic systems. The analysis carried out within a general

framework is also made deeper on the closed-loop robustness.

Finally, three perspectives are outlined. The first aims to build a universal framework for the control of modular power electronics converters. In this sense, it extends the results obtained on parallel buck converters and the 3-phases inverter. The challenges identified justify a series of research directions around IR and its exploitation in control, aimed at completing and extending the results of this manuscript. Finally, the expected benefits of co-designing the system, its control and the specifications are highlighted. To this end, the importance of inversion in the context of constrained dynamic systems is emphasized.

Keywords: input redundancy, hierarchical control, control of power electronic converters, control allocation, inversion, output regulation, co-design.

Résumé

Remplacer un unique actionneur de grande capacité par plusieurs fonctionnant de concert constitue une tendance technologique de plus en plus répandue. L'objectif est d'accroître non seulement la capacité globale du système d'actionnement, mais également sa robustesse systémique vis-à-vis des défaillances de l'un de ses composants.

Le cahier des charges de la commande d'un tel système est naturellement hiérarchisé, puisque les préférences des composants ne doivent être prises en compte que si leur contribution globale à l'effort de commande est préservée. Le strict respect de cette hiérarchie est en lien étroit avec la notion de Redondance d'Entrée (RE). Cette propriété est redéfinie comme l'existence de trajectoires d'entrée distinctes donnant lieu à une même trajectoire de sortie. Autrement dit, la RE est le contraire de l'inversibilité à gauche. Dans le cas de systèmes linéaires associés à des espaces vectoriels pour l'entrée et l'état, la RE est équivalente à l'existence d'un annihilateur, dont la sortie peut être injectée à l'entrée du système sans modifier sa trajectoire de sortie. Sous ces mêmes hypothèses, il est possible d'isoler la partie de l'entrée qui influence la sortie. Ces trois points de vue (inversion, annihilateur, décomposition de l'entrée) sont illustrés en traitant le cas de l'onduleur triphasé en étoile, puis généralisés aux systèmes statiques et affines soumis à des contraintes d'entrée.

Dans le cas où le système est dynamique, la structuration de la loi de commande s'appuie classiquement sur l'allocation de commande. Cette stratégie formule la distribution de l'effort d'actionnement global comme un problème d'optimisation, dont la résolution est effectuée de manière quasi-continue, en ligne. Une analyse approfondie de la littérature dédiée à cette approche est proposée, en adoptant un point de vue historique et en illustrant les techniques présentées sur un unique exemple académique.

Cette analyse s'ouvre naturellement sur l'extension aux systèmes dynamiques de la discussion adoptant les trois points de vue précédents. La RE est formellement définie pour cette classe de systèmes. La prise en compte de la trajectoire d'état donne naissance à une taxonomie des systèmes redondants en entrée, dans le cas linéaire. Sous cette dernière hypothèse, des caractérisations de la RE et de sa taxonomie sont proposées. L'existence, la construction et la mise en œuvre d'un annihilateur sont également discutés, de même que l'influence des contraintes d'entrée et d'état sur la RE.

Le problème central de la régulation de sortie est également revisité au prisme de la RE. L'inadéquation des équations du régulateur pour tirer profit des degrés de libertés offert par la RE est mise en évidence. Au contraire, équiper le générateur de trajectoires d'un annihilateur spécifiquement conçu pour cet objectif permet une paramétrisation exhaustive des régimes permanents acceptables, et offre ainsi la possibilité d'en faire un choix optimal, en ligne. Ce faisant, la notion de RE est affaiblie, puis façonnée en une version spécifiquement adaptée à la régulation de sortie : la RE faible, bornée et persistante. Le cadre obtenu permet une comparaison en profondeur des définitions existantes de la RE, qui sont également reliées à plusieurs notions d'inversibilité à gauche.

Le problème de la régulation de sortie d'une interconnexion parallèle de hacheurs série est abordé. En plus d'être pertinent pour la recherche en électronique de puissance, ce problème est source d'inspiration pour l'automatique. Il permet en effet de concrétiser et d'enrichir les discussions sur les trois points de vue précédent, dans le cas des systèmes dynamiques. L'analyse conduite dans un cadre général est également approfondie pour ce qui concerne la robustesse de la boucle fermée.

Finalement, trois perspectives sont esquissées. La première vise la construction d'un cadre universel pour la commande de convertisseurs d'électronique de puissance modulaire. En ce sens, elle prolonge les résultats obtenus sur les hacheurs séries en parallèle et sur l'onduleur triphasé. Les verrous identifiés justifient une série de directions de recherche autour de la RE et de son exploitation en automatique, visant à compléter et à étendre les résultats présentés. Enfin, les bénéfices attendus d'une co-conception du système, de sa commande et du cahier des charges qu'elle remplie sont mis en lumière. Dans cet objectif, la centralité de l'inversion des systèmes dynamiques sous contraintes est exhibée.

Mots-clés: redondance d'entrée, commande hiérarchique, commande de convertisseurs électroniques de puissance, allocation de commande, inversion, régulation de sortie, co-conception.